REFERENCE ONLY

UNIVERSITY OF LONDON THESIS

Degree PhD Year 2005 Name of Author OHOMEN, N-C

COPYRIGHT

This is a thesis accepted for a Higher Degree of the University of London. It is an unpublished typescript and the copyright is held by the author. All persons consulting the thesis must read and abide by the Copyright Declaration below.

COPYRIGHT DECLARATION

I recognise that the copyright of the above-described thesis rests with the author and that no quotation from it or information derived from it may be published without the prior written consent of the author.

LOANS

Theses may not be lent to individuals, but the Senate House Library may lend a copy to approved libraries within the United Kingdom, for consultation solely on the premises of those libraries. Application should be made to: Inter-Library Loans, Senate House Library, Senate House, Malet Street, London WC1E 7HU.

REPRODUCTION

University of London theses may not be reproduced without explicit written permission from the Senate House Library. Enquiries should be addressed to the Theses Section of the Library. Regulations concerning reproduction vary according to the date of acceptance of the thesis and are listed below as guidelines.

A. Before 1962. Permission granted only upon the prior written consent of the author. (The Senate House Library will provide addresses where possible).

B. 1962 - 1974. In many cases the author has agreed to permit copying upon completion of a Copyright Declaration.

C. 1975 - 1988. Most theses may be copied upon completion of a Copyright Declaration.

D. 1989 onwards. Most theses may be copied.

This thesis comes within category D.

☑ This copy has been deposited in the Library of UCL

☐ This copy has been deposited in the Senate House Library, Senate House, Malet Street, London WC1E 7HU.

Investigation of Chx10 in Development of the Neural Retina and Microphthalmia

Nathalie Sophie Dhomen

A thesis submitted for the degree of Doctor of Philosophy

University of London

2005

Developmental Biology Unit

Institute of Child Health

University College London

30 Guilford Street

London WC1N 1EH

ProQuest LLC
789 East Eisenhower Parkway
P.O. Box 1346
Ann Arbor, MI 48106-1346

Abstract

Chx10 is a homeobox transcription factor essential for the development of the vertebrate eye. A mutation in the human gene *CHX10* causes microphthalmia and a similar phenotype is observed in the ocular retardation, *Chx10* null mouse. Lack of Chx10 causes a reduction in proliferation of neural retinal progenitor cells (RPCs) in the developing retina, resulting in a reduction in the size of the eye. The aim of this study was threefold: to identify downstream targets of the *Chx10* gene and discover more about the role of Chx10 at a molecular level, to further characterise the *Chx10*$^{-/-}$ phenotype and the behaviour of the mutant RPCs, and to investigate the possibility that the *Chx10*$^{-/-}$ retina harbours stem cell-like cells.

Firstly, Affymetrix GeneChip technology was used to compare the gene expression profile of wild type retina with that of the *Chx10* null retina during early development. Significant differential expression was observed for 34 characterised genes; genes involved in neuronal differentiation were down-regulated whereas genes involved in retinal pigmented epithelium (RPE) specification were up-regulated. These findings highlight a novel role for Chx10 in maintaining the neural retina/RPE boundary.

Secondly, experiments aimed at characterising *Chx10*$^{-/-}$ RPCs showed that they exhibit altered cycling properties compared to wild type RPCs and that their differentiation to neural retinal cells is delayed. The data resulting from these studies support a model in which the transition from G1 phase of the cell cycle to S phase or to differentiation is disrupted in the *Chx10*$^{-/-}$ retina. Finally, a population of proliferating cells was discovered in the adult *Chx10*$^{-/-}$ retina, which showed neurogenic properties and formed neurospheres in culture, a point of interest in the context of retinal stem cell research.

The study conducted here has offered valuable clues as to how Chx10 affects retinal progenitor cell proliferation and differentiation at both a molecular and a cellular level. It is hoped this work will contribute to the current knowledge of eye development in general, and Chx10's involvement in this process in particular.

Acknowledgements

First and foremost, I would like to thank my primary supervisor Jane Sowden and my secondary supervisor Patrizia Ferretti for all their help, support and advice during the last four years. In addition there are several people who have given me technical assistance and advice as well as contributing to the work presented in this thesis. They are Dr. Mike Hubank, Danielle Fletcher, and Nipurna Jina, who run the Affymetrix GeneChip facility at ICH, Jo Sinclair in the Molecular Immunology Unit at ICH, who runs the flow cytometry unit and has helped with the analysis of the flow cytometry experiments described in Chapter 5, Brian Young at the Institute of Neuroscience who prepared the semithin retinal sections described in Chapter 5, Professor Robin Ali, Dr. James Bainbridge, and Kam Balaggan from the Institute of Ophthalmology, who contributed to Chapter 6 - and I would like to specifically thank Jim and Kam for performing the BrdU injections described therein-, Joel Rae for his contribution of data to the orientation of cell division experiment described in Chapter 5, and Deborah Ridout who provided statistical advice. Funding for this project was provided by a Fight for Sight studentship and I would like to thank the organisation for their support and interest.

On a personal note, I would like to thank everyone in the Developmental Biology and Neural Development units who have made my day to day life interesting and enjoyable. I don't want to offend anyone by accidental omission, so I'm just going to say you know who you are, although I'd like to say a special thank you to Joel Rae for his help in the final production of this thesis. I feel privileged to have known and worked with you all. Special mention also goes to 'the Coven', Bronwen Herbert, Kerra Pearce, Katy Newton, Sarah Horton, Chantelle Hudson and Emily Towers, who have kept me sane and shared with me the ups and downs of phd-dom. I would especially like to thank Bronwen and Kerra for their close personal friendship in addition to their technical help in the labs. I would like to thank my family, and especially my parents, for their unstinting love and support throughout my studies and research. Their encouragement has contributed greatly to the completion of this thesis. Finally, I would like to thank Marc, whose endless love, support, and patience have meant the world to me.

Table of Contents

List of Figures

List of Tables

List of Abbreviations

Abbreviation	Full Title
ANOVA	Analysis of variance
bHLH	Basic helix-loop-helix
BMP	Bone morphogenetic protein
BrdU	Bromodeoxyuridine
CB	Ciliary body
CDS	Coding sequence
CE	Ciliary epithelium
CHX10	C. elegans ceh-10 homeo domain containing homolog
CMZ	Ciliary marginal zone
CNS	Central nervous system
CRALBP	Cellular retinaldehyde-binding protein
DAPI	4'6-diamidino-2-phenylindole
DEPC	Diethylpyrocarbonate
EGF	Epidermal growth factor
EST	Expressed sequence tags
EtOH	Ethanol
FACS	Flourescence activated cell sorting
FEVR	Familial exudative vitreoretinopathy
FGF	Fibroblast growth factor
GAPDH	Glyceraldehyde-3-phosphate dehydrogenase
GCL	Ganglion cell layer
GFAP	Glial fibrilary acidic protein
GFP	Green flurorescent protein
GO	Graves' ophthalmopathy
H3	Histone H3
INL	Inner nuclear layer
ISH	*In situ* hybridisation
IVT	In vitro transcription
MeSH	Medical subject heading
Mitf	Microphthalmia-associated transcription factor
NBL	Neuroblastic layer
NeuN	Neuronal nuclear antigen
NMD	Nonsense-mediated mRNA decay
NNO1	Nanophthalmos 1
NR	Neural retina
OMIM	Online Medelian Inheritance in Man
ONL	Outer nuclear layer
PBS	Phosphate buffered saline
PCNA	Proliferating cell nuclear antigen
PI	Propidium iodide
PKC	Protein kinase C
PNA	Peanut agglutinin
pRB	Protein retinoblastoma
RA	Retinoic acid
RGCs	Retinal ganglion cells
RPC	Retinal progenitor cell
RPE	Retinal pigmented epithelium
RT-PCR	RT-PCR
SAGE	Serial analysis of gene expression
TUNEL	TdT-mediated dUTP digoxigenin nick end labelling

CHAPTER 1

Introduction

1.1 The importance of vision loss drives the study of eye development

The World Health Organization (WHO) estimated in 1996 that approximately 38 million people worldwide were blind and more than 110 million had low vision. With the world's population estimated at 5.3 billion at the time, this translated roughly into an overall blindness rate of 7 per 1000. (Schaumberg and Dana, 1996). By 2002, the WHO reported that the number of people with visual impairment worldwide was in excess of 161 million (Resnikoff et al., 2004). Normal vision provides a key source of information about one's environment, and any loss of vision soon becomes debilitating. As such a large number of people are affected by vision loss, a great deal of effort is being made to examine the causes and possible solutions to blindness. The causes of blindness are wide-ranging, from genetic abnormalities to vitamin insufficiencies. In this study, microphthalmia, a form of congenital blindness characterised by small eyes, is being examined. Congenital blindness is usually either caused by genetic factors (e.g. mutations in single genes or chromosome abnormalities) or is prenatally acquired because of environmental factors such as maternal drug use, irradiation poisoning or maternal disease (Warburg, 1993). Simple, non-syndromic microphthalmia results from genetic alterations at various chromosomal loci (see section 1.4).

The well-characterised physiology and anatomy of the eye facilitates research into its developmental aberrations. A large number of patients and murine models with eye malformations are available for genetic and biological analysis because a) the eye is not essential for viability, b) gene mutations affecting the eye and retina generally produce readily recognised phenotypes and c) the importance of normal vision to humans means that virtually any significant dysfunction of the retina is brought to clinical attention (Freund et al., 1996). Thus, more mutations affecting the eye have been documented in humans than in any other species. Genetic abnormalities of the eye were found to be involved in 2% of the 2811 phenotypes recorded in a 1985 analysis of McKusick's Mendelian Inheritance in Man (Costa et al., 1985), making it the fourth most common system affected by genetic disease in humans (Freund et al., 1996).

In addition, the retina is an ideal developmental system for study. The eye is effectively a highly specialised extension of the brain (Chow and Lang, 2001) and the retina in particular is recognised as an 'approachable part of the brain' (Dowling, 1987; Freund et al., 1996). This accessibility exists even *in utero*, and has enabled the use of the eye as a model system for the study of mechanisms of development in general, and central nervous system development in particular, in a variety of vertebrates (Cepko et al., 1996; Chow and Lang, 2001; Dyer and Cepko, 2001; Harris, 1997; Jean et al., 1998). Relatively few types of cells (only seven main classes of cells are present in the vertebrate retina) proliferate, differentiate and organise themselves into functional structures in the developing eye, so the eye represents the various processes of development, including tissue induction, formation of highly specialised structures and neurogenesis, in an easily accessible system. Thus, a great deal of information is available on the process of eye development, several aspects of which will be examined below.

However, many questions remain to be answered about the molecular basis of retinal development and it is clear that elucidating the regulatory mechanisms that underlie eye and retinal development will be a difficult task. The human and mouse genome projects, together with knowledge of eye development in other model organisms such as *Drosophila melanogaster*, will eventually make it possible to understand how the eye is made in cellular and molecular detail. In the coming years, the main goals of basic and applied developmental research of the eye will be: 1) to identify all of the regulatory molecules which control eye formation and to determine their relationship to genetic eye diseases; 2) to understand the function of these molecules, as well as the relationship between them (i.e. which molecules control which and when); and 3) to identify and characterise the retinal stem cells and progenitor cells which give rise to the mature retina.

The medical benefits of this work will, in the long run, be enormous. First, it will be possible to make specific molecular diagnoses in many patients with congenital eye defects, and to provide their families with accurate genetic counselling. Second, and in the longer term, it may be possible to prevent the retinal cell death associated with various eye defects by using gene therapy or pharmacological approaches. Finally knowledge of retinal stem cells and progenitor cells is likely to make feasible the

replacement of damaged retinal or other ocular tissue, by cell transplantation approaches using cells derived from the eye or elsewhere in the patient's nervous system, or from other stem cell sources, such as embryonic stem cells or bone marrow.

1.2 Embryonic Development of the Vertebrate Eye

1.2.1 Overview

The vertebrate eye develops from an area of the neuroectoderm (specifically the forebrain) that evaginates towards the surface ectoderm early in development, around 22 days of human embryonic development and embryonic day 8 (E8) in mouse. This forms the optic pit. By the time the evaginating tissue abuts the surface ectoderm, around 4 weeks in the human embryo (Sadler, 1990) and by E9 in the mouse (Chow and Lang, 2001; Freund et al., 1996; Jean et al., 1998); Figure 1.1A), it has formed the optic vesicle, the anterior part of which will become the neural retina, and the posterior part of which will become the retinal pigmented epithelium (RPE) and optic stalk. The vesicle induces changes in the ectoderm necessary for lens formation and the surface ectoderm thickens. As development progresses, during embryonic weeks 5 and 6 in the human, and by E10 in the mouse (Chow and Lang, 2001; Freund et al., 1996; Jean et al., 1998; Sadler, 1990), the optic vesicle and the surface ectoderm begin to invaginate, forming the optic cup and lens placode. The interior layer of the optic cup will differentiate to become the neural retina and the outer layer of the cup will become the RPE, with the most posterior part of the optic cup forming the optic stalk, which will develop into the optic nerve. The invaginating lens placode will pinch off from the surface ectoderm to form the lens. The invagination is not restricted to the central portion of the optic cup, but also involves part of the ventral surface, forming the choroid (or optic) fissure (Figure 1.1B). Formation of this fissure allows the hyaloid artery to reach the inner chamber of the eye (Figure 1.1B). From week 6 to week 11 in the human and E10 to E11 in the mouse, the inner layer of the optic cup, the neural retina, thickens as retinal progenitor cells proliferate, whilst the outer layer of the cup, the RPE, becomes a thin, pigmented cellular layer (Chow and Lang, 2001; Freund et al., 1996; Jean et al.,

Figure 1.1: Overview of early eye vertebrate eye development. A: the eye first develops from evaginations of the forebrain which form the optic vesicle. This abuts an area of the surface ectoderm which becomes the lens placode. Both the optic vesicle and lens placode then invaginate to form the optic cup. B: The optic cup invaginates such that it becomes a two layered structure, the interior of which will differentiate to become the neural retina. Invagination also occurs in the ventral portion of the optic cup, forming the choroid fissure, allowing the hyaloid artery to reach the inner chamber of the eye. C: As development progresses, the inner layer of the optic cup thickens and differentiates into the neural retina, whilst the outer layer becomes a relatively thin pigment layer, the retinal pigmented epithelium (RPE). The choroid fissure fuses ventrally around the optic nerve, completing formation of the optic cup which will grow into a mature eye. Figure adapted from: Sadler, 1990.

A

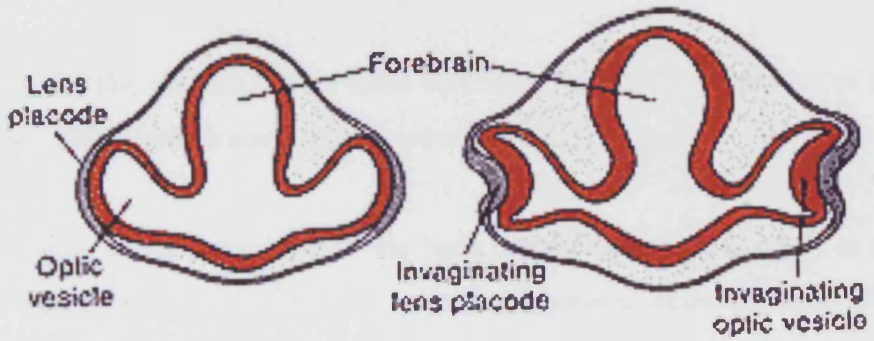
Lens placode
Forebrain
Optic vesicle
Invaginating lens placode
Invaginating optic vesicle

B

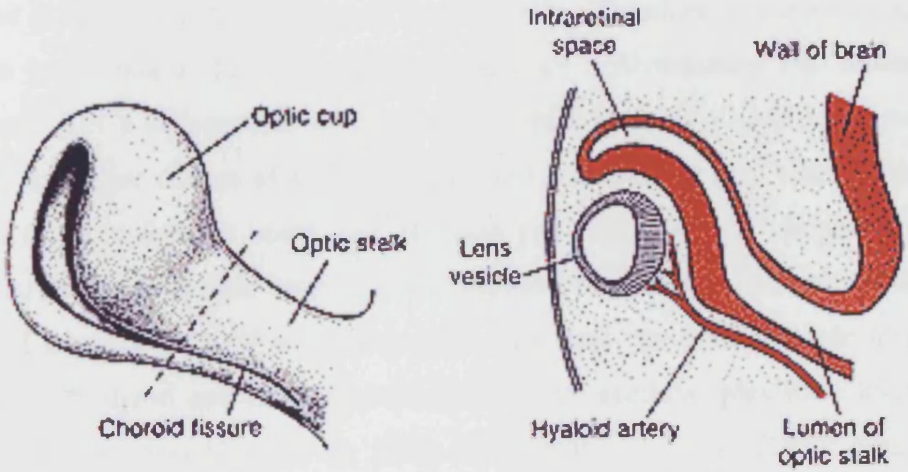
Optic cup
Optic stalk
Choroid fissure
Intraretinal space
Wall of brain
Lens vesicle
Hyaloid artery
Lumen of optic stalk

C

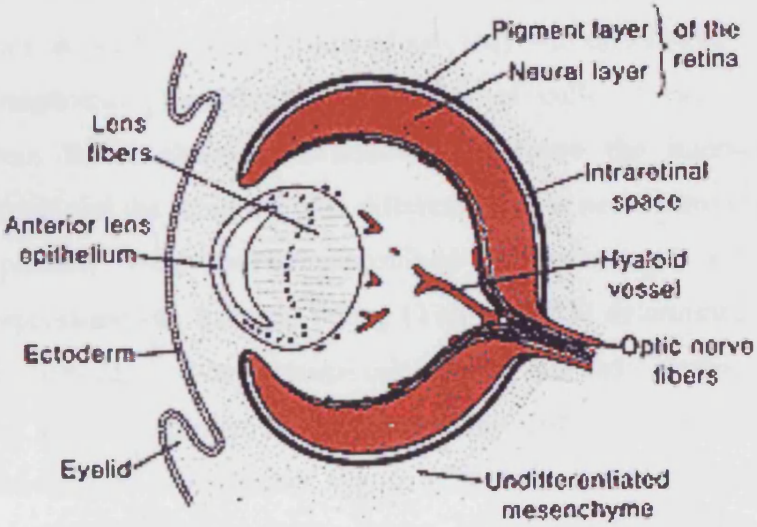
Pigment layer
Neural layer
of the retina
Lens fibers
Intraretinal space
Anterior lens epithelium
Hyaloid vessel
Ectoderm
Optic nerve fibers
Eyelid
Undifferentiated mesenchyme

1998; Sadler, 1990). The choroid fissure fuses ventrally, completing formation of the optic cup (Sadler, 1990), which continues to grow into a mature eye.

The initial thickening of the inner layer of the optic cup between E10 and E11 in the mouse results from the proliferation of retinal progenitor cells (RPCs). This proliferation continues throughout development, until about postnatal day 11 (P11), but at the same time, from about E10.5 onwards, a number of cells begin to leave the cell cycle and become post-mitotic, and differentiate into one of seven retinal cell types (Freund et al., 1996; Marquardt and Gruss, 2002). Therefore, some RPCs are continuing to proliferate at the same time as others are differentiating into mature retinal neurons. RPCs differentiate in a conserved order to form a stratified tissue composed of six major classes of neuronal cells, and one class of glial cells. These are arranged in three cellular strata: the ganglion cell layer (GCL), composed of ganglion cells, the inner nuclear layer (INL), composed of amacrine, horizontal, and bipolar retinal neurons as well as Muller glial cells, and the outer nuclear layer (ONL), composed of rod and cone photoreceptors. Two acellular plexiform layers separate these three layers (Jean et al., 1998; Marquardt and Gruss, 2002); Figure 1.2A).

RPCs in the neuroblastic multi-potential retina become post-mitotic at different overlapping times, depending on what type of cell they will differentiate to (Young, 1985). As retinogenesis proceeds, the proportion of cells of each type which differentiate from RPCs changes continuously. Because the interval between cessation of mitosis and the onset of overt differentiation is not a constant, the order of cell differentiation could not be determined by microscopic assessment of morphological specialisation. Instead, Young (Young, 1985) determined the day of final mitosis (or birth-date) of each retinal cell type by autoradiographic analysis of nuclear labelling in the mature retina in animals injected with tritiated thymidine during the period of RPC proliferation. Figure 1.2B, left, depicts a summary of the time-course of multiplication and differentiation of the neural retina in the mouse that resulted from this study. It was determined that ganglion cells are the first to become post-mitotic, followed by horizontal cells and amacrine cells in the INL, and cone photoreceptors in the ONL. Rod photoreceptors soon follow, and last to be born are the bipolar cells and Muller glial cells of the INL (Figure 1.2B, right, summarises

Figure 1.2: Cells of the neural retina. A: Diagrammatic representation and semithin section, stained with toluene blue, of the wild type adult mouse retina, depicting the rod and cone photoreceptors of the outer nuclear layer, the horizontal, amacrine, bipolar and Muller glial cells of the inner nuclear layer, and the retinal ganglion cells of the retinal ganglion cell layer. The cell layers are separated by two acellular plexiform layers. B: Left: summary of the time-course of multiplication and differentiation of neural retinal cells as elucidated by Young, 1985. Retinal progenitor cells of the developing retina exit the cell cycle and differentiate to the various different types of retinal cells in a conserved order, starting with the earliest born ganglion cells, horizontal cells and cone photoreceptors at E11, to the last born bipolar cells and Müller glial cells up to 11 days after birth. (G.C. - ganglion cells, H.C. - horizontal cells, adapted from Young, 1985). Right: summary of the time of birth of each retinal cell type. Figure adapted from Marquardt and Gruss, 2002.

A

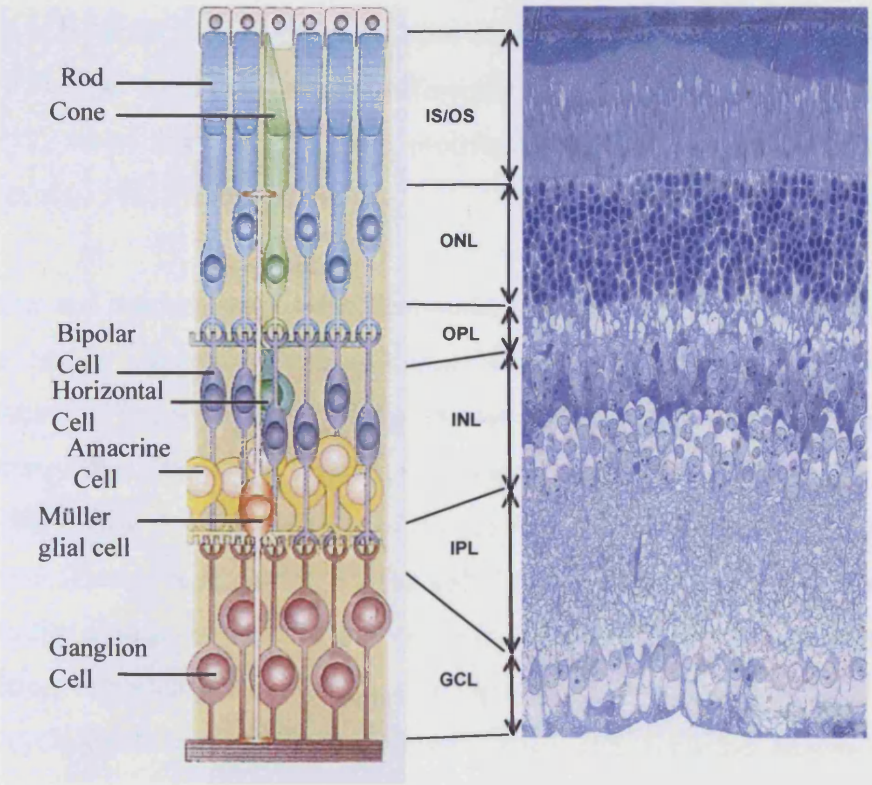
Rod
Cone
Bipolar Cell
Horizontal Cell
Amacrine Cell
Müller glial cell
Ganglion Cell
IS/OS
ONL
OPL
INL
IPL
GCL

B

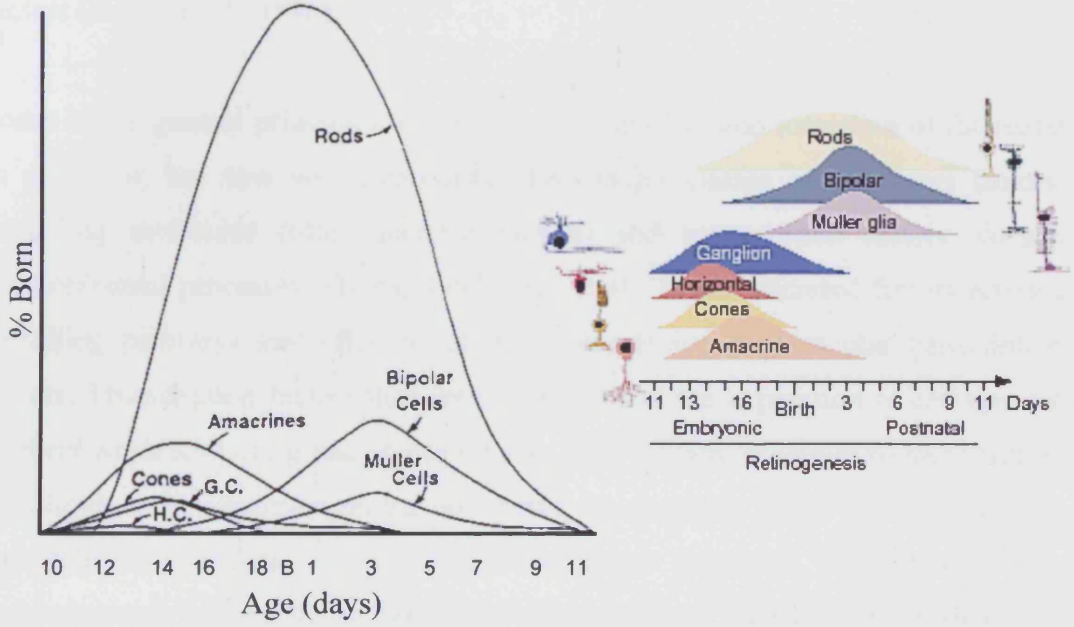
% Born
Rods
Bipolar Cells
Amacrines
Muller Cells
Cones
G.C.
H.C.
10 12 14 16 18 B 1 3 5 7 9 11
Age (days)
Rods
Bipolar
Müller glia
Ganglion
Horizontal
Cones
Amacrine
11 13 16 Birth 3 6 9 11 Days
Embryonic
Postnatal
Retinogenesis

the time of birth for each cell type) (Cepko et al., 1996; Marquardt and Gruss, 2002; Young, 1985). In the mouse, retinal differentiation is complete around postnatal day 11 or P11, when there are no more proliferating retinal progenitor cells present (Cepko et al., 1996; Young, 1985).

The timing and mechanisms of the commitment of an RPC to become a specific cell type are largely unknown. Seminal lineage studies using intracellular injection of either tracers or retroviruses in various species including *Xenopus* and mouse, have demonstrated that the embryonic RPC is multipotent, i.e. each RPC has the potential to form any of the six major classes of mature neurons as well as Muller cells (Holt et al., 1988; Turner et al., 1990; Turner and Cepko, 1987; Wetts and Fraser, 1988). These studies also show that the multipotency of RPCs appears to extend to the last cell division, suggesting they are committed to a specific cell fate only after they exit the cell cycle (Holt et al., 1988; Turner and Cepko, 1987). Further studies indicated that at a given time during development, an RPC can generate only a subset of cell types (Austin et al., 1995; Belliveau et al., 2000; Belliveau and Cepko, 1999), leading to the development of the competence model: RPCs pass through a series of competence states, thought to be intrinsically defined, during each of which they are competent to produce only a subset of retinal cell types in response to environmental factors (Cepko et al., 1996)

Some of the general principles underlying development, and formation of the retina in particular, are now well established. Two major classes of regulatory factors, signalling molecules (often secreted factors) and transcription factors, control developmental processes (Harris, 1997; Jean et al., 1998). Secreted factors activate signalling pathways that often result in the expression of particular transcription factors. Transcription factors then intrinsically direct the expression of cell-specific markers while restricting fate choice (Harris, 1997). Many examples of these factors are known to be important during embryonic development of the vertebrate eye. A comprehensive review of the numerous genes involved in vertebrate eye development is beyond the scope of this overview, but a number of them should be addressed, with regards to the work discussed in this study. Table 1.1 displays a list of genes whose products are essential for eye formation, as an aberrant ocular phenotype can be observed if these genes are affected by a mutation, either in mouse

Gene	Phenotype	Reference
Chx10, CHX10	Reduction in retinal proliferation, microphthalmia	(Burmeister et al., 1996)
Pax6	No eyes visible and no nasal cavities develop in homozygotes, heterozygotes have small eyes and are blind	(Hill et al., 1991)
Rx, RX	Failure to develop eyes	(Zhang et al., 2001)
Pitx3	Bilateral microphthalmia due to failure of lens morphogenesis	(Rieger et al., 2001)
Mitf	Microphthalmia	(Hodgkinson et al., 1993)
Cyclin D1	Severe retinopathy caused by impaired development of all layers of the retina	(Fantl et al., 1995)
Hes1	Premature and accelerated differentiation, resulting in a small eye	(Tomita et al., 1996)
Lhx2	Anophthalmia due to failure of optic cup and lens placode formation	(Porter et al., 1997)
Gas1	Remnant mutant eyes are ingressed from the surface with minimal RPE and lens, and disorganised eyelid, cornea and NR	(Lee et al., 2001)
Gli3	Variable ocular phenotypes from normal optic cup and lens pit to persistent optic vesicle with no evidence of lens development	(Franz and Besecke, 1991; Hui and Joyner, 1993)
Otx2, OTX2	Missing forebrain and hindbrain structures in mice, micro/anopthalmia in humans	(Matsuo et al., 1995; Ragge et al., 2005a)
Pax2	Defects in optic nerve development, coloboma	(Favor et al., 1996)
Foxg1	Ventrally rotated ellipsoid eyes, defective nasal retina	(Freund et al., 1996)
Hesx1	Anophthalmia	(Dattani et al., 1999)
Msx1,2	Double null: arrest in eye development, *Msx2* overexpression: microphthalmia	(Rauchman et al., 1997; Wu et al., 2003)
Bmp7	Anophthalmia	(Wawersik et al., 1999)
SOX2	Anophthalmia	(Fantl et al., 1995; Ragge et al., 2005b)
SIX6	Bilateral anophthalmia and pituitary anomalies	(Gallardo et al., 2004)

Table 1.1 List of genes known to cause microphthalmia in the mouse or in humans (capitalised italics).

or chick, or in the human. Many of them are expressed early during eye development, and their absence often leads to a loss of entire parts of the eye. In addition, expression of a large number of other genes has been observed in the developing eye, at various time points and in various areas, contributing to patterning of the eye. Finally, a number of genes are involved specifically in retinal development, in particular in specification of the various cell types of the retina. These genes are summarised in Figure 1.3.

1.2.2 Genes expressed early during eye development and those causing eye phenotypes

Many of the genes in Table 1.1, such as *Pax6, Rx, Hesx1, Six3* and *Otx1* and *Otx2*, are expressed very early in eye development, and are thought to be involved in initial specification of the eye. The majority of them are anterior neural plate transcription factors, a group of genes whose expression is required for specification of the eye field (Chow and Lang, 2001). *Pax6*, in particular, has been studied in great detail and is thought to be a master regulator of eye development. It is a paired class homeobox gene that has maintained an extremely high level of conservation throughout evolution (Halder et al., 1995) and orthologues have been identified in vertebrates (Hirsch and Harris, 1997; Krauss et al., 1991; Li et al., 1997; Martin et al., 1992; Walther and Gruss, 1991), *Drosophila* (Quiring et al., 1994) and squid (Tomarev et al., 1997). In the murine eye, *Pax6* is first expressed in the optic pit at E8, and by E9, expression is seen in the neural epithelium of the optic vesicle, the optic stalk and the prospective lens ectoderm and it continues to be expressed in all these cell types through to E12. The essential requirement for this gene can be deduced from the malformation of eyes when over- or under-expressed in a variety of species (Schedl et al., 1996) and its ability to induce ectopic eyes in *Drosophila* (Quiring et al., 1994), squid (Tomarev et al., 1997), and *Xenopus* (Chow and Lang, 2001) when misexpressed.

In mice, null mutations of *Hesx1*, a member of the paired-like family of transcription factors, lead to variable anterior CNS defects and pituitary dysplasia, as well as anophthalmia or microphthalmia (Dattani et al., 1999). It is expressed early in the mouse gastrula and anterior neural plate. *Six3* and *Six6* are closely-related members

of the SIX-homeodomain family. Severe brain defects and microphthalmia in 6 cases of holoprosencephaly suggest a role for *SIX3* in the developing anterior neural plate and eye (Wallis et al., 1999). In *Medaka* fish, misexpression of *Six3* results in conversion of the midbrain and prospective cerebellum to RPE-containing, optic cup like structures, and in the appearance of ectopic *Rx*, *Pax6* and endogenous *Six3* expression (Loosli et al., 1999). *Six3* is expressed in the eye field at early gastrula stage whilst both *Six3* and *Six6* are expressed throughout optic vesicle at later stages. Expression of both continues in optic stalk and neural retina. Misexpression studies suggest importance of *Six6* in retinal determination. In chick RPE cells, *Six6* misexpression leads to expression of *Chx10* (C. elegans *ceh-10* homeo domain containing homolog) and visinin, two neural retinal markers normally excluded from the RPE (Toy et al., 1998).

Another gene expressed early during eye development is the paired-like homeobox gene *Rx*. Its role in the early events of eye development has been established based on its expression pattern and gain/loss of function studies (Mathers et al., 1997; Zhang et al., 2000). First expressed throughout the anterior plate, and following neurulation, it is expressed most abundantly in the optic vesicles and later throughout the neural retina. By postnatal day 6.5 in the mouse, *Rx* is restricted to photoreceptor cells and the inner nuclear layer, and by 13.5, it is no longer detectable (Bailey et al., 2004). *Rx* misexpression in *Xenopus* can expand endogenous *Pax6*, *Six3*, and *Otx2* expression in the optic region at late neurula stages (Zhang et al., 2001). Mice homozygous for the *Rx* gene are anophthalmic as optic vesicles fail to develop (Voronina et al., 2004).

Otx2, a member of the orthodenticle-related family of transcription factors, is expressed in the optic vesicle, and eventually becomes restricted to the RPE (Bovolenta et al., 1997; Simeone et al., 1993). In $Otx2^{-/-}$ mutants, forebrain and midbrain structures are completely missing, due to a defect in neural induction, making it difficult to determine its precise role in the developing eye. However, in chimeric embryos in which the neuroectoderm is made up of $Otx2^{-/-}$ cells, the expression of the forebrain/eye markers *Six3* and *Hesx1* is initiated but not maintained, suggesting that *Otx2* is not required cell-autonomously for the induction of anterior neural tissue, but is required for its maintenance and regional specification

(Rhinn et al., 1998). In the human, mutations in OTX2 cause a range of severe ocular malformations, including bilateral anophthalmia (Ragge et al., 2005a).

1.2.3 Patterning of the developing eye

As eye development progresses, a number of genes are involved in patterning of the optic vesicle and subsequently the optic cup, and their expression patterns are restricted to various fields of the eye cup. In addition, a variety of genes are required for specification of the lens, which develops from the overlying ectoderm. Misexpression of a number of these genes, such as *Pax2, Lhx2, Msx1* and *2, Chx10 and Mitf*, result in abnormal eye phenotypes (Table 1.1), but many genes expressed later in development appear more robust, i.e. show no abnormal eye phenotype upon misexpression, perhaps due to redundancy.

Pax2 and *Vax2* are both expressed early in the ventral half of the optic cup (Barbieri et al., 2002; Dressler et al., 1990; Nornes et al., 1990; Schulte et al., 1999), whereas *Xbr-1* and *Tbx5* are restricted to the dorsal half (Gibson-Brown et al., 1998; Isaac et al., 1998; Papalopulu and Kintner, 1996; Sowden et al., 2001). Misexpression of *Vax2* in the chick dorsal neural retina leads to the ectopic expression of the ventral markers *Pax2, Ephb2, Ephb3* and the downregulation of the dorsal markers *Tbx5, Ephrinb2 and Ephrinb3* (Schulte et al., 1999). By contrast, *Tbx5* misexpression in the ventral retina leads to the down-regulation of both *Vax2* and *Pax2* and the ectopic induction of *EphrinB2* and *EphrinB3* (Koshiba-Takeuchi et al., 2000). These experiments suggest that *Vax2* and *Tbx5* play important roles in specifying ventral and dorsal fates and also highlight the potential role of ephrin signalling in the determination of dorsal/ventral polarity in the neural retina (Chow and Lang, 2001). It has been suggested that the developing retina is in fact divided into four domains along the dorso-ventral axis, with *EphrinB2* expression localised to the dorsal-most domain, *Tbx5* expression extending through to the two dorsal domains, and *Vax* expression localised to the ventral-most domain (Peters and Cepko, 2002).

Experiments in zebrafish and mice have provided evidence suggesting that retinoic acid (RA) also plays a role in establishing ventral polarity within the developing optic cup. RA-soaked beads induced a secondary choroidal fissure in any region of

the zebrafish optic cup, and RA treatment also resulted in an enlarged optic stalk and in the expansion of *Pax[b]*, the zebrafish homologue of *Pax2*, in dorsal region of the eye (Hyatt et al., 1996). In retinoid-responsive transgenic reporter mice, the importance of RA for morphological changes involved in choroidal fissure formation was also demonstrated, however it could not ventralise the retina as observed in zebrafish (Schulte et al., 1999). RA receptor loss-of-function mutants also highlight the importance of RA in the ventral retina, for example, *Rxra*$^{-/-}$ mice are characterised by a reduction in size of the ventral retina and by the failure of the optic fissure to close (Kastner et al., 1994).

Segregation of gene expression can also be observed along the anterior (nasal)-posterior (temporal) axis of the developing eye. Expression of *BF-1/Foxg1*, a winged-helix transcription factor, is restricted to the anterior half and *BF-2/Foxd1*, another winged-helix transcription factor, is restricted to the posterior half (Hatini et al., 1994). The two may regulate each other perhaps in the same manner as *Pax6* and *Pax2*. In addition, two homeodomain factors of the hmx family, *Soho1* and *Gh6*, are expressed in the anterior neural retina. Misexpression studies in chick have shown that either *Soho1* or *Gh6* can down-regulate expression of *EphA3*, which is normally restricted to the posterior neural retina (Schulte and Cepko, 2000).

Induction and development of the lens requires the expression of a variety of genes, including *Pax6* (Ashery-Padan et al., 2000; Collinson et al., 2000; Quinn et al., 1996), bone morphogenetic protein genes *Bmp4* and *Bmp7* (Furuta and Hogan, 1998; Wawersik et al., 1999), fibroblast growth factor (FGF) signalling (McAvoy et al., 1991), members of the Group B1 *Sox* family of transcription factors (Chow and Lang, 2001), and forkhead transcription factors *Foxe3* and *Lens1* (Blixt et al., 2000; Brownell et al., 2000; Kenyon et al., 1999).

1.2.4 Neural Retina versus RPE

Of particular interest is how the two layers of the optic cup, both derived from the neuroectoderm, become specified such that that anterior layer develops into the neural retina, and the posterior layer into the RPE. A variety of genes, as well as an

interaction with the surrounding tissue, are involved in specifying and segregating the two domains.

The earliest known transcription factor expressed specifically in the presumptive retinal region upon close contact with the surface ectoderm (with which the presumptive retina interacts to achieve correct development) is encoded by the paired-like homeobox gene *Chx10* (Burmeister et al., 1996; Liu et al., 1994b). Explant studies support the idea that *Chx10* expression in the presumptive neural retina occurs in response to inductive signals from the presumptive lens ectoderm (Nguyen and Arnheiter, 2000). Interaction with the surface ectoderm appears to be a requirement for retinal development, as it does not develop if the surface ectoderm is removed (Hyer et al., 1998; Nguyen and Arnheiter, 2000). Along with Chx10, other genes that appear to play an important role during this period of close contact include *Lhx2*, a LIM homeodomain-containing transcription factor, whose loss of function in knock out mice results in anophthalmia (Porter et al., 1997), and members of the fibroblast growth factor (FGF) family (Hyer et al., 1998; Nguyen and Arnheiter, 2000). Both FGF1 and FGF2 are expressed in the surface ectoderm and their ectopic expression leads to a thickening of the presumptive RPE that retains *Pax6* and *Chx10* expression, normally restricted to the neural retinal layer, and lacks expression of the helix-loop-helix transcription factor *Mitf* (microphthalmia associated transcription factor) and pigmentation, both normally associated with the developing RPE (Nguyen and Arnheiter, 2000).

In addition, further genes are implicated in the correct development of the retina e.g. *Msx1, Msx2* and *Dlx1*. Both *Msx1* (formerly known as *Hox7.1*) and *Msx2* (*Hox 8.1*) are expressed in the mouse embryo during early stages of mouse development in a distinct spatial and temporal manner (Monaghan et al., 1991). Their expression pattern indicates that the inner layer of the optic cup is differentiated into three distinct compartments even before cellular differentiation becomes obvious. It is suggested that both *Msx1* and *Msx2* are involved in regulation of the development of the iris, ciliary body and retina. The *Msx1* and *Msx2* double knock out mouse shows an arrest in eye development, whilst overexpression of *Msx2* leads to microphthalmia (Rauchman et al., 1997; Wu et al., 2003). *Dlx1* is expressed in prospective retina at E11.5 to E14.5. Expression is restricted to the neural retinal layer, while more ventral

parts of the eye epithelium, the prospective ciliary body and iris, are not labelled. Within the differentiating neural retina, labelling seems stronger in the neuroblastic layer (in more compacted cells). *Dlx1* can be used as a molecular marker of the prospective neural retina prior to its morphological differentiation (Dolle et al., 1992).

RPE specification, on the other hand, is dependent on signals from the extraocular mesenchyme and the transcription factor *Mitf*. In mice, *Mitf* is initially expressed throughout the dorsal optic vesicle, but is down-regulated in the presumptive retinal region soon after the initiation of *Chx10* expression (Bora et al., 1998), after which it becomes restricted to the presumptive RPE. In chick optic vesicle explants, it was observed that initiation of *Mitf* expression does not occur and that expression of Chx10 expands throughout the entire explant, suggesting that extraocular mesenchyme is required for both RPE development and for inhibition of neural retina development (Chow and Lang, 2001; Fuhrmann et al., 2000). The ability of exogenously applied activin A to rescue *Mitf* expression and RPE development makes it a good candidate for secreted mesenchymal factor that induces RPE (Fuhrmann et al., 2000).

When *Mitf* is rendered non-functional (at least 17 mutant alleles are known for this gene (Graw, 1996)), the RPE hyperproliferates, remains unpigmented and displays areas developing into a second retina, presumably through a process of transdifferentiation (Bumsted and Barnstable, 2000; Nakayama et al., 1998; Nguyen and Arnheiter, 2000). It has been speculated that formation of the secondary transdifferentiated neural retina in *Mitf* mutants depends on signals such as *Bmp7* which are expressed on the dorsal side of the optic cup. *Bmp7* mutants are anophthalmic, suggesting that BMP signalling plays an important role in the development of the neural retina (Wawersik et al., 1999).

The specification of the two layers of the optic cup is the result of an early inductive decision: neural retina versus RPE. Although morphologically distinct from an early stage as well as biochemically identifiable (*Chx10*, *Pax6* and *Msx2* are preferentially expressed in the presumptive neural retina, for example), this determination is nevertheless extremely plastic. For example, regulation can occur as late as optic cup

stages when the inner and outer layers are interchanged. Even after the RPE has begun to differentiate, most vertebrates can regenerate neural retina from the RPE if the retina is removed or damaged (Saha et al., 1992). RPE has been shown to transdifferentiate in response to FGF *in vitro* and its ability to do so is restricted to a specific period during development (Pittack et al., 1991). The fact that removal of the neural retina can result in a transformation of the RPE into neural retina indicates that these two layers interact during normal development. In addition, it is known that the RPE plays a critical role in later development of the neural retina; contact with the RPE is required for photoreceptor differentiation specifically, and laminar organisation in general (Reh, 1992). What factors the RPE and neural retina provide for each other is not yet resolved and needs further experimentation.

1.3. Differentiation of Retinal Cells

Birthdating and morphological studies have demonstrated that the various cell layers of the presumptive neural retina undergo their final mitosis and begin to differentiate in a precise and stereotypical fashion (Cepko et al., 1996; Young, 1985). Studies suggest that retinal cell determination involves cell-cell interactions together with an intrinsic timing mechanism that regulates the differing ability of cells to respond to inductive stimuli, mechanisms that are paralleled in embryonic lens and mesoderm induction (Cepko et al., 1996; Marquardt and Gruss, 2002).

The timing and mechanisms of the commitment of a retinal progenitor cell to become a specific cell type are largely unknown, but it appears that progenitors usually become committed to a specific fate only after they exit the mitotic cycle (Cepko et al., 1996). Commitment of a retinal progenitor cell to a specific cell fate appears to depend on both intrinsic properties (regulating their competence to differentiate to a particular cell fate) and signals from the microenvironment. Identification of the environmental cues necessary to initiate the differentiation pathways for each specific retinal cell type is still ongoing. Nevertheless it is clear that the cornerstones of developmental regulation - in the eye as in other tissues – are the signalling events within and between cells, and the endogenous control by transcription factors of the competence of cells to respond to signals (Freund et al., 1996). Thus transcription factors may serve to make post-mitotic retinal cells competent to respond to

appropriate environmental stimuli, and initiate the production of signals by the cells that modify the microenvironment, thereby influencing the developmental program of neighbouring cells (Cepko et al., 1996; Freund et al., 1996).

The three successive processes that make up retinogenesis - proliferation of progenitors, neurogenesis, and gliogenesis - rely on changing states of RPCs over time. Whilst it has been proven that a single RPC can generate all 7 types of retinal cell, at any specific point in development, discrete populations of RPCs co-exist, which display differing preferences for various cell fates (Lillien, 1998). These inherent differences are mediated by a range of basic helix-loop-helix (bHLH) transcription factors, which function as cell-intrinsic regulators (Marquardt and Gruss, 2002). These factors lie broadly within two distinct functional groups – repressors and activators (Hatakeyama and Kageyama, 2004). Repressors such as *Hes1* and *Hes5* (homologues of *Drosophila hairy* and *enhancer of split* genes) inhibit neuronal differentiation, instead promoting maintenance of progenitor cell status and also gliogenesis. In the mature mouse retina, *Hes1* is expressed only in CRALBP-positive (Furukawa et al., 2000) cells, the latest born of the retinal cell types (Furukawa et al., 2000), indicative of the fact that the expressing cells have resisted or not been susceptible to all previous signals to differentiate. Activators, such as *Mash1* and *Math5* (homologues of *Drosophila* proneural genes *achaete-scute* and *atonal*) override repressor activity and promote neural differentiation (Tomita et al., 2000).

As well as maintaining progenitor cells or promoting differentiation, bHLH factors have been shown to contribute to the specification of many neuronal types from precursor cells during neurogenesis. The activating bHLH factor *Neurod1*, for instance, has a regulatory role in several processes in the developing rodent neural retina (Morrow et al., 1999a). In retinal explants from *Neurod1*-null mice, an increased Muller glial cell population was observed, and misexpression of *Neurod1* blocked gliogenesis, indicating a role for *Neurod1* in the regulation of the neuronal versus glial cell fate decision. A role in interneuron development was also suggested after the observation that lack of *Neurod1* promoted bipolar cell differentiation at the expense of amacrine cells, and conversely the amacrine interneuron population was expanded at the expense of bipolar cells under forced *Neurod1* expression (Inoue et

al., 2002). The fact that *Neurod1* expression remains within a subset of mature photoreceptors and that in retinal explants from *Neurod1*-null mice a subset of photoreceptors underwent apoptosis also suggests *Neurod1* is required for the survival of retinal neurons (Morrow et al., 1999a).

Although activating bHLH factors promote neurogenesis and play a role in determining cell fate, they cannot alone specify retinal neuron subtypes. For instance, the bHLH genes *Math3* and *Neurod1* are expressed by differentiating amacrine interneurons and in the double knock out mice, amacrine cells are completely absent (Inoue et al., 2002). In addition, an increase in the numbers of ganglion and Muller glial cells is observed in the double mutant retina, suggesting an alteration in the fate adopted by a distinct population of cells. However, retinal culture studies showed that induced expression of either *Math3* or *Neurod1* is not sufficient to cause an increase in the amacrine cell population, although gliogenesis was inhibited. Misexpression of *Pax6* with *Math3*, however, increased amacrine and horizontal cell genesis and *Pax6* with *Neurod1* increased amacrine cell genesis alone (Inoue et al., 2002). These results indicate that a combination of bHLH and homeobox genes is required to confer specific cell fates.

Current research suggests that homeodomain transcription factors determine layer specificity, while bHLH transcription factors regulate neuronal fate within the specified layers (Hatakeyama and Kageyama, 2004). In the example above, *Pax6* specifies the INL, but without further signalling, cells do not mature. *Neurod1* is required to specify an identity from the three available cell types in the INL. Various combinations of transcription factors required for cell fate have been elucidated, as shown in Figure 1.3. Misexpression of the repressing bHLH factor *Hes1* during retinal development inhibits neuronal differentiation, instead promoting progenitor cell status (Tomita et al., 1996). This is in agreement with the suggested function of *Hes1*, which is to maintain cells in a progenitor state such that there is sufficient time for expansion of the retinal cell population and also a sufficient supply of RPCs remaining at late stages of development for generation of all retinal cell types. Those cells that do not stop expression of *Hes1* adopt the last-born cell fate (Muller glia, Figure 1.3)(Tomita 1996).

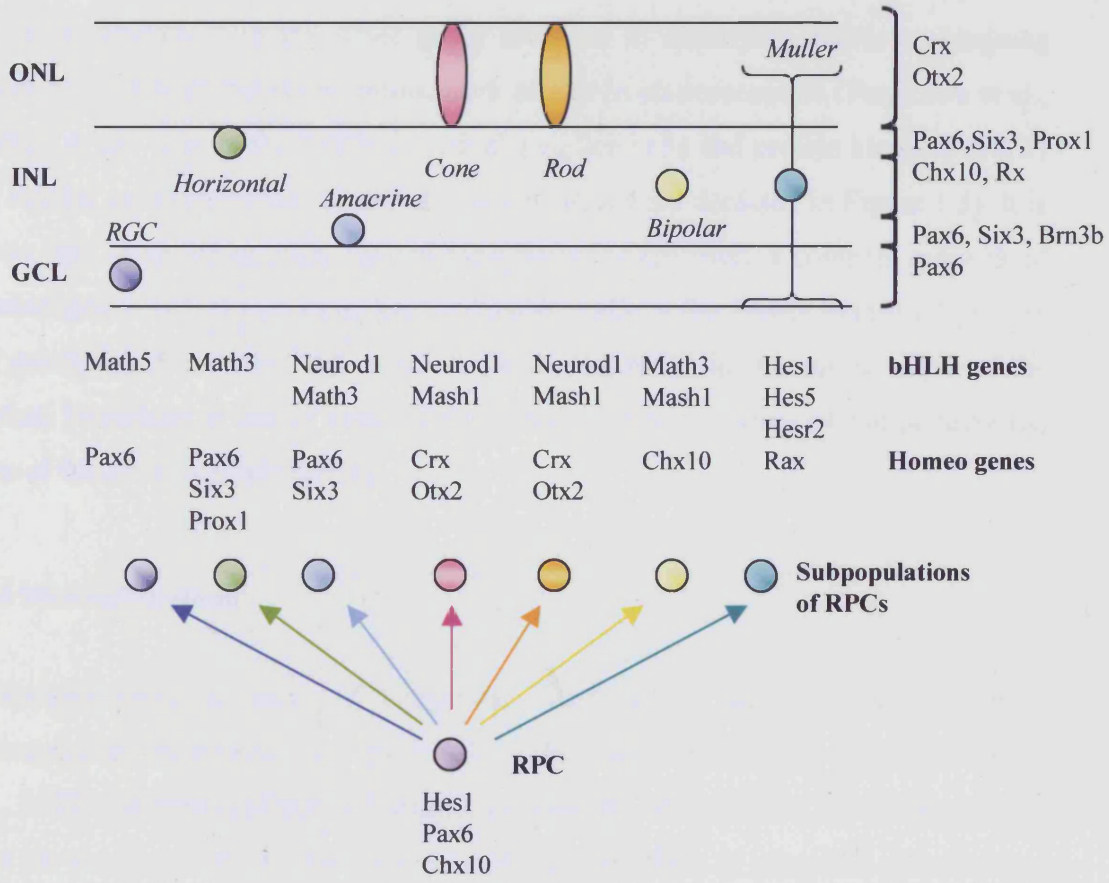

Figure 1.3: Cascade of progressive differentiation of retinal progenitor cells to the seven different cell types of the neural retina. RPCs express Hesx1, Pax6 and Chx10. At particular points in development, subpopulations of RPCs express combinations of bHLH and homeobox transcription factors required for differentiation into a particular cell type. RPC = retinal progenitor cell, RGC = retinal ganglion cell, INL = inner nuclear layer, ONL = outer nuclear layer.

As time progresses, many other genes involved in specifying and/or maintaining identity of cells of the neural retina, such as *Crx* in photoreceptors (Furukawa et al., 1997), *Brn3b* (Liu et al., 2000b) in retinal ganglion cells and protein kinase C (*PKC*) in bipolar cells, are being identified (some of which are depicted in Figure 1.3). It is clear that, from the moment the eye field becomes specified, a complex network of transcription factors and signalling molecules controls the highly organised process of producing the correct cell types in the correct ratios in the correct areas of the retina. Mutations in one or more of these factors cause a variety of eye phenotypes, one of which is microphthalmia.

1.4 Microphthalmia

Microphthalmia, a cause of congenital blindness, is an ocular malformation characterised by a small eye, specifically a short total axial length (TAL) (Weiss et al., 1989). Examples of microphthalmic eyes are shown in Figure 1.4. It may or may not be accompanied by other ocular abnormalities, such as cataracts, microcornea, sclerocornea, and retinal or optic-nerve coloboma (a gap in structure of the eye). There are thought to be over 150 causes of microphthalmia, ranging from a variety of genetic mutations to disruption of the intrauterine environment (Bateman, 1984; Warburg, 1993) and it may manifest itself as a part of a syndrome. Severity of the disease often ranges from mild to clinical anophthalmia (Kubo et al., 2005), even within a single family, suggesting variable gene expression (Warburg, 1993). There are more than 100 inherited conditions inducing microphthalmos and coloboma; approximately 50 different autosomal dominant, 67 autosomal recessive, and 16 X-linked syndromes with microphthalmia and coloboma, and this wide spectrum of genetic microphthalmia conditions is reflected in the volume and variety of entries regarding microphthalmia entered onto the Online Mendelian Inheritance in Man (OMIM) database. In some disorders, ocular manifestations are isolated signs, (Pearce, 1986), but it is more common that systemic features are part of the symptomology. A variety of deletions and translocations, occurring in a variety of chromosomes, may give rise to microphthalmia or coloboma (Warburg, 1993). The reported prevalence of these conditions has varied between 0.22 and 3.48 per 10000, partly due to a great variability in the inclusion criteria used in different registers

A

B

Normal eye

Microphthalmic eye

Figure 1.4: Examples of microphthalmia in human patients. *A*: an example of bilateral microphthalmia. Photo from Ferda et al, 2000. *B*: Comparison of a normal eye versus a microphthalmic eye. Photos kindly provided by Dr. Bart Leroy, Dept. of Ophthalmology, Ghent University Hospital, Ghent, Belgium.

(Bermejo and Martinez-Frias, 1998; Busby et al., 1998; Castilla, 1994; Kallen et al., 1996; Morrison et al., 2002; Stoll et al., 1992; Warburg, 1993). For example, in some studies, a distinction was made between isolated microphthalmia or anophthalmia and those that were associated with a syndrome (Bermejo and Martinez-Frias, 1998; Castilla, 1994), whilst others grouped all ocular malformations together (Busby et al., 1998; Kallen et al., 1996; Morrison et al., 2002).

Microphthalmos appears to be a fairly common ocular malformation in all races. The high incidence, which would be unusual for a disorder caused by a single gene suggests multiple etiologies (Bateman, 1984). Thus, nonsyndromic simple microphthalmia is clinically and genetically heterogeneous, and may be inherited in a number of manners. A number of families have been studied in which simple microphthalmos seems to be inherited in an autosomal dominant (Fryns, 1995; Othman et al., 1998; Pearce, 1986; Vingolo et al., 1994), autosomal recessive (Bateman, 1984; Bessant et al., 1998; Ghose et al., 1991; Kohn et al., 1988; Warburg, 1993; Zlotogora et al., 1994), and X-linked manner (Graham et al., 1991; Hoefnagel et al., 1963).

For all of the above forms, one or more loci have been identified. Two loci have been identified in families in which the disease is inherited in an autosomal dominant manner: one shows linkage to chromosome 15q12-q15 (Morle et al., 2000), and another is the NNO1 locus, on chromosome 11 (Othman et al., 1998). In a family with autosomal recessive inheritance of the disease, a locus for isolated microphthalmia was mapped to chromosome 14q32 (Bessant et al., 1998), and in a family with X-linked inheritance of clinical anophthalmos, a gene is localised to the Xq27-28 (Graham et al., 1991). Another locus (Male et al., 2002) was identified through the association of microphthalmia and anophthalmia with chromosome rearrangements involving distal 3q (Male et al., 2002; Yokoyama et al., 1992), whilst another locus has been inferred by the co-segregation of a translocation, t(2:16), with the phenotype, suggesting a gene on the 16p13.3 band is responsible (Yokoyama et al., 1992).

Although a number of loci have been identified, very few genes have been shown to cause microphthalmia. The first to be identified was CHX10 (Ferda et al., 2000).

Table 1.2 summarises the known loci and genes for non-syndromic simple microphthalmia.

Known Loci	**Reference**
15q12-q15	(Morle et al., 2000)
11p	(Othman et al., 1998)
14q32	(Bessant et al., 1998)
Xq27-q28	(Graham et al., 1991)
16p13.3	(Yokoyama et al., 1992)
3q26.33-q28	(Male et al., 2002)
Known Genes	
CHX10	(Ferda et al., 2000)
SOX2	(Fantes et al., 2003; Ragge et al., 2005b)
RX	(Voronina et al., 2004)
OTX2	(Ragge et al., 2005a)

Table 1.2: Known loci and genes for non-syndromic simple microphthalmia

1.5 The CHX10 gene

In a recent study, a locus for isolated human microphthalmia has been mapped on chromosome 14q24.3, and the gene at this locus identified as human homeobox transcription factor *CHX10* (Ferda et al., 2000). As described above, CHX10 is known to be an important gene for neural retinal specification. A point mutation in the DNA recognition helix of the homeodomain renders the CHX10 protein unable to bind to DNA and thus abolishes its function. This was the first human microphthalmia gene to be identified – three others, the *RX* (Voronina and Mathers, 2000), SOX2 (Fantes et al., 2003) and OTX2 (Ragge et al., 2005a) genes, have been recently discovered – and accounts for approximately 2% (2/117) of the patients with nonsyndromic microphthalmia examined (Ferda et al., 2000).

The discovery of *CHX10* as a gene for human microphthalmia can be attributed to the similarity that was observed between human microphthalmia and a mouse mutant with an effective null mutation in the homologous gene *Chx10*. In 1962 a mutant mouse with small eyes, a soft and irregular lens, and a thin and undifferentiated retina was described, and designated *ocular retardation, or* (Truslove, 1962). A second allele of the mutation, or^J, was discovered in 1973 (Theiler et al., 1976), demonstrating recessive inheritance with complete penetrance. Its phenotype has been described in detail by a number of authors, and includes a reduction in the size

of the eye with an uneven retina in which most of the cell layers are disorganised (Burmeister et al., 1996; Robb et al., 1978; Theiler et al., 1976).

Chx10 co-segregates with the *or*^{J} locus, and this *ocular retardation* allele is an effective null allele of *Chx10*. A point mutation near the midpoint of *Chx10* mRNA, leading to a premature stop codon, is thought to result in a truncated form of the protein, which is quickly degraded (Burmeister et al., 1996). The similarity between this phenotype and that of human microphthalmia led to the cloning of the human *CHX10* gene (Liu et al., 1994b), and the identification of mutations in this gene giving rise to a recessively inherited form of the disease (Ferda et al., 2000).

The murine *Chx10* gene encodes a 361 amino acid polypeptide with a predicted mass of 39 kDa. The homeodomain is situated between residues 148 and 207. Like many other homeobox transcripts, the *Chx10* mRNA has a long 3' untranslated region (Liu et al., 1994b). The Chx10 homeodomain is 58-65% identical to a series of paired (prd)-like homeodomains, and the deduced protein contains an octapeptide between residues 33 and 39, much like several other putative transcription factors with prd-like homeodomains (Figure 1.5; (Liu et al., 1994b). It has been speculated that conserved homeodomain sequence also indicates a conserved function. One example of this is the *Drosophila eyeless* gene, highly related in protein sequence to mammalian *Pax-6* genes (Quiring et al., 1994). Both are expressed in the developing eye of their respective embryos and eye formation is severely affected by their mutation. In the same way, *Chx10* is thought to be related in function to the prd-like homeodomain genes goldfish *vsx-1* and *C. elegans ceh-10*. In addition to a high level of sequence identity in the homeodomain, all three express a second domain, termed the CVC domain. The function of this domain is unclear but may serve as a DNA or protein binding site (Svendsen and McGhee, 1995).

1.5.1 *Chx10* Expression During Eye Development

Chx10 expression in the eye is observed as early as embryonic day 9.5 (E9.5) (Burmeister et al., 1996). At this stage of eye development, the optic vesicle, an evagination from the diencephalon, is in contact with the surface ectoderm (Chow and Lang, 2001). *Chx10* expression is restricted to the anterior (outermost) region of

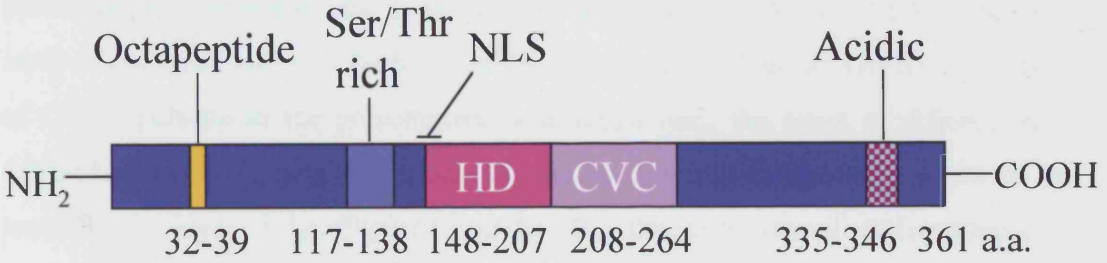

Figure 1.5: Organisation of the Chx10 polypeptide sequence. The octapeptide is found close to the N-terminus in Chx10 and related homeodomain proteins, a serine/threonine region is located N-terminal to the homeodomain, and a potential nuclear localisation signal overlaps the N-terminus of the homeodomain. The CVC domain lies C-terminal to the homeodomain, and there is a small region high in acidic amino acids in the C terminus.

the optic vesicle, which will form the future neuroretina (Liu et al., 1994b); Figure 1.6A). At E10, invagination of the optic vesicle is initiated, creating the optic cup, composed of two layers. The overlying ectoderm thickens to form the lens placode, from which the lens and cornea will develop. *Chx10* remains expressed in the presumptive neuroretina, the inner layer of the optic cup (Figure 1.6A). The outer layer of the optic cup will form the retinal pigmented epithelium (RPE). Expression of *Chx10* persists in the presumptive neuroretina until the onset of differentiation (around E11), after which it is maintained in dividing neural progenitors of the neuroblastic layer only (Figure 1.6B-E). By the time retinal differentiation is complete (around postnatal day 11 or P11) (Young, 1985); (Cepko et al., 1996) and there are no more proliferating retinal progenitor cells, *Chx10* expression is restricted to the inner nuclear layer (INL) of the retina, specifically to the bipolar cells, although a recent study using a novel multifunctional BAC transgenic reporter identified the expression of *Chx10* in a subset of Muller glial cells, also located in the INL (Rowan and Cepko, 2004). This expression in the INL is maintained in the mature retina.

Although Chx10 is a transcription factor, its downstream target or targets have yet to be identified. Examination of the mouse mutant *Chx10*$^{-/-}$ has provided some clues to the function of this transcription factor, but a clear picture is yet to be established. In a broader sense, the mutant is one of several models of microphthalmia that are providing information about the various genes involved in eye development. Thus, examination of the mutant and elucidation of downstream targets may not only provide clues to the function of Chx10 itself, but also provide more information about genes required for eye development, necessary to understand and treat microphthalmia and other retinal disorders.

1.5.2 A Role in Specification and Differentiation of the Neural Retina

Based on its expression pattern, a number of roles for the Chx10 gene have been proposed: as it is expressed at an early stage, and throughout the presumptive neural retina, Chx10 may specify the presumptive neuroretina in the early optic vesicle and optic cup, most likely in combination with other transcription factors, such as

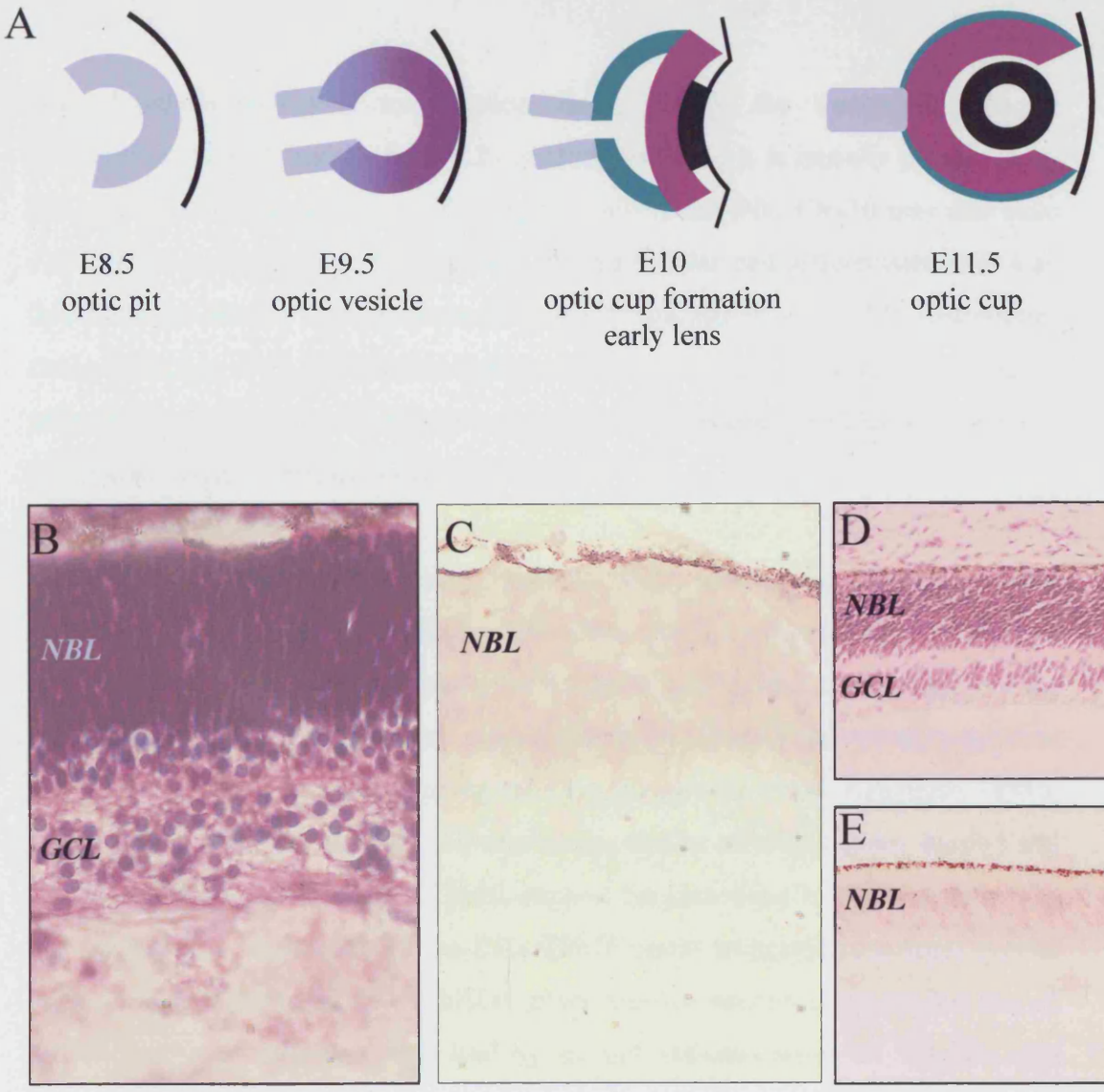

Figure 1.6: Chx10 expression during retinal development. *A*: Schematic representation of early eye development, with expression of Chx10 depicted in purple. Chx10 is first observed throughout the anterior part of the optic vesicle at E9.5 in the mouse. Chx10 expression then continues to be expressed in proliferating retinal progenitor cells of the neural retina. *B-E*: As development progresses, and cells of the neural retina begin to differentiate, Chx10 becomes restricted to the proliferating neuroblastic layer of the developing retina. *B* and *D*: Haematoxylin and eosin staining of mouse E18.5 and human 13 week retina respectively. *C* and *E*: *In situ* hybridisation at the same time points showing *Chx10* expression in neural progenitors of the proliferative neuroblastic layer (NBL). GCL = ganglion cell layer. *In situ* data kindly provided by Dr. A. Rutherford, a former member of the Sowden lab.

microphthalmia-associated transcription factor (*Mitf*), the transcription factor necessary for specifying the RPE (Liu et al., 1994b). As it is initially present in all RPCs, and then becomes restricted to bipolar cells in the INL, Chx10 may also have a specific role later in eye development, during bipolar cell differentiation. It may determine the identity of cells in the INL and/or boundaries of the INL (Burmeister et al., 1996; Liu et al., 1994b) and in the mature retina, the differentiated cells of the neuroretina, particularly the bipolar cells, may be maintained by Chx10 expression (Burmeister et al., 1996; Liu et al., 1994b).

Such roles in differentiation are consistent with observations regarding other homeobox genes. As described earlier, homeobox genes are frequent determinants of pattern formation, and in many cases, their activity may extend over a region of the embryo containing a variety of cell types, such as the layers of the retina, rather than being restricted to a single developing cell type (Krumlauf, 1993a; Krumlauf, 1993b; Liu et al., 1994b; Morata, 1993). Misexpression studies of bHLH genes *Mash-1* and *Math3*, and the homeobox gene *Chx10*, support the idea that Chx10 is important for the specification of the cells of the INL. Chx10 seems to provide the inner nuclear layer specific identity, while the bHLH genes regulate neuronal versus glial fate of the INL retinal neurons, thus leading to the differentiation of bipolar cells (Hatakeyama et al., 2001). Both sets of genes are necessary for the differentiation of bipolar cells, but they play different roles. In the *Chx10*$^{-/-}$ mutant, differentiation of neural retinal cells other than bipolar cells also seems to be indirectly affected, with a delay in the differentiation of some of the other cells such as the photoreceptors, and a decrease in size of the inner and outer segments of photoreceptor rods (Burmeister et al., 1996). Thus, Chx10 may play a role (direct or indirect) in differentiation of all retinal cell types.

1.5.3 A Role in Retinal Progenitor Cell Proliferation

Chx10 is also thought to be important in undifferentiated precursors. The primary role of Chx10 in these RPCs seems to be to promote proliferation, as has been concluded from studies of the *Chx10*$^{-/-}$ mutant mouse. Using bromodeoxyuridine (BrdU) incorporation as an assay for cell proliferation, it was observed that by E11.5, there was an 83% reduction in BrdU incorporation in the periphery of the retina, and

that total cell number throughout the retina was decreased by 30-50% (Burmeister et al., 1996). The apparent decrease in proliferation in the periphery was observed between E10.5 and E18.5. It was suggested that this might account for the fact that the volume of the mutant retina is only one half that of controls at E10.5 and one tenth that of controls at E18.5 (Burmeister et al., 1996). These data suggest that Chx10 influences RPC division during much or all of retinal formation.

In another study, it was observed that the phenotype is partly ameliorated when expressed on a different background (*Mus musculus castaneus* instead of 129/SV) (Bone-Larson et al., 2000). However, one prominent feature of the original mutant phenotype was not rescued: the periphery of the modified *Chx10*$^{-/-}$ retina showed both incomplete growth and a lack of differentiated cells. Since this aspect of the *ocular retardation* phenotype was not ameliorated, it is likely that *Chx10* plays a fundamental role in the central-to-peripheral gradient of retinal development. Thus, again a decrease in proliferation in the periphery of the retina was observed, with relatively few changes in the central retina. A decrease in proliferation is one of three developmental mechanisms proposed to explain the resulting phenotype (a decrease in only peripheral proliferation, but a reduction in cell number throughout the entire retina). There are a number of other possibilities that may account for the reduction in cell number observed in the above study. The first is an increase in cell death, but this is unlikely, as cell death has been shown to decrease in *Chx10*$^{-/-}$ mutants (Robb et al., 1978; Theiler et al., 1976). A second possibility is that the population of progenitors selected to continue along a neurogenic line could be reduced at the outset of ocular morphogenesis. Even at a normal rate of proliferation, (which seems to be occurring in the central retina according to the above study) a small reduction in the number of progenitors can lead to the reduction in cell numbers observed throughout the retina (Bone-Larson et al., 2000). This possibility has yet to be explored.

However, even though an apparent decrease in cell proliferation, as assayed by BrdU incorporation, is observed only in the periphery of the mutant retina, a change in cell proliferation seems to be the most likely explanation of the mutant phenotype. One suggestion that would be consistent with the observed data is that Chx10 prolongs G1, an observation made in studies using ^{3}H-thymidine injections to estimate the

percentage of mitotic figures present in the developing wild type and Chx10 null mutants (Konyukhov and Sazhina, 1966). In this way, apparently normal proliferation in the central retina, as assayed by BrdU incorporation, may still give rise to a smaller retina. That a homeobox gene such as *Chx10* might regulate cell proliferation is in agreement with recent proposals of a similar function for some Hox genes during development (Condie and Capecchi, 1993; Condie and Capecchi, 1994; Dolle et al., 1993; Duboule, 1995). For example, it was shown that disruption of the *Hoxd-13* gene induces localised heterochrony – retardation in morphogenesis during development - leading to mice with neotenic limbs (Dolle et al., 1993).

1.5.4 Chx10 and the Cell Cycle

It is reasonable to speculate that if Chx10 plays a role in proliferation, it may play a role in control of the cell cycle. Some evidence for this is coming to light. A relatively well-known mechanism for cell cycle exit is the dephosphorylation of the negative cell cycle regulators protein retinoblastoma (pRB), p107 and p130 and their subsequent binding to E2F family proteins that encourage proliferation (Figure 1.7). A loss of pRB results in the formation of retinoblastoma tumours. Despite their ubiquitous expression during embryogenesis, however, the specific loss of pRB or p107 together with p130 disrupts the normal development of only a very limited spectrum of tissues (Wiggan et al., 1998). Previously such disruptions have been attributed to deregulation of E2F activity and consequent failure to exit cells cycle to allow differentiation.

It has been suggested that the tissue specific effects of losing specific pRB-family proteins (including effects in the retina) may also be a consequence of deregulation of the activity of other novel pRB-associated factors that are involved in determining cell fate. This led to the discovery of an interaction between the pRB-family proteins and a class of homeoprotein domain-containing developmental factors, including *Mhox*, *Pax3*, and *Chx10 in vitro*. As with the interaction with E2F, the consequence of these interactions is repression of activated transcription by these proteins (Wiggan et al., 1998). Thus, it can be postulated that activated unphosphorylated pRB may bind to Chx10 and repress either its transcription of cell differentiation genes, or its repression of cell cycle genes – it is unknown which action Chx10

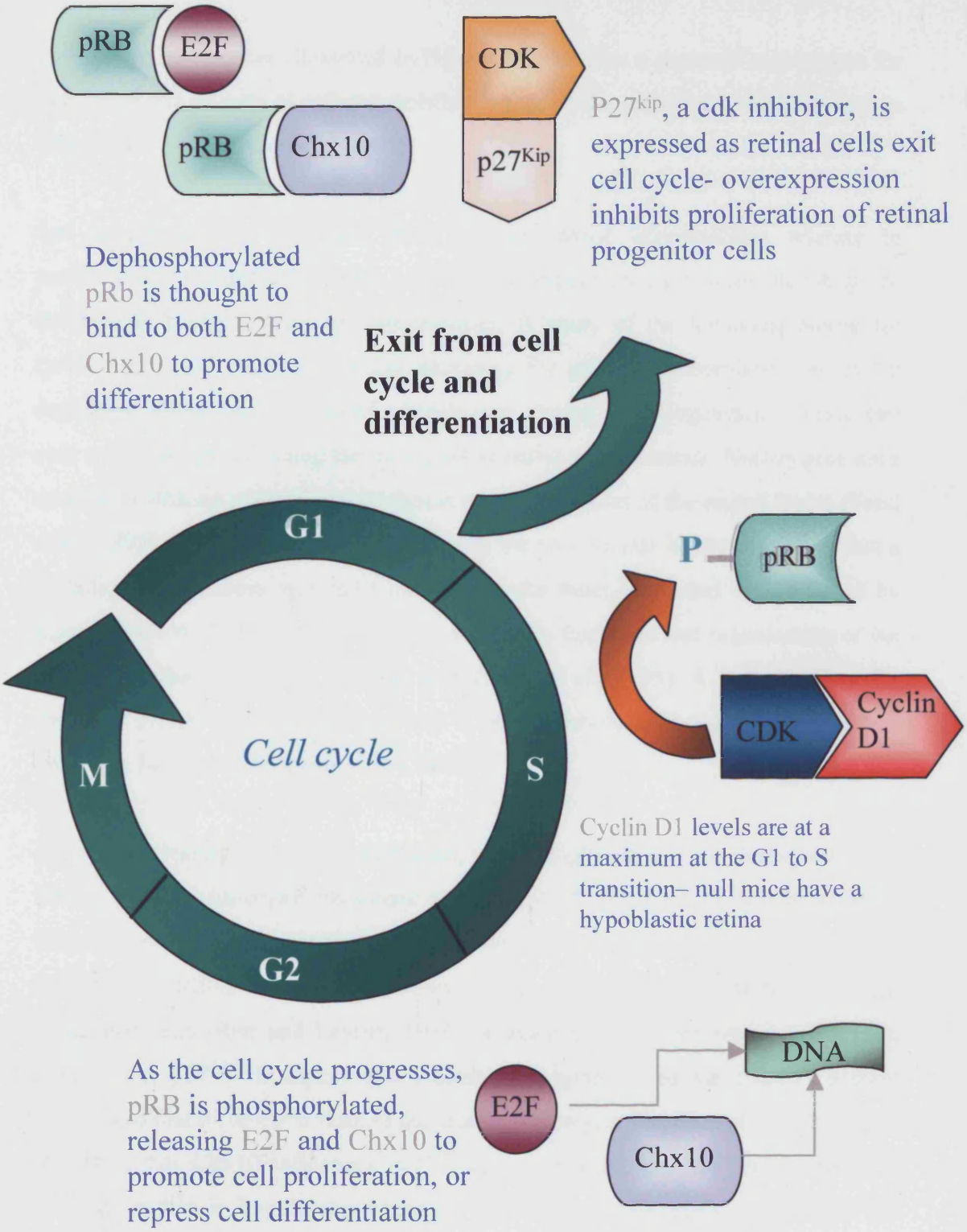

Figure 1.7: Depiction of the cell cycle and how various cell cycle proteins interact with or are affected by Chx10. Upon exit from the cell cycle, pRB is thought to bind to E2F and Chx10 to promote differentiation. $P27^{Kip1}$ is upregulated upon exit from the cell cycle, and its overexpression inhibits proliferation. Cells continuing into the cell cycle, require expression of cyclin D1, whose absence results in a hypoblastic retina. As pRB is phosphorylated, E2F and Chx10 are released and can bind to DNA to promote proliferation/repress differentiation.

exerts. This interaction, illustrated in Figure 1.7, provides a potential mechanism for integrating the process of cellular proliferation and differentiation – two processes in which Chx10 appears to be involved.

Just as deregulation of pRB gives rise to retinal abnormalities relating to proliferation, a number of other cell cycle components have been shown to be involved in retinal disease or abnormalities. A study of the knockout mouse for *cyclin D1*, a cell cycle component necessary for pRB phosphorylation by cyclin dependent kinase and expressed ubiquitously during embryogenesis, reveals that only a few tissues, including the retina, are sensitive to its absence. Nullizygous mice revealed a striking reduction in thickness and organisation of the retinal layers (Fantl et al., 1995). Comparison of cell numbers in the two nuclear layers confirmed that a reduction in thickness was most marked for the outer layer and accompanied by disorganisation of nuclear polarity. A reduction in thickness and organisation of the surface ganglion cell layer was also seen (Fantl et al., 1995). A lack of cyclin D1 seems to affect only proliferation, and it would therefore be interesting to see if cyclin D1 has any relationship with Chx10.

Another interesting cell cycle component, which might have some relationship with Chx10, is the cyclin-dependent kinase inhibitor $p27^{Kip1}$ (Figure 1.7). *In vitro* analyses show that $p27^{Kip1}$ accumulation in retinal cells correlates with cell cycle withdrawal and differentiation, and when overexpressed, it inhibits proliferation of the progenitor cells (Reh and Levine, 1998). Results from another recent publication suggest that $p27^{Kip1}$ is abnormally present in progenitors of the *Chx10*$^{-/-}$ mutant mouse, and that its deletion rescues the mutant phenotype (Green et al., 2003). It was suggested that Chx10 influences $p27^{Kip1}$ at a post-transcriptional level, through a mechanism that is largely dependent on cyclin D1. Additionally, deletion of the *p27*^{Kip1} gene restores normal development of cyclin D1 deficient mice (Geng et al., 2001). Thus, these cell cycle regulators may play an important role in Chx10 regulation of neural retinal progenitor proliferation. Table 1.3 summarises how Chx10 is thought to interact with various cell cycle proteins.

Cell Cycle Component	Role in Cell Cycle	Phenotype upon deletion	Relationship with Chx10?
pRb	Negative cell cycle regulator, binds E2F to cause exit of cell cycle	Retinoblastoma tumours – uncontrolled proliferation	Yes (Wiggan et al., 1998)
Cyclin D1	Activates cyclin dependent kinases cdk4 and cdk6, drives cell cycle progression	Severe retinopathy – impaired development of all retinal layers	Suspected (Green et al., 2003)
$P27^{Kip1}$	Inhibits cyclin dependent kinases, required for timing of cell cycle withdrawal	Normal period of histogenesis of photoreceptors and Müller glia is extended	Yes (Green et al., 2003)

Table 1.3: Cell cycle components potentially affected by or under control of Chx10

1.6 Retinal Stem Cells

The role of Chx10 in proliferation of neural retinal progenitor cells is of great interest because of the profound reduction in volume of the retina observed in the microphthalmia phenotype. There is however, an additional reason why this role is of interest: contrary to past belief, there is a possibility that a RPC- or stem cell-like cells may exist in adult warm-blooded vertebrates, which may be a source of new strategies in treating retinal degenerative disease. There is some evidence that both birds and mammals may have a source of proliferating retinal progenitors in the equivalent of the frog and fish ciliary marginal zone (CMZ) (Figure 1.8A, B) (Ahmad et al., 2000; Fischer and Reh, 2000; Perron and Harris, 2000b; Tropepe et al., 2000). It has long been clear that amphibian and fish eyes grow postnatally, with cells from the ciliary marginal zone at the periphery of the retina exiting a pool of progenitors, differentiating and migrating and integrating within the retina (Reh and Levine, 1998; Wetts et al., 1989) (Figure 1.8A and B). An upregulation of these proliferating cells is observed upon retinal damage (Reh and Levine, 1998). Until recently, no such mechanism was believed to exist in birds or mammals. However, a proliferating marginal zone of retinal progenitors equivalent to the frog CMZ has recently been identified in chickens (Fischer and Reh, 2000). These cells show many similarities with embryonic RPCs: they expressed both *Pax6* and *Chx10*, a pattern of

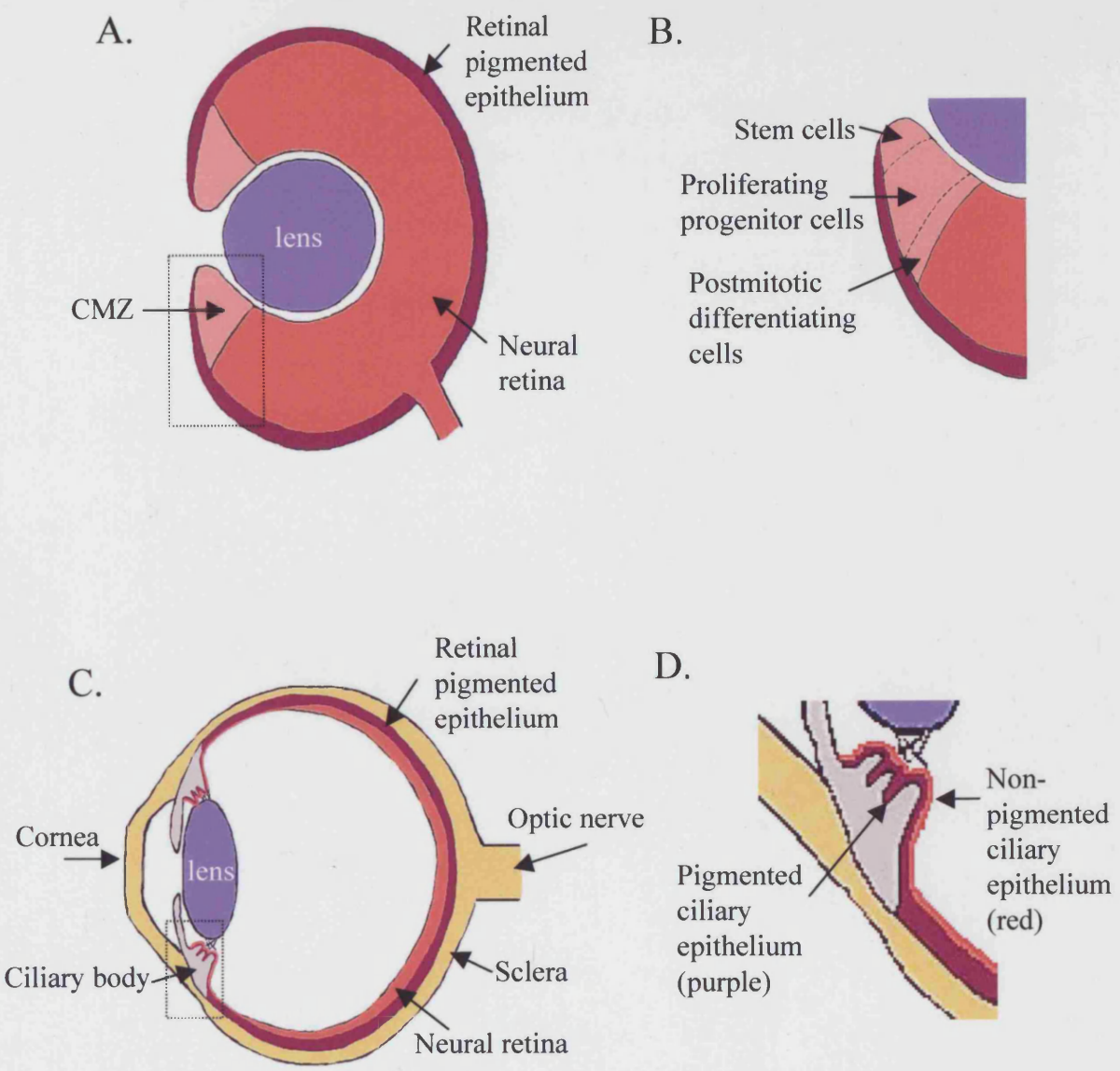

Figure 1.8: Stem cells and progenitor cells in the Xenopus and mammalian eye. (*A*) Schematic diagram of a section of the adult Xenopus retina. The ciliary marginal zone (CMZ, pink) is located at the periphery of the retina (red). (*B*) The box in *A* is magnified in *B*. The retinal stem cell-containing region is located at the peripheral edge of the CMZ. More centrally, progenitors mature progressively and new neurons are added to the retina at the most central region of the CMZ. (*C*) Schematic diagram of a section of an adult mouse retina. (*D*) The box in *C* is magnified in *D*. Stem cells have been isolated from the pigmented ciliary epithelium (purple), a forward continuation of the retinal pigmented epithelium overlying the ciliary body. This, in turn, is overlaid by a non-photosensitive forward continuation of the neural retina (red), the non-pigmented ciliary epithelium. Figure adapted from Perron and Harris, 2000.

Figure 1.9: Model of cycling behaviour in wild type and *Chx10*$^{-/-}$ CE cell culture. In the wild type CE (A), a stem cell-like cell gives rise to progenitor cells that can cycle and/or produce differentiating cells. Chx10 expression in progenitors regulates a feedback mechanism (blue arrow), limiting the number of stem cell divisions and therefore the number of colonies observed, however cycling of progenitors results in a large colony. In the *Chx10*$^{-/-}$ retina, progenitor cells do not express Chx10, and without its inhibiting effects, the population of stem cell-like cells expands (blue arrow), resulting in relatively more neurosphere colonies than in the wild type CE. However, lack of Chx10 also decreases proliferation of progenitors (red arrow), resulting in relatively smaller colonies.

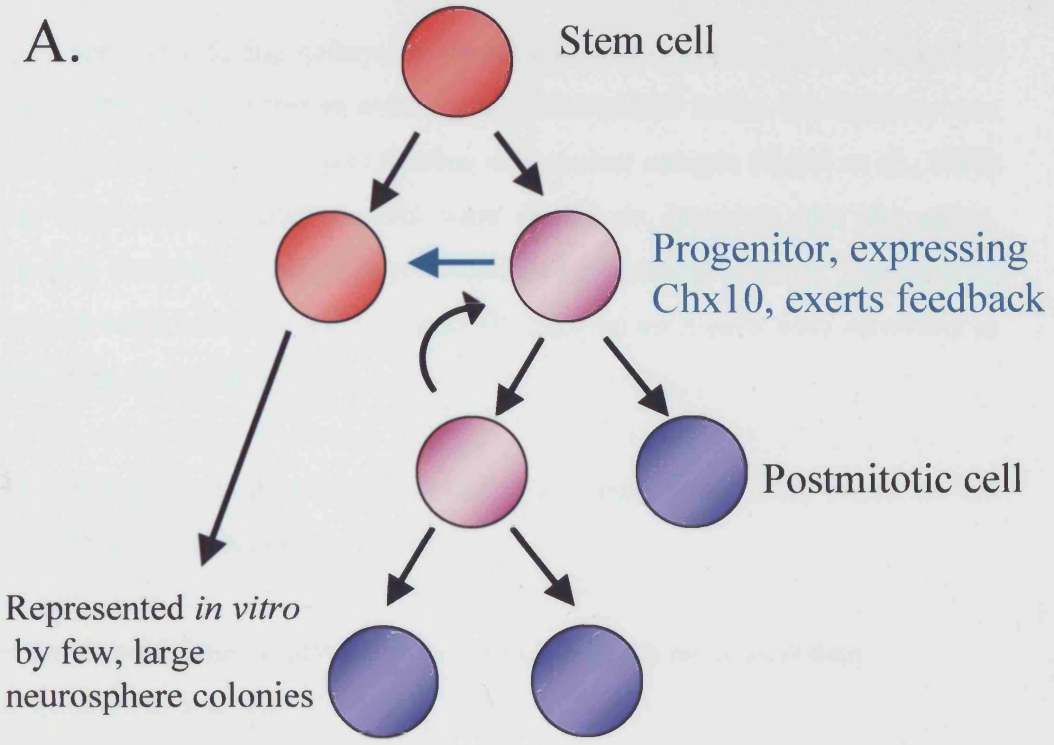
A.
Stem cell
Progenitor, expressing
Chx10, exerts feedback
Postmitotic cell
Represented *in vitro*
by few, large
neurosphere colonies

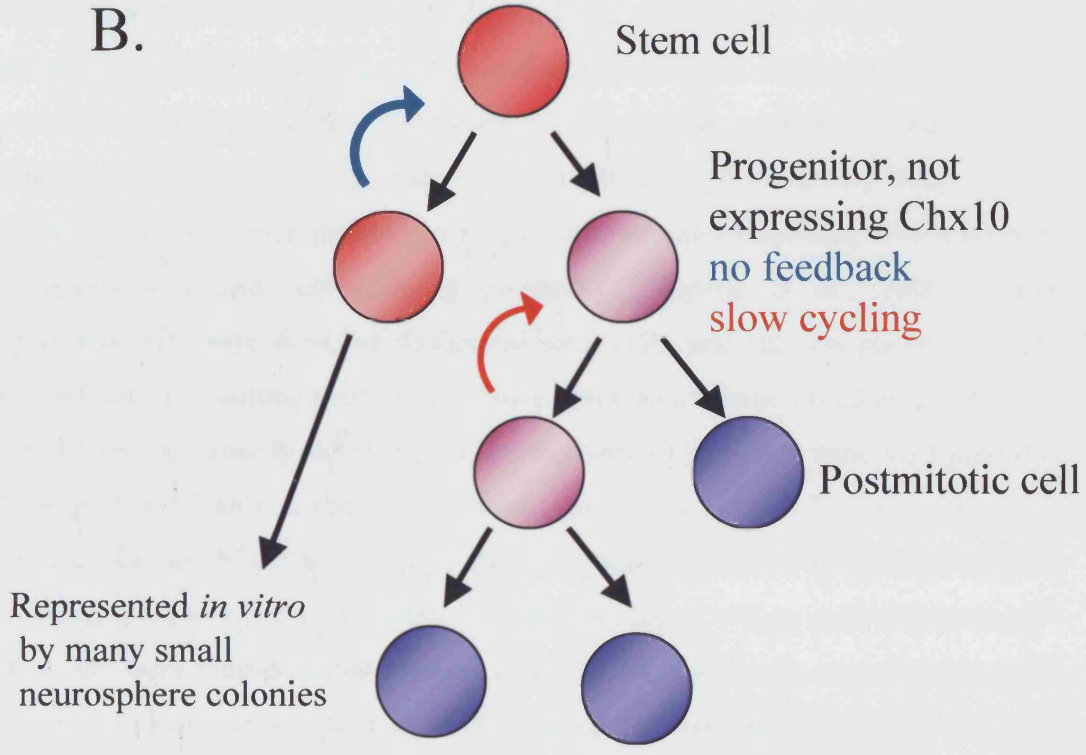
B.
Stem cell
Progenitor, not
expressing Chx10
no feedback
slow cycling
Postmitotic cell
Represented *in vitro*
by many small
neurosphere colonies

expression seen only during embryonic retinal progenitor proliferation, as *Pax6* and *Chx10* are expressed in different cells in the differentiated retina. Proliferation was observed with both BrdU and proliferating cell nuclear antigen (Kurki et al., 1988) labelling. Such undifferentiated cells were shown to integrate into the retina, although they showed no change in proliferation upon retinal damage. Similar cells have been identified in quail and opossum although no such cells were identified in mouse (Kubota et al., 2002).

The cells described above may be classified as neural stem cells based on the following definition of neural stem cells:

a) They are derived from embryonic stem cells or from the nervous system.
b) They generate neural cells.
c) They have some capacity for self-renewal.
d) They can give rise to cells other than themselves through asymmetric division (Gage, 2000).

It remains difficult to deduce the difference between stem cells and progenitor cells derived from them, which may have similar properties but only undergo a limited number of divisions and give rise to fewer cell types. In a culture system, a small number of cells from the pigmented ciliary epithelium of the ciliary body of both embryos and adult mice grew from single cells into small spheres, which showed multipotentiality and self-renewing properties (Tropepe et al., 2000). These pigmented cells were therefore designated stem cells, and the non-pigmented cells arising from the resulting neurospheres were designated neural retinal progenitors, as they showed no capacity to self-renew, but expressed *Chx10* and were multipotential (Tropepe et al., 2000). A similar experiment using cells isolated from the pigmented ciliary epithelium of the adult rat eye also led to the designation of a number of cells as "retinal progenitor cells with stem cell like properties" – they were shown to self-renew and were multipotential (Ahmad et al., 2000). These cells were thought to be quiescent *in vivo*, with only a fraction dividing, and responding to treatment with fibroblast growth factor 2 (FGF2) *in vitro*.

Embryonic neural retinal progenitor cells, from human foetuses at 6-13 weeks after conception, have also been cultured and maintained for over 300 days and passaged more than 10 times. These cultures were expanded with addition of epidermal growth factor (EGF) and FGF2 (Kelley et al., 1995a). This expansion of primary cultures of human retinal progenitors was thought to have potential for providing a source for transplantation to treat degenerative conditions of the retina such as macular degeneration and retinitis pigmentosa. Whilst this is still true, the above-mentioned experiments suggest that there may now be an additional source in adults, one that may be exploited by encouraging proliferation rather than by transplantation.

The role Chx10 plays in these putative stem cells is of great interest. In the above-mentioned experiment using mouse retinal cell cultures, it was observed that the number of spheres arising from the pigmented ciliary epithelium in *Chx10*$^{-/-}$ mouse increased compared to controls, but the spheres were also smaller. It was postulated that the presumptive stem cells observed give rise to Chx10-expressing neural retinal progenitor cells, which in turn exerted a form of feedback on the stem cells. Without the presence of Chx10, this feedback would be decreased, leading to a larger number of stem cells, but the colonies would be smaller due to the lack of proliferation as a result of Chx10 absence (Figure 1.9). Although this is an interesting premise, an important question that arises is whether presumptive stem cell and neural retinal progenitor cell are one and the same, as is suggested by other studies, in which such cells are labelled as neural retinal progenitor cells with stem cell-like properties. The peripheral region of the eye is of particular interest, as it is where the presumptive stem cells are located, as well as the area of the eye where proliferation seems most affected in the *Chx10*$^{-/-}$ mutant eye.

1.7 Aims

In this study, I wished to achieve the following objectives:

1. To identify downstream targets of Chx10 and potential genes involved in microphthalmia through use of microarray technology. By this method I aimed to discover the molecular basis of the phenotype i.e. learn more about the genetic

pathway in which Chx10 is involved, how it might control retinal size, and identify new candidate genes for microphthalmia.

2. To further characterise the cellular defect observed in the Chx10 null phenotype, and in particular examine how the behaviour of RPCs may be altered.

3. To explore the possibility that dividing cells exist in the adult mutant and wild type retina and to test the hypothesis that lack of Chx10 causes a persistence of stem cell-like cells in the adult retina. This should lead to a greater understanding of the biology of stem cells and clearer view of the potential of stem cell therapy in retinal disease.

I have used the *Chx10*$^{-/-}$ (Chx10 null) mouse as a model for microphthalmia, as similar phenotypes are observed in mice and humans when a mutation occurs in their respective *Chx10* genes (Ferda et al., 2000). With use of gene microarrays, which allows the investigation into the expression of thousands of genes, differential gene expression was studied in order to discover what genes are up- or down-regulated as a result of Chx10 absence. As Chx10 is a transcription factor, it is possible that it may have one or more direct downstream targets, which could be identified using this approach.

To explore how Chx10 affects cell proliferation during development and in the adult retina/ciliary margin, a series of immunocytochemistry experiments were undertaken on sections of eyes from both wild type and mutant mice at different time points during development and in the adult. Cell cycle markers including histone 3 (H3) and proliferating cell nuclear antigen (Kurki et al., 1988) were used in conjunction with neural/retinal cell markers in order to ascertain whether the lack of Chx10 has any effect on their expression. In addition, flow cytometry experiments were conducted to examine RPCs in various stages of the cell cycle.

To explore how Chx10 affects cell proliferating in the adult retina/ciliary margin, a BrdU study was initiated to identify and localise any cycling cells *in vivo*. In addition, cell cultures of dissected wild type and *Chx10*$^{-/-}$ retina were set up to examine whether adult retinal or ciliary margin cells could proliferate *in vitro*.

It is hoped the results presented here will give a greater understanding of the role of Chx10 in proliferation and differentiation of neural retinal progenitors, which might be the basis for future strategies to address such conditions as microphthalmia or neural retinal degenerative diseases.

CHAPTER 2

Materials and Methods

2.1 Materials

2.1.1. General lab reagents and solutions

2.1.1.1 General Reagents

AnalaR grade reagents obtained from either British Drug Houses (BDH) or Sigma Aldrich were used except where indicated otherwise.

Glassware, solutions and media were autoclaved at 15psi, 121°C for 20 minutes as required.

Distilled water (dH_2O): Water was purified using a MilliRo 15 Water Purification System (Millipore, SA), or further purified using a Milli-Q Plus Ultra Pure Water System (Millipore), and sterilised by autoclaving as necessary.

A 1:1000 dilution of diethylpyrocarbonate (DEPC, Sigma) was added to solutions stated to be DEPC-treated, left at 37° C overnight, and subsequently autoclaved.

2.1.1.2. General Solutions

Phosphate buffered saline (PBS):	0.16M sodium chloride, 0.003M potassium chloride, 0.008M disodium hydrogen phosphate, 0.001M potassium dihydrogen phosphate, as PBS tablets from Oxoid, 1 tablet per 100 mls.
PBST:	PBS with 0.1% Tween-20
4% PFA:	16 g paraformaldehyde was dissolved in 350 ml DEPC-treated PBS, heated to 65°C on stirrer until solution was clear. The solution was then adjusted to 400 ml.

0.5 M EDTA:	186.1g of disodiumethylene-diaminetetraacetate.2H_2O was added to 800 ml dH_2O, adjusted to pH 8.0 with NaOH pellets, adjusted to pH 7.5 with HCl if required, made up to 1L with dH_2O and autoclaved.
1M Tris (also referred to as TrisHCl):	121 g Tris base (Trizma base, Sigma) was dissolved in 800 ml dH_2O and the pH adjusted by adding concentrated HCl. Solution was allowed to cool to room temperature before making final pH adjustment. The solution was made up to 1L with dH_2o and autoclaved.
5M NaCl:	292.2 g of NaCl were dissolved in 800 ml dH_2O. The solution was adjusted to 1L and autoclaved.
1M $MgCl_2$:	203.3g of $MgCl_2.6H_2O$ was dissolved in 800 ml dH_2O. The solution was adjusted to 1L and autoclaved.

2.1.1.3 Other general materials

TESPA (3-aminopropyltriethoxysilane, Sigma) coated slides:

Slides (1 mm Superfrost, VWR) were loaded into glass holders and dipped successively in troughs containing:

10%HCl/70%EtOH in DEPC H_2O

DEPC H_2O

95% EtOH in DEPC H_2O for 30 seconds each.

Slides were left to dry in a 65°C oven. Slide holders were then dipped successively in troughs containing:

2% TESPA in acetone,

2 x 100% acetone,

DEPC H_2O for 30 seconds each.

Slides were left to dry in a 37°C oven.

2.1.2 Reagents for GeneChip Assay

2.1.2.1. RNA preparation

Tri Reagent:	Sigma
Isopropanol:	Sigma
Pellet Paint NF Co-Precipitant:	Novagen

2.1.2.2. RNA gel electrophoresis

Agarose:	Gibco
Formaldehyde:	Sigma
Ethidium bromide:	Sigma
0.24-9.5 kb RNA ladder:	Gibco
10x MOPS buffer:	0.2M 3-(N-morpholino) propanesulfonic acid (MOPS), 50 mM sodium acetate trihydrate, 10 mM EDTA
RNA denaturing loading buffer:	For 3.72 ml: 24 mg Orange G (Sigma), 300 µl glycerol, 450 µl 10x MOPS, 720 µl formaldehyde, 2.25 ml formamide

2.1.2.3 Agilent 2100 Bioanalyser Reagents

RNA 6000 Nano LabChip$^{(R)}$ Kit:	Molecular Probes, Inc.
	RNA Nano Chips
	Electrode Cleaners
RNA 6000 Nano Reagents and Supplies:	Molecular Probes, Inc.
	RNA Nano Dye Concentrate
	RNA 6000 Nano Marker
	RNA 6000 Nano Gel Matrix
	Spin filters
RNA 6000 ladder:	Ambion

2.1.2.4. Target cRNA preparation

-First cycle of amplification – cDNA synthesis:

T7-oligo(dT) promoter primer,
HPLC-purified: Affymetrix

200U/µl Superscript II, 5x first strand buffer, 0.1M DTT, 10mM dNTP mix, 5x second strand buffer, DNA ligase (*E. coli*), DNA polymerase I (*E. coli*), RNase H,

T4 DNA polymerase: Invitrogen

RNasin (recombinant): Promega

Glycogen: Roche

5M ammonium acetate: 385g ammonium acetate was dissolved in 800 ml dH_2O

-First cycle - IVT for cRNA amplification:

MegaScript T7 kit: Ambion

RNeasy Mini Kit: Qiagen

-Second cycle of amplification and labelling – cDNA synthesis:

Random primers: Invitrogen

Reagents as in first cycle cDNA synthesis

GeneChip Sample Cleanup
Module: Affymetrix

-Second cycle – IVT for cRNA amplification and labeling:

ENZO BioArray High Yield RNA Transcript Labelling kit – Affymetrix GeneChip Sample Cleanup Module: Affymetrix

2.1.2.5. Fragmentation

5x Fragmentation buffer composed of: 200 mM Tris-acetate pH 8.1, 150 mM magnesium acetate, 500 mM potassium acetate.

2.1.2.6. Hybridisation

Hybridisation	Control Kit: Affymetrix Control oligonucleotide B2 20x Eukaryotic hybridisation controls
Herring sperm DNA:	Promega
Acetylated BSA:	Gibco
GeneChips: U74Av2:	Affymetrix
Hybridisation buffer:	2-(N-Morpholino)ethanesulfonic acid (MES) stock (see below), NaCl (Ambion), EDTA, 10% Tween-20, H_2O. Final 1x concentration: 100mM MES, 1 M [Na^+], 20 mM EDTA, 0.01% Tween-20.
12x MES stock:	MES free acid monohydrate, MES sodium salt, H_2O. Final concentration: 1.22 M MES, 0.89 M [Na^+]

2.1.2.7. Washing and staining

SAPE stain solution (per array):	600 µl 2x stain buffer (see below), 540 µl water, 2 µg/µl acetylated BSA, 10 µg/ml of streptavidin phycoerythrin (SAPE, Molecular Probes)
Antibody solution (per array):	300 µl 2x stain buffer, 266.4µl water, 2 mg/ml acetylated BSA, 0.1 mg/ml normal goat IgG (Sigma), 3 µg/ml biotinylated goat anti-streptavidin antibody (Vector laboratories)

2x stain buffer:	MES stock buffer, NaCl, 10% Tween-20, H_2O, Antifoam (Sigma). Final 1x concentration: 100 mM MES, 1M [Na^+], 0.05% Tween-20, 0.005% Antifoam
Stringent wash buffer:	MES stock buffer, NaCl, 10% Tween-20, H_2O. Final concentration: 100 mM MES, 0.1M [Na^+], 0.01% Tween-20
Non-stringent wash buffer:	20x SSPE buffer (Sigma), 10% Tween-20, water, Antifoam. Final concentration: 6x SSPE, 0.01% Tween-20, 0.005% Antifoam

2.1.3. Real Time PCR Reagents

2.1.3.1. Preparation of RNA

See **2.1.2.1**

2.1.3.2. Reverse Transcription

Random hexamers, dNTPs:	Amersham Biosciences
Rnase inhibitor:	Invitrogen
PCRII buffer, $MgCl_2$ and MLV-RT:	Applied Biosciences

2.1.3.3. Real time PCR

TaqMan Universal PCR Mastermix:	Applied Biosystems
96-well optical plates, optical tubes and caps:	Applied Biosystems

Gene mixes (in Table 2.1): Applied Biosystems, Assays-on-Demand™ Gene Expression Products

Gene	ABI assay ID	Sequence Surrounding Probe	Exon/Exon boundaries
Rxrg	Mm00436410_m1	AGCTCCCAGCTAAATGTGGTCAACA	2/3
Si	Mm00498996_m1	CATCATCAATGGGAGCCAGGTGTGG	3/4
Dct	Mm00494456_m1	TGCAAATGCACAGGAAACTTTGCTG	1/2
Dlx2	Mm00438427_m1	AAACTCAGGTCAAAATCTGGTTCCA	2/3
Cdh8	Mm00483238_m1	CTGAGATCAGGAACCACAGTCAGAT	8/9
Gapdh	Mm99999915_g1	TGAACGGATTTGGCCGTATTGGGCG	Exon 1, no boundaries

Table 2.1: Gene mix information from Applied Biosystems for Assays-on-Demand gene mixes

Gene mix Neurod1: Applied Biosystems, Assays-by-Design™ Gene Expression Service

Sequence on which primers and probe were based:

5'-TCGATAGCCATTCGCATCATGAGCGAGTCATGAGTGCCCAGCTTAATGCCATCTTTCACGATTAGAGGC

Forward primer: 5'-TCGATAGCCATTCGCATCATGAG

Reverse primer: 5'-GCCTCTAATCGTGAAAGATGGCATT

MGB probe: 5'-CTGGGCACTCATGACTC (binds to same strand as reverse primer)

Eukaryotic 18s rRNA Endogenous Control:

Applied Biosystems, MGB probe and two unlabelled primers, non-primer limited

2.1.4 Preparation of riboprobes

Plasmids with the cDNA inserts used for probe synthesis together with the enzymes (all from Promega) used to linearise and transcribe them for antisense and sense probes are listed in **Table 2.2**. Simple plasmid maps are shown in Figure 2.1. All vectors had ampicillin resistance.

Gene	Source	Antisense	Sense
Rxrg	Prof. R. Evans, Howard Hughes Medical Institute, The Salk Institute for Biological Studies, La Jolla, California and Prof. D. Mangelsdorf, Southwestern Medical Centre, University of Texas, Dallas, Texas	(after subcloning) HindIII, T3	BamHI, T7
Si	Dr. W. Pavan, National Institutes of Health, Genetic Disease Research Branch, Department of Health and Human Services, Bethesda, MD	KpnI, T3	Information not supplied
Dct	Dr. W. Pavan, National Institutes of Health, Genetic Disease Research Branch, Department of Health and Human Services, Bethesda, MD	HindIII, T7	Information not supplied
Dlx2	Prof. J. Rubenstein, University of California, San Francisco, California	HindIII or EcoRI, T3	NotI, T7
Neurod1	Prof. M. Tsai, Baylor College of Medicine, Houston, Texas	HindIII, T7	EcoRV, Sp6
Cdh8	Dr. M Takeichi, Riken Centre For Developmental Biology, Kobe	BglII, T3	XbaI, T7

Table 2.2. Enzymes and RNA polymerases used to make antisense and sense riboprobes for the genes listed.

Figure 2.1: Simple plasmid maps of the vectors and inserts obtained to make riboprobes for *in situ* hybridisation. A: Original vector/insert received for *Rxrg* (left) and final vector/insert used for riboprobe synthesis (right). B-F: Plasmid maps for vectors/inserts of *Dlx2*, *Neurod1*, *silver*, *Dct* and *Cdh 8* respectively, including vector names and sizes, insert sizes, enzyme restriction sites, and polymerases required to make sense and antisense probes where known.

A.

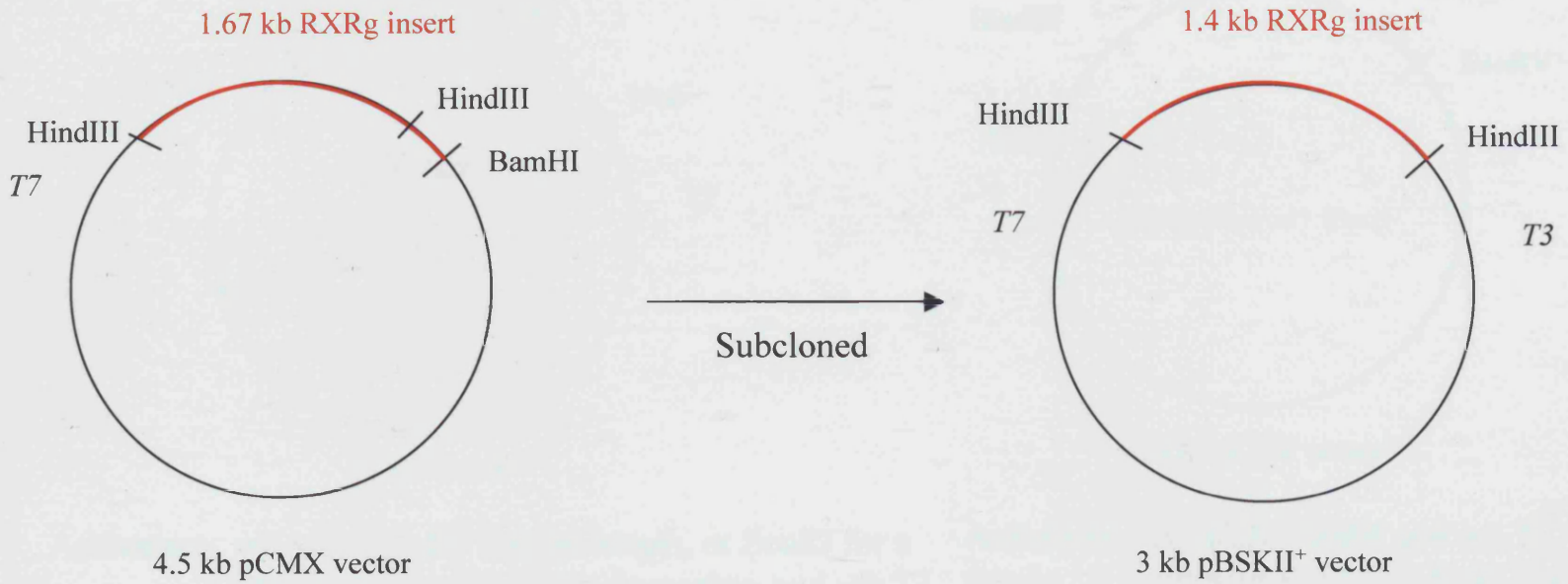

4.5 kb pCMX vector

3 kb pBSKII^{+} vector

Determined sense/antisense direction using restriction digests

B.

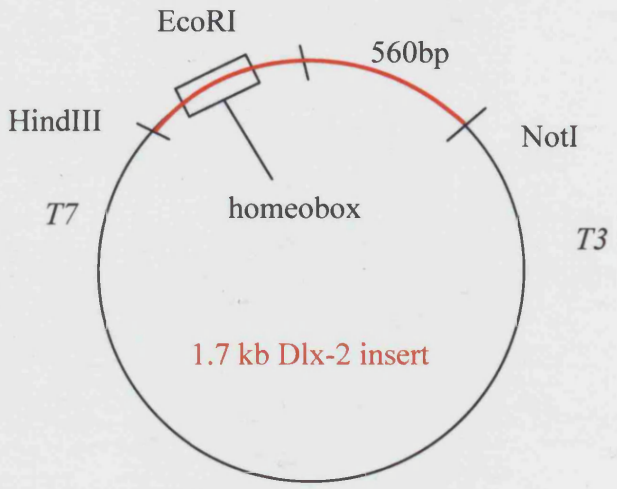

Antisense: cut with HindIII for full length, or EcoRI for a 560 bp probe without the homeobox and use T3

Sense: cut with NotI and use T7

C.

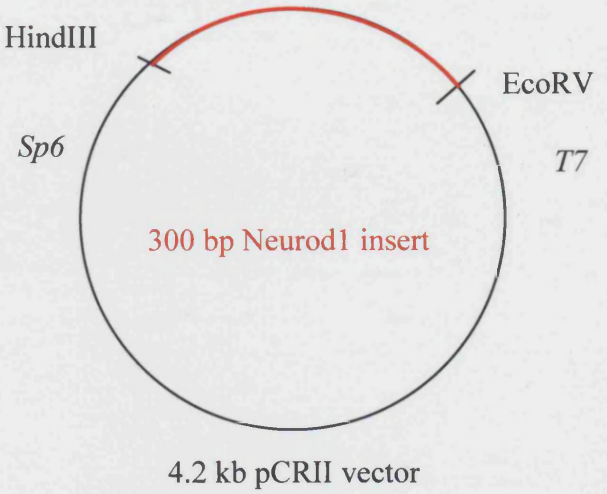

Antisense: cut with HindIII and use T7

Sense: cut with EcoRV and use Sp6

D.

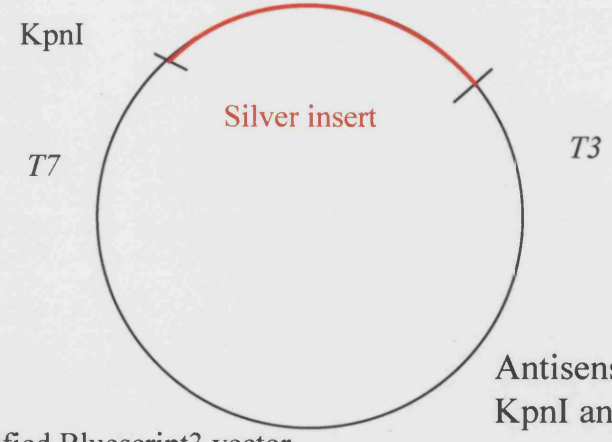

Antisense: cut with KpnI and use T3

E.

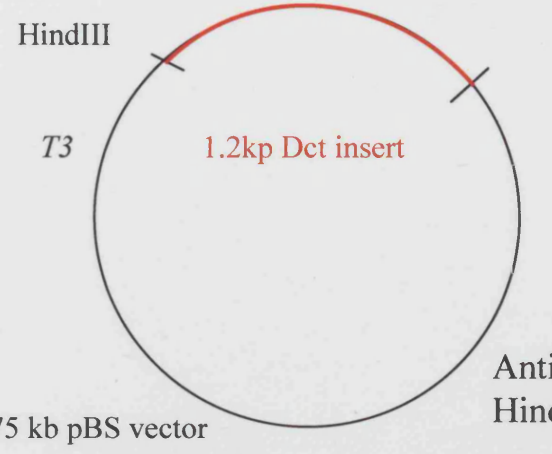

Antisense: cut with HindIII and use T7

F.

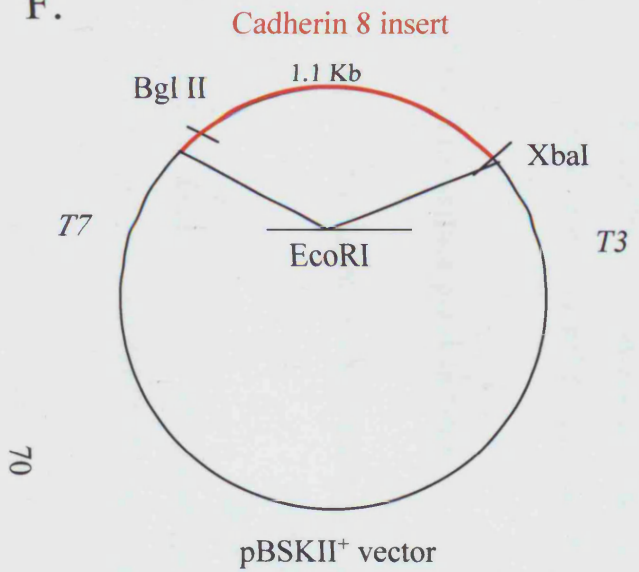

Antisense: cut with Bgl II and use T3
Sense: cut with XbaI and use T7

2.1.4.1. Transforming chemically competent cells

E. coli DH5α cells:	Invitrogen
LB Broth:	Invitrogen, 20g of Lennox L LB broth base per 1L of dH_2O, autoclave.
LB agar:	Invitrogen, 32g of Lennox L agar per 1L of dH_2O, autoclave.
LB agar plates:	LB agar was melted in microwave, poured into cell culture plates, and allowed to cool to solid form. Plates were stored at 4°C and used within a week of preparing.
Treatment with ampicillin:	0.05g ampicillin (Sigma) was dissolved per ml of dH_2O. 1 ml of this solution was added per 1L of LB broth or LB agar (0.05 mg/ml)

2.1.4.2. Isolating plasmid DNA

Glycerol: Sigma

QIAprep® Miniprep from Qiagen, contains:

Buffer P1	50mM Tris-Cl, pH 8.0; 10mM EDTA; 100μg/ml RnaseA
Buffer P2	200mM NaOH, 1% SDS
Buffer N3	3M KAc pH 5.5
Buffer PE	Concentrate (Qiagen)
Buffer EB	10mM Tris Cl, pH 8.5

2.1.4.3. Linearising plasmid DNA

10x restriction enzyme reaction buffers, restriction enzymes (as shown in **Table 2.2**): Promega /Roche

TE buffer: Qiagen, 10 mM Tris-Cl, pH 8.0, 1 mM EDTA

3M sodium acetate: 408.1g of sodium acetate was dissolved in 800 ml dH_2O. The pH was adjusted to 5.2 with

glacial acetic acid. The solution was made up to 1L with dH_2O and autoclaved.

2.1.4.3.1 DNA Agarose Gel Electrophoresis

Agarose:	Gibco
Ethidium bromide,10 mg/ml:	Sigma
5x Loading buffer:	Bioline
Hyperladders I and IV:	Bioline

Tris-acetate/EDTA (TEA) electrophoresis buffer:

Working solution 1x:	0.04M Tris-acetate 0.001M EDTA
Stock solution 50x:	242g Tris base
	57.1 ml glacial acetic acid
	100 ml EDTA pH 8.0 per 1L

Tris-borate/EDTA (TBE) electrophoresis buffer:

Working solution 1x:	0.045M Tris-borate
	0.001M EDTA
Stock solution 5x:	54 g Tris base
	27.5 g boric acid
	20ml 0.5M EDTA pH 8.0 per 1L

2.1.4.3.2. Subcloning of *Rxrg* plasmid

10x NEBuffer 2, BSA (100x): NEB (New England Biolabs)

10x NEBuffer BamHI, BSA (100x): NEB

Calf Intestinal Alkaline Phosphatase (CIP) 10,000U/ml: NEB

Qiaquick Gel Extraction Kit: Qiagen

Buffer QG: Qiagen, composition undisclosed

Buffer PE: Concentrate (Qiagen)

Buffer EB: 10mM Tris·Cl, pH 8.5

Low DNA Mass ladder: Invitrogen

T4 DNA ligase 2,000,000U/ml and 10x ligation reaction buffer: NEB

E. coli TOP10 one shot cells, S.O.C. medium: Invitrogen

PCR mastermix:

dNTPs: Bioline,

5U/µl Taq polymerase, 10x Buffer, 50mM $MgCl_2$ solution: Bioline

T7 and T3 primers: Genosys (Sigma)

Primer sequences:

T7 (5' to 3')	GTAATACGACTCACTATAGG
T3 (5' to 3')	AATTAACCCTCACTAAAGGG

2.1.4.4. Production of Riboprobe

5x polymerase buffer, DTT, RNase inhibitor: Promega/Roche

DIG labelling mix: Roche

Polymerases (T3, T7, Sp6): Promega/Roche

10 M ammonium acetate: 770g ammonium acetate was dissolved in 800 ml dH_2O, the solution was adjusted to 1L.

2.1.5 Whole mount *in situ* hybridisation

Proteinase K:	Sigma
Glycine:	BDH
Glutaraldehyde:	Sigma
Sheep Serum:	Sigma
Anti DIG antibody:	Roche
NBT/BCIP:	Roche

SSC: 20x SSC (3 M sodium chloride, 0.3 M sodium citrate) was made up by dissolving 175.3 g of sodium chloride and 88.2 g of sodium citrate into 900 ml of DEPC-treated water. The pH was adjusted to 7.0 with concentrated sodium hydroxide solution and made up to a litre with DEPC-treated water. For SSC pH 4.5, citric acid was used to adjust the pH.

10% SDS: 25g sodium dodecyl sulphate (SDS) was dissolved in 200 ml DEPC-treated H_2O and heated to 68° C to dissolve. pH is adjusted to 7.2 with HCl. The solution was made up to 250 ml with DEPC-treated H_2O.

Hybridisation mix: 50 ml whole mount hybridisation mix was made up at a time and stored in 10 ml aliquots at –20°C. 25 ml formamide, 12.5 ml 20x SSC pH 4.5, 5 ml 10% SDS, 250 µl 10 mg/ml yeast tRNA (Sigma) and 250 µl 10 mg/ml heparin (Sigma) were mixed and made up to 50 ml with DEPC-treated water.

Solution 1: 50% formamide, 5x SSC pH 4.5, 1% SDS in DEPC treated H_2O

Solution2: 50% formamide and 2x SSC pH 4.5 in DEPC treated H_2O

TBST: 250 ml TBST was made from 25 ml sterile 10x TBST stock, 2.5 ml Tween-20 (to give a 1% concentration), 24 mg levamisol and distilled water. 10x TBST stock contained 8% w/v NaCl, 0.2% w/v KCl, and 0.25 M Tris HCl (pH 7.5).

NTMT: 50 ml NTMT was made up from 1 ml 5M NaCl, 5 ml Tris pH 9.5, 2.5 ml 1M $MgCl_2$, 1% Tween-20 and 24 mg levamisol in DEPC H_2O.

2.1.6. Embedding and vibratome sectioning of whole mount *in situ* hybridized embryos

25% glutaraldehyde solution: Sigma

Gelatin/albumin embedding mixture:

200 ml embedding mixture was made by adding 0.9 g gelatin (300 Bloom; Sigma) to 20 ml PBS and heating to dissolve with continuous stirring. A further 160 ml PBS was added once the mix had dissolved. The solution was cooled to room temperature. 56 g albumin grade II (Sigma) was stirred in by mixing overnight with a stirrer. 36 g sucrose was added and stirring was continued until dissolution. The embedding mixture was stored at –20°C in 5 ml aliquots.

2.1.7. *In situ* hybridisation for cryostat sections

Anti Digoxigenin (Dig) antibody: Roche

Nitro blue tetrazolium chloride/5-Bromo-4-chloro-3-indolyl phosphate NBT/BCIP: Roche

Histoclear: National Diagnostics

Yeast tRNA: 50 mg yeast tRNA (Sigma) was dissolved in 5 ml DEPC-treated distilled water to give a concentration of 10 mg/ml.

Dextran sulphate: 5 g dextran sulphate (Sigma) was dissolved in DEPC-treated water by vigorous vortexing to give a 50% solution.

Salts solution: 10 times Salts solution (2 M sodium chloride, 0.05 M sodium dihydrogen orthophosphate monohydrate, 0.05 M di-sodium hydrogen orthophosphate anhydrous, 0.05 mM EDTA, 0.1 M Tris pH 7.5) was made up with: 57g sodium chloride, 3.45g sodium dihydrogen orthophosphate monohydrate, 3.55g di-sodium hydrogen orthophosphate anhydrous, 50 ml 0.5 mM EDTA, 50 ml 1 M Tris (pH 7.5), made up to 500 ml with DEPC-treated water and autoclaved.

Cryosection hybridisation buffer (CSHB):	50 ml made up from, 25 ml formamide, 10 ml 50% dextran sulphate, 5 ml 10 mg/ml tRNA, 5 ml 10x Salts, 250 µl Denhardts solution (Sigma), 4.75 ml DEPC-treated water, final concentration 50% formamide, 10% dextran sulphate, 0.5% Denhardts solution, 0.1% tRNA, 1x Salts, stored in 10 ml aliquots at -20°C
Washing Solution:	1x SSC, 50% formamide, and 0.1% Tween-20 in DEPC H_2O
MABT:	Made from a sterile 5 times MABT stock, diluted in distilled water and mixed with Tween-20 to give a 0.1% concentration. 5 times MABT (0.5 M maleic acid, 0.75 M sodium chloride) was made up with 58.1 g maleic acid dissolved into 900 ml distilled water. Sodium hydroxide was added to raise the pH to 7.5, causing the maleic acid to first come out of solution, and then go back into solution. 43.8 g of sodium chloride was added, the pH checked again and the solution made up to 1 litre with distilled water.
M-block:	50 ml M-block was made up and stored at –20°C in 10 ml aliquots: a) a 10% Blocking Reagent (Roche Molecular Biochemicals) solution was made up in MABT and stored at –20°C in 10 ml aliquots. 10 ml 10% Blocking Reagent was added to 10 ml heat-inactivated (by heating to 56°C for 30 minutes) sheep serum and made up with 5 times MABT stock and Tween-20 to give 50 ml blocking solution in 1 times MABT (M-block).
Staining buffer:	2% 5M NaCl, 5% 1M $MgCl_2$, 10% 1M Tris pH 9.5, 0.1% Tween-20 in DEPC H_2O.

2.1.8. Preparation of frozen and paraffin-embedded sections

OCT compound:	BDH
Isopentane:	Sigma
20% sucrose:	20g of sucrose (Sigma) were dissolved per 100 ml DEPC treated PBS and filter sterilised. 5 ml aliquots were stored at -20°C until use.

2.1.9. Staining with Eosin and Haematoxylin

Ehrlich's haematoxylin:	VWR
Eosin (1% aqueous):	Raymond Lamb
Vecta-Mount mounting medium (Vector Laboratories)	
Histoclear:	National Diagnostics

2.1.10. Immunohistochemistry on frozen and paraffin-embedded sections

2.1.10.1. Primary antibodies

All primary antibodies used in immunohistochemistry are listed in **Table 2.3**

Rhodamine conjugated anti peanut agglutinin (PNA): Vector laboratories

Antibody	Host	Subtype	Working Conc.	Source
Anti-phosphohistone 3 (H3)	Rabbit Polyclonal	IgG	1:100	Upstate
Anti-proliferating cell nuclear antigen (PCNA)	Mouse Monoclonal	IgG_{2a}	1:100	Santa Cruz
Anti-numb	Mouse Monoclonal	IgG_1	1:500	BD Transduction Laboratories
Anti-brn3b (Pou4f)	Goat Polyclonal	IgG	1:100	Santa Cruz
Anti-β3 tubulin	Mouse Monoclonal	IgG_1	1:1000	Promega
Anti- blue "S" cone opsin	Chicken		1:5000	Tiansen Li, Harvard Medical School, Boston (Zhao et al., 2003)
Anti-rhodopsin	Goat Polyclonal	IgG	1:50	Santa Cruz
Anti recoverin	Rabbit Monoclonal		1:100	Chemicon
Anti syntaxin	Mouse Monoclonal	IgG_1	1:100	Sigma
Anti-VC1.1	Mouse Monoclonal	IgM	1:100	Sigma
Anti-bromodeoxyuridine (BrdU)	Rat Monoclonal	IgG2a	1:100	Oxford Biotech (Immunologicals Direct)
Anti nestin	Mouse Monoclonal	IgG_1	1:10	Developmental Studies Hybridoma Bank
Anti-NeuN	Mouse Monoclonal	IgG_1	1:50	Chemicon
Anti-β1 integrin	Mouse	IgG_1	1:100	Transduction Laboratories
Anti CRALBP	Rabbit		1:1000	Jack Saari, University of Washington, Seattle (Bunt-Milam and Saari, 1983)
Anti GFAP	Rabbit Monoclonal		1:100	DAKO
Anti PKC	Mouse Monoclonal		1:100	Amersham Biosciences
Anti Calbindin	Rabbit Polyclonal		1:50	Santa Cruz

Table 2.3 Primary antibodies used in immunohistochemistry

2.1.10.2. Secondary antibodies

Secondary Antibody	Working Conc.	Source
Fluorescein (FITC)-conjugated Affinipure goat anti-rabbit IgG	1:100	Jackson Immunoresearch Laboratories
Cy3-conjugated Affinipure goat anti mouse IgG	1:100	Jackson Immunoresearch Laboratories
Cy3-conjugated Affinipure rabbit anti goat IgG	1:100	Jackson Immunoresearch Laboratories
FITC-conjugated Affinipure donkey anti-goat IgG	1:100	Jackson Immunoresearch Laboratories
Rhodamine Red-X-conjugated Affinipure donkey anti rabbit IgG	1:100	Jackson Immunoresearch Laboratories
Alexa Fluor 594-conjugated goat anti-chicken IgG		Molecular Probes (Invitrogen)
Fluorescein-labelled affinity purified goat anti-rat IgG	1:100	Insight Biotechnology (KPL)
Rhodamine (TRITC)-conjugated Affinipure goat anti rabbit IgG	1:100	Jackson Immunoresearch Laboratories

Table 2.4 Secondary antibodies used in immunohistochemistry

2.1.10.3. Blocking sera and detergents, other reagents

Foetal Calf Serum (also used for cell culture): Sigma

Normal Goat Serum: DAKO

Normal Donkey Serum: Santa Cruz

Bovine Serum Albumin (BSA): Sigma

Citifluor glycerol/PBS solution: Citifluor Ltd.

Declere: Cell Marque

Hoechst nuclear dye: Hoechst 33258 (Sigma) diluted at 1.2 mg/ml in water

0.01M citric acid buffer: 2.1 g of citric acid monohydrate added to 950 ml dH_20, adjusted to pH 6.0 with NaOH, and made up to 1l with dH_20.

2.1.11. Fluorescence activated cell sorting (FACS) analysis of cell cycle

Leibovitz's L15 Medium with L-Glutamine:
Gibco

0.05% trypsin/0.53 mM EDTA: Gibco

Hypotonic buffer containing propidium iodide:
(50 μg/ml propidium iodide in 0.1% sodium citrate and 0.1% Triton X-100). A sodium citrate/Triton X-100 stock solution was made by dissolving 250 mg of sodium citrate and 250 μl of Triton X-100 in 250 ml H_2O. 50 μl of 20x propidium iodide stock solution (1 mg/ml) could then be added to every ml of sodium citrate/Triton X 100 solution used.

2.1.12. Analysis of mitotic spindle orientation during cell division

Vectashield mounting medium containing DAPI:
Vector Laboratories

2.1.13 Dissociation and Numb-labelling of retinal cells (see also 2.1.10 and 2.1.11)

DMEM/F-12 (1:1) with Glutamax I:
Gibco

Hanks Balanced Salt Solution (HBSS):
Gibco

Anti-numb and other: see tables 2.3 and 2.4

2.1.14 Immunohistochemistry on sections of BrdU injected mice

2.1.14.1. Preparation of BrdU injected mouse eyes

BrdU: Sigma

Carnoy's fixative: 60% EtOH, 30% chloroform, 10% acetic acid

2.1.14.2. Primary antibodies

See **Table 2.3**

2.1.14.3. Secondary antibodies

See **Table 2.4**

2.1.14.4. Blocking sera and detergents, other reagents

See **2.1.10**

Histoclear: National Diagnostics

0.1M sodium borate (pH 8.5):19.04 g added to500 ml H_2O, pH adjusted with HCl

2.1.15. Dissociation and immunohistochemistry of retinal cells (See also 2.1.10, 2.1.13)

DMEM/F-12 (1:1) with Glutamax I:
Gibco

Dispase: Gibco

2.1.16. TUNEL labelling

In situ Cell death Detection kit: Roche

Proteinase K solution: 915 µl dH_2O
50 µl 1 M Tris
25 µl 200 mM EDTA
10 µl 1mg/ml Proteinase K

2.1.17. Cell Culture Reagents

Media:

NSA medium: Euroclone

Leibovitz's L15 Medium with L-Glutamine: Gibco

DMEM/F-12 (1:1) with Glutamax I: Gibco

N-2 Supplement (containing insulin, human transferrin, progesterone, putrescine and selenite): Gibco

Dispase: Gibco

0.05% trypsin/0.53 mM EDTA: Gibco

Penicillin/streptomycin solution: Sigma

Epidermal growth factor, human, recombinant (EGF): Promega

Fibroblast growth factor, basic, human, recombinant (FGF-2): Promega

Fetal Calf Serum: Sigma

Poly-l-lysine (PLL) and laminin coated coverslips were prepared as follows:

Sterile coverslips in culture wells were coated with 100µl of 20 µg/ml of PLL (Sigma, 20 µl of a 1 mg/ml stock solution made up to 1 ml with distilled water), for 30 minutes, after which the PLL was siphoned out and the coverslips were allowed to air dry in the hood for 30 minutes. Coverslips were then coated with 100 µl of 50µg/ml of laminin (Sigma, stock solution 1 mg/ml, 50 µl of 1 mg/ml stock solution made up to 1 ml with PBS) for 30 minutes after which the laminin was siphoned out and the coverslips allowed to air dry.

2.2 Methods

2.2.1 Animals and timed matings

129/Sv wild type and *Chx10*$^{-/-}$ (*Mus musculus* colony with a homozygous mutation of Chx10 on a 129/Sv background) colonies were housed in the animal housing facility at the Institute of Child Health in accordance with Home Office Licensing stipulations and all procedures involving animals were carried out under Home Office Licensing approval and in accordance with the Animals (Scientific Procedures) Act 1986. Timed matings were set up on the evening of a given day and if vaginal plugs were subsequently found, the following morning was designated embryonic day 0.5 (E0.5). On required day of embryonic development, pregnant mice were sacrificed by cervical dislocation. Embryos were removed from the uterus for use in all experiments described, e.g. for fixing and producing sections, or further dissection. When required, eyes from the sacrificed mother were proptosed and removed using bent forceps.

E11.5 *Chx10*$^{-/-}$/ *p27*$^{Kip1-/-}$ double null mice embryos were received from Edward Levine (Department of Ophthalmology and Visual Sciences, Department of Neurobiology and Anatomy, University of Utah, Salt Lake City, UT, USA). *Chx10*$^{-/-}$ / *p27*$^{Kip1-/-}$ double null mice were generated by inter-crossing *Chx10*$^{-/-}$ and *p27*$^{Kip1-/-}$ mice. *Chx10*$^{-/-}$ and *p27*$^{Kip1-/-}$ animals were on a 129/Sv background. Genotyping of mouse-tail DNA was performed as described by Green et al (Green et al., 2003).

2.2.2. Affymetrix GeneChip assay

2.2.2.1. Preparation of RNA

Retinal dissection

Eyes were dissected using no.5 Watchmaker's forceps from embryonic day 11.5 (E11.5) day old 129/Sv (wild type) and *Chx10*$^{-/-}$ (mutant) embryos in cold DEPC-treated PBS. In all cases, somites were counted, by adding all somites from the hind limb to the tail to 27, the number of somites known to

have developed from the head to the hind limb. The mesenchyme was removed from the outside of the eyes, and the RPE was subsequently teased away to leave only the neural retina and the lens. To ensure purity of the material, the dissected tissue was moved to a new dish of PBS with every step. Eyes from one litter were placed together in a 0.5 ml microfuge tube and placed in a -80°C freezer until the day of RNA extraction.

RNA extraction

Without letting the tissue thaw, TRI Reagent was added to the tissue, in a volume of roughly ten times the amount of tissue. The tissue was triturated and allowed to stand for 5 minutes at room temperature to allow complete dissociation of nucleoprotein. 0.2 ml of chloroform was added per ml of TRI Reagent and the sample was vortexed and allowed to stand for 10 minutes at room temperature. The resulting mixture was centrifuged at 13,000 rpm (approx. 11,000x g) for 15 minutes in a Heraeus Biofuge 13R refrigerated centrifuge at 4° C. The upper aqueous phase of the mixture, containing RNA, was transferred to a fresh tube. 0.5 ml of isopropanol was added per ml of TRI Reagent used, and this was left to precipitate overnight at -20° C. In some cases 0.5 µl of pellet paint was added to aid visualisation. The precipitate was centrifuged at 13,000 rpm (approx. 16,000x g) for 30 minutes and an RNA pellet was formed in the bottom of the tube. The supernatant was removed, and the pellet was allowed to air dry for 5-10 minutes and resuspended in an appropriate amount of distilled water.

The extracted RNA was tested for quality and quantity on a formamide RNA gel and/or on an Agilent 2100 Bioanalyser.

2.2.2.2. RNA gel electrophoresis

A 1% w/v agarose gel was prepared by dissolving 0.95g of agarose in 9.5 ml 10x MOPS buffer and 5 ml formaldehyde. 16 µl RNA denaturing loading buffer and 1 µl of 1 mg/ml ethidium bromide was added to 3 µl samples and 0.24-9.5kb ladder and incubated at 70° C for 5 minutes. The samples were loaded onto the gel and run at

maximum current and 100 V. Gels were visualized on an Alpha Innotech Corporation MultiImage Light Cabinet using AlphaImager 1220 software.

2.2.2.3. Agilent 2100 Bioanalyser

The Agilent 2100 Bioanalyser system comprises of the Chip Priming Station, the IKA vortex mixer, the 2100 Bioanalyser itself and the 2100 Expert Software. RNA samples were analysed according to the manufacturer's protocol.

Reagents were allowed to equilibrate to room temperature. RNA 6000 Nano dye concentrate was vortexed and spun down. 1 µl of dye was added to 65 µl of filtered gel matrix and vortexed thoroughly to produce a gel-dye mix. 9 µl of gel-dye mix was added to the gel-dye mix well of the RNA Nano Chip. The chip was placed on the correctly adjusted chip priming station and the plunger of the syringe was depressed and held in place for 30 seconds. After releasing the plunger and opening the priming station, 9 µl of gel-dye mix was added to the other two gel-dye wells of the chip. 5 µl of RNA 6000 Nano Marker was added to the ladder well and each of the sample wells. The RNA 6000 ladder and samples were heat denatured at 70° C for 2 minutes. 1 µl of ladder was added to the ladder well, and 1 µl of sample RNA was added to the sample wells. The chip was placed on the vortex mixer and vortexed for 1 minute at the IKA vortexer set point (2400 rpm). The chip was then placed on the Bioanalyser and the analysis program was initiated.

2.2.2.4. Preparation of cRNA target (schematic shown in Figure 2.2)

-First cycle of amplification, first strand cDNA synthesis

The total RNA samples were mixed with the T7-oligo(dT) promoter primer and incubated at 70°C for 6 minutes, then cooled to 4°C for 2 minutes. RT_Premix_1 was prepared from DEPC-treated water, 5x first strand buffer, DTT, 0.1M, dNTP mix, 10mM, RNase inhibitor, 40 U/µl, and SuperScript II, 200 U/µl, and added to the denatured RNA and primer mixture. These were incubated for 1 hour at 42°C. The samples were heated at 70°C for 10 minutes to inactivate the SuperScript II, then cooled to 4°C.

Figure 2.2: Schematic of the preparation of the cRNA targets to hybridise to the GeneChips. This consists of two rounds of cDNA synthesis and *in vitro* transcription in order to amplify the total RNA extracted from the tissue. The first cycle is the amplification step: total RNA is converted to cDNA and subsequently to cRNA through *in vitro* transcription using unlabelled ribonucleotides. The second cycle results in the production of labelled cRNA target: the cRNA from the first cycle is converted to cDNA and subsequently converted to labelled cRNA through *in vitro* transcription using biotinylated ribonucleotides. Figure from www.affymetrix.com.

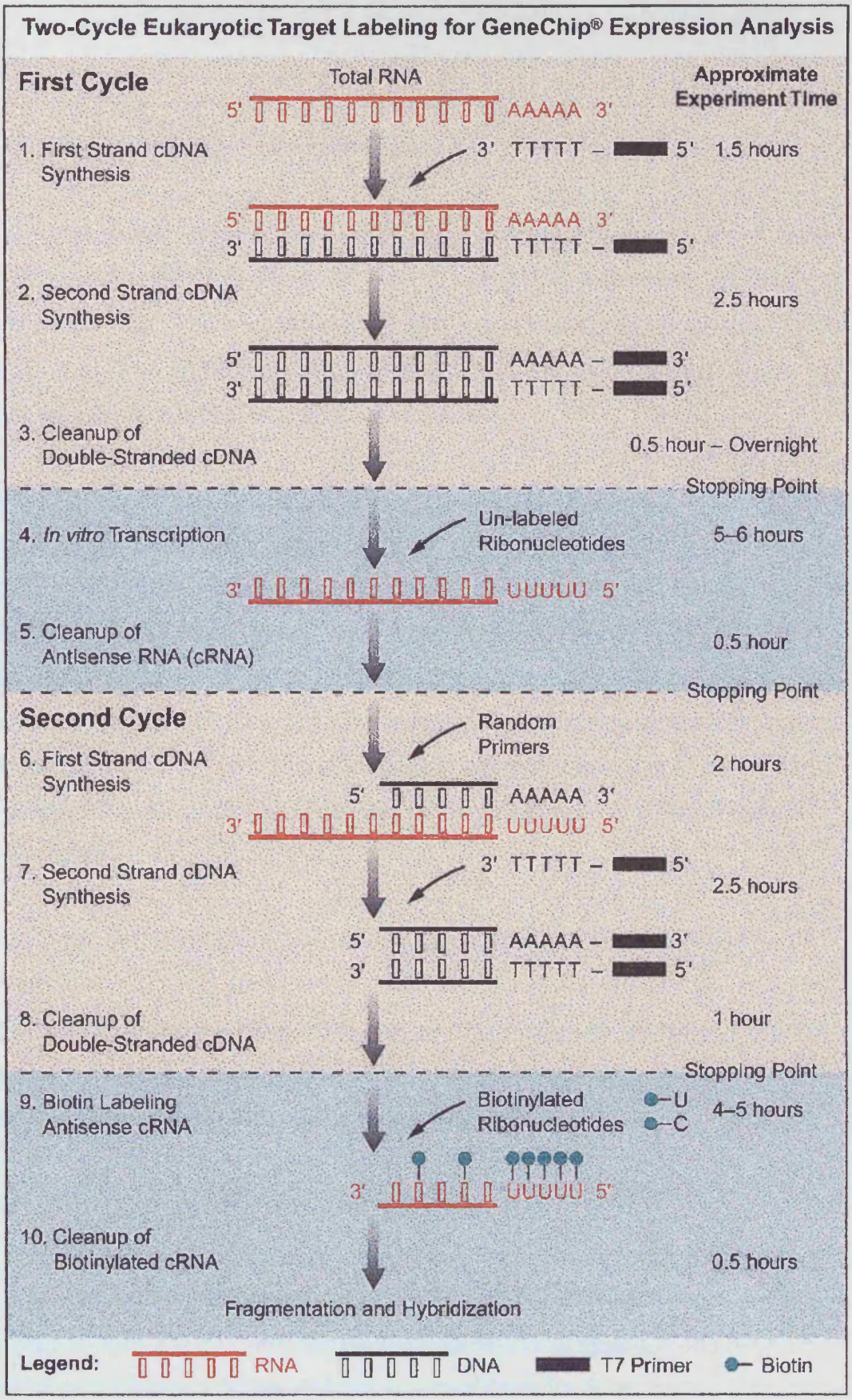
Two-Cycle Eukaryotic Target Labeling for GeneChip® Expression Analysis
First Cycle
Total RNA
Approximate Experiment Time
5' AAAAA 3'
1. First Strand cDNA Synthesis
3' TTTTT – 5'
1.5 hours
5' AAAAA 3'
3' TTTTT – 5'
2. Second Strand cDNA Synthesis
2.5 hours
5' AAAAA – 3'
3' TTTTT – 5'
3. Cleanup of Double-Stranded cDNA
0.5 hour – Overnight
Stopping Point
4. In vitro Transcription
Un-labeled Ribonucleotides
5–6 hours
3' UUUUU 5'
5. Cleanup of Antisense RNA (cRNA)
0.5 hour
Stopping Point
Second Cycle
Random Primers
6. First Strand cDNA Synthesis
2 hours
5' AAAAA 3'
3' UUUUU 5'
7. Second Strand cDNA Synthesis
3' TTTTT – 5'
2.5 hours
5' AAAAA – 3'
3' TTTTT – 5'
8. Cleanup of Double-Stranded cDNA
1 hour
Stopping Point
9. Biotin Labeling Antisense cRNA
Biotinylated Ribonucleotides
U
C
4–5 hours
3' UUUUU 5'
10. Cleanup of Biotinylated cRNA
0.5 hours
Fragmentation and Hybridization
Legend:
RNA
DNA
T7 Primer
Biotin

-First cycle, second strand cDNA synthesis

SS_Premix_1 was prepared from DEPC-treated water, 5x second strand buffer, dNTP mix, *E. coli* DNA ligase, 10 U/µl, *E. coli* DNA polymerase, 10 U/µl, and RNase H, 2 U/µl. This was added to the first strand reaction and incubated at 16°C for 2 hours. 1 µl of T4 DNA polymerase (5 U/µl) was added to each sample and these were further incubated at 16°C for 10 minutes.

-First cycle double-stranded cDNA cleanup by ethanol precipitation

DEPC-treated water, glycogen, 0.6 volumes of 5M ammonium acetate and 2.5 volumes of cold absolute ethanol were added to the reaction and mixed. The cDNA was precipitated at -20°C for 30 minutes to 2 hours and subsequently centrifuged at 13,000 rpm (approx. 16,000x g) for 20 minutes at 4°C. The supernatant was removed and the pellets washed with 70% cold ethanol. After centrifuging at 13,000 rpm for 5 minutes at 4°C, the ethanol was removed and the pellets dried in a Speed Vacuum for 5-10 minutes.

-First cycle, IVT for cRNA amplification using Ambion MEGAscript T7 kit

DEPC-treated water, premixed NTPs, 10x reaction buffer and 10x enzyme mix were added to the dried double-stranded cDNA pellets at room temperature and mixed. These were incubated at 37°C for 5-6 hours.

-First cycle, cRNA cleanup with RNeasy columns

The samples were adjusted to a volume of 100 µl with RNase-free water, and 350 µl Buffer RLT was added to each sample, followed by 250 µl ethanol. Each sample was applied to an RNeasy mini spin column and centrifuged for 15 seconds at 10,000 rpm (approx. 9,000x g). The flowthrough was discarded. 500 µl Buffer RPE was added and the column was centrifuged for 15 seconds at 10,000 rpm. 500 ml Buffer RPE was added and the column was centrifuged for 2 minutes at maximum speed to dry

the RNeasy membrane. The column was transferred to a new collection tube and 30 µl of RNase-free water was pipetted onto the membrane. This was centrifuged for 1 minute at 10,000 rpm to elute. This was followed by a second elution with 20 µl of water. One µl of this was used to examine IVT yield on the Agilent 2100 Bioanalyser.

-Second cycle, first strand cDNA synthesis

Random primers were added to the cDNA samples and incubated at 70°C for 10 minutes. The samples were cooled on ice for 2 minutes. RT_Premix_2 was prepared from the same reagents as RT_Premix_1 and added to the denatured RNA and primer mixture. This was incubated at 42°C for 1 hour. To remove the RNA template, RNase H was added and the samples were incubated for 20 minutes at 37°C, then heated at 95°C for 5 minutes to inactivate the RNase H. The samples were chilled on ice for 2 minutes.

-Second cycle, second strand synthesis

T7-Oligo(dT) promoter primer was added to the chilled samples and incubated at 70°C for 6 minutes. The samples were then cooled to 4°C. SS_Premix_2 was prepared from DEPC-treated water, 5x second strand buffer, dNTP mix, and *E. coli* DNA polymerase I and added to the samples. The samples were incubated at 16°C for 2 hours, T4 DNA polymerase was then added and the samples were incubated at 16°C for a further 10 minutes.

-Second cycle, double-strand cDNA cleanup using the GeneChip sample cleanup module

600 µl of cDNA binding buffer was added to each of the samples and mixed. These were each applied to a cDNA cleanup spin column and centrifuged for 1 minute at 10,000 rpm (approx. 9,000x g). 750 µl wash buffer was then applied to each spin column and the columns were centrifuged for 1 minute at 10,000 rpm. The cap of each spin column was opened and the columns were centrifuged for 5 minutes at

maximum speed to allow complete drying of the membrane. Each spin column was transferred to a 1.5 ml collection tube and 14 µl of cDNA elution buffer was pipetted directly onto the membrane. This was incubated for 1 minute at room temperature and centrifuged for 1 minute at maximum speed to elute.

-Second cycle, IVT for cRNA amplification and labelling with ENZO BioArray High Yield Transcript Labelling Kit

DEPC-treated water, 10x HY reaction buffer, 10x biotin-labelled ribonucleotides, 10x DTT, 10x RNase inhibitor mix and 20x T7 RNA polymerase were added to the double-stranded cDNA sample and incubated at 37°C for 4-5 hours.

-Second cycle, labelled cRNA target cleanup using GeneChip sample cleanup module

60 µl water, 750 µl IVT cRNA binding buffer and 250 µl ethanol were added to the samples and each sample was applied to a spin column. The columns were centrifuged for 15 seconds at 10,000 rpm (approx. 9,000x g). 500 µl IVT cRNA wash buffer was applied to each column and the columns were spun for 15 seconds at 10,000 rpm. 500 µl 80% of ethanol was then applied to each column, and the columns centrifuged for 15 seconds at 10,000 rpm. The cap of each spin column was opened and the columns were centrifuged for 5 minutes at maximum speed. The columns were transferred to a 1.5 ml collection tube and 11 µl of RNase-free water was pipetted directly onto the membrane. The columns were centrifuged for 1 minute at maximum speed to elute. One µl of this sample was used to examine IVT yield and quality on the Agilent 2100 Bioanalyser.

2.2.2.5. Fragmentation

2 µl of 5x fragmentation buffer is added for every 8 µl of RNA + H_2O and incubated at 94°C for 35 minutes. This was put on ice following incubation.

2.2.2.6. Hybridisation

A hybridisation cocktail was prepared with 15 μg fragmented cRNA, 5 μl control oligonucleotide B2, 15 μl 20x Eukaryotic hybridisation controls, 3 μl herring sperm DNA, 3 μl acetylated BSA, 150 μl 2x hybridisation buffer, and water to make up to 300 μl (per chip). This was heated to 99°C for 5 minutes. After this, the hybridisation cocktail is transferred to a 45°C heat block for 5 minutes. The probe array cartridges (GeneChips) are filled with 1x hybridisation buffer and incubated at 45°C for 10 minutes. The hybridisation cocktail was spun at maximum speed in a microcentrifuge for 5 minutes to remove any insoluble material from the mixture. The buffer solution was removed from the probe array cartridges and filled with clarified hybridisation cocktail. This was placed in a rotisserie box rotating at 60 rpm in a 45°C oven. This was left to hybridise for 16 hours.

2.2.2.7. Washing and staining

The GeneChip cartridges were inserted into the designated modules of the GeneChip Fluidics Station 400, which automates the introduction of the nucleic acid target to the probe array cartridge and controls the delivery of reagents. The washing and staining program was set up follows:

Post hyb wash 1:	10 cycles of 2 mixes/cycle with non-stringent wash buffer at 25° C
Post hyb wash 2:	4 cycles of 15 mixes/cycle with stringent wash buffer at 50°C
Stain:	Stain the probe array for 10 minutes in SAPE solution at 25°C
Post stain wash:	10 cycles of 4 mixes/cycle with non-stringent wash buffer at 25°C
2nd Stain:	Stain the probe array for 10 minutes in antibody solution at 25°C
3rd Stain:	Stain the probe array for 10 minutes in SAPE solution at 25°C
Final Wash:	15 cycles of 4 mixes/cycle with non-stringent wash buffer at 30°C.

Table 2.5: Washing and staining protocol for Affymetrix GeneChips

The probe arrays were removed from the fluidics station modules and checked for bubbles or air pockets. If bubbles were present, the chips were refilled either by hand or on the fluidics station. The probe arrays were then scanned in the HP GeneArray scanner.

2.2.3 Real time PCR analysis

2.2.3.1. Preparation of RNA

Retinal dissection and extraction of RNA as described in 2.2.2.1.Quality and quantity of RNA was tested on a spectrophotometer and by electrophoresis on a formamide gel as described in 2.2.2.2.

2.2.3.2. Reverse transcription

1 μg of RNA in 10 μl dH_2O was added to 5 μl of RT mix 1 (2 μl of 50 μM random hexamers, 2 μl of dNTPs at 2.5 mM each, and 1 μl of 20U/μl RNase inhibitor) on ice and incubated at 70°C for 10 minutes. The mixture was placed on ice for a further 1 minute after which 5 μl of RT mix 2 (2 μl 10x PCRII buffer, 2 μl of 25 mM $MgCl_2$, and 1 μl of 50U/μl MLV-RT) was added. This was incubated at 42°C for 1 hour. For non-RT controls, dH_2O was added to RT mix 2 instead of MLV-RT.

2.2.3.3. Real time PCR

Enough gene mix was made for the number of wells/reactions required per gene.
Per reaction:

25 μl TaqMan universal PCR mastermix

2.5 μl 20x Gene mix (details section 2.1.1.3)

20.5 μl dH_2O

2 μl cDNA (or H_2O for non-template controls) was added to each, making a total reaction of 50 μl per well. In some experiments, all amounts were halved with no significant changes to the results.

The 96-well plate or optical tubes were briefly spun and placed in the ABI 7000 Sequence detector. The standard conditions for PCR were set as follows:

2 min at 50° C
10 min at 95° C
40 cycles of: 15 sec at 95° C
60 sec at 60° C

using the 9600 emulation (the ramping of the block is controlled to mimic the performance of the ABI 7000 Sequence detector predecessor, the 9600)

2.2.3.4. Data analysis

The threshold line for each experiment was set at the level where all runs were in the linear range of amplification. A threshold cycle (Ct) was determined for each amplification. Using the CTs, relative differences in starting material between the wild type and *Chx10*$^{-/-}$ retinae could be determined. The method used here is the ΔΔCt method and is as follows:

Subtraction of Gapdh Ct from Sample Ct to normalise against Gapdh:

$$\text{Sample Ct} - \text{Gapdh Ct} = \Delta\text{Ct Sample}$$

Set one of samples as a reference (e.g. wild type) and subtract reference ΔCt from other sample ΔCts (e.g. *Chx10*$^{-/-}$):

$$\Delta\text{Ct}[\text{Chx10}^{-/-}] - \Delta\text{Ct [wild type]} = \Delta\Delta\text{Ct}$$

Amount of *Chx10*$^{-/-}$ relative to wild type is then calculated:

$$= 2^{-\Delta\Delta CT}$$

This will produce the fold-change difference between the reference sample, in this case the wild type sample, and the other samples, in this case the *Chx10*$^{-/-}$ sample.
This method is based on the assumption that the targets all have a 100% amplification efficiencies leading to a doubling of DNA product per cycle, or 2^n amount of DNA after n cycles. This assumption is made here because the primers

and probes for the PCR study were produced as kits by Applied Biosystems (Assays-on-Demand), which have been optimised to 100% efficiency.

Only one set of primers and probes was made through the Assays-by-Design system, where a sequence is sent to Applied Biosystems and primers and probes are designed based on this sequence. To test whether the efficiency of this primer/probe set, Neurod1, is also optimal, dilutions of cDNA were run for Gapdh and Neurod1. Data points were plotted and the slope of the Neurod1 line matched that of the Gapdh line, indicating the same efficiencies.

2.2.4. Preparation of riboprobes for *in situ* hybridisation

2.2.4.1. Chemically competent cells were transformed with plasmid DNA

E. coli DH5α cells were removed from -80°C freezer and thawed on ice. 100 µl of cells were transferred to a microfuge tube and 1 µl of plasmid DNA (see Table 2.2) was added directly to the competent cells and mixed in by gentle tapping. The tube was incubated on ice for 30 minutes, then heat shocked for 45 seconds in a 37°C waterbath. The tube was then placed on ice for 2 minutes. 900 µl of pre-warmed LB broth was added to the tube and the vial was shaken for 1 hour at 225 rpm in a 37°C shaking incubator. Two volumes (50 and 200 µl) from each transformation were spread on separate LB agar plates treated with ampicillin. The plates were inverted and incubated overnight in a 37°C oven. The following day, 1-2 colonies would be selected and grown in 5 ml LB broth with ampicillin overnight in a 37°C shaking incubator.

2.2.4.2. Isolating plasmid DNA

The following day, glycerol stocks of the transformed cells were made by adding 300 µl of autoclaved 80% glycerol to 700 µl bacteria to be kept at -80°C for future use. The rest of the cells were spun down in a Sorvall RC5B Plus centrifuge at 4°C at 600 rpm (approx. 30x g) for 15 minutes.

Plasmid DNA was isolated using the Qiagen QIAprep Miniprep Kit according to manufacturer's protocol:

1ml of a total 5ml overnight culture was harvested by centrifugation at 13000 rpm (approx. 15,000x g) for 1 minute. Bacterial cell pellets were resuspended in 250µl of buffer P1, with subsequent of addition of 250µl of P2.These were then inverted 4-6 times to mix. 350µl of N3 was then added and samples inverted 4-6 times to mix. Precipitates were harvested by centrifugation at 13,000 rpm for 10 minutes. Supernatants were bound to Qiagen spin miniprep columns by centrifugation at 13,000 rpm for 1 minute and washed with 750µl of PE using centrifugation as above. The columns were centrifuged to remove excess PE and DNA eluted from the column by incubation with 50µl of buffer EB for 1 minute, followed by centrifugation at 13,000 rpm for 1 minute.

2.2.4.3. Linearising plasmid DNA

A digest was set up with a final volume of 30 µl: 8-10 µg of plasmid, 3 µl of appropriate 10x restriction enzyme reaction buffer, 1 µl of restriction enzyme, made up to 30 µl with DEPC H_2O. This was allowed to digest overnight. 1 µl of digest was run on a 1% agarose gel to confirm digestion. The rest was made up to 400 µl with dH_2O and 400 µl of phenol/choloroform was added. The mixture was vortexed for a few seconds and spun at full power on a microfuge for 5 minutes. The top layer was transferred to a new microfuge tube and 400 µl of chloroform was added. The mixture was again vortexed and spun. The top layer was again transferred to a new microfuge tube and 40 µl of 3M sodium acetate (pH5.3) and 1 ml of EtOH was added. The mixture was left to precipitate overnight at -20°C. The mixture was then spun for 40 minutes at full speed (approx. 16,000x g) on a microfuge and washed with 70% EtOH and another spin for 10 minutes. The pellet was air dried for 5-10 minutes and diluted in TE buffer at approx 1 µg/µl, taking into account a roughly 30% loss from the original 8-10 µg digested. 1 µl of the linearised DNA was tested for quality and quantity on an agarose gel and/or a spectrophotometer.

2.2.4.3.1 DNA Agarose Gel Electrophoresis

The appropriate amount of electrophoresis grade agarose was added to the appropriate volume of TAE buffer (e.g. a 1% gel was made up of 1g of agarose per 100 ml dH_2O) and placed in a microwave at full power for a few minutes depending on the volume (the mixture was not allowed to boil, and heated until the agarose was fully dissolved). A 1:10000 dilution of 10 mg/ml ethidium bromide was added to the gel and the gel poured in a mould and allowed to cool. When gel was cooled, the gel was placed in a gel tank with 1x TAE (used when running l>1 kb DNA fragments or when running a gel for gel extraction) or TBE buffer (used when running <1 kb fragments).

1 µl of 5x loading buffer was added per 4 µl of sample DNA and samples were loaded onto the gel. One of the wells was loaded with a molecular weight marker, e.g. hyperladder I or IV. The gel was run at maximum current and 100V. Gels were visualized on an Alpha Innotech Corporation MultiImage Light Cabinet using AlphaImager 1220 software, unless stated otherwise.

2.2.4.3.2 Spectrophotometry

2 µl of sample DNA was diluted in 48 µl of appropriate buffer or water in Eppendorf cuvettes. A cuvette with 50 µl buffer or water was first placed in the Eppendorf Biophotometer and used to set a reference. The appropriate dilution was entered onto the Biophotometer and the samples were measured one by one for DNA quality and quantity. The spectrophotometer measures absorbance at 230, 260, and 280 nm, and calculates DNA concentration and 260/280 and 260/230 ratios, taking into account the dilution factor, giving and indication of amount and purity.

2.2.4.3.3. Subcloning of *Rxrg* plasmid

The plasmid obtained for *Rxrg* was received in an expression vector. As antisense probe could not be produced from this plasmid (see Figure 2.1) a 1.4 HindIII fragment was subcloned into the Bluescript $pSKII^+$ plasmid. Cmx-Rxrg plasmid and

pSKII$^+$ plasmid (available in the lab from glycerol stocks) were isolated and linearised as follows:

30 µl of pSKII$^+$ at 0.09 mg/ml, 1.5 µl HindIII, 3 µl 10x NEBuffer 2, and 0.4 µl BSA were incubated at 37° C for 1 hour, then 4 µl 10x NEBuffer BamH1 and 2 µl BamH1 were added and the mixture further incubated at 37° C for 1 hour. 2.5 µl CIP (about 1:10) was added to the pSKII$^+$ digest at 37° C for 1 hour.

5 µl Cmx-Rxrg plasmid at 0.37 µg/µl, 1 µl HindIII, 1 µl 10x NEBuffer 2, 0.2 µl BSA and 3 µl H_2O were incubated at 37° C for 1 hour, then 1.5 µl 10x NEBuffer BamH1,1 µl BamH1 and 7 ml H_2O were added and the mixture further incubated at 37° C for 1 hour.

Both vector and Rxrg insert were run on a 1.5% agarose gel, which was visualised on a BioRad ChemiDoc imager using BioRad QuantityOne software. The vector and insert were excised from the gel and gel purified using a Qiagen QIAquick Gel Extraction Kit according to the manufacturer's protocol:

3 volumes of Buffer QG were added to 1 volume of gel (100mg = approx 100 µl) in a colorless tube. This was incubated at 50° C until gel was completely dissolved (approx 10 min), while vortexing every 2-3 min. 1 volume of isopropanol was added per volume of gel and the sample was applied to the QIAquick spin column and centrifuged for 1 minute. The flow-through was discarded. 0.75 ml Buffer PE was added to the spin column and sample was centrifuged for 1 min. The column was placed in a clean collection tube and 20 µl dH_2O was applied to the centre of the spin column membrane. The column was allowed to stand for 1 min, then centrifuged for 1 min.

2 µl of the linearised plasmids were run on a 2% gel with a low DNA mass ladder to determine their relative concentrations. The insert and plasmid were incubated in a 2:1 or 5:1 ratio of insert:vector using the following equation:

ng insert – (ng vector x kb inert)/ kb vector = ratio insert:vector

and made up to 8 µl with dH_2O and incubated at 45°C for 5 minutes. The mixture was put on ice and 1 µl of concentrated T4 DNA ligase and 1 µl of 10x ligation buffer was added and the mixture was incubated for 1 hour at 25°C.

4 µl of the ligation mix was added to 50 µl of TOP10-One shot cells and was mixed by gentle tapping and incubated on ice for 20 minutes. Cells were heat shocked for 45 seconds at 45°C and returned to ice for a further 2 minutes. 250 µl of prewarmed S.O.C. medium was added and the tube incubated for 1 hour in a shaking incubator at 37°C. 150 µl of the cells were plated out on LB plates with ampicillin together with appropriate control plates. Plates were incubated overnight at 37°C. Controls included a ligation mix with the cut vector and cells without ligation mix.

The following PCR mastermix was made up:

1:20 dNTPs 25mM each final conc, 1:10 10x buffer, 1:40 $MgCl_2$ solution, 1:200 BIOTaq polymerase, and 1:200 T7 and T3 primers (100 µM stock) .

The 31 colonies resulting from the 2:1 ratio ligation were picked up with a pipette tip, and each tip was dipped into an aliquot of PCR mix and kept. The PCR was set up on an Eppendorf Mastercycler as follows:

5 min 95° C

Followed by 25 cycles of:

15 sec 95° C

15 sec 52° C

1.5 min 72° C

Followed by:

10 min 72° C

The pipette tips that had been dipped into those colonies found to contain the insert were subsequently dipped into 5 ml ampicillin treated LB broth and treated as above to isolate the cDNA.

2.2.4.4. Production of riboprobe

A reaction mixture containing the following was prepared on ice:

9 µl DEPC H_2O

4 µl 5x polymerase buffer

2 µl DTT

2 µl DIG labelling mix

1 µl linearised DNA

1 µl RNase inhibitor

1 µl Polymerases (T3, T7 or Sp6)

The mixture was spun briefly on a microfuge and incubated at 37°C for 1 hour to overnight.

To precipitate the probe, 130 µl of DEPC H_2O, 50 µl 10M ammonium acetate, and 400 µl 100% EtOH was added and the mixture placed at -20°C overnight. The mixture was then spun for 30 minutes, washed with 70% EtOH for 10 minutes and resuspended in 20 µl DEPC H_2O. 1 µl was used to run an RNA gel (see 2.2.2.2). 20 µl formamide was added to the probe together with 1 µl RNase inhibitor and the probe was stored at -20°C until used. DIG-labelled probes were used for whole mount ISH and section ISH usually by diluting 1 µl of probe in 150 µl of hybridization buffer (approx. 1 µg/ml). Probes were tested for specificity of binding to mRNA either by comparing hybridization of sense and Antisense probes or by reproduction of wild type expression pattern reported elsewhere.

2.2.5 Whole mount *in situ* hybridisation

Mouse embryos for whole mount ISH (E11-E12) were harvested and fixed overnight in 4% PFA in PBT. They were subsequently washed 3 x 15 minutes in PBT and dehydrated through a series of methanols: 20 minutes each in 25%, 50%, and 75% v/v methanol in PBT and 2 x 20 minutes in 100% methanol. Embryos could be stored at -20°C for several weeks in 100% methanol at this point.

To begin the procedure embryos were rehydrated through methanols and washed twice for 10 minutes in PBT. The embryos were then permeabilised in proteinase K in PBT at room temperature. Strength and length of treatment depended on embryos and probes, and required optimisation. Approximate concentrations and times are shown below:

10 μg/ml for 15 minutes for E12.5 embryos
10 μg/ml for 8 minutes for E11.5 embryos

The reaction was stopped by incubating embryos with 2 mg/ml of freshly made glycine/PBT for 10 minutes. Embryos were then washed 2 x 5 minutes in PBT. The embryos were subsequently post-fixed in 4% PFA and 0.2% glutaraldehyde (0.2% of a 25% glutaraldehyde solution) in PBT for 20 minutes and washed 2 x 10 minutes PBT. Embryos were bleached in 6% H_2O_2 in PBT for 1 hour, then washed again 2 x 10 minutes in PBT. The embryos were then placed in 1 ml hybridisation mix without probe and transferred to 2 ml microfuge tubes. The hybridization mix was replaced with another 1 ml of hybridisation mix and the embryos were incubated (pre-hybridised) overnight in a 70°C waterbath.

The following day, embryos were transferred to prewarmed fresh hybridisation mix containing probe at chosen dilution (~1 μg/ml), and incubated at 70°C overnight.

The hybridisation mix was removed and saved for re-use, and embryos were washed 2 x 30 minutes in Solution 1 at 70°C. The embryos were then washed 2 x 30 minutes in Solution 2 at 65°C.

After washing 3 x 5 minutes in TBST at room temperature, embryos were pre-blocked with 20% sheep serum (heat inactivated at 70°C) in TBST for 1 hr at room temperature or 2-3 hr at 4°C. Embryos were then incubated with a 1:1000 dilution of anti-DIG antibody in above block at 4°C overnight.

The following day, the antibody was recovered for reuse and the embryos washed with TBST at 40 minute intervals as many times as possible at room temperature (at least 5), then overnight at 4°C

Embryos were then washed 3 x 10 minutes in NTMT, after which NBT/BCIP in NTMT (18 µl/ml) was added. Vials containing embryos were wrapped in foil and developed by rocking in a light tight box. Embryos were examined every 10-20 minutes until staining was complete. Embryos were then washed 2 x 10 minutes in PBT and stored in the dark with 0.018% thimerosol in PBT. Embryos were examined on a Leica MZFLIII dissecting microscope and digital images were captured using a Jenoptik ProgRes C14 camera and Improvision Openlab software.

2.2.6. Embedding and vibratome sectioning of whole mount *in situ* hybridized embryos

Embryos were washed in PBS and transferred to 2-5 ml gelatin/albumin embedding mixture and incubated 30 minutes to overnight. Each embryo was coated in embedding mix and placed on the side of an embedding mould. With instruments and microscope readied, 0.1 volume of 25% glutaraldehyde was added to 1 volume of embedding mixture and mixed thoroughly and swiftly by pipetting. Embryo was immediately placed in mixture and orientated under microscope (setting occurred within 2 minutes). Blocks were placed at 4°C for 1 hour to overnight to set. Blocks could be kept wrapped in cling film or in PBS for several weeks at 4°C.

For vibratome sectioning, blocks were trimmed and superglued to vibratome mount. Blocks were cut in a bath of DEPC PBS and 30-50µm sections were cut and placed on TESPA coated slides. Slides were mounted with 50% glycerol in PBT and stored in a flat slide holder at 4°C. Slides were examined on a Zeiss Axioplan 2 using DIC

and digital images were captured using a Leica DC500 camera and Adobe Photoshop software.

2.2.7. *In situ* hybridisation for cryostat sections

Slides with cryosectioned tissue were removed from −80°C and laid out for 15 minutes at room temperature to thaw. Preparation of cryo-sectioned retina is described in 2.2.8. RNA probes to be hybridised were diluted to an appropriate concentration (~1 ng/µl), usually around 1 part in 100 (this is best determined empirically), in cryostat section hybridisation buffer, allowing 75-100 µl for each slide. Probe mixes were incubated at 70°C for 5 minutes to denature the RNA. 75-100 µl mix was then added to each of the thawed out slides. Probe mix was evenly spread across the slides with no bubbles over the sections. 20 x 40 mm coverslips were washed in 100% ethanol, dried, and carefully placed on the slides so as to cover the sections entirely. Slides were placed on a slide moat (Grant Instruments Ltd., Shepreth, UK) heated to 65°C and humidified with DEPC-treated distilled water and left overnight.

Slides were removed from the slide moat, placed in coplin jars (maximum 5 slides per coplin jar) and immersed in preheated Washing Solution within a glass trough in a 65°C water bath for 1 hour. Slides were then carefully transferred into new coplin jars containing preheated Washing Solution. Any coverslips that had not fallen off the slides were gently nudged off using a 200 µl pipette tip. After 30 minutes, the Washing Solution was replaced (in a fume hood) and slides were washed a further 30 minutes at 65°C. The slides were transferred in a fume hood to fresh coplin jars containing MABT and washed 2 x 30 minutes at room temperature. Slides were then removed one by one from the coplins, their edges dried with a tissue and the sections encircled using a grease pen, and placed in a humidified incubation chamber. 200-300 µl M-block was immediately applied to each slide. The slides were incubated for a minimum of 1 hour at room temperature. Anti-digoxygenin antibody tagged with alkaline phosphatase was diluted 1:1000 in M-block and applied to the slides. The slides were then incubated overnight at 4°C.

The slides were removed from 4°C and transferred back into coplin jars to be washed 4 x 5 minutes in MABT. The slides were placed in fresh coplins to be washed 2 x 10 minutes in Staining Buffer. They were then returned to the incubation chamber. 200-300 µl of Staining Buffer with 18 µl/ml NBT/BCIP stock solution were applied to each slide and incubated at room temperature protected from light for 1-24 hours until satisfactorily developed. The length of time necessary for development is related to the strength of the probe during hybridisation. The reaction can be slowed by placing at 4°C. Labelling was checked under a dissecting microscope and slides were washed in distilled water. Slides were dehydrated in 100% butanol for 5 minutes and washed 2 x 5 minutes in Histoclear. Slides were immediately mounted with Vectamount™ and left to dry at room temperature. Slides were examined on a Zeiss Axioplan 2 using DIC and digital images were captured using a Leica DC500 camera and Adobe Photoshop software.

2.2.8. Preparation of frozen and paraffin-embedded retinal sections

2.2.8.1. Frozen sections

Cryo-sections were used fore a variety of experiments, for *in situ*, immunostaining, and DAPI staining. Sections were prepared of mouse embryos and adult eyes. Tissue required for sectioning was fixed in 4% paraformaldehyde overnight. After a brief wash in PBS, the tissue was placed in 20% sucrose solution and again left overnight. After another brief wash in PBS, the tissue was placed in a polystyrene or foil mould containing O.C.T. compound. The mould was placed in a container of isopentane, which in turn was placed in liquid nitrogen. The O.C.T. compound was allowed to freeze completely and either sectioned straight away or placed in a -80° C freezer until sectioned. The block was sectioned using a Bright cryostat (model OTF with a 5040 microtome) and Bright solid microtome knife (B1009DR) in 7 µm thick sections. The sections were collected onto slides which were coated with 2% TESPA. The slides were kept at room temperature overnight to allow them to dry, and stored at -80° C until used.

2.2.8.2. Paraffin-embedded sections

Tissue required for sectioning was fixed in 4% paraformaldehyde overnight. The tissue was partially dehydrated through a succession of ethanol (EtOH)/PBS solutions from 30% to 50% to 70% to 90% to 100% EtOH for 5-30 minutes depending on size of tissue. If not fully processed immediately, the process was stopped at the 70% EtOH/PBS stage and the tissue kept in 70% EtOH/PBS at room temperature until required for embedding. The tissue was then cleared in a 1:1 solution of ethanol and Histoclear, and subsequently placed in a 60°C oven in 100% Histoclear. The tissue was then transferred successively to a wash of 1:1 Histoclear:paraffin wax, and two washes of paraffin wax. The tissue was taken out of the oven and positioned and the wax allowed to cool and harden overnight. The wax blocks were sectioned on a Microm microtome (HM325) at 7μm, and the sections collected onto a film of dH_2O on TESPA-coated slides. Slides were placed on a heated surface where sections were allowed to flatten over the warmed water's surface. The water was pipetted off and the slides were allowed to dry in a 37°C incubator overnight and stored at room temperature until use.

2.2.9. Staining with Eosin and Haematoxylin

2.2.9.1. Frozen sections

Slides were removed from -80°C and allowed to thaw for about 10 minutes at room temperature. The sections were incubated in distilled water to remove O.C.T. compound, then placed in Ehrlich's haematoxylin solution for 5 minutes. They were then washed in distilled water for 1 minute and placed in a trough to be washed for 5 minutes under running tap water. Slides were then immersed in 10% hydrochloric acid, 70% ethanol in distilled water for 10 seconds only and returned to the trough and the running tap water for a further 5 minutes. This was followed by immersion in 1% eosin solution for 5 minutes and a further five minutes in the trough with running tap water. Slides were then dehydrated through a series of alcohol solutions: 2 minutes in 70% ethanol (in distilled water), 2 minutes in 95% ethanol, and 2 x 5 minutes in 100% ethanol. After 2 x 5 minute washes in Histoclear, slides were immediately mounted with coverslips using Vecta-Mount mounting medium and

allowed to dry at room temperature. Slides were examined on a Zeiss Axioplan 2 Imaging microscope and digital pictures were captured using a Jenoptik ProgRes C14 camera and Improvision Openlab software.

2.2.9.2. Paraffin-embedded sections

Sections were deparaffinized in Histoclear for ten minutes and rehydrated through graded concentrations of EtOH as follows:

100% EtOH – 3 minutes
90%, 70%, 50%, 25% EtOH – 1 minute each
Distilled H_2O – 5 minutes

They were then placed in Ehrlich's haematoxylin for 5 minutes and the protocol was followed as described above for frozen sections.

2.2.10. Immunohistochemistry on frozen and paraffin-embedded sections

2.2.10.1. Anti-phosphohistone H3 on frozen sections

Slides of retinal sections were taken from the –80°C freezer and laid out to thaw for 15 minutes. After three washes with PBS, a grease pen was used to draw around the sections. The sections were then treated with blocking solution (10% foetal calf serum (FCS), 1% bovine serum albumin (BSA), and 0.1% Tween-20 in PBS) for 1 hour. Anti-phosphohistone 3 antibody (1:100) was made up in blocking solution and the sections were incubated with the primary antibody overnight at 4°C. After three washes with PBS, the sections were incubated with FITC-conjugated anti-rabbit secondary antibody (1:100) and Hoechst nuclear dye (1:1000), made up in blocking solution, for 1 hour. The sections were then washed three times in PBS and mounted with Citifluor. Slides were examined on a Zeiss Axiophot and digital images were captured using a Hamamatsu Orca camera and Improvision Openlab software. Alternatively, slides were examined using a Zeiss Axioplan 2 Imaging microscope

and digital images were captured using a Jenoptik ProgRes C14 camera and Improvision Openlab software.

Statistical analysis: The total number of retinal cells (Hoechst-stained) and the number of mitotic cells (H3-labelled) were counted on nine midline retinal sections from three eyes from mutant and wild type animals at all time points (E11.5, E13.5, E15.5 and E18.5). An H3 labelling index was obtained by dividing the number of H3-labelled cells by the total number of cells in each section. Two-way analysis of variance was performed using SPSS 11 to check for an interaction between mutant and wild type mice and the various time points. After an interaction was found, the significant simple main effects were further analysed by pairwise comparisons using the Sidak adjustment for multiple comparisons ($p<0.05$ was considered significant). Refs: http://web.uccs.edu/lbecker/SPSS/glm_sme.htm; (Becker and Coolidge, 1991; Rosnow and Rosenthal, 1989).

2.2.10.2. Anti-proliferating cell nuclear antigen (PCNA) on paraffin-embedded sections

Sections from embryonic eyes were deparaffinized in Histoclear for ten minutes and rehydrated through graded concentrations of EtOH as follows:

100% EtOH – 3 minutes
90%, 70%, 50%, 25% EtOH – 1 minute each
Distilled H_2O – 5 minutes

The slides were heated in a microwave at 540W in 0.01 M citric acid buffer (pH 6.0) for 10 minutes and cooled 10 minutes under running tap water before being rinsed two times in PBS. Sections were incubated with blocking solution (10% FCS, 1% BSA and 0.1%Tween-20 in PBS) for 30 minutes. Slides were subsequently incubated with mouse anti PCNA primary antibody (diluted 1:100 in blocking solution) at 4°C overnight. After 3 x 5 minute washes with PBS, slides were incubated with Cy3-conjugated anti mouse secondary antibody (diluted 1:100 in blocking solution) for 40 minutes, together with 1:1000 Hoechst nuclear dye. Slides were then washed again 2 x 5 minutes in PBS and mounted with Citifluor. Slides were examined on a Zeiss

Axiophot and digital images were captured using a Hamamatsu Orca camera and Improvision Openlab software.

2.2.10.3. Immunohistochemistry using retinal cell markers on frozen sections

Sections were thawed for 15 minutes, rinsed in PBS for a further 15 minutes and then blocked with 10% fetal calf serum,1% BSA and 0.1% Tween-20 in PBS for 30 minutes, 10% normal goat serum and 0.2% Triton X-100 in PBS for two hours (for PNA), 2% normal donkey serum and 0.1% Tween-20 in PBS for 30 minutes (for anti-brn3b), 10% normal goat serum, 3% BSA and 0.1% Tween-20 in PBS for 30 minutes (for anti-blue cone opsin), or 4% normal donkey serum and 1% Triton X-100 in PBS for two hours (for anti-rhodopsin). The sections were incubated with mouse anti-β3 tubulin (1:100), mouse anti-syntaxin (1:100), mouse anti-vc1.1, (1:100), rabbit anti-recoverin (1:100), goat anti-brn3b (1:100), rhodamine-conjugated PNA (1:10), chicken anti-blue cone opsin antibody (1:5000), or goat anti-rhodopsin antibody (1:50) at 4°C overnight. PNA treated sections were then incubated with Hoechst nuclear dye (1:1000) for 40 minutes and mounted with Citifluor. Anti-β3 tubulin, anti-syntaxin, and anti-vc1.1 treated sections were incubated with Cy3-conjugated anti-mouse antibody (1:100). Anti-recoverin, anti-brn3b, anti-blue cone opsin and anti-rhodopsin treated sections were incubated with rhodamine Red-X-conjugated anti-rabbit (1:100), Cy3-conjugated anti-goat (1:100), Alexa594-conjugated goat anti-chicken (1:100) and FITC-conjugated donkey anti-goat (1:100) antibodies respectively for two hours. The sections were then treated with Hoechst nuclear dye for 40 minutes and mounted with Citifluor. Slides were viewed using a Zeiss Axiophot and digital images were captured using a Hamamatsu Orca camera and Improvision Openlab software. Alternatively, slides were viewed using a Zeiss Axioplan 2 Imaging microscope and digital images were captured using a Jenoptik ProgRes C14 camera and Improvision Openlab software.

2.2.11. Fluorescence activated cell sorting (FACS) analysis of cell cycle

Retinal dissection from E11.5 embryos occurred as described in 2.2.2.1 but in Leibovitz's L15 medium. In addition, retinae were dissected in a similar manner

from E13.5, E15.5, and E18.5 embryos, with a further step in which the lens was separated from the retina, leaving a clean retina. Retinae from littermates were pooled. They were treated with 0.05% trypsin/0.53 mM EDTA for 10 minutes at 37°C, and the reaction was subsequently quenched with a small amount of fetal calf serum. The tissue was triturated gently to form a single cell suspension. The cells were centrifuged for 1 minute at 8000 rpm (approx. 6,000x g) and washed with PBS and counted on a haemocytometer. The cells were then briefly centrifuged and resuspended in 70% ethanol and kept at 4°C until used for analysis (1-14 days). Cells were briefly centrifuged and resuspended in 300 µl hypotonic buffer containing propidium iodide (50 µg/ml propidium iodide (Sigma) in 0.1% sodium citrate and 0.1% Triton X-100). The samples, containing $5x10^5$ to $1x10^6$ cells, were immediately run on a Beckman Coulter Epics XL flow cytometer. 30,000 events were collected and, with Expo 32 software (Beckman Coulter), gated using doublet discrimination. In this way, only single cells in the cell cycle were selected for analysis. The data were subsequently modelled using Multicycle software (Phoenix Flow Systems), using an appropriate modelling system.

Statisical analysis: 3 pools of wild type and 3 pools of *Chx10*$^{-/-}$ retinae were collected at E11.5 and run on the flow cytometer. The data were averaged and means and standard deviations calculated, after which student t-tests were performed.

2.2.12. Analysis of mitotic spindle orientation during cell division

Frozen sections of embryonic mouse retinae were laid out to thaw at room temperature for 15 minutes. They were then washed twice in PBS and mounted with Vectashield mounting medium containing DAPI. Slides were viewed using a Zeiss Axioplan 2 Imaging microscope and digital images were captured using a Jenoptik ProgRes C14 camera and Improvision Openlab software. The angle between a line running through the mitotic spindle of the dividing cell and a tangent to the closest part of the ventricular surface was measured. Vertical mitotic spindles (line through spindle 90^0 +/- 45^0 to ventricular surface) were classified as asymmetric cell divisions and horizontal spindles (line through spindle 0^0 +/- 45^0 to the ventricular surface) as symmetric.

Statistical analysis: *Chx10$^{-/-}$, Chx10$^{-/-}$/ p27$^{Kip1+/-}$ and Chx10$^{-/-}$/ p27$^{Kip1-/-}$* and wild type 129/Sv mice were analysed blind. The percentage of vertical divisions was determined per eye (at least 4 eyes were analysed per genotype) and the mean and standard error was calculated for each genotype. Genotypes were analysed for significant differences using pairwise 2-tailed Mann Whitney U tests.

2.2.13 Dissociation and Numb-labelling of retinal cells

Retinae were dissected as described in 2.2.2.1 but in DMEM/F-12 medium, then washed with Hanks balanced salt solution (HBSS). The tissue was centrifuged for 5 minutes at 900 rpm (approx. 80x g) and the supernatant replaced with 0.5 ml of 1 mM EDTA in HBSS. The cells were subsequently placed in culture incubator for 20-30 minutes, at 37°C with 5% CO_2. The tissue was then mechanically dissociated by trituration and washed with HBSS by centrifuging the cells for 5 minutes at 900 rpm for three minutes and replacing the supernatant. This was repeated in order to resuspend cells in DMEM/F-12. After cell counting using a haemocytometer, cells were plated on poly-l-lysine and laminin coated coverslips at 6-12 x 10^4 cells/ml. The cells were placed in a cell culture incubator at 37°C with 5% CO_2 and left overnight. The cells were subsequently fixed for 10 minutes in 4% PFA. The coverslips were then washed three times in Leibovitz's L15 medium. Cells were treated with blocking solution (10% NGS and 0.1% Triton X-100 in PBS) for 20 minutes. Anti-Numb antibody was diluted 1:500 in 5% NGS and 0.1% Triton X-100 and applied to the cells for 1 hour. The coverslips were washed three times in Leibovitz's L15 medium, after which Cy3-conjugated anti-mouse antibody, diluted 1:50 in blocking solution, was applied for 30 minutes. The coverslips were then washed three times in Leibovitz's L15 medium and once in dH_2O. Each coverslip was then mounted onto a glass slide using CITIFLUOR.

2.2.14 Histological examination of semithin retinal sections

For histological examination, retinal tissue was fixed in 3% glutaraldehyde (pH 7.4), 0.1M sodium cacodylate, and 5 mM calcium chloride; rinsed; and transferred to 1% osmium tetroxide for 2 hours before being processed and embedded in resin

(Agar100, DDSA, MNA, DMP30) using standard procedures. Semithin sections were cut on a microtome (Ultracut E; Leica, Cambridge, UK) with glass knives and stained with 1% toluidine blue in 1% borax. Observations were made in four P12 $Chx10^{-/-}$ and four 129/Sv mice. For each retina, replicate counts of the number of cells in the inner and outer nuclear layers were made from 1-μm semithin sections. For each retina, sections were prepared at 20-μm intervals at four positions across the central retina. Observations were restricted to the central retinal zone, avoiding the peripheral region where the cell layers are thinner. For the mutant, the analysis was performed on the thickest region of central retina in each section.

2.2.15 Immunohistochemistry on sections of BrdU injected mice

2.2.15.1. Preparation of BrdU injected mouse eyes

Animals were given an intraperitoneal injection with 100μg/g of body weight of BrdU diluted at 10 mg/ml in 0.1M Tris pH7. Tissue was prepared either the following day or 1 day to 3 weeks after the last injection when injecting every other day over a period of time (See injection schedules Chapter 6). Animals were given a terminal anaesthetic and perfused with saline to remove blood. The eyes were removed and fixed in Carnoy's fixative: 60% EtOH, 30% chloroform, 10% acetic acid for no longer than 15 minutes. The eyes were embedded in wax as described in section 2.2.8.2, going from Carnoy's fixative straight to 90% EtOH. The wax blocks were sectioned and treated as described in section 2.2.8B. Alternatively, animals were perfused with 4% paraformaldehyde rather than saline, and required no further fixing.

2.2.15.2. Anti-BrdU immunolabelling on paraffin-embedded sections

Sections were deparaffinized in Histoclear for ten minutes and rehydrated through graded concentrations of EtOH as follows:

100% EtOH – 3 minutes
90%, 70%, 50%, 25% EtOH – 1 minute each
Distilled H_2O – 5 minutes

The slides were heated in a microwave at 540W in 0.01 M citric acid buffer (pH 6.0) for 6 minutes and cooled 10 minutes under running tap water before being rinsed two times in PBS. Alternatively, sections were treated with Declere (1:20 Declere:dH_2O) for 4 minutes at full power and 15 minutes at 540W in the microwave and rinsed with PBS, replacing the deparaffinising, rehydrating and citric acid buffer steps. The sections were then incubated in 0.1M HCl for 30 minutes at room temperature. They were subsequently incubated in 2M HCl for 30 minutes at 37° C, followed by a 10 minute incubation in 0.1M sodium borate (pH 8.5) at room temperature. After three washes in PBS, non-specific binding sites were blocked with 10% FCS and 1%BSA in PBS for 1 hour at room temperature. This was followed by incubation with rat anti-BrdU antibody (1:100 in blocking solution) at 4°C overnight in a humid chamber. After three washes in PBS, the slides were incubated with the FITC-labelled anti-rat secondary antibody (1:100 in blocking solution) for 40 minutes. After three washes with PBS, the slides were mounted with Citifluor. Slides were viewed using a Zeiss Axiophot and digital images were captured using a Hamamatsu Orca camera and Improvision Openlab software. Alternatively, slides were viewed using a Zeiss Axioplan 2 Imaging microscope and digital images were captured using a Jenoptik ProgRes C14 camera and Improvision Openlab software.

Statistical analysis: BrdU labelled cells were counted on midline retinal sections from 3-7 eyes from treated mutant and wild type animals at 4 weeks and 8 weeks of age. Student t-tests were performed between mutant and wild type counts at the two time points to determine significance ($p<0.05$).

2.2.15.3. Retinal cell markers on BrdU injected paraffin-embedded sections

For double labelling of BrdU and nestin, β3 tubulin, β1-integrin, NeuN, Brn3b (Pou4f2), rhodopsin, blue cone opsin, recoverin, CRALBP (cellular retinaldehyde-binding protein), GFAP, protein kinase C (PKC), syntaxin, or VC1.1, sections were treated as above, but after the blocking step, sections were incubated with either mouse anti-nestin antibody (1:10), anti-β3 tubulin (1:1000), anti-β1-integrin (1:100), anti-NeuN (1:50), anti-PKC (1:100), anti-syntaxin (1:100), or anti-VC1.1 (HNK-1) antibody (1:100), goat anti-Brn3b (1:100) or anti-rhodopsin antibody (1:50), chicken anti-blue cone opsin antibody (1:5000), and rabbit anti-calbindin (1:50) antibody, anti-recoverin antibody (1:100), anti-CRALBP antibody (1:1000) or anti-GFAP antibody (1:100) at 4°C overnight. Incubation with primary antibody was followed by a 1 hour incubation with the appropriate species-specific secondary antibody: Cy3-conjugated anti-mouse antibody (1:100), Cy3-conjugated anti-goat antibody (1:100), Alexa-594-conjugated anti-chicken antibody (1:100), or rhodamine (TRITC)-conjugated anti-rabbit antibody (1:100, GFAP) or rhodamine Red-X-conjugated anti rabbit antibody (1:100, calbindin, recoverin and CRALBP). After washing in PBS, the slides were then incubated with anti-BrdU antibody (1:100) for two hours, followed by 3 x 5 minute washes in PBS and incubation in FITC-conjugated anti-rat secondary antibody for 40 minutes. After three washes with PBS, the slides were mounted with Citifluor. Slides were viewed using a Zeiss Axiophot and digital images were captured using a Hamamatsu Orca camera and Improvision Openlab software. Alternatively, slides were viewed using a Zeiss Axioplan 2 Imaging microscope and digital images were captured using a Jenoptik ProgRes C14 camera and Improvision Openlab software.

2.2.16. Dissociation and immunohistochemistry of retinal cells

To immuno-label neuronal sub-types of dissociated retinal cells, wild type (n=5) and *Chx10* $^{-/-}$ mutant mice (n=12) were injected with BrdU at P25, P27, and P29 and tissue was prepared 3 weeks after the first injection. Retinae were dissected as described in 2.2.2.1 but in DMEM/F-12 medium, then treated with 2 units/ml dispase for 10-20 minutes and triturated to dissociate cells. Cells were spun onto slides using a Shandon cytospin (500 rpm for 5 mins), air dried for 10 minutes and fixed for 10

minutes with 4% paraformaldehyde. Slides were treated with 2M HCl for 10 minutes, sodium borate for 10 minutes and incubated with 10% FCS and 1% BSA in PBS blocking solution for 20 minutes. Immunohistochemistry was performed as described above for double labelling studies, with the following alterations: primary antibody incubations and anti-BrdU antibody incubations were performed for one hour, secondary antibody incubations were performed for 30 minutes. Slides were viewed using a Zeiss Axioplan 2 Imaging microscope and digital images were captured using a Jenoptik ProgRes C14 camera and Improvision Openlab software.

2.2.17. TUNEL labelling

The terminal deoxynucleotidyl transferase (TdT) -mediated deoxyuridine triphosphate (dUTP) nick end labeling (TUNEL) assay was performed using the *In situ* Cell death Detection kit. This procedure was performed on both frozen and paraffin-embedded sections. Frozen sections were laid out to thaw for 10-15 minutes and washed in dH_2O for five minutes. Paraffin-embedded sections were deparaffinized in Histoclear for ten minutes and rehydrated through graded concentrations of EtOH as follows:

100% EtOH – 3 minutes
90%, 70%, 50%, 25% EtOH – 1 minute each
Distilled H_2O – 5 minutes

Alternatively, sections were treated with Declere (1:20 Declere:dH_2O) for 4 minutes at full power and 15 minutes at 540W in the microwave and rinsed with PBS, replacing the deparaffinising and rehydrating step.

All sections were then permeabilised by incubating with Proteinase K solution (100 µl/section) for 15 minutes at room temperature. After washing 2 x 5 minutes in PBS, sections were incubated with the TUNEL reaction mixture (5 µl enzyme solution and 45 µl labelling solution per section) for 1 hour at 37°C. Sections were rinsed and washed 3 x 5 minutes in PBS and mounted with Citifluor. Slides were viewed using a Zeiss Axiophot and digital images were captured using a Hamamatsu Orca camera

and Improvision Openlab software. Alternatively, slides were viewed using a Zeiss Axioplan 2 Imaging microscope and digital images were captured using a Jenoptik ProgRes C14 camera and Improvision Openlab software.

2.2.18. Cell Culture from adult retina

Retinae were dissected from adult wild type 129/Sv and *Chx10*$^{-/-}$ mutant eyes in Leibovitz's L15 medium. The retinal tissue was placed in a small amount of dispase (2.5 U/ml) at 37°C for ten minutes, and subsequently broken up mechanically. The tissue was then placed in small amount of trypsin/EDTA for 10 minutes at 37°C. 10% FCS in medium was added to neutralise the trypsin, and the samples were centrifuged at 1000 rpm (approx. 200x g) for 5 minutes. The supernatant was removed and replaced with NSA (used initially but then replaced by DMEM/F-12) or DMEM/F-12 medium containing 10 µl/ml N2 supplement, 10 ng/ml FGF-2, 20 ng/ml EGF, and a penicillin/streptomycin solution (50 U/ml penicillin, 50 µg/ml streptomycin). The tissue was triturated to fully dissociate the cells and the cells were examined on a haemocytometer to assess their numbers. Cells were plated at roughly 100,000 cells per well in a 24-well plate. Medium (half the amount of medium already present in the well) was added to the wells every five to seven days and cells and medium transferred to larger wells as necessary. Cells were incubated at 37°C with 5% CO_2.

After 28 days, cultures which had formed neurospheres were passaged. Neurospheres were spun down in a microfuge and fresh medium was added. The cells were then mechanically dissociated by triturating. Cells were subsequently replated in 24-well plates in the medium described above. This procedure was repeated on day 56, in one case on day 86. Cells generally did not survive a second passage, and in one case a third passage.

On some occasions, at the same time as passaging, some of the passaged cells were plated with differentiating medium, DMEM/F-12 medium containing 10 µl/ml N2 supplement, 10% FCS and penicillin/streptomycin solution, but without the growth factors. Cells were plated onto poly-L-lysine and laminin coated cover slips in 24 well plates. Medium was replaced with fresh medium every other day.

Images of cells were captured using a Zeiss inverted stereo microscope, with a Yashica 108 Multiprogram camera and Kodak Ektachrome 160T film. Film was then processed and scanned into digital images using an Epson FilmScan 200 and Adobe Photoshop.

CHAPTER 3

Identifying Genes Downstream of Chx10

3.1 Introduction

From the time it was first characterised in some detail (Liu et al., 1994b), Chx10 has been regarded as a putative transcription factor, due to the presence of a homeodomain sequence. More specifically, it is thought to belong to the paired class of homeodomain transcription factors, as it is 58%-65% identical to a series of paired-like homeodomains and like several other putative transcription factors with prd-like homeodomains, contains an HSIDGILG octapeptide in addition to its homeodomain (Liu et al., 1994b). However, little is known about the genes it may regulate. It has been shown that Chx10 acts as both a transcriptional activator and repressor (Dorval et al., 2005; Ferda et al., 2000), but thus far, although its DNA binding site has been determined (Ferda et al., 2000), no direct targets have been identified. Identifying Chx10 target genes and elucidating the genetic pathway in which Chx10 is involved may lead to the identification of other genes involved in microphthalmia. Characterisation of genes that control retinal proliferation and differentiation will provide increased understanding of the underlying molecular mechanisms and in the longer term may lead to the development of novel therapeutic strategies.

In order to identify possible downstream targets of the Chx10 transcription factor, the Affymetrix GeneChip Expression Probe Array system was used to examine differential gene expression between *Chx10*$^{-/-}$ and wild type retinal tissue. Microarray studies have become a widely used tool for examining gene expression in recent years. Before their introduction, existing expression monitoring technologies included differential colony (plaque) hybridisation of cDNA clones (Yamamoto et al., 1983), the use of subtractive hybridisation (Hubank and Schatz, 1994; Kavathas et al., 1984), and a more recent differential display method (Liang and Pardee, 1992); (Paraoanu et al., 2005; Welsh et al., 1992). In addition, sequencing of cDNA libraries by EST was used to identify unknown genes expressed in given cells or tissues (Adams et al., 1991). However, using hybridisation gels is cumbersome and insensitive and whilst the sequencing of cDNA libraries is more direct, it is not designed to quantify expressed genes, requires some effort and is not sensitive in the presence of less abundant messages (Constantine and Harrinton, 2001; Yamamoto et al., 2001).

Serial analysis of gene expression (SAGE) is an efficient variation of cDNA sequencing, which allows for quantitative and simultaneous analysis of a large number of transcripts in any particular cell or tissue (Velculescu et al., 1995; Yamamoto et al., 2001), but requires relatively complicated procedures for sample preparation, requires large amounts of sequencing and is not very sensitive (Constantine and Harrinton, 2001). So more recently, array based methods involving spotting or printing clones or cDNAs onto various surfaces have been developed. The advantage of this is that it is parallel, but to monitor many genes, large numbers of cDNAs or PCR products must be prepared, purified, quantitated, catalogued and spotted onto a support. If derived from a cDNA library, low abundance cDNAs are unlikely to be spotted and the library must be normalised to reduce redundant spotting of genes from highly expressed genes (Constantine and Harrinton, 2001). Once prepared, the arrays can be used for comparative hybridisations using cDNA prepared from different sources.

A further refinement has been the development of GeneChip Expression Probe Arrays, which are synthesised *in situ* on a glass support using light-directed, solid-phase combinatorial chemistry. Labelled cRNA targets derived from the mRNA of an experimental sample are hybridised to DNA oligonucleotide probes attached to the solid support of the chip. By monitoring the amount of label associated with each DNA location, it is possible to infer abundance of each mRNA species represented (www.affymetrix.com, Figure 3.1). The direct, combinatorial synthesis of oligonucleotides based on sequence information offers several advantages: because oligonucleotide probes for each gene or EST are specifically chosen and synthesised in known locations on the arrays, hybridisation patterns and signal intensities can be interpreted in terms of specific gene or EST identity and relative amounts of mRNA without additional sequencing or characterisation (Constantine and Harrinton, 2001; Lockhart et al., 1996; Wodicka et al., 1997). Use of specifically chosen oligonucleotide probes allows for the sensitive, quantitative detection of alternatively spliced mRNAs and the differentiation of closely related members of gene families. This procedure eliminates the necessity of preparing and handling clones, PCR

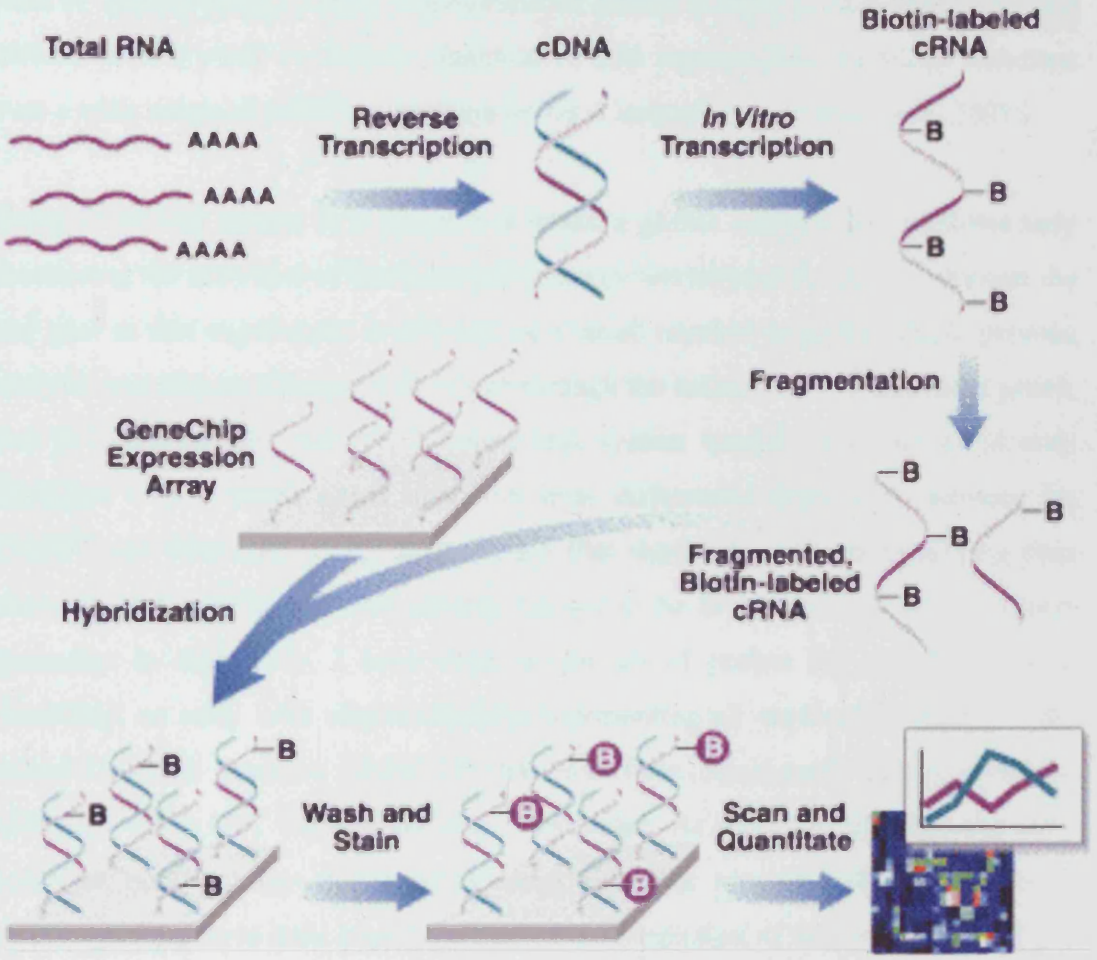

Figure 3.1: Standard eukaryotic gene expression assay. The target, biotin labelled cRNA, is produced from total RNA extracted from the relevant tissue. The target is fragmented and hybridised to the nucleic acid probes attached to the GeneChip expression array. By monitoring the amount of label associated with each DNA location, after washing, staining and scanning, it is possible to infer the abundance of each mRNA species represented. (Adapted from a figure on www.affymetrix.com)

products and cDNAs. In contrast to many of the spotting methods where a single clone is used to analyse each mRNA, GeneChip Arrays use approximately sixteen pairs of specific unique 25mer oligonucleotide probes to analyse each transcript. This method allows users to achieve quantitative and reproducible transcript detection over a wide range of mRNA expression levels (Constantine and Harrinton, 2001).

Using GeneChip arrays, it is possible to make a global analysis by simultaneously monitoring the activities of thousands of genes (www.affymetrix.com). Although the end goal in this experiment is to focus on a small number of genes, whole genome analysis provides an efficient tool to sort through the activities of thousands of genes, and to recognise key players. I hoped this system would allow me to identify candidate Chx10 target genes based on their differential expression between the *Chx10*$^{-/-}$ and wild type retina; an approach that should be more wide-ranging than choosing and examining genes already known to be involved in eye development generally. In this study, I have used as the set of probes the murine U74Av2 GeneChip, an array with oligonucleotides representing all sequences (~6000) in the mouse UniGene database (Build 74) that have been functionally characterised. In addition, ~6000 EST clusters are also represented. At the time, this was the most complete murine array available, as chips with the recently fully characterised murine genome have only been produced after completion of this experiment. A list of forty genes/ESTs showing a significant 1.5-fold difference in expression and eight genes showing a significant at least two-fold difference in expression between the *Chx10*$^{-/-}$ retina and the wild type retina was produced from this study. In addition, thirty genes/ESTs showed a more than 1.5-fold change in expression similar to the two most changed genes. Several of these genes are involved in regulation of transcription, cell fate determination, and/or the cell cycle, offering clues to the molecular pathways in which Chx10 is involved.

3.2 Results

3.2.1 Embryonic day 11.5 was selected as an appropriate time point for GeneChip analysis

cRNA derived from total RNA collected from pools of wild type and *Chx10*$^{-/-}$ E11.5 retinae was used as the target for the GeneChip probes. Chx10 is first expressed in retinal progenitor cells of the presumptive neuroretina at E9.5 in the optic vesicle. However, the invagination of the optic vesicle and formation of the optic cup, including increased initial proliferation of the neuroretina relative to the RPE, occurs normally in the *Chx10*$^{-/-}$ retina, and its appearance at E10.5 is grossly normal (Burmeister et al., 1996), indicating that Chx10 is not essential for this process. Instead it seems most important in proliferation and regulation of retinal progenitor cells later in development.

To explore this idea further, the total number of cells in midline sections from both wild type (n = 9) and *Chx10*$^{-/-}$ (n = 9) eyes at various time points during development were counted to examine the relative change in total cell number between the two. At E10.5, when the optic cup has just been formed and the initial thickening of the presumptive neuroretina is occurring, no significant difference was observed between the number of retinal cells per midline sections counted in the wild type retina and those counted in the *Chx10*$^{-/-}$ retina (2-way ANOVA and post hoc multiple comparisons using the Sidak adjustment, $p < 0.97$, Figure 3.2A). Only a 1.7% reduction in average number of total cells per section was observed. At Ell.5 this reduction increases to 24%, although the difference in cell number is not yet significant ($p < 0.23$, Figure 3.2A). As development progressed, the wild type eye showed a much larger increase in cell number compared to the *Chx10*$^{-/-}$ retina, with the difference between the wild type and *Chx10*$^{-/-}$ becoming larger and showing higher significance than at E11.5 ($p < 0.001$ from 13.5 onwards, asterisks Figure 3.2A). A previous study reported a 30-50% reduction in cell number between the wild type and *Chx10*$^{-/-}$ retina and a reduction in proliferation in the peripheral but not the central retina at E11.5 (Burmeister et al., 1996). On haematoxylin and eosin stained frozen sections of E11.5 retinae, some differences can be observed between the wild type and *Chx10*$^{-/-}$ retina. Although the presumptive neural retina has

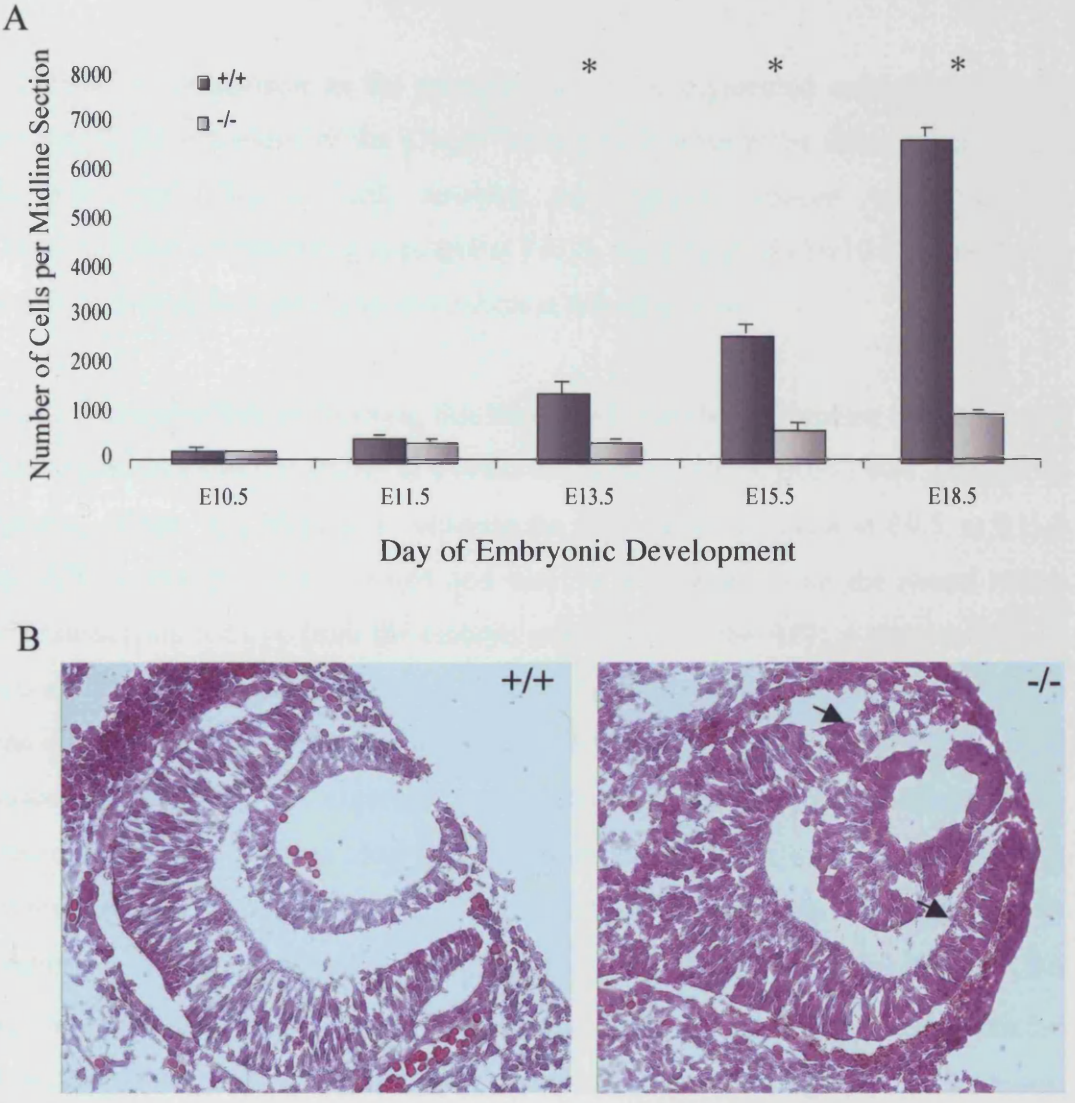

Figure 3.2: Differences between wild type and *Chx10*$^{-/-}$ retinae during development. (*A*) Change in total cell number during development. Difference in the total number of cells between wild type and *Chx10*$^{-/-}$ midline retinal sections at various time points during development. The total number of cells in 9 midline retinal sections from wild type and *Chx10*$^{-/-}$ eyes per time point were counted. At E10.5, no significant difference is observed between wild type and *Chx10*$^{-/-}$ cell counts ($p < 0.97$, 2-way ANOVA and post hoc multiple comparisons using Sidak adjustment). At E11.5, a 24% reduction in total RPC number is observed in the Chx10$^{-/-}$ retina, but this difference is not yet significant ($p < 0.23$). As development progresses, the difference in cell number increases, as the number of cells in the wild type retina increases to a greater extent than the number of cells in the *Chx10*$^{-/-}$ retina, and the difference between the wild type and *Chx10*$^{-/-}$ cell numbers is highly significant (* $p < 0.001$). Error bars = 1 standard deviation, n = nine midline sections taken from three eyes. (*B*) Haematoxylin and eosin stained frozen section of an E11.5 wild type (+/+) retinal section and an E11.5 *Chx10*$^{-/-}$ (-/-) retinal section. The periphery of the *Chx10*$^{-/-}$ retina is thinner than that of the wild type (arrows).

thickened in comparison to the presumptive retinal pigmented epithelium in both genotypes, the periphery of the *Chx10*$^{-/-}$ retina does seem to be thinner than that of the wild type (Figure 3.2B, arrows). As changes between wild type and *Chx10*$^{-/-}$ retinae are becoming apparent at E11.5, the effects of Chx10 absence should be reflected in differential gene expression at this time point.

Another consideration in choosing this time point was the importance of achieving a clean dissection and the ability to extract RNA successfully from small amounts of material. Whilst it is difficult to separate the RPE from the retina at E9.5, at E11.5 the RPE is relatively well formed and easy to tease away from the neural retina. After dissecting the eye from the embryo and removing the RPE, a clean retina and lens are left (Figure 3.3). Even at E11.5, it was technically difficult to remove the lens cleanly from the retina at this stage, and thus the lens was left in place in all dissections. Chx10 is not expressed in the lens, but possible indirect effects on the gene expression in the lens must be kept under consideration when comparing gene expression from the GeneChip data. The initial aim was to collect enough RNA to hybridise to the chips without the need for an amplification step, a total of 5 μg RNA per chip. Pilot experiments showed that roughly 5 μg of total RNA can be extracted from the retinae of about 35-40 E11.5 embryos – thus requiring the need to dissect 210-240 embryos to collect enough RNA for six chips (3 wild type replicates and 3 *Chx10*$^{-/-}$ replicates). Setting up timed matings and dissecting the material is a time-consuming task, and the numbers of embryos required would have increased significantly if an earlier time point was chosen, where the retinae are far smaller.

3.2.2 High quality RNA was extracted and amplified from pools of retinae

An important step in performing GeneChip analysis is acquiring sufficient high quality RNA to convert to cRNA to hybridise to the chips. As discussed above, the initial aim of this study was to extract sufficient RNA from embryonic retinae to avoid the necessity of amplification, a potential source of bias. However, this proved to be technically difficult. In a preliminary experiment, enough dissections were performed to acquire the minimum 5 μg of RNA required per chip as recommended by Affymetrix. However, after cDNA synthesis and *in vitro* transcription, the

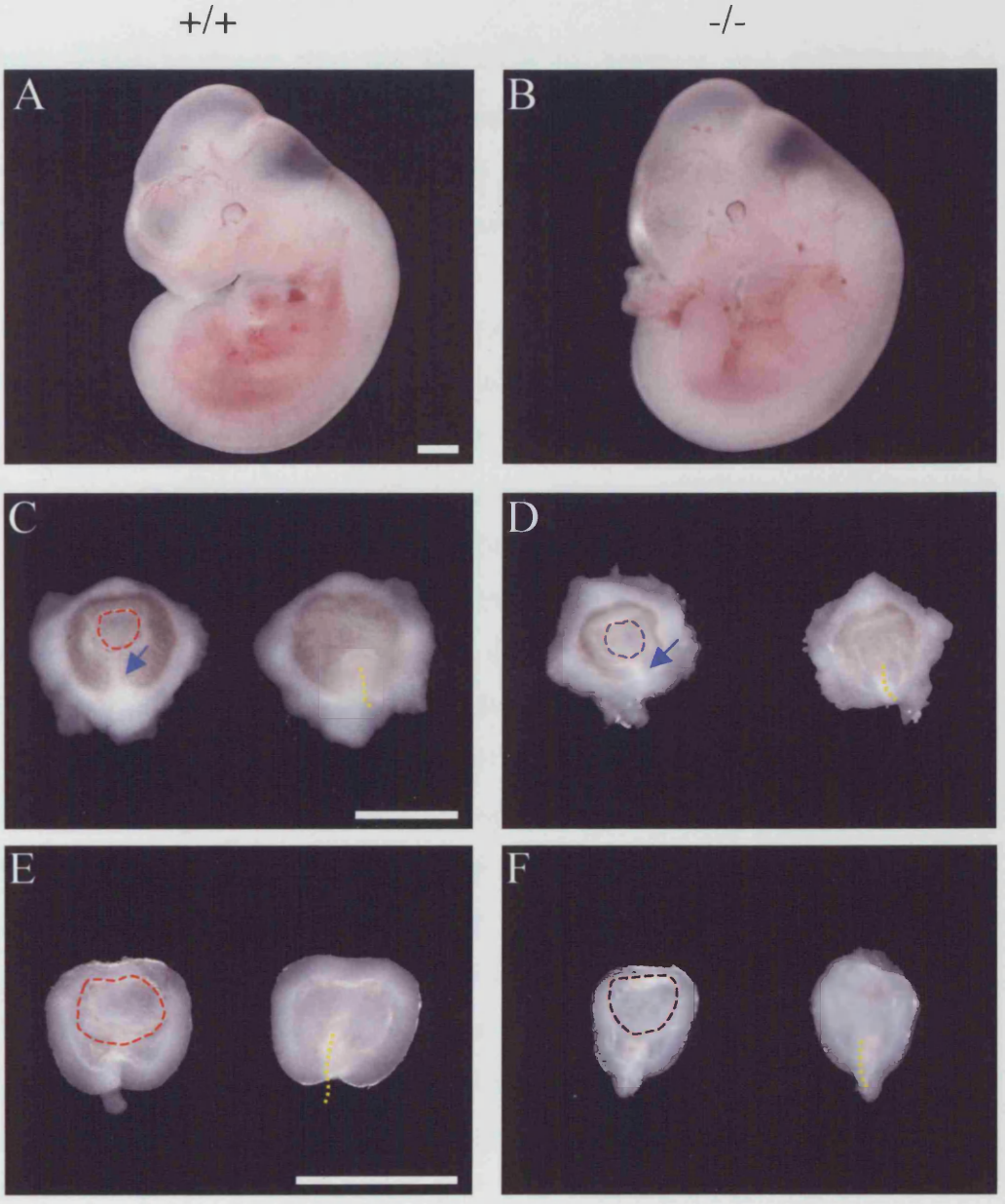

Figure 3.3: Progression of retinal dissection. A and B depict whole wild type *(A)* and *Chx10*$^{-/-}$ *(B)* embryos at E11.5. Eyes were teased away from both the wild type *(C)* and *Chx10*$^{-/-}$ *(D)* embryos, shown in each panel from the front (left) and back (right). The lens is outlined with red dashed lines, the optic fissure indicated by a blue arrow and the optic stalk outlined in dashed yellow lines. The retinal pigmented epithelium is subsequently teased away, leaving a clean wild type *(E)* or *Chx10*$^{-/-}$ *(F)* retina. Again both panels depict views from the front (left) and back (right) of the retina, with the lens outlined in red dashed lines and the optic stalk outlined in yellow dashed lines. Scale bars: 1 mm.

resulting cRNA produced was not sufficient to fragment and hybridise to the GeneChips. It became clear that in this study, 5 μg of RNA per chip would not be sufficient to produce enough material for hybridisation, and that realistically, to perform triplicate hybridisations, the study would require an amplification step.

The Affymetrix standard labelling protocol of a single round of cDNA synthesis and subsequent *in vitro* transcription is effectively already a linear amplification step. Based on a protocol first described by Eberwine and colleagues (Van Gelder et al., 1990), it has been shown to faithfully maintain relative mRNA levels when starting with 1 μg of poly(A)$^+$ or 10 μg of total RNA (Lockhart et al., 1996; Mahadevappa and Warrington, 1999). Aplication of additional rounds of amplification from much smaller amounts of RNA have since been shown to give reproducible results for a single RNA sample (Luo et al., 1999), and to allow detection of differences between samples consistent with those detected without amplification (Wang et al., 2000). A technical note produced by Affymetrix examines the use of an additional round of cDNA synthesis and *in vitro* transcription protocol as a method for amplifying small amounts of starting material. The protocol produces a good cRNA yield from as little as 1 ng of RNA. A comparison of hybridisation to GeneChips indicated the amplified transcripts are a close match to those produced from a single round of cDNA synthesis and IVT, although when amplifying from as little as 1 ng of RNA, some transcripts are lost. Linearity of amplification was tested by spiking samples with predetermined amounts of exogenous poly (A)$^+$ transcripts and was shown to be preserved, when amplifying as little as 100 ng of RNA (GeneChip Eukaryotic Small Sample Target Labelling Technical Note, http://www.malaria.mr4.org/MArray/Affy_small_technote.pdf). The protocol does exhibit a 3' bias compared to the standard protocol however, but it was generally found to produce similar results to the standard protocol when amplifying 10 ng of RNA or more, and thus this protocol was chosen for use in this study (for schematic, see Chapter 2.2.2.4). For each chip, 100-600 ng of RNA was amplified.

High quality RNA was extracted from pools of retinae dissected from embryos that were in the 40-47 somite range (Table 3.1). Collecting tissue from a large number of individuals should reduce the possibility that observed gene expression is specific to any one individual, and limiting the somite range should allow observation of gene

expression at a fairly specific window during development. The quality of the extracted RNA was tested initially using formaldehyde RNA gels, and all samples were tested for quantity and quality on an Agilent 2100 Bioanalyser. The Bioanlayser is a microfluidics based platform for the analysis of DNA, RNA, proteins and cells and is often used in the context of gene expression analysis via microarray technology (www.agilent.com). RNA is injected into microchannels and separated according to molecular size, after which the fragments are detected by fluorescence. The system calculates the ratio of ribosomal bands in total RNA samples and shows the percentage of ribosomal impurities in as little as 5 ng of mRNA, as well as giving a good estimation of concentration. Figure 3.4 is an example of quality control on RNA extracted from both wild type, and *Chx10*$^{-/-}$, retinae.

Chip	Tissue Collected	Somite Range
129/Sv 1	80 retinae from 45 individuals	40-45
129/Sv 2	59 retinae from 30 individuals	42-47
129/Sv 3	29 retinae from 15 individuals	41-43
Chx10$^{-/-}$ 1	82 retinae from 41 individuals	41-47
Chx10$^{-/-}$ 2	30 retinae from 15 individuals	41-44
Chx10$^{-/-}$ 3	30 retinae from 15 individuals	41-45

Table 3.1: Number of retinae collected per GeneChip used in this study and the somite range for each pool of retinae collected.

3.2.3 Acquisition and normalisation of GeneChip data

cRNA from three independent pools of wild type and *Chx10*$^{-/-}$ retinae were hybridised to separate U74v2 chips, producing a total of six chips, three replicates of each type. All were stained with the single dye phycoerythrin and scanned twice by the HP GeneArray scanner for fluorescence. The data for all three replicates of each type were pooled and analysed using Genespring 5.1 and later Genespring 6 software. The data was normalised in two consecutive steps, in order to eliminate variations between the three hybridisations. Firstly, the data was normalised per chip. Because global expression is being examined, it is expected that in general, fluorescence of all six chips should be of a similar intensity – whilst a proportion of the transcripts may be up- or down-regulated in some of the chips compared to others, most of the transcripts are expected to be expressed at similar levels. Thus the fluorescence signal of all chips is normalised to the 50th percentile. Secondly, the data is normalised per gene. On every chip, sixteen probe pairs are present per

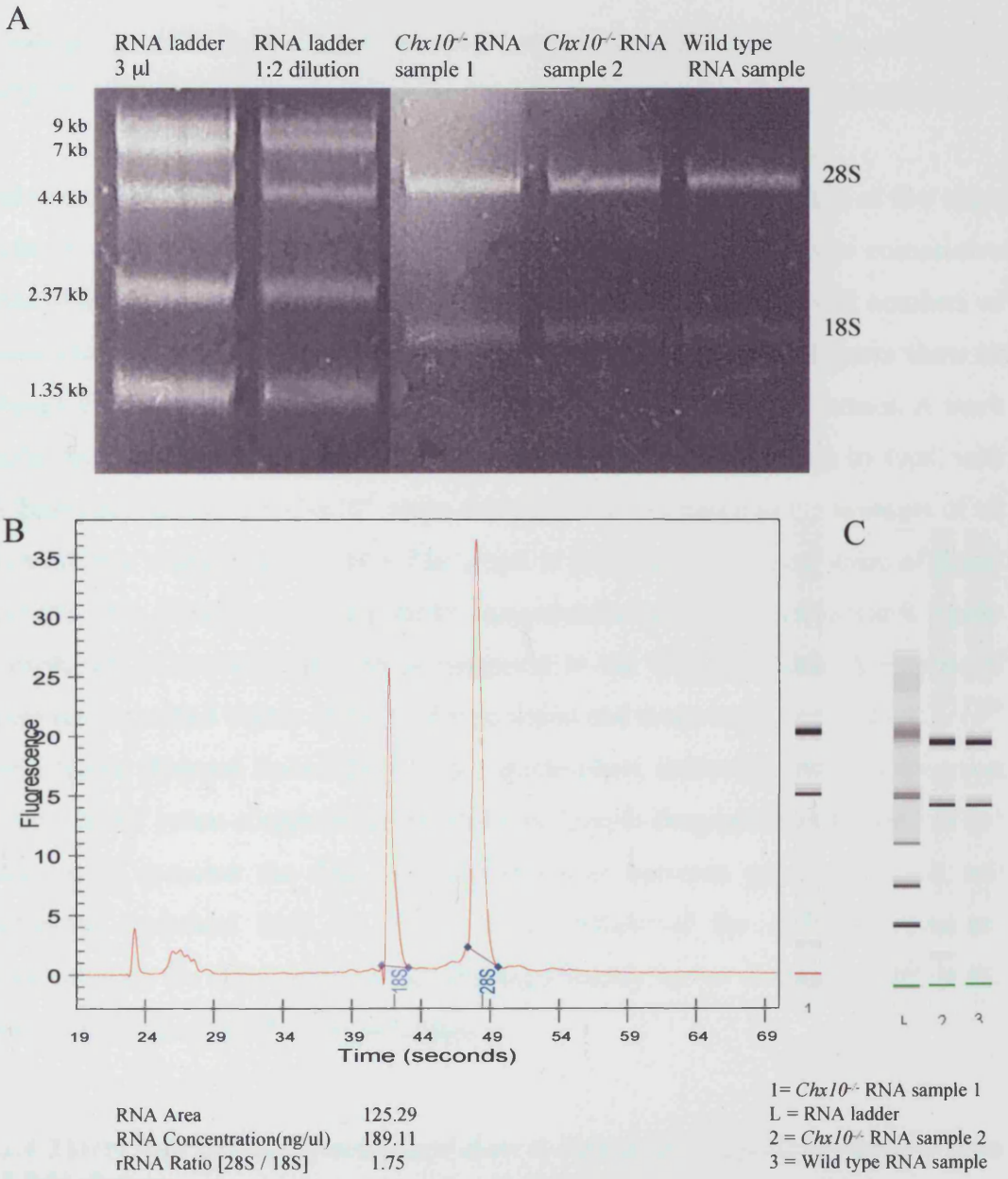

Figure 3.4: Quality and quantity control of RNA samples extracted from pools of E11.5 *Chx10*$^{-/-}$ and wild type retinae. *(A)* Samples were run on an RNA gel to check for the presence of RNA. In this case, samples from one pool of wild type and two pools of *Chx10*$^{-/-}$ retinae were tested. The presence of RNA is indicated by the typical 18S and 28S ribosomal RNA bands. A rough estimate of quantity could be acquired based on the brightness of the bands as compared to the brightness of the ladder bands at various dilutions. 3 µl of ladder contains approximately 500 ng of each component. *(B)* The RNA was also tested on an Agilent Bioanalyser 2100, producing a graph and gel equivalent, again clearly depicting 18S and 28S bands for the first mutant sample tested on the gel in *A*. Peaks were in the correct proportion (1.75, 1.7-2 is considered optimal) and a smooth baseline indicated no contamination by DNA. An estimate of the quantity of RNA present was also produced (RNA concentration ng/µl). *(C)* 'Gels' produced by the Bioanalyser for the RNA ladder and other two samples tested on the gel in *A*.

transcript (gene/EST), and their fluorescent signal is expected to be the same. Thus for every chip, the data is normalised to the median expression of every sequence.

The normalised data could then be displayed per chip, where expression of five chips could be compared to any one chip (Figure 3.5A; Figures 3.5-3.9 show consecutive steps of analysing data and producing gene lists). For each chip, small numbers of genes show very low or very high expression, whilst the majority of genes show an average expression and are therefore grouped in between the two extremes. A more useful display of the normalised data, however, was graphing the data by type, with all three replicates of the *Chx10*$^{-/-}$ chips averaged and compared to the averages of all the wild type chips (Figure 3.5B). The graph is produced on a linear scale of signal intensity, thus giving a relatively direct representation of the extent to which a gene is expressed in the wild type retina compared to the *Chx10*$^{-/-}$ retina. A number of genes are expressed highly in the wild type retina and down-regulated in the *Chx10*$^{-/-}$ retina (green diagonal lines Figure 3.5B), while others showed increased expression in the *Chx10*$^{-/-}$ retina compared to the wild type (purple diagonal lines Figure 3.5B). I went on to examine the fold change differences between gene expression and performed statistical tests to narrow down which of the ~12000 transcripts represented on the chips were statistically significantly up- or down-regulated in the *Chx10*$^{-/-}$ retina compared to the wild type.

3.2.4 Thirty four characterised genes show a statistically significant greater than 1.5 fold change

The data was organised into a two-dimensional plot of the hybridisation signal for ease of comparison (Figure 3.6A). Values of the majority of the transcripts fall along the central diagonal line and in between the parallel lines. Subsequent analysis of the data continued by eliminating all transcripts that were given an Absent signal for either set of RNA. A restriction was set for transcripts that were Present in at least two out of three wild type chips or two out of three *Chx10*$^{-/-}$ chips. Thus, only the genes that were expressed by either the wild type or *Chx10*$^{-/-}$ retinae were displayed, narrowing down the number of genes to analyse to 7218 (Figure 3.6). Genes were then restricted to those that showed at least a 1.5-fold difference in expression between the wild type and *Chx10*$^{-/-}$ retina – a total of 293 genes (Figure 3.7A, for a

Figure 3.5: Normalised GeneChip data from 6 chips.

(*A*) Normalised data is displayed per chip (SV 1-3 are the wild type replicates, ORJ 1-3 are the *Chx10*$^{-/-}$ replicates). All expression data is compared to SV1, thus the expression data for this sample is coloured according to the legend on the right: genes that show the least expression are represented with a purple colour at the bottom of the graph(low signal intensity), and genes that show high expression are represented with a green colour at the top of the graph (high signal intensity). The colour of each gene is maintained in the other samples, but their position on the graph (signal intensity) is higher or lower compared to the SV1 sample (see also Figure 3.8).

(*B*) Normalised data is displayed as a graph, in which the signal intensities of the three wild type replicates (SV, left) and the three *Chx10*$^{-/-}$ replicates (ORJ, right) are averaged. Expression of the *Chx10*$^{-/-}$ replicates is compared to that of the wild type replicates, and thus the lines are coloured according to wild type expression: green for highly expressed transcripts with high signal intensity at the top of the graph, and purple for transcripts with lower signal intensity.

A

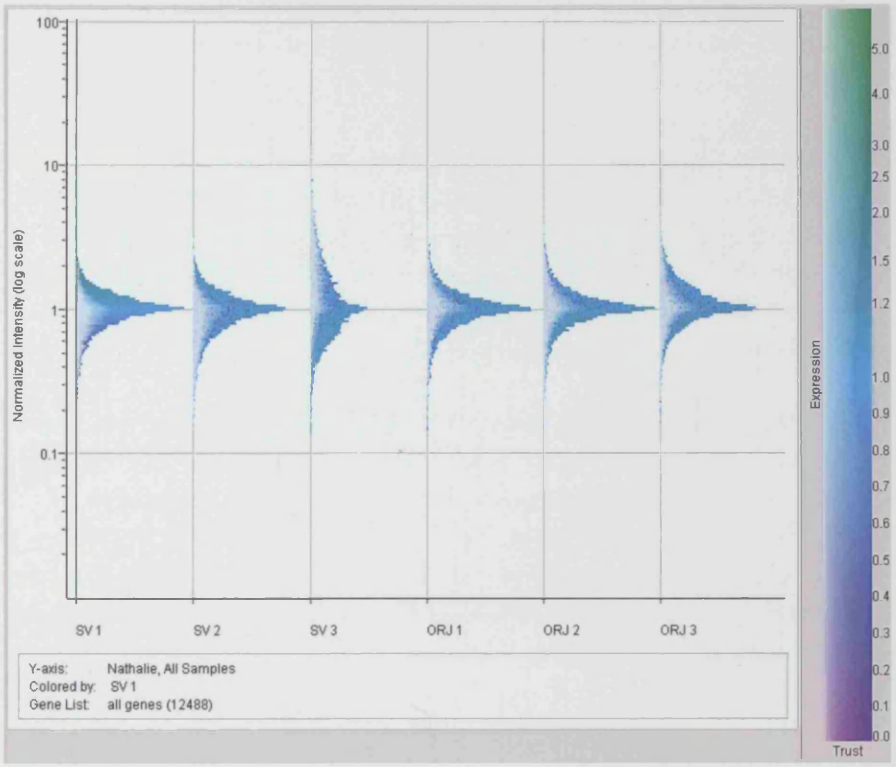
100
10
1
0.1
Normalized Intensity (log scale)
SV 1
SV 2
SV 3
ORJ 1
ORJ 2
ORJ 3
Y-axis: Nathalie, All Samples
Colored by: SV 1
Gene List: all genes (12488)
Expression
5.0
4.0
3.0
2.5
2.0
1.5
1.2
1.0
0.9
0.8
0.7
0.6
0.5
0.4
0.3
0.2
0.1
0.0
Trust

B

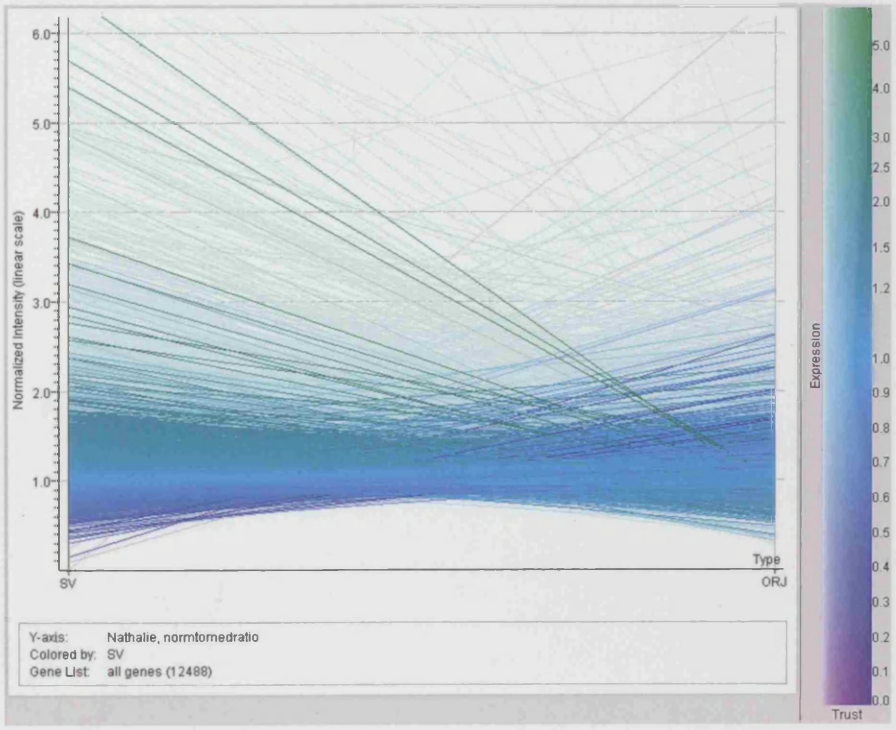
6.0
5.0
4.0
3.0
2.0
1.0
Normalized Intensity (linear scale)
SV
Type
ORJ
Y-axis: Nathalie, normtornedratio
Colored by: SV
Gene List: all genes (12488)
Expression
5.0
4.0
3.0
2.5
2.0
1.5
1.2
1.0
0.9
0.8
0.7
0.6
0.5
0.4
0.3
0.2
0.1
0.0
Trust

Figure 3.6: Normalised data showing relative expression of genes between wild type replicates and *Chx10*$^{-/-}$ replicates.

(*A*) Normalised data for all genes represented on the GeneChip is displayed as a two-dimensional plot of the average hybridisation signal intensities of the three wild type replicates (SV, x-axis) and the three *Chx10*$^{-/-}$ replicates (ORJ, y-axis). Values for the expression of the majority of the genes fall along the central diagonal line, representing equal expression in the two genotypes. Parallel lines indicate a two-fold change in expression.

(*B*) The 7218 genes that are detected as 'Present' in at least two out of three wild type replicates or two out of three *Chx10*$^{-/-}$ replicates are displayed as a two-dimensional plot of the average hybridisation signal intensities of the three wild type replicates (SV, x-axis) and the three *Chx10*$^{-/-}$ replicates (ORJ, y-axis). Values for the expression of the majority of the transcripts fall along the central diagonal line, representing equal expression in the two genotypes. Parallel lines indicate a two-fold change in expression.

A

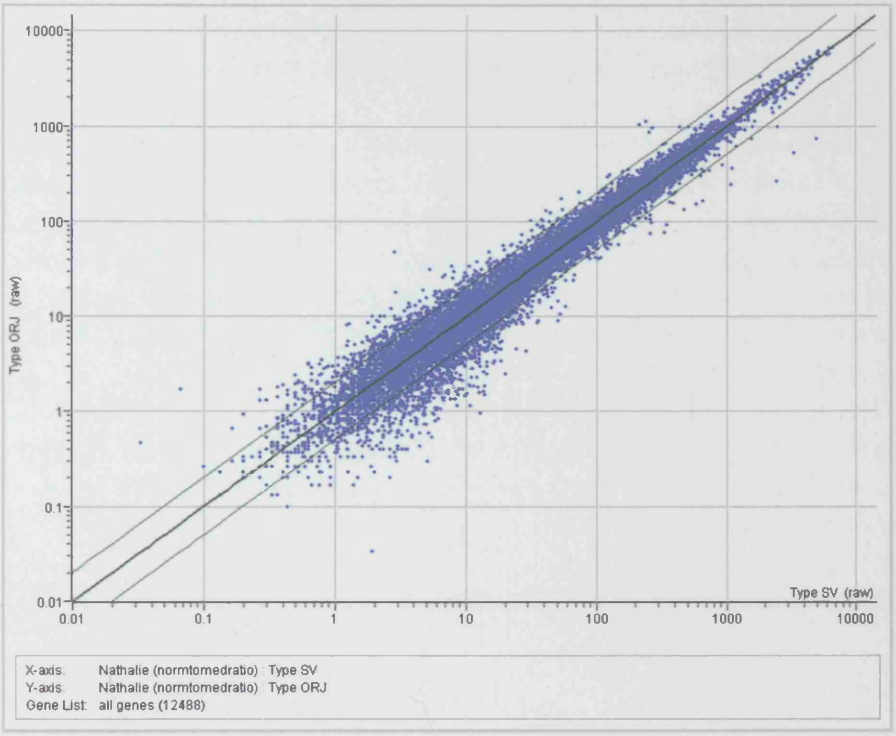
10000
1000
100
10
1
0.1
0.01
Type ORJ (raw)
0.01
0.1
1
10
100
1000
10000
Type SV (raw)
X-axis: Nathalie (normtomedratio) : Type SV
Y-axis: Nathalie (normtomedratio) : Type ORJ
Gene List: all genes (12488)

B

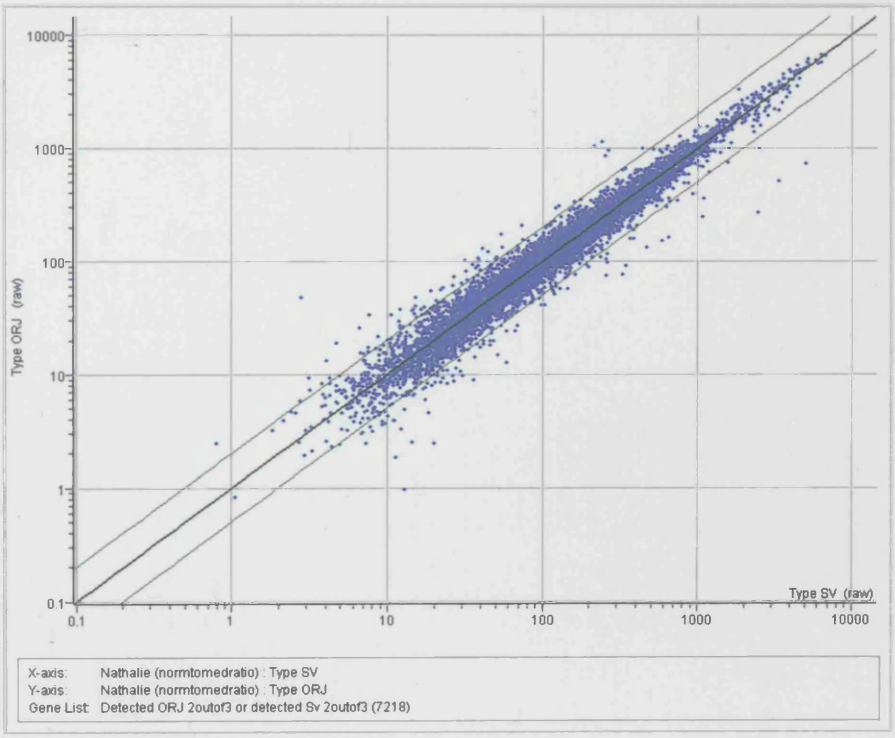
10000
1000
100
10
1
0.1
Type ORJ (raw)
0.1
1
10
100
1000
10000
Type SV (raw)
X-axis: Nathalie (normtomedratio) : Type SV
Y-axis: Nathalie (normtomedratio) : Type ORJ
Gene List: Detected ORJ 2outof3 or detected Sv 2outof3 (7218)

Figure 3.7: Normalised data showing genes with a greater than 1.5-fold or 2-fold change in expression between the wild type and *Chx10*$^{-/-}$ replicates.

(*A*) Signal intensity of 293 of the 7218 genes expressed in either the wild type or *Chx10*$^{-/-}$ retinae are up- or down-regulated more than 1.5-fold times in the *Chx10*$^{-/-}$ retina compared to the wild type. Data is displayed as a two-dimensional plot of the average hybridisation signal intensities of the three wild type replicates (SV, x-axis) and the three *Chx10*$^{-/-}$ replicates (ORJ, y-axis). The central diagonal line represents equal expression in the two genotypes. Parallel lines indicate a two-fold change in expression.

(*B*) 43 of the 7218 genes expressed in either the wild type or *Chx10*$^{-/-}$ retinae are up- or down-regulated more than 2-fold times in the *Chx10*$^{-/-}$ retina compared to the wild type.

A

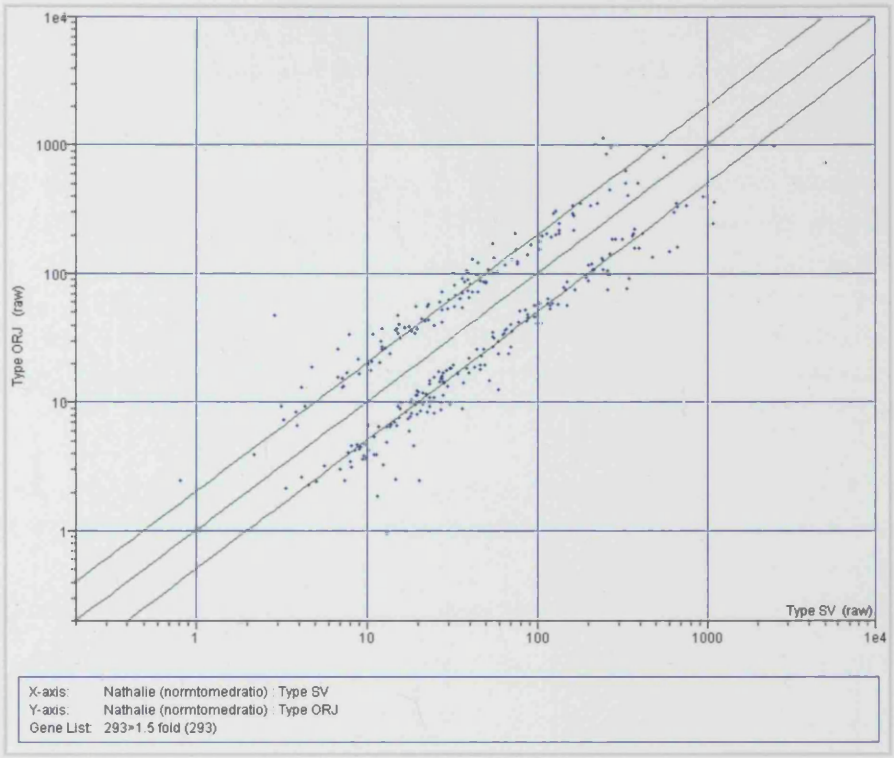
1e4
1000
100
10
1
Type ORJ (raw)
1
10
100
1000
1e4
Type SV (raw)
X-axis: Nathalie (normtomedratio) : Type SV
Y-axis: Nathalie (normtomedratio) : Type ORJ
Gene List: 293>1.5 fold (293)

B

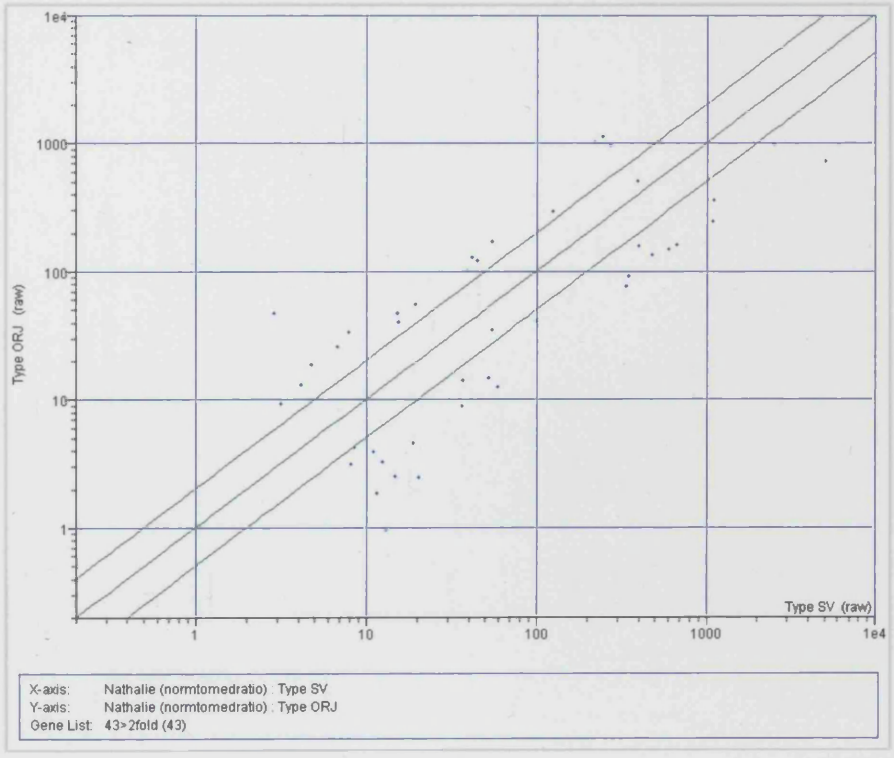
1e4
1000
100
10
1
Type ORJ (raw)
1
10
100
1000
1e4
Type SV (raw)
X-axis: Nathalie (normtomedratio) : Type SV
Y-axis: Nathalie (normtomedratio) : Type ORJ
Gene List: 43>2fold (43)

Figure 3.8: Normalised data showing genes with a statistically significant greater than 1.5-fold or 2-fold change in expression between the wild type and *Chx10*$^{-/-}$ replicates.

(*A*) 40 of the 293 genes showing a greater than 1.5-fold change in expression between the wild type and *Chx10*$^{-/-}$ retina passed the parametric analysis of variance test for significance. Data is displayed as a two-dimensional plot of the average hybridisation signal intensities of the three wild type replicates (SV, x-axis) and the three *Chx10*$^{-/-}$ replicates (ORJ, y-axis). The central diagonal line represents equal expression in the two genotypes. Parallel lines indicate a two-fold change in expression.

(*B*) 8 of the 43 genes showing a greater than 2-fold change in expression between the wild type and *Chx10*$^{-/-}$ retina passed the parametric analysis of variance test for significance.

A

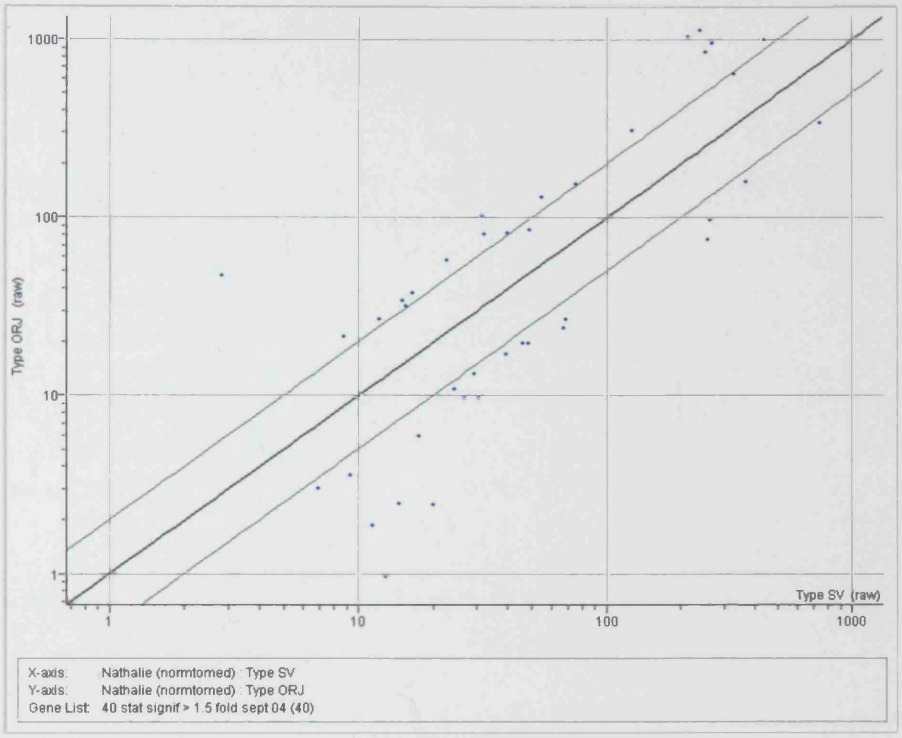
1000
100
10
1
Type ORJ (raw)
1
10
100
1000
Type SV (raw)
X-axis: Nathalie (normtomed) : Type SV
Y-axis: Nathalie (normtomed) : Type ORJ
Gene List: 40 stat signif > 1.5 fold sept 04 (40)

B

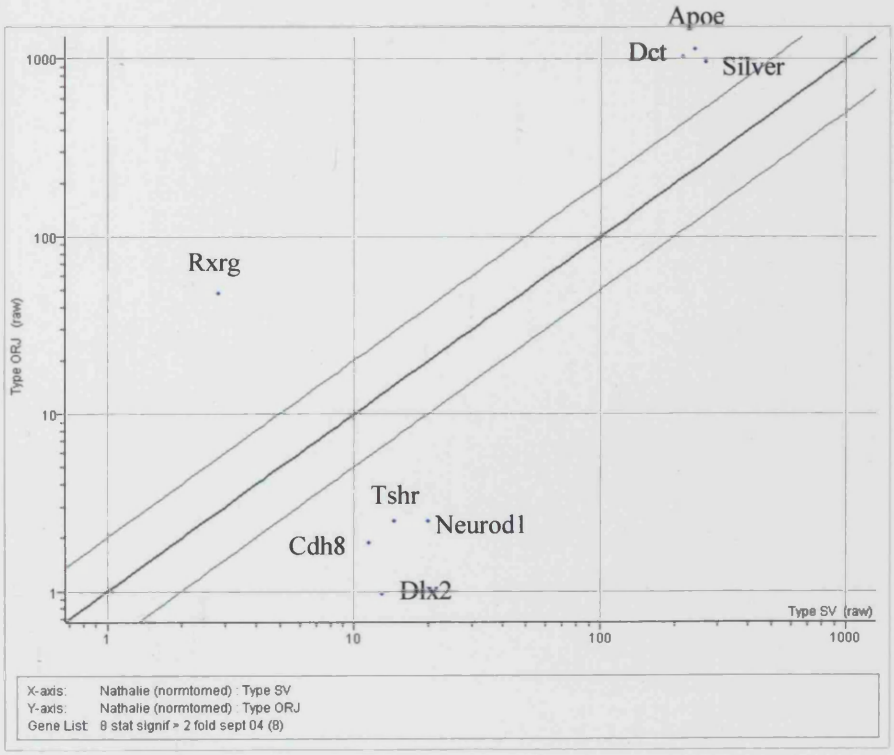
Apoe
Dct
Silver
Rxrg
Tshr
Neurod1
Cdh8
Dlx2
1000
100
10
1
Type ORJ (raw)
1
10
100
1000
Type SV (raw)
X-axis: Nathalie (normtomed) : Type SV
Y-axis: Nathalie (normtomed) : Type ORJ
Gene List: 8 stat signif > 2 fold sept 04 (8)

Figure 3.9: Normalised data showing genes with a statistically significant greater than 1.5-fold or 2-fold change in expression between the wild type and *Chx10*$^{-/-}$ replicates.

(*A*) Normalised data of the 40 genes/ESTs showing a statistically significant greater than 1.5-fold change is displayed per chip (SV 1-3 are the wild type replicates, ORJ 1-3 are the *Chx10*$^{-/-}$ replicates). All expression data is compared to SV1, thus the expression data for this sample is coloured according to the legend on the right: genes that show the least expression are represented with a purple colour at the bottom of the graph (low signal intensity), and genes that show high expression are represented with a green colour at the top of the graph (high signal intensity). The colour of each gene is maintained in the other samples, but their position on the graph (signal intensity) is higher or lower compared to the SV1 sample.

(*B*) Normalised data of the 8 genes showing a statistically significant greater than 2-fold change is displayed per chip.

A

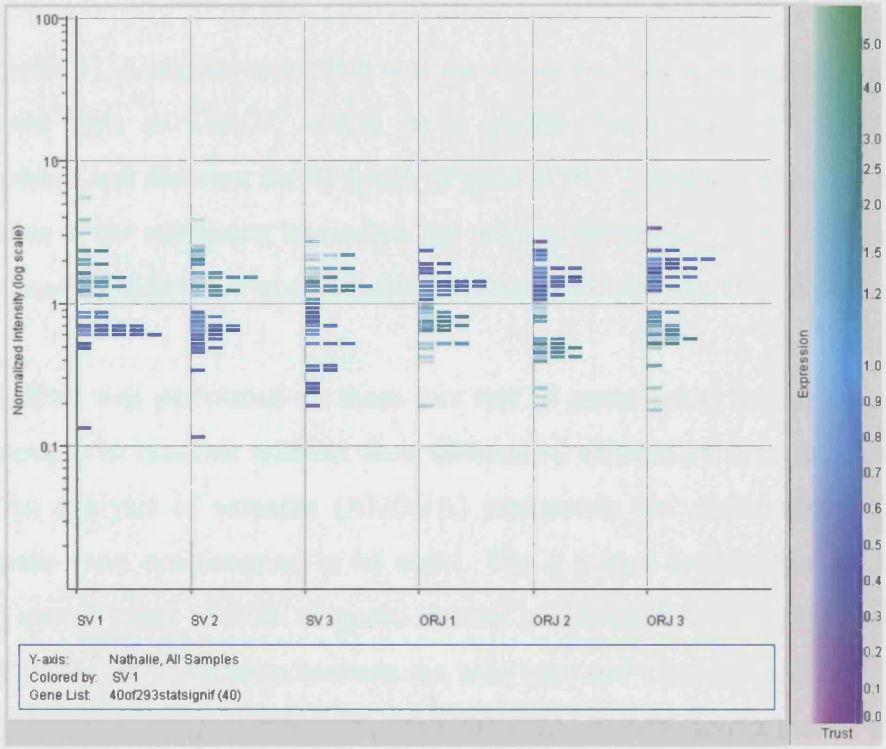
100
10
1
0.1
Normalized Intensity (log scale)
SV 1
SV 2
SV 3
ORJ 1
ORJ 2
ORJ 3
Y-axis: Nathalie, All Samples
Colored by: SV 1
Gene List: 40of293statsignif (40)
Expression
5.0
4.0
3.0
2.5
2.0
1.5
1.2
1.0
0.9
0.8
0.7
0.6
0.5
0.4
0.3
0.2
0.1
0.0
Trust

B

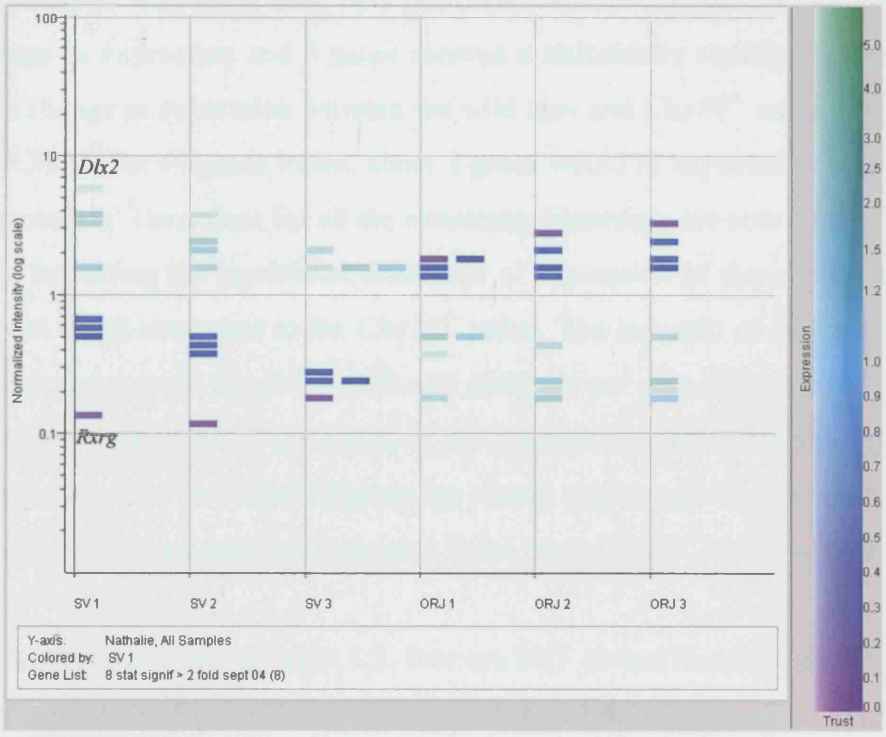
100
10
1
0.1
Normalized Intensity (log scale)
Dlx2
Rxrg
SV 1
SV 2
SV 3
ORJ 1
ORJ 2
ORJ 3
Y-axis: Nathalie, All Samples
Colored by: SV 1
Gene List: 8 stat signif > 2 fold sept 04 (8)
Expression
5.0
4.0
3.0
2.5
2.0
1.5
1.2
1.0
0.9
0.8
0.7
0.6
0.5
0.4
0.3
0.2
0.1
0.0
Trust

list see Appendix 1). A similar restriction was set to test the 7218 genes expressed in either the wild type or *Chx10*$^{-/-}$ retina for a greater than two-fold change in expression, which was the case for 43 genes (Figure 3.7B). Already the values of a large proportion of the remaining transcripts fall outside the parallel lines, indicating a more than two-fold difference in expression between wild type and *Chx10*$^{-/-}$ retina.

Statistical analysis was performed on these two sets of genes using the log ratio of the signal intensity to examine whether their differential expression was statistically significant. An analysis of variance (ANOVA) parametric test was performed in which variances were not assumed to be equal. The p values for the Welch t-test were given a cut-off value of 0.05. 40 genes showed a statistically significant greater than 1.5 fold change in expression between the wild type and *Chx10*$^{-/-}$ retina (Figure 3.8A, Table 3.2). It should be noted that of the 293 genes that showed a greater than 1.5-fold differential expression, about 14 genes would be expected to pass the restriction by chance. The same tests were performed on those genes that showed a two-fold change in expression and 8 genes showed a statistically significant greater than two-fold change in expression between the wild type and *Chx10*$^{-/-}$ retina (Figure 3.8B, Table 3.3). Of the 43 genes tested, about 3 genes would be expected to pass the restriction by chance. The values for all the remaining transcripts are now outside the parallel lines, indicating the significant difference of expression of these transcripts in the wild type retina compared to the *Chx10*$^{-/-}$ retina. The log ratio of the intensity signals of these genes could then be specifically observed per chip (Figure 3.9). This comparison between chips gives some idea of the consistency and reproducibility of the microarray study. The two labelled genes are clearly expressed at a different level in all three wild type retinal samples compared to the three *Chx10*$^{-/-}$ retinal samples.

Of the forty transcripts listed in Table 3.2, four are EST clones that have as yet not been further characterised. In addition, there is some redundancy, as there are two transcripts representing *C. elegans* ceh-10 homeo domain containing homolog (*Chx10*) and two transcripts representing protein kinase C, beta 1 (*Pkcb1*). Thus a total of thirty four characterised genes show a significant, more than 1.5-fold change, in expression between the wild type retina and the *Chx10*$^{-/-}$ retina. Fifteen of these are up-regulated in the *Chx10*$^{-/-}$ retina, and eighteen are down-regulated. Eight show a significantly greater than two-fold change (Table 3.3).

Gene Title	Trend	Fold-change	Genbank Accession Number
Apolipoprotein E (*Apoe*)	+	4.70	D00466
Biglycan (*Bgn*)	+	2.18	X53928
Brain and kidney protein (*Bk*)	+	2.26	AW046243
Cyclin E2 (*Ccne2*)	-	2.44	AF091432
Cadherin 8 (*Cdh8*)	-	6.00	X95600
C. elegans ceh-10 homeo domain containing homolog (*Chx10*)*	-	2.61	L34808
C. elegans ceh-10 homeo domain containing homolog (*Chx10*)*	-	2.69	AV246437
Claudin 1 (*Cldn1*)	-	2.75	AI604314
Cytochrome P450, family 1, subfamily b, polypeptide 1 (*Cyp1b1*)	-	3.41	X78445
Dopachrome tautomerase (*Dct*)	+	4.80	X63349
Distal-less homeobox 2 (*Dlx2*)	-	13.83	M80540
Fibroblast growth factor 9 (*Fgf9*)	-	2.75	U33535
Forkhead box C2 (*Foxc2*)	-	2.29	X74040
Frizzled homolog 4 (Drosophila) (*Fzd4*)	+	2.07	AW122897
Growth arrest specific 2 (*Gas2*)	-	2.14	M21828
GATA-binding protein 3 (*Gata3*)	-	2.27	X55123
G protein-coupled receptor 175 (*Gpr175*)	+	2.50	AI842363
Heparan sulfate (glucosamine) 3-O-sulfotransferase 1 (*Hs3st1*)	+	2.32	AF019385
Insulin-like growth factor binding protein 5 (*Igfbp5*)	+	2.41	L12447
Indolethylamine N-methyltransferase (*Inmt*)	+	3.26	M88694
Insulinoma-associated 1 (*Insm1*)	-	2.14	AF044669
Myeloblastosis oncogene (*Myb*)	-	2.31	M12848
Neurogenic differentiation 1 (*Neurod1*)	-	8.29	U28068
Pleckstrin homology-like domain, family A, member 1 (*Phlda1*)	-	3.04	U44088
Phospholipase D3 (*Pld3*)	+	2.12	AF026124
Protein kinase C, beta 1 (*Prkcb1*)*	+	2.56	X53532
Protein kinase C, beta 1 (*Prkcb1*)*	+	2.50	X59274
Renin binding protein (*Renbp*)	+	2.46	AA600645
Retinoid X receptor gamma (*Rxrg*)	+	17.93	X66225
Silver (*Si*)	+	3.54	U14133
Stathmin-like 2 (*Stmn2*)	-	2.21	AI839868
Transducin-like enhancer of split 1, homolog of Drosophila E(spl) (*Tle1*)	-	2.48	U61362
Tenascin C (*Tnc*)	-	2.30	X56304
Transient receptor potential cation channel, subfamily M, member (*Trpm1*)	+	3.34	AF047714
Thyroid stimulating hormone receptor (*Tshr*)	-	5.76	U02602
UDP-glucose ceramide glucosyltransferase (*Ugcg*)	+	2.30	D89866
EST	+	2.50	AA717225
EST	+	2.09	AA691628
EST	+	1.84	AA763466
EST	-	2.09	AI153421

Table 3.2: Table of 40 genes/ESTs that showed a statistically significant greater than 1.5-fold change in expression between the wild type and *Chx10*$^{-/-}$ retina. Trend indicates whether the gene is up- (+) or down-regulated (-) in the *Chx10*$^{-/-}$ retina compared to the wild type. * Indicates a gene that is represented twice.

Gene Title	Trend	Fold-change	Genbank Accession Number
Silver (*Si*)	+	3.54	U14133
Thyroid stimulating hormone receptor (*Tshr*)	-	5.76	U02602
Dopachrome tautomerase (*Dct*)	+	4.80	X63349
Cadherin 8 (*Cdh8*)	-	6.00	X95600
Distal-less homeobox 2 (*Dlx2*)	-	13.83	M80540
Apolipoprotein E (*Apoe*)	+	4.70	D00466
Neurogenic differentiation 1 (*Neurod1*)	-	8.29	U28068
Retinoid X receptor gamma (Saga et al., 1999)	+	17.93	X66225

Table 3.3: Table of 8 genes that showed a statistically significant greater than 2-fold change in expression between the wild type and *Chx10*$^{-/-}$ retina. Trend indicates whether the gene is up- (+) or down-regulated (-) in the *Chx10*$^{-/-}$ retina compared to the wild type.

3.2.5 Examining genes that show a correlation to the two most changed genes

The lists of genes/ESTs above were obtained through a series of relatively stringent steps. One of the problems of analysing the volume of data obtained from a microarray experiment is that various approaches will result in different lists of genes showing changes in expression. There is no correct or definitive list. It is important to be aware that taking one approach to analysing the GeneChip data may lead to the exclusion of differentially expressed genes that are important to the study because of stringent analysis conditions. Whilst the approach described above is used as a standard method in the microarray facility at the Institute of Child Health, UCL, at which this study was performed, it is important try to ensure no genes have been unnecessarily eliminated.

Statistical tests will not necessarily pinpoint only those genes that are important to a particular study. They simply exclude genes that do not exhibit a sufficiently different change in expression. In order to examine the data a little further, a common procedure is to look for genes whose pattern of altered expression correlates with some of the most significantly altered genes. The 293 genes that showed a 1.5-fold change in expression were analysed for a correlation with the two most changed genes: retinoid X receptor gamma (*Rxrg*), the gene most increased in expression, and distal-less homeobox 2 (*Dlx2*), the gene most decreased in expression in the *Chx10*$^{-/-}$ retina. Twenty one transcripts showed an increase in expression similar to that of

Rxrg (Figure 3.10) and twenty three transcripts showed a decrease in expression similar to that of *Dlx2* (Figure 3.11).

Of the twenty one transcripts showing an increase in expression, eighteen did not pass the statistical analysis performed earlier, and thus are not observed in Table 3.2. Upon examination of the data per chip (Figure 3.10C), it is clear that the reason for this is that these samples showed variable levels of expression. Whilst overall it is clear that there is a difference between the wild type and *Chx10*$^{-/-}$ expression of the genes, the difference would not have been clear-cut enough to pass the statistical analysis. Similarly, of the twenty three transcripts that show a decrease in expression, another twelve failed the statistical analysis, excluding them from the list in Table 3.2. The transcripts that failed the statistical analysis are listed in Table 3.4. Eight of the transcripts represent ESTs, and twenty two of the transcripts represent characterised genes.

3.2.6 Functional classification of genes with altered expression

One of the challenges of analysing microarray data is extracting meaningful information from often very large lists of genes. In order to assign some meaning to the fifty six characterised genes that show a change in expression, ontology information from Netaffix, the Affymetrix online analysis facility (www.affymetrix.com), and the Mouse Genome Informatics website (www.informatics.jax.org) were used to assign the expressed genes to a functional class, based on the biological processes they are involved in. A number fit into more than one category, due to having either more than one function or because of an overlap between functional classes themselves. The results are listed in Table 3.5, giving an initial glance at what types of genes show a difference in expression.

Figure 3.10: Normalised data showing genes that show a correlation with Rxrg

(*A*) 21 genes show a correlation in expression to *Rxrg*. Data is displayed as a graph, in which the log ratio of signal intensities of the three wild type replicates (SV, left) and the three *Chx10*$^{-/-}$ replicates (ORJ, right) are averaged. Expression of the *Chx10*$^{-/-}$ replicates is compared to that of the wild type replicates, and thus the lines are coloured according to wild type expression: green for highly expressed genes with high signal intensity at the top of the graph, and purple for genes with lower signal intensity.

(*B*) 18 of the 21 genes showing a correlation in expression to *Rxrg* did not pass the statistical analysis performed on the 293 genes showing a change in expression between the wild type and *Chx10*$^{-/-}$ retinae.

(*C*) Normalised data of the genes in (*B*) is displayed per chip (SV 1-3 are the wild type replicates, ORJ 1-3 are the *Chx10-/-* replicates). All expression data is compared to SV1, thus the expression data for this sample is coloured according to the legend on the right: genes that show the least expression are represented with a purple colour at the bottom of the graph (low signal intensity), and genes that show high expression are represented with a green colour at the top of the graph (high signal intensity). The colour of each gene is maintained in the other samples, but their position on the graph (signal intensity) is higher or lower compared to the SV1 sample.

A

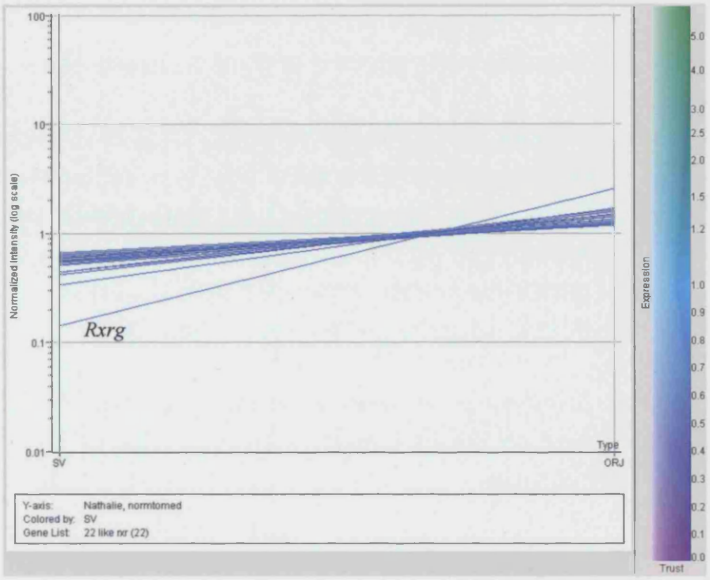
Normalized Intensity (log scale)
100
10
1
0.1
0.01
Rxrg
SV
Type
ORJ
Y-axis: Nathalie, normtomed
Colored by: SV
Gene List: 22 like nr (22)
Expression
5.0
4.0
3.0
2.5
2.0
1.5
1.2
1.0
0.9
0.8
0.7
0.6
0.5
0.4
0.3
0.2
0.1
0.0
Trust

B

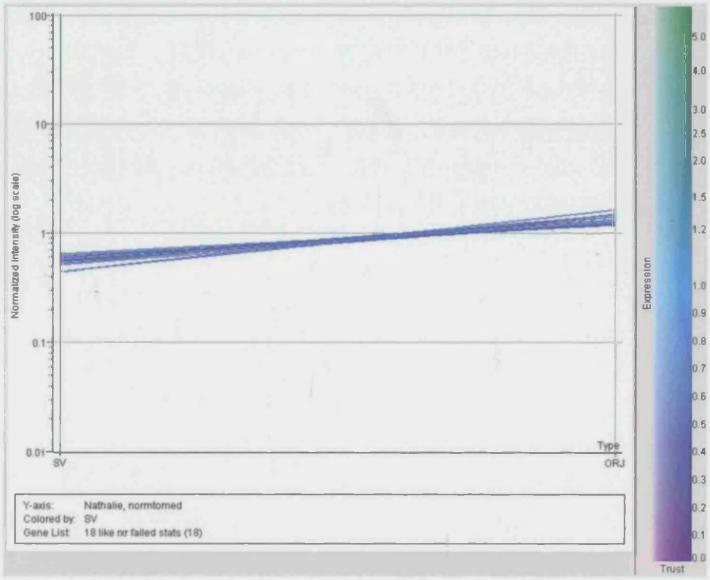
Normalized Intensity (log scale)
100
10
1
0.1
0.01
SV
Type
ORJ
Y-axis: Nathalie, normtomed
Colored by: SV
Gene List: 18 like nr failed stats (18)
Expression
5.0
4.0
3.0
2.5
2.0
1.5
1.2
1.0
0.9
0.8
0.7
0.6
0.5
0.4
0.3
0.2
0.1
0.0
Trust

C

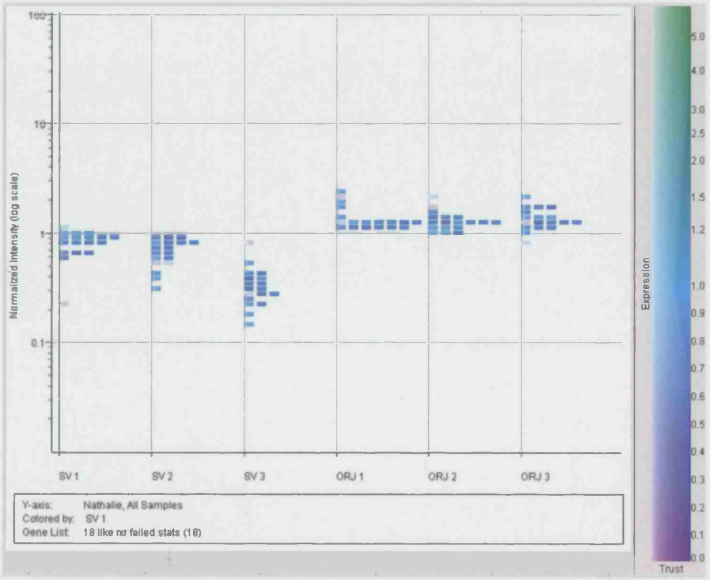
Normalized Intensity (log scale)
100
10
1
0.1
SV 1
SV 2
SV 3
ORJ 1
ORJ 2
ORJ 3
Y-axis: Nathalie, All Samples
Colored by: SV 1
Gene List: 18 like nr failed stats (18)
Expression
5.0
4.0
3.0
2.5
2.0
1.5
1.2
1.0
0.9
0.8
0.7
0.6
0.5
0.4
0.3
0.2
0.1
0.0
Trust

Figure 3.11: Normalised data showing genes that show a correlation with *Dlx2*

(*A*) 23 genes show a correlation in expression to *Dlx2*. Data is displayed as a graph, in which the log ratio of signal intensities of the three wild type replicates (SV, left) and the three *Chx10*$^{-/-}$ replicates (ORJ, right) are averaged. Expression of the *Chx10*$^{-/-}$ replicates is compared to that of the wild type replicates, and thus the lines are coloured according to wild type expression: green for highly expressed genes with high signal intensity at the top of the graph, and purple for genes with lower signal intensity.

(*B*) 12 of the 23 genes showing a correlation in expression to *Dlx2* did not pass the statistical analysis performed on the 293 genes showing a change in expression between the wild type and *Chx10*$^{-/-}$ retinae.

(*C*) Normalised data of the genes in (*B*) is displayed per chip (SV 1-3 are the wild type replicates, ORJ 1-3 are the *Chx10-/-* replicates). All expression data is compared to SV1, thus the expression data for this sample is coloured according to the legend on the right: genes that show the least expression are represented with a purple colour at the bottom of the graph (low signal intensity), and genes that show high expression are represented with a green colour at the top of the graph (high signal intensity). The colour of each gene is maintained in the other samples, but their position on the graph (signal intensity) is higher or lower compared to the SV1 sample.

A

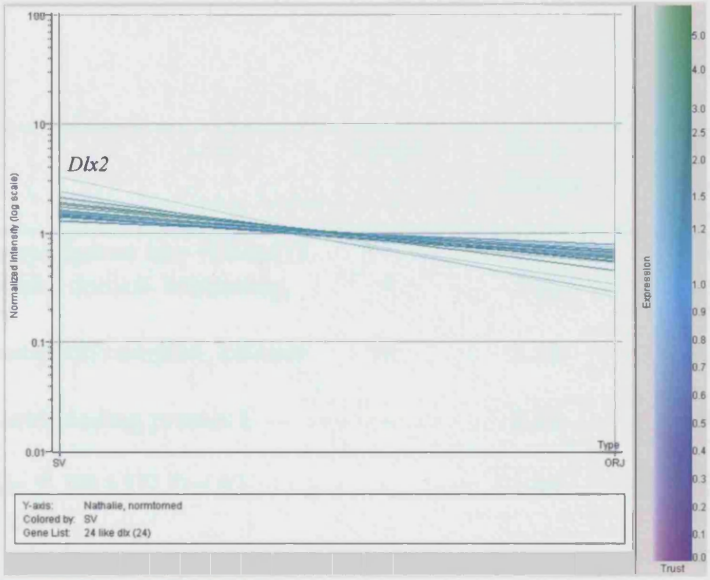
Dlx2
Normalized Intensity (log scale)
100
10
1
0.1
0.01
SV
Type
ORJ
Expression
5.0
4.0
3.0
2.5
2.0
1.5
1.2
1.0
0.9
0.8
0.7
0.6
0.5
0.4
0.3
0.2
0.1
0.0
Trust
Y-axis: Nathalie, normtomed
Colored by: SV
Gene List: 24 like dlx (24)

B

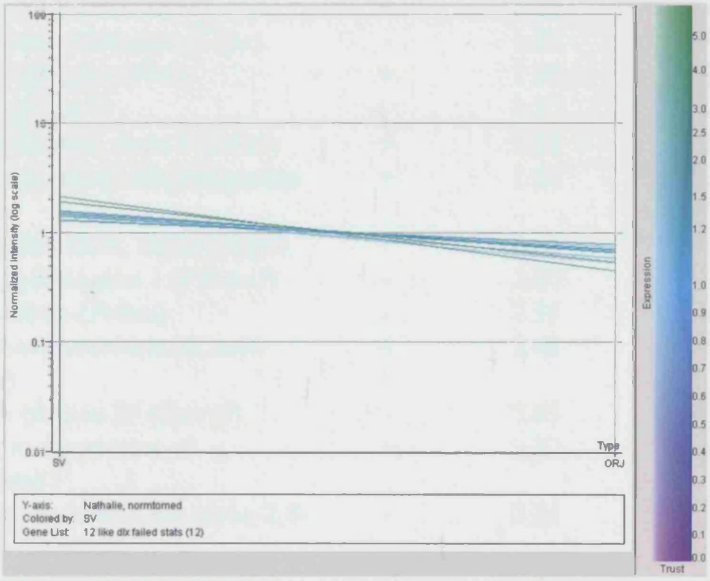
Normalized Intensity (log scale)
100
10
1
0.1
0.01
SV
Type
ORJ
Expression
5.0
4.0
3.0
2.5
2.0
1.5
1.2
1.0
0.9
0.8
0.7
0.6
0.5
0.4
0.3
0.2
0.1
0.0
Trust
Y-axis: Nathalie, normtomed
Colored by: SV
Gene List: 12 like dlx failed stats (12)

C

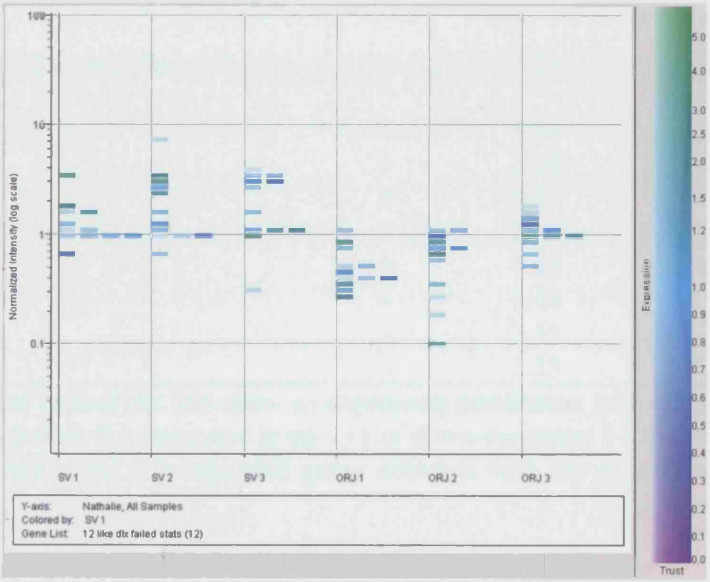
Normalized Intensity (log scale)
100
10
1
0.1
SV 1
SV 2
SV 3
ORJ 1
ORJ 2
ORJ 3
Expression
5.0
4.0
3.0
2.5
2.0
1.5
1.2
1.0
0.9
0.8
0.7
0.6
0.5
0.4
0.3
0.2
0.1
0.0
Trust
Y-axis: Nathalie, All Samples
Colored by: SV 1
Gene List: 12 like dlx failed stats (12)

Gene Title	Trend	Fold-Change	Genbank Accession Number
Adenylosuccinate synthetase like 1(*Adssl1*)	+	1.91	M74495
Basic helix-loop-helix domain containing, class B2 (*Bhlhb2*)	+	2.95	Y07836
CCR4-NOT transcription complex, subunit 7 (*Cnot7*)	+	3.31	AI931748
Cellular retinoic acid binding protein I (*Crabp1*)	-	2.29	X15789
DNA segment, Chr 2, ERATO Doi 93, expressed (*D2Ertd93e*)	-	1.94	C77278
DNA segment, Chr 6, Wayne State University 176, expressed (*D6Wsu176e*)	-	2.07	AA733372
Enolase 2, gamma neuronal (*Eno2*)	+	2.28	AC002397
Farnesyl diphosphate synthetase (*Fdps*)	-	1.83	AW045533
Fragile histidine triad gene (*Fhit*)	+	1.80	AF047699
Forkhead box G1 (*Foxg1*)	-	3.57	U36760
Glutathione S-transferase, theta 2 (*Gstt2*)	+	2.06	X98056
Leukotriene B4 12-hydroxydehydrogenase (*Ltb4dh*)	+	1.84	AA596710
N-acetyl galactosaminidase, alpha (*Naga*)	+	2.18	AJ223966
Polo-like kinase, pseudogene 1 (*Plk-ps1*)	-	2.67	U73170
Protein kinase C, alpha (*Prkca*)	-	2.35	M25811
Sphingomyelin phosphodiesterase, acid-like 3A (*Smpdl3a*)	+	2.42	Y08135
Small proline-rich protein 2F (*Sprr2f*)	-	2.03	AJ005564
Signal transducer and activator of transcription 6 (*Stat6*)	+	3.02	L47650
ST8 alpha-N-acetyl-neuraminide alpha-2,8-sialyltransferase 3 (*St8sia3*)	-	2.25	X80502
Transmembrane protein 30B (*Tmem30b*)	+	2.13	AA619554
Transmembrane 4 superfamily member 8 (*Tm4sf8*)	+	2.18	AI843488
Vascular endothelial growth factor B (*Vegfb*)	+	1.84	U43836
EST	+	2.51	AA607758
EST	+	2.08	AA656550
EST	+	2.07	AI839150
EST	+	2.00	AV303935
EST	+	1.96	AI020029
EST	-	4.18	AW214136
EST	-	3.51	AW122834
EST	-	2.33	AA867778

Table 3.4: Table of transcripts that show an expression correlation with either *Rxrg* or *Dlx2*. Trend indicates whether the transcript is up- (+) or down-regulated (-) in the *Chx10*$^{-/-}$ retina compared to the wild type. Up-regulated genes correlate with *Rxrg*, down-regulated genes with *Dlx2*.

Classification	Genes
Carbohydrate metabolism	***Eno2, Naga, Renbp, Smpdl3a***
Cell adhesion	*Cdh8, Cldn1*
Cell Cycle/Proliferation	*Ccne2, Crabp1, Fgf9, Foxg1, Gas2, Myb,* ***Vegfb***
Cell differentiation/cell fate determination	***Bhlhb2****, Chx10, Crabp1, Dlx2, Fgf9, Foxg1, GATA 3, Neurod1, Tle1*
Cell growth/ regulation of cell growth	***Apoe,*** *Gas2,* ***Igfbp5****, Myb, Prkcbl, Stat6, Vegfb*
Cell signalling	*Fgf9, Foxc2, Fzd4 , Prkca,* ***Prkcb1, Stat6****, Stmn2, Tle1, Tshr*
Electron transport	*Cyp1b1*
Glutathione metabolism	***Gstt2***
Lipid metabolism/transport	***Apoe****, Fdps,* ***Pld3, Ugcg***
Melanin Biosynthesis	***Dct, Si***
Nucleotide biosynthesis	***Adssl1***
Protein biosynthesis	***Phlda1****, St8sia3*
Regulation of transcription	***Bhlhb2****, Chx10,* ***Cnot7****, Foxc2, Dlx2, Myb, Neurod 1,* ***Rxrg, Stat6****, Tle1*
Unclassified	***Bgn, Bk****, D2Ertd93, D6Wsu176e,* ***Fhit, Gpr175, Hs3st1, Inmt****, Insm1,* ***Ltb4dh****, Plk-ps1, Sprr2,* ***Tmem30B, Tm4sf8****, Tnc,* ***Trpm1***

Table 3.5: Functional characterisation of the fifty six genes that show a change in expression in the *Chx10*$^{-/-}$ retina compared to the wild type. Genes in bold type are up-regulated, those in normal type are down-regulated.

A few of the genes exhibiting changes in expression are involved in cell metabolism and thus may reflect some physical differences between the wild type and *Chx10*$^{-/-}$ eye. Nine genes are involved in carbohydrate, lipid, and glutathione metabolism, and all but one (*Fdps*, involved in lipid metabolism) of those are up-regulated in the *Chx10*$^{-/-}$ retina. A further three are important for protein and nucleotide biosynthesis. *Phlda1* and *St8sia3*, involved in protein biosynthesis, are both down-regulated, whilst *Adssl1*, involved in nucleotide biosynthesis, is up-regulated in the *Chx10*$^{-/-}$ retina. In addition, two genes whose products are play a part in melanin biosynthesis, *Si* and *Dct* show an increase in expression in the *Chx10*$^{-/-}$ retina compared to the wild type. A further two genes, *Cldn1* and *Cdh8*, are involved in cell adhesion, and are both down-regulated in the *Chx10*$^{-/-}$ retina, as is *Cyp1b1*, which has a function in electron transport.

However, the majority of the genes whose expression is affected by a lack of Chx10 seem to be important for proliferation and cell cycle regulation, cell growth, differentiation and cell fate determination, or cell signalling. Twelve genes are transcription factors or involved in transcriptional regulation, and eight of these play roles in cell fate determination and differentiation. A further three are involved in regulation of cell growth and/or in cell proliferation. In addition, gene products of two of the genes, *Gas2* and *Ccne2* are part of the cell cycle machinery, and both are down-regulated in the *Chx10*$^{-/-}$ retina. Altogether, eleven genes are involved in either cell growth or cell proliferation; nine are involved in cell differentiation or cell fate determination, and nine in cell signalling.

A number of the differentially expressed genes are known to play a part in various disorders affecting the eyes. *Fzd4* is involved in retinal angiogenesis and familial exudative vitreoretinopathy (FEVR) is a hereditary ocular disorder characterised by failure of peripheral vascularisation that has been linked to the *Fzd4* locus (Robitaille et al., 2002). *Cyp1b1* is affected in primary congenital glaucoma. A cytochrome P450-dependent arachidonate metabolite that inhibits Na^+K^+-ATPase in the cornea is thought to cause ocular drainage abnormalities (Schwartzman et al., 1987). Optic atrophy and blindness are characteristics of *Naga* deficiency (Schindler et al., 1988), a disorder characterised by neurologic abnormalities and progressive psychomotor deterioration (van Diggelen et al., 1988). *Foxc2* is also associated with eye abnormalities: *Foxc2*$^{+/-}$ mice have anterior segment abnormalities similar to those reported in humans with Axenfeld-Rieger anomaly (Smith et al., 2000). *Foxc1* and *Foxc2* are expressed in the mesenchyme from which ocular drainage structures derive. Mutations in the human homologue of *Foxc1*, *FOXC1/FKHL7*, cause dominant anterior segment defects and glaucoma and various families (Smith et al., 2000). *Tshr* expression is detectable in normal orbital adipose tissues, with increased levels found in orbital tissues from patients with Graves' ophthalmopathy (GO), and in orbital preadipocyte cultures following differentiation (Bhattacharyya et al., 2005).

In addition, a number of the other genes are known to be expressed in the retina. *Foxg1* is normally expressed in most, if not all, nasal RGCs but not in most temporal RGCs (Pratt et al., 2004). Studies show that the gene product of *Foxg1* is involved in brain development, specifically in negative regulation of neuron differentiation and

regulation of the mitotic cell cycle (Hanashima et al., 2002; Vyas et al., 2003; Xuan et al., 1995). *Foxg1* is also involved in axon midline choice point recognition (Pratt et al., 2004) and dorsal/ventral pattern formation (Vyas et al., 2003). The gene showing the most significant change, *Rxrg*, has been shown to be important in photoreceptor development, and is expressed in retinal progenitor cells during eye development in the rat (Azadi et al., 2002; Kelley et al., 1995b; Ying et al., 2000). Both *Dlx2* and *Neurod1,* transcription factors that are involved in cell fate determination, have been shown to be present in the developing eye. *Dlx2* is expressed quite early during retinal development in retinal progenitor cells, whilst *Neurod1* is expressed a little later in development and is thought to be important for regulating neural versus glial fate (de Melo et al., 2003; Morrow et al., 1999a).

A significant number of the differentially expressed genes are expressed in the retinal pigmented epithelium (RPE) of the eye. As the RPE was removed from the retinae in the GeneChip study, this was intriguing. Two of the genes, *Si* and *Dct*, involved in melanin biosynthesis from tyrosine, are specific to the melanocytes present in the RPE (Baxter and Pavan, 2003; Steel et al., 1992). In addition, the RPE is thought to be the source of *Apoe*, specific alleles of which are related to age-related macular degeneration (Anderson et al., 2001). *Trpm1* is expressed in the normal eye and in melanosomal cell lines (Duncan et al., 1998) and its promoter contains 4 consensus binding sites for microphthalmia-associated transcription factor (*Mitf*), a gene required for determining RPE cell fate (Hunter et al., 1998). *Fgf9* is also known to be expressed in a subpopulation of RPE cells as well as in photoreceptors and other neurons of the retina. It is thought to be an autocrine/paracrine factor in the outer retina (Alizadeh et al., 2003). Moreover, activation of FGF receptors in the presumptive RPE by ectopic expression of FGF9 in transgenic mice has been shown to result in a second retina (Zhao and Overbeek, 1999), indicating it may form part of the FGF signalling network thought to regulate RPE versus neural retinal fate.

3.3 Discussion

3.3.1 Considerations for interpreting microarray data

The purpose of this study was to examine differential expression between the wild type and the *Chx10*$^{-/-}$ E11.5 retina in order to ascertain whether the expression of any genes are affected by the absence of Chx10. As Chx10 is a transcription factor, it would be logical to assume it will exert some effect, either directly or indirectly, on a number of other genes expressed at a similar point in development as Chx10. Such genes could then become the basis of further study to examine their own role in the genetic pathway of retinal development as well as their possible roles in the causes of microphthalmia. In the past, potential candidates would have been picked for study based on the knowledge that they are expressed at a similar time point to Chx10 and important for eye development. However, GeneChip technology is an excellent tool for carefully targeting potentially interesting genes, as it is possible to examine a list of genes known to be affected by Chx10. It is possible, for example, to observe differentially expressed genes that would not normally be considered for further study as their role in eye development might be unknown.

A few limits must be taken into consideration upon analysis, however. To date, much of the interest of researchers in microarrays has been directed towards identifying individual genes, the regulated expression of which can explain particular biological phenomena (Schulze and Downward, 2001). This is also the case in this study, where changes in expression of certain genes may lead to clues as to how the *Chx10*$^{-/-}$ phenotype may result from the absence of Chx10. The problem is that microarray experiments, whether based on oligonucleotides or cDNA, are highly capable of generating long lists of genes with altered expression, but they provide few clues as to which of these changes are important in establishing a given phenotype. A given stimulus could potentially lead to changes in the mRNA levels of hundreds of genes, particularly in mammalian systems (Schulze and Downward, 2001). It is important to avoid the temptation to look for genes that conform to existing ideas of how the system might work.

In most cases, careful analysis of the published literature is required before direct experimental investigation of gene function is undertaken. This is complicated by the lack of unified gene ontology. For the examination of human expression arrays, the use of advanced sophisticated literature-searching tools, such as Medminer or high-density array-pattern interpreter (HAPI) which correlates gene accession numbers with MeSH (medical subject heading) keywords, can be very useful for known genes. Functional annotation of new sequences and expressed sequence tags remains a challenge, but is crucial for the interpretation of genome-wide expression data (Schulze and Downward, 2001). In this study, a dedicated Affymetrix data analysis website, Netaffix, and the Mouse Genome Informatics website were used as the first point of call to examine the function of genes that show a change in expression, and further information was retrieved from the Online Inheritance in Man (OMIM) website and research articles about the genes concerned.

The approach to data analysis undertaken in this study mirrors those undertaken in a variety of microarray studies. The use of commercial, and specifically Affymetrix, microarrays is becoming a common phenomenon. They have been used to examine such wide-ranging subjects as the effects of short- and long-term caloric restriction on the liver of aging mice (Cao et al., 2001), the development of the mouse hippocampus (Mody et al., 2001), the regulation of gene expression by Brn3a in developing sensory ganglia (Eng et al., 2004), and gene expression in the eye of a mouse model for Batten Disease (Chattopadhyay et al., 2004). In all cases, a cut-off in the change in expression levels is chosen below which changes are unlikely to signify an important contribution to the study. In this study, the cut-off point chosen was a 1.5-fold change. Rather than suggesting that all genes that show a greater than 1.5-fold change in expression are responding to the absence of Chx10, it suggests that any genes that show a less than 1.5-fold change in expression are more likely to be showing a natural variation in expression rather than a response to Chx10 absence. In other studies, the cut-off point ranged from 1.5- (Cao et al., 2001) to 3-fold (Mody et al., 2001) changes in expression. Similar to the study performed by Eng et al, the genes showing changes in expression were then sorted into functional groups, based on literature and ontology resources. This is a relatively subjective area of the analysis, and is approached in different manners in different studies, but

an attempt at classification is always made (Cao et al., 2001; Chattopadhyay et al., 2004; Eng et al., 2004; Mody et al., 2001).

One final problem that limits the usefulness of microarrays in the analysis of individual pathways is the fact that regulation of mRNA levels is only one aspect of biological control. Protein levels are also controlled at several post-transcriptional steps, and protein activity is controlled by post-translational modification (Schulze and Downward, 2001). Thus, whilst a valuable tool in identifying potentially novel genes and proteins involved in biological processes for which little information exists, this is by no means an all-encompassing, definitive approach.

3.3.2 Chx10 seems to exert a significant effect on cell proliferation, growth and differentiation

Strikingly, many of the identified genes are involved in cell proliferation or regulation of cell growth. As the *Chx10*$^{-/-}$ retina is significantly smaller than the wild type retina, this is an encouraging result. It is interesting that a 2.4-fold decrease in cyclin E2 (*Ccne2*) is observed in *Chx10*$^{-/-}$ retina, as expression of another cyclin, cyclin D1, has previously been shown to be decreased in the *Chx10*$^{-/-}$ retina (Green et al., 2003). Cyclins A, D and E are required for mammalian cells to traverse G1 and enter S phase. Cyclin E controls the initiation of DNA synthesis by activating CDK2; the KIP1 and CIP1 proteins bind and inhibit the cyclin E-CDK2 complex (Gudas et al., 1999; Lauper et al., 1998). It has been suggested that cyclin D1 is necessary for proliferation to progress in the *Chx10*$^{-/-}$ retina, as it may be required for *Chx10*$^{-/-}$ dependent-modulation of $p27^{Kip1}$. It is possible that Cyclin E may play a similar role.

Gas2 is another cell cycle gene that shows a decrease in expression. It tends to be expressed during growth arrest and is a component of the microfilament system (Brancolini et al., 1992). When expressed in mammalian cells, human *Gas2* localised at the actin cytoskeleton, along the stress fibres and at the plasma membrane (Collavin et al., 1998). Its decrease in expression in the *Chx10*$^{-/-}$ retina is another indication that the small size of the *Chx10*$^{-/-}$ retina may in some way arise from a mis-regulation of the cell cycle.

Not all genes with a function in proliferation that showed a change in expression are necessarily known to be expressed in the eye. For example, the *Myb* gene encodes proteins that are critical for hematopoietic cell proliferation and development, and there is evidence that disrupting *Myb* function might be an effective therapeutic strategy for controlling leukemic cell growth (Ratajczak et al., 1992). Detailed analysis of hematopoiesis in *Myb* homozygous mutant mice revealed distinct blocks in T-cell, B-cell, and red blood cell development, as well as a 10-fold increase in the number of hematopoietic stem cells. Cell cycle analysis showed that twice as many hematopoietic stem cells were actively cycling in mutant mice compared with wildtype mice (Sandberg et al., 2005). *Vegfb,* a growth factor expressed in muscle and in the heart, can promote angiogenesis (Olofsson et al., 1996; Silvestre et al., 2003). Cellular retinoic acid-binding protein (*Crabp1*) is assumed to play an important role in various retinoic acid-mediated differentiation and proliferation processes (OMIM entry *180230; Vogel). *Foxg1* has been shown to be involved in the regulation of the cell cycle in the brain (Vyas et al., 2003). To see a change in such genes in this study is interesting because of their known roles in proliferation generally or specifically in other cell types. It would be of interest if these roles are retained in the developing eye.

In addition to changes in expression of genes important for proliferation and growth, a number of the changed genes are involved in cell differentiation or signalling. Chx10 itself is shown to be down-regulated in the *Chx10*$^{-/-}$ retina, with both sets of probe pairs for this gene showing a similar fold-change in expression (Table 3.2). It is interesting that Chx10 shows a change in expression, but not entirely surprising. The Chx10 mRNA is detected in the *Chx10*$^{-/-}$ retina (Rutherford et al., 2004), but the mRNA contains a premature stop codon and is likely to be degraded by a process such as nonsense-mediated mRNA decay (NMD), in which the cell is rid of non-functional mRNAs arising from mutations and processing errors (Weischenfeldt et al., 2005). Thus a decrease in the *Chx10* mRNA transcript is reflected in the microarray study. Five genes, *Neurod1*, *Dlx2*, *Fgf9*, *Foxg1*, and *Rxrg*, are expressed specifically in the eye. As stated in section 3.2.6, both *Dlx2* and *Neurod1* are expressed early in retinal development and play roles in cell fate determination (de Melo et al., 2005; Morrow et al., 1999a) and *Fgf9* is also known to be expressed in a subpopulation of RPE cells as well as in photoreceptors and other neurons of the

retina (Alizadeh et al., 2003). *Foxg1* is normally expressed in most, if not all, nasal RGCs but not in most temporal RGCs (Pratt et al., 2004) and *Rxrg* has been shown to be important in photoreceptor development, and is expressed in retinal progenitor cells during eye development in the rat (Azadi et al., 2002; Kelley et al., 1995b; Ying et al., 2000). In addition, *Cnot7*, another gene showing differential expression, is a transcriptional cofactor, known to co-regulate *Rxrb* by binding to its AF-1 domain in testicular somatic cells. *Rxrb* malfunctions in the absence of *Cnot7* (Nakamura et al., 2004).

A number of transcription or signalling factors that are known to play a role in other cell types have also shown a change in expression. It's been shown that expression of individual *Tle* genes correlated with immature epithelial cells that are progressing toward that terminally differentiated state, suggesting a role during epithelial differentiation. In both normal tissues and tissues resulting from incorrect or incomplete maturation events, *Tle* expression was elevated and coincided with Notch expression, implicating these molecules in the maintenance of the undifferentiated state in epithelial cells (Liu et al., 1996). *Bhlhb2* is a transcription factor involved in the regulation of chondrocyte differentiation via the cAMP pathway (Shen et al., 1997). The gene product of *Prkca* is involved in the induction of positive chemotaxis, neutrophil chemotaxis, the positive regulation of inflammatory response, and the induction of apoptosis by intracellular signals (Cataisson et al., 2003). As with the cell proliferation genes expressed in tissues other than the eye, changes in these genes may indicate novel roles for them in the retina, or conversely, previously unidentified roles for Chx10.

3.3.3 Changes in expression of genes involved in cell adhesion and fat metabolism and the immune system

Two of the differentially expressed genes are involved in cell adhesion, *Cdh8* and *Cldn1*. Cadherins mediate calcium-dependent cell-cell adhesion and cadherin 8 has been shown to be expressed during retinal development and in the adult eye (Honjo et al., 2000). Claudin 1 is associated with tight junctions (Furuse et al., 1998). *Cldn1* is a member of a superfamily of epithelial membrane proteins (EMPs), which may have multiple potential functions, including maintenance and regulation of cell

polarity and permeability, perhaps through mechanisms involving tight junctions (Swisshelm et al., 1999). It is interesting that these two genes show a difference in expression, as *Chx10*$^{-/-}$ retinal progenitor cells may have different adhesive properties to those of the wild type.

Four genes involved in adipocyte metabolism or differentiation, *Foxc2*, *Tpra40*, *GATA3,* and *Tshr*, have shown a change in expression. Cederberg et al identified *Foxc2* as a key regulator of adipocyte metabolism. In mice over-expressing *Foxc2* in white adipose tissue (WAT) and brown adipose tissue (BAT), the intra-abdominal WAT depot was reduced and has acquired a brown fat-like histology, whereas interscapular BAT was hypertrophic (Cederberg et al., 2001). *Tshr* expression is increased in orbital tissues from patients with Graves' ophthalmopathy (GO), and in orbital preadipocyte cultures following differentiation (Bhattacharyya et al., 2005). The orbit of the *Chx10*$^{-/-}$ eye contains what appear to be large deposits of fatty tissue, described as hypertrophied Harderian and lachrymal glands in one study (Truslove, 1962), and thus it would be of interest to examine whether changes in adipocyte metabolism or differentiation are an effect of Chx10 absence.

Three of the differentially expressed genes are normally associated with the immune system: *Prkcb1*$^{-/-}$ mice are immuno-deficient, showing characteristics similar to X-linked immunodeficiency (Leitges et al., 1996). *GATA3* is expressed in T cells and participates in T cell receptor activation. *GATA3* is necessary and sufficient for Th2 cytokine gene expression (Zheng and Flavell, 1997), and is critical for the expression of the *IL5* gene in Th2 cells (Zhang et al., 1997). Tong showed that murine *GATA2* and *GATA3* are specifically expressed in white adipocyte precursors and that their down-regulation sets the stage for their terminal differentiation. Constitutive *GATA2* and *GATA3* expression suppressed adipocyte differentiation and trapped cells at the preadipocyte stage (Tong et al., 2000). *Stat6* activates *IL4* and is involved in Th2 cell differentiation. As yet there is no indication that Chx10 plays any significant part in the immune system, but it could be an interesting subject for research.

Thus, the microarray data provide an interesting overview of the mechanisms potentially controlled by Chx10. A few genes controlling cell proliferation have changed in expression, but more strikingly, a large number of transcription factors,

particularly ones that control various aspects of cell differentiation, have changed in expression in the *Chx10*$^{-/-}$ retina. Although cell proliferation and differentiation are often intricately linked, it seems Chx10 may be exerting its effects more through cell differentiation mechanisms than through changes in the cell cycle.

Whilst encouraging, it is important to remember, however, the data obtained from this experiment are not necessarily the definitive list of genes whose expression is altered in the developing eye by a lack of Chx10. It is important to note, for example that three genes previously shown to be up- or down-regulated in the *Chx10*$^{-/-}$ retina, retinoid related orphan receptor B (Chow et al., 1998), *Foxn4* (Gouge et al., 2001) and cyclin D1 (Green et al., 2003) and that were present on the microarray, did not show any significant difference in expression in this study. The analysis of the data is to some extent subjective, depending on such factors as correctly, linearly amplified high quality RNA, the type of parametric tests selected to analyse the microarray data, the restrictions I've chosen to impose on the data, and even the type of chips available at the time. The amplification step used in this study was chosen based on its success in previous studies, but there is no guarantee that no targets were lost as a result of the amplification strategy. The statistical analysis used here is also quite stringent, thus producing a relatively small list of differentially expressed genes. To some extent I have tried to look at some genes that did not pass the statistical analysis based on their correlation with other differentially expressed genes, but it is possible that genes that are in fact regulated by Chx10 did not pass the analysis. It is important to consider that a different approach to the analysis of the raw data may have produced different results.

3.3.4 Genes selected for further study

Once a set of genes has been identified, their function has to be modulated in such a way as to directly determine their degree of involvement. The gene list produced in this study seems to present a plausible snapshot of gene expression at E11.5 in the wild type and *Chx10*$^{-/-}$ retina. Many of the genes in the list are known to be expressed in the eye at this time point and examination of the literature available regarding these genes has produced some idea of how Chx10 affects retinal development. However, it is important to verify whether these genes are indeed differentially

expressed and whether they are directly regulated by Chx10. Ideally, all genes would be examined further, but time constraints have led me to choose some of the most interesting and most significantly changed genes to examine initially.

Some of the genes that show the most significant changes in expression, such as *Rxrg* or *Dlx2*, are genes that would not immediately be considered as potential candidates for Chx10 regulation, as they have not been studied in detail in the developing retina and thus their potential importance is as yet unknown. These genes, along with *Neurod1*, seem to play a large part in cell differentiation and cell fate determination, processes Chx10 appears to exert a large effect upon. In addition, a number of genes that show differential expression are normally expressed in the RPE (*Dct, Si, Apoe, Fgf9*). This pattern of expression change suggests that perhaps one way in which Chx10 regulates retinal development is through the specification of the retina in favour of the RPE.

Thus, of the list of genes in Tables 3.2 an 3.3, I have chosen to examine in further detail the expression of retinoid X receptor (Saga et al., 1999), dopachrome tautomerase (*Dct*), silver (*Si*) – the three most up-regulated genes-, distal-less homeobox 2 (*Dlx2*), neurogenic differentiation 1 (*Neurod1*) and cadherin 8 (*Cdh8*) – the three most down-regulated genes, with the exception of silver, which was selected in preference to *Apoe* because of its early RPE expression and close association with *Dct*. All six are shown to be significantly up- or down-regulated more than 2-fold in the $Chx10^{-/-}$ retina compared to the wild type retina and five of these genes may be part of a $Chx10^{-/-}$ regulated retinal versus RPE specification system as discussed above. This study will form the subject of the following chapter.

CHAPTER 4

Analysis of Putative Chx10 Target Genes

4.1 Introduction

The aim of the microarray study described in the previous chapter was to identify genes that are regulated by Chx10 and in this way discover the molecular basis for the *Chx10*$^{-/-}$ microphthalmic phenotype. The expression of a number of genes has been shown to be either up- or down-regulated in the E11.5 *Chx10*$^{-/-}$ retina compared to the wild type. As discussed, the nature of these genes and their various functions give some indication as to how Chx10 might control various aspects of eye development. However, before any conclusions can be drawn, it is important to verify whether these are genuine changes in expression, and to compare their patterns of expression to begin to determine whether these changes are likely to result from direct transcriptional regulation by Chx10, or as an indirect effect of its function. Ideally, all 54 characterised genes that showed a change in expression would be examined further to verify their expression in the wild type and *Chx10*$^{-/-}$ retina and tested for regulation by Chx10. However, as is the case with many microarray experiments, examining all the genes that show a change in expression in further detail is a daunting and time consuming task and was beyond the scope of this thesis. A more realistic approach taken here was to choose a small number of genes that are potentially interesting and by analysis of these, validate the broader set of data from the microarray.

The microarray experiment has yielded a list of eight genes statistically significantly up- or down-regulated by more than 2-fold in the absence of Chx10. I have chosen to study six of these in further detail. The three genes shown to be most significantly up-regulated in the absence of Chx10 are retinoid x receptor gamma (*Rxrg*), silver *(Si,)* and dopachrome tautomerase *(Dct)*. Their up-regulation suggests that these three genes are normally repressed in the presence of Chx10. In addition, I further examined three genes that were down-regulated in the absence of Chx10: distal-less 2 *(Dlx2)*, neurogenic differentiation 1 (*Neurod1*), and cadherin 8 *(Cdh8)*. Their down-regulation in expression suggests that these three genes are normally activated in the presence of Chx10. Whether any of these genes are directly regulated by Chx10 remains to be seen, but in at least an indirect manner, it seems Chx10 may play a dual role as an activator and a repressor.

Rxrg showed the greatest change in expression in the *Chx10*$^{-/-}$ retina compared to the wild type. Retinoic acid is of vital importance for proper function of the retina and retinoic acid activity is mediated by interaction with nuclear retinoic acid receptors and retinoid X receptors (Janssen et al., 1999). Retinoid X receptors respond to 9-cis-retinoic acid and also serve as heterodimeric partners for the vitamin D receptor, thyroid hormone receptors, and retinoic acid receptors, A, B and G (Mangelsdorf et al., 1992). A lack of Chx10 causes it to be up-regulated nearly 18-fold, suggesting a link between Chx10 and retinoic acid signalling. The other two up-regulated genes I have selected are dopachrome tautomerase (*Dct*) and silver (*Si*). Both of these genes are normally expressed in the developing retinal pigmented epithelium (RPE) and are thought to be important for the specification of melanocytes (Baxter and Pavan, 2003). Their expression in the *Chx10*$^{-/-}$ retina is therefore unusual and hints at a role for Chx10 in specification of the neural retina by repression of RPE genes.

Two of the genes that are down-regulated, *Dlx2* and *Neurod1*, are known to be involved in development of the forebrain. Their role in retinal development is less well studied, but as with *Si* and *Dct*, the *Dlx2* and *Neurod1* proteins seem to be involved in cell fate specification, both in the CNS and in the developing retina (Liu et al., 2000a; Miyata et al., 1999; Qiu et al., 1995). The final gene chosen for examination is cadherin 8 (*Cdh8*), an integral membrane protein that mediates calcium-dependent cell adhesion. It has been proposed that cadherins are involved in the sorting and aggregation of early neurons during central nervous system development and in the formation of brain nuclei and cortical laminae (Korematsu and Redies, 1997). A similar role during early retinal development is as yet unclear.

In order to confirm the differential expression of the genes obtained from the microarrays, real time RT-PCR (RT-PCR) was used. Because differences in gene expression between the wild type and *Chx10*$^{-/-}$ retina were mostly within a ten-fold change of each other (excepting *Rxrg* and *Dlx2*), it was important to use a sensitive method to verify these changes. Traditional end-point RT-PCR using agarose gels is only semi-quantitative, showing at best only a 10-fold change, as ethidium bromide is not very sensitive and agarose gel resolution poor. Real-time RT-PCR can accurately detect a 2-fold difference in expression. In addition, real time PCR allows one to measure the product of amplification during the early exponential phase of

amplification, when product is doubling with every cycle, whilst end-point RT-PCR only allows measurement of product at the end of the plateau stage of amplification, when products can be highly variable (http://www.appliedbiosystems.com/support/tutorials/pdf/rtpcr_vs_tradpcr.pdf). This is illustrated in Figure 4.1 where PCR amplification of a series of 10-fold dilutions is displayed on both a linear scale and a logarithmic scale. As the sample is diluted, it takes more cycles before the amplification is detectable. If the reactions were stopped at, for example, 33 cycles, as would be the case in traditional end-point PCR, the blue, red and purple reactions would indicate the same amount of product even though the reactions shown by the purple and red lines differ by a factor of 100 in the amount of cDNA. The logarithmic graph illustrates the importance of examining the product in the much earlier, exponential phase of amplification. The orange threshold line is set at the point where the reactions show a series of equally spaced curves in order of dilution. On the linear graph this is at the very beginning of the upturn of the curve and not in what appears to be the linear region of the curve. In real time PCR, it is possible to measure the cycle number at which the increase in fluorescence (and therefore cDNA) is logarithmic.

The measured fluorescence is a result of the chemistry of real time PCR. A number of approaches are available. The one used in this study is the TaqMan probe system. In addition to forward and reverse primers, a TaqMan probe is designed to hybridise to a given sequence between the forward and reverse primer sequences. The TaqMan probe is a linear oligonucleotide probe that contains a 5' reporter fluorophore and a 3' quencher at the ends of the probe. When the probe is intact, the quencher dye absorbs the fluorescence of the reporter dye due to their close proximity to each other. When the probe is hybridised to the target, it is hydrolysed by the exonuclease activity of the Taq DNA polymerase, resulting in the separation of the reporter dye from the quencher and an increase in the fluorescence emission (Figure 4.2).

In addition to using RT-PCR, I used whole mount *in situ* hybridisation (ISH) to examine the expression of the differentially expressed genes in the E11.5 and E12.5 wild type and *Chx10*$^{-/-}$ mouse and retina. Frozen sections of retinae at later time points were also examined through ISH. The ISH studies were designed to give a

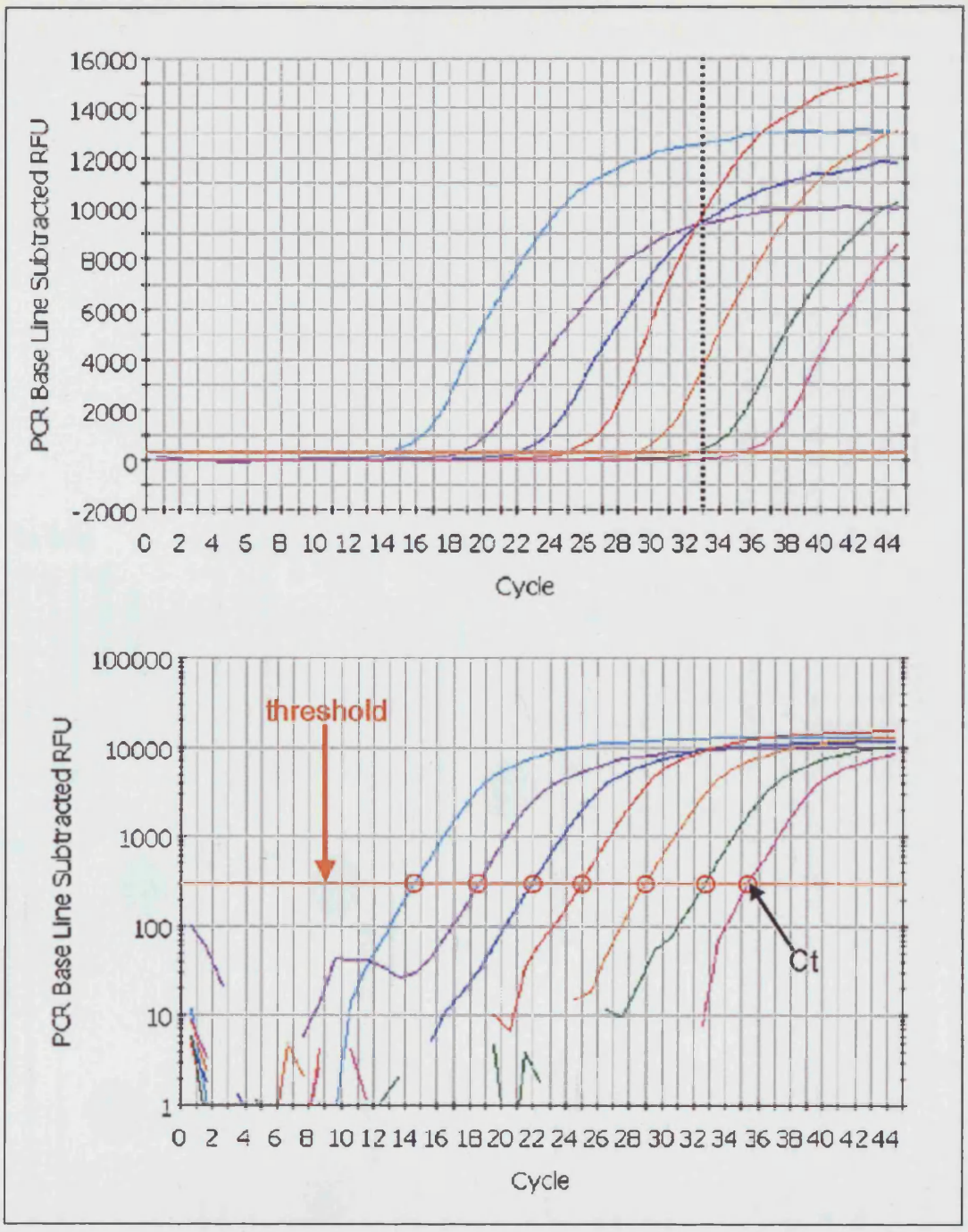

Figure 4.1: PCR amplification of a series of 10-fold dilutions is displayed on both a linear scale and a logarithmic scale. As the sample is diluted, it takes more cycles before the amplification is detectable. If the reactions were stopped at, for example, 33 cycles, blue, red and purple reactions would indicate the same amount of product even though the reactions shown by the purple and red lines differ by a factor of 100 in the amount of cDNA. The orange threshold line is set at the point where the reactions show a series of equally spaced curves in order of dilution on the logarithmic (bottom) scale and the threshold cycle (Ct) is shown for each sample. On the linear graph (top) this is at the very beginning of the upturn of each curve and not in what appears to be the linear region of the curve. In real time PCR, it is possible to measure the cycle number at which the increase in fluorescence (and therefore cDNA) is logarithmic. Figure adapted from online real time pcr tutorial by Dr. Margaret Hunt at Unifersity of South Carolina School of Medicine (http://pathmicro.med.sc.edu/pcr/realtime-home.htm)

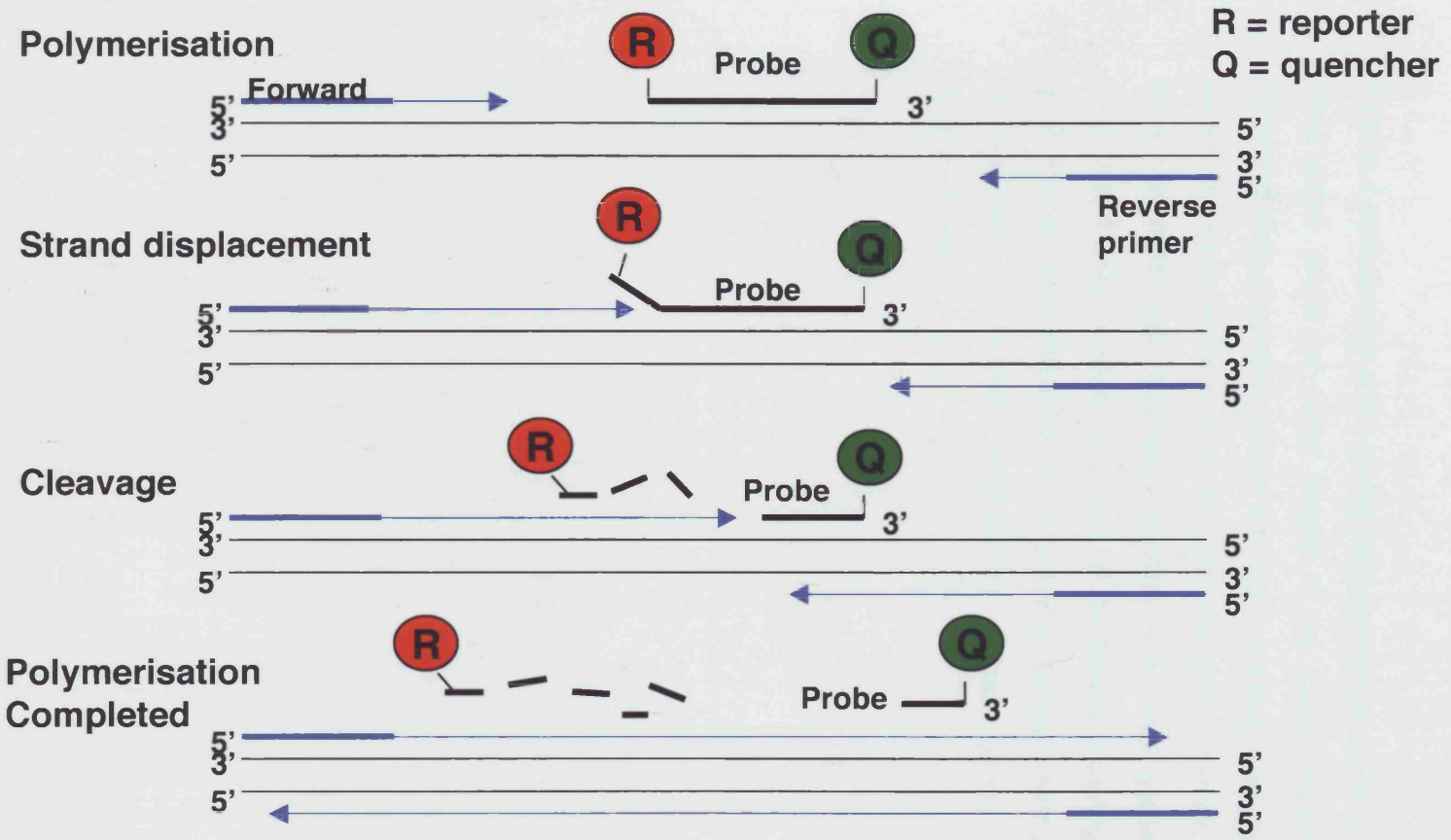

Figure 4.2: Quantitative real time RT-PCR chemistry. In addition to forward and reverse primers, a TaqMan probe is designed to hybridise to a given sequence between the forward and reverse primer sequences. The TaqMan probe is a linear oligonucleotide probe that contains a 5' fluorophore and a 3' quencher at the ends of the probe. When the probe is intact, the quencher dye absorbs the fluorescence of the reporter dye due to their close proximity to each other. When the probe is hybridised to the target, together with the primers, it is hydrolysed by the exonuclease activity of the Taq DNA polymerase as the DNA strand is being synthesised , resulting the separation of the reporter dye from the quencher and an increase in the fluorescence emission upon completion of strand synthesis.

visual confirmation of expression changes in the wild type and *Chx10*$^{-/-}$ retinae, as well as allowing the observation of specific areas of expression within the embryo and the retina. In addition, they served to test whether patterns of expression overlapped with Chx10 and therefore whether RPC expression of Chx10 is likely to directly regulate their expression

Finally, I performed *in silico* studies of the above genes. In order to examine whether these genes might be direct targets of the Chx10 transcription factor, I have examined their promoter regions for Chx10 binding sites. Potential Chx10 binding sites found close to the start of the CDS of a given gene were further examined for conservation through sequence alignment with other species. In addition, I have compared the chromosome positions of the human homologues of these genes, as well as other genes identified in the previous chapter, with known microphthalmia loci in order to discover whether any of these genes might be a cause of microphthalmia.

4.2 Results

4.2.1 Retinoid X receptor gamma

The most dramatic change in expression observed in the microarray study was that of retinoid X receptor gamma. Expression of this gene was increased 17.9-fold in the *Chx10*$^{-/-}$ retina compared to the wild type. In order to verify this change in expression by RT-PCR, for *Rxrg* as well as for the other genes examined in this chapter, total RNA from three pools of E11.5 wild type and *Chx10*$^{-/-}$ retinae were collected in addition to one pool for a pilot experiment (Table 4.1). This approach mirrors the conditions used for the microarray study.

Pool	Tissue Collected	Somite Range
129/Sv pilot	16 retinae from 8 individuals	40-44
129/Sv 1	30 retinae from 15 individuals	41-44
129/Sv 2	36 retinae from 19 individuals	41-45
129/Sv 3	35 retinae from 18 individuals	42-46
Chx10$^{-/-}$ pilot	26 retinae from 13 individuals	41-48
Chx10$^{-/-}$ 1	30 retinae from 15 individuals	41-45
Chx10$^{-/-}$ 2	36 retinae from 18 individuals	42-46
Chx10$^{-/-}$ 3	34 retinae from 17 individuals	41-47

Table 4.1: Number of retinae collected per pool of tissue used in the real time RT-PCR study and the somite range for each pool

A pilot study was conducted using primers and probe for the two most changed genes, *Rxrg* and *Dlx2*, in order to test sensitivity, as RT-PCR is a relatively new approach as yet untested in our laboratory. Reverse transcription, using 1 μg of RNA, was performed once using the pilot RNA samples and a single PCR run performed, using for each gene, with the housekeeping gene, glyceraldehyde-3-phosphate dehydrogenase (*Gapdh)* as a control. Reverse transcription was performed twice on RNA samples in pool 1, and RT-PCRs run using cDNA from both RTs. Reverse transcription was performed once for samples in pools 2 and 3. 18s RNA was used as a control in addition to *Gapdh* for pools 2 and 3. H_2O non-template controls were used for every gene to check for possible contamination. This applies to all genes tested through RT-PCR described below.

The real time PCR results are depicted as amplification graphs in Figure 4.3. In all cases, the amplification products from the *Chx10*$^{-/-}$ retina were detectable at earlier cycles than those from the wild type retina, with any replicates showing very close correlation. This indicates that there was more of the target cDNA present in the *Chx10*$^{-/-}$ retina than in the wild type 129/Sv retina. An example of a control *Gapdh* amplification curve is also shown on Figure 4.3. There was little detectable difference in *Gapdh* amplification curves between the wild type and *Chx10*$^{-/-}$ retina for Pool 1, RT1, suggesting that the difference in *Rxrg* amplification product between the wild type and the *Chx10*$^{-/-}$ retina is due to a difference in *Rxrg* expression rather than a difference in loading. The threshold was set within the lower part of the linear range for every experiment (horizontal green lines, Figure 4.3). As the product of amplification doubles with every cycle number, the difference between the threshold cycles (Ct, where the fluorescence passes the threshold) of the wild type and *Chx10*$^{-/-}$ samples, after normalisation against *Gapdh*, allows calculation of the fold-change in expression between the two (see ΔΔCt method described in Chapter 2). The fold-change values for *Rxrg* expression in the *Chx10*$^{-/-}$ retina compared to the wild type retina are as detailed in Table 4.2. *Chx10*$^{-/-}$ pool 1 was compared to wild type pool 1, *Chx10*$^{-/-}$ pool 2 compared to wild type pool 2, etc. All are normalised against *Gapdh* expression.

Pool	Increase/Decrease	Fold-change
Pilot	Increase	6.2
Pool 1 RT1	Increase	13.9
Pool 1 RT2	Increase	7.1*
Pool 2	Increase	10.7* (8.8-13.1)
Pool 3	Increase	12* (10.3-14.2)

Table 4.2: Relative change in expression of *Rxrg* in *Chx10*$^{-/-}$ retinae compared to wild type retinae for each set of retinal pools collected for real time PCR. * Indicates result of fold-change calculation based on average of Cts of duplicate runs. Numbers in parentheses indicate a range of fold-changes, based on calculations including a standard deviation between duplicate runs.

The above table indicates that there is an increased amount of expression of *Rxrg* in the *Chx10*$^{-/-}$ retina compared to the wild type retina. The fold changes are slightly variable, but it seems *Rxrg* expression is increased roughly 10-fold in the *Chx10*$^{-/-}$ retina. These data correspond with the microarray data, where a 17.9-fold increase in *Rxrg* expression was observed in the *Chx10*$^{-/-}$ retina compared to the wild type. Pools 2 and 3 were also normalised against 18s RNA with similar results. However, some

Figure 4.3: RT-PCR amplification curves for *Rxrg*. Amplification curves depicted as cycle number versus Delta Rn (baseline corrected normalised fluorescence). Amplification curves shown for the pilot experiment and for cDNA from all 3 cDNA pools. For Pools 2 and 3, the PCRs were run as duplicates. *Chx10*$^{-/-}$ amplification curves are consistently to the left of the wild type curves. An amplification curve is also shown for GAPDH, to which the products were normalised. H_2O controls were used in all experiments, with fluorescence above the threshold level considered as contamination. An H_2O control run can be seen on the GAPDH graph.

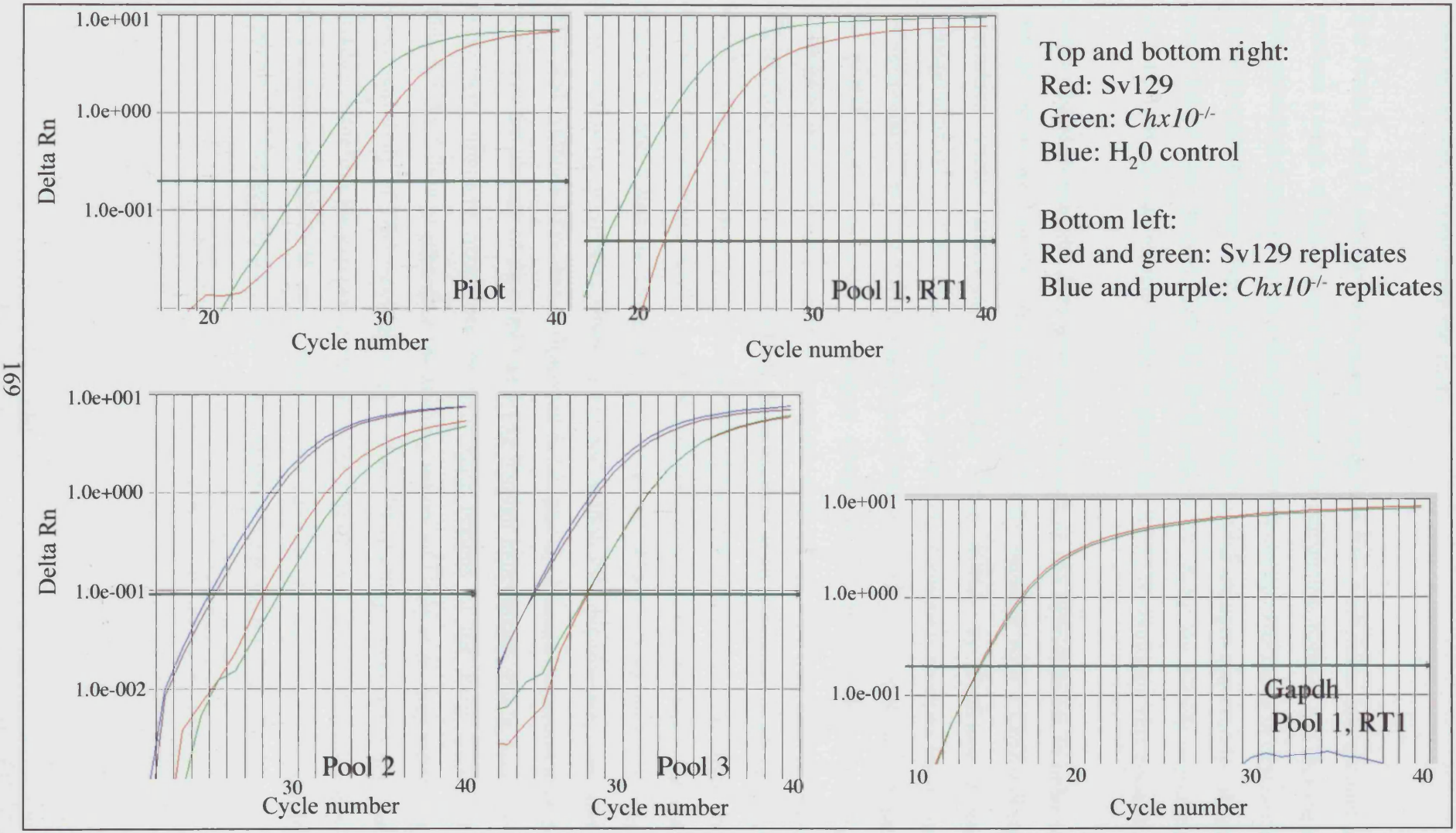
1.0e+001
1.0e+000
1.0e-001
Delta Rn
Pilot
20
30
40
Cycle number
Pool 1, RT1
20
30
40
Cycle number
Top and bottom right:
Red: Sv129
Green: Chx10-/-
Blue: H20 control
Bottom left:
Red and green: Sv129 replicates
Blue and purple: Chx10-/- replicates
1.0e+001
1.0e+000
1.0e-001
1.0e-002
Delta Rn
Pool 2
30
40
Cycle number
Pool 3
30
40
Cycle number
1.0e+001
1.0e+000
1.0e-001
Gapdh
Pool 1, RT1
10
20
30
40
Cycle number

contamination was observed in the H_2O control for 18s rRNA and thus *Gapdh* was used as the control throughout the study.

For Pools 2 and 3, standard deviations of duplicate runs were taken into account to produce a range of fold-change (see chapter 2 for calculation method) and thus these data provide the most complete reflection of the fold-change difference in expression of the five experiments. Figure 4.4 summarises the fold-changes observed for all six genes tested (see below). The RT-PCR results for *Rxrg* are clearly consistent between runs, and this reproducibility suggests the RT-PCR results are very accurate.

I also wished to examine *Rxrg* expression through *in situ* hybridisation. In order to produce riboprobes for the ISH study, I was kindly supplied with a CMX-mRxrg expression vector containing the mouse *Rxrg* cDNA by Professor Evans (Mangelsdorf et al., 1992) (See Chapter 2 for details of plasmids received for *in situ* hybridisation). The *Rxrg* cDNA was excised from the CMX vector and inserted into the $pSKII^+$ vector, in order to prepare riboprobes for ISH experiments. *Rxrg* expression was previously reported in various areas of the wild type embryo using ^{35}S-labelling probes in ISH, including the myotomes at all segmental levels of trunk and tail and facial muscle primordia, the central nervous system, including the forebrain and striatum, and in sensory and endocrine tissues, including the otic epithelium and retina by Dolle et al (Dolle et al., 1994). These data were not reproduced here, in repeated whole mount and section ISH experiments, even after replicated synthesis of probes as described in Chapter 2, although restriction digests confirmed the identity of the cDNA as *RXRg*. Further experiments will be necessary to generate effective riboprobes by subcloning regions of the *Rxrg* cDNA. In addition, the failure to reproduce the staining pattern of Dolle et al. may reflect the lower sensitivity of DIG labelling compared to ^{35}S labelling. Although it was not possible to confirm the expression change in the *Chx10*$^{-/-}$ retina by ISH in this study, nevertheless, the RT-PCR data obtained here confirm the significant change in expression of this gene in the *Chx10*$^{-/-}$ retina as observed in the previous chapter.

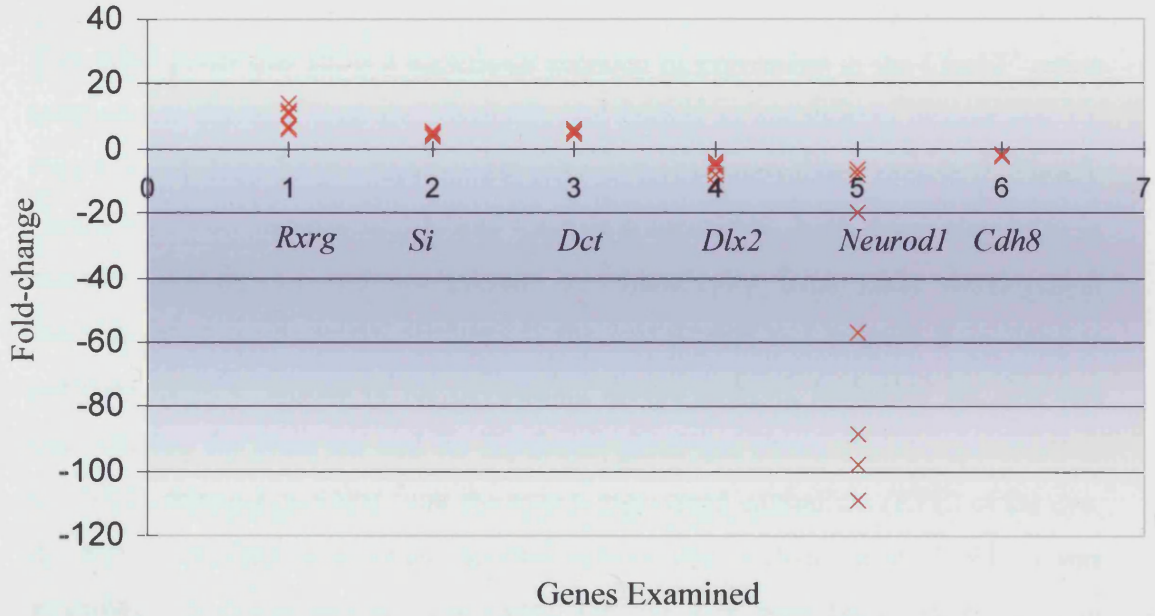

Figure 4.4: Fold-change data from real time PCR experiments for all six genes examined. The fold-changes calculated for each experiment, based on the ΔΔCt method, are given for each gene, as listed along the X-axis. An increase in expression in the *Chx10*$^{-/-}$ retina compared to the wild type is depicted by a positive fold-change value, whilst a decrease in expression is depicted by a negative fold-change value. Very little variation was found between repeated experiments for all but one gene, *Neurod1*, from which highly varied results were obtained. Fold-changes per gene were either all positive or all negative, and their change in expression correlated with the mircroarray data obtained in Chapter 3.

4.2.2 Silver and dopachrome tautomerase

Two other genes that show a significant increase in expression in the *Chx10*$^{-/-}$ retina compared to the wild type are silver (*Si*, also known as melanocyte protein mel 17, *Pmel17*) and dopachrome tautomerase (*Dct* or tryosinase-related protein 2, *Tyrp2*). They showed an increase of 3.5- and 4.8-fold respectively. Both genes play roles in melanin biosynthesis and are present in melanocytes from early development onwards. Most melanocytes originate in the neural crest and migrate from there to populate specific regions of the developing mouse embryo, including the skin and hair follicles, the inner ear and the Harderian gland and choroid of the eye (Steel et al., 1992). Melanocytes that form the retinal pigmented epithelium (RPE) of the eye, in contrast, develop from locally derived neuroectoderm (Steel et al., 1992). It was surprising that genes normally associated with the RPE were being up-regulated in the *Chx10*$^{-/-}$ retina. The presence of RPE-specific genes in the *Chx10*$^{-/-}$ retina may indicate some disruption in the specification of the retina and/or RPE.

Real time RT-PCR was performed as described in section 4.2.1. Amplification curves obtained from the RT-PCR study are provided in Appendix 2. The comparative Ct method was used to calculate the fold-change in gene expression in the *Chx10*$^{-/-}$ retina compared to the wild type and the normalised results summarised in Table 4.3. The amplification for Pool 1 RT1 failed for *Dct*, and thus no change in expression is noted for this run. As for *Rxrg*, standard deviations of duplicate runs were taken into account to produce a range of fold-change for Pools 2 and 3 (see chapter 2 for calculation method) and thus these data provide the most complete reflection of the fold-change difference in expression of the four experiments.

	Si			*Dct*	
Pool	**Increase/Decrease**	**Fold-change**		**Increase/Decrease**	**Fold-change**
Pool 1RT1	Increase	4.6		-	-
Pool 1RT2	Increase	3.4		Increase	6.3*
Pool 2	Increase	5.5* (4.8-6.2)		Increase	5.4* (4.6-6.4)
Pool 3	Increase	3.6* (2.7-4.9)		Increase	4.2* (2.8-6.3)

Table 4.3: Relative change in expression of *Si* and *Dct* in *Chx10*$^{-/-}$ retinae compared to wild type retinae for each set of retinal pools collected for real time PCR. * Indicates result of fold-change calculation based on average of Cts of duplicate runs. Numbers in parentheses indicate a range of fold-changes, based on calculations including a standard deviation between duplicate runs.

The above table indicates that there is an increased amount of expression of both *Si* and *Dct* in the *Chx10*$^{-/-}$ retina compared to the wild type retina. As with *Rxrg*, the fold changes are slightly variable (see Figure 4.4 for comparison), but it seems expression of *Si* is increased roughly 4-fold and of *Dct* roughly 5-fold in the *Chx10*$^{-/-}$ retina. These data correspond well with the microarray data, where a 3.54 and 4.8-fold increase in *Si* and *Dct* expression respectively were observed in the *Chx10*$^{-/-}$ retina compared to the wild type. These figures fall into the fold-change ranges produced for Pools 2 and 3, and the results were reproducible across several runs. Pools 2 and 3 were also normalised against 18s RNA with similar results.

In addition to RT-PCR, silver and dopachrome tautomerase expression were also examined using *in situ* hybridisation. Figure 4.5A-D shows whole mount ISH staining for silver at both E11.5 and E12.5 in wild type and *Chx10*$^{-/-}$ embryos. At E11.5 melanocytes can be observed migrating away from the neural crest (Figure 4.5A, B, arrows). An abundant presence of silver mRNA was also observed in the retinal pigmented epithelium of the eye (Figure 4.5A, inset). At E12.5, the silver expression can be observed in the limbs of both the wild type, and *Chx10*$^{-/-}$, embryos (Figure 4.5C, D). Again, the RPE was darkly stained in both genotypes, but it was difficult to tell if there was any difference in expression between the two, either in the RPE or the retina (Figure 4.5C, D insets).

30 μm vibratome sections of the retinae of the treated embryos were examined (Figure 4.5E-H) in order to assess whether any differences in silver expression could be observed between the wild type and *Chx10*$^{-/-}$ retinae. A few individual melanocytes can be observed just outside the RPE of all sections. At both E11.5 and E12.5 the wild type RPE shows high silver expression, whilst silver mRNA was faintly detected in the retina at E11.5 but not at E12.5 (Figure 4.5E, G). In the *Chx10*$^{-/-}$ eye, the RPE is also exhibits high silver expression, and expression seems more extensive, especially around the periphery of the RPE and retina (Figure 4.5F, H, arrows). The border between the RPE and retina is obscured by heavy staining. The retina itself shows a greater presence of silver mRNA at both time points compared to the wild type retina, suggesting increased silver expression in the retina as well as the RPE.

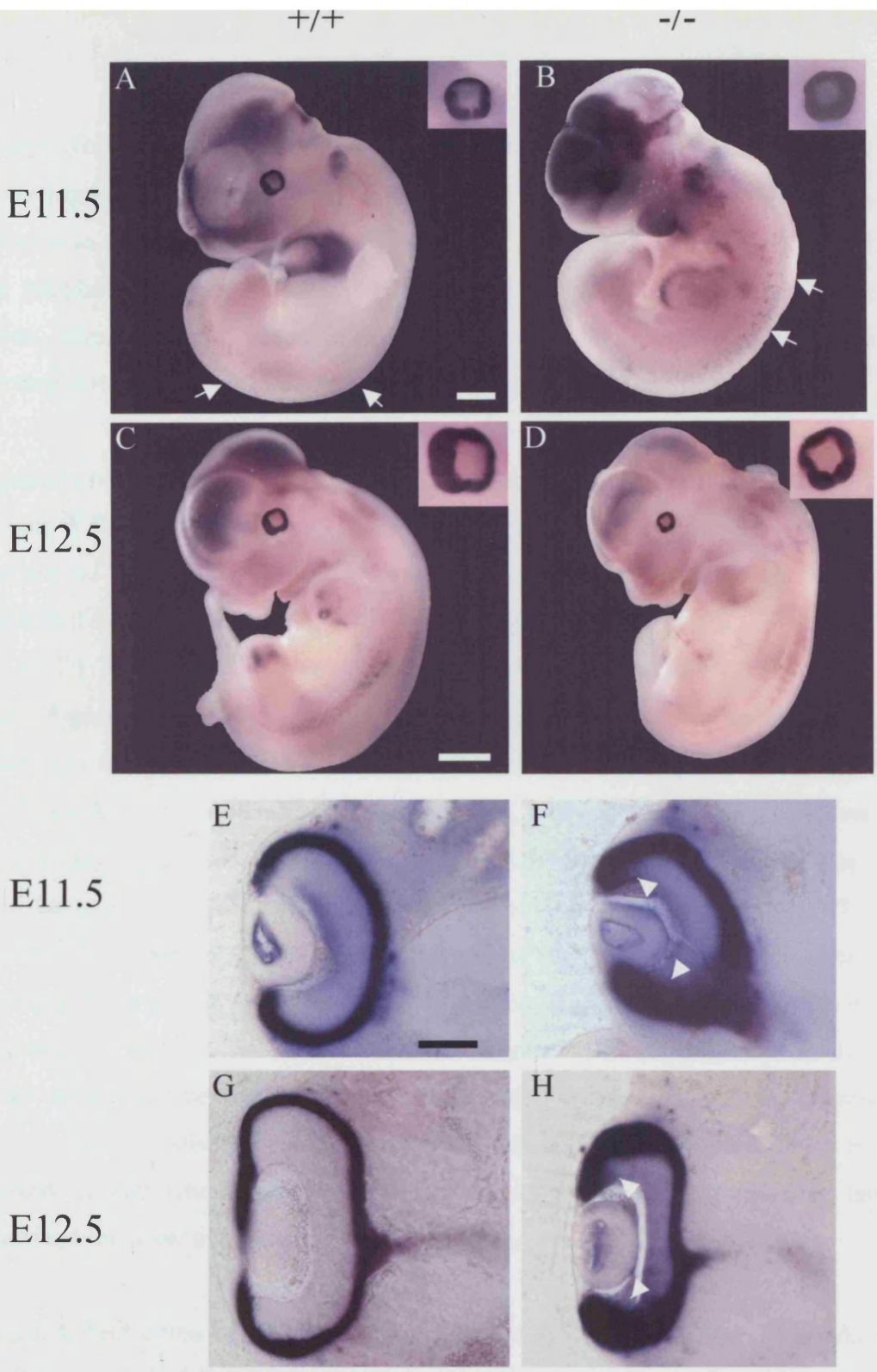

Figure 4.5: Whole mount *in situ* hybridisation of E11.5 and E12.5 wild type and *Chx10*$^{-/-}$ embryos for silver. *A-D*: E11.5 *(A,B)* and E12.5 *(C, D)* wild type and *Chx10*$^{-/-}$ embryos with staining of melanocytes migrating from the neural crest along the length of the body (*A,B* arrows). Inserts show magnified eyes. *E-H*: 30 μm vibratome sections of whole mount ISH from E11.5 *(E,F)* and E12.5 *(G,H)* wild type *(E,G)* and *Chx10*$^{-/-}$ *(F,H)* embryos. Very dark staining is observed in the RPE of all eyes. Some staining is observed in the wild type E11.5 retina, but little staining is observed in the E12.5 wild type retina. In the *Chx10*$^{-/-}$ eyes, staining is extended into the periphery of the retina at both ages (*F,H* arrowheads), and the rest of the retina is also lightly stained. Scale bar = 1 mm for *A-D*, 100 μm for *E-H*

In situ hybridisation of much thinner (14 μm) frozen sections at E13.5, clearly show silver expression being restricted to the RPE of the wild type retina (Figure 4.6A), whereas in the *Chx10*$^{-/-}$ retina, silver expression is observed both in the RPE and in the periphery of the neural retina (Figure 4.6B and C). Especially in the ventral retina, silver expression seems to have extended from the boundary of the RPE and the neural retina toward the central retina.

A pattern similar to silver expression can be observed after whole mount ISH for *Dct* (Figure 4.7). Again, melanocytes can be observed migrating from the neural crest and around the eye (Figure 4.7A-D, arrows and insets, and G). However, *Dct* is not expressed in the limbs at E12.5 like silver is (compare Figure 4.7 C, D with Figure 4.7 C, D). The *Chx10*$^{-/-}$ eye seems more darkly stained than the wild type at both ages (Figure 4.7A-D, insets). 30 μm vibratome sections of the treated embryos confirmed this observation. In the wild type sections at both E11.5 and E12.5 the wild type RPE shows significant *Dct* expression, whilst the retina does not seem to express any significant amount of *Dct* (Figure 4.7E-H). In contrast, in the *Chx10*$^{-/-}$ eye, the retina itself shows more *Dct* expression at both time points (Figure 4.7F, H). *Dct* mRNA is also abundant in the RPE and as with silver, expression seems to extend into the periphery of the retina. In addition, it seems that expression is more extensive in the ventral retina and RPE (Figure 4.7F, H, arrows). A similar observation could be made upon close examination of silver expression, especially after *in situ* hybridisation on frozen sections; however, the difference seems more marked in *Dct* whole mount *in situ* hybridisation sections compared to those examined for silver expression.

In situ hybridisation of E13.5 frozen sections with *Dct* probe show a remarkable similarity to those hybridised with silver probe. Again, expression is restricted to the RPE of the wild type eye (Figure 4.8A) whilst it is extended into the periphery of the retina in the *Chx10*$^{-/-}$ eye (Figure 4.8B and C). Again, staining seems to be more extensive in the ventral retina than in the dorsal retina.

The observed expression in the wild type embryos closely matches *Si* and *Dct* expression described in the literature (Baxter and Pavan, 2003), and thus hybridisation appears to be specific. However, the silver expression observed in the

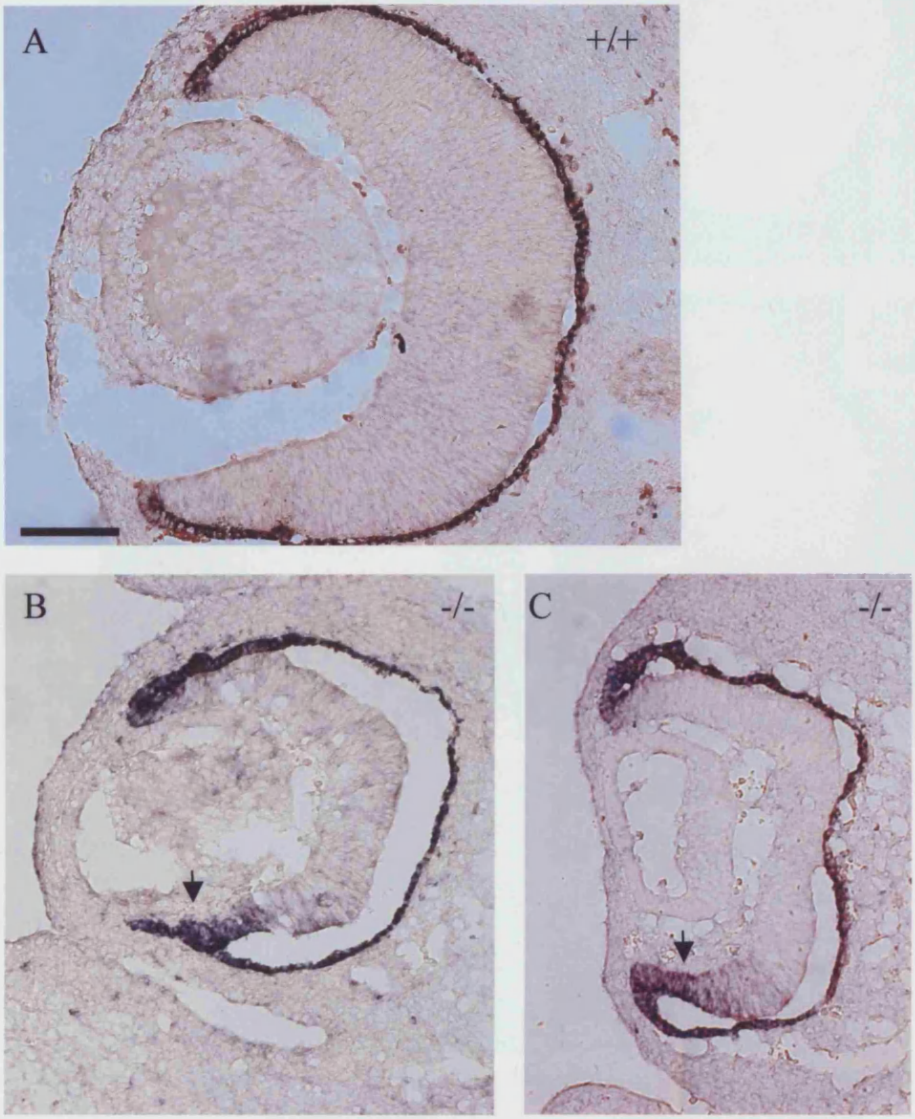

Figure 4.6: *In situ* hybridisation of E13.5 wild type and *Chx10*$^{-/-}$ retinal sections for *Si*. *A*: E13.5 wild type retinal section with *Si* staining restricted to the retinal pigmented epithelium. No *Si* staining is observed in the retina. *B* and *C*: E13.5 *Chx10*$^{-/-}$ retinal sections with *Si* staining observable in the retinal pigmented epithelium as well as in the periphery of the retina, especially in the ventral peripheral retina (arrows). Scale bar = 100 μm for all.

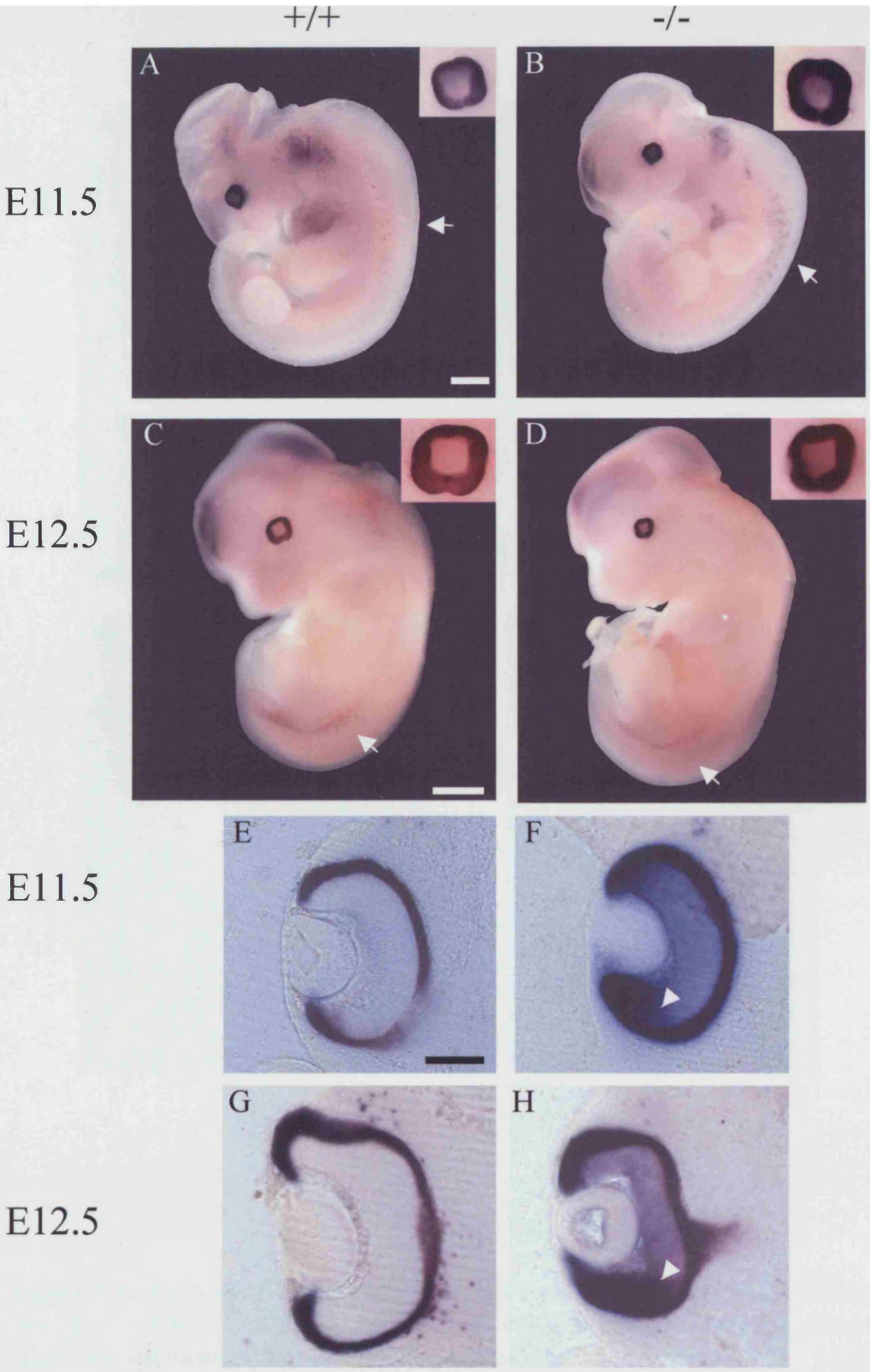

Figure 4.7: Whole mount *in situ* hybridisation of E11.5 and E12.5 wild type and *Chx10*$^{-/-}$ embryos for *Dct*. *A-D*: E11.5 *(A,B)* and E12.5 *(C, D)* wild type and *Chx10*$^{-/-}$ embryos with staining of melanocytes migrating from the neural crest along the length of the body. Inserts show magnified eyes, with darker staining in mutant eyes. *E-H*: 30 μm vibratome sections of whole mount ISH from E11.5 *(E,F)* and E12.5 *(G,H)* wild type *(E,G)* and *Chx10*$^{-/-}$ *(F,H)* embryos. Very dark staining is observed in the RPE of all eyes. No staining is observed in the wild type retinae. In the *Chx10*$^{-/-}$ eyes, staining is extended into the periphery of the retina, especially in the ventral retina, at both ages (*F,H* arrowheads), and the rest of the retina is also stained. Scale bar = 1 mm for *A-D*, 100 μm for *E-H*.

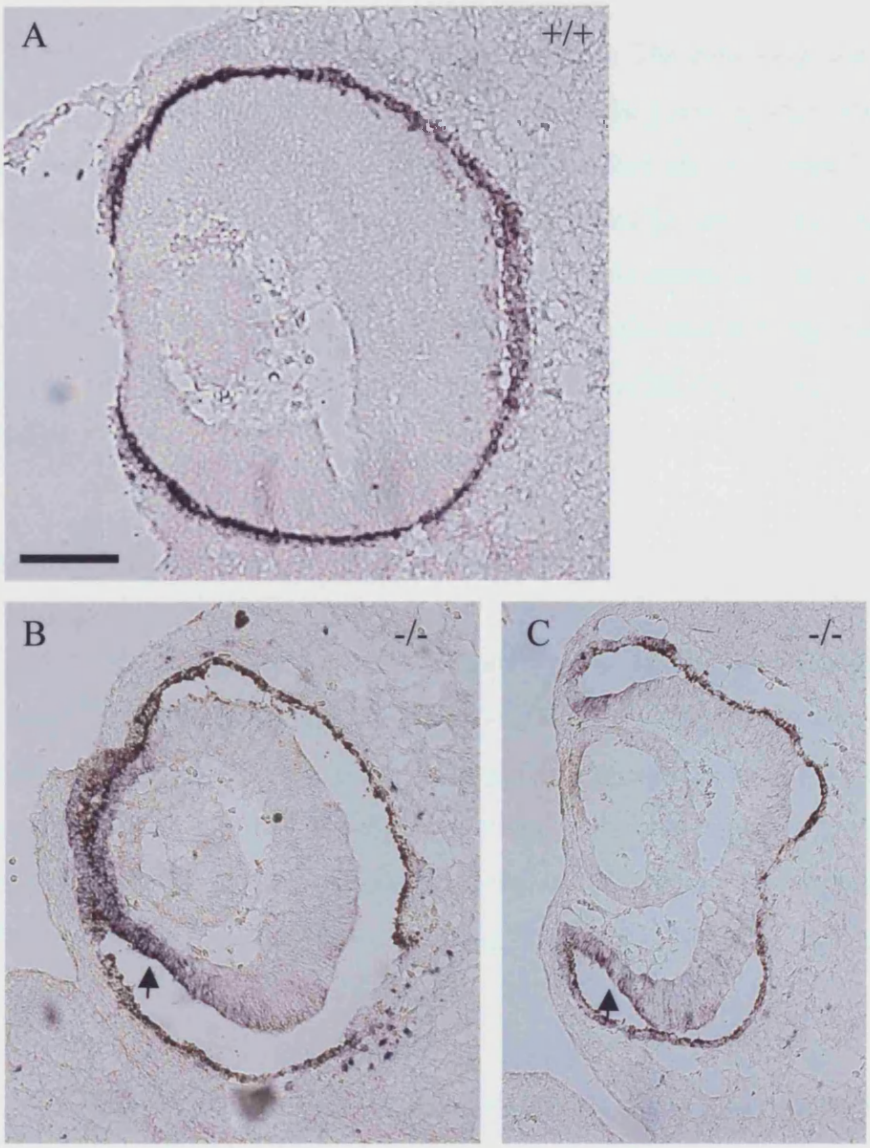

Figure 4.8: *In situ* hybridisation of E13.5 wild type and *Chx10*$^{-/-}$ retinal sections for *Dct*. *A*: E13.5 wild type retinal section with silver staining restricted to the retinal pigmented epithelium. No *Dct* staining is observed in the retina. *B* and *C*: E13.5 *Chx10*$^{-/-}$ retinal sections with *Dct* staining observable in the retinal pigmented epithelium as well as in the periphery of the retina, especially in the ventral peripheral retina (arrows). Scale bar = 100 μm for all.

limbs of the E12.5 retina is not reported in other literature. The data were also highly reproducible as at least three embryos of each genotype were treated with each probe, with similar results. The above *in situ* hybridisation and real time RT-PCR data indicate that both *Si* and *Dct* are indeed up-regulated in the *Chx10*$^{-/-}$ retina at E11.5 and suggest that normal specification of the neural retina and the boundary between the RPE and the NR at the periphery of the optic cup is disrupted in the absence of Chx10. These data correspond with the microarray data discussed in the previous chapter.

4.2.3 Distal-less homeobox 2

After *Rxrg*, the gene that shows the most dramatic change in expression between the wild type and *Chx10*$^{-/-}$ retina is distal-less homeobox 2 (*Dlx2*), which shows a 13.8-fold reduction in expression in the *Chx10*$^{-/-}$ retina compared to the wild type. *Dlx2* is thought to play a large role in forebrain specification and development but little is known about the role of *Dlx2* in retinal development. I examined the expression of *Dlx2* during early retinal development using real time RT-PCR and *in situ* hybridisation.

Real time RT-PCR was performed as described in section 4.2.1. Amplification curves obtained from the *Dlx2* RT-PCR study are supplied in Appendix 2. In contrast to the data observed for *Rxrg*, the amplification products from the wild type retina were detectable at earlier cycles than those from the *Chx10*$^{-/-}$ retina. This indicates that there was more of the target cDNA present in the wild type retina than in the *Chx10*$^{-/-}$ retina. The comparative Ct method was used to calculate the fold-change in gene expression in the *Chx10*$^{-/-}$ retina compared to the wild type and the normalised results summarised in Table 4.4. Standard deviations of duplicate runs were taken into account to produce a range of fold-change for Pools 2 and 3.

Pool	Increase/Decrease	Fold-change
Pilot	Decrease	7.7
Pool 1 RT1	Decrease	11.0
Pool 1 RT2	Decrease	4.5*
Pool 2	Decrease	6.1* (3.6-10.6)
Pool 3	Decrease	4.6* (2.6-8.3)

Table 4.4: Relative change in expression of *Dlx2* in *Chx10*$^{-/-}$ retinae compared to wild type retinae for each set of retinal pools collected for real time PCR. * Indicates result of fold-change calculation based on average of Cts of duplicate runs. Numbers in parentheses indicate a range of fold-changes, based on calculations including a standard deviation between duplicate runs.

The RT-PCR data indicate that there is indeed a decreased amount of *Dlx2* expression in the *Chx10*$^{-/-}$ retina compared to the wild type retina. Expression is decreased roughly 7-fold in the *Chx10*$^{-/-}$ retina. A seven-fold change in expression falls into the fold-change ranges calculated for the last two runs. These ranges are relatively large as compared to the genes described earlier (Figure 4.4 provides a comparison). This is because the standard deviations between replicates are slightly larger, represented by the greater difference between replicates on the amplification curves. The microarray data indicate there is a 13.83 fold decrease in *Dlx2* expression in the *Chx10*$^{-/-}$ retina compared to the wild type, which suggests that the microarray study may have been more sensitive to changes in expression compared to the RT-PCR method. The biggest change in expression observed using RT-PCR was an eleven-fold decrease for Pool 1 RT1. However, the results do not show a particularly large variation between runs, and thus the RT-PCR data confirm to a large extent the data obtained from the microarray study. Pools 2 and 3 were also normalised against 18s RNA with similar results.

Figure 4.9 summarises whole mount *in situ* hybridisation results for *Dlx2* at E11.5 and E12.5. High expression can be observed in the forebrain and branchial arches of both wild type, and *Chx10*$^{-/-}$, embryos at E11.5 (Figure 4.9A, B). The expression in the forebrain remains high at E12.5 for both genotypes, but is decreased in the branchial arches of E12.5 embryos (Figure 4.9C, D). High magnification views of the eyes of all embryos are also shown in Figure 4.9 (insets). Very little presence of *Dlx2* mRNA can be observed in any of the eyes, with exception of the E12.5 wild type eye (Figure 4.9C, inset), where some expression can be seen within the area enclosed by the RPE. This suggests *Dlx2* expression begins at around E12.5 in the

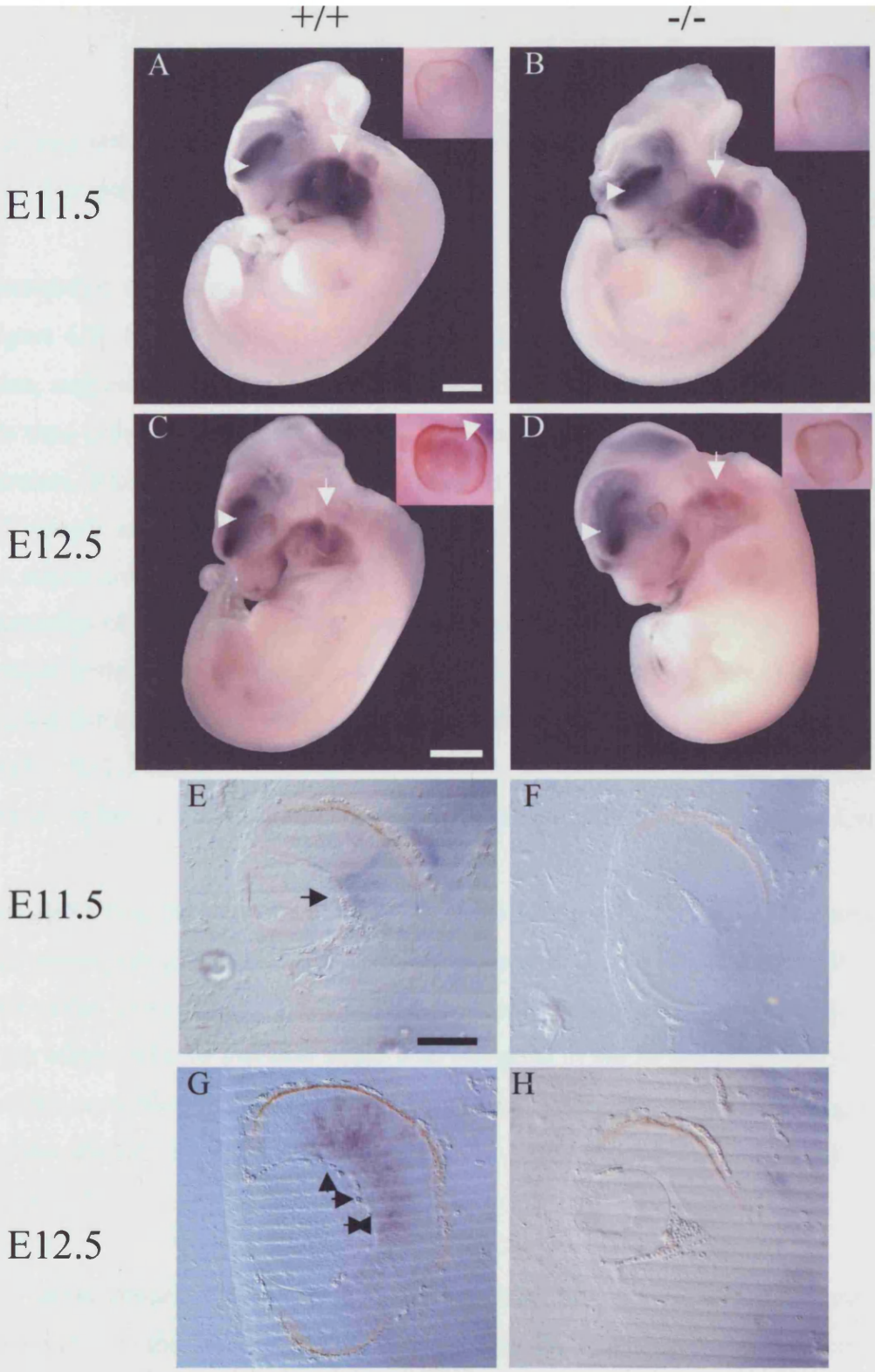

Figure 4.9: Whole mount *in situ* hybridisation of E11.5 and E12.5 wild type and *Chx10*$^{-/-}$ embryos for *Dlx2*. *A-D*: E11.5 *(A,B)* and E12.5 *(C, D)* wild type and *Chx10*$^{-/-}$ embryos with *Dlx2* expression in the branchial arches (arrows) and the forebrain (arrowheads). Inserts show magnified eyes, with staining visible in the wild type E12.5 retina (arrowhead). *E-H*: 30 μm vibratome sections of whole mount ISH from E11.5 *(E,F)* and E12.5 *(G,H)* wild type *(E,G)* and *Chx10*$^{-/-}$ *(F,H)* embryos. Faint radial staining can be observed across the central area of the wild type retina at E11.5 (*E*, arrow). By E12.5, *Dlx2* staining is extended in the central area of the wild type retina, predominantly into the dorsal retina and to a lesser extent the ventral retina (*G*, arrows). No staining is observed in the *Chx10*$^{-/-}$ retina at any time. Scale bar = 1 mm for *A-D*, 100 μm for *E-H*.

wild type retina, but that little or no *Dlx2* is expressed in the *Chx10*$^{-/-}$ retina at the same time point.

Examination of 30 μm vibratome sections of the embryos confirms this observation (Figure 4.9E-F). Very little *Dlx2* expression can be detected in the E11.5 wild type retina, suggesting that *Dlx2* is only beginning to be expressed in the central retina at this time point (Figure 4.9E, arrow). This observation is in accordance with the literature, which indicates that *Dlx2* staining in the wild type retina begins centrally and extends radially across the retina (de Melo et al., 2003; Eisenstat et al., 1999). No expression is observed in the *Chx10*$^{-/-}$ retina (Figure 4.9F). The pattern of expression observed at E11.5 in the wild type retina is expanded at E12.5, and extends further into the dorsal area of the retina than the ventral area (Figure 4.9G, arrows). No expression is observed in the periphery. No expression is observed in the *Chx10*$^{-/-}$ E12.5 retina, indicating that if *Dlx2* is expressed at this time point in the *Chx10*$^{-/-}$ retina, it is at a very low level in comparison to the wild type (Figure 4.9H).

This also seems the case at E13.5. *In situ* hybridisation of E13.5 frozen sections for *Dlx2* show clear presence of *Dlx2* mRNA in the wild type retina (Figure 4.10A, B). *Dlx2* seems to be expressed in a punctuate pattern throughout the neuroblastic layer of the whole retina by this time point, with exception of the far periphery. In contrast, no *Dlx2* expression can be detected in the *Chx10*$^{-/-}$ retina (Figure 4.10C), suggesting that the absence of Chx10 seems to inhibit *Dlx2* expression for at least a day, from E12.5 to E13.5.

Dlx2 sense probes did not result in any staining, and the published literature is consistent with the data obtained here, suggesting the anti-sense probe is specific for *Dlx2* (de Melo et al., 2003; Eisenstat et al., 1999; Qiu et al., 1997). In addition, at least three embryos of each genotype were treated for each probe, with reproducible results. The above ISH data, combined with the real time RT-PCR data indicate that *Dlx2* is indeed down-regulated in the *Chx10*$^{-/-}$ retina during early development, confirming the change in *Dlx2* expression observed in the microarray experiment.

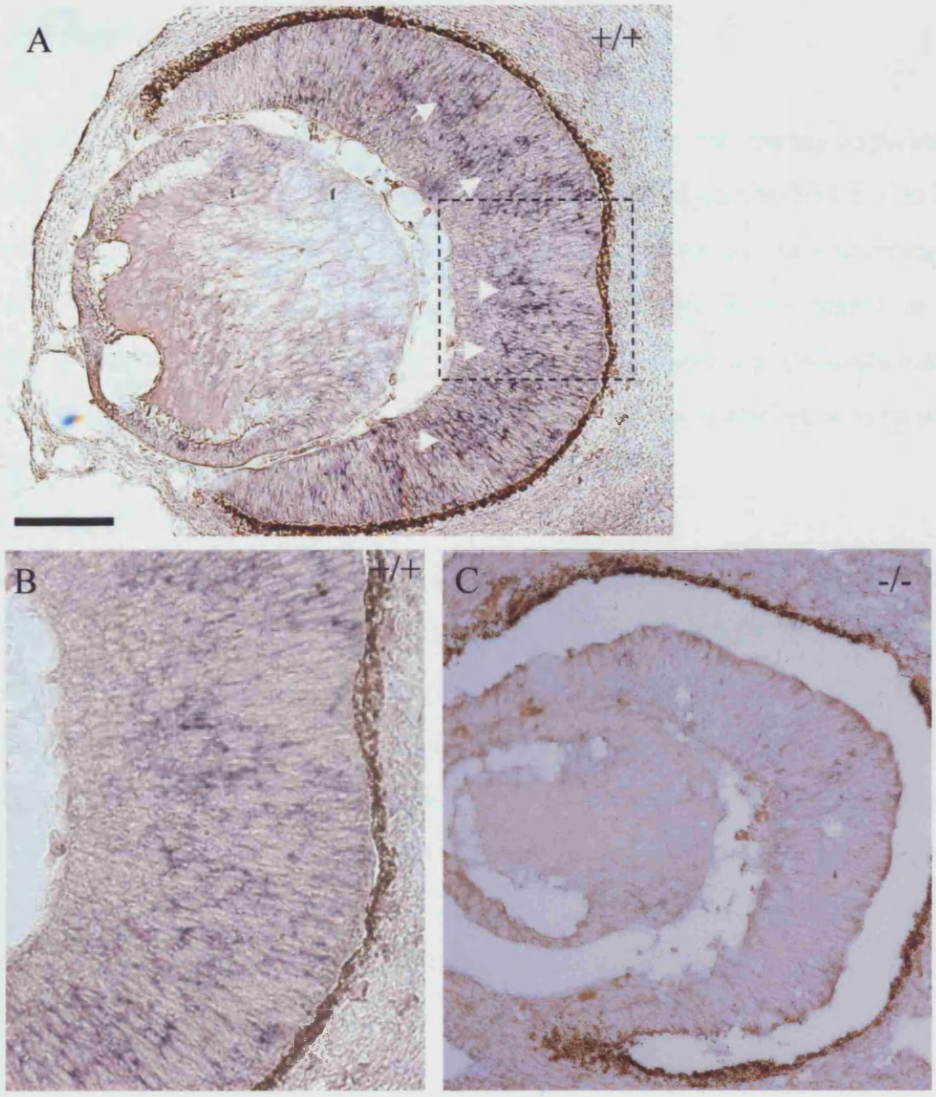

Figure 4.10: *In situ* hybridisation of E13.5 wild type and *Chx10*$^{-/-}$ retinal sections for *Dlx*. *A and B*: E13.5 wild type retinal section with *Dlx* expression observable throughout the retina (arrows), box in A is magnified in B. *C*: E13.5 *Chx10*$^{-/-}$ retinal section with no *Dlx* staining in the retina. Scale bar = 100 μm for *A* and *C*, 50 μm for *B*.

4.2.4 Neurogenic differentiation 1

Another gene that showed significant down-regulation in the microarray experiment is *Neurod1*. Expression of this gene was decreased 8.3-fold in the E11.5 *Chx10*$^{-/-}$ retina compared to the wild type in the microarray study. *Neurod1* is a homolog of the Drosophila *atonal* gene and is widely expressed during development in the mammalian brain and the pancreas (Liu et al., 2000a). It plays a significant role in retinal cell specification and possibly in proliferation, and is therefore a very good candidate for Chx10 regulation.

Real time RT-PCR was performed as described in section 4.2.1. Amplification curves from the *Neurod1* RT-PCR study are provided in Appendix 2. In contrast to the RT-PCR studies performed for the other genes, the results for *Neurod1* were highly variable. The normalised results are summarised in Table 4.5 and depicted in Figure 4.4. Standard deviations of duplicate runs were taken into account to produce a range of fold-change for Pools 2 and 3. Amplification of cDNA from Pool 1 initially indicated a 57.3-fold decrease in *Neurod* expression in the *Chx10*$^{-/-}$ retina compared to the wild type. A smaller difference was observed after a second RT and PCR run from Pool 1 (Table 4.5).

cDNA from Pools 2 and 3 were run simultaneously. The difference between the wild type and *Chx10*$^{-/-}$ cDNAs is far greater in Pool 3 and in Pool 2. Even though the replicates showed a high correlation, the cDNA for Pools 2 and 3 were run again to examine whether this change could have been caused by some outside factor. Again a large difference between wild type and *Chx10*$^{-/-}$ was observed. As a final confirmation, the RT was performed again for Pools 2 and 3 and run on the PCR. Again a large difference between the two was observed.

Because the same results were produced three times within Pools 2 and 3, even after a second round of RT was performed from the starting material, it seems the variation between the two is a result of a genuine difference in *Neurod1* mRNA present in the two pools of *Chx10*$^{-/-}$ retinae (the wild type pools consistently show a Ct of just under 30 cycles, suggesting no difference in starting material). The non-

template H_2O controls used did not indicate any contamination. Pools 2 and 3 were also normalised against 18s RNA with similar results.

Pool	Increase/Decrease	Fold-change
Pool 1 RT1	Decrease	57.3
Pool 1 RT2	Decrease	19.56
Pool 2	Decrease	6.5* (5.7-7.3)
Pool 2 2nd run	Decrease	6.6
Pool 2 RT2	Decrease	8.3
Pool 3	Decrease	88.3* (73.3-106.5)
Pool 3 2nd run	Decrease	97.7
Pool 3 RT2	Decrease	109.1

Table 4.5: Relative change in expression of *Neurod1* in *Chx10*$^{-/-}$ retinae compared to wild type retinae for each set of retinal pools collected for real time PCR. * Indicates result of fold-change calculation based on average of Cts of duplicate runs. Numbers in parentheses indicate a range of fold-changes, based on calculations including a standard deviation between duplicate runs.

Despite the variability, the RT-PCR data indicate that there is indeed a decreased amount of *Neurod1* expression in the *Chx10*$^{-/-}$ retina compared to the wild type retina. However, it is unclear to what extent *Neurod1* is down-regulated in the *Chx10*$^{-/-}$ retina. In the microarray experiment, an eight-fold difference in expression was observed. A similar change in expression is observed when comparing *Chx10*$^{-/-}$ Pool 2 to wild type Pool 2. However, a much greater apparent decrease in expression is observed for Pools 1 and 3.

To further examine *Neurod1* expression in the wild type and *Chx10*$^{-/-}$ retinae, whole mount *in situ* hybridisation was performed on E11.5 and E12.5 embryos (Figure 4.11A-D). At E11.5, *Neurod1* seems to be strongly expressed in the somites and otic vesicle in both genotypes (Figure 4.11A, B arrows). Extensive expression is also observed in the brain. By E12.5, the same pattern of expression is observed, but staining is not as dark, suggesting that perhaps *Neurod1* is becoming down-regulated. This is especially true for the brain regions (Figure 4.11C, D). No apparent expression was observed in the eyes of any of the embryos at either time point (Figure 4.11A-D, insets). Staining for *Neurod1* was reproducible (at least three embryos of each genotype tested) and specific, as a similar pattern was not observed when using the *Neurod1* sense probe and previous findings confirm that expression should be observed in areas containing differentiating neurons of the central and peripheral nervous system, for example in the otic vesicle (Kim et al., 2001).

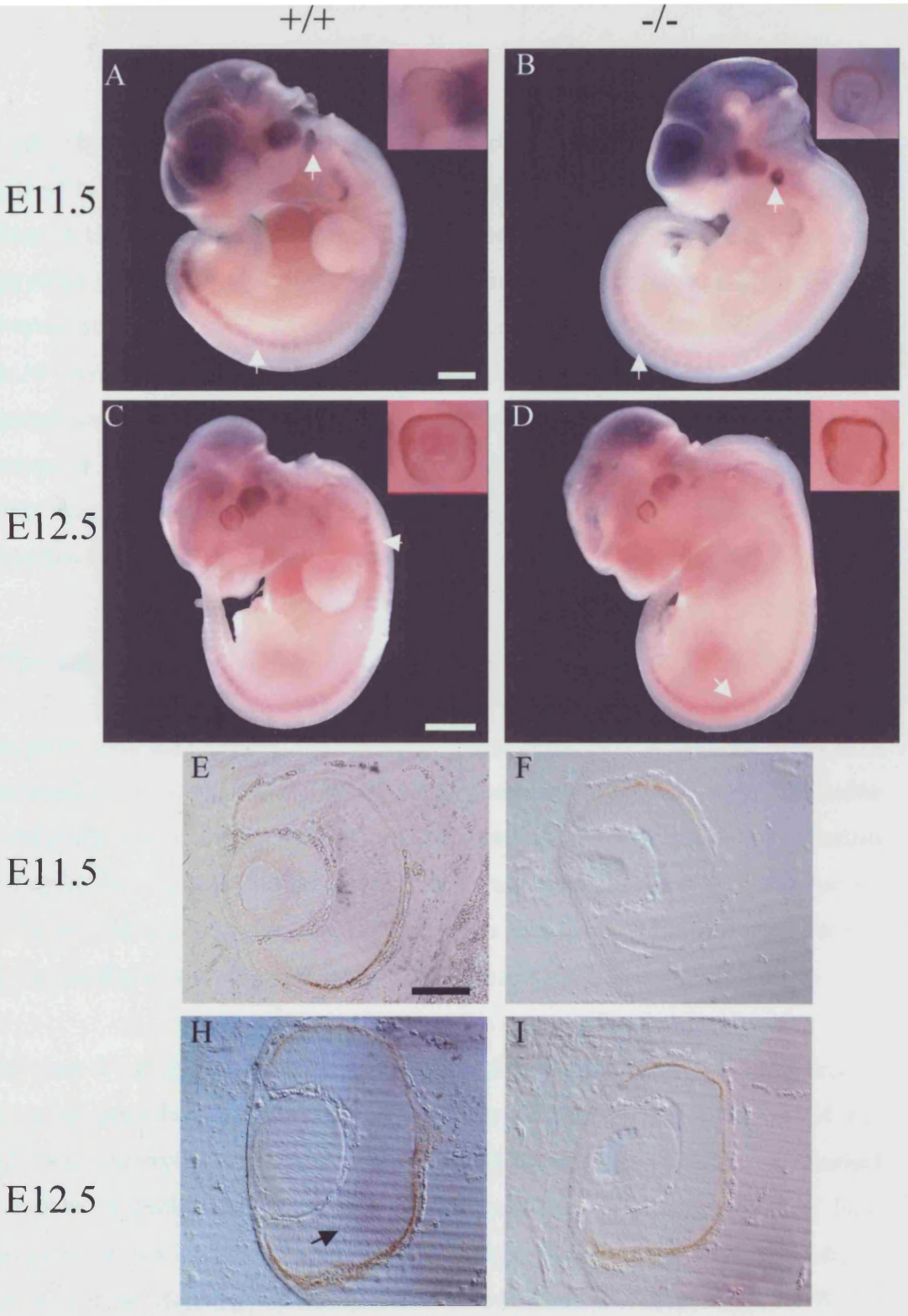

Figure 4.11: Whole mount *in situ* hybridisation of E11.5 and E12.5 wild type and *Chx10*$^{-/-}$ embryos for *Neurod1*. *A-D*: E11.5 *(A,B)* and E12.5 *(C, D)* wild type and *Chx10*$^{-/-}$ embryos with *Neurod1* staining in otic vesicles and somites (*A-D* arrows). Inserts show magnified eyes. *E-H*: 30 μm vibratome sections of whole mount ISH from E11.5 *(E,F)* and E12.5 *(G,H)* wild type *(E,G)* and *Chx10*$^{-/-}$ *(F,H)* embryos. No apparent staining can be observed in the retinae of E11.5 wild type and *Chx10*$^{-/-}$ eyes. At E12.5 some faint staining can be observed in the wild type central retina (*H,* arrow), whilst no apparent staining is observed in the *Chx10*$^{-/-}$ retina. Scale bar = 1 mm for *A-D*, 100 μm for *E-H* .

30 μm vibratome sections of the embryos treated for whole mount ISH confirm an apparent lack of *Neurod1* expression in the wild type and *Chx10*$^{-/-}$ retinae at E11.5 (Figure 4.11E, F). By E12.5 however, some expression can be observed in the wild type retina (Figure 4.11G). This is not observed in the *Chx10*$^{-/-}$ retina (Figure 4.11H), however, suggesting *Neurod1* expression is not yet expressed at this time point in the *Chx10*$^{-/-}$ retina or that its expression is severely down-regulated. Kim et al report that *Neurod1* expression in the retina cannot be observed until E13 (Kim et al., 2001) and Morrow et al report it is not strongly observed until E17 (Morrow et al., 1999a), which may account for the lack of strong staining in the retina at any time point examined here.

4.2.5 Cadherin 8

The microarray data suggest that the integral membrane protein cadherin 8 is down-regulated 6-fold in the E11.5 *Chx10*$^{-/-}$ retina compared to the wild type. Cadherins mediate calcium-dependent cell-cell adhesion and are thought to play an important role in the development and maintenance of various tissues (Korematsu and Redies, 1997). As with the genes described above, I have examined cadherin 8 expression of the developing retina using real time RT-PCR and *in situ* hybridisation.

Real time RT-PCR was performed as described in section 4.2.1 and amplification curves are provided in Appendix 2. The results are summarised in Figure 4.4 and Table 4.6. The replicates observed here generally show a close correlation. Standard deviations of duplicate runs were taken into account to produce a range of fold-change for Pools 2 and 3. Because of the greater difference between replicates in Pool 3 (and therefore a greater standard deviation), the fold-change range for Pool 3 is also higher than that of Pool 2. However, the change in expression of cadherin 8 in the *Chx10*$^{-/-}$ retina compared to the wild type seems consistent and reproducible. As was the case for *Dlx2*, the microarray data suggest a larger difference in expression (6-fold versus 2-fold) than the RT-PCR study, suggesting again that the microarray experiment may be more sensitive to gene expression changes. Pools 2 and 3 were also normalised against 18s RNA with similar results.

Pool	Increase/Decrease	Fold-change
Pool 1 RT1	Decrease	1.8
Pool 1 RT2	Decrease	1.8
Pool 2	Decrease	1.6* (1.4-1.8)
Pool 3	Decrease	2.3* (1.2-4.7)

Table 4.6: Relative change in expression of cadherin 8 in *Chx10*$^{-/-}$ retinae compared to wild type retinae for each set of retinal pools collected for real time PCR. * Indicates an average of a duplicate run.

Whole mount *in situ* hybridisation of E11.5 wild type and *Chx10*$^{-/-}$ embryos indicates that there is *Cdh8* expression in various areas of the embryo at this time point, including the brain and the anterior limb bud (Figure 4.12A, B), as well as along the somites. By E12.5, expression is observed in a similar pattern, although expression seems to have decreased in the anterior limb buds and appeared in the posterior limb buds in both genotypes (Figure 4.12C, D). There is more extensive *Cdh8* staining in the E12.5 *Chx10*$^{-/-}$ embryo, but it is difficult to assess whether this staining is real as staining in the brain regions is often a result of trapping in the ventricles and can also be observed when using sense probes. *Cdh8* expression has been reported in various areas of the CNS by E11.5, including various areas of the forebrain and developing grey matter structures (Korematsu et al., 1998); (Korematsu and Redies, 1997).

In 30 μm vibratome sections of the E11.5 wild type embryo, some expression can be observed in the central and dorsal area of the retina (Figure 4.12E, arrow), but does not extend into the periphery of the retina. In contrast, no apparent expression can be observed in the same area in the *Chx10*$^{-/-}$ retina, suggesting expression of cadherin 8 may be down-regulated in the E11.5 *Chx10*$^{-/-}$ retina. At E12.5, *Cdh8* mRNA can still be detected in the wild type retina, but seems to be localised more to the dorsal area of the retina, rather than the central retina, as was the case at E11.5 (Figure 4.12G). Again, no expression is observed in the *Chx10*$^{-/-}$ retina (Figure 4.12H). The *in situ* hybridisation, performed on at least three embryos of each genotype, and real time RT-PCR data suggest *Cdh8* is down-regulated in the *Chx10*$^{-/-}$ retina compared to the wild type, mirroring the data obtained from the microarray experiment.

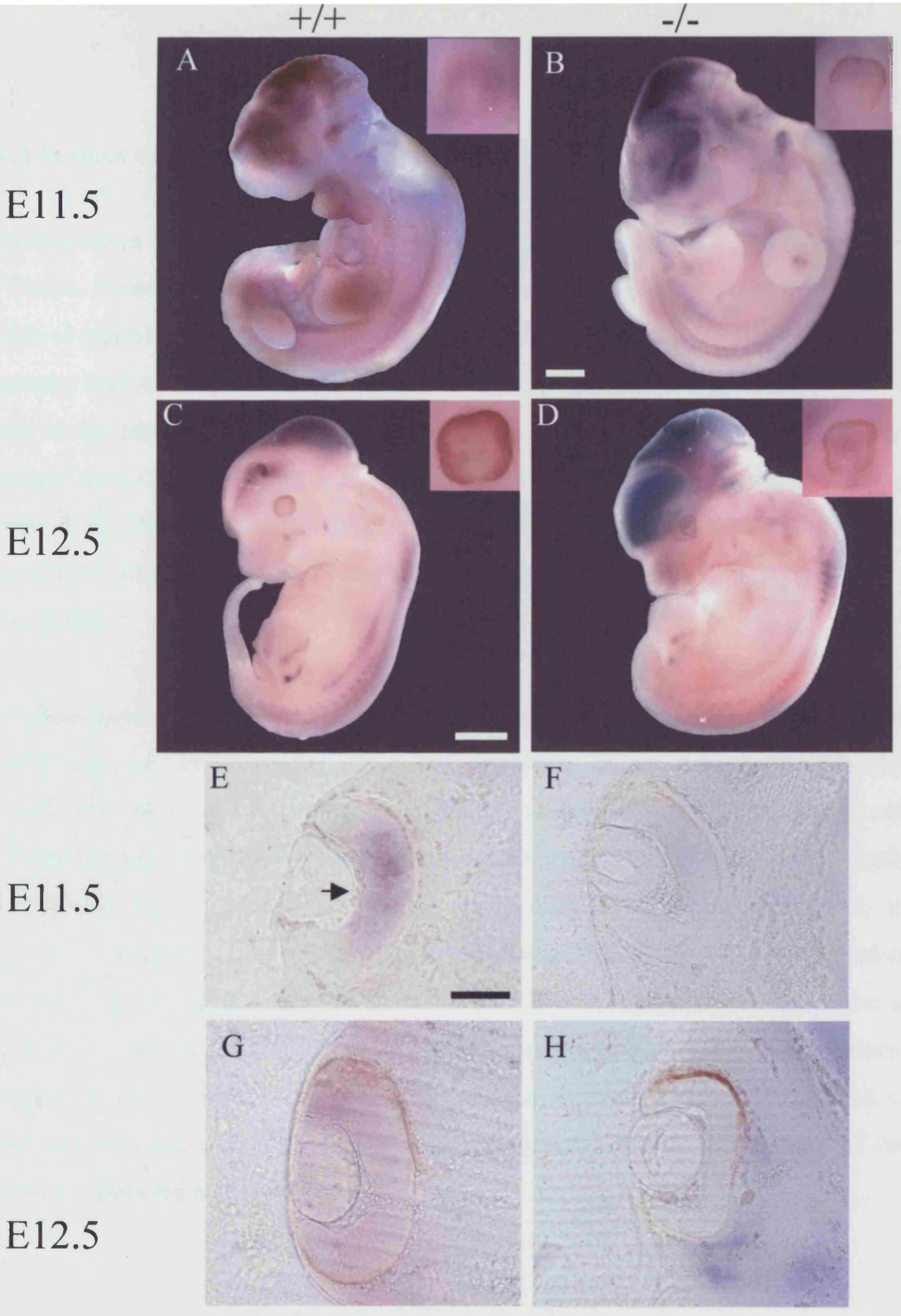

Figure 4.12: Whole mount *in situ* hybridisation of E11.5 and E12.5 wild type and *Chx10*$^{-/-}$ embryos for *Cdh8*. *A-D*: E11.5 *(A,B)* and E12.5 *(C, D)* wild type and *Chx10*$^{-/-}$ embryos with *Cdh8* staining in brain, somites and limbs. Inserts show magnified eyes. *E-H*: 30 μm vibratome sections of whole mount ISH from E11.5 *(E,F)* and E12.5 *(G,H)* wild type *(E,G)* and *Chx10*$^{-/-}$ *(F,H)* embryos. *Cdh8* staining is observed in the central retina of the E11.5 wild type eye (*E*, arrow), whereas no staining is observed in the *Chx10*$^{-/-}$ retina at the same age. There is no apparent staining in the E12.5 Chx10$^{-/-}$ retina. Scale = 1 mm for *A-D*, 100 μm for *E-H*.

4.2.6 *In silico* examination of Chx10-regulated genes

The expression of the genes discussed above all appear to be affected by the absence of Chx10. Whether Chx10 exerts a direct or indirect effect is yet unclear. One way in which to examine this more closely is by searching for Chx10 binding sites in the promoter regions of these genes. If such sites are present, this may indicate Chx10 binds to the promoters of these genes in order to activate or repress them directly. The preferred Chx10 binding site, identified through a binding site selection assay (Ferda et al., 2000) is TAATTAGC, where TAAT is a conserved homeobox binding motif, and TAGC are thought to confer further specificity for the Chx10 gene (Ferda et al., 2000).

For all six genes, the 10 kb region upstream of the first codon of the coding sequence (CDS) was searched for the consensus sequence of the Chx10 binding site (TAATTA). The CDS was entered into a BLAST search of nucleotide databases, and a genomic clone was located. Nucleotides upstream of the CDS were subsequently analysed for the Chx10 binding site. If no genomic clone could be located, an alternative method was used. A link to the 'map viewer' on the NCBI Entrez database (http://www.ncbi.nlm.nih.gov/mapview) allowed targeting of the beginning of the CDS and examination of the genomic sequence around it, based on genomic contigs. As the consensus site is palindromic, the sites identified on one strand of DNA are effectively also sites on the complementary strand. A summary of the results is displayed in Table 4.7.

Gene	Search type	Genbank accession number of genomic clone or contig	Number of Chx10 binding sites found on sense strand	Location of Chx10 binding sites (bp upstream from CDS)
Rxrg	Map Viewer	NT078306	3	3393 6136 8664
Dct	BLAST	AC108833	3	6842 7913 6842
Si	BLAST	AC117232	1	7498
Dlx2	BLAST	AL928931	4	103 1738 1902 9254
Neurod1	BLAST	AL928696	8	844, 1258 1320, 1512 4887, 6617 6901, 10724
Cdh8	Map Viewer	NT078586	2	485 5943

Table 4.7: Summary of promoter searches of differentially expressed genes. Two types of searches were employed (BLAST or Map Viewer) using the CDS of the genes indicated. Genomic clones or contigs were examined for Chx10 binding sites and their location determined.

Of the six genes examined, *Neurod1* contains the largest number of Chx10 binding sites, 4 of which are within 2 kb of the CDS start site, suggesting that this would be the most likely candidate gene to whose promoter region Chx10 might be able to bind. *Cdh8* and *Dlx2* each have a Chx10 binding site consensus sequence within 500 bp of their CDS start codon and in addition *Dlx2* has two Chx10 consensus binding sites within 2 kb of its CDS start codon. Although both *Rxrg* and *Dct* have three Chx10 consensus binding sites, these are all more than 2 kb from the CDS start site, and the same is true for the *Si* consensus binding site. This makes them less likely candidates for direct Chx10 regulation than the other three.

In order to investigate the Chx10 binding sites further, sequence alignments with homologues from other species were made to discover whether any of the Chx10 consensus binding sites within roughly 5 kb of a starting site, occurred within conserved areas of the upstream coding region of these genes. The rat, human, dog and chicken homologues of the genes and their upstream regions were compared

using Zpicture (http://zpicture.dcode.org) and MultAlin (http://prodes.toulouse.inra.fr/multalin/multalin.html). Z-picture allows one to visualise areas of homology between species (Figures 4.13A and 4.14A). Multiple sequence alignments with hierarchical clustering were produced by entering such areas of homology into the MultAlin website (Figures 4.13B and 4.14B).

Of the five potential Chx10 binding sites within 5 kb of the *Neurod1* start codon, one was conserved in all species examined, the site 4.9 kb upstream of the CDS. The site closest to the start codon, 844 bases upstream, is conserved in human, rat and dog. The site 1.5 kb upstream of the CDS is conserved in the human and the rat. The other two potential Chx10 binding sites were only conserved in the rat (Figure 4.13).

The *Dlx2* potential Chx10 binding sites at 1.7 and 1.9 kb upstream were also conserved in human, rat and dog (Figure 4.14). The site 103 upstream was situated in the 5' UTR and thus unlikely to be a real Chx10 binding site. No comparison could be made with chicken as no appropriate homologue was found.

The cadherin 8 site 485 upstream of the start site was not conserved in other species and neither was the *Rxrg* site 3.3 kb upstream of the start site.

Another aim of the study is to identify genes that may be involved in microphthalmia. Several microphthalmia loci have been identified for various forms of microphthalmia including 15q12-q15 (Morle et al., 2000), NNO1 locus on 11p (Othman et al., 1998), 14q32 (Bessant et al., 1998), Xq27-28 (Graham et al., 1991), and 16p13.3 (Yokoyama et al., 1992). To assess whether any of the six genes discussed above may map to microphthalmia loci, I examined the chromosome positions of their human homologues. Table 4.8 summarises these results.

A

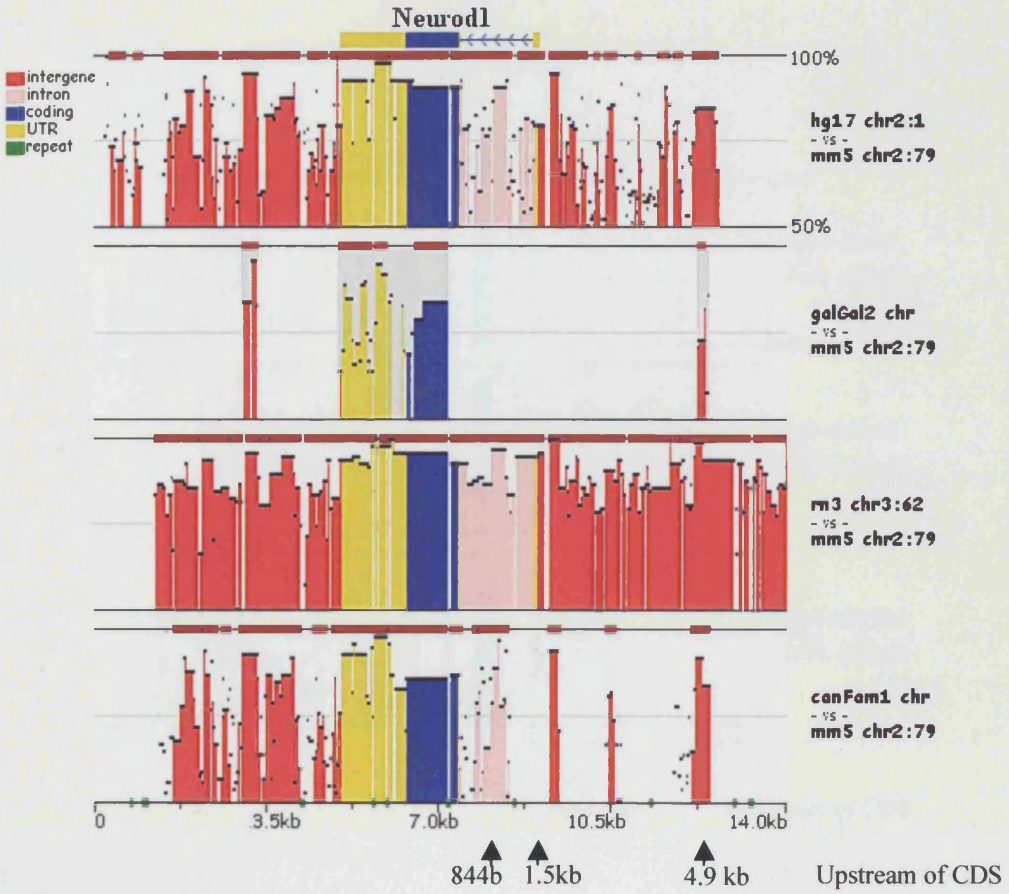

B

```
Neurod1 4.9 kb upstream
     mouse  GCTTGCGGCA TAATCTTAAT TAAGATAATT GATTCATATT GCACCTGCGA
     human  GCTTGCGGCA TAATCTTAAT TAAGATAATT GATTCATATT GCACCTGCGA
       dog  GCTTGCGGCA TAATCTTAAT TAAGATAATT GATTCATATT GCACCTGCGA
       rat  GCTTACGGCA TAATCTTAAT TAAGATAATT GATTCATATT GCACCTGCGA
   chicken  GTTTGCGGCA TTATCTTAAT TAAAATAATT GATTCATATT GCACCTGCGA
 Consensus  GcTTgCGGCA TaATCTTAAT TAAgATAATT GATTCATATT GCACCTGCGA

Neurod1 844b upstream
     mouse   CTCCCTTTA AAAGATGGAG TAATTACAAT GGTCAGCGAC
       rat   CTCGCTTTA AAAGATGGAG TAATTACAAT GGTCAGCGAC
     human   CTCCCTTTA AAAGATTGAG TAATTATAAT GGTCAGCGAT
       dog  CTCTCTTTAA AAAGATTGAG TAATTATGAT GGTCAGCGAT
 Consensus  .ctcccTTtA AAAGATgGAG TAATTAcaAT GGTCAGCGAc

Neurod1 1.5 kb upstream
     mouse   ATTCTCGGG AGAGTAAAAA ATAGGAATCA TAATTACCT- -GTTGTTAAA
       rat   ATTCTCGGG AGAATAAAAA ATAGGAATCG TAATTACCT- -GTTGTTAAA
     human  TATTCTGGGG CAAAAAAATG AAAGAACT-G TAATTACCTT TGTTGTTAGT
 Consensus  .ATTCTcGGG agAatAAAaa AtAGgAaTcg TAATTACCT. .GTTGTTAaa
```

Figure 4.13: Sequence alignments of the *Neurod1* promoter region. (A) Zpicture visualisation of the *Neurod1* gene. Each of the human (hg17), chicken (galGal2), rat (rn3) and dog (canFam1) sequences is compared to the mouse (mm5) sequence and each comparison then compared to the others. The positions of the three potential Chx10 binding sites shown in B are depicted with arrows. (B) Sequence alignments of three potential Chx10 binding sites in the *Neurod1* promoter region.

A

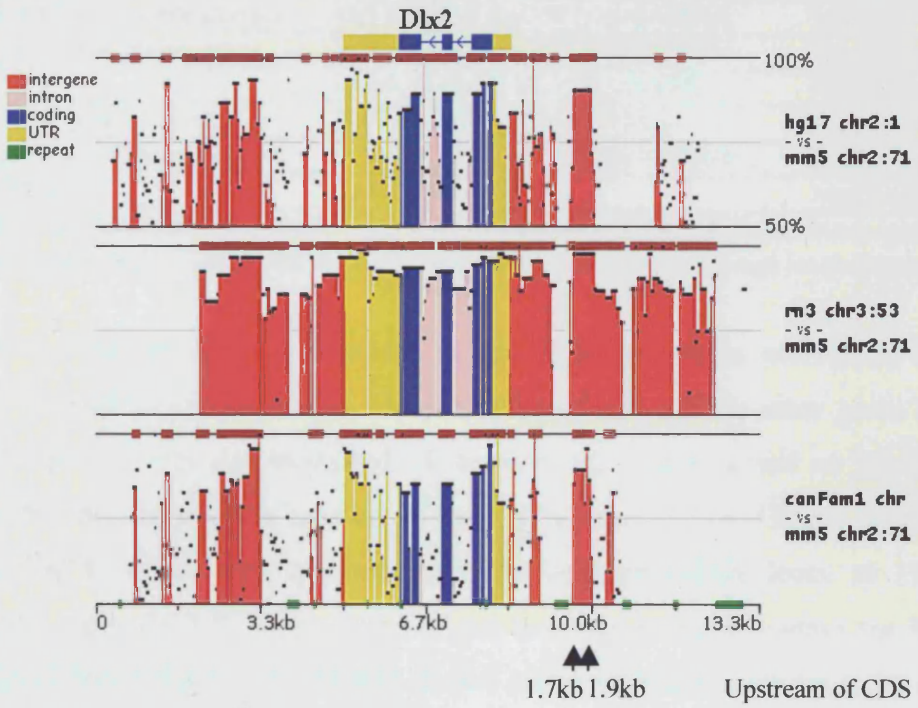

B

```
Dlx2 1.7 kb upstream
     mouse  AAAAGAACAA AATAGTAATT AAAAGCCACA AAA
       rat  AAAAGAACAA AATAGTAATT AAAAGCCACA AAA
       dog  AAAAGAACAA AATAGTAATT AAAAGCCACA AAA
     human  AAAAGAACAA AATAGTAATT AAAAGCCACA AAA
 Consensus  AAAAGAACAA AATAGTAATT AAAAGCCACA AAA

Dlx2 1.9 kb upstream
     mouse  AAAAAGCAAG TGTGTAATTA AAACTCCAGC ATT
     human  AAAAAGCAAG TGTGTAATTA AAACTCCAGC ATT
       rat  AAAAAGCAAG TGTGTAATTA AAACTCCAGA ATT
       dog  AAAAAGCAAG TGTGTAATTA AAACTCCAGC ATC
 Consensus  AAAAAGCAAG TGTGTAATTA AAACTCCAGc ATt
```

Figure 4.14: Sequence alignments of the *Dlx2* promoter region. (A) Zpicture visualisation of the *Dlx2* gene. Each of the human (hg17), rat (rn3) and dog (canFam1) sequences is compared to the mouse (mm5) sequence and each comparison then compared to the others. The positions of the two potential Chx10 binding sites shown in B are depicted with arrows. (B) Sequence alignments of two potential Chx10 binding sites in the *Dlx2* promoter region.

Mouse Gene	Human homologue	Location of Human Homologue
Retinoid X receptor gamma	RETINOID X RECEPTOR GAMMA	1q22-q23
Dopachrome tautomerase	DOPACHROME TAUTOMERASE	13q31-q32
Silver	HOMOLOG OF MOUSE SILVER	12q13-q14
Distal-less homeobox 2	DISTAL-LESS HOMEOBOX 2	2q32
Neurogenic differentiation 1	NEUROGENIC DIFFERENTIATION 1	2q32
Cadherin 8	CADHERIN 8	16q21-q22.1

Table 4.8: The six differentially expressed mouse genes obtained from the microarray study, their human homologues, and the chromosome location of their human homologues

None of the chromosome locations of the six human genes correspond to known microphthalmia loci. However, the human homologues of the other genes identified in Chapter 1 were also examined. Of these, *GAS2* was localised on 11p15.2-p14.3 which coincides with the location of the NNO1 locus at 11p. *TRPM1* is localised to 15q13-q14, which also coincides with the microphthalmia locus at 15q12-q15. Finally, both *BIGLYCAN* and *RENBP* are localised to Xq28, within the Xq27-q28 locus to which a form of X-linked clinical anophthalmia was shown to be localised. It would be interesting to examine whether any cases of microphthalmia segregate to the loci of the genes listed in Table 4.8. Interestingly, both *Dlx2* and *Neurod1* are located in the same position, which would make this a particularly interesting locus to examine for microphthalmia.

In summary, the data obtained from the various approaches described in this and the previous chapter is brought together below in the Table 4.9.

Gene	Microarray (E11.5)	RT-PCR (E11.5)	In situ hybridisation (E11.5-E12.5)	Possible Chx10 binding sites
Rxrg	↑ 17.9x	↑ 10x	Not done (technical failure – p170)	Unlikely (only >2kb from start)
Si	↑ 3.5x	↑ 4x	RPE but also peripheral neural retina in *Chx10*$^{-/-}$	Unlikely (only >2kb from start)
Dct	↑ 4.8x	↑ 5x	RPE but also peripheral neural retina in *Chx10*$^{-/-}$	Unlikely (only >2kb from start)
Dlx2	↓ 13.8x	↓ 7x	Absent in *Chx10*$^{-/-}$ (weak stain in E11.5 +/+; stronger by E12.5)	Possibly: 3 ≤2kb from start 2 conserved in 3 species 1 in 5' UTR - unlikely
Neurod1	↓ 8.3x	↓ 6-109x	Absent in *Chx10*$^{-/-}$ (weak stain in E12.5 +/+)	Yes: 4 ≤ 2kb from start 1 conserved: 5 species 1 conserved: 4 species 1 conserved: 3 species
Cdh8	↓ 6.0x	↓ 2x	Absent in *Chx10*$^{-/-}$ (stained in +/+)	Possibly: ≤500 bp from start but not conserved

Table 4.9: Summary of expression data obtained for six genes in the wild type and *Chx10*$^{-/-}$ retinae

4.3 Discussion

4.3.1 Retinoid signalling gene up-regulated in the *Chx10*$^{-/-}$ retina

The studies described above have provided new information on how early retinal development is regulated. It has been hypothesised that Chx10 is important for retinal progenitor cell proliferation and the cell fate determination of bipolar cells (Burmeister et al., 1996). However, three of the genes examined here, *Rxrg*, *Dlx*, and *Neurod1*, are involved in retinal cell fate determination and two are involved in RPE specification (Budd and Jackson, 1995). The picture emerging from the studies in this and the previous chapter is that the lack of retinal progenitor cell proliferation in the *Chx10*$^{-/-}$ retina may be a result of misspecification of retinal progenitor cells, rather than directly related to cell cycle machinery.

Whilst it has been established that retinoic acid is an important signalling molecule both for development and vision (Brickell and Tickle, 1989; Hyatt and Dowling, 1997; Morriss-Kay, 1993; Rando, 1994), only a few studies have examined the expression of *Rxrg* in the developing retina. Dolle et al report the presence of *Rxrg* transcripts in the neuroblastic layer of the developing mouse retina and Kelley et al report the presence of *Rxrg* transcripts in amacrine and ganglion cells as well as in progenitor cells in the developing retina of the rat (Dolle et al., 1994; Kelley et al., 1995b). Five chicken retinoid receptor genes were examined throughout chicken retinal development. Of these, *Rxrg* was observed as early as day 4 of embryonic development in the central retina, with expression spreading to more peripheral regions by day 8. The first few *Rxrg* expressing cells were observed in the neuroblastic layer of the developing retina, but with increasing *Rxrg*-expressing cell numbers, expression became localised to the ventricular layer. By day 10, when photoreceptors and ganglion cells have been generated and begun to establish their definitive layers, *Rxrg* positive cells became restricted to the photoreceptor layer and continued to do so post-hatching (Hoover et al., 1998).

Thus *Rxrg* is expressed in retinal progenitor cells and subsequently restricted to a subset of retinal cells, specifically the photoreceptors. In another study, thyroid hormone beta 2 receptor and retinoid receptor (which form heterodimers with *TR-b2*)

mRNAs were examined in long term neonatal mouse retinal cultures. Long term cultures lacked green cone photoreceptors and showed a loss of *TR-b2* and *Rxrg* mRNA, indicating these proteins are involved in determination of green cone identity (Azadi et al., 2002). *Rxrg* is also detected in the nuclei and outer segments of cone photoreceptor cells of the mature human retina (Janssen et al., 1999). In contrast, Kelley et al have shown that 9-cis RA can promote rod differentiation and propose that a balance between TR and RXR activation determines whether photoreceptors differentiate into cones or rods in the mammalian retina, with predominant RXR activation biasing toward rod differentiation (Kelley et al., 1994; Kelley et al., 1995b). Thus retinoic acid promotion of differentiation of photoreceptors may be mediated through *Rxrg*. A similar role of *Rxrg* was suggested in developing myotomes, where it is expressed from an early age. Retinoic acid has a differentiating effect on myogenic cells and *Rxrg* is thought to mediate this effect (Dolle et al., 1994).

Rxrg expression has been studied in most detail in the central nervous system, where it is expressed in two domains early during development, in the developing hypothalamus and the neostriatum (Dolle et al., 1994). In fact, *Rxrg* and *Rxrg1* (one of two *Rxrg* isoforms) knock outs have been created to examine how the striatum was affected, as *Rxrg* and other retinoid receptors are expressed at high levels in this area and thought to be important for regulation of brain functions (Krezel et al., 1998; Saga et al., 1999). Interestingly, *Rxrg* expression in the developing hypothalamus is similar to that of the *Nkx-2* family of homeobox genes (Dolle et al., 1994). In the retina, *Rxrg* expression is initially similar to *Chx10* expression. In addition, *Rxrg* is also expressed in the ventral horns of the foetal spinal cord, where *Chx10* expression has also been observed (Dolle et al., 1994; Liu et al., 1994a).

Why is *Rxrg* up-regulated in the *Chx10*$^{-/-}$ retina? As different studies give contrasting evidence of the function of *Rxrg* (with one study showing the necessity for *Rxrg* in green cone photoreceptor differentiation, and another study showing a bias toward rod photoreceptor differentiation in the presence of predominant *Rxrg* expression (Janssen et al., 1999; Kelley et al., 1995b), it is difficult to asses what the effect of *Rxrg* up-regulation might be, and how it may be controlled by Chx10. Perhaps Chx10 is required to limit *Rxrg* expression early during development, to prevent

premature differentiation of photoreceptors. However, this would mean that one would expect to see an excess of photoreceptors in the *Chx10*$^{-/-}$ retina, and that photoreceptor differentiation occurs at an earlier time point. This does not seem to be the case, as rod, and possibly cone, photoreceptor differentiation seems to be delayed (Rutherford et al., 2004)(see also chapter 5).

Perhaps photoreceptor differentiation is only one role for *Rxrg*. It is initially expressed in retinal progenitor cells, as is Chx10, and thus may function together with Chx10 in retinal progenitor cells before causing photoreceptor differentiation, in the same way that Chx10 seems to play a role both in retinal progenitor cell proliferation and subsequently bipolar cell differentiation. Other retinoid signalling molecules showing a change in expression in the *Chx10*$^{-/-}$ retina include *Crabp1* and *Cnot7* (see Table 3.4 in Chapter 3). Thus Chx10 exerts a significant effect on retinoid signalling in the developing retina. However, it is unclear how this is done, as no Chx10 binding sites were found in the *Rxrg* promoter region, suggesting *Rxrg* is not a direct target for Chx10 regulation.

There is little indication that *Rxrg* is an up-regulated RPE gene in the same way that *Dct* and *Si* are. No *Rxrg* expression has been observed in the RPE, and in fact, no retinoic acids of any kind are expressed in the RPE, although their precursor retinols are (Hoover et al., 1998). However, there is some link between the RPE and *Rxrg* expression in the retina. Levels of the selected retinoid receptor transcripts are differentially affected by short- or long-term culture and in the latter case, an attached RPE seems to play a protective role (Azadi et al., 2002).

4.3.2 Another homeobox transcription factor down-regulated in the *Chx10*$^{-/-}$ retina

Dlx2 plays a role in cell fate determination during development. *Dlx2* is best-known for its role in forebrain and branchial arch development, where it regulates patterning and differentiation. In one study of forebrain development, *Dlx2* was shown to be expressed in the same cells as *Mash-1*, a bHLH gene and marker of relatively undifferentiated cells, but in a reciprocal fashion to *Map-2*, a marker of terminal neuron differentiation. Thus, like *Chx10* in the retina, *Dlx2* was thought to be

expressed at the transition from proliferation to terminal differentiation (Porteus et al., 1994). It has been suggested that alternate cell fate choices in the developing telencephalon are controlled by coordinated functions of bHLH and homeobox transcription factors through their differential effects on Notch signalling (Yun et al., 2002). This echoes studies in the retina, where *Mash-1* and *Math-3* (bHLH genes) and *Chx10* are required to direct bipolar cell differentiation (Hatakeyama et al., 2001) and the combination of Notch and bHLH transcription factor signalling are generally thought to be a mechanism in which retinal cell type specification occurs (Perron and Harris, 2000a).

One study examines the expression of *Dlx2* at various stages during mouse retinal development. *Dlx2* can be detected in retinal progenitors at E12.5 and this was confirmed in the current study (Figure 4.9B). At E13.5 expression of *Dlx2*, *Brn3b*, *Pax6* and *Chx10* define distinct yet overlapping domains in the retinal neuroepithelium (de Melo et al., 2003). The *Dlx1* and *Dlx2* double knock out retina shows reduced cellularity in the ganglion cell layer, whilst amacrine and horizontal cells seem to develop relatively normally, and it has been suggested that *Dlx2* is required for late-born retinal ganglion cell differentiation (de Melo et al., 2003). In the adult, *Dlx2* is co-expressed with *Brn3b* in ganglion cells, *Pax6* in amacrine, horizontal, and ganglion cells, and *Chx10* in some bipolar cells. These data support a role for *Dlx2* in inner retinal development and in the retinal differentiation and/or maintenance of the inner nuclear layer interneurons and ganglion cells in the adult. It has been suggested that a subset of retinal progenitors require *Dlx1/2* expression to down-regulate *Chx10* expression in order to begin their terminal differentiation as retinal ganglion cells (de Melo et al., 2003). However, the data obtained here suggest that *Chx10* is upstream of *Dlx2* and is needed for its induction. Perhaps a lack of *Chx10* arrests the induction of *Dlx2* expression, and this may lead to a decreased number of retinal ganglion cells in the *Chx10*$^{-/-}$ retina.

4.3.3 *Neurod1* is a candidate for Chx10 regulation

Of the three genes involved in cell fate determination, the third is a bHLH gene (where *Rxrg* was a retinoid receptor and *Dlx2* was a homeobox gene). In this study, *Neurod1* seems the most likely candidate for direct Chx10 regulation. *Neurod1* is

known to play a role in cell specification in a variety of organs. The role of *Neurod1* in the developing pancreas has been studied in depth, as the *Neurod1* knock out mouse shows abnormal pancreatic islet morphogenesis and overt diabetes. *Neurod1* also plays are role in the proliferation and differentiation of enteroendocrine cells of the small intestine. Over-expression of *Neurod1* leads to cell cycle arrest and apoptosis, whilst the re-entry into the cell cycle of normally quiescent cells and disrupted cell number are observed in the null (Mutoh et al., 1997). Interestingly, cyclin D1, a gene thought to be down-regulated in the *Chx10*$^{-/-}$ retina, is thought to repress *Neurod1* in enteroendocrine cells, in manner independent of its effects on the cell cycle (Ratineau et al., 2002).

Neurod1 is also transiently expressed in a subset of neurons in the central and peripheral nervous systems at the time of their terminal differentiation. Ectopic expression of *Neurod1* in Xenopus causes conversion of epithelial cells into neurons (Lee et al., 1995). Mice homozygous for a *Neurod1* deletion fail to develop a granule cell layer within the dentate gyrus. Whilst early cell populations in the dentate gyrus are present and normally organised, and migration of dentate precursor cells and newly born granule cells from the neuro-epithelium to the dentate gyrus remains intact, a dramatic defect in proliferation of precursor cells is observed once they reach the dentate gyrus and a significant delay in the differentiation of granule cells occurs (Liu et al., 2000a). It seems *Neurod1* is required for the differentiation of granule cells in the cerebellum and hippocampus and is critical for postnatal neurogenesis in the mouse brain (Miyata et al., 1999).

In the retina, *Neurod1* is expressed in areas of undetermined retinal cells as well as in developing photoreceptors and amacrine cells (Morrow et al., 1999b). Strong expression is first observed at E17, although expression of *Neurod1* is strong elsewhere in the CNS from E13. In the current study weak Neurod1 expression was observed at E12.5 in the wild type. Expression is maintained in a subset of mature photoreceptors in the adult (Morrow et al., 1999a). *Neurod1* is thought to be a critical regulator of neuronal versus glial fate, a regulator of interneuron development, favouring amacrine over bipolar differentiation, and essential for the terminal differentiation and survival of a subset of photoreceptors (Inoue et al., 2002; Morrow et al., 1999a; Pennesi et al., 2003). A loss of *Neurod1* results in age-related

degeneration of rods and cones (Pennesi et al., 2003). It has also been found to suppress glial differentiation and stimulate some cells from the toxin damaged chicken retina to acquire some neuronal phenotypes (Fischer et al., 2004).

Like *Rxrg* and *Dlx2*, *Neurod1* is expressed in retinal progenitors and then becomes localised to a subset of retinal neurons. Both *Rxrg* and *Neurod1* seem to be required for normal photoreceptor differentiation and *Dlx2* seems to be required for a subset of retinal ganglion cell differentiation. A change in expression in all three of these genes is therefore likely to significantly affect the proportions and morphology of retinal neurons, going some way to explaining the apparent lack of properly differentiated cells observed in the *Chx10*$^{-/-}$ retina. An examination of when and how well the various retinal cell types begin to differentiate in the *Chx10*$^{-/-}$ retina may lead to further insights in how Chx10 regulates retinal development, and forms the subject of the following chapter.

4.3.4 RPE genes up-regulated in the *Chx10*$^{-/-}$ retina

Two of the genes examined here are known to be expressed in the RPE. Silver and dopachrome tautomerase are expressed in all developing melanocytes. Silver encodes a pigment cell-specific transmembrane protein that resides in the melanosomal matrix and is a diagnostic marker for melanoma (Adema et al., 1996; Kobayashi et al., 1994; Kwon et al., 1991). The carboxyl terminus of silver is truncated in the classical coat colour mutant *silver*, resulting in dilution of hair coloration (Kwon et al., 1991; Martinez-Esparza et al., 1999). Silver can accelerate melanin synthesis *in vitro* and direct melanosomal matrix assembly (Berson et al., 2001; Lee et al., 1996b); however a complete understanding of the function of silver in melanocytes remains elusive. *Dct* converts L-dopachrome into 5,6-dihydroxyindole-2-carboxylic acid. Mutations in the *Dct* gene are responsible for the phenotype of the classic pigmentation mutation slaty (Budd and Jackson, 1995; Jackson et al., 1992). *Dct* can be detected in migratory melanocytes as early as 10 days of gestation and is also expressed in the neuroectoderm destined to become RPE (Steel et al., 1992).

Silver is expressed in the presumptive RPE starting at E9.5 and in neural crest-derived melanoblasts starting at E10.5. Its expression in dorsal regions precedes dopachrome tautomerase expression, suggesting it identifies melanoblasts at an earlier developmental stage than *Dct*. (Baxter and Pavan, 2003). Silver expression is not detectable in embryos mutated for microphthalmia associated transcription factor (*Mitf*), demonstrating transcriptional dependence of Silver on *Mitf* in the RPE. Interestingly, another gene shown to be differentially expressed in the microarray study, *Trpm1*, is also transcriptionally dependent on *Mitf*. Mutations in *Mitf* in the mouse cause RPE to thicken, lose pigmentation and expression of a number of pigment epithelium transcription factors, and eventually trans-differentiate into a laminated second retina (Bumsted et al., 2001; Mochii et al., 1998; Nakayama et al., 1998; Packer, 1967; Scholtz and Chan, 1987). It is thought that the progressive restriction of *Mitf* expression to the future RPE is instrumental for the separation of the mammalian optic vesicle into NR and RPE (Nguyen and Arnheiter, 2000).

Two other published studies have also identified the expression of RPE-specific genes within the *Chx10*$^{-/-}$ retina. Horsford et al. suggested that *Chx10* is not necessary for the initial specification of the neural retina, but is required for its maintenance (Horsford et al., 2005). They report ectopic expression of *Mitf* in the *Chx10*$^{-/-}$ retina, and by using *Chx10* and *Mitf* transgenic mice to misexpress these two genes in the NR and RPE, show an antagonistic interaction between *Chx10* and *Mitf*. It was suggested that *Chx10* repression of *Mitf* ensures the maintenance of the neural retinal identity, and that in its absence, ectopic expression of *Mitf* results in cells previously specified as NR to transdifferentiate to RPE cells. (Horsford et al., 2005). In the second study, electroporation of Chx10 into chick optic vesicles resulted in strong down-regulation of *Mitf* and other RPE-specific genes. In addition, the authors of this study used a Chx10 BAC reporter mouse to perform cell lineage studies in the *Chx10*$^{-/-}$ retina in mixed genetic backgrounds, and demonstrate that neural retinal cells transdifferentiate to RPE (Rowan et al., 2004). *Mitf* was not found to be up-regulated in the microarray study performed here however, but the up-regulation of RPE-specific genes, some of which are dependent on *Mitf* expression, does support a role for Chx10 in maintaining a boundary between RPE and NR. The early time point used here to examine expression makes it unclear whether this change in gene expression is a result of an early misspecification event or a gradual trans-

differentiation event. A change in expression of these genes suggests that Chx10 seems to play a greater role in retinal cell specification than in the actual cell cycle of retinal progenitor cells, and exerts its effects through various transcription factors that control exit from the cell cycle and commitment to a differentiation pathway, rather than through the regulation of cell cycle machinery.

4.3.5 Cadherin 8 may be involved in bipolar cell fate specification

Finally differential expression for cadherin 8 was observed between the wild type and *Chx10*$^{-/-}$ retina. In the developing central nervous system, cadherins are thought to play a role in neural connectivity: based on their preferential homotypic binding and the localisation of cadherins in synaptic junctions (Honjo et al., 2000; Korematsu and Redies, 1997; Uchida et al., 1996). Cadherin 8 expression is restricted to particular subdivisions of early central nervous system and the thalamus. Korematsu et al studied cadherin 8 expression in the central nervous system in detail from early during embryogenesis to postnatal stages and suggest its expression pattern indicates that *Cdh8* is involved in the formation of striatal compartmentalised structures during brain development (Korematsu et al., 1998; Korematsu and Redies, 1997). No report was made of cadherin 8 expression in the eyes in these studies.

Few studies have examined cadherin 8 expression in the developing retina. Wohrn et al examined cadherin 6B and cadherin 7 expression during chicken retinal development, and studies of R-cadherin, N-cadherin and B-cadherin have been reported (Wohrn et al., 1998 and references therein). A study of five cadherins (N-cad, R-cad, cad-6, cad-8, cad-11) in the mouse postnatal retina suggests each may be expressed in a restricted population of retinal cells (Honjo et al., 2000). Cadherin 8 is expressed in the ganglion cell layer and the inner nuclear layer between postnatal days 0 and 3 (P0-P3). By P7 it is expressed in a deeper zone of the INL and by P14 expression in the INL is prominent, whilst expression in the GCL is diminished. A similar pattern is observed in the adult, but overall less *Cdh8* expression is observed. It is thought that these *Cdh8* positive cells may be bipolar cells, as they do not co-label with calbindin-D, a horizontal and amacrine cell marker (Honjo et al., 2000). Here, the first report of expression of *Cdh8* within the early embryonic wild type retina was made, and microarray, *in situ*, and RT-PCR data support an early function

in the retina which is disrupted by a lack of Chx10. Its down-regulation in the *Chx10*$^{-/-}$ retina may be an early indication that bipolar cell specification is not occurring normally.

4.3.6 Conclusions

Real time PCR and *in situ* hybridisation have confirmed the changes in expression observed in the microarray study described in the previous chapter of all six genes chosen for further examination. In addition, the *in silico* study performed here suggests *Neurod1* may be a target for direct Chx10 regulation. Further functional studies will be required to confirm or refute this interaction. The microarray study and the further investigation of some of the genes showing a change in expression have revealed that as well as affecting the transcript levels of proteins regulating proliferation, Chx10 also seems to exert early effects on genes thought to be important for retinal cell differentiation and cell fate specification. As all cell types, with the exception of bipolar cells, are present in the *Chx10*$^{-/-}$ retina (Burmeister et al., 1996), little investigation has been done into how cell differentiation has been affected by a lack of Chx10. Thus, one of the aims of the following chapter is to examine how early proliferation and differentiation of retinal neurons is affected by a lack of Chx10.

CHAPTER 5

Chx10$^{-/-}$ retinal progenitor cells exhibit altered properties during retinal development

5.1. Introduction

Chx10 is essential for RPC proliferation. DNA synthesis in the *Chx10*$^{-/-}$ mutant has been examined by quantifying incorporation of the thymidine analogue bromodeoxyuridine (Kee et al., 2002). A large reduction in BrdU labelling was found at the periphery of the embryonic retina but labelling indices were not significantly altered in the central retina (Bone-Larson et al., 2000; Burmeister et al., 1996). Lack of proliferation in the *Chx10*$^{-/-}$ mutant is partially rescued by deletion of the cell cycle regulatory gene p27^{Kip1} (Green et al., 2003). It is clear that proliferation of RPCs is affected by an absence of Chx10; however it is unclear how this occurs.

The microarray data described in Chapter 1 shows a relationship between Chx10 and regulation of expression of cell cycle proteins. Altered regulation of a single cell cycle protein could be all that is necessary to reduce proliferation, as has been observed when a decrease in proliferation was observed in cyclin D1 knock out mice (Fantl et al., 1995). However, data does not currently exist showing that lack of, for example, *Gas2* or *Ccne2* causes small eyes. In addition, genes of cell cycle proteins were in the minority amongst the genes identified by the microarray study.

Instead, the picture that emerged was that Chx10 affects a variety of transcription factors involved in the specification of the neural retina and the surrounding RPE, and in regulating RPC development. A variety of transcription factors are known to affect eye size. Over-expression of several eye-specific transcription factors results in giant eyes (Kobayashi et al., 2001; Zuber et al., 2003). Lack of other transcription factors reduce eye size(Chow and Lang, 2001; Fantl et al., 1995; Lee et al., 1996a). However, none of the transcription factors identified in the microarray study are known to regulate proliferation levels or eye size.

Conversely, Chx10 is known to be important for differentiation and maintenance of a specific cell type, the bipolar cell (Burmeister et al., 1996; Liu et al., 1994b). Other transcription factors, such as *Crx* and *Brn3b* are important for differentiation of other specific retinal cell types, photoreceptors and retinal ganglion cells respectively (Furukawa et al., 1999; Liu et al., 2000b). The relationship between the effects on RPC proliferation and differentiation in the Chx10 retina is unclear. Perhaps changes

in cell cycle that result in a smaller retina are a secondary effect of transcriptional regulation of retinal progenitor cell development.

As described in Chapter 1, the aims of this thesis are to understand the causes of the *Chx10*$^{-/-}$ phenotype, and the disease aetiology of microphthalmia. The microarray study was designed to do this at a molecular level, through examination of the genetic pathway in which Chx10 is involved. The studies described in this chapter were performed to better characterise the abnormal behaviour of RPCs in the absence of Chx10, and thus examine the *Chx10*$^{-/-}$ phenotype at a cellular level. Elucidating how RPCs behave differently in the *Chx10*$^{-/-}$ retina should offer clues to how the small eye phenotype is caused. The studies described here were designed to further elucidate how lack of Chx10 affects RPC behaviour and examined two hypotheses:

1. The cell cycle of RPCs is altered in the *Chx10*$^{-/-}$ retina
2. Differentiation of retinal cell types is affected by a lack of Chx10.

In order to examine cycling behaviour, three studies were undertaken. Firstly, anti-phosphohistone H3 and proliferating cell nuclear antigen (Kurki et al., 1988) immuno-labelling was used to examine the distribution of mitotic/cycling cells in the wild type eye and in the *Chx10*$^{-/-}$ mutant eye during embryonic development.

Secondly, flow cytometry was used to examine what proportions of retinal progenitor cells were in various stages of the cell cycle. Flow cytometry is a common approach to monitor the cell cycle of mammalian cells. It can measure DNA content of individual cells at a great speed, and thus conveniently reveal cell distribution over DNA content, which indicates the locations of cells in the cell cycle. Dyes such as propidium iodide (PI), which bind DNA, provide a rapid and accurate means for quantitating both total nuclear DNA content and the fraction of cells in each phase of the cell cycle. The fluorescence signal intensity of the PI is directly proportional to the amount of DNA in each cell. DNA content distribution of a typical exponentially growing cell population is composed of two peaks of G1/G0 and G2/M phase and a valley of S phase. G2/M phase cells have twice the amount of DNA of G1/G0 phase cells, and S phase cells possess varying amounts of DNA between G1 and G2 cells (Krishan, 1975; Nicoletti et al., 1991).

Thirdly, I examined the dividing behaviour of newly born cells. Investigations in the rat and chick retina have indicated that the mitotic spindle orientation during cell division is associated with whether an RPC divides asymmetrically, to give one daughter that remains as a progenitor and one that adopts a differentiation pathway, or symmetrically, giving rise to two daughter cells that divide again (Cayouette and Raff, 2003; Cayouette et al., 2001; Silva et al., 2002). RPCs with horizontal spindle orientations (i.e. parallel to the ventricular surface) tend to produce daughters that become the same cell type (symmetric cell division) whereas RPCs with vertical spindles (i.e. perpendicular to the ventricular surface) tend to produce daughters that with different fates (asymmetric) (Cayouette et al., 2001). Based on the hypothesis that the types of divisions are important for expansion and initiation of differentiation of the RPC pool I compared the mitotic spindle orientations in E11.5 mutant and wild type retinae.

Finally, in order to examine how cell differentiation is affected in the *Chx10*$^{-/-}$ retina, and test the second hypothesis, various markers of immature and mature neural retinal cells were used in order to compare their initiation of expression. β3 tubulin is an early pan-neuronal marker that labels maturing retinal cells (Snow and Robson, 1994; Watanabe et al., 1991). In addition, cell-type specific markers were used at various stages of early retinal development, between E11.5, when the first ganglion cells are born and begin to differentiate, until P20, when differentiation of the latest born cells, the rod photoreceptors, is occurring. In addition, the numbers of nuclei in the various cell layers of the P12 wild type and *Chx10*$^{-/-}$ were counted to examine whether there is a difference in the relative numbers of various types of cells.

5.2. Results

5.2.1 Mitotic cells in the *Chx10*$^{-/-}$ mutant retina fail to amplify the size of the retinal progenitor cell population

To examine the cycling behaviour of Chx10-expressing RPCs in the central retina, anti-phospho-histone H3, which strongly labels cells during mitosis, was used to compare the distribution of mitotic cells in the wild type eye and in the *Chx10*$^{-/-}$ mutant mouse, during embryonic development. The anti phospho-histone H3 antibody used here is highly specific for the phosphorylated form of histone H3, whose phosphorylation at Ser10 initiates at the end of G2, and is complete just prior to the formation of prophase chromosomes at the beginning of mitosis. Dephosphorylation begins in anaphase and is completed just as detectable chromosome decondensation occurs in telophase (Hendzel et al., 1997).

H3-positive mitotic cells located at the ventricular edge of the neuroblastic cell layer, where mitosis occurs (see Figure 5.4), were detected in the wild type and *Chx10*$^{-/-}$ retina at various points of development, from E11.5 to E18.5. At E11.5, wild type and *Chx10*$^{-/-}$ central retinal sections are roughly similar in size, and a similar number of cells are undergoing mitosis at the ventricular edge (two examples each of wild type and *Chx10*$^{-/-}$ E11.5 retinal sections are shown in Figure 5.1A-D). By E13.5 the *Chx10*$^{-/-}$ retina is visibly smaller and thinner than the wild type retina (compare Figure 5.1E and F). Fewer cells seem to be undergoing mitosis and a lack of H3 labelling was observed in the periphery of the mutant retina (Figure 5.1F) which is consistent with previous reports of reduced BrdU incorporation at the periphery (Bone-Larson et al., 2000; Burmeister et al., 1996). The same phenomenon was observed during the rest of embryogenesis - no H3-labelled cells are observed in the periphery *Chx10*$^{-/-}$ retina at E15.5 or E18.5 (Figure 5.2C and D). By contrast H3-positive cells were detected in the central retina of both genotypes throughout embryogenesis.

Whilst H3-labelled cells were observed along the entire ventricular edge of the wild type retina at later stages of embryogenesis (Figure 5.2A, B), few labelled cells were observed in the E15.5 and E18.5 *Chx10*$^{-/-}$ retina, and these were limited to the central

Figure 5.1: H3-labelled cells in the developing *Chx10*$^{-/-}$ retina at E11.5 and E13.5. Midline sections from wild type (*A,C,E,*) and *Chx10*$^{-/-}$ (*B,D,F*) eyes at E11.5 (*A-D*) and E13.5 (*E,F*), labelled with H3 antibody (green) and counter-stained with Hoechst nuclear dye (blue). At E11.5, wild type (*A,C*) and *Chx10*$^{-/-}$ (*B,D*) retina show a similar number of mitotic H3-positive cells along the ventricular surface. At E13.5, the wild type retina (*E*) is larger than the *Chx10*$^{-/-}$ (*F*). More cells were labelled in the wild type retina than in the *Chx10*$^{-/-}$ retina, and no cells were labelled in the periphery of the *Chx10*$^{-/-}$ retina (dashed white lines demarcating central retina in *F*). Scale bars = 100 μm, scale bar in A applies to A-D.

E11.5

+/+ -/-

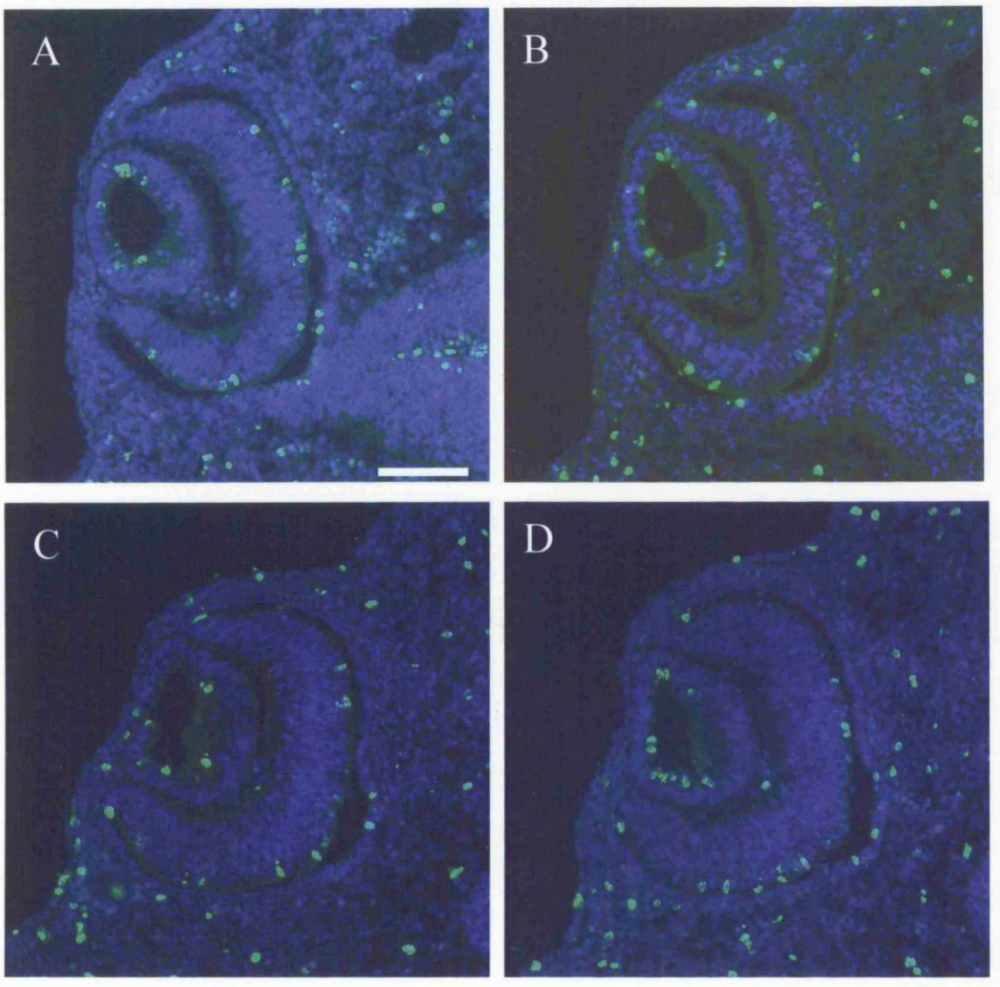

E13.5

+/+ -/-

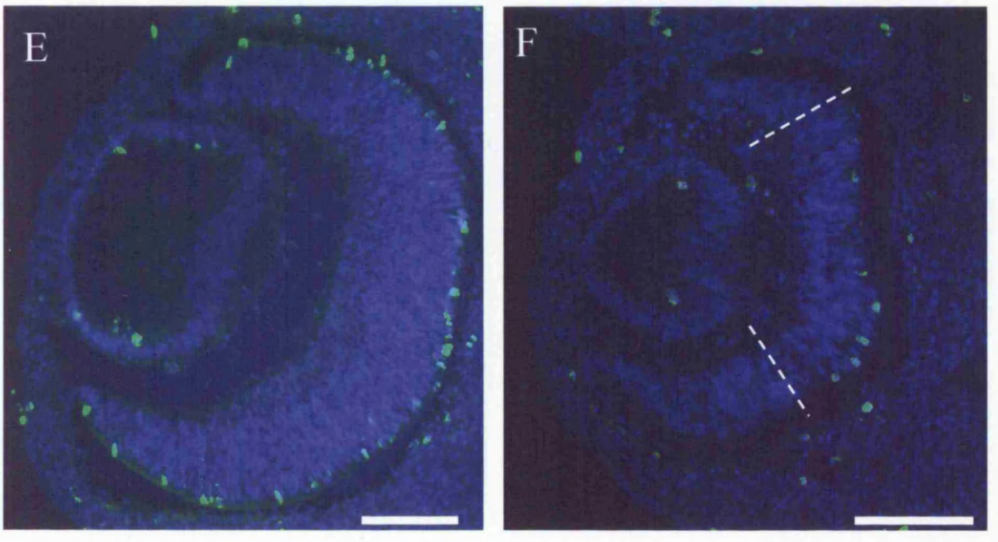

Figure 5.2: H3-labelled cells in the developing *Chx10*$^{-/-}$ retina at E15.5 and E18.5. Midline sections from wild type (*A,B,E,F*) and *Chx10*$^{-/-}$ (*C,D,G,H*) eyes at E15.5 (*A,C,E,G*) and E18.5 (*B,D,F,H*), labelled with H3 antibody (green) and counterstained with Hoechst nuclear dye (blue). *A-D* show mitotic cells in whole retinal sections of the E15.5 (*A,C*) and E18.5 (*B,D*) *Chx10*$^{-/-}$ and wild type central retinae. Fewer labelled cells are present in the *Chx10*$^{-/-}$ retinae, and mitotic cells tend to be located more dorsally in the E18.5 *Chx10*$^{-/-}$ retina (*D*). High magnification views of retinal sections are depicted in (*E-H*). H3-positive cells displaced from the ventricular surface were seen in the in the *Chx10*$^{-/-}$ retina at both E15.5 (*G*) and E18.5 (*H*) (arrowheads) retina. Scale bars = (in A) 200 μm for A and B and 100 μm in C and D, (in E) 50 μm for E-H.

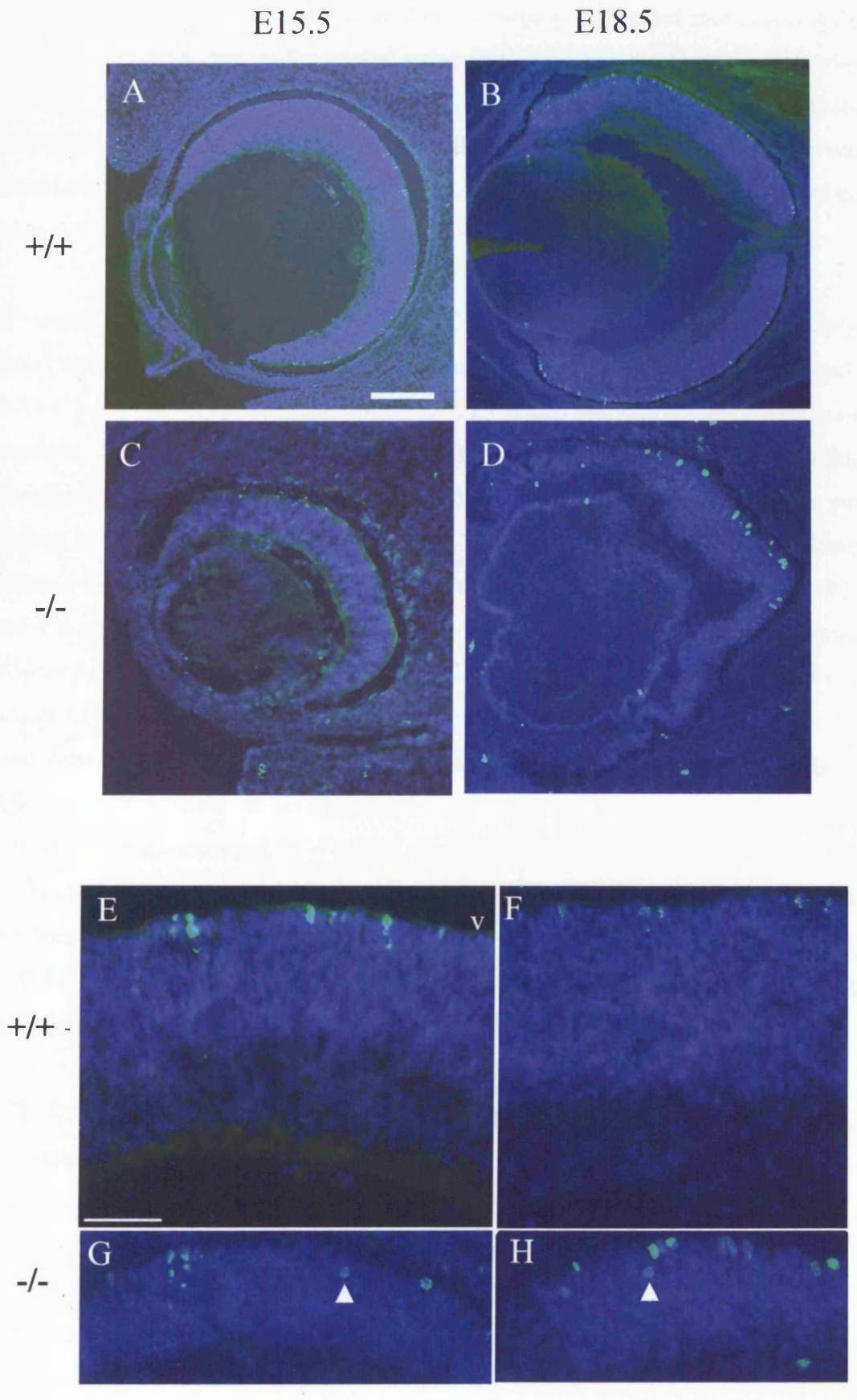
E15.5
E18.5
A
B
+/+
C
D
-/-
E
v
F
+/+
G
H
-/-

retina. In addition, at E18.5, H3-lablled cells tended to be located more specifically towards the dorsal area of the central retina (Figure 5.2C, D). High magnification images of wild type and *Chx10*$^{-/-}$ retina at E15.5 and E18.5 (Figure 5.2E-H) revealed abnormal positioning of mitotic cells was in the *Chx10*$^{-/-}$ retina. H3 labelling was found not only in cells at the ventricular edge, but also in cells displaced towards the vitreal edge (Figure 5.2G, H, arrowheads).

To compare the number of mitotic cells in *Chx10*$^{-/-}$ and wild type retina, the mitotic labelling index was estimated at each stage from midline retinal sections (Figure 5.3A-C). A count of total cell numbers in central retinal sections reveals a significant increase in total cell number in the wild type retina at each time point during development. In contrast, there is no significant increase in total cell number per section in the *Chx10*$^{-/-}$ retina from time point to time point up to E15.5. A significant increase in average total cell number per section is observed from E11.5 to E18.5, but it is only a 3-fold increase compared to a 13-fold increase in the wild type retina (Figure 5.3A). Numbers of H3-labelled cells were counted and divided by total cell counts to estimate the mitotic labelling index. At E11.5, a similar proportion of the total cells in the wild type and mutant are undergoing mitosis ($p = 0.16$) (Figure 5.3C), whereas there is a significant difference between genotypes at each subsequent stage analysed ($p < 0.001$). In both the mutant and the wild type, the mitotic index decreased significantly from E11.5 to E13.5 (Figure 5.3C). When the absolute numbers of H3-labelled cells were compared during this period it was observed that there is a significant increase in dividing cells in the wild type retina whereas the number is constant in the mutant, over the same period (Figure 5.3B).

At E15.5 and E18.5, the wild type pattern of growth (significantly increasing total cell number) and significantly decreasing mitotic index continued (Figure 5.3A-C). By contrast, no significant change is observed between the mitotic index at E13.5 and E18.5 in the mutant retina; a small increase in both total cell number and the number of H3 labelled cells was observed (Figure 5.3A-C). Despite the presence of mitotic cells throughout embryogenesis in the mutant, in numbers similar to the number of mitotic cells present at E11.5 in the wild type (compare E18.5 mutant with E11.5 wild type in Figure 5.3B), a large expansion in the size of the pool of dividing RPCs was not observed in the mutant.

Figure 5.3: Comparison of total cell number and H3 labelled cells in wild type and *Chx10*$^{-/-}$ retina. (*A*) Total cell number of wild type retina increases steadily in the wild type retina during development. Significant increases in total cell number were observed between every time point in the wild type (*p<0.001). In the *Chx10*$^{-/-}$ retina, a small but significant overall increase is observed between E11.5 and E18.5 (**, p<0.001). (*B*) The number of H3-labelled mitotic cells in the wild type retina increases significantly between E11.5 and E18.5 (*p<0.001) and between E11.5 to E13.5 (p=.024). In the *Chx10*$^{-/-}$ retina, no overall significant increase is observed in H3-labelled cells between E11.5 and E18.5. (*C*) The number of H3-labelled cells was divided by the total number of cells per section, to create the mitotic labelling index. Early in development, at E11.5, a similar proportion of cells are undergoing mitosis in the *Chx10*$^{-/-}$ and wild type retina. At E13.5 there is a significant decrease in the mitotic index of both the *Chx10*$^{-/-}$ and wild type retina (*p=0.002,**p=0.008). This trend continued in the wild type retina throughout development, with a significant difference in mitotic labelling index between E13.5 and E18.5 (*p=0.003), but no significant change was observed in the mitotic labelling index from E13.5 onwards in the *Chx10*$^{-/-}$ retina. Columns indicate means, error bars = sd. n = nine midline sections taken from three eyes.

A

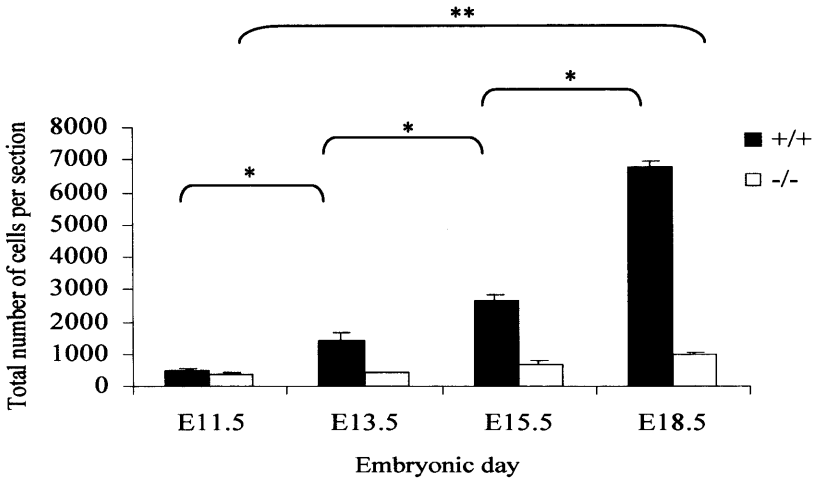
**
*
*
*
Total number of cells per section
8000
7000
6000
5000
4000
3000
2000
1000
0
E11.5
E13.5
E15.5
E18.5
Embryonic day
+/+
-/-

B

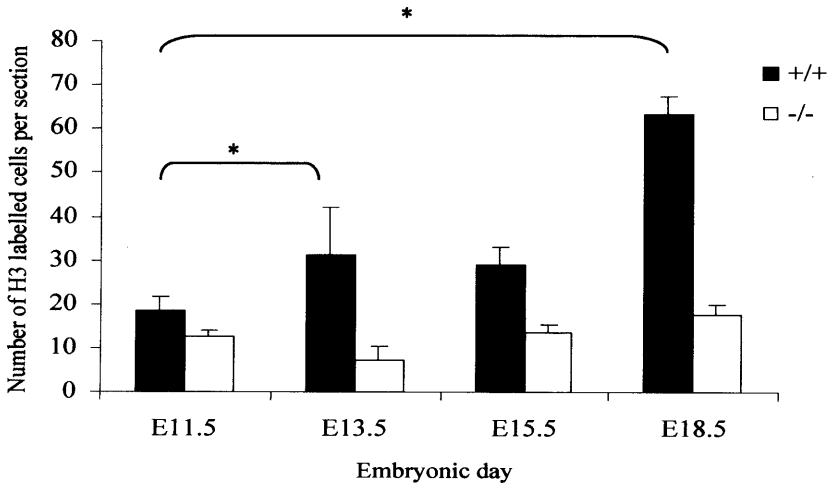
*
*
Number of H3 labelled cells per section
80
70
60
50
40
30
20
10
0
E11.5
E13.5
E15.5
E18.5
Embryonic day
+/+
-/-

C

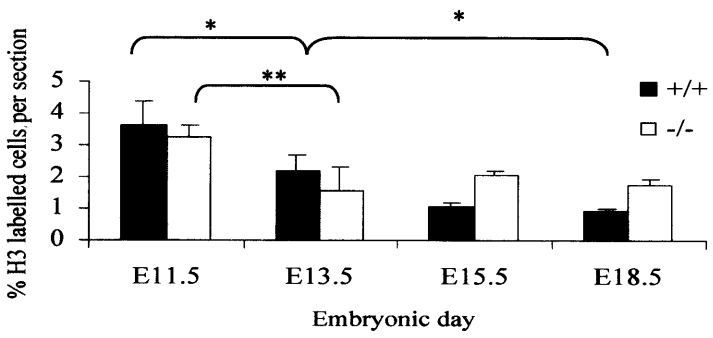
*
*
**
% H3 labelled cells per section
5
4
3
2
1
0
E11.5
E13.5
E15.5
E18.5
Embryonic day
+/+
-/-

5.2.2 PCNA labelling confirms a lack of proliferation at the periphery

Immunostaining with PCNA (proliferating cell nuclear antigen), which labels cells during the G1 and S phases of the cell cycle (Kurki et al., 1988), Figure 5.4) confirmed the pattern of reduced proliferation at the retinal periphery compared to central retina. At E13.5, a differentiating cell layer has developed along the vitreal edge of the retina, where cells have exited the cell cycle to differentiate to their final retinal cell types. The RPCs still cycling are located in the neuroblastic layer towards the ventricular edge of the retina. PCNA staining can be observed throughout the neuroblastic layer of the retina, particularly, along the ventricular edge of the retina, where cells are undergoing mitosis, and in the vitreal edge of the neuroblastic layer - adjacent to the differentiated cell layer - where most cells are thought to be in S phase (Figure 5.5A). PCNA staining is seen in both the central retina and the periphery (Figure 5.5A, C). In contrast, PCNA staining in the *Chx10*$^{-/-}$ retina is restricted to the central retina (Figure 5.5B, D). PCNA labelled cells are located throughout the retina, from the ventricular edge to the vitreal edge (Figure 5.5D), in contrast to labelling in the wild type retina. This suggests that no differentiating cell layer has become established yet at this point.

A similar pattern of staining can be observed at E15.5 (Figure 5.5E-H). PCNA labelled cells in the wild type retina are restricted to the neuroblastic layer, where cells are proliferating, whilst no PCNA labelling is observed in the differentiated cell layer toward the vitreal edge (Figure 5.5G). As was observed at E13.5, staining seems brightest at the ventricular edge of the neuroblastic cell layer, (Figure 5.5E). In the *Chx10*$^{-/-}$ retina, however, PCNA labelled cells are again observed from the ventricular edge to the vitreal edge of the entire retina, suggesting that differentiating cells are not forming a separate layer to RPCs (Figure 5.5H). PCNA staining is limited to the central retina, and no PCNA labelled cells are observed in the periphery (Figure 5.5F).

By E18.5, PCNA labelling in the wild type retina is becoming fainter in the neuroblastic layer. Although staining can still be observed in the neuroblastic layer of the wild type retina (Figure 5.6A, C), the strongest staining is confined to cells along the ventricular edge of the retina (Figure 5.6C). A high power confocal microscope

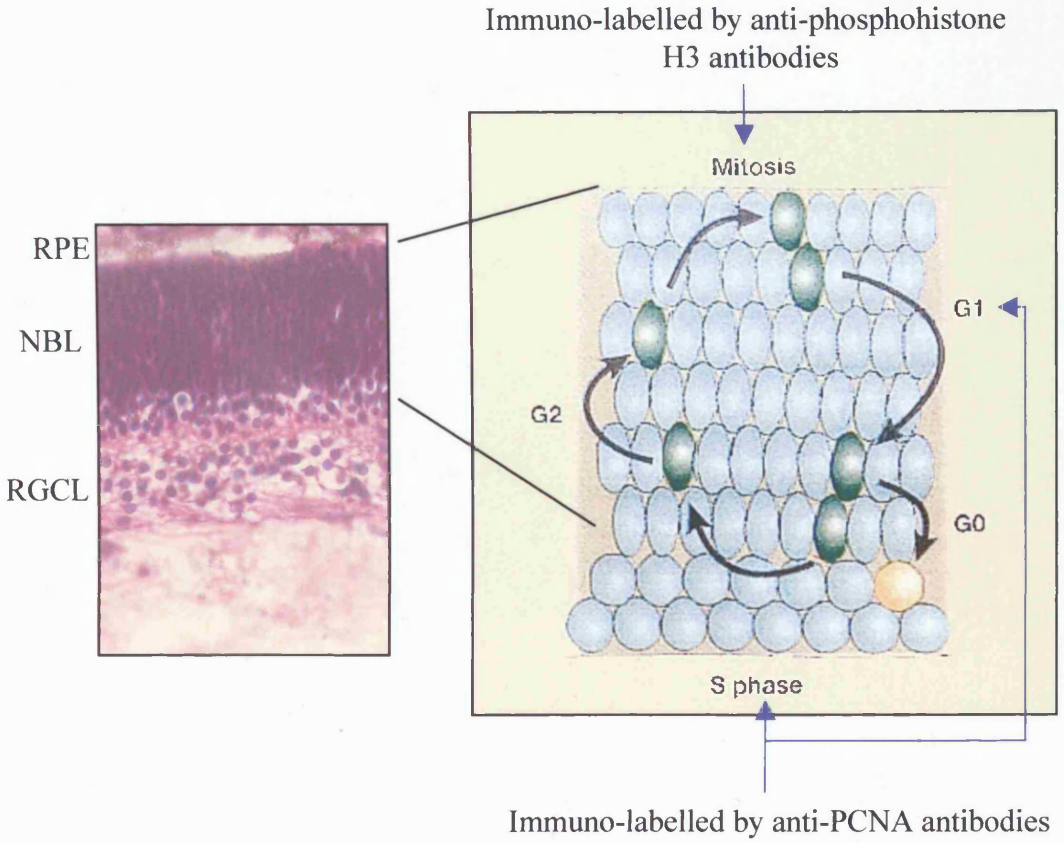

Figure 5.4: Localisation of cells in various phases of the cell cycle in the developing retina. Cells underoing mitosis are situated at the ventricular edge of the neuroblastic layer, and as they progress through G1 and S phase, they migrate toward the vitreal edge of the neuroblastic layer. Cells that exit the cell cycle and go on to differentiate migrate further towards the vitreal edge, away from the neuroblastic layer, whilst cells that will divide again migrate back toward the ventricular edge.

Figure 5.5: PCNA labelling of wild type and *Chx10*$^{-/-}$ retina at various time points during development. At E13.5 (*A-D*) PCNA labelling (red, with blue Hoechst nuclear counter-stain) in the wild type retina (*A,C*) can be observed throughout the proliferating neuroblastic layer from the centre of the retina to the very periphery (*C*). In the *Chx10*$^{-/-}$ retina, PCNA labelling is observed in the central retina (*B, D*) from the vitreal layer to the ventricular layer, but no staining is observed in the periphery (*B*, arrows indicate boundaries of staining). A similar pattern is observed at E15.5 (*E-G*), where PCNA staining is still observed in the neurobalstic layer of the wild type retina (*E,G, NBL*), with no staining in the differentiated cell layer (*G*). In the *Chx10*$^{-/-}$ retina, PCNA labelling remains confined to the central retina (*F*, arrows indicate boundaries of PCNA labelling) and is still present from the vitreal to the ventricular edge of the retina (*H*). Scale bar in A = 100 μm for A, 50 μm for B and C; scale bar in D = 50 μm; scale bar in E = 100 μm for E and F, 50 μm for G and H.

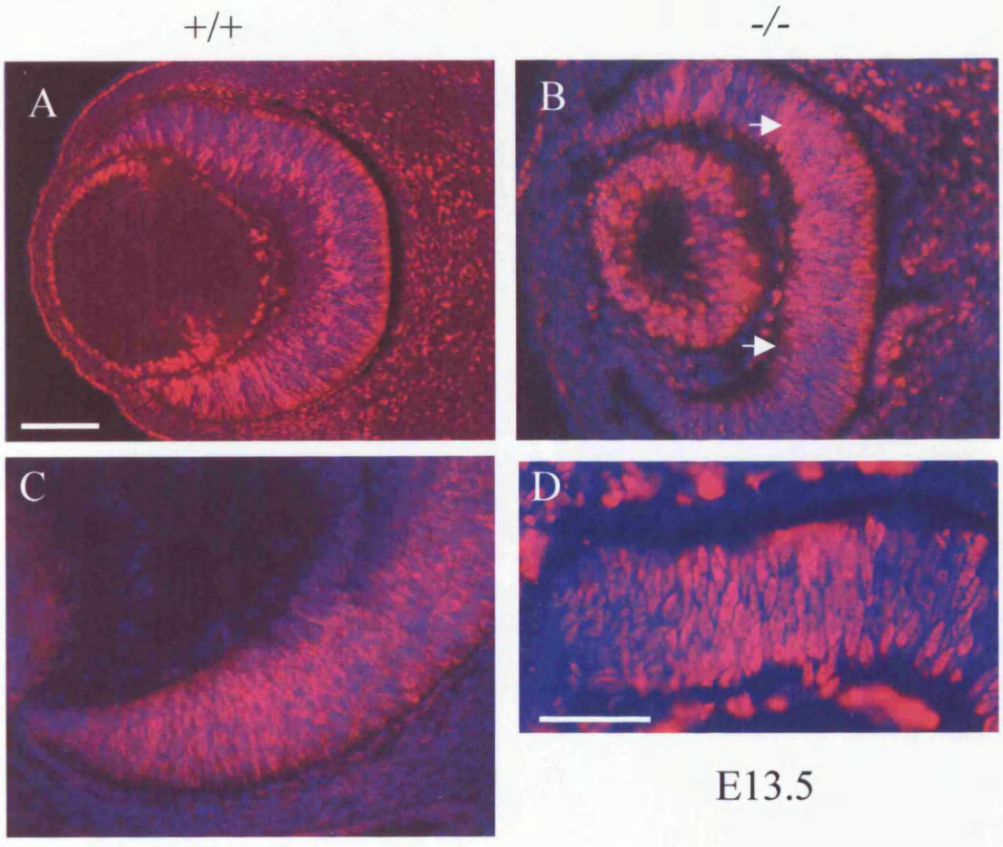
+/+
-/-
A
B
C
D
E13.5

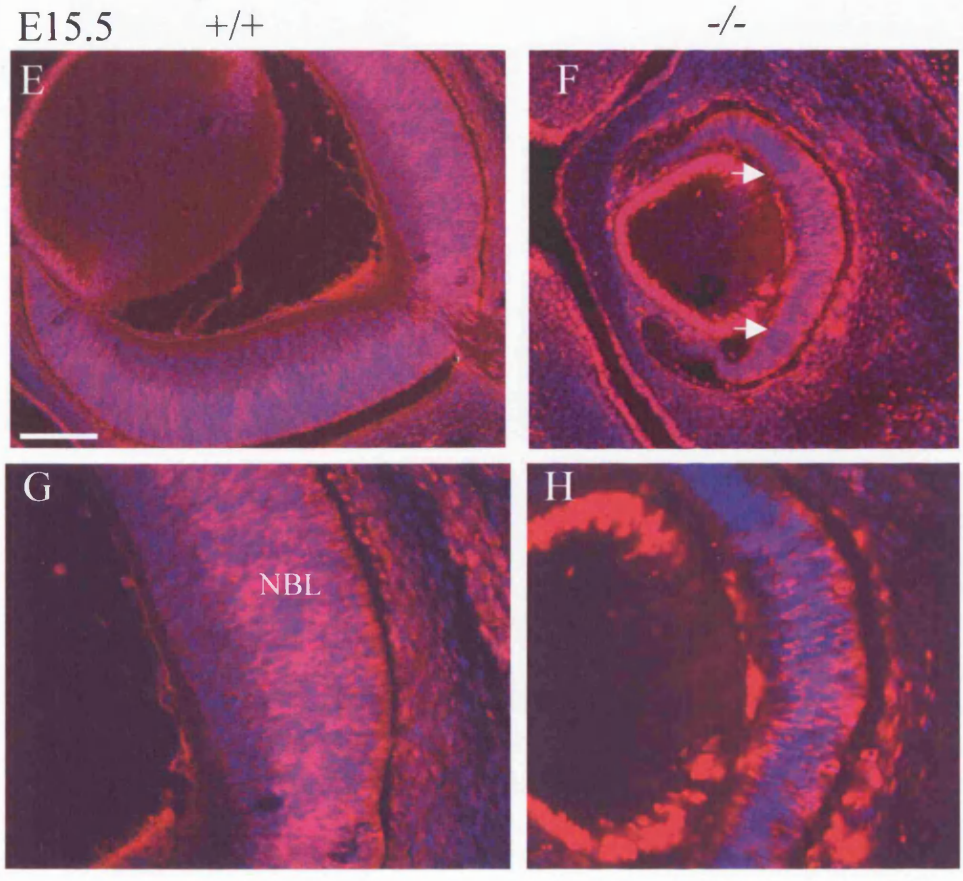
E15.5
+/+
-/-
E
F
G
NBL
H

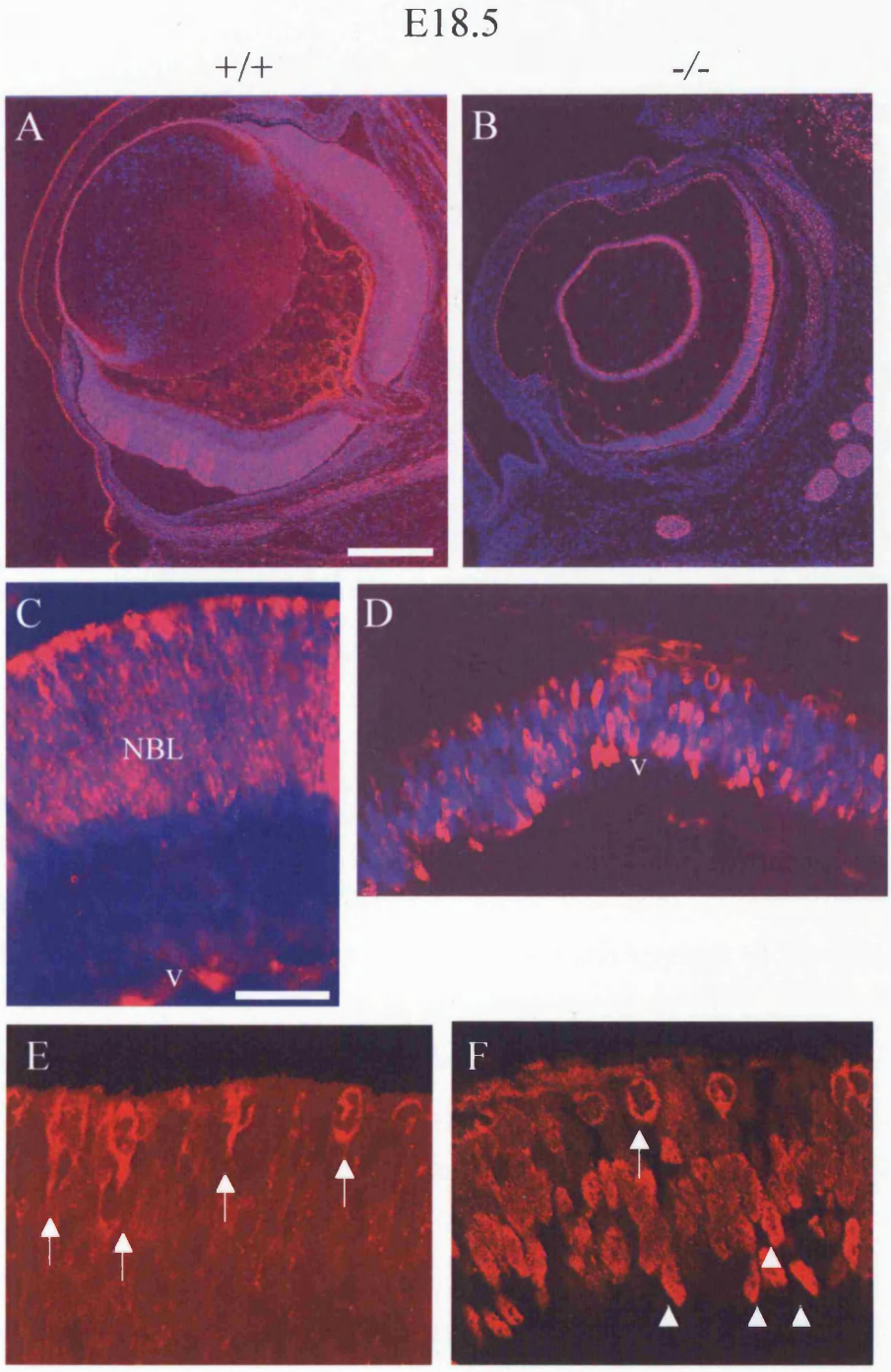

Figure 5.6: PCNA labelling (red, with blue Hoechst nuclear counter-stain in *A-D*) of wild type (A,C,E) and *Chx10*$^{-/-}$ (B,D,F) retina at E18.5. PCNA labelling in the wild type retina is strongest at the ventricular edge of the retina and is observed in the proliferating neuroblastic layer (C, NBL), whilst the postmitotic cells toward the vitreal edge (v) of the retina no longer express PCNA. In the *Chx10*$^{-/-}$ retina, PCNA labelling still occurs throughout the retina (*D*). E and F are confocal images. Strong PCNA staining is observed in mitotic cells at ventricular edge of wild type retina (E, arrows), and in both mitotic cells at the ventricular edge of the retina (F, arrow) and in nuclei of proliferating cells throughout the *Chx10*$^{-/-}$ retina (F, arrowheads). Scale bar in A = 200 μm for A and B; scale bar in C = 50 μm for C and D.

image of the wild type retina at this time point shows bright PCNA labelling in dividing cells along the ventricular edge of the retina (Figure 5.6E, arrows). In contrast, PCNA labelling is observed throughout the width of the *Chx10*$^{-/-}$ retina, although staining again is confined to the central retina, and in particular the dorsal area of the retina (Figure 5.6B). Both mitotic cells at the ventricular edge of the *Chx10*$^{-/-}$ retina and cycling cells in the rest of the retina are strongly labelled (Figure 5.6D, F, arrows point to mitotic cells and arrowheads to cycling cells). Thus PCNA labelling confirms that there is a lack of proliferation occurring in the periphery of the *Chx10*$^{-/-}$ retina from E13.5 onwards, and suggests that a greater proportion of cells are cycling in the *Chx10*$^{-/-}$ retina than in the wild type retina at later time points, mirroring the H3 data.

5.2.3 Apoptosis does not contribute to the cell number deficit or differentiation delay in the early embryonic *Chx10*$^{-/-}$ retina

TdT-mediated dUTP nick end labelling (TUNEL) was used to assess whether increased levels of apoptosis were occurring during development of the *Chx10*$^{-/-}$ retina, which could explain the low level of retinal growth in the *Chx10*$^{-/-}$ retina. Between E11.5 and E18.5 the total cell number has increased 13 times compared to less than 4 times in the mutant (Figure 5.3A). The TUNEL procedure was used to examine whether this difference might have resulted from an increase in apoptosis in the *Chx10*$^{-/-}$ retina.

7 retinal sections from 4 eyes were examined from the wild type retina. Very few apoptotic cells were observed in most sections (Figure 5.7), with the exception of sections from the ventral retina including the optic fissure, where an increased number of apoptotic cells were observed. On average, 9.8 +/- 5.0 apoptotic cells were observed per midline retinal section in the wild type retina. Similarly, only a very small number of apoptotic figures were observed in the *Chx10*$^{-/-}$ retina. In fact, fewer apoptotic cells were observed in the *Chx10*$^{-/-}$ retina than in the wild type. On average, only 3.4 +/- 2.2 apoptotic cells were observed per retinal section, counted in 17 sections from 2 eyes. A significant difference ($p<0.015$ student's t-test) was observed between the number of apoptotic cells in central E11.5 in the wild type and mutant retina. This corresponds with previous data on apoptosis in the *Chx10*$^{-/-}$ retina (Robb

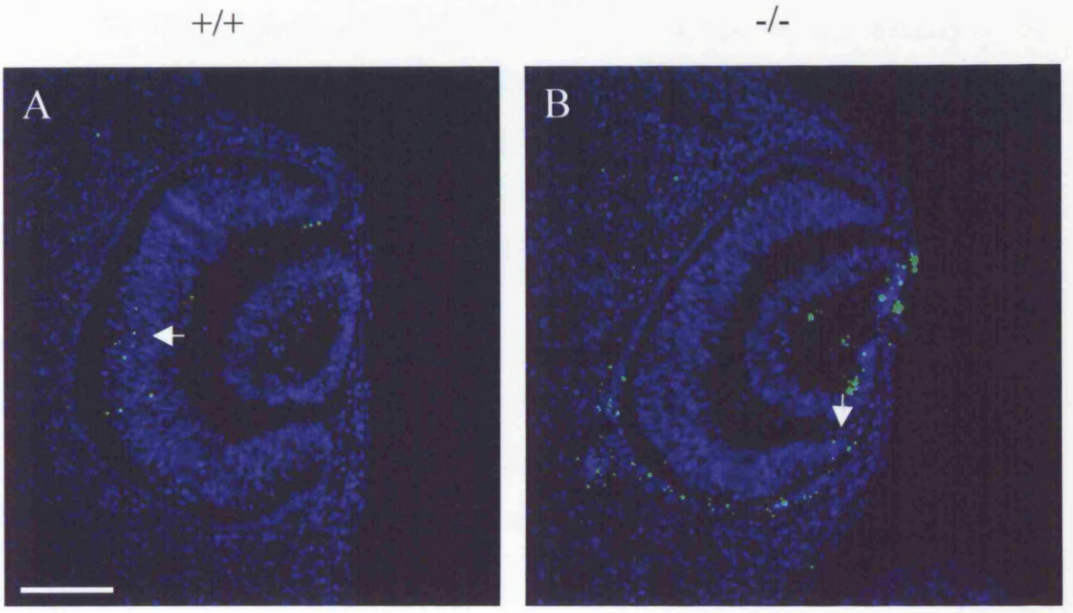

Figure 5.7 TUNEL labelling (green) of E11.5 wild type (*A*) and *Chx10*$^{-/-}$ (*B*) retina. Apoptotic bodies can be observed in the central area of the wild type retina (*A*, arrow), whilst apoptotic bodies seem to be localised at the periphery of the *Chx10*$^{-/-}$ retina (*B*, arrow)

et al., 1978; Theiler et al., 1976). Thus changes in apoptosis are unlikely to be involved in the reduced size of the retina, as fewer apoptotic cells were observed in the *Chx10*$^{-/-}$ retina than in the wild type.

Interestingly, the positioning of the apoptotic figures in the *Chx10*$^{-/-}$ retina was different to that of the apoptotic cells in the wild type. In the wild type retina, apoptotic figures were generally observed in the central retina (Figure 5.7A, arrow). In contrast, apoptotic figures in the *Chx10*$^{-/-}$ retina were observed in the periphery of the retina (Figure 5.7B, arrow). As this is the same area in which cell proliferation is observed to be reduced, this difference is particularly striking.

5.2.4 Changes in the cell cycle

The H3 data indicated that RPCs in the *Chx10*$^{-/-}$ retina do seem to proliferate, do not die, but also do not expand in number. In order to investigate in what ways RPCs of the *Chx10*$^{-/-}$ retina differed from those of the wild type retina, flow cytometry was used to measure the DNA content of dissociated RPCs and compare the percentage of cells at G1/G0, G2 and S stage of the cell cycle. Neural retinae from 3 pools of E11.5 wild type and 3 somite matched pools of *Chx10*$^{-/-}$ mouse embryos were dissociated, labelled with propidium iodide and analysed using an Epics XL flow cytometer (Beckman Coulter). For each sample, 30,000 events were collected on the flow cytometer, using doublet discrimination to exclude clumps of cells. The data was analysed using Expo32 software (Beckman Coulter) to only select single cells in the cell cycle (i.e. excluding dead or fragmented cells). The data was subsequently modelled using Multicycle software (Phoenix flow systems), using an appropriate modelling system (the 'aggregates' modelling system). The data closely fit this model, used for analysis of single cells, and this was verified by low Chi squared values upon fitting the data to the model.

The graphs obtained using Multicycle software are shown in Figures 5.8. Each graph shows an initial G1/G0 peak, and a final G2 peak, with an S phase curve between the two. This S phase curve is visibly smaller in the *Chx10*$^{-/-}$ retina.

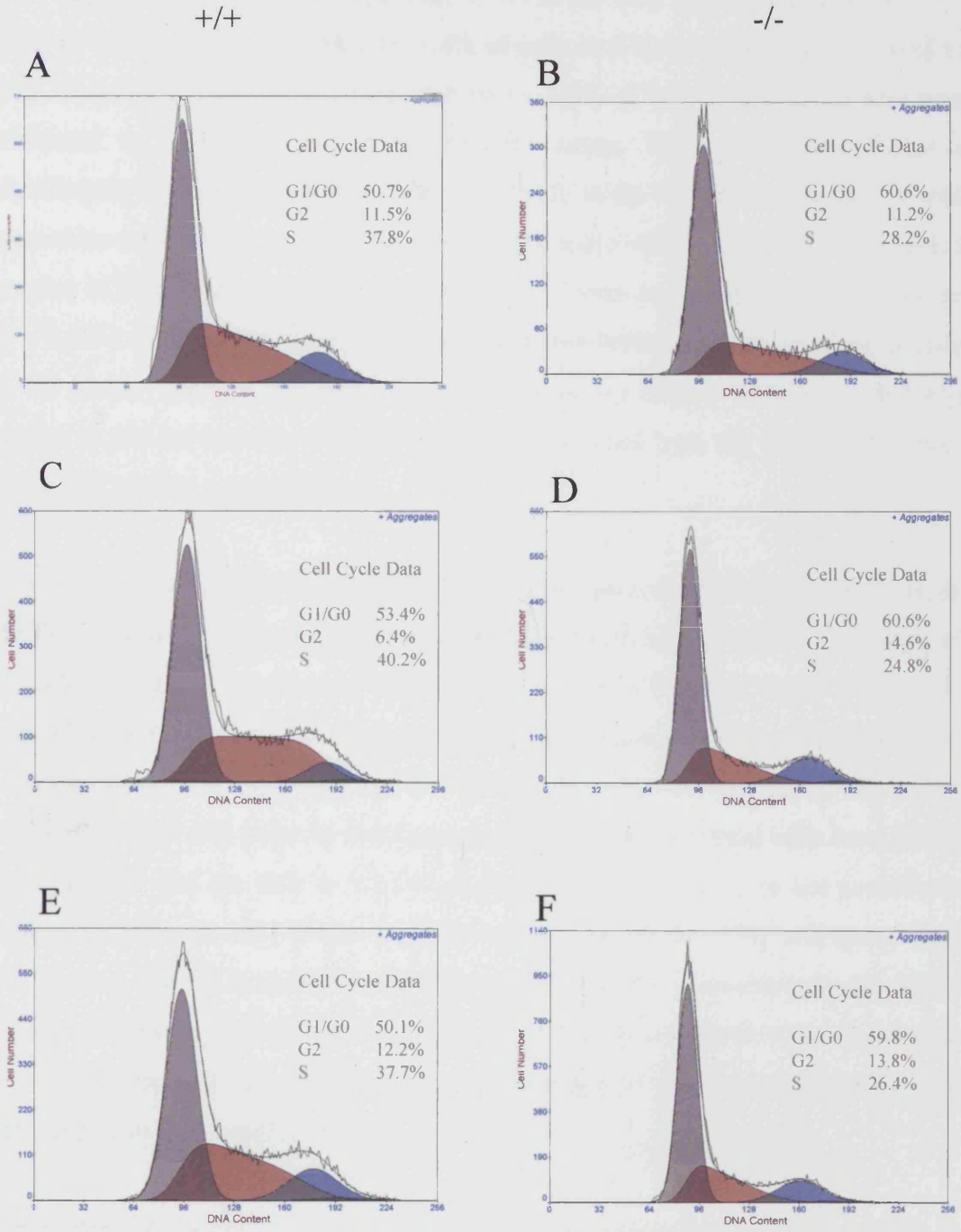

Figure 5.8: Flow cytometry data of retinal progenitor cells at E11.5. Graphs representing proportions of retinal progenitor cells in the various stages of the cell cycle at E11.5 in the wild type (*A,C,E*) and *Chx10*$^{-/-}$ (*B,D,*F) retinae. G1/G0 phase is shown in grey, S phase in red, and G2 phase in blue. A larger proportion of cells reside in the G1/G0 phase of the cell cycle in the *Chx10*$^{-/-}$ retina than in the wild type, whilst a smaller proportion reside in S phase (compare cell cycle data of B, D, F to A, C, E).

On average, 51.4 +/- 1.8 % of cells were in G1 in the wild type compared to 60.3 +/- 0.5% in the *Chx10*$^{-/-}$ retina, 38.6 +/- 1.4% of cells in S in the wild type compared to 26.5 +/- 1.7% in the *Chx10*$^{-/-}$ retina and 10 +/- 3.2% of cells in G2 in the wild type compared to 13.2 +/- 1.8% in the *Chx10*$^{-/-}$ retina. These data showed that a significantly higher proportion of cells were in G1 in the *Chx10*$^{-/-}$ retina than in wild type retina (student t-test, $p = 0.001$, Figures 5.8 and 5.10E). Conversely a decreased number of RPCs were in S-phase in the *Chx10*$^{-/-}$ retina compared with the wild type ($p < 0.001$). No significant difference was observed between the proportions of cells in G2 phase. Thus, at the stage when the retinae are largely undifferentiated and similar in size between the *Chx10*$^{-/-}$ mutant and the wild type, the cycling properties of the RPCs differ considerably.

Three pools of wild type and *Chx10*$^{-/-}$ retinae were also collected at E13.5 and run on the flow cytometer (Figure 5.9A-F). The proportions of cells in the various stages of the cell cycle have not changed significantly between E11.5 and E13.5 in the wild type. However, two out of the three pools showed a markedly reduced proportion of cells undergoing G2, and there was a corresponding increase in cells in the G1/G0 and S phases. At this point in development, a proportion of retinal cells have exited the cell cycle and are thus in the G0 phase of the cell cycle. It is not possible to distinguish between cells in the G1 phase and the G0 phase of the cell cycle using this method. Thus it is not clear whether a decrease in the proportion of cells in G2 phase and a corresponding increase in the proportion of cells in G1/G0 compared to E11.5 is a result of cells differentiation or a change in the relative lengths of the various phases of the cell cycle.

Again there is a significant difference between the proportion of cells residing in G1/G0 phase and in S phase ($p = 0.02$ and 0.001 respectively) between the wild type and the *Chx10*$^{-/-}$ retina. By this point, in the *Chx10*$^{-/-}$ retina, an even larger proportion of the retinal progenitor cells tested (70.6 +/- 3.0%) were in G1/G0 (Figure 5.9 and 5.10B) than at E11.5, whilst a smaller proportion of RPCs are in S phase (19.8 +/- 3.4%). It is possible that the G1 phase of the cell cycle is extended in the *Chx10*$^{-/-}$ retina, or that a large proportion of cells have exited the cell cycle and are residing in G0.

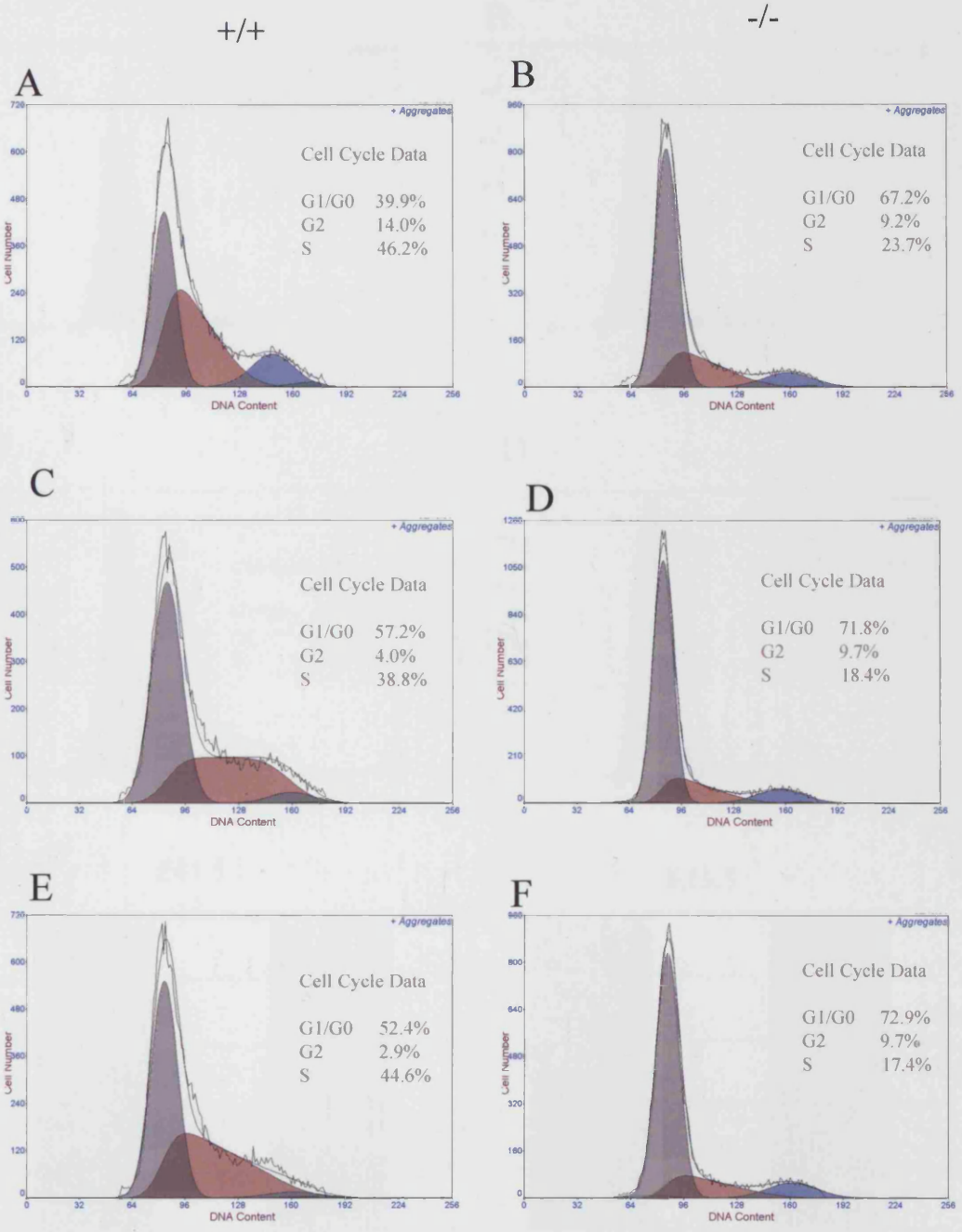

Figure 5.9*:* Flow cytometry data of retinal progenitor cells at E13.5. Graphs representing proportions of retinal progenitor cells in the various stages of the cell cycle at E13.5 in the wild type (*A,C,E*) and *Chx10*$^{-/-}$ (*B,D,F*) retinae. G1/G0 phase is shown in grey, S phase in red, and G2 phase in blue. A larger proportion of cells reside in the G1/G0 phase of the cell cycle in the *Chx10*$^{-/-}$ retina than in the wild type, whilst a smaller proportion reside in S phase (compare cell cycle date of B, D, F to A, C, E).

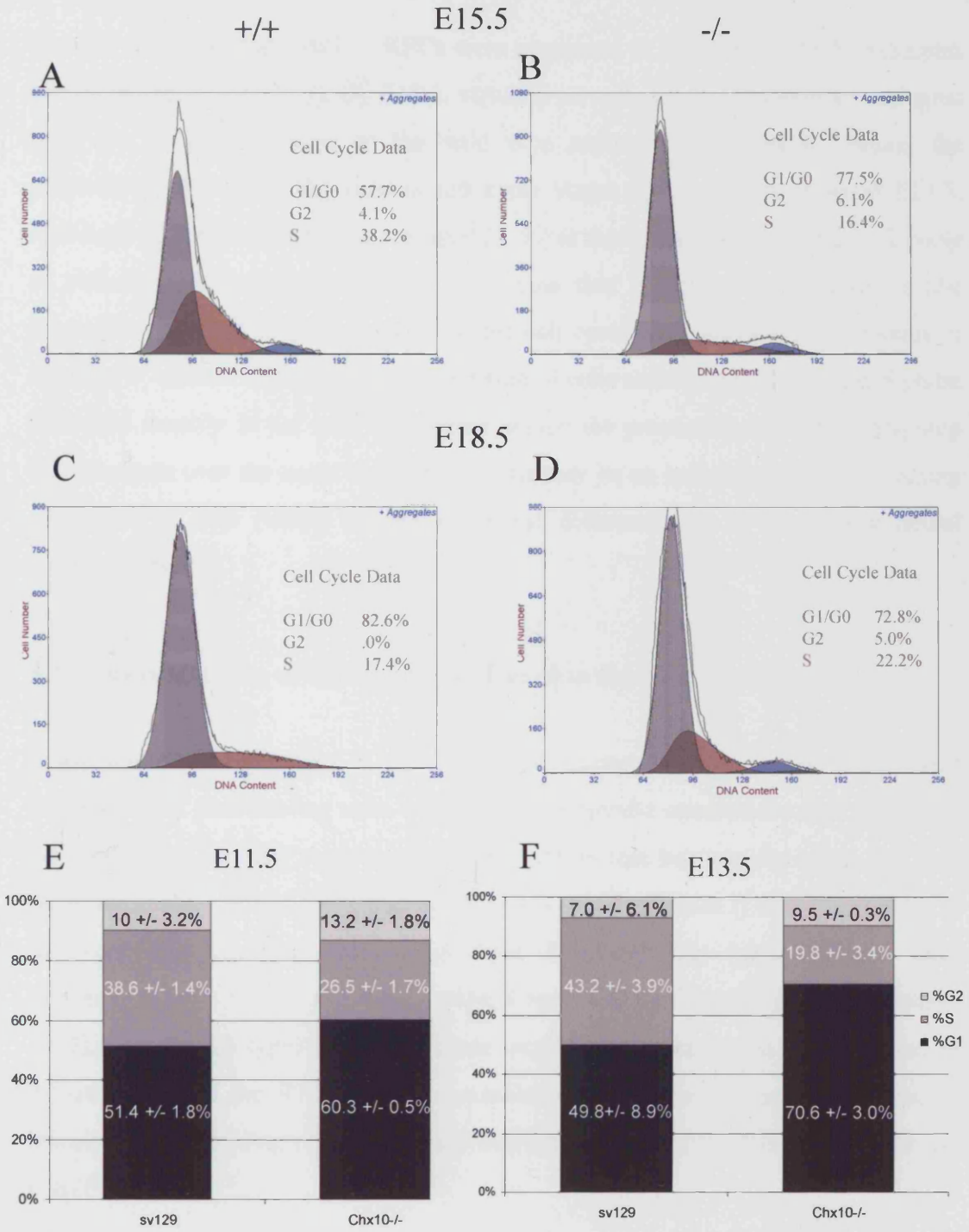

Figure 5.10: Flow cytometry data of retinal progenitor cells. *A-D:* Graphs representing proportions of retinal progenitor cells in the various stages of the cell cycle at E15.5 (*A, B*) and 18.5 (*C, D*) in the wild type (*A,C*) and *Chx10*$^{-/-}$ (*B,D*) retinae. G1/G0 phase is shown in grey, S phase in red, and G2 phase in blue. A larger proportion of cells reside in the G1/G0 phase of the cell cycle in the *Chx10*$^{-/-}$ retina than in the wild type at E15.5, whilst the proportions are similar at E18.5. No cells reside in the G2 phase of the cell cycle in the wild type retina by E18.5 (*C*). *E-F*: Summary of flow cytometry results for retinal progenitor cells at E11.5 (*E*) and E13.5 (*F*) in the wild type and *Chx10*$^{-/-}$ retina. A comparison of wild type versus *Chx10*$^{-/-}$ RPCs shows that a higher proportion of cells reside in the G1/G0 phase of the cell cycle in the *Chx10*$^{-/-}$ retina at both time points.

Finally, wild type and *Chx10*$^{-/-}$ RPCs were examined at E15.5 and E18.5 (examples shown in Figure 5.10A-D). By E18.5, virtually no cells are in G2 anymore and most cells are in G1/G0 phase in the wild type retina. In the *Chx10*$^{-/-}$ retina, the proportions of cells in the various cell cycle stages are similar to those at E13.5. Although no statistical analysis was carried out at these time points as only 1-2 pools of retinae were collected for each, it seems that there is little change in the proportions of cells at various stages of the cell cycle from about E13.5 onwards in the *Chx10*$^{-/-}$ retina. In contrast, the proportion of cells undergoing G1/G0 and S phase increased steadily in the wild type retina, whilst the proportion of cells undergoing G2 decreases over the same time period. This may be an indication of the increasing proportion of cells exiting the cell cycle and differentiating to the various neural retinal cell types.

5.2.5 The orientation of cell division is altered in the *Chx10*$^{-/-}$ retina

Some studies, in particular in the developing cortex but also in the retina, have suggested that proliferating cells with horizontal spindle orientations (i.e. parallel to the ventricular surface) tend to produce daughters that become the same cell type (symmetric cell division) whereas those with vertical spindles (i.e. perpendicular to the ventricular surface) tend to produce daughters that have different fates (asymmetric) (Cayouette and Raff, 2003a; Chenn and McConnell, 1995; Zamenhof, 1987). Perhaps the types of divisions are important for expansion and initiation of differentiation of the RPC pool. To examine this hypothesis, the mitotic spindle orientations of dividing cells were classified and counted in the E11.5 wild type and *Chx10*$^{-/-}$ retinae.

Retinal sections were stained with 4'6-diamidino-2-phenylindole (DAPI), which allows the identification of cells in late anaphase and telophase when condensed chromosomes are separating (Hamada and Fujita, 1983; Otto and Tsou, 1985). As in section 5.2.1, mitotic figures were localised and counted along the ventricular edge of the retina. If a line drawn through the spindle of a mitotic figure was 0^0 +/- 45^0 to the ventricular surface of the retina, the division was classified as horizontal (Figure 5.9A). If the line through the mitotic spindle was 90^0 +/- 45^0 to the ventricular surface, the mitotic figure was classed as a vertical division (Figure5.11B). Only

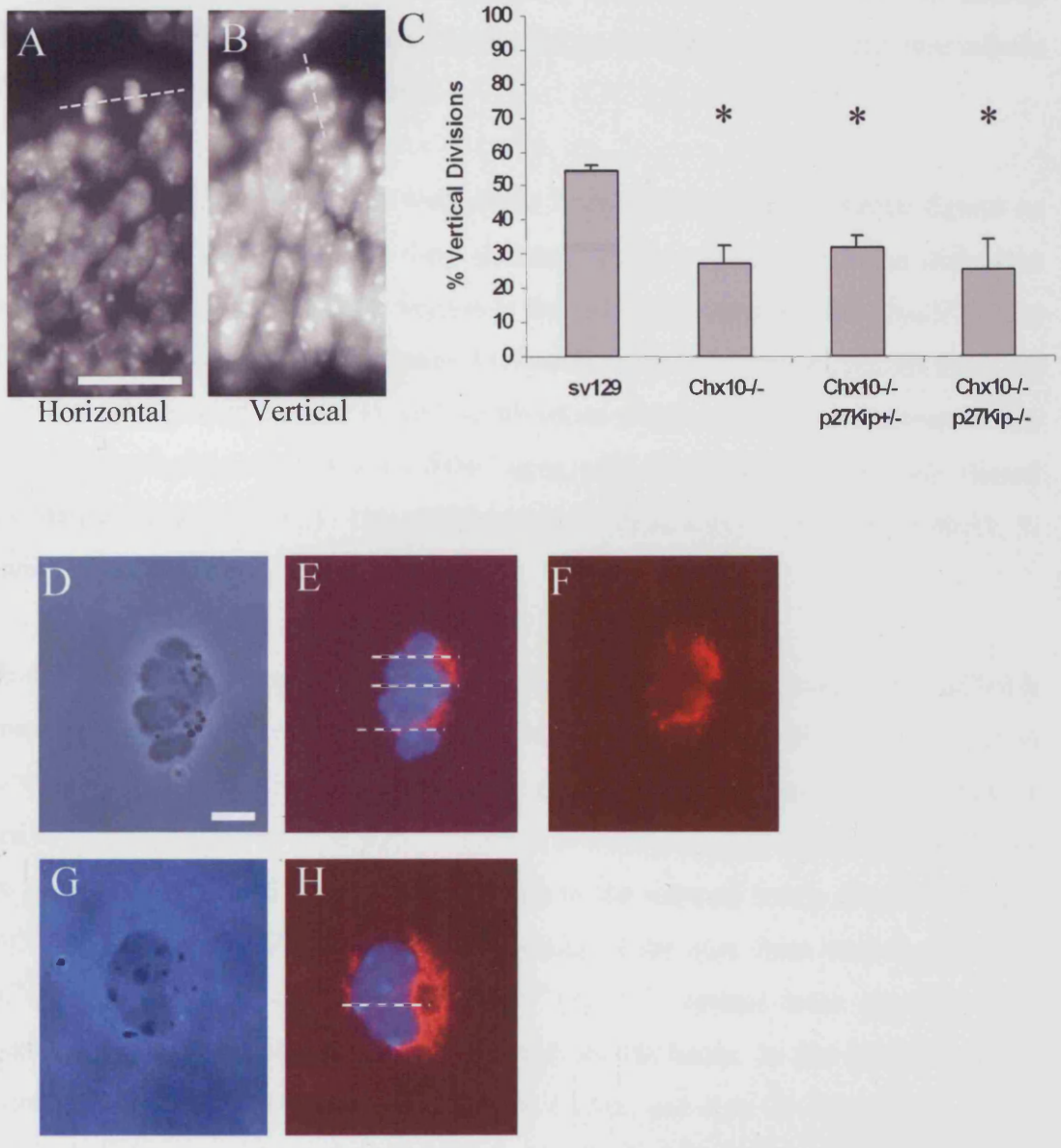

Figure 5.11: Examining symmetry of division of retinal progenitor cells. *A,B:* DAPI staining of the E11.5 retina – cells dividing with a horizontal (*A*, dashed lines) and a vertical (*B*, dashed lines) mitotic spindle orientation were observed in both the wild type and mutant retinae of E11.5 mice. *C*: Percentage vertical spindles observed in the wild type retina, the *Chx10*$^{-/-}$ retina, the *Chx10*$^{-/-}$ / *p27*$^{Kip+/-}$ and the *Chx10*$^{-/-}$/*p27*$^{Kip-/-}$ double knock out, +SE. All mutant genotypes differ significantly from the wild type (asterisks, $p<0.01$ Mann Whitney U test) but not from each other. *D-F*: Numb staining of dissociated wild type (*D-F*) and *Chx10*$^{-/-}$ retinal cells. *D* and *G* are phase images of the dissociated cells, *E* and *H* show red numb staining and blue Hoechst nuclear counter stain. In both cases, numb staining appears to be localised on one side of the mitotic cells, perpendicular to plane of cleavage (indicated by dashed lines). This is more clearly visible in *F*, where only numb staining is shown. Scale bar = 10 μm.

figures where both daughter cells were clearly visible were counted. Overall, mitotic figures were clearly identifiable as horizontal or vertical, with only the rare mitotic figure requiring angle measurement.

Wild type and *Chx10*$^{-/-}$ embryos were cut in 7 μm sections, and all mitotic figures on all high-quality retinal sections were counted. There was no significant difference between the number of cells per section in the wild type retina and the *Chx10*$^{-/-}$ retina ($p = 0.4$). In total, 191 mitotic figures were analysed in 6 wild type eyes. Of these, on average 54.5% were classed as vertical divisions (Figure 5.11C). In contrast, of the 100 mitotic figures counted in 4 *Chx10*$^{-/-}$ eyes, only 27.7% of divisions were classed as vertical (Figure 5.11C). This difference was statistically significant ($p<0.01$, 2-tailed Mann Whitney U test).

In addition to examining wild type and *Chx10*$^{-/-}$ eyes, spindle orientations of RPCs in mice generated by intercrossing *Chx10*$^{-/-}$ and *Kip1*$^{-/-}$ mice were also examined. It has been shown that growth of the retina in the *Chx10*$^{-/-}$ mutant is rescued by deletion of the cell cycle regulatory gene *p27*^{Kip1} (Green et al., 2003). This study was carried out to examine whether *p27*^{Kip1} could contribute to the reduced levels of cells dividing vertically in the *Chx10*$^{-/-}$ retina. Mitotic figures of the eyes from both the *Chx10*$^{-/-}$ *p27*$^{Kip-/-}$ double knockout, and the *Chx10*$^{-/-}$ *p27*$^{Kip+/-}$ retinae were counted. Both showed a significant bias towards horizontal cell divisions. In the *Chx10*$^{-/-}$p27$^{Kip-/-}$ mice, 95 mitotic figures were counted from 4 eyes, and only 25.49% of these were vertical divisions (Figure 5.11C). Similarly, in the *Chx10*$^{-/-}$ *p27*$^{Kip+/-}$ mouse, 74 mitotic figures from 4 eyes respectively were counted, and 31.75% of these were vertical divisions (Figure 5.11C). These results were not significantly different from those obtained from the *Chx10*$^{-/-}$ mouse eyes ($p = 0.39$ for *Chx10*$^{-/-}$*p27*$^{Kip-/-}$ and 0.34 for *Chx10*$^{-/-}$*p27*$^{Kip+/-}$), but significantly different to those obtained from the wild type mouse eyes ($p < 0.006$ for *Chx10*$^{-/-}$*p27*$^{Kip-/-}$ and < 0.005 for *Chx10*$^{-/-}$ *p27*$^{Kip+/-}$, 2-tailed Mann Whitney U test). This indicates that the difference in cell division type between wild type and *Chx10*$^{-/-}$ RPCs was not ameliorated by lack of p27^{Kip1} suggesting that it is independent of the proliferation defect.

To further examine the orientation of division, anti-numb antibody was used on dissociated retinal progenitor cells. In previous studies, a correlation was observed

between asymmetric localisation of numb, an intrinsic factor that regulates cellular competence through the *Notch* pathway, and cellular competence to differentiate. Cells with an asymmetric numb distribution differentiated more readily in culture (Dooley et al., 2003). In the rat retina, cells that divided with their mitotic spindles perpendicular to the ventricular edge showed asymmetrical numb distribution, with the more vitreal cell inheriting numb (Cayouette et al., 2001; Cayouette and Raff, 2003b; Dooley et al., 2003). RPCs from wild type and *Chx10*$^{-/-}$ developing retinae were dissociated and allowed to remain in culture for 24 hours. Cells were then fixed and mitotic figures were examined for numb localisation. Very few mitotic figures were observed amongst the dissociated cells, and thus only a few observations could be made. Figure 5.11D-H show examples of both wild type and *Chx10*$^{-/-}$ dissociated RPCs, with numb staining perpendicular to the mitotic spindles (dashed lines in Figure 5.11E, H). Thus, numb would be distributed between both daughter cells in these instances. In other mitotic figures, it was difficult to ascertain whether numb staining was distributed evenly across two dividing cells or not. In no case was numb staining observed in only one pole, away from the mitotic spindle. As the aim of this experiment was to compare the number of cells with different numb distributions between mutant and wild type, it was not pursued here due to a low number of numb-labelled mitotic cells observed in culture.

5.2.6 Altered profile of cell fate determination

A mutation in the *p27*^{Kip1} gene has previously been shown to rescue the proliferation defect in the *Chx10*$^{-/-}$ mouse. However, it does not seem to ameliorate the bias toward horizontal divisions observed in the *Chx10*$^{-/-}$ retina. If the orientation of cell division is related to what fate the daughter cells will assume, the question arises whether onset of differentiation of retinal neurons is affected in the *Chx10*$^{-/-}$ retina. To test this idea, I used immunostaining for β3 tubulin on E11.5 retina. β3 tubulin is a marker of maturing neurons, first expressed around E11.5 when the first ganglion cells are born (McCabe et al., 1999);(Snow and Robson, 1994; Watanabe et al., 1991).

Retinae from wild type, *Chx10*$^{-/-}$, and *Chx10*$^{-/-}$*p27*$^{Kip-/-}$ mice were examined by β3 tubulin labelling at E11.5. In the wild type retina, β3 tubulin labelling could be observed in the central retina, in particular at the vitreal edge, where ganglion cells first mature (Figure 5.12A, B arrow). Processes could be observed projecting radially from the ganglion cells toward the ventricular edge. In contrast, no β3 tubulin labelling was observed in the *Chx10*$^{-/-}$ retina at E11.5 (Figure 5.12C). Similarly, no β3 tubulin staining was observed in the *Chx10*$^{-/-}$*p27*$^{Kip-/-}$ retina at the same time point (Figure 5.12D). Together these data suggest that the decrease in vertical cell division is associated with delayed differentiation of retinal neurons.

A lack of β3 tubulin staining suggests that the maturation of the earliest-born retinal cells, the retinal ganglion cells, is delayed. The question arises as to whether other neural retinal cell types are similarly affected. Is an effect observed in later-born cells? To examine this, a number of retinal markers were used at various points during development. Antibodies against syntaxin and VC1.1 were used to examine the development of amacrine and horizontal cells (the same antibodies were used in Chapter 6, with amacrine and horizontal cells in the adult wild type retina serving as clear positive controls), which begin to become postmitotic shortly after retinal ganglion cells begin to exit the cell cycle and differentiate (see Figure 1.2). At E13.5, syntaxin-labelled cells can be observed at high magnification in the wild type retina (Figure 5.13A, C, arrows). In contrast, no syntaxin labelling can be observed in the *Chx10*$^{-/-}$ retina at the same point during development (Figure 5.13B, D). By E15.5, syntaxin labelling is still widespread throughout the wild type retina (Figure 5.13E, G, arrowheads), whilst in *Chx10*$^{-/-}$ eyes only a few cells in the central retina are labelled with the syntaxin antibody (Figure 5.13F, H, arrows).

A similar pattern of expression can be observed using the anti-VC1.1 antibody. VC1.1 is expressed in both amacrine and horizontal cells (Arimatsu et al., 1987), whilst syntaxin is more restricted to amacrine cells (Barnstable et al., 1985). At E13.5, VC1.1 labelling can be observed in several cells in the wild type central retina, especially in the most central retinal areas, which are the first to mature, and towards the ventricular edge, where cells exit the cell cycle and begin to differentiate (Figure 15.14A, C, arrows). Mirroring observations made using anti-syntaxin

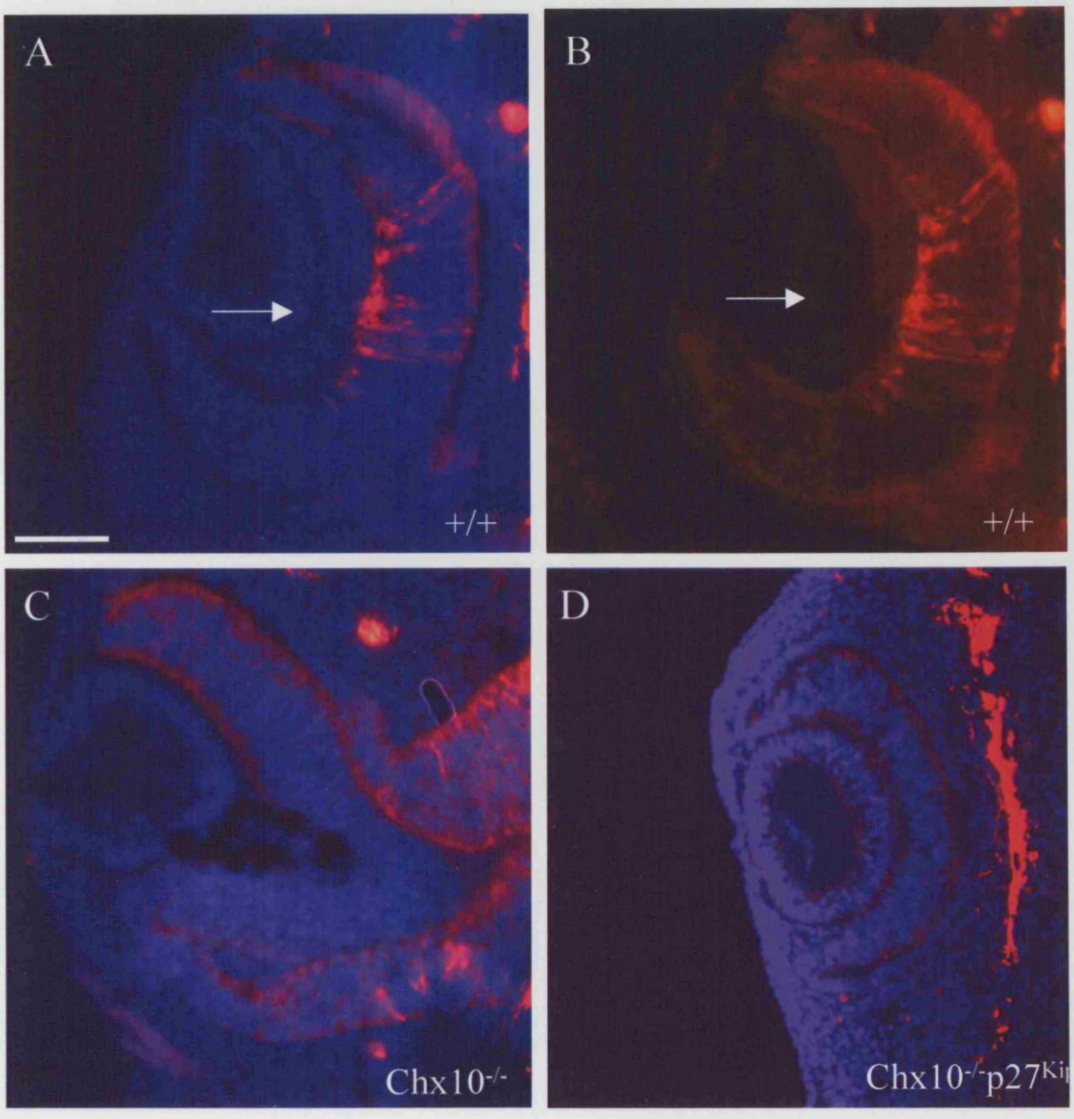

Figure 5.12: Immunostaining for β3-tubulin (red, with blue Hoechst nuclear counter-stain in *A,C,D*) in the wild type shows differentiating neurons in the E11.5 wild type central retina (*A*, *B* arrows), but not in the E11.5 *Chx10*$^{-/-}$ retina (*C*) or the E11.5 *Chx10*$^{-/-}$/*p27*$^{Kip-/-}$ double knock out (*D*). Scale bar = 100μm.

Figure 5.13: Syntaxin labelling (red, with blue Hoechst nuclear counter-stain) of wild type (*A,C,E,G*) and *Chx10*$^{-/-}$ (*B,D,F,H*) retina at E13.5 (*A-D*) and E15.5 (*E-H*). At E13.5 (*A-D*) syntaxin labelling in the wild type retina is difficult to discern at low magnification (*A*) but can be observed in larger areas of the retina at higher magnification (*C*, arrows). In the *Chx10*$^{-/-}$ retina, no syntaxin labelling can be observed, either at low (*B*) or high magnification (*D*). At E15.5, syntaxin labelling can still be observed in large areas of the wild type retina (*G*, arrowheads) and is also seen in a few cells of the *Chx10*$^{-/-}$ retina (*F,H*, arrows). Scale bars = 100 μm in A and B; scale bar in C = 50 μm for C and D; scale bar in E = 100 μm in E, 50 μm in F; scale bar in G = 50 μm for G and H.

E13.5

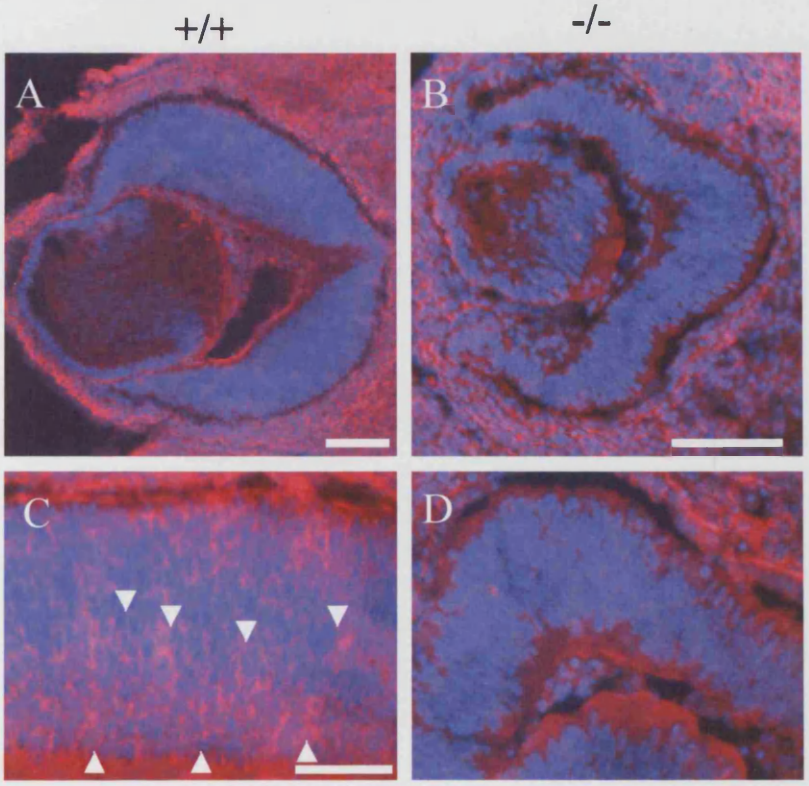

E15.5

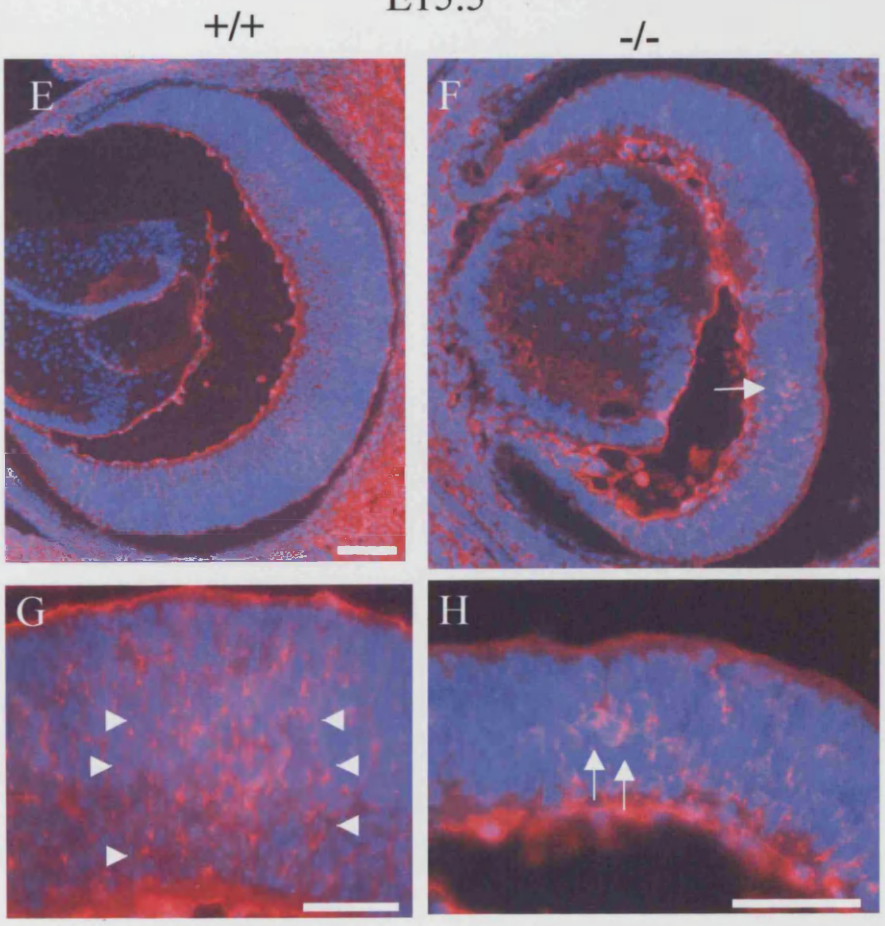

Figure 5.14: VC1.1 labelling (red, with blue Hoechst nuclear counter-stain) of wild type (*A,C,E,G*) and *Chx10*$^{-/-}$ (*B,D,F,H*) retina at E13.5 (*A-D*) and E15.5 (*E-H*). At E13.5, VC1.1 labelling in the wild type retina can be observed at low and high magnification (*A, C,* arrows), whilst no VC1.1 staining can be observed in the *Chx10*$^{-/-}$ retina (*B,D*). At E15.5, VC1.1 labelling can still be observed in large areas of the wild type retina (*G,* arrows) and is also seen in a few cells of the *Chx10*$^{-/-}$ retina (*H,* arrows). Scale bar in A = 100 μm in A, 50 μm in B; scale bars in C and D = 50 μm; scale bar in E = 100 μm in E, 50 μm in F; scale bars in G and H = 50 μm.

E13.5

+/+ -/-

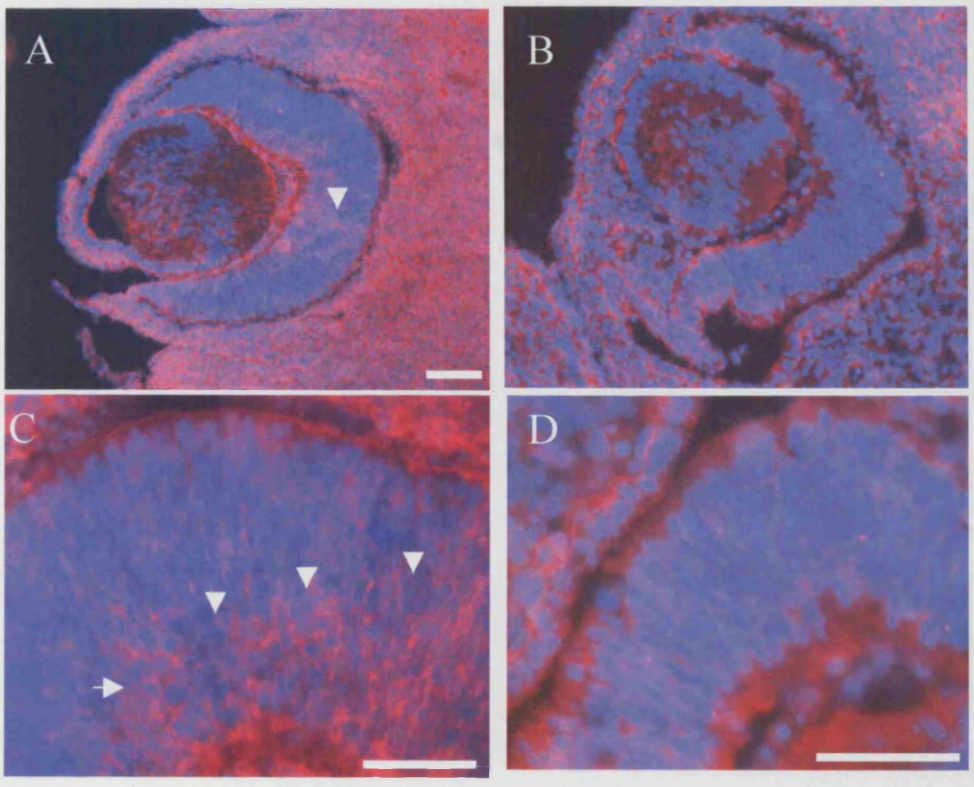

E15.5

+/+ -/-

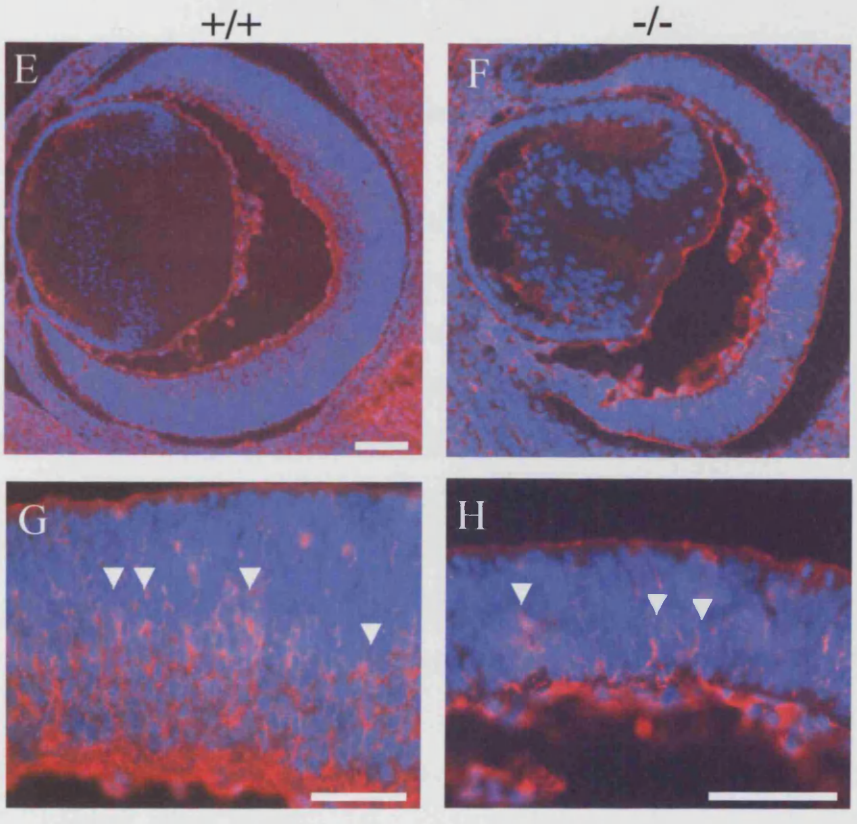

antibody, no VC1.1 staining can be observed in the *Chx10*$^{-/-}$ retina at the same time point. At E15.5, differentiating amacrine and horizontal cells can be observed in the differentiating layers of the wild type retina (Figure 5.14E, G, arrows), and VC1.1 labelling can also be observed in the *Chx10*$^{-/-}$ retina, although to a lesser extent than in the wild type retina. Both syntaxin and VC1.1 labelling suggest that the birth and/or differentiation of amacrine and horizontal cells may be delayed in the *Chx10*$^{-/-}$ retina.

To examine whether there is a change in photoreceptor differentiation in the *Chx10*$^{-/-}$ retina compared to the wild type, recoverin labelling was examined at E18.5 (Dizhoor et al., 1991). At this point during development, a small number of differentiating photoreceptors can be observed at the ventricular edge of the wild type retina (Figure 5.15A, C, arrows). This is not the case, however, in the *Chx10*$^{-/-}$ eye; no recoverin labelling can be observed anywhere in the retina at E18.5 (Figure 5.15B, D). This again suggests that differentiation of a variety of neural retinal cell types is delayed or disrupted in the *Chx10*$^{-/-}$ retina.

Previous data indicate that the development of photoreceptors is disrupted in the *Chx10*$^{-/-}$ retina, and that expression of the *Crx* gene, a gene necessary for photoreceptor differentiation, is delayed (Rutherford et al., 2004). However it is not clear whether both rods and cones are similarly affected. As cones are generated early along with amacrine and ganglion cells and rods and bipolars are late born cells, it is of interest to examine whether both types of photoreceptor are disrupted and whether early and late-born cells are differentially affected. Cone cell-specific peanut agglutinin (PNA)-rhodamine staining and immunostaining for the blue short wave-sensitive "S" cone opsin gene were used to compare cone development in the post-natal *Chx10*$^{-/-}$ and wild-type retina. Immunostaining for rhodopsin was also performed to compare rod development at the same stages (Molday, 1989).

PNA labels all developing cone types (Zhang et al., 1994). By P14 in both the wild type and the mutant retina distinct cone outer segments were detected with PNA (Figure 5.16B and E). Blue cone opsin-positive outer segments were detected in both the *Chx10*$^{-/-}$ (Figure 5.16J) and the wild-type retina at P7 (Figure 5.16G) and at later stages (Figure 5.16H, I, K, L), consistent with previous reports of wild-type

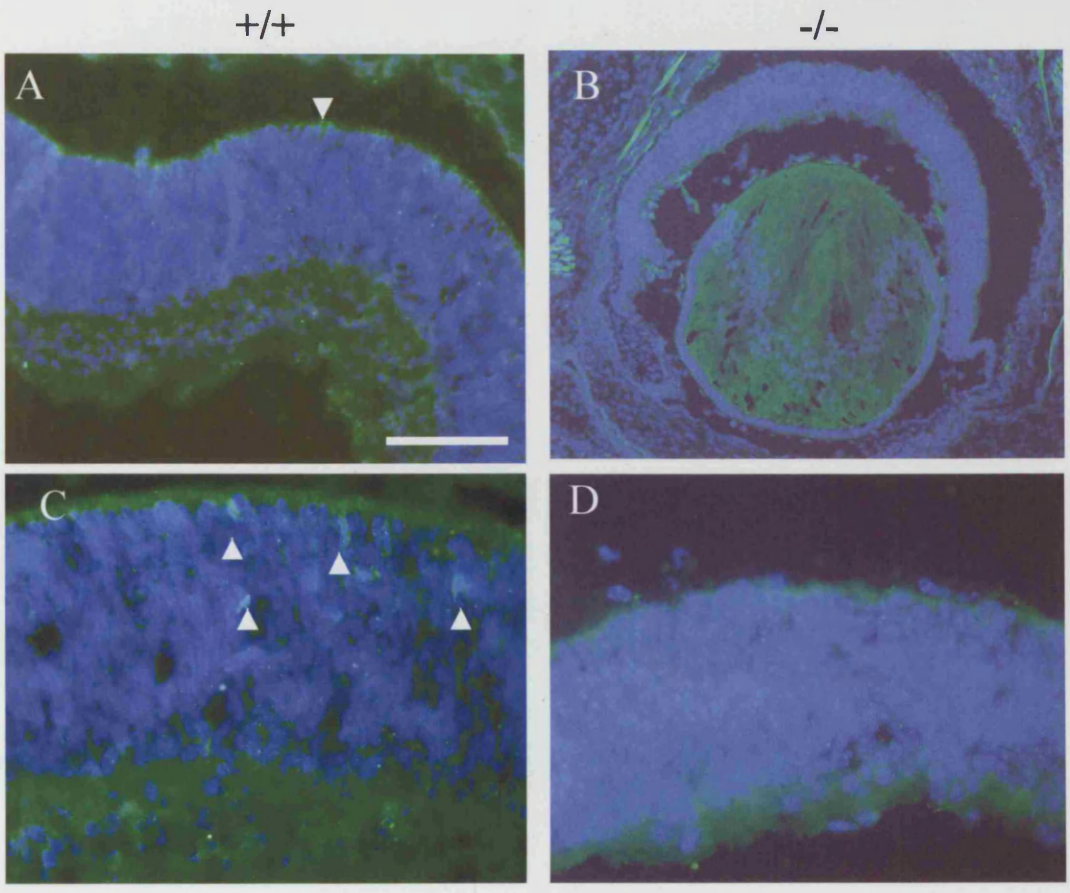

Figure 5.15: Recoverin labelling (green, with blue Hoechst nuclear counter-stain) of wild type (*A,C*) and *Chx10*$^{-/-}$ (*B,D*) retina at E18.5. In the wild type retina, a few recoverin-labelled cells can be observed at the ventricular edge of the retina (*A,C*, arrows), where developing photoreceptors are located. No recoverin labelling can be observed in the *Chx10*$^{-/-}$ retina (*B,D*). Scale bar = 100 μm for A, 200 μm for B, and 50 μm for C and D.

Figure 5.16. Examination of photoreceptor differentiation in the postnatal retina. Cone photoreceptors of both wild type and *Chx10*$^{-/-}$ mutant retina were labelled with PNA (*A-F*, red) and blue cone opsin (*G-L*, red) at postnatal days 7, 14-15 and 20. PNA staining of cone pedicles is first observed at P14 in both the wild type (*B*, arrowheads), and *Chx10*$^{-/-}$ (*E*, arrowheads) retina, and cones seem to be present at similar densities. By P20 it is clear that the outer segments of the cone photoreceptors of the *Chx10*$^{-/-}$ retina are shorter and abnormal looking compared to the cones of the wild type retina at the same stage (compare *F*, arrowhead with *C*, arrowheads). Labelling with blue cone opsin labels blue cone outer segments as early as P7 in both the wild type and *Chx10*$^{-/-}$ retina and expression persists at later stages (*H, I, K, L*) in both. By contrast, rhodopsin labelling (*M-R*, green) was observed at P7 in the developing outer segments of rod photoreceptors (*M*, arrowhead) and remains expressed in the outer segments of the wild type retina at later stages (*N, O*), but is not expressed in the mutant retina until P20 (*R*), where it is only sparsely distributed (arrowheads). Hoechst 33258 nuclear dye was used to label the nuclei of the photoreceptor layer blue in all sections. Scale bars = 20 μm.

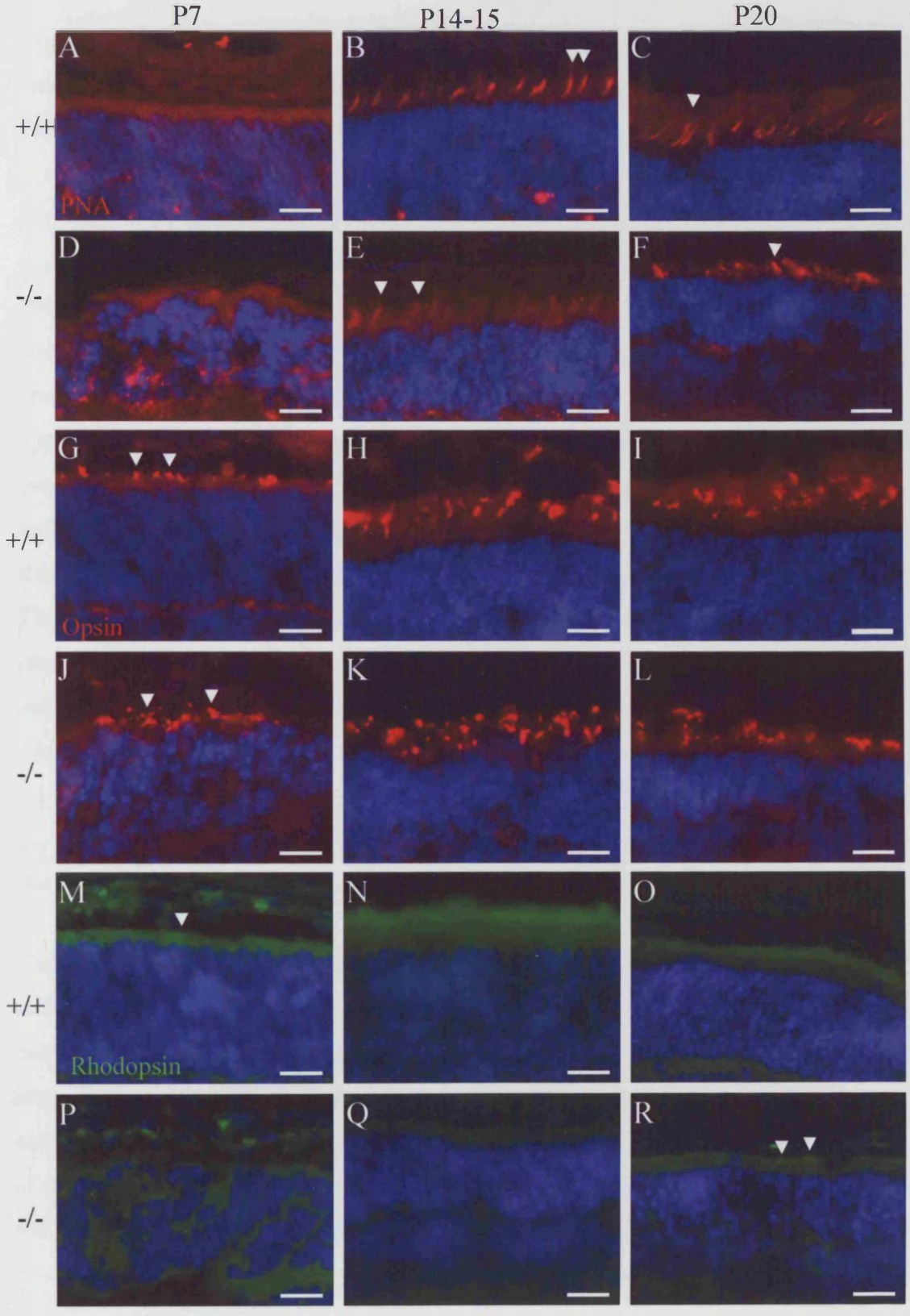
P7
P14-15
P20
A
B
C
+/+
PNA
D
E
F
-/-
G
H
I
+/+
Opsin
J
K
L
-/-
M
N
O
+/+
Rhodopsin
P
Q
R
-/-

expression patterns. The cones were present at similar densities within the *Chx10*$^{-/-}$ and the wild-type retinae (Figure 5.16B and E). At P20 the cone outer segments were reduced in length in the *Chx10*$^{-/-}$ retina (Figure 5.16F) compared with the wild-type (Figure 5.16C). By contrast, rhodopsin was localised in the developing outer segments at P7 (Figure 5.16M) and P15 (Figure 5.16N) in the wild-type but similar expression was markedly absent in the *Chx10*$^{-/-}$ retina (Figure 5.16P, Q). At P20 the rhodopsin was specifically localised throughout the rod outer segment layer in the wild-type retina (Figure 5.16O). By this stage the mutant retina showed more sparsely distributed rhodopsin positive outer segments with an abnormal truncated appearance (Figure 5.16R). These data show that the cone photoreceptors are being generated relatively normally in the absence of Chx10, suggesting that generation of early born photoreceptors is less disrupted than late born photoreceptors. It follows that the reduction in cell number in the outer nuclear layer is due to a rod deficit. These data also indicate that lack of Chx10 is affecting the differentiation of photoreceptors as outer segment morphogenesis is abnormal for rods and cones. It seems likely that this phenotype could result from the delay in *Crx* expression in the *Chx10*$^{-/-}$ mutant.

5.2.7 Cell numbers are decreased in both the inner and outer nuclear layers of the *Chx10*$^{-/-}$ retina

Use of specific retinal cell type markers indicated that the differentiation of several cell types is affected by a loss of Chx10. However, expression of *Brn3b* and *Pax6*, markers of postmitotic retinal ganglion cells and amacrine cells/retinal ganglion cells respectively, in the *Chx10*$^{-/-}$ retina suggest cells of the inner retina were being born in early embryonic stages (Rutherford et al., 2004). To address whether the reduced size of the *Chx10*$^{-/-}$ retina was due to a reduction in specific types of cells, for example of rod photoreceptors, semithin histological sections of wild type and *Chx10*$^{-/-}$ retinae were examined. These sections offer the advantage of being only one cell layer thick, allowing relative cell counts in the various cell layers. All retinal layers are present in the wild type retina by P12 (Figure 5.17A, B). Each layer is of an even thickness throughout the retina (Figure 5.17B) and the retina tapers off towards the periphery, and the ciliary body has a characteristic folded shape (Figure 5.17C). The P12 *Chx10*$^{-/-}$ retina, however, is far less organised and of variable thickness. Thick areas

Figure 5.17: Semithin sections of wild type (*A-C,J,K*) and *Chx10*$^{-/-}$ (*D-I, L*) retina stained with toluidine blue. The P12 wild type retina is of an even thickness throughout, tapering towards the periphery and ciliary body (*A-C*), and contains three well-organised cell layers. The P12 *Chx10*$^{-/-}$ retina, in contrast, shows variable thickness and organisation, with some well organised thick areas of retina (*D,E*, arrows and *F,H*) and some thin areas where retinal cell layers are far less organised (*D,E* arrowheads, and *G,I*). *J-L* show P12 wild type and *Chx10*$^{-/-}$ retinae compared to an adult wild type retina, all at the same magnification. The wild type P12 retina is slightly smaller than the mature adult retina, and the photoreceptors are less well developed. The P12 *Chx10*$^{-/-}$ retina is about half as small as the wild type retina at this time point – a relatively thick, well-organised area of *Chx10*$^{-/-}$ was used for this comparison.

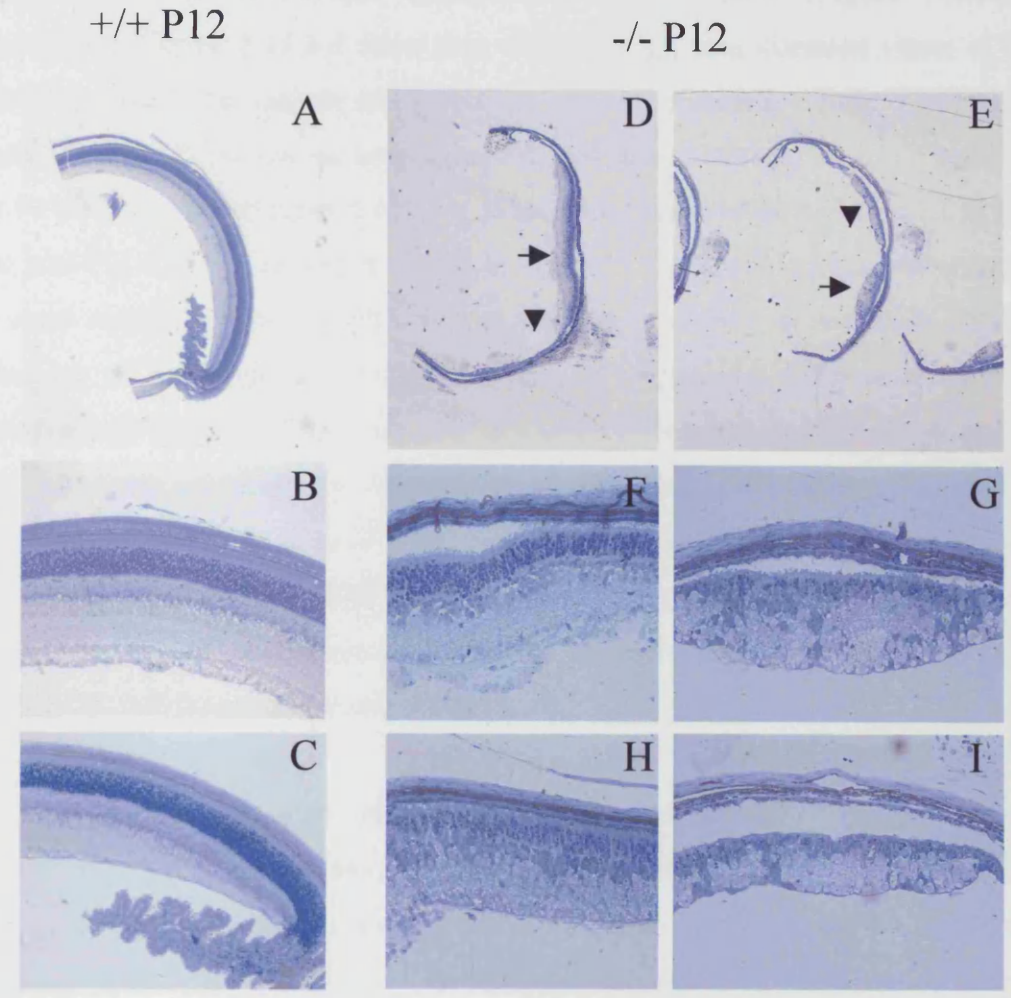
+/+ P12
-/- P12
A
D
E
B
F
G
C
H
I

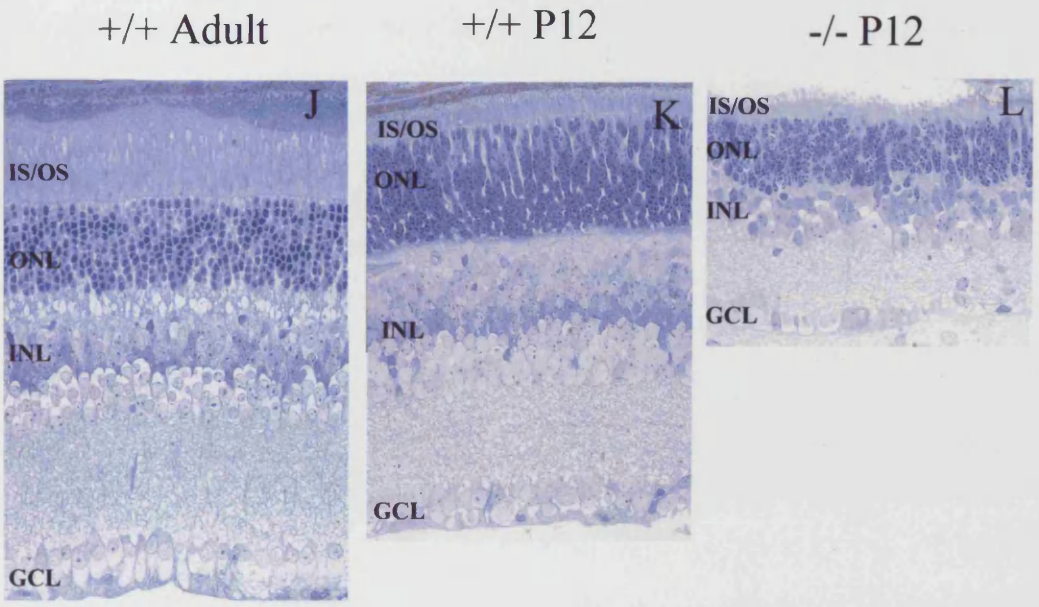
+/+ Adult
+/+ P12
-/- P12
J
IS/OS
ONL
INL
GCL
K
IS/OS
ONL
INL
GCL
L
IS/OS
ONL
INL
GCL

(Figure 5.17D, E arrows) are interspersed with thin areas (Figure 5.17D, E, arrowheads). Figure 5.17 F-I show four different high magnification views of P12 *Chx10*$^{-/-}$ retinae. The various cell layers are present, especially in the thicker areas (Figure 5.17F, H) but are far less organised, and in some areas, only one cell layer can be distinguished (Figure 5.17I). A direct comparison of the adult and P12 wild type and P12 *Chx10*$^{-/-}$ retinae is shown in Figure 5.17J-L. All images were taken at the same magnification. The P12 wild type retina is slightly thinner than the adult retina, but all cell layers are present and the most significant differences are in the photoreceptor layers: the cells are not fully differentiated in the P12 retina, and the inner and outer segments are significantly smaller than in the adult. At its thickest and most organised, the *Chx10*$^{-/-}$ P12 retina is only about half the size of the wild type P12 retina. Morphologically distinct cell types are present in both, but the cell layers of the *Chx10*$^{-/-}$ retina are thinner than in the wild type and the plexiform layers between the cell layers are greatly reduced.

A comparison was made of the thickness of the inner and outer nuclear layers by making replicate counts of the number of nuclei along the length of each nuclear layer. Table 5.1 summarises the cell nuclei counts. Both layers show a significant reduction in cell number, with a more marked reduction in the outer nuclear layer. It seems likely that a lack of cells in the outer nuclear layer is due to a low number of mitotic RPCs being present in the *Chx10*$^{-/-}$ retina around birth, the normal peak of rod genesis.

Genotype	**Nuclear Cell layer (no of nuclei)**	
	Inner	**Outer**
+/+	8.8 +/- 1.2	11.7 +/- 0.8
-/-	4.0 +/- 0.9	4.2 +/- 1.4

Table 5.1. Comparison of thickness , by nuclei, of retinal tissues from wild type (+/+) *and* *Chx10*$^{-/-}$ (-/-) mice. Observations were made on four eyes in each category. Numbers refer to the mean values +/- SD.

5.3. Discussion

5.3.1 A decrease in proliferation in the periphery of the *Chx10*$^{-/-}$ retina may be due to misspecification of neural retina

The aim of the study described here was to examine if and how the properties of retinal progenitor cells in the *Chx10*$^{-/-}$ retina are affected by the lack of Chx10 during early retinal development. Previous studies, using the cell cycle marker BrdU, have indicated that there is an apparent decrease in proliferating cells in the periphery of the retina from E10.5 onwards. However, proliferation seemed to occur normally in the central retina, as there was no apparent difference in the percentage of BrdU-labelled cells in this area (Bone-Larson et al., 2000; Burmeister et al., 1996).

The results obtained here correlate to some extent with these studies. H3 and PCNA labelling confirm that the apparent number of cycling cells is diminished in the periphery of the retina. Thus far, no real explanation has been put forth for this phenomenon. Why should a lack of Chx10 affect a population of RPCs in the periphery of the retina in a different manner? However, in the previous chapter, it became clear that RPE markers are expressed in the periphery of the *Chx10*$^{-/-}$ retina. It seems likely that the decrease in proliferation observed in the periphery of the *Chx10*$^{-/-}$ retina may not occur as a result of Chx10 directing some aspect of the cell cycle, but of a possible misspecification of the peripheral retina.

The neural retina and the RPE are adjacent tissues and are both patterned from the optic vesicle. However, total cell number of the neural retina is much larger than that of the RPE, due primarily to differential regulation of proliferation, which first occurs during optic vesicle morphogenesis to form the optic cup (Green et al., 2003). It is possible that a lack of Chx10 causes the border between RPE and neural retina, at the periphery of the retina, to become less accurately specified. A proportion of the RPCs at the periphery of the retina may in this way acquire some RPE-like characteristics, such as expression of RPE- markers and a decrease in proliferation compared to the rest of the retina. This would explain why this area of the retina seems to be most severely affected by a lack of proliferation.

Interestingly, the few apoptotic cells observed in the *Chx10*$^{-/-}$ retina early on in development are located in the periphery of the retina, in contrast to the wild type, in which a few apoptotic cells are located in the central retina, but most are located around the optic fissure. Although rare, and unlikely to be playing a direct role in the apparent decrease in cell number compared to the wild type, this cell death in the periphery of the *Chx10*$^{-/-}$ may reflect a certain level of disorganisation, where the border between RPE and neural retina is 'blurred'.

5.3.2 H3 labelled cells and orientation of cell division offer clues to how *Chx10*$^{-/-}$ RPCs proliferate

In addition to a decrease in the proliferation of RPCs in the periphery of the *Chx10*$^{-/-}$ retina, RPCs are not cycling in a manner similar to that of the wild type throughout the entire retina. In the wild type retina, cells undergo a highly proliferative phase between E9.5 and E10.5, resulting in a thickened presumptive neural retina and a thinner presumptive RPE. By E11.5, a small proportion of cells start to differentiate whilst other cells continue to cycle. If cell orientation during division is a reflection of the proportion of cell undergoing symmetric and asymmetric divisions (Chenn and McConnell, (Cayouette and Raff, 2003b), our data suggest that about 50% of divisions are symmetric (horizontal divisions), resulting in two daughter cells that will divide again. About 50% of divisions are asymmetric (vertical divisions), resulting in one daughter cell that will exit the cell cycle and differentiate, and one daughter cell that will go on to divide again.

In this model, as development continues, the proportion of dividing cells that divide asymmetrically will increase, whilst symmetric divisions resulting in two proliferative daughter cells will decrease. Instead, more symmetric divisions will result in two post-mitotic cells, which will go on to differentiate. This shift from symmetrical divisions resulting in two further dividing daughter cells to asymmetrical divisions or symmetrical divisions resulting in two post-mitotic cells would result in the proportion of H3-labelled cells in the wild type retina decreasing throughout development, even as total cell number increases.

However, this pattern of proliferation is not observed in the *Chx10*$^{-/-}$ retina. The H3 study revealed that following an early decrease in proliferation in the mutant compared with the wild type retina, between E11.5 and E13.5, later, a small population of RPCs continues to proliferate steadily in the mutant. The H3 study suggests that rather than a steady decrease in the proportion of mitotic cells during development, as one might expect if cells are not proliferating normally, a small population of progenitors seem to cycle continually, maintaining a stable mitotic labelling index that does not decrease with development as observed in the wild type retina. These cycling cells, however, do not expand the RPC population in a significant manner.

In addition, at E11.5 a larger proportion of cells are undergoing horizontal divisions than in the wild type, which may suggest that a larger proportion of divisions are symmetrical. This seems counter-intuitive, as a larger proportion of symmetrical divisions, over time, should result in larger numbers of cells. Thus, the data do not fit a model in which symmetric divisions are important for expansion of the RPC population in the early optic cup. At present, there is some controversy over whether this model represents the events occurring in the early retina. Studies by Cayouette and Raff suggesting the orientation of division reflects the types of divisions cells undergo in the developing retina (Cayouette and Raff, 2003b) have been questioned by other groups, who have found no evidence for a relationship between spindle orientation and type of cell division (Silva et al., 2002; Tibber et al., 2004).

It is possible that the increased horizontal divisions suggest that a proportion of cells are dividing symmetrically to become post-mitotic and subsequently differentiate. This would explain why there is no apparent expansion in the RPC population from early on in development, but might be expected to involve early onset of expression markers of cell differentiation. However, this explanation is not supported by labelling with the marker β3-tubulin for differentiated neurons, which suggested that differentiation is delayed, not advanced, in the *Chx10*$^{-/-}$ retina, and this was confirmed with the use of retinal specific markers, which indicated that the differentiation of most, if not all, retinal cell types is delayed. Thus, it is unlikely that at this early point in development, these increased putative symmetrical divisions result in two post-mitotic cells which differentiate.

A relative increase in the proportion of cells dividing symmetrically in the *Chx10*$^{-/-}$ retina at E11.5 may mean that cells that should be dividing asymmetrically and producing daughter cells that will go on to differentiate are actually dividing symmetrically and thus a delay in cell differentiation would be observed. This is supported by a relative lack of β3-tubulin expression at this time point in the *Chx10*$^{-/-}$ retina compared to the wild type. A subsequent delay in expression of other retinal cell type markers was similarly observed. Such a delay in differentiation of various cell types has also been observed in various other studies (Bone-Larson et al., 2000; Burmeister et al., 1996). It is possible that these symmetrically dividing cells produce daughter cells that arrest in G1/G0, and therefore do not go on to either further proliferate or differentiate. This would explain why there is no apparent expansion of the RPC population whilst a small proportion of cells appears to be proliferating throughout development, and in addition, why there is an apparent delay in retinal cell differentiation in the *Chx10*$^{-/-}$ retina. In order to draw firmer conclusions, it will be necessary in future work to identify the fate of cells resulting from the different types of division, for example through the use of time lapse microscopy.

The presence of continually dividing cells throughout development raises the question as to what becomes of these proliferating cells. Do they continue proliferating after development, in similar proportions? This question forms the basis of the following chapter.

5.3.3 The cell cycle of the *Chx10*$^{-/-}$ RPCs is likely to be increased in length

If cells are proliferating constantly, RPC number should, as a consequence be growing steadily as well. However, there is some evidence that in addition to a change in the pattern of cycling, there is also an increase in the length of the cell cycle, such that the number of cycles over time is decreased in the *Chx10*$^{-/-}$ retina. Studies using ^{3}H thymidine have indicated that the length of G1 may be increased in the *Chx10*$^{-/-}$ RPCs (Konyukhov and Sazhina, 1971). In addition, a recent study suggests that cyclin D1, a G1 regulator, is decreased in the *Chx10*$^{-/-}$ retina (Green et al., 2003). It was suggested that this decrease in cyclin D1 allows p27^{Kip1} to be

ectopically localised in retinal progenitor cells, and that $p27^{Kip1}$ lengthens the cell cycle by causing an extension of the G1 phase (Green et al., 2003).

The flow cytometry data obtained in this study indicate that a larger proportion of RPCs are in the G1/G0 phase of the cell cycle in the *Chx10*$^{-/-}$ retina than in the wild type retina. One interpretation of this is that in the *Chx10*$^{-/-}$ RPCs, the length of G1 is increased as suggested by Konyukhov (Konyukhov and Sazhina, 1971). However, an increase in the length of the cell cycle alone would be insufficient to explain the small size of the *Chx10*$^{-/-}$ retina. If proliferation is merely decreased, a full complement of cells ought to be produced, only over a longer period of time. However, if cells arrest in the G1 phase of the cell cycle, and neither proliferate or differentiate, as suggested above, this may result in an abnormally small retina.

Cell death certainly does not seem to contribute to the decreased retinal size of the *Chx10*$^{-/-}$ eye. In accordance with various earlier studies, cell death does not seem to be increased in the developing *Chx10*$^{-/-}$ retina (Burmeister et al., 1996; Robb et al., 1978; Theiler et al., 1976). In fact, as noted in these earlier studies, apoptotic cell death seems to be decreased in the *Chx10*$^{-/-}$ retina. This seems to be particularly true around the optic fissure area, and may relate to the abnormal development of the optic nerve, another feature of the *Chx10*$^{-/-}$ eye (Burmeister et al., 1996).

5.3.4 Conclusions

In summary, the results obtained in this study suggest that *Chx10*$^{-/-}$ retinal cells do indeed exhibit an abnormal pattern of proliferation. Not only does this study to some extent support an increase in the length of G1, through flow cytometry analysis, but an abnormal pattern of proliferation was observed throughout development. A difference in the orientation in cell divisions observed at E11.5 between the wild type and *Chx10*$^{-/-}$ retina could suggest that this abnormal pattern of proliferation is a result of a change in the proportion of symmetrical and asymmetrical divisions occurring throughout development.

CHAPTER 6

Absence of Chx10 causes embryonic neural progenitor-like cells to persist in the adult retina

6.1. Introduction

The data from the studies described thus far indicate that retinal progenitor cell proliferation is severely disrupted in the *Chx10*$^{-/-}$ retina (Chapter 5), and that this disruption is in part caused by misregulation of transcription factors necessary for retinal cell fate determination and/or differentiation (Chapters 3 and 4). The abnormalities in RPC behaviour are associated with a severe decrease in retinal cell number, as well as improper differentiation and structure of various retinal cell types, such as bipolar cells and rod photoreceptors, by the time the *Chx10*$^{-/-}$ mouse reaches adulthood. As the normal pattern of histogenesis is disrupted in the *Chx10*$^{-/-}$ retina, are there any compensatory mechanisms to correct for it? This question was of particular interest in view of the small population of dividing cells observed to be cycling throughout development (Chapter 5). The mitotic cells present in the slow growing *Chx10*$^{-/-}$ retina during embryonic development could be primitive neuroepithelium cells, perhaps self-renewing stem or precursor cells, which require Chx10 for expansion and/or transition to a pool of RPCs that undergo a finite number of divisions before differentiating. If this model is correct, one might expect that the cells cycling consistently throughout embryogenesis persist into adulthood in the *Chx10*$^{-/-}$ retina.

Of further interest is that the ciliary epithelium (CE) at the periphery of the adult retina has recently been shown to harbour cells which when isolated and cultured *in vitro* exhibit stem cell properties of multi-potentiality and self-renewal (Ahmad et al., 1999; Tropepe et al., 2000). The CE, which forms part of the ciliary body and consists of both pigmented and non-pigmented layers, is derived during development from the neuroepithelium at the periphery of the optic cup. Adult CE cells cultured in conditions that promote stem cell propagation (neurosphere cultures) express Chx10 and the neural progenitor marker nestin and can be differentiated to express retinal neuron specific markers (Ahmad et al., 1999). Notably, more neurospheres arose from the CE of the *Chx10*$^{-/-}$ mouse compared to wild type cultures (Tropepe et al., 2000). The question arises as to why more of such presumptive stem cells would reside in the CE of the *Chx10*$^{-/-}$ mouse than in the wild type. Does reduced proliferation of RPCs, caused by the absence of Chx10 in the microphthalmic embryonic retina, lead to increased number of 'stem cells' in the adult?

As discussed in Chapter 1, it has long been known that most of the retina in fish and amphibians is formed by the addition of new retinal neurons from a growth zone at the retinal margin, the ciliary marginal zone (CMZ), rather than during embryogenesis (Figure 6.1)(Moshiri et al., 2004). The CMZ of teleost fish and frogs continue to generate new retinal neurons throughout life (Johns, 1977; Johns and Easter, Jr., 1977; Wetts et al., 1989), and accordingly, this region of stem cells persists. Recently it has been shown that the post-hatch chicken retina has ongoing neurogenesis at the retinal margin, similar to that in lower vertebrates. Although most of the chick retina is derived from embryonic RPCs (Figure 6.1), the CMZ cells of the chicken are capable of generating new retinal neurons that are incorporated into the retina (Fischer and Reh, 2000). In all these species, cells in the CMZ expressed retinal progenitor cell markers such as nestin and *Pax6*, suggesting they formed a colony of self-renewing progenitor cells derived from the embryonic neural cells. They were also able to generate neurons, and thus they satisfy the criteria for neural retinal stem cells set out in Chapter 1. No such stem cell-like cells are thought to exist in the mammalian ciliary margin, and it has been suggested that the CMZ has decreased over the course of evolution with lower vertebrates possessing a large CMZ, capable of renewing retinal cells throughout life, and mammals lacking a CMZ altogether (Figure 6.1) (Perron and Harris, 2000b). Yet the possibility that the CE may harbour such cells is intriguing, especially if this population of putative stem cells is expanded in the *Chx10*$^{-/-}$ retina. They may offer some hope to an otherwise bleak prospect for replacing damaged retinal neurons in adult mammals.

In this chapter, a series of experiments were designed to explore whether reduced proliferation of RPCs, caused by the absence of Chx10 in the microphthalmic embryonic retina was associated with an increased number of 'stem cells' in the adult. A BrdU study was performed to identify any cycling cells in the adult wild type and *Chx10*$^{-/-}$ retina *in vivo*. In addition, retinal cultures were set up to examine whether cells from the adult wild type and *Chx10*$^{-/-}$ neural retina, ciliary epithelium, or RPE were able to proliferate and form neurospheres *in vitro*.

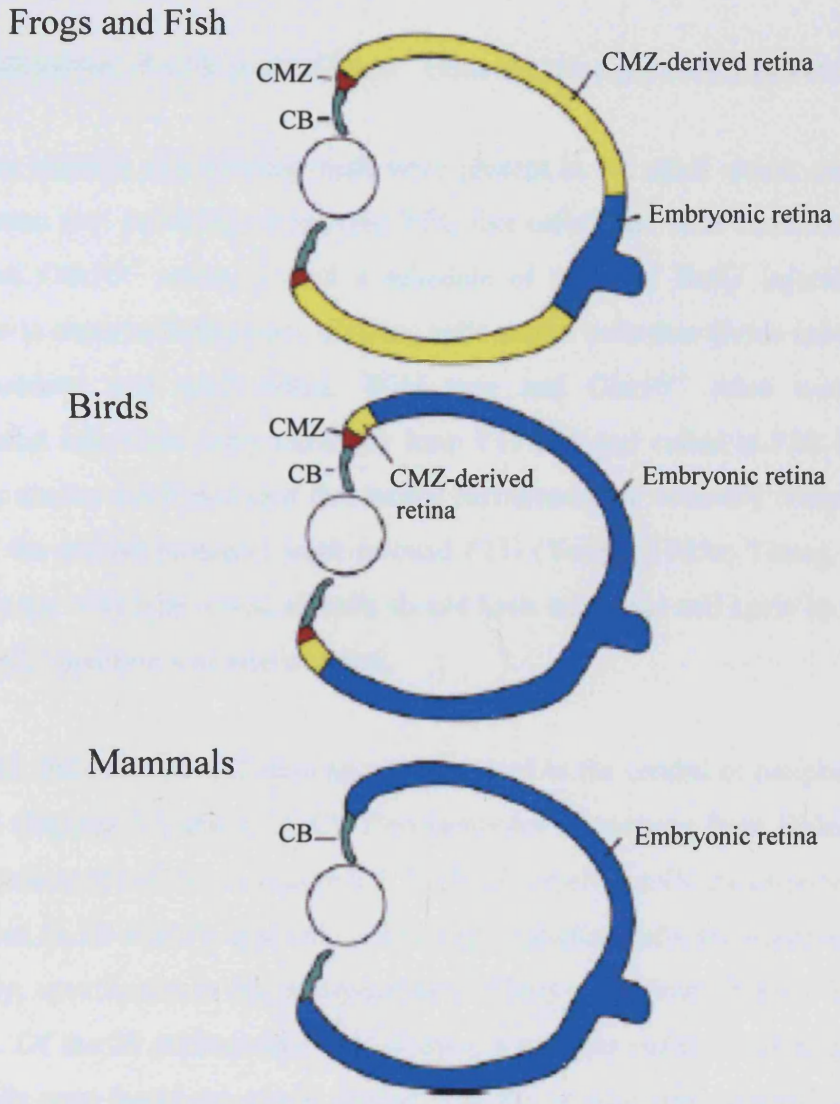

Figure 6.1: The relative contribution of the CMZ to retinal growth has been progressively reduced in homeothermic vertebrates and is shown in drawings of the adult eyes. The region of retina generated in the embryonic/neonatal period is shown in blue, while that generated by the CMZ is shown in yellow for various vertebrate classes. The CMZ itself is indicated in red the show the relationship to the ciliary body, coloured green. Figure adapted from Moshiri et al., 2004.

6.2. Results

6.2.1. Proliferation of cells in the *Chx10*$^{-/-}$ central retina persists into adulthood

To examine whether any dividing cells were present in the adult retina, and to test the hypothesis that persisting embryonic RPC-like cells/stem cells continue cycling in the adult *Chx10*$^{-/-}$ retina, I used a schedule of repeated BrdU injections that allowed me to observe both slowly dividing cells and/or cells that divide infrequently in the postnatal and adult retina. Wild type and *Chx10*$^{-/-}$ mice were given intraperitoneal injections every other day from P15-P29 and culled at P30. Previous birthdating studies have indicated that retinal histogenesis is normally completed by the end of the second postnatal week (around P11) (Young, 1985a; Young, 1985b), and thus, in the wild type retina, all cells should have exited the cell cycle by the time the first BrdU injection was administered.

As expected, little or no BrdU staining was observed in the central or peripheral wild type retina (Figures 6.2 and 6.5A-C). Two examples of sections from Brdu-treated, wild type retinae are shown in Figure 6.2. No BrdU labelled cells are observed in the central retina (6.2B and F), and only a few BrdU labelled cells are observed in the ciliary body, specifically in the non-pigmented ciliary epithelium (Figure 6.2G and H, arrows). Of the 28 sections analysed (7 eyes, 4 sections each), an average of 0-2 labelled cells were found per retinal section. The site of such rare, labelled cells was often within the inner layers of the retina (an example of this is shown in Figure 6.5B).

The *Chx10*$^{-/-}$ retina showed a remarkable contrast. A relatively large number of cells were labelled throughout the central retina (Figures 6.3, 6.4 and 6.5D and E). Three *Chx10*$^{-/-}$ sections are shown in Figures 6.3 and 6.4. The arrows in Figure 6.3 indicate the BrdU labelled cells present throughout the central retina as well as in the ciliary body. These sections also show that the ciliary body (CB) is considerably enlarged in the *Chx10*$^{-/-}$ eye compared to the wild type. More BrdU labelled cells are highlighted in the retinae of the sections in Figure 6.4C and E by arrows, whilst BrdU labelled cells in the ciliary bodies are highlighted with arrowheads in Figure 6.4B and E. It is

Figure 6.2: Two sections of wild type retina taken from mice injected with BrdU between P15 and P29. Plates *A* and *E* show phase views of the whole retinal sections. These were labelled with anti-BrdU antibody (green) and counterstained with Hoechst nuclear dye (blue). *B-D* are higher magnification views of the central (*B*) and peripheral (*C,D*) areas of the section shown in *A*. No cells were labelled with BrdU antibody in this section. *F-H* are high magnification views of the central (*F*) and peripheral (*G,H*) areas of the section shown in *E*. No cells were labelled for BrdU in the central retina, and only 1-2 BrdU-labelled cells were observed in the non-pigmented ciliary epithelium of the ciliary body at the periphery of the retina (arrows). Scale bar = 400 μm for *A* and *E*, 100 μm for *B-D* and *E-G*, 50 μm in *H*, L = lens.

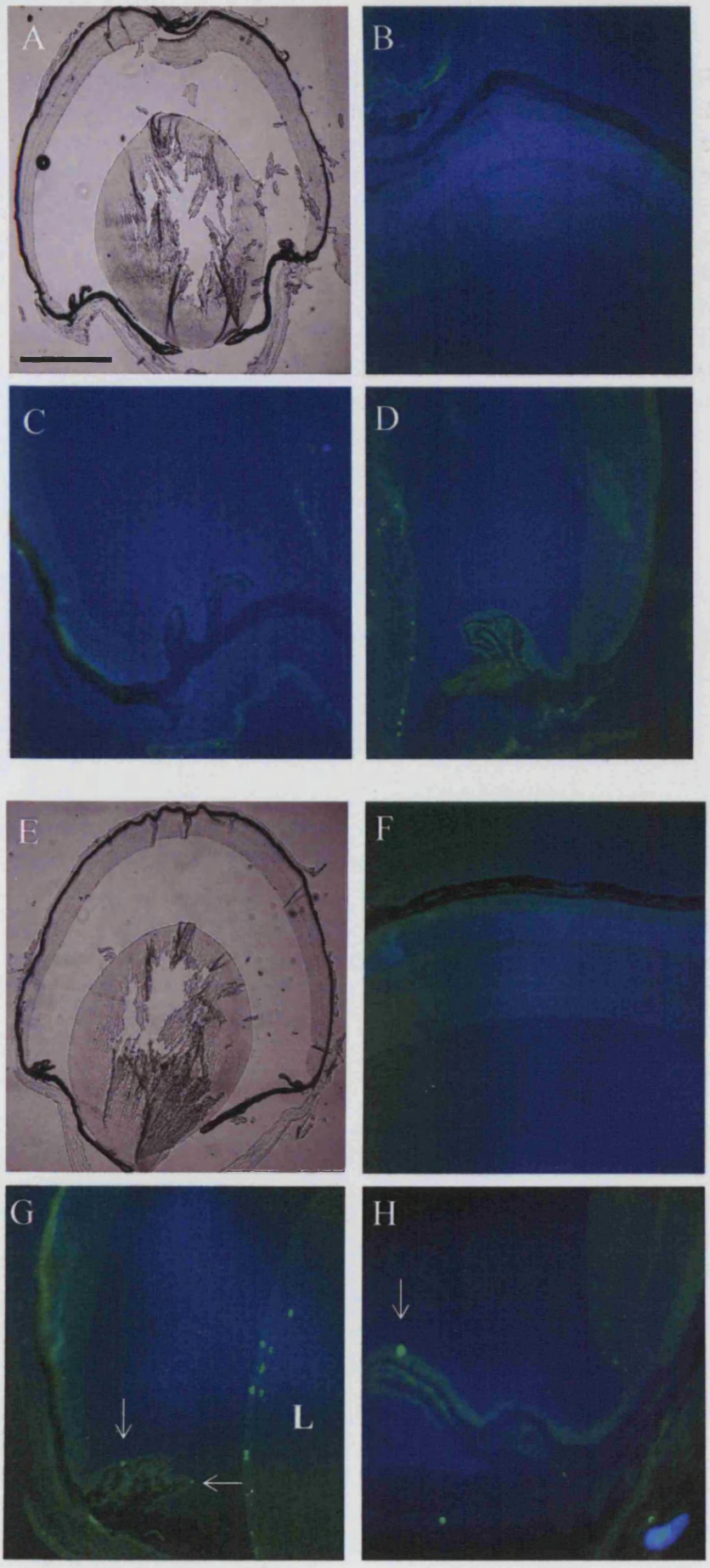
A
B
C
D
E
F
G
L
H

Figure 6.3: Section of *Chx10*$^{-/-}$ retina taken from mouse injected with BrdU between P15 and P29. *A* is a phase view of the whole retinal section. The pigmented ciliary epithelium of the ciliary body is greatly expanded in the *Chx10*$^{-/-}$ retina, and there is very little vitreous space between the lens and the retina. The section was labelled with anti-BrdU antibody (green) and counterstained with Hoechst nuclear dye (blue), shown in *B*. A large number of BrdU labelled cells could be observed along the length of the retina (arrows), as well as in the ciliary body, although it is difficult to discern whether labelled cells are in the pigmented or non-pigmented epithelium. Scale bars = 500 μm in *A*, 100 μm in *B*, L = lens, CB = ciliary body.

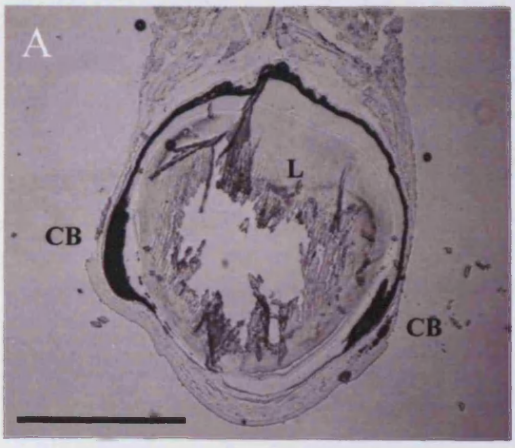
A
L
CB
CB

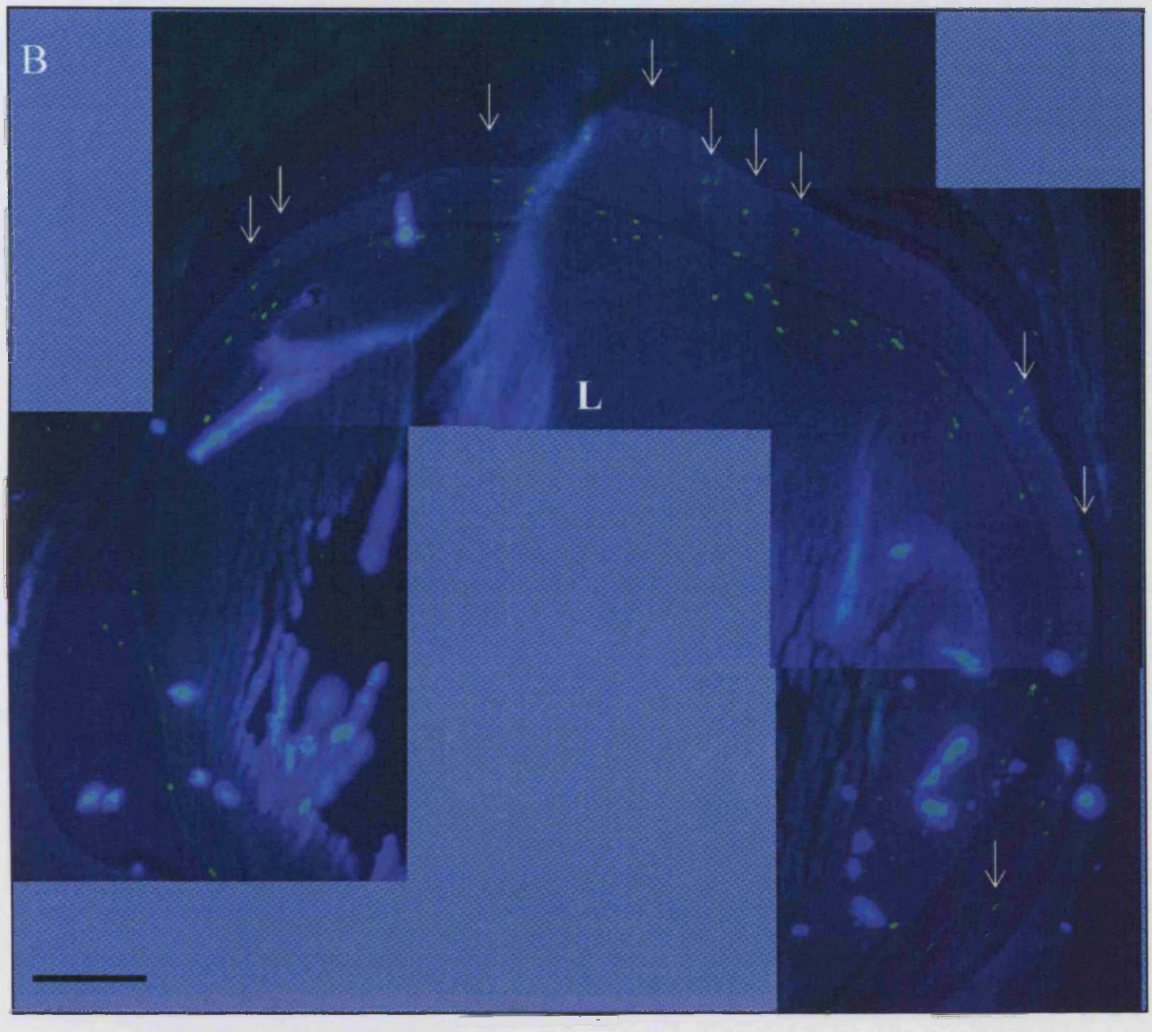
B
L

Figure 6.4: Two sections of *Chx10*$^{-/-}$ retina taken from mice injected with BrdU between P15 and P29. Plates *A* and *D* show whole retinal midline sections, *B* and *C* are high magnification views of green and purple boxed areas in A respectively, *E* is a high magnification view of boxed area in *D*. A number of BrdU labelled cells can be observed in both the *Chx10*$^{-/-}$ retina (*C* and *E*, arrows) and in the ciliary body (*B* and *E*, arrowheads). Scale bar in *A* = 500 μm in *A* and *D*, in *B* = 100 μm in others, L = lens.

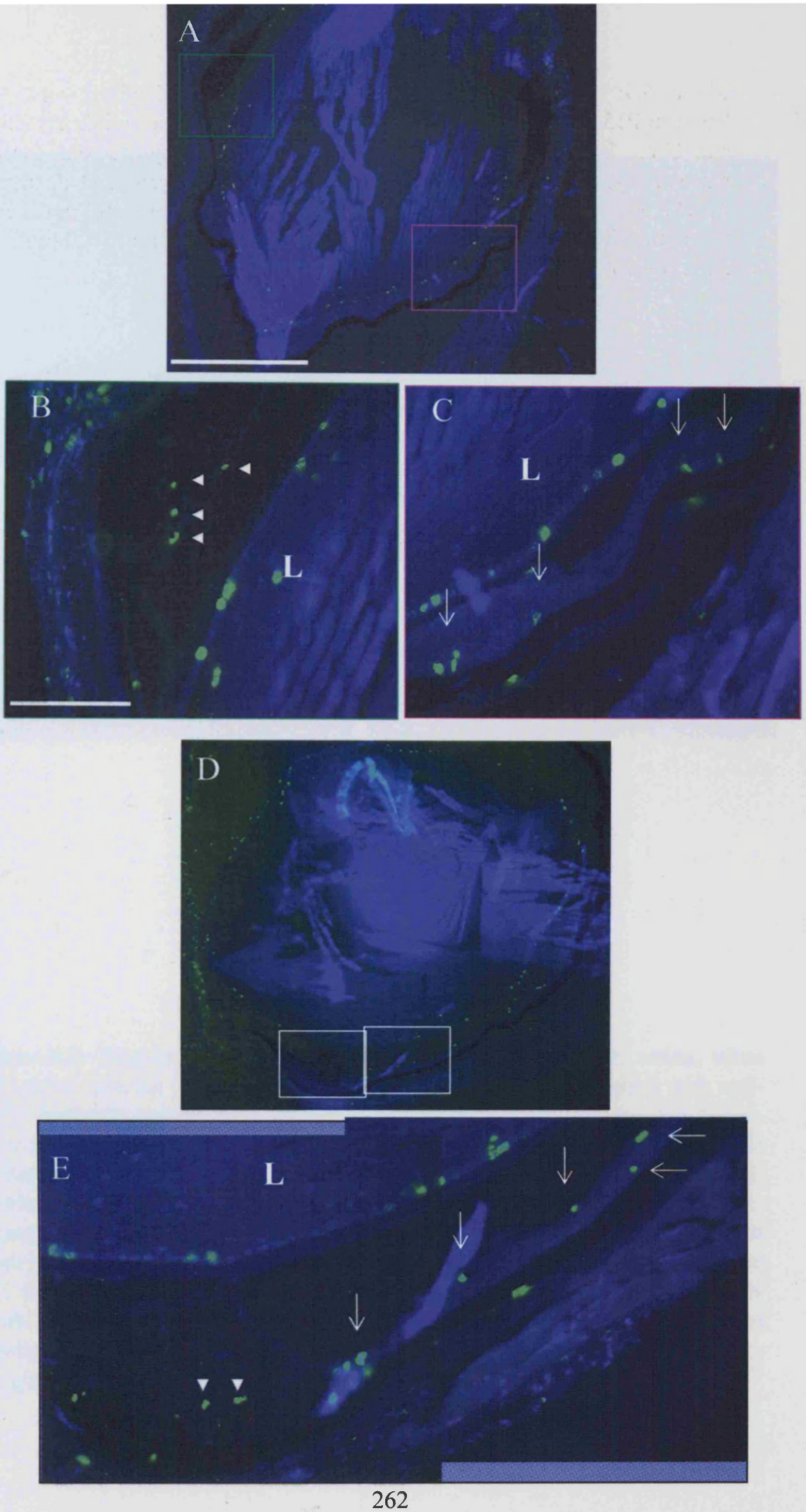
A
B
L
C
L
D
E
L

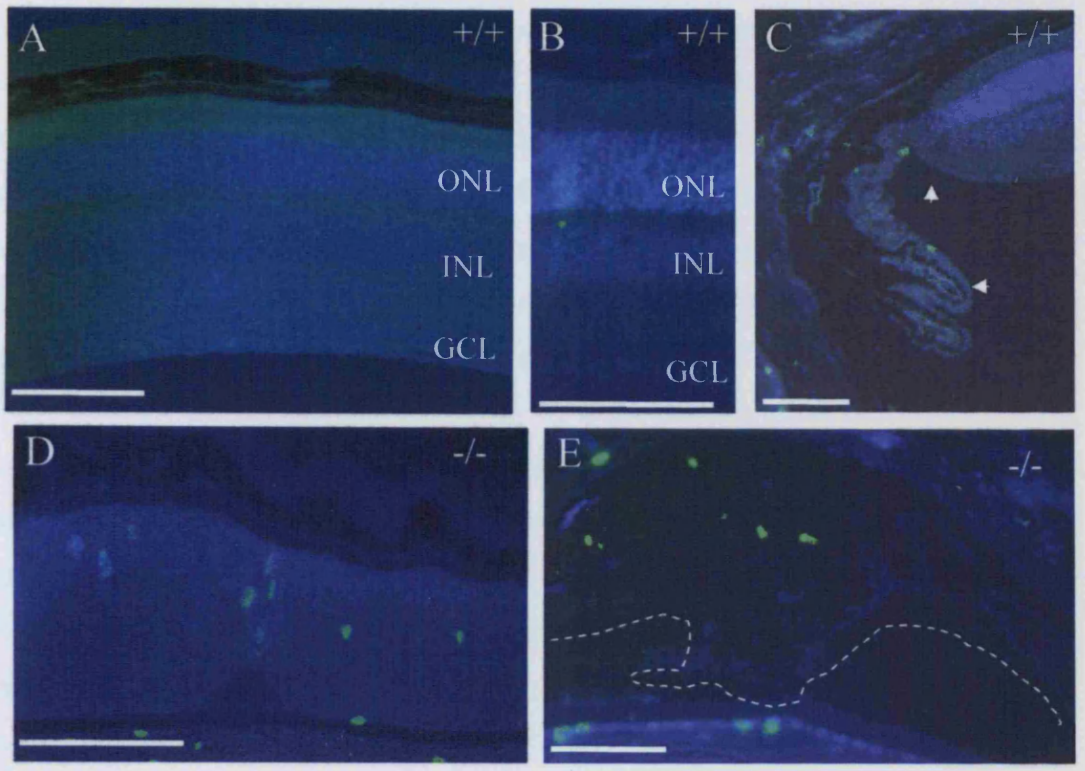

Figure 6.5: Sections of wild type (*A, B, C*) and *Chx10*$^{-/-}$ (*D, E*) retina, taken from mice injected with BrdU between P15 and P29, were labelled with anti-BrdU antibody (green) and counterstained with Hoechst nuclear dye (blue). Very few cells were labelled in the wild type retina (*A*), and any labelled cells tended to be located in the inner nuclear (*B*) or ganglion cell layer. A small number of cells were labelled in the ciliary body, in most cases in the non-pigmented ciliary epithelium (*C*, arrowheads). In the *Chx10*$^{-/-}$ retina, many cells were labelled throughout (*D*), indicating that proliferation is occurring between P15 and P29. The expanded pigmented epithelium of the mutant ciliary body (with its vitreous edge marked by dashed line, E) contains a small number of labelled cells as well. (ONL - outer nuclear layer, INL - inner nuclear layer, GCL - ganglion cell layer, scale bars = 100μm)

difficult to ascertain whether labelled cells in the ciliary bodies of *Chx10*$^{-/-}$ eyes are located in the pigmented or non-pigmented epithelia. Figure 6.5 is a comparison of BrdU treatment of wild type eyes and *Chx10*$^{-/-}$ eyes. A dramatic difference is observed between the wild type (A, B) and *Chx10*$^{-/-}$ (D) central retinae, in which a substantial number of cells are labelled with BrdU. BrdU labelling can be observed in the ciliary bodies of both the wild type (C) and *Chx10*$^{-/-}$ (E) eyes, but those in the wild type are clearly residing in the non-pigmented ciliary epithelium, whilst it is difficult to discern whether this is also the case in the *Chx10*$^{-/-}$ ciliary body.

To quantify the number of BrdU-labelled cells observed in *Chx10*$^{-/-}$ and wild type retinae, four to six midline sections were examined from three to seven eyes of each genotype and the average number of BrdU-labelled cells per section were compared using student's t-tests. The number of BrdU-labelled cells counted in the *Chx10*$^{-/-}$ retinae was substantially higher ($p = 1.75 \times 10^{-5}$) than the occasional labelled cell observed in the wild type retina (Figure 6.6A, 4 weeks), but the variation in the number of labelled cells per section was highly variable in the *Chx10*$^{-/-}$ retina, as can be seen in a graph of the raw cell counts (Figure 6.6C). In addition to an increase in BrdU-labelled cells in the central retina of the *Chx10*$^{-/-}$ eye compared to the wild type, a significantly larger number of cells were BrdU-labelled in the *Chx10*$^{-/-}$ ciliary body as well (Figure 6.6B; $p = 0.01$).

In order to examine whether proliferation in the *Chx10*$^{-/-}$ retina continues further into adulthood, a follow-up set of injections was performed between 3 to 5 weeks and 6 to 8 weeks after birth. In the wild type retina, few or no dividing cells were detected at either additional time point (Figure 6.6A, C). In the *Chx10*$^{-/-}$ retina, a significantly larger number of cells ($p = 0.02$) divide during both two-week periods compared to the wild type retina (Figure 6.6A, C). A similar range of BrdU labelled cell numbers was observed in the *Chx10*$^{-/-}$ retina at three to five weeks of age as at two to four weeks. However, fewer cells were labelled at six to eight weeks than at two to four weeks of age. Examples of *Chx10*$^{-/-}$ retinal sections at each time point are shown in Figure 6.7. BrdU labelled cells are still present throughout the central retina, from the periphery to the centre (arrows). These data indicate that a population of cells in the retina continues to proliferate well into adulthood.

Figure 6.6: Mice were injected with BrdU for two weeks before culling at 4, 5 or 8 weeks, and labelled cells were counted in midline retinal sections and compared. Labelled cells in the *Chx10*$^{-/-}$ and wild type retina were counted. Quantitative results were obtained in the central retina at 4 and 8 weeks (*A*), and in the ciliary epithelium at 4 weeks (*B*). At 4 weeks, less than five cells per section were labelled in the wild type retina, whereas more than 20 cells per section were labelled in the *Chx10*$^{-/-}$ retina on average - a highly significant difference. By 8 weeks, very few BrdU labelled cells were observed in the wild type retina, whilst a significantly higher average of 12 labelled cells per section was observed in the *Chx10*$^{-/-}$ retina (*A*). A small but significant difference between the number of labelled cells in the ciliary epithelia of the wild type and mutant retinae was observed in sections from 4 week old mice (*B*). Columns indicate means and error bars = sd. Numbers in brackets denote number of sections examined. At four weeks, sections were taken from 7 wild type and 6 mutant mouse eyes, at 8 weeks, sections were taken from 3 wild type and 7 mutant mouse eyes.(*C*) Raw data of cell counts of BrdU-labelled cells in the central retina at 4, 5 and 8 weeks. Each point indicates a cell count in a single section.

A

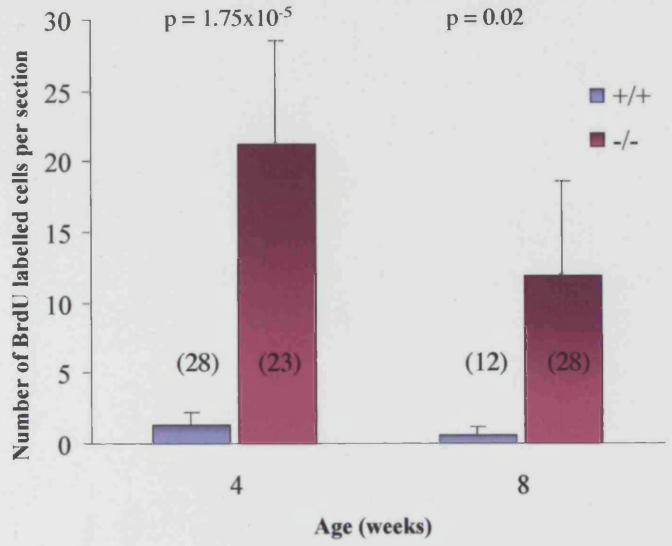
p = 1.75x10-5
p = 0.02
+/+
-/-
Number of BrdU labelled cells per section
30
25
20
15
10
5
0
(28)
(23)
(12)
(28)
4
8
Age (weeks)

B

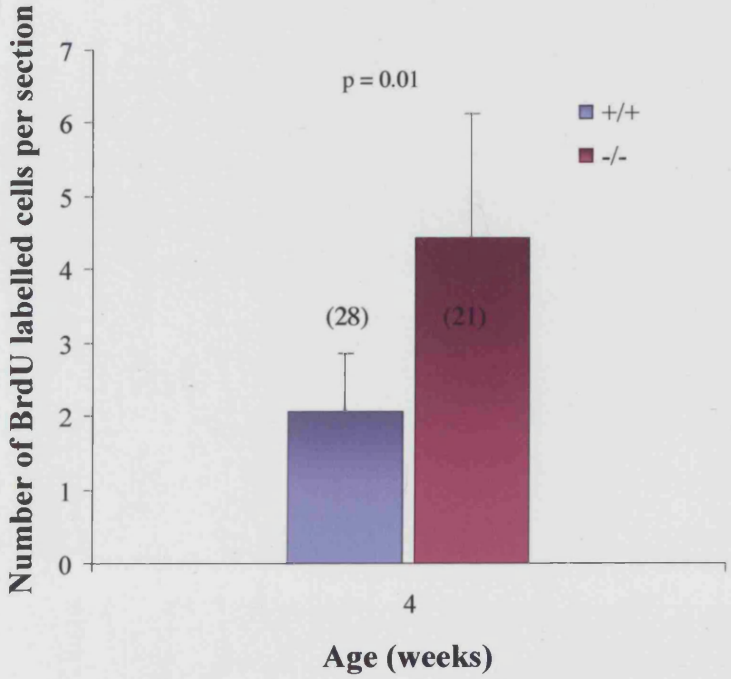
p = 0.01
+/+
-/-
Number of BrdU labelled cells per section
7
6
5
4
3
2
1
0
(28)
(21)
4
Age (weeks)

C

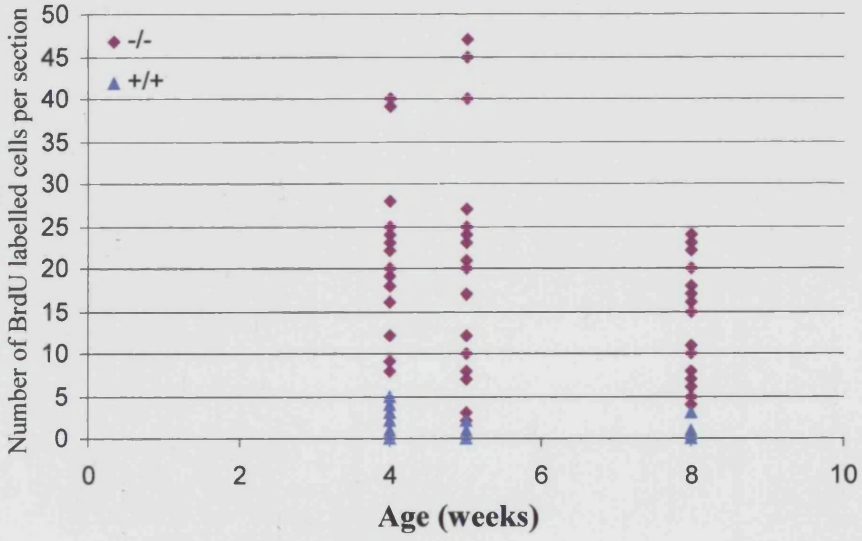
-/-
+/+
Number of BrdU labelled cells per section
50
45
40
35
30
25
20
15
10
5
0
0
2
4
6
8
10
Age (weeks)

Figure 6.7: Sections of *Chx10*$^{-/-}$ retina taken from mice injected with BrdU every other day for two weeks, from three to five weeks of age (*A*) and from six to eight weeks of age (*B*). In both sections BrdU-labelled cells can be observed throughout the central retina (arrows). It is difficult to discern any BrdU labelled cells in the ciliary bodies of the retinae. Scale bar = 100 μm, L = lens, CB = ciliary body.

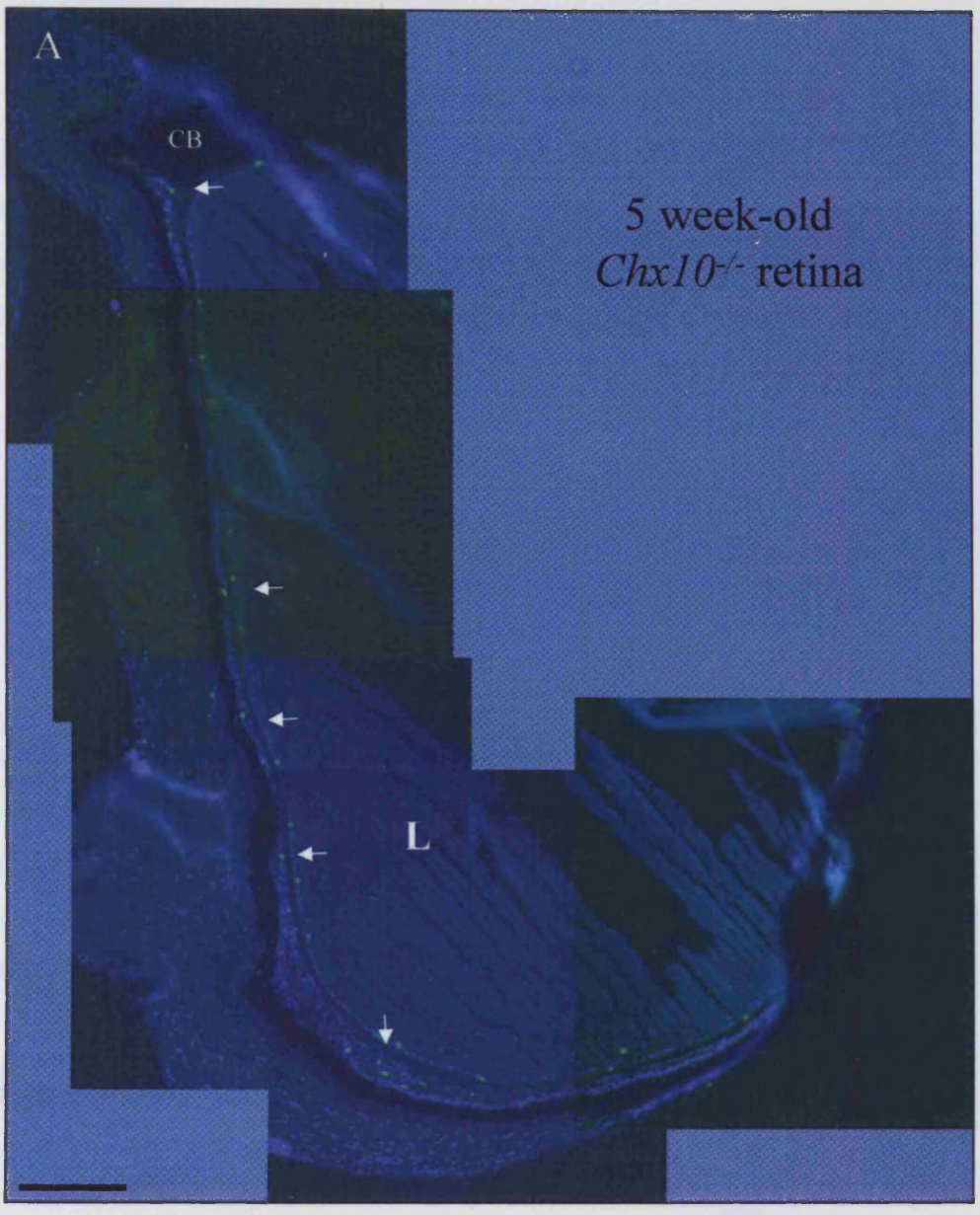
A
CB
5 week-old
Chx10-/- retina
L

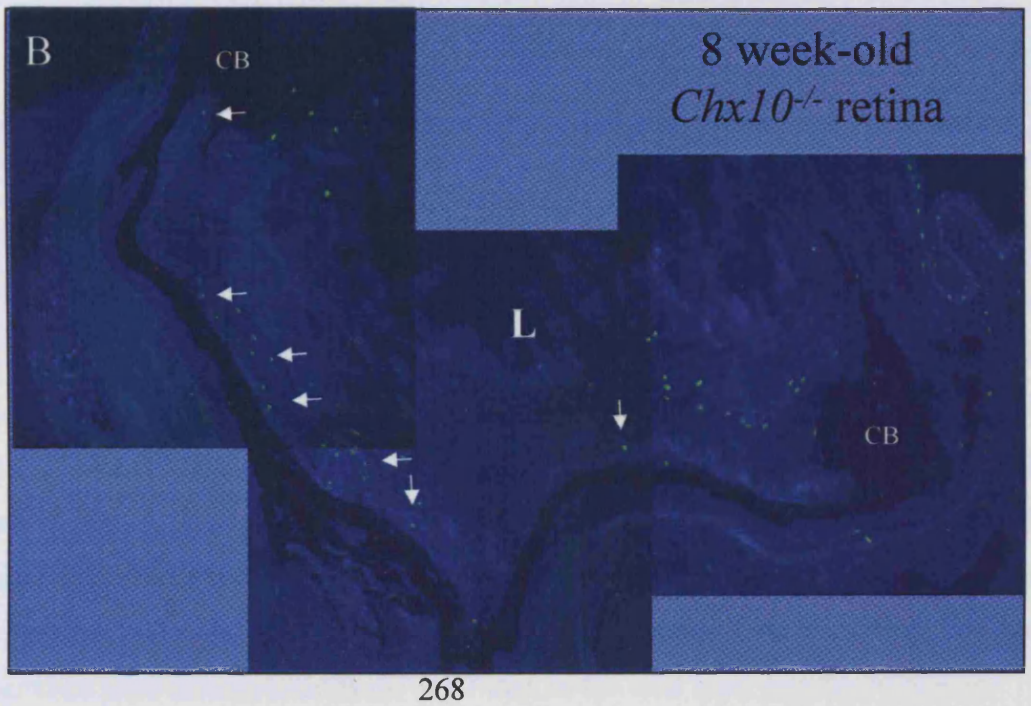
B
CB
8 week-old
Chx10-/- retina
L
CB

In order to verify that cells continued to cycle in the adult *Chx10*$^{-/-}$ retina, H3 immunostaining was also carried out on a series of postnatal retinal sections. Whereas H3-positive mitotic cells were not detected at P20 in the wild type retina, in the *Chx10*$^{-/-}$ eye occasional H3-positive cells were seen at the ventricular surface in the central retina (Figure 6.8), confirming that cell cycling is taking place in the *Chx10*$^{-/-}$ well after histogenesis is complete in the wild type retina. This study identified a unique feature of the pattern of proliferation in the *Chx10*$^{-/-}$ retina that is very different to that of the wild type retina.

6.2.2. Pattern of proliferation after birth

In addition to the injection schedule described above, 2 other types of injection schedules were followed, and these are listed in Table 6.1. These schedules were designed to examine the pattern of proliferation that occurs at the end of wild type retinal cell histogenesis and how this compares to the pattern of proliferation occurring in the *Chx10*$^{-/-}$ retina.

Schedule	Age at first injection	Injected	Culled
1	P15, P21, or P42	Every other day for two weeks	Culled on day after last injection
2	P7, P10, P13 or P15	Once	Culled P8, P11, P14, or P16
3	P10, P15, P20, or P25	Injected every other day for five days (3 times)	Culled on day after last injection (P15, P20, P25 or P30)

Table 6.1: BrdU injection schedules employed to examine cell proliferation in the postnatal wild type and *Chx10*$^{-/-}$ retina

Schedule 2 was designed to examine how proliferation changed from day to day in the last few days of normal retinal histogenesis (completed at P11). It is clear from raw data of BrdU labelled cell counts in Figure 6.9A that in the wild type retina, the number of cells synthesizing DNA decreases fairly drastically from P7 to P15. At P7 and P10, many cells are still cycling in the periphery of the retina, the last part of the retina to mature, and a few BrdU-labelled cells can also be observed in the central retina (Figure 6.10A, C, F). By P15, histogenesis is complete, and only a few cells can be observed in the wild type retina (Figure 6.9A, 6.10, H). In the *Chx10*$^{-/-}$ retina, fewer cells have incorporated BrdU at P7 than in the wild type, and the pattern of

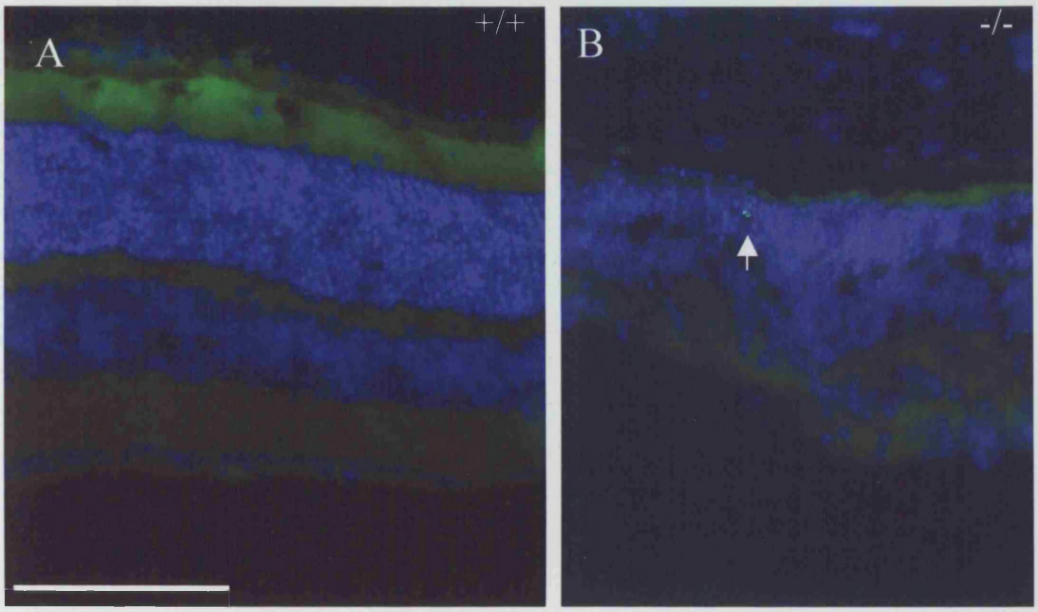

Figure 6.8: H3 labelling in the wild type (*A*) and *Chx10*$^{-/-}$ (*B*) retina at postnatal day 20. No H3 labelling can be observed in the wild type retina, only some auto-fluorescence caused by the outer segments of the photoreceptor cell layer. In the *Chx10*$^{-/-}$ retina, an occasional H3 labelled cell can be observed near the ventricular edge of the retina (*B, arrow*). Scale bar = 100 μm in *A*, 200 μm in *B*.

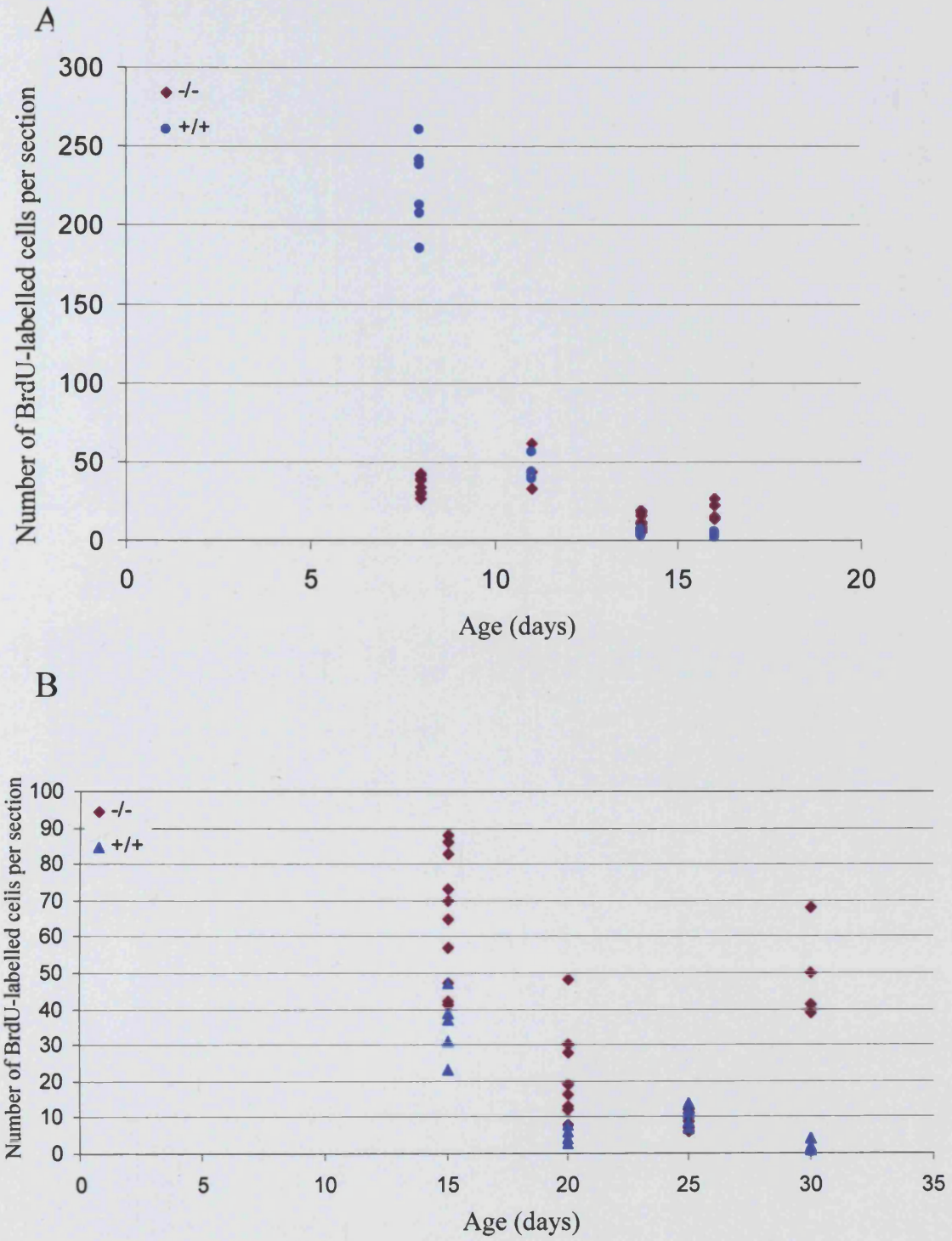

Figure 6.9: BrdU labelled cell counts of midline retinal sections from mice injected overnight and culled the following day (*A*) or injected every other day for five days and culled on the day after last injection (*B*). Each data point represents a count of one section. Age corresponds to day of culling.

Figure 6.10: BrdU labelled cells in retinae of mice injected once and culled the following day. *A* and *B*: BrdU labelled cells in section of wild type (*A*) and *Chx10*$^{-/-}$ (*B*) retinae injected at P7. In the wild type retina, BrdU labelled cells tend to be located at the periphery of the retina, the last area of the retina to fully mature, whilst BrdU labelled cells are observed throughout the retina in the *Chx10*$^{-/-}$ eye. *C-H*: BrdU labelled cells in wild type retinae injected at P10 (*C, F*), P13 (*D,G*) and P15 (*E, H*). BrdU labelled cells slowly diminish in number in the periphery of the retina with increasing age (*C-E*). In the central retina (*F-H*), a decrease of BrdU labelled cells with age is also readily apparent. Few BrdU labelled cells remain in the retina at P10 (*F*), only one can be observed at P13 (*G, arrow*), and no BrdU labelled cells can be observed at P15 (*H*) in the central retina. BrdU labelled cells are green and the sections are counterstained with Hoechst nuclear dye (blue). Scale bar in *A* = 500 μm, in *B* = 100 μm, and in *C* = 100 μm for *C-H.*

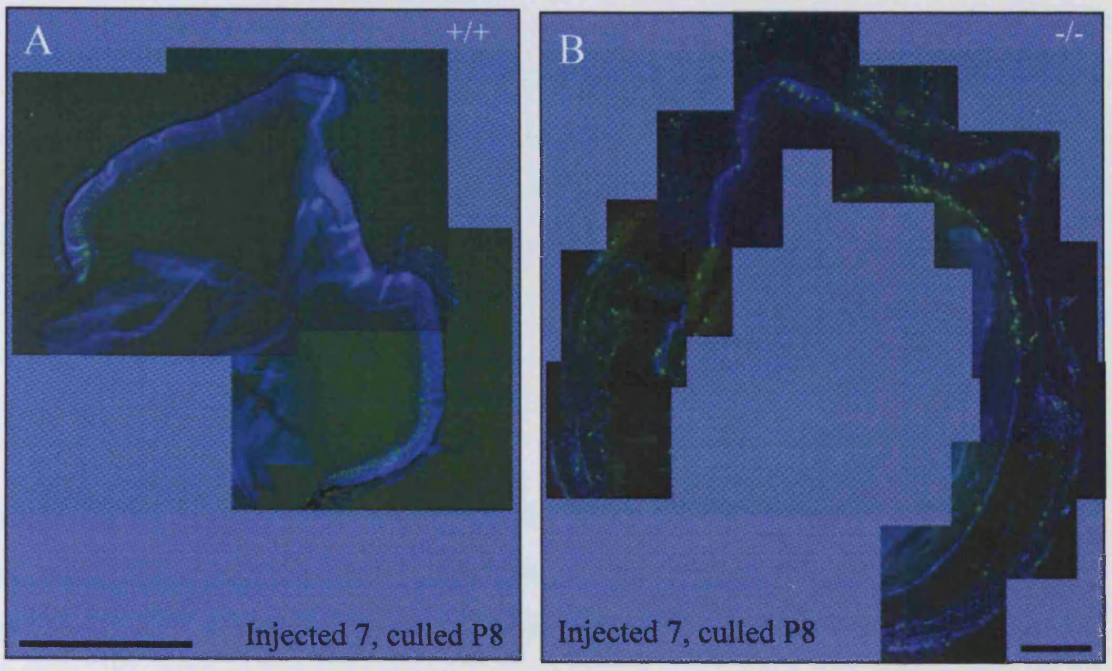

Injected P10, culled P11 Injected P13, culled P14 Injected P15, culled P16

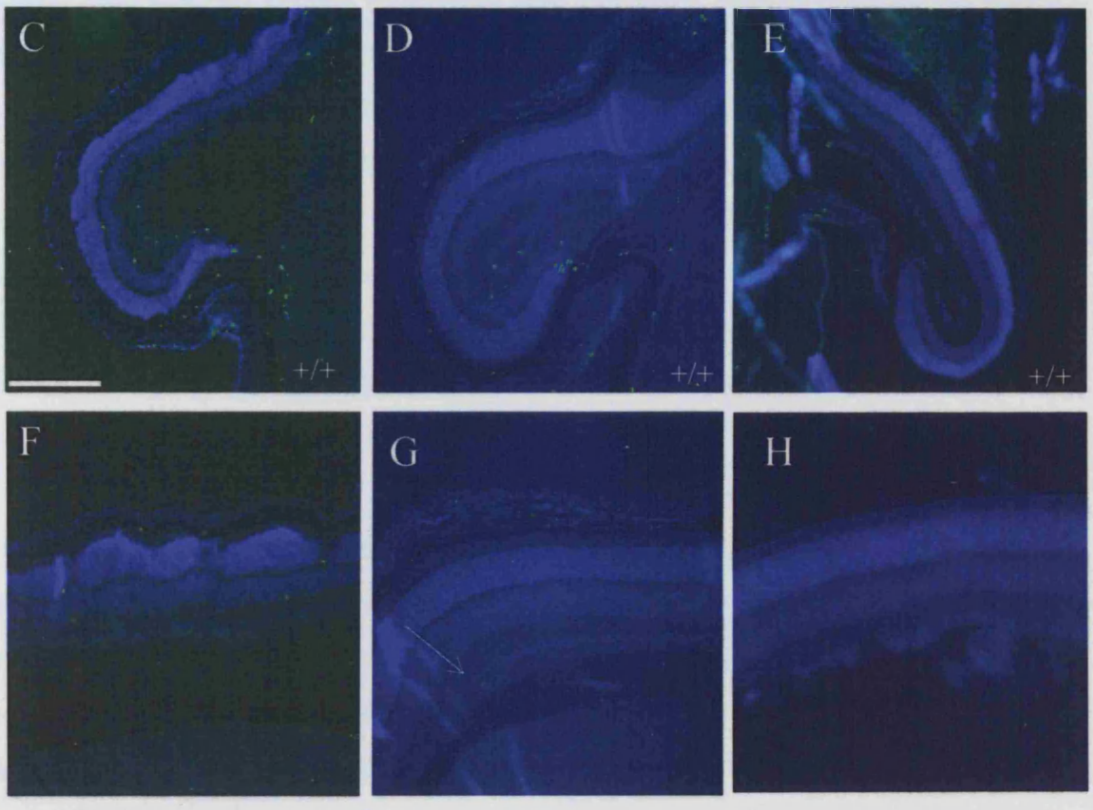

BrdU labelling is different: BrdU-labelled cells are present throughout the retina, not restricted to the periphery (Figure 6.10B). By P10, a similar amount of BrdU labelled cells were observed in the *Chx10*$^{-/-}$ retina as in the wild type (Figure 6.9A), after which the number of BrdU labelled cells is higher in the *Chx10*$^{-/-}$ retina than in the wild type, a pattern that subsequently seems to carry on into adulthood, as the number of BrdU-labelled cells are similar to those observed after 2-4 weeks of BrdU injections, described above.

Mice were also injected every other day for five days. The purpose of this was to examine whether any relatively short burst of proliferation was taking place in a specific window of development that could account for the large numbers of BrdU labelled cells observed in the *Chx10*$^{-/-}$ retina during the two-week injection periods. It is possible, for instance that a large burst of proliferation takes place between P15 and P21, and that cell cycling diminishes after this point. This is illustrated to some extent in the wild type retina. Between P10 and P15, a large number of cells seem to be cycling and are therefore labelled with BrdU. Most of the labelled cells will have divided at P10, at the periphery of the retina, where the last retinal progenitor cells divide and mature. This can be seen from the overnight injection and culling treatments described above, and after P10, cell cycling diminished substantially (Figure 6.9B, Figure 6.11A). At all later time points, BrdU labelling is rarely observed (Figure 6.9B, 6.11B), consistent with the observation that retinal histogenesis is complete by P11.

In the *Chx10*$^{-/-}$ retina, large numbers of BrdU labelled cells are observed at every time point (Figure 6.9B), both in the first five days of the two-week period and in the last five days. Only between P20 and P25 can a decrease in cycling cells be observed. BrdU-labelled cells are spread throughout the retina, as originally observed after two weeks of BrdU injections (Figure 6.11C). This suggests that, in contrast to the pattern of proliferation observed in the wild type retina, the BrdU labelling observed in the *Chx10*$^{-/-}$ retina is a result of regularly cycling cells. As fewer BrdU labelled cells are observed later in adulthood, even after two weeks of BrdU injections, this could indicate cell cycling decreases slowly through adulthood, with large numbers of cells cycling between P10 and P20 and fewer cells cycling six to eight weeks after birth. Cycling cells also do not seem to become restricted to the

Figure 6.11: BrdU labelled cells in retinae of mice injected every other day for five days before culling. *A*: wild type retina injected from P15-P20. A few BrdU labelled cells can be observed towards the periphery of the retina (*arrows*), the last area of the retina to fully mature. B and C: Retinae of wild type (B) and *Chx10*$^{-/-}$ (C) mice injected from P25-P30. No BrdU labelled cells can be observed in either the periphery or the central area of the retina of the, by now, adult wild type eye. By contrast, BrdU labelled cells are observed throughout the *Chx10*$^{-/-}$ retina at the same time point (*C, arrows*). BrdU labelled cells are green and the sections are counterstained with Hoechst nuclear dye (blue). Scale bar in *A* = 100 μm in *A*, 200 μm in *B*, scale bar in *C* = 100 μm.

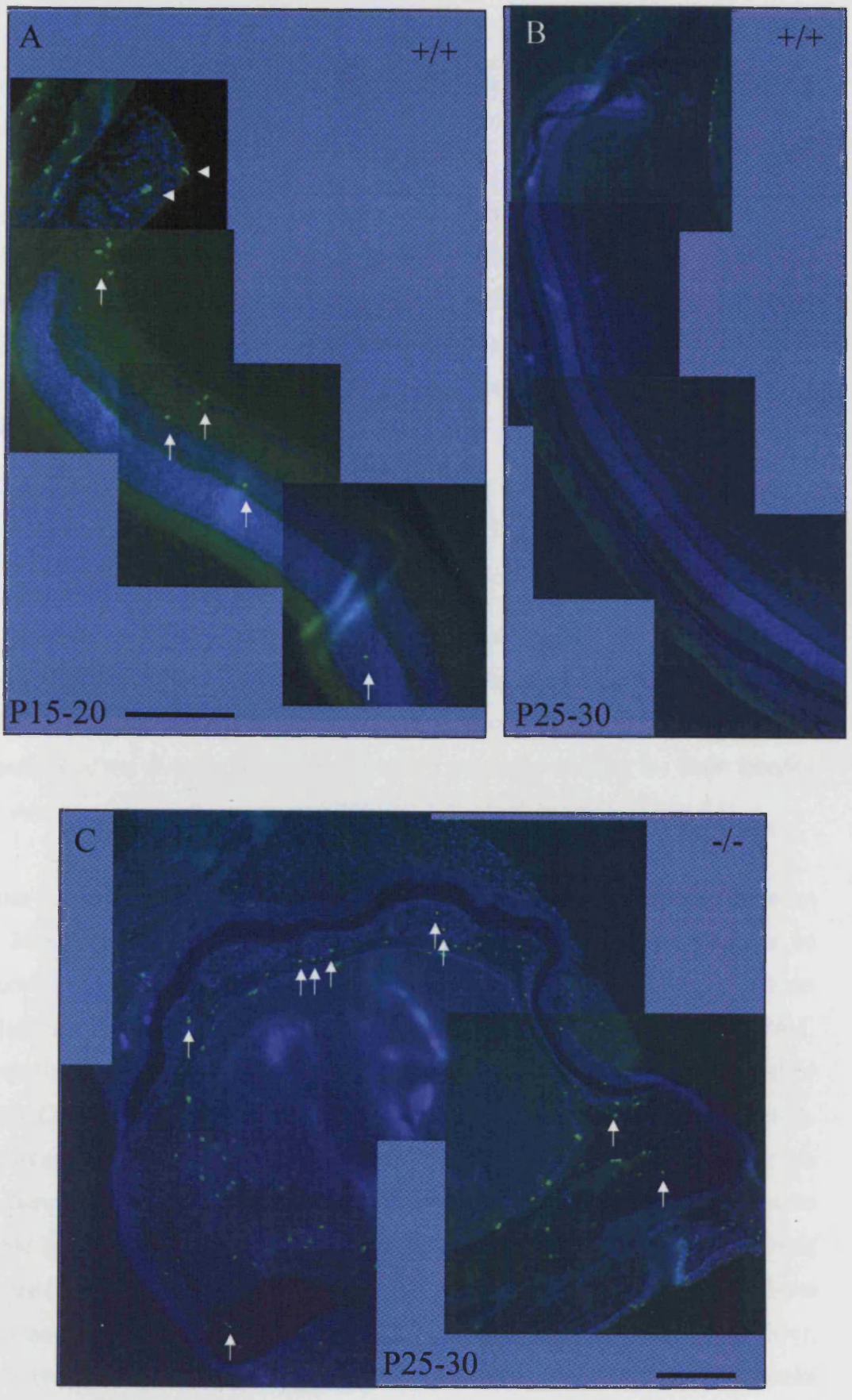
A
+/+
P15-20
B
+/+
P25-30
C
-/-
P25-30

periphery of the retina in the same way that the final cycling cells observed during wild type retinal histogenesis are.

Statistical significance was not tested for data obtained from schedules 2 and 3, as sections were only counted from 1-2 eyes. The data described in section 6.2.1, however, show that the number of BrdU labelled cells in *Chx10*$^{-/-}$ retinal sections is highly variable (see raw cell count numbers, Figures 6.6C and 6.9), and even between sections of the same eye, and that variability is higher between sections of the *Chx10*$^{-/-}$ eye than the wild type eye.

6.2.3. Some BrdU labelled cells differentiate and form new neurons in the adult *Chx10*$^{-/-}$ retina

The presence of cycling cells in the *Chx10*$^{-/-}$ retina is interesting and raises the question of what type of cells they are. Are they retinal progenitor cells? Retinal stem cells? Can they differentiate to become retinal neurons? In order to examine the phenotype of the dividing BrdU labelled cells I examined whether the BrdU labelled cell would co-label with a variety of RPC and retinal cell markers (Table 6.1).

Nestin is a marker for neural progenitor/stem cells (Ahmad et al., 1999; Ahmad et al., 2000; Messam et al., 2000). Nestin-labelled retinal progenitor cells can be detected in the early postnatal wild type retina. Typically nestin-labelled progenitors project radially across the retinal laminar axis (Insua et al., 2003). Figure 6.12A-C shows BrdU labelled cells in wild type P8 mice (BrdU injected at P7 and mice culled at P8). Co-labelling of BrdU with nestin was observed in the periphery of the retina, the last area of the retina to mature and cease proliferation, where nestin staining can be observed to project across the whole of the retina (Figure 6.12A and B), but no double labelling was detected in the central retina which is largely post-mitotic (Figure 6.12C) and where nestin-labelled cells are restricted to the ganglion cell layer and inner plexiform layer. BrdU labelled cells are observed in the neuroblastic layer, where retinal progenitor cells reside before they become post-mitotic. By four weeks of age in the wild type, no nestin labelling of RPCs was observed (Figure 6.12D), and BrdU labelled cells were rarely detected, as described above. By contrast, nestin labelling was widespread in the *Chx10*$^{-/-}$ retina at four weeks of age. Nestin-labelled

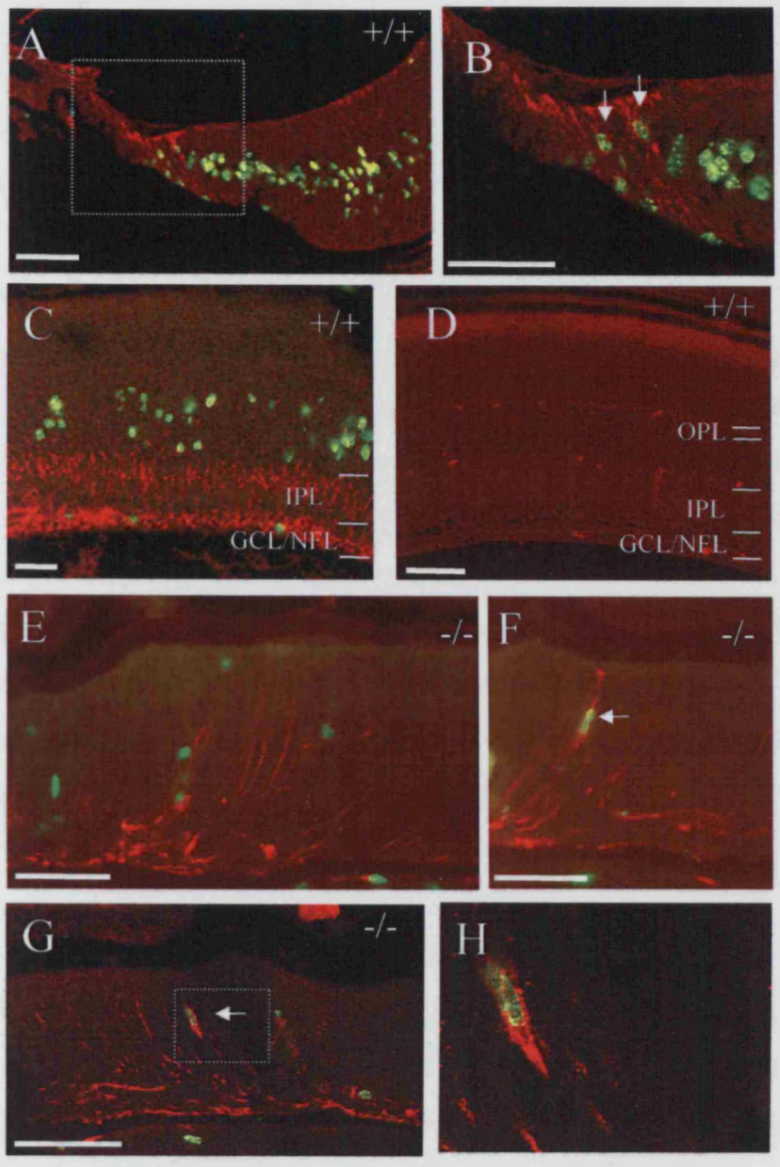

Figure 6.12: Sections from wild type and *Chx10*$^{-/-}$ eyes double labelled for BrdU (green) and nestin (red). *A-C*: At postnatal day 8 (P8), after a single BrdU injection on P7, BrdU labelling is observed primarily in the periphery of the retina (*A,B*), and decreases towards the central retina (*C*). Nestin labelling is observed radially across the retina at the periphery, where it double labels with a few BrdU labelled cells (box in *A* magnified in *B,* arrows), but in the central retina is restricted primarily to the ganglion cell layer and the inner plexiform layer, and is rarely observed to double label with cycling BrdU labelled cells (C). *D*: By four weeks of age, after two weeks of BrdU injections, BrdU labelled cells are rarely observed in the wild type retina, and nestin labelling is no longer apparent (bright red areas caused by auto-fluorescence of outer segments and vasculature). In contrast, nestin labelling is observed in cells projecting radially across the retina in 4 week old *Chx10*$^{-/-}$ retinae (*E, F, G*), and occasionally double labels with BrdU labelled cells (*F* and *G*, arrows, box in *G* magnified in *H*), more abundant in the *Chx10*$^{-/-}$ retina than in the wild type. (OPL - outer plexiform layer, IPL - inner plexiform layer, GCL/NFL - ganglion cell layer/nerve fibre layer, all scale bars = 50 μm, apart from scale bar in *G* which = 100 μm in *G*, 15 μm in *H*).

cells were observed projecting radially across the retina (Figure 6.12E-H) in a similar manner to nestin-labelled cells of the early wild type retina. Co-localisation of BrdU and nestin was detected in a small number of cells (Figure 6.12F, G, H), although the majority of BrdU labelled cells did not co-label with nestin.

To further examine whether the cycling cells observed in the *Chx10*$^{-/-}$ adult retina are retinal progenitor-like cells another marker for RPCs was employed. CRALBP is often used as a Muller cell and RPE marker in adult retinae (Bunt-Milam and Saari, 1983), but is also known to be a retinal progenitor cell marker (Walcott and Provis, 2003). Co-labelling of BrdU-labelled cells with CRALBP, in conjunction with the co-labelling observed with nestin, would suggest that the BrdU labelled cells observed in adult *Chx10*$^{-/-}$ have RPC-like properties. It is important to keep in mind, however, that co-labelling with CRALBP could equally suggest that the cycling cells observed are Muller or RPE cells. In addition, the marker would also allow investigation of the expanded ciliary epithelium, which can be observed in the adult retinal sections.

CRALBP staining is observed in the Muller cells and RPE of the wild type adult retina (Figure 6.13A, B). Bright labelling is observed in the inner nuclear layer of the retina, where Muller cell bodies reside. The end-feet of the Muller cells are brightly labelled at the vitreal edge of the ganglion cell layer/inner limiting membrane, and processes running from the Muller cell bodies to the inner segments of the photoreceptors can be observed throughout the outer plexiform layer, outer nuclear layer and in the inner segments. Labelling can also be seen in the RPE, but is less bright. Muller cell and RPE labelling is seen throughout the wild type retina, but ends abruptly at the periphery of the retina, and no CRALBP labelling can be observed in either the pigmented or non-pigmented epithelium of the ciliary body (Figure 6.13B). In the *Chx10*$^{-/-}$ retina, CRALBP labelling is abundant, disorganised and difficult to examine. However, a small number of double labelled cells were observed (Figure 6.13E, F, and box in F magnified in G). F and G are confocal images depicting a BrdU labelled cell with CRALBP-labelled processes.

Were the co-labelled BrdU/CRALBP cells retinal progenitor cells or cycling Muller glial cells? To examine this further, another glial marker, GFAP, was used. GFAP

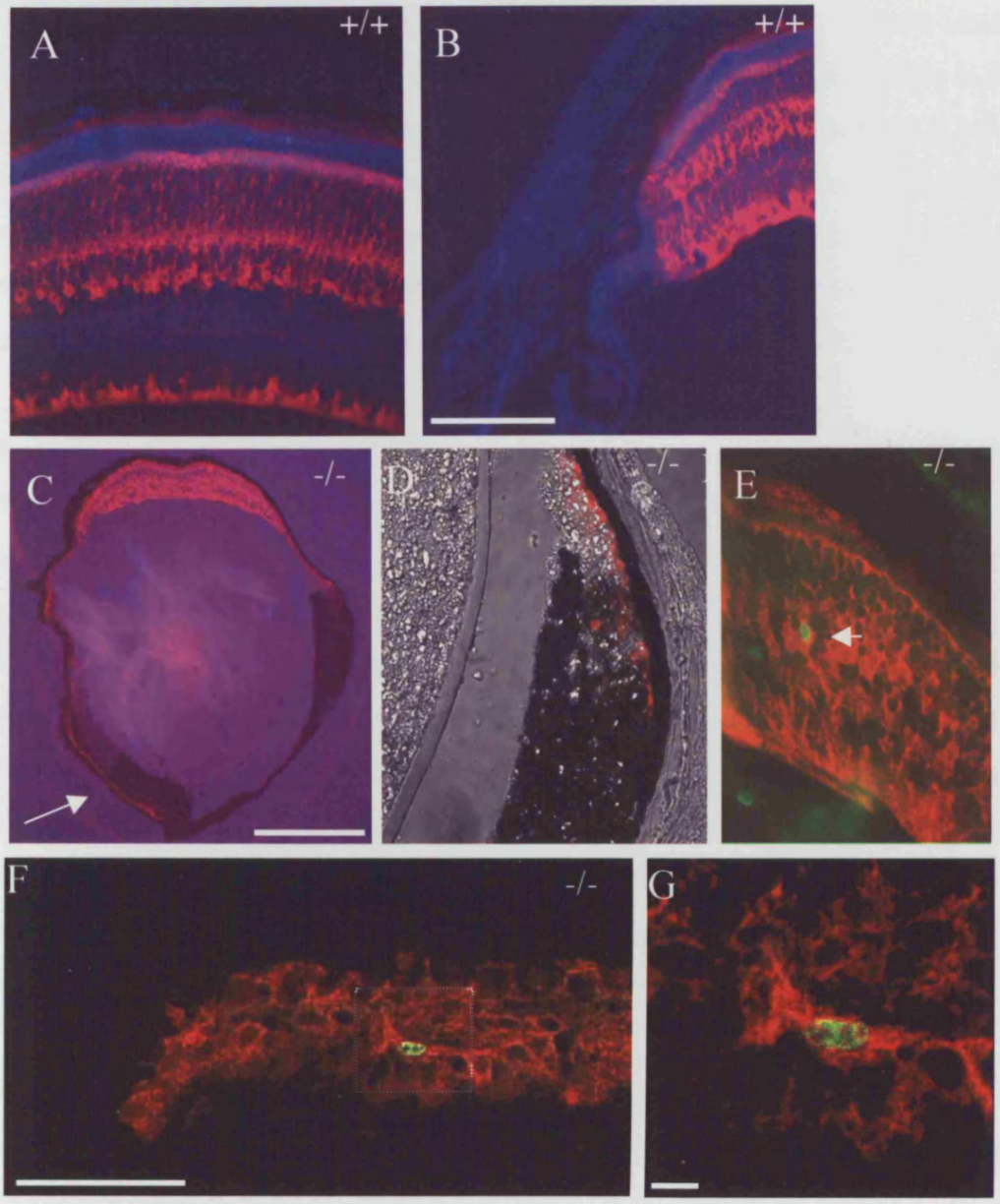

Figure 6.13: Sections from wild type (*A and B*) and *Chx10*$^{-/-}$ eyes (*C-G*) labelled for CRALBP (red) and BrdU (*E-G*, green) at four weeks of age. CRALBP staining in the wild type central retina (*A*) is observed in the Muller cells of the inner nuclear layer, their processes extending toward the ventricular edge of the retina, their endfeet at the vitreal edge of the retina, and in the RPE. No CRALBP staining is observed in either the pigmented or non-pigmented ciliary epithelium of the wild type retina (*B*). In the *Chx10*$^{-/-}$ retina, CRALBP staining can be observed in the central retina of the *Chx10*$^{-/-}$ retina and the RPE, which extends beyond the expanded ciliary epithelium of the *Chx10*$^{-/-}$ retina (*C*, arrow). In a phase photograph of CRALBP staining of the *Chx10*$^{-/-}$ retina (*D*), it is clear no CRALBP staining is observed in the ciliary epithelium of the *Chx10*$^{-/-}$ retina. The retinae have been injected every other day with BrdU for two weeks, and some BrdU labelled cells in the *Chx10*$^{-/-}$ retina are co-labelled with CRALBP (*E*, arrow, *F*, box in *F* magnified in *G*). Scale bar in *B* = 50 μm in *A* and *B*, scale bar in *C* = 200 μm for *C* and 50 μm for *D* and *E*, scale bar in *F* = 100 μm, in *G* = 25 μm.

labelling can normally be observed in the outer plexiform layer and, to some extent, the ganglion cell layer of the wild type retina (Figure 6.14A, B). Some staining in the inner nuclear layer can be seen in the very periphery of the retina (Figure 6.14A). GFAP labelling in the *Chx10*$^{-/-}$ retina is far less organised, less discretely localised, and seems more widespread (Figure 6.14C, D). However, no double labelling of BrdU and GFAP was observed, suggesting the BrdU/CRALBP double-labelled cells described above are more likely to be retinal progenitor cells than Muller glial cells.

Interestingly, CRALBP staining was not observed in the majority of the *Chx10*$^{-/-}$ ciliary epithelium. As can be observed in Figure 6.13C and D, CRALBP staining is localised to the RPE along the outer edge of the retina (arrow) and extends past the expanded ciliary epithelium at the peripheral edge of the ciliary body. However, CRALBP labelling does not extend into the ciliary body (Figure 6.13D), which suggests that the pigmented cells observed in the expanded CE of the *Chx10*$^{-/-}$ retina do not express this particular RPE marker. Rowan et al recently proposed that the expanded ciliary body is a result of transdifferentiation of neural retina to RPE, associated with expansion of RPE gene expression (Rowan et al., 2004). However the CRALBP staining showed that at this point, these cells are not expressing the full complement of RPE markers.

To examine whether dividing cells differentiate and give rise to new neuronal cells in the adult retina, retinal sections from BrdU injected animals were double-labelled with the neuronal markers β3-tubulin and NeuN, both markers of mature neuronal cells. At P8, a large proportion of cells in the wild type retina, specifically those in the ganglion cell layer and many in the inner nuclear layer, will have fully matured into retinal neurons. Accordingly, β3-tubulin is strongly localised in the ganglion cell/nerve fibre layer, the inner plexiform layer, and in a proportion of cells of the inner nuclear layer (Figure 6.15A-C) and weakly detected in the photoreceptor layer at this time point. Cycling cells are localised in the neuroblastic layer of the retina, toward the ventricular edge, and thus BrdU-labelled cells are localised in this area of the retina. A few BrdU-positive cells with β3-tubulin labelled processes are located toward the vitreal edge of the inner nuclear layer, especially in the periphery of the retina, where the last of cycling cells are differentiating (Figure 6.15A, box in A

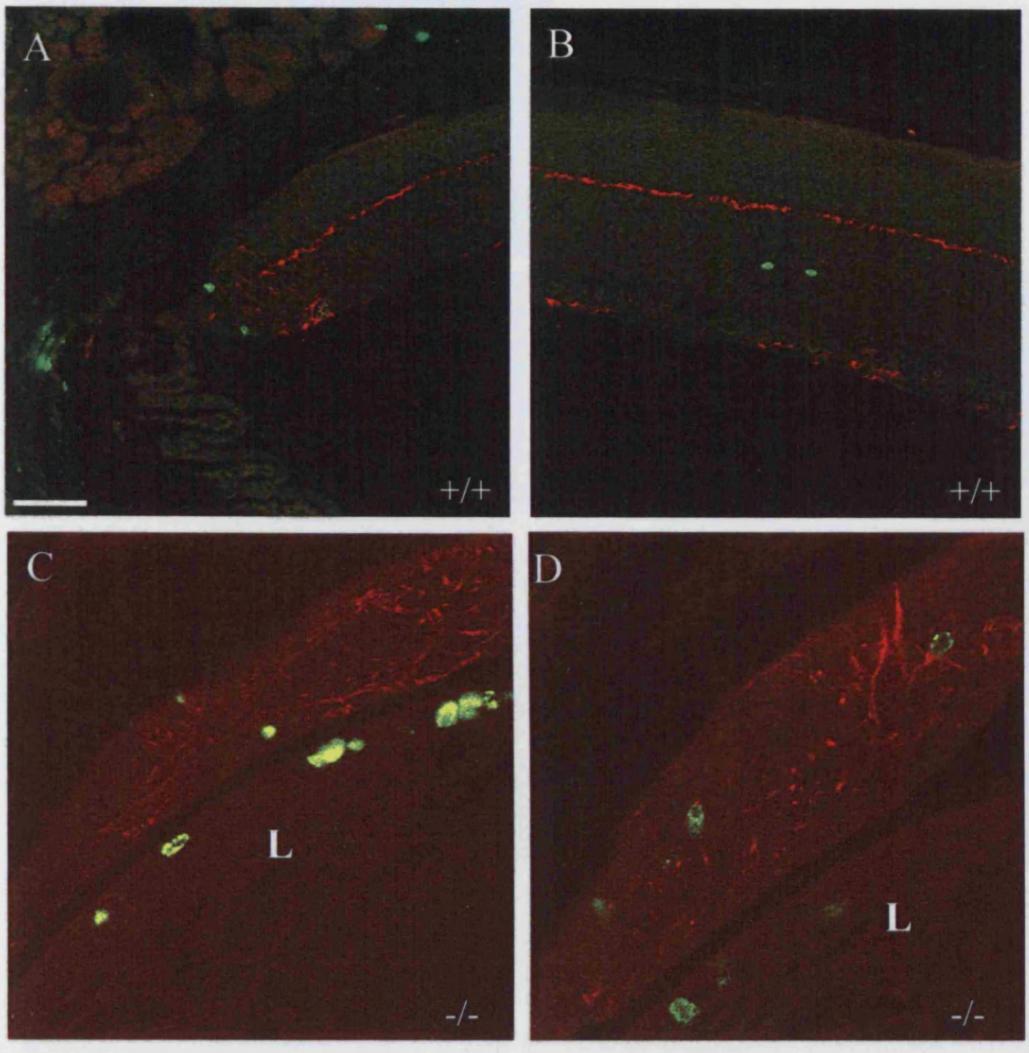

Figure 6.14: Sections from wild type (*A and B*) and *Chx10*$^{-/-}$ (*C* and *D*) eyes labelled for GFAP (red) and BrdU (green) at four weeks of age. GFAP staining in the wild type periphery (*A*) and central retina (*B*) is limited to astrocytic cells within the inner plexiform layer, and no double labelling with BrdU is observed. In the *Chx10*$^{-/-}$ retina, GFAP staining is more extensive throughout, as is clear in both examples of central retinal sections depicted here (*C, D*) but as was the case for the wild type retina, no GFAP and BrdU double labelling was observed. L = lens, scale bar = 80 μm.

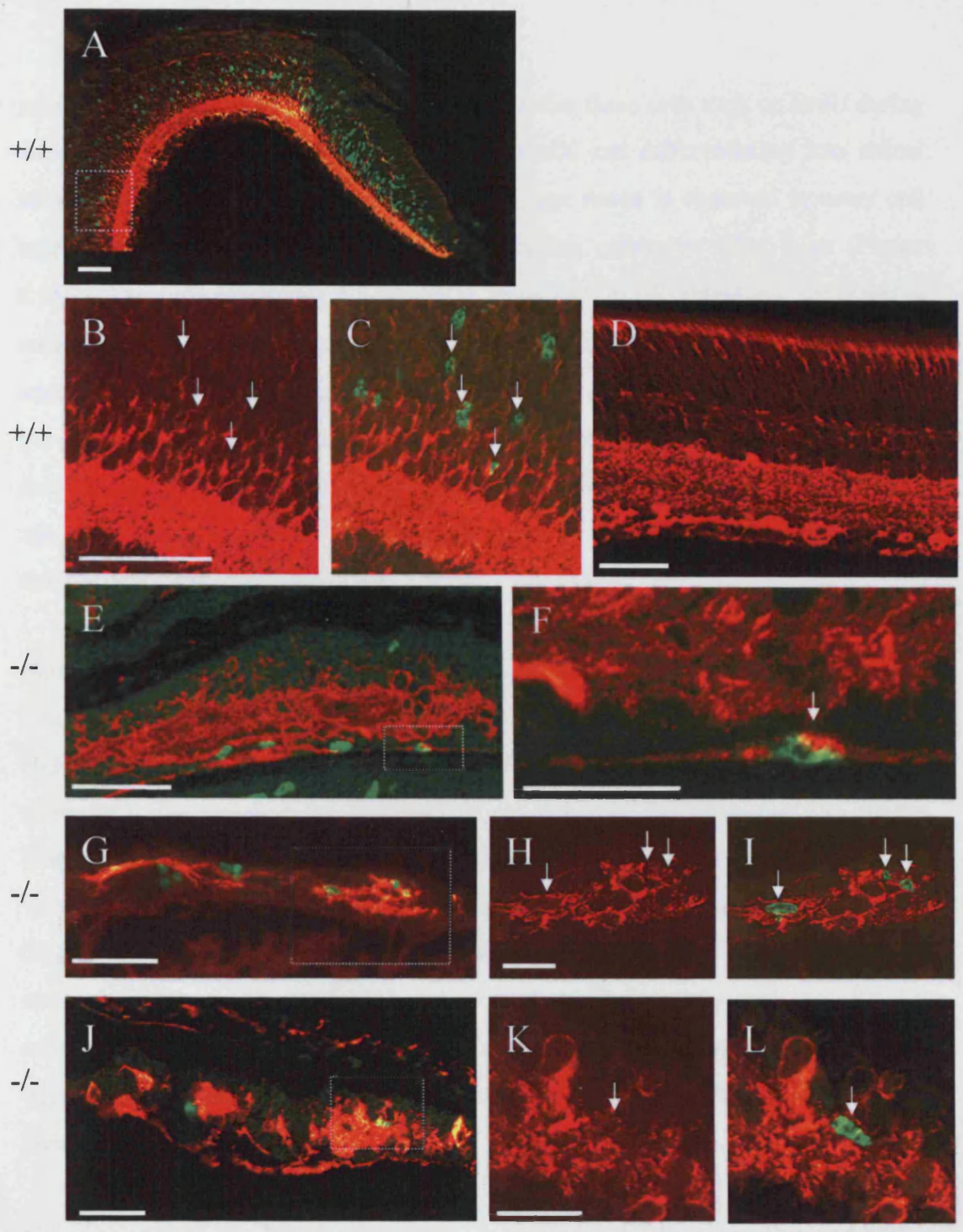

Figure 6.15: Sections from wild type and *Chx10*$^{-/-}$ eyes double labelled for BrdU (green) and β3 tubulin (red). At P8, after a single BrdU injection on P7, β3 tubulin is localised to the ganglion cell and the inner plexiform layers of the wild type retina, and to a proportion of cells in the inner nuclear layer (*A-C*). BrdU labelled cells that contribute to the inner nuclear layer are double labelled with β3 tubulin (box in *A* magnified and rotated in *B* and *C*, arrows). In the adult wild type retina, β3-tubulin labelling can be observed in all layers of the retina in an organised pattern (*D*). In the mutant retina, β3 tubulin labelled cells are observed at 4 (*E-F*), 5 (*G-I*), and 8 (*J-L*) weeks of age in an apparently disorganised pattern. After two weeks of BrdU injections administered every other day before culling, BrdU labelled cells are observed in the retina at all time points and some cells label for both β3 tubulin and BrdU at each time point (arrows in *F,H,I,K,L*). Scale bar = 50 μm in all but *F,H, I,K, L* where it = 20 μm

rotated and magnified in B and C). It is possible that these cells took up BrdU during their final cell cycle before becoming post-mitotic and differentiating into retinal neurons. β3 tubulin staining in the adult wild type retina is observed in every cell layer, with the strongest staining in the ganglion cell/nerve fibre layer (Figure 6.15D). The cells expressing β3-tubulin in the adult *Chx10*$^{-/-}$ retina are disorganised compared to the highly organised pattern of β3-tubulin expression observed in the adult wild type retina. Using confocal microscopy I detected BrdU-positive cells in the adult *Chx10*$^{-/-}$ retina with β3-tubulin labelled processes, examples are shown at four (Figure 6.15 E-F), five (Figure 6.15G-I) and eight (Figure 6.15J-L) weeks of age. This suggests that some of the cycling cells observed in the adult *Chx10*$^{-/-}$ retina exit the cell cycle and differentiate to become neurons.

NeuN labelling was also used to examine mature neurons in the wild type and *Chx10*$^{-/-}$ retina, offering the advantage of labelling cell nuclei rather than the cell bodies and process labelled by β3-tubulin. In the adult wild type retina, NeuN is restricted to the ganglion cell and inner retinal cell layer, but photoreceptors are not labelled by NeuN (Figure 6.16A, B). In the *Chx10*$^{-/-}$ retina, NeuN labelling is not widespread, but a few NeuN labelled cells can be observed in various retinal sections (Figure 6.16C-E). BrdU and NeuN co-labelled cells were only observed in a few sections (Figure 6.16E, magnified in F, arrow), much less frequently than the β3-tubulin and BrdU co-labelled cells, which may reflect cell immaturity, as NeuN is a late neuronal marker, or the fact that a smaller proportion of cells are labelled with NeuN in the adult retina.

No nestin, CRALBP, GFAP, β3-tubulin, or NeuN localisation was observed within the ciliary body of either the *Chx10*$^{-/-}$ or the wild type eye.

6.2.4. New amacrine-like cells develop in the adult *Chx10*$^{-/-}$ retina

To determine whether the neurons generated from RPCs in the adult *Chx10*$^{-/-}$ retina, expressed markers characteristic of specific retinal neurons, immuno-labelling with a range of antibodies was carried out on BrdU injected mouse retinae. To extend the time for BrdU labelled cells to differentiate, a final BrdU injection schedule was

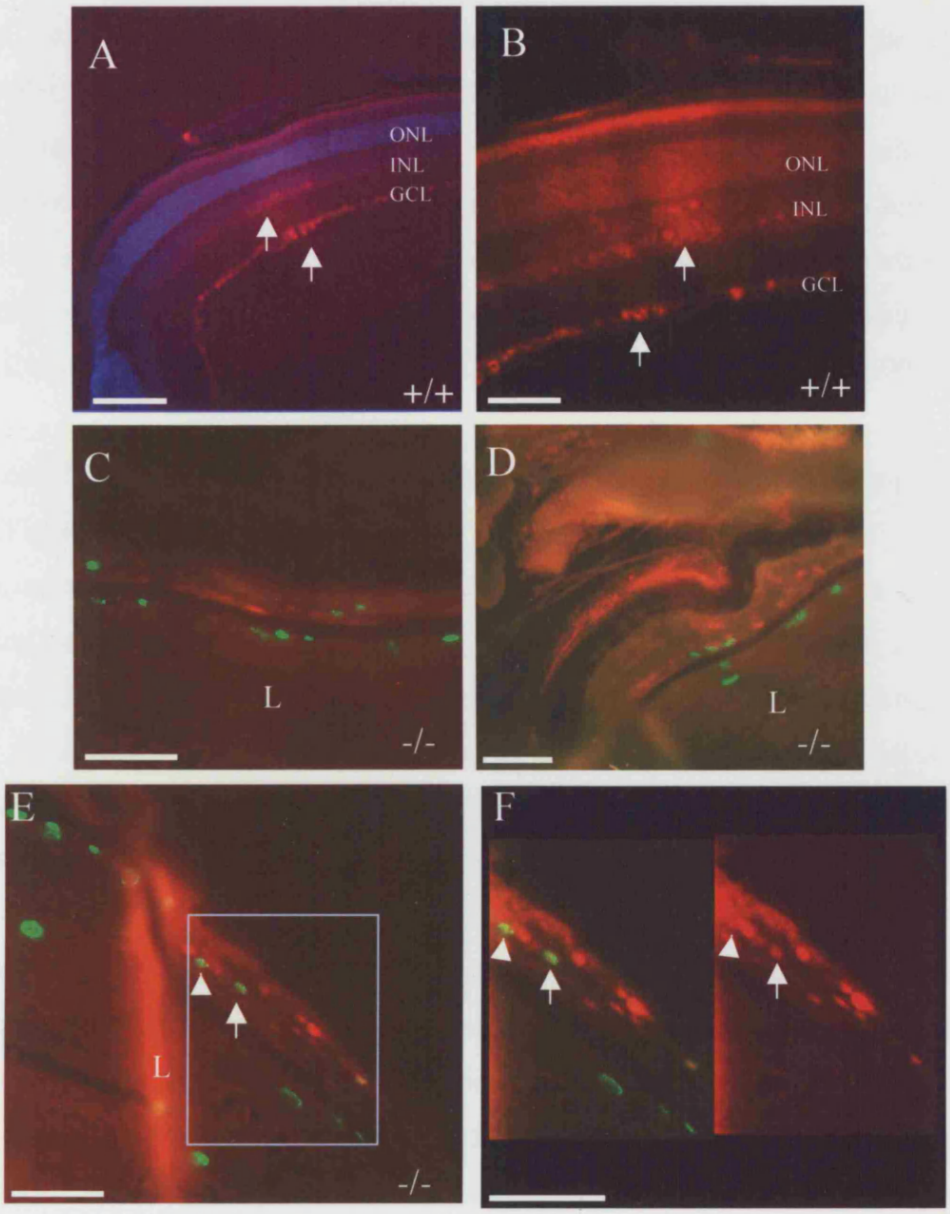

Figure 6.16: Sections from wild type and *Chx10*$^{-/-}$ eyes double labelled for BrdU (green) and NeuN (red). In the adult wild type eye (*A,B*), cells in the ganglion cell layer and towards the vitreal edge of the inner nuclear layer are most brightly stained for NeuN (*A, B, arrows*), whilst cells in the rest of the inner nuclear layer and the outer nuclear layer are less brightly labelled (*B*). *C-E* are examples of sections taken from *Chx10*$^{-/-}$ retinae at 4 weeks of age after two weeks of BrdU injections. NeuN labelling is disorganised and scattered in all three sections. Higher magnification views of the box in *E*, (*F*) show one BrdU labelled cell that does not co-label with NeuN (arrowhead) and one BrdU labelled cell that does co-label with BrdU (arrow). ONL = outer nuclear layer, INL = inner nuclear layer, GCL = ganglion cell layer, L = lens, scale bars = 50 μm.

devised. Cells were injected every other day from P25 to P29 and then culled three weeks after the last injection. Sections were then examined for BrdU and cell marker co-labelling. Brn3b (Pou4f2) was used as a marker for ganglion cells, blue cone opsin for cones, rhodopsin for rods, recoverin for photoreceptors, protein kinase C (PKC) for bipolar cells, and syntaxin and the VC1.1 epitope for amacrine and horizontal cells (Alexiades and Cepko, 1997; Rutherford et al., 2004; Xiang et al., 1993). Calbindin was also used as a marker for horizontal cells (Chu et al., 1993).

As expected, whilst bipolar cells in the adult wild type retina stained brightly with PKC (Figure 6.17A), no PKC staining was observed in the *Chx10*$^{-/-}$ retina, confirming that bipolar cells are not present in the *Chx10*$^{-/-}$ retina (Figure 6.17D). Labelling with cone opsin and rhodopsin proved to be problematic. Both markers label the outer segments of the respective photoreceptors, whilst BrdU labels the nuclei of dividing cells. The adult *Chx10*$^{-/-}$ retinal cell layers are relatively disorganised compared to the wild type retina, thus making it very difficult to match the nuclei of any photoreceptors to their respective outer segments, a task that is already difficult in the organised wild type retina. Thus, the photoreceptor marker recoverin was also employed. All cells in the outer nuclear layer, where the photoreceptors reside, are brightly labelled in the adult wild type retina (Figure 6.17B). Recoverin also labelled cells towards the ventricular edge of the *Chx10*$^{-/-}$ retina, however, no double staining of BrdU and recoverin was observed (Figure 6.17E). Brn3b labels ganglion cells (Figure 6.17C), but as was observed with recoverin labelling, no Brn3b/BrdU double labelling was observed in the adult *Chx10*$^{-/-}$ retina. This suggests that the neurons observed to be double labelled with β3-tubulin and BrdU are unlikely to be ganglion cells or photoreceptors.

Whilst no BrdU-labelled cells co-labelled for ganglion cell layer or outer nuclear layer cell markers, some BrdU labelled cells in the adult *Chx10*$^{-/-}$ retina, however, did express inner nuclear layer cell markers. Figure 6.17F shows a BrdU-labelled cell co-labelled with calbindin; a cross section through a confocal image of a *Chx10*$^{-/-}$ retinal section, taken at 0.2 μm increments. The green BrdU-labelled nucleus indicated by the arrows is surrounded by red calbindin staining, causing a yellow area where the two markers overlap. BrdU-labelled cells also co-labelled for both VC1.1 (Figure 6.18) and syntaxin (Figure 6.19). In the adult wild type retina, VC1.1 is expressed in

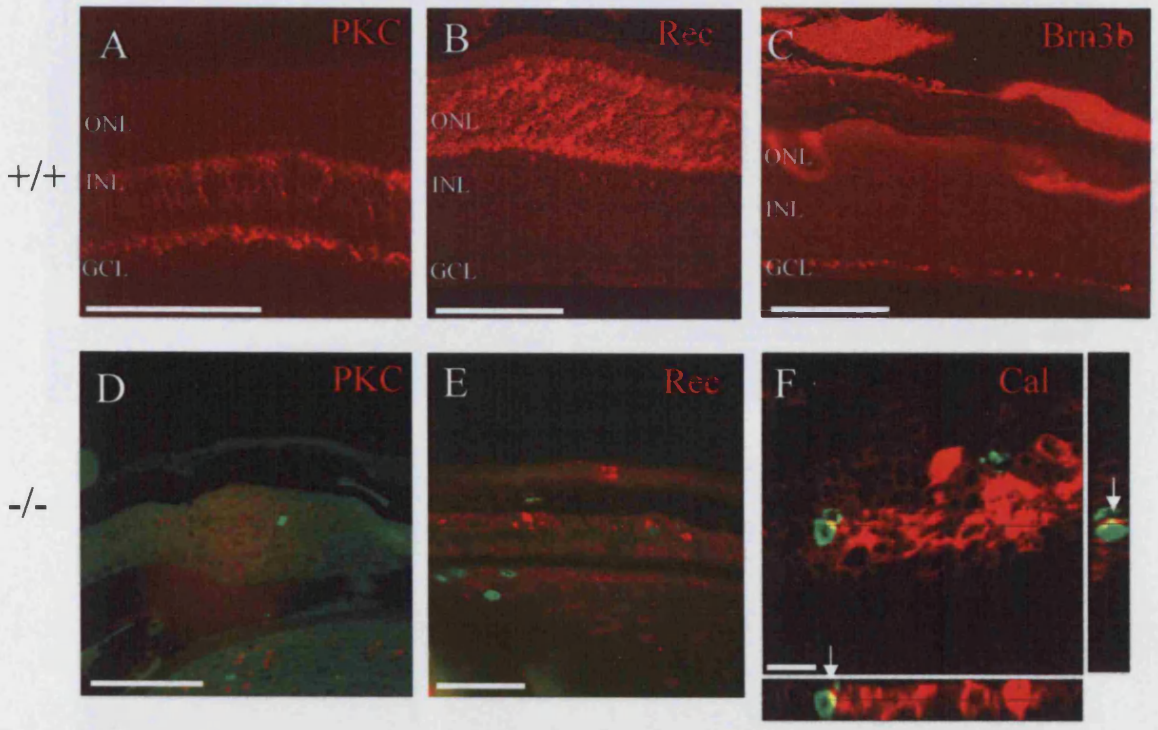

Figure 6.17: Sections from wild type eyes (*A-C*) or *Chx10*$^{-/-}$ eyes (*D-F*) labelled with a variety of retinal cell markers (red) and (in *D-F*) BrdU (green). *A – C* are wild type sections from 4-week old wild type mice. PKC (A) labels the bipolar cells located in the inner nuclear layer of the retina and their processes towards the ganglion cell layer. Recoverin (B, rec) labels all the photoreceptors in the outer nuclear layer of the retina. Brn3b (C) labels the ganglion cells in the ganglion cell layer. *D-F* are sections of retina from 4-week old *Chx10*$^{-/-}$ mice that have been injected with BrdU every other day for two weeks before culling. No PKC labelling can be observed in *D*, confirming that no bipolar cells are present in the mutant retina. Some recoverin labelled cells can be observed towards the ventricular layer of the retina (*E*), but no recoverin and BrdU double-labelling can be observed. *F* is a view through a series of 0.2 μm increments through the retinal section taken with a confocal microscope. The cross hairs indicate the position of a BrdU labelled cell that seems to be co-labelled with calbindin (cal). Views through the section at the level of the cross hairs, show an overlap of some of the red and green labelling (yellow areas, arrows).ONL = outer nuclear layer, INL = inner nuclear layer, GCL = ganglon cell layer, scale bars = 100 μm except in *F* where it = 25 μm.

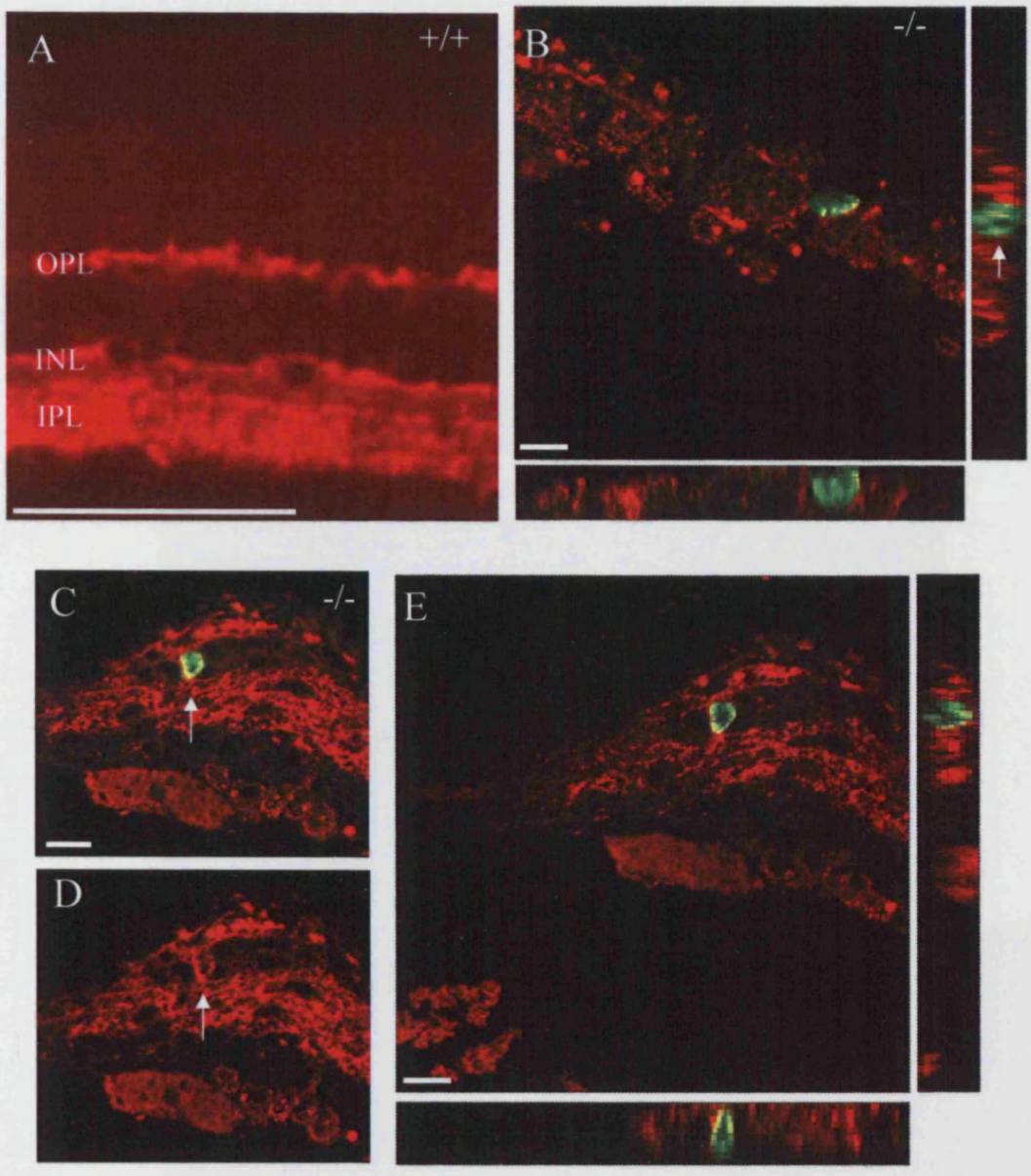

Figure 6.18: Sections from wild type and *Chx10*$^{-/-}$ eyes labelled for VC1.1 (red) and (in *B-E*) BrdU (green). VC1.1 staining in the 4-week old wild type retina is localised to the inner plexiform layer, some of the inner nuclear layer cells, and the outer plexiform layer. *B-E* are two sections of retinae of 4-week old *Chx10*$^{-/-}$ mice injected with BrdU for two weeks before culling. B and E are views through a series of 0.2 μm increments through the retinal sections taken with a confocal microscope. The cross hairs indicate the position of a BrdU labelled cell. In *B*, views through the section at the level of the cross hairs, shows some overlap of the red and green labelling (yellow areas, arrow). In *E*, BrdU-labelling more clearly overlaps with VC1.1 labelling. This is confirmed by *C* and *D*, an average projection of the 0.2 μm increments (C), and a view of only the VC1.1 labelling (D), where the BrdU labelled cell is clearly stained red (arrow). ONL = outer nuclear layer, INL = inner nuclear layer, GCL = ganglion cell layer, scale bar = 50 μm in *A*, 20 μm in *B*, 25 μm in *C* and *D*, 25 μm in *E*.

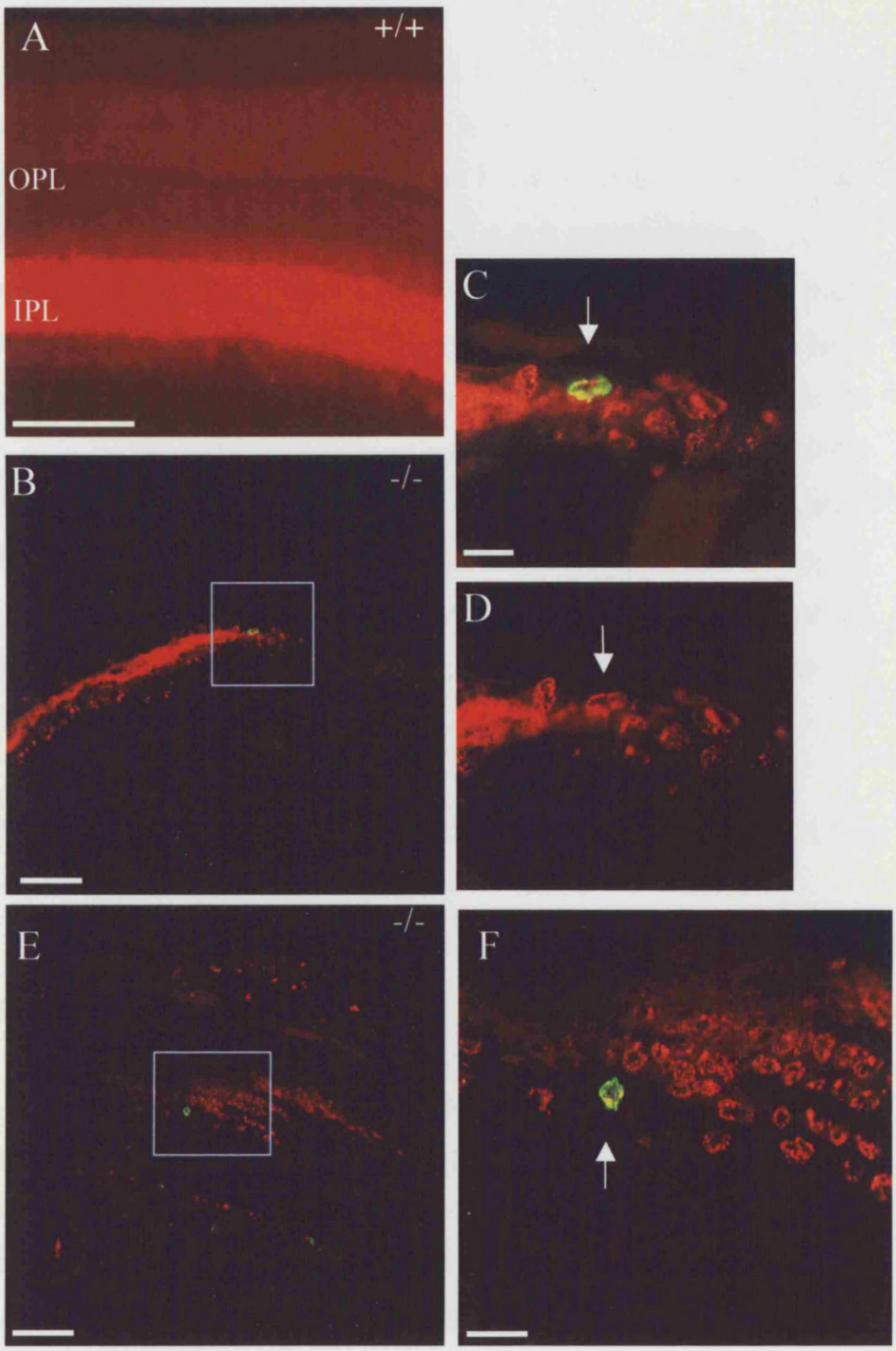

Figure 6.19: Sections from wild type and *Chx10*$^{-/-}$ eyes labelled for syntaxin (red) and (in *B-F*) BrdU (green). Syntaxin staining in the 4-week old wild type retina is localised to the inner plexiform layer and some of the inner nuclear layer cells. *B-F* are two sections of retinae of 4-week old *Chx10*$^{-/-}$ mice injected with BrdU for two weeks before culling. *C* and *D* are high magnification views of the section in *B*, with (*C*) and without (*D*) the BrdU labelling imposed, showing clearly that the BrdU labelled cell (arrows) is also labelled with syntaxin. *F* is a high magnification view of the section in *E*, and shows a cell double labelled for BrdU and syntaxin (arrow), giving it a yellow colour. ONL = outer nuclear layer, INL = inner nuclear layer, GCL = ganglion cell layer, scale bar in *A* = 50 μm, in *B* and *E* = 100 μm, in *C* = 25 μm and in *F* = 30 μm.

the inner and outer plexiform layers and the vitreal cells of the inner nuclear layer, the amacrine and horizontal cells (Figure 6.18A). Two examples of BrdU/VC1.1 co-labelled cells are shown in Figure 6.18B-E. B and E show cross sections through confocal images of *Chx10*$^{-/-}$ retinal sections, taken at 0.2 μm increments. Yellow labelling indicates overlapping red and green staining from VC1.1 and BrdU labelling respectively. Syntaxin, like VC1.1, is expressed in the inner plexiform layer and amacrine cells of the inner nuclear layer, but unlike VC1.1, is not detected in the outer plexiform layer of the adult wild type retina (Figure 6.19A). Figure 6.19B-F show two examples of BrdU/syntaxin co-labelled cells, with the high-magnification images C, D and F clearly depicting the yellow staining caused by the overlapping green BrdU and red syntaxin labelling. These experiments suggest that some of the cycling cells observed in the *Chx10*$^{-/-}$ retina not only differentiate to become neuronal cells, but acquire specific retinal cell type markers.

Immuno-staining for neuronal markers was not detected in the ciliary body of the *Chx10*$^{-/-}$ eye in these experiments.

6.2.5. Labelling of dissociated cells

To confirm double-labelling of BrdU and retinal neuron markers and to attempt to quantify the types of cells, immunostaining was performed on dissociated retinal cells from BrdU injected *Chx10*$^{-/-}$ and wild type mice. A similar injection schedule was used to the one described in 6.2.4; mice were injected every other day for five days from P25-P29 and left for three weeks after the first injection. The retinae were dissociated and spun using a cytospin, onto microslides, for immunolabelling. Antibodies against β3-tubulin, CRALBP, VC1.1, syntaxin, Brn3b, calbindin and recoverin were used together with anti-BrdU antibodies.

Whilst wild type retinae were relatively easy to dissociate and spin down, *Chx10*$^{-/-}$ retinae tend to be very difficult to both dissect and dissociate. This, coupled with their decreased size compared to the wild type retina, meant that only a small number of *Chx10*$^{-/-}$ retinal cells were recovered for analysis. Labelling with β3-tubulin and Brn3b was unsuccessful. In addition, no cells were co-labelled with CRALBP or

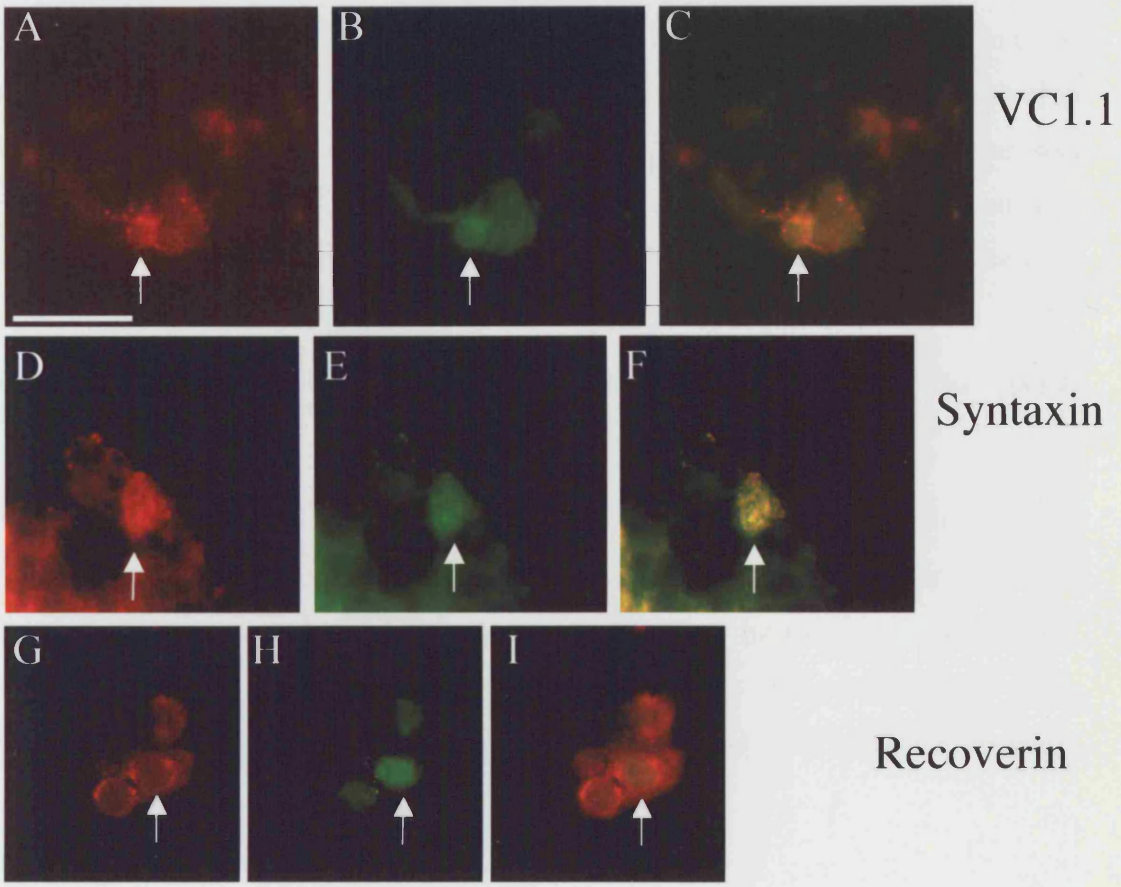

Figure 6.20: Dissociated *Chx10*$^{-/-}$ retinal cells from BrdU injected mice, co-labelled for BrdU (green) and VC1.1 (red, *A-C*), syntaxin (red, *D-F*) or recoverin (*G-I*). C, F, and I are overlays of the green and red figures to their left. Arrows indicate co-labelled cells. Scale bar = 30 μm.

calbindin. BrdU labelled cells were, however, found to be co-labelled with VC1.1 (Figure 6.20A-C) and syntaxin (Figure 6.20D-F). This supports the observation made in the retinal sections and suggests cycling cells are capable of differentiating to inner nuclear layer cells of the retina. In addition, co-labelling with recoverin was observed (Figure 6.20G-I). Due to the very small amount of dissociated retinal cells being recovered, no analysis could be made of the relative amount of labelled cells.

6.2.7. BrdU labelled cells in the adult wild type form part of the retinal vasculature

Occasionally BrdU labelled cells were observed in the adult wild type retina (Figure 6.5B). These cells did not double label with either nestin or β3-tubulin and were restricted to the inner layers of the retina. Based on their location, it is possible that these cells may be part of the developing capillary plexus of the inner retina, which develops during the first few postnatal weeks (Feeney et al., 2003; Friedlander et al., 1996).

In order to discover if these cells were part of the retinal vasculature, retinal sections were examined for expression of the endothelial marker, β1-integrin. In the adult wild type retina, β1-integrin labelling can be observed in vascular cells of the inner nuclear layer (Figure 6.21A, C). Whilst no BrdU labelled cells expressed β1-integrin in the adult *Chx10*$^{-/-}$ retina (Figure 6.21B) occasional BrdU labelled cells observed in the adult wild type retina also expressed β1-integrin (Figure 6.21C, magnified in inset), confirming that these cells are more likely to be associated with the retinal vasculature than persisting dividing progenitor cells.

6.2.6. Cell death is not a common fate of cells in the *Chx10*$^{-/-}$ retina

As not all BrdU labelled cells observed in the *Chx10*$^{-/-}$ retina co-labelled with nestin or β3-tubulin, it still remains unclear what the identity is of the majority of cycling cells observed. One possibility is that the cells continue to cycle beyond normal development but are unable to contribute to the retina as fully functioning cells. Thus, it is possible that these cells eventually stop cycling and die.

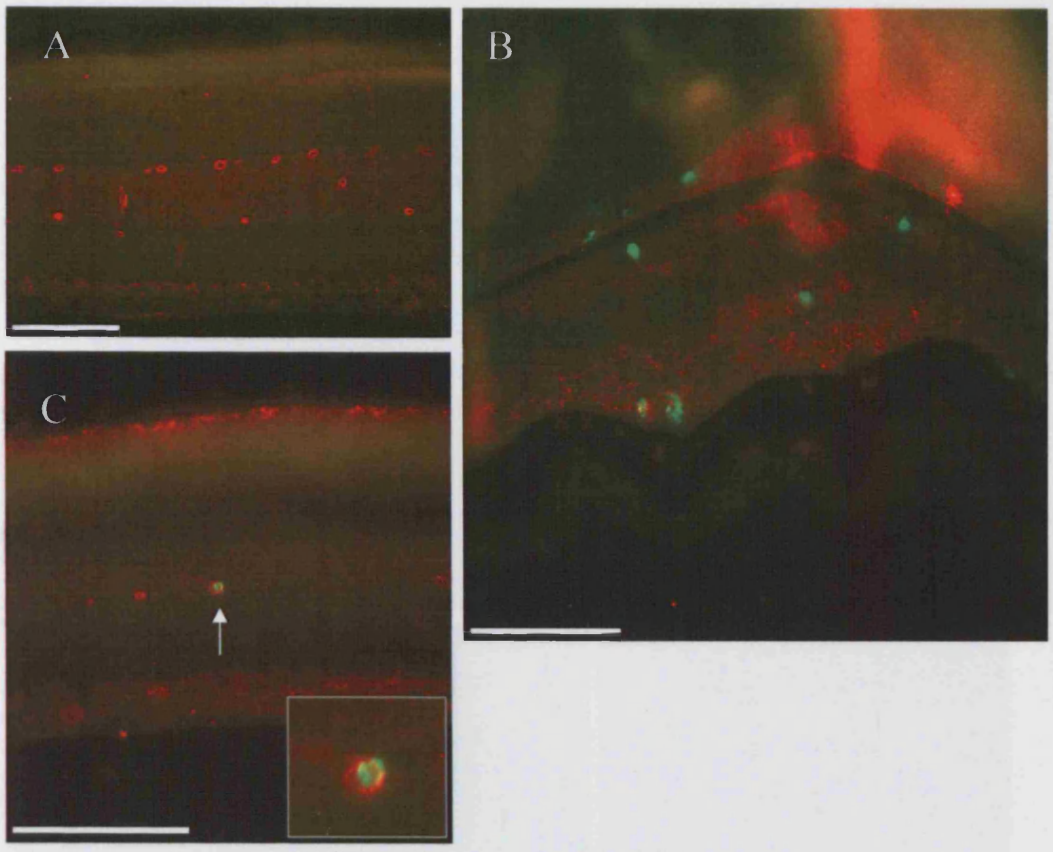

Figure 6.21: Sections from wild type (*A,C*) and *Chx10*$^{-/-}$ (*B*) eyes double labelled for BrdU (green) and β1 integrin (red). Eyes were injected every other day from P15 to P29 and culled on P30. In the wild type retina, β1 integrin labels cells of the vasculature, mostly within the inner nuclear layer (*A*). A few cells incorporate BrdU during the time of BrdU injection (*C, arrow*) and these cells co-label for β1 integrin (arrow *C* and magnified in *inset*), suggesting these cells are part of the retinal vasculature. BrdU labelled cells observed in the *Chx10*$^{-/-}$ retina do not co-label for β1 integrin (B). Scale bars = 50 μm.

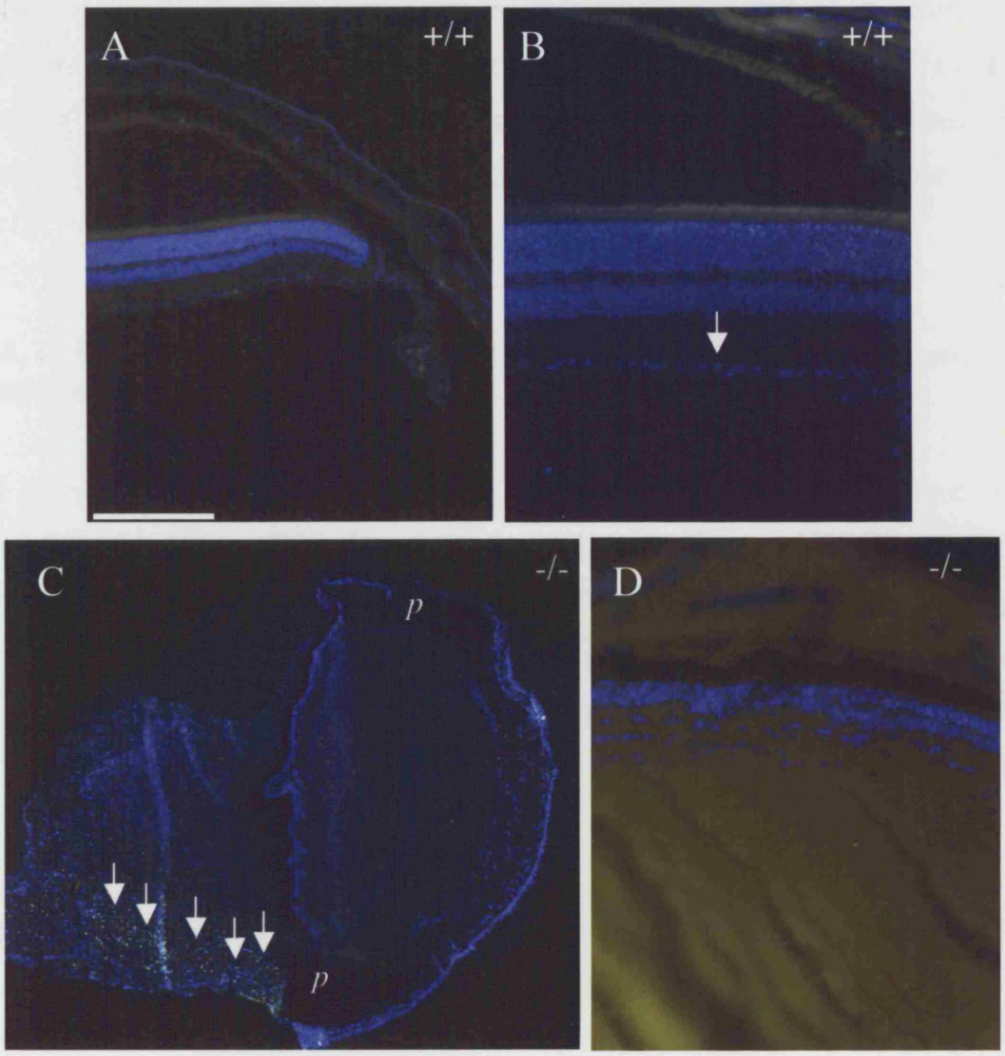

Figure 6.22: Sections from 4-week-old wild type (+/+, *A, B*) and *Chx10*$^{-/-}$ (-/-, *C ,D*) eyes stained with the TUNEL detection kit for apoptotic bodies (green) and counterstained with Hoechst nuclear dye (blue). Both in the wild type and *Chx10*$^{-/-}$ retina, few apoptotic bodies can be seen in the retina, either in the periphery (*A* and *C (p)*) or in the central retina (*B* and *D*). Some faintly labelled green bodies can be observed wild type retina (*B*, arrow), but these are faint, compared to brightly labelled apoptotic bodies in other areas of the sections (*C*, arrows), suggesting little or no cell death is occurring in either the wild type or *Chx10*$^{-/-}$ retina. Scale bar = 200 μm in *A*, 100 μm in *B* and *D*, 400 μm in C.

In order to discover whether cell death is occurring in the adult *Chx10*$^{-/-}$ retina, TUNEL labelling of retinal sections at postnatal week four and eight (after BrdU labelling according to schedule 1) was performed in both the wild type and *Chx10*$^{-/-}$ retina. In both cases, apoptotic cell death was not detected in the central or peripheral retina (Figure 6.22). This suggests that cell death was not a common fate in the *Chx10*$^{-/-}$ retina.

6.2.8. Cell cultures of adult retinal cells suggest retinal progenitor-like cells are present in the *Chx10*$^{-/-}$ central retina

The presence of BrdU labelled cells in the *Chx10*$^{-/-}$ retina suggests there is a population of cycling cells in the *Chx10*$^{-/-}$ central retina. If this is the case, it should be possible to observe this phenomenon in culture. Previous studies have indicated that no neurosphere cultures can be grown from *Chx10*$^{-/-}$ retinae (Tropepe et al., 2000), whilst such cultures can be grown from the CE of both wild type and *Chx10*$^{-/-}$ eyes. In view of the BrdU results presented here, I re-examined whether progenitor cells could be cultured from the central retina.

At varying time points, four primary cultures were set up, using defined conditions for neurosphere propagation (Ahmad et al., 1999; Kelley et al., 1995a), made up of the central neural retina of both wild type and *Chx10*$^{-/-}$ retinae, as well as cultures of the CE and RPE. Cells were treated with growth factors EGF and FGF-2. In all cases, dissociated wild type cells had a tendency to remain unchanged in the culture dishes (Figure 6.23A, B). The cells rounded up and showed no processes for several days. Trypan blue staining at 32 days *in vitro* indicated the cells did not die, however, they did not divide or show any signs of being mature neurons (Figure 6.23B). This state lasted for three weeks and seemed unchanged.

In the *Chx10*$^{-/-}$ retina, a remarkable difference was observed. Cells dissociated from the central neural retina started to proliferate and form small spheres, neurospheres, within days of being in culture (Figure 6.23C). The neurospheres grew to various sizes, and by approximately 15 days in culture, the neurospheres began to look darker and necrotic in their centres (6.23D). After 28 days *in vitro*, the spheres were passaged – dissociated and replated. Fewer neurospheres seemed to arise from the

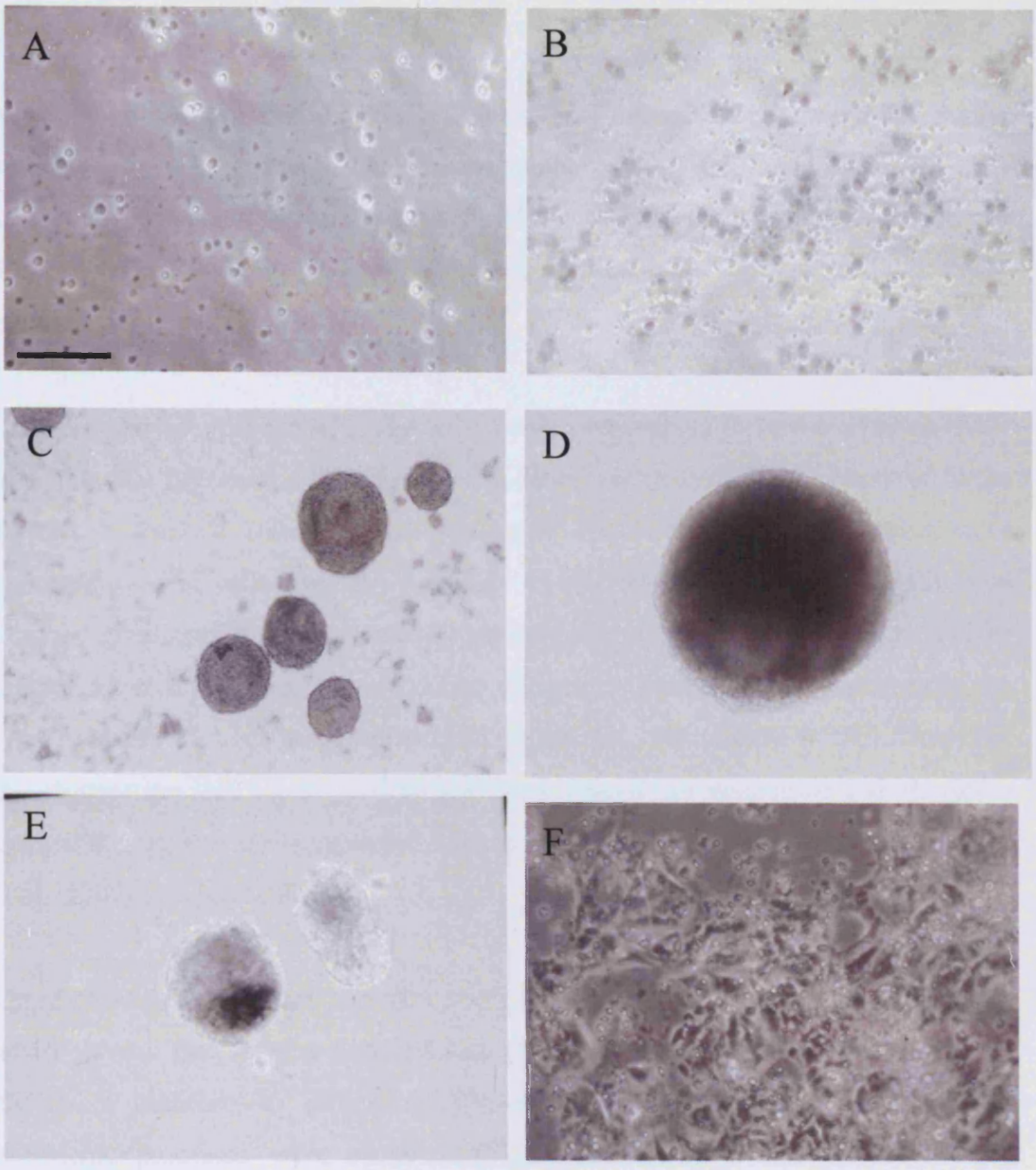

Figure 6.23: Cell cultures of dissociated wild type (*A and B*) and *Chx10*$^{-/-}$ (*C-F*) retinal cells. *A.* Dissociated wild type retinal cells after 1 day *in vitro*. Cells are small and round and don't have any processes. After 32 days *in vitro* (*B*), cells show no change in phenotype and trypan blue staining indicates cells are still viable, as no trypan blue can be observed inside the cells. Cells of the *Chx10*$^{-/-}$ retina proliferate to form neurospheres, observed in *C* after 7 days in *vitro*. Neurospheres grow progressively larger, as observed in *D* after 15 days *in vitro*, and the centres begin to look necrotic. Neurospheres from the ciliary epithelium (*E*) are both pigmented and non-pigmented. After 28 days *in vitro*, neural retina-derived neurospheres are dissociated and placed in differentiating conditions (*F*) and flatten and adhere to the culture dish. Scale bar = 50 μm.

passaged cells, suggesting that either a substantial number of cells were lost during passaging, or the capacity to self-renew in the cycling cells was depleting. In 3 separate experiments, neurospheres were maintained for 60 days and passeaged 2-3 times during this period. However with each passage, cells were lost and eventually no neurospheres were observed.

Cells dissociated from the RPE, did not grow in neurosphere culture conditions either from the wild type eye or the *Chx10*$^{-/-}$ eye. Some neurospheres were observed in the cultures dissociated from the CE of the *Chx10*$^{-/-}$ eyes (Figure 6.23E). However, these cultures included cells from the periphery of the retina and so the possibility that these neurospheres arose from retinal cells cannot be ruled out. Separating the ciliary epithelium from the retina is a difficult dissection. Neurospheres arising from the ciliary margin cultures tended to contain pigmented cells (Figure 6.23E). However, the observation that CE-derived neurospheres started out pigmented and showed a gradual change to a non-pigmented state, as observed in previous literature (Tropepe et al., 2000) was not made here.

Upon passaging, some of the cells were transferred to differentiating conditions, where growth factors were replaced with fetal calf serum. In these conditions, cells showed a tendency to adhere and flatten to the culture dishes, and on some occasions, processes were observed (Figure 6.23F). However, immunostaining results were not conclusive for these cultures, and thus future experiments will be needed to ascertain whether the cells could differentiate to specific neural retinal cell fates.

6.3. Discussion

6.3.1 An aberrant pattern of proliferation observed in the *Chx10*$^{-/-}$ retina during development continues after birth

The data obtained in this study show that when Chx10 function is disrupted, cells with RPC-like behaviour persist in the adult retina. In accordance with the results obtained in Chapter 5, cells seem to be cycling steadily from birth onwards into adulthood. Interestingly, these RPC-like cells in the adult mutant retina are present in both central and peripheral regions. Putative stem-cell like cells have thus far only been isolated from the ciliary epithelium (CE) at the very periphery of the retina (Ahmad et al., 2000; Tropepe et al., 2000), whilst cells taken from the neural central retina apparently did not proliferate to form neurosphere colonies (Tropepe et al., 2000).

In this study, dividing cells were identified *in vivo* in the CE of the wild type and *Chx10*$^{-/-}$ eye, and in the neural retina of the *Chx10*$^{-/-}$ eye. The only other examples of neurogenic progenitor-like cells present in the central retina of adult vertebrate organisms are the rod-precursor lineages of teleost fish (Reh and Levine, 1998) and Muller glial cells in postnatal chicks (Fischer and Reh, 2001). In damaged gold fish retina, the rod-precursor cells regenerate all types of retinal neuron, whereas acute damage of the postnatal chick retina induced Muller glial cells to undergo a single round of cell division and express markers characteristic of retinal progenitors and occasionally retinal neurons. Similar progenitor-like cells have not been observed in mammalian retina which does not regenerate following injury, although in other regions of the nervous system evidence exists that glial cells can give rise to neurons (Doetsch et al., 1999). Transdifferentiation of the RPE to neural retina, can also provide a source of new neurons after retinal damage, and has been shown to occur in amphibians, and in chick and mammalian embryonic eyes (Reh and Levine, 1998).

That single genetic changes can result in the presence of RPC-like cells in the mature retina of mammals is a novel concept and supported by recent studies that identified persistent progenitors at the retinal margin of adult Shh receptor patched (ptc) +/- mice (Moshiri and Reh, 2004) and in the central retina of $p27^{Kip1}$ null and

$p27^{Kip1}$/$p19^{INK4d}$ double-null mice at P18 (Cunningham et al., 2002). Like Chx10, these genes affect proliferation of retinal progenitors but their deficiency has different effects on the adult retina. In the Ptc+/- mice, which have constitutively activated Shh signalling, proliferating cells were present in the retinal margin and in the CE, and only those at the margin generated new photoreceptors in response to retinal degeneration (Moshiri and Reh, 2004). Whereas loss of the cyclin dependent kinase inhibitors, $p27^{Kip1}$ and $p19^{INK4d}$ which mediate cell cycle exit, prolonged the normal period of retinal cell proliferation and caused retinal dysplasia including an increase in the number of horizontal cells (Cunningham et al., 2002).

The analysis of the profile of mitotic cells during development performed in the previous chapter, using H3 labelling, supports a model in which lack of Chx10 extends the longevity of a population of embryonic RPCs. The H3 study revealed that following an early decrease in proliferation in the mutant compared with the wild type retina, later, a small population of RPCs continues to proliferate steadily in the mutant. These cells are a possible source of the dividing cells observed in the adult retina. Previous studies concluded that RPCs have a limited life-span, as neuro-sphere colonies could not be isolated from the adult neural retina (Tropepe et al., 2000). By contrast here we find that in retina lacking Chx10, RPC-like cells persist into adulthood. Although one cannot exclude a non-neuroepithelial source for the BrdU-positive cells, the expression data make this unlikely. Since Chx10 is not expressed in the retinal pigmented epithelium (RPE) and BrdU-labelled cells were not observed in the RPE, migrating RPE cells are an unlikely alternative source. Moreover, a recent analysis of expression using a Chx10-GFP BAC reporter transgene in *Chx10* null retina showed that in the P14 retina, GFP-positive cells expressed the Muller glial/progenitor markers CRALBP and Pax6 (Rowan and Cepko, 2004). Although the data do not exclude the possibility that the dividing cells initially have a Muller glial origin, the rarity of BrdU and CRALBP double labelling suggests instead that they may be occasionally adopting a glial or RPE fate after division. These findings are consistent with the idea that RPC-like cells persist in the absence of Chx10.

6.3.2 Misspecification of the retina through the absence of Chx10 may contribute to the continued cycling of retinal progenitor cells

Two recent studies and the results in chapters 3 and 4 give insight to the data obtained in these BrdU experiments. Crossing the $Chx10^{orJ}$/ 129/Sv into a mixed genetic background produced a more severe phenotype, with a progressive appearance of ectopic pigmentation in the neural retina (Rowan et al., 2004). Labelling with a Chx10-GFP BAC transgene suggested that these pigment cells arose from cells in the neural retina, and the authors concluded that these arose by direct transdifferentiation of neural retinal cells. In addition, ectopic RPE gene expression (of *Tfec* and *Dct*) was also found in the neural retina from early embryonic stages (Rowan et al., 2004), mirroring the results of chapters 3 and 4, in which both silver and dopachrome tautomerase were upregulated in the $Chx10^{-/-}$ developing retina. A recent study by Horsford et al, discussed in detail in Chapter 4, suggests that Chx10 acts to maintain the neural retina by repressing expression of RPE determinants such as the Mitf transcription factor (Horsford et al., 2005). This study, however, did not explore whether the adult mutant retina contains proliferating cells. The presence of proliferating cells in the adult retina likely reflects this instability of neural retinal identity in the absence of Chx10. Nestin, VC1.1 and CRALBP immuno-staining of BrdU-positive cells is consistent with their progenitor state as these markers have been used to label neural progenitors (Alexiades and Cepko, 1997; Walcott and Provis, 2003). It remains possible that the observed cells are neural retinal cells that may be dividing as part of a process of transdifferentiation, but the altered pattern of proliferation observed throughout development and into adulthood suggests this is unlikely. In addition, proliferating cells were observed throughout the retina whereas studies suggesting that transdifferentiation may be taking place in the $Chx10^{-/-}$ retina, report that this process occurs at the periphery (Rowan et al., 2004). Alternatively, the dividing cells may have failed to complete normal retinal histogenesis due to RPE gene expression, and therefore retain progenitor-characteristics.

6.3.3 RPC-like cells maintain neurogenic potential, but are unable to expand retinal cell numbers

The data obtained here suggest that neurons are being generated in the adult mutant retina, albeit in small numbers and expressing only a subset of retinal neuron markers. Previous work has shown that over expression of Chx10 increased generation of all types of inner nuclear layer (INL) cells in mouse and suppressed photoreceptor development in chick, whereas lack of Chx10 prevents bipolar cell development (Burmeister et al., 1996);(Hatakeyama et al., 2001; Toy et al., 2002). That RPC-like cells in the adult mutant preferentially express INL markers (syntaxin, VC1.1) may relate to Chx10's role in providing INL-identity. One possibility is that progenitors that were predestined in part to produce amacrine cells selectively persisted in the mutant retina post-natally. Consistent with this idea, we found no evidence of ganglion cell, bipolar cell, or photoreceptor production, with the exception of an occasional recoverin-labelled cell seen upon retinal dissociation and immunolabelling. No recoverin-labelled cells were observed in retinal sections, which is more likely to be an indication of the rarity of such double-labelled cells than of a difference between data obtained from sections and data obtained from dissociated cells, as retinae were treated in an identical manner. However, the finding that the adult mutant retina is apparently permissive for neurogenesis is surprising and suggests that the environment is not inhibitory.

While the Chx10 null adult retina contains RPCs with neurogenic potential, it remains markedly deficient in cell number. In the previous chapter it has been shown that, consistent with other studies, very low levels of apoptosis were detected in the embryonic wild type retina (Pequignot et al., 2003), and we found that apoptosis is not likely to contribute to the cell number deficit in the mutant during development (Green et al., 2003; Robb et al., 1978). The data obtained from this study suggest that the same is true in the adult retina. In both the wild type and *Chx10*$^{-/-}$ mature retina, very few apoptotic bodies were observed, suggesting that there is no widespread cell death resulting from the absence of Chx10. This suggests that the Chx10 null adult RPC-like cells thus seem to harbour the same proliferative defects found in the embryonic RPCs and are unable to drive cell number expansion and growth of the retina.

6.3.4 *In vivo* demonstrations of stem-cell like properties of cycling cells in the adult retina

Properties of multi-potentiality and self-renewal have been demonstrated *in vitro* for putative stem cells isolated from the adult CE of the rodent retina (Ahmad et al., 1999; Tropepe et al., 2000). In this study, cells isolated from the *Chx10*$^{-/-}$ retina have also exhibited self-renewing properties, although their multi-potentiality has not been tested. In addition, this study has identified cycling cells in the CE of the ciliary body in the adult wild type mouse eye *in vivo*. These cells are a likely source of the CE stem cells characterised *in vitro*. Cycling cells were not identified however, at the peripheral edge of the retina (the ciliary margin). By contrast, proliferating RPCs in the ciliary margin have been identified in adult chickens (Fischer and Reh, 2000), and in quail and opossum (Kubota et al., 2002) which show similarities with embryonic RPCs, such as expression of both *Pax6* and *Chx10*.

An increased number of dividing cells was observed *in vivo* within the adult CE of the *Chx10*$^{-/-}$ eye, compared with the wild type. Likewise, in a previous *in vitro* study, *Chx10* mutant CE produced more neurospheres containing fewer cells than the wild type CE (Tropepe et al., 2000). Both mutant and wild type neurosphere colonies differentiated to produce neurons (Tropepe et al., 2000). However, *in vivo*, the adult CE showed no evidence of neurogenesis, in contrast to the dividing cells in the mutant central retina. The different behaviours of these dividing cell populations are likely influenced by differences in their extracellular environments. The relationship between the progenitor-like cells observed here in the CE and the central retina, the putative retinal stem cells isolated from the CE (Ahmad et al., 1999; Tropepe et al., 2000), and the transdifferentiating pigment generating cells (Horsford et al., 2005; Rowan et al., 2004) have not been established and will be the subject of future investigation. These findings are of interest as they suggest that manipulation of Chx10 expression and/or extracellular factors could influence the number of cells with neurogenic potential within the mature retina.

CHAPTER 7

Final Discussion

7.1 Identification of genes previously not known to be under Chx10 control

The first aim of this study was to identify genes that are controlled, either directly or indirectly by the transcription factor Chx10. It was hoped more could be learned about the genetic pathway in which Chx10 is involved, and thus discover the molecular basis for the *Chx10*$^{-/-}$ retinal phenotype. The microarray system employed for this purpose was an ideal tool for examining the expression of thousands of genes simultaneously in the *Chx10*$^{-/-}$ and wild type retinae early in development. It has resulted in the identification of 293 genes whose expression is changed in the *Chx10*$^{-/-}$ retina, of which 34 are characterised genes that are significantly up- or down-regulated at least 1.5-fold in the absence of Chx10. Although many of these genes are expressed in the developing eye, few of these genes would have been chosen for examination as potential Chx10 targets, either because loss-of-function mutants do not show a significant phenotype, or because very little is as yet known about their function in the developing eye.

7.1.1 Cell cycle proteins affected by the absence of Chx10

One group of genes of particular interest with regards to our understanding of Chx10 function, is the group of genes known to play a role in the cell proliferation. These include the cell cycle machinery-regulating genes growth arrest specific 2 (*Gas2)* and cyclin E2 (*Ccne2)*. The role of Chx10 in cell proliferation in general, and its involvement in the cell cycle in particular, has been under a great deal of scrutiny, as a markedly reduced retinal cell number is one of the major phenotypic effects of its absence. As described in Chapter 1, Chx10 has been shown to interact with the pRB family of proteins, and the levels of both cyclin D1 and $p27^{Kip1}$ in retinal progenitor cells are thought to be influenced by Chx10. The results obtained in this study indicated that both *Gas2* and *Ccne2* are down-regulated in the *Chx10*$^{-/-}$ retina.

Gas2 and other growth arrest specific genes were initially identified due to their high level of expression in murine fibroblasts under growth arrest conditions followed by down-regulation after re-entry into the cell cycle (Schneider et al., 1994). In contrast, *Gas2* was found to be expressed more strongly in proliferative murine keratinocytes than in differentiating cells, and there was a higher expression of *Gas2* during

exponential growth than during growth arrest in this cell population, suggesting regulation of *Gas2* is cell specific (Manzow et al., 1996). In this study, *Gas2* down-regulation as a result of Chx10 absence (Chapter 3) is observed in conjunction with a decrease in exponential growth, suggesting *Gas2* may be regulated in a similar manner in the retina. In addition, *Gas2* has been shown to be involved in the execution of the apoptotic program in hindlimb interdigital tissues by acting as a death substrate for caspase enzymes (Lee et al., 1999). These data are of interest in light of the findings in Chapter 5 and previous studies, suggesting apoptosis is reduced in the *Chx10*$^{-/-}$ developing retina. It raises the possibility that a decrease in *Gas2* expression as a result of Chx10 absence affects the apoptotic process.

CCne2, together with other E cyclins, is expressed during the late G1 phase of the cell cycle until the end of the S-phase. The activity of cyclin E is limiting for the passage of cells through the restriction point which marks a "point of no return" for cells entering the division cycle from a resting state or passing from G1 into S-phase (Moroy and Geisen, 2004). It has been shown that *Ccne2*-associated kinase activity is regulated in a cell cycle dependent manner with peak activity at the G1 to S transition and that ectopic expression of cyclin E2 in human cells accelerates G1, suggesting that it is rate limiting for G1 progression (Payton and Coats, 2002). The data obtained in Chapter 5 suggest that the length of G1 is increased in the *Chx10*$^{-/-}$ retina, and thus the down-regulation of *Ccne2* in response to Chx10 may be associated with this phenomenon.

Figure 7.1 summarises the interactions of various cell cycle proteins shown to be affected by the absence of Chx10 (see Chapter 1 for details), and also highlights the cell cycle proteins identified in this study. Neither of these cell cycle proteins has previously been shown to play a significant role in eye development, but their apparent change in expression in response to Chx10, and the fact that the human homologue of *Gas2* maps to a microphthalmia locus (Chapter 4) provides strong reasons to further examine their role in the progression of RPC proliferation and differentiation.

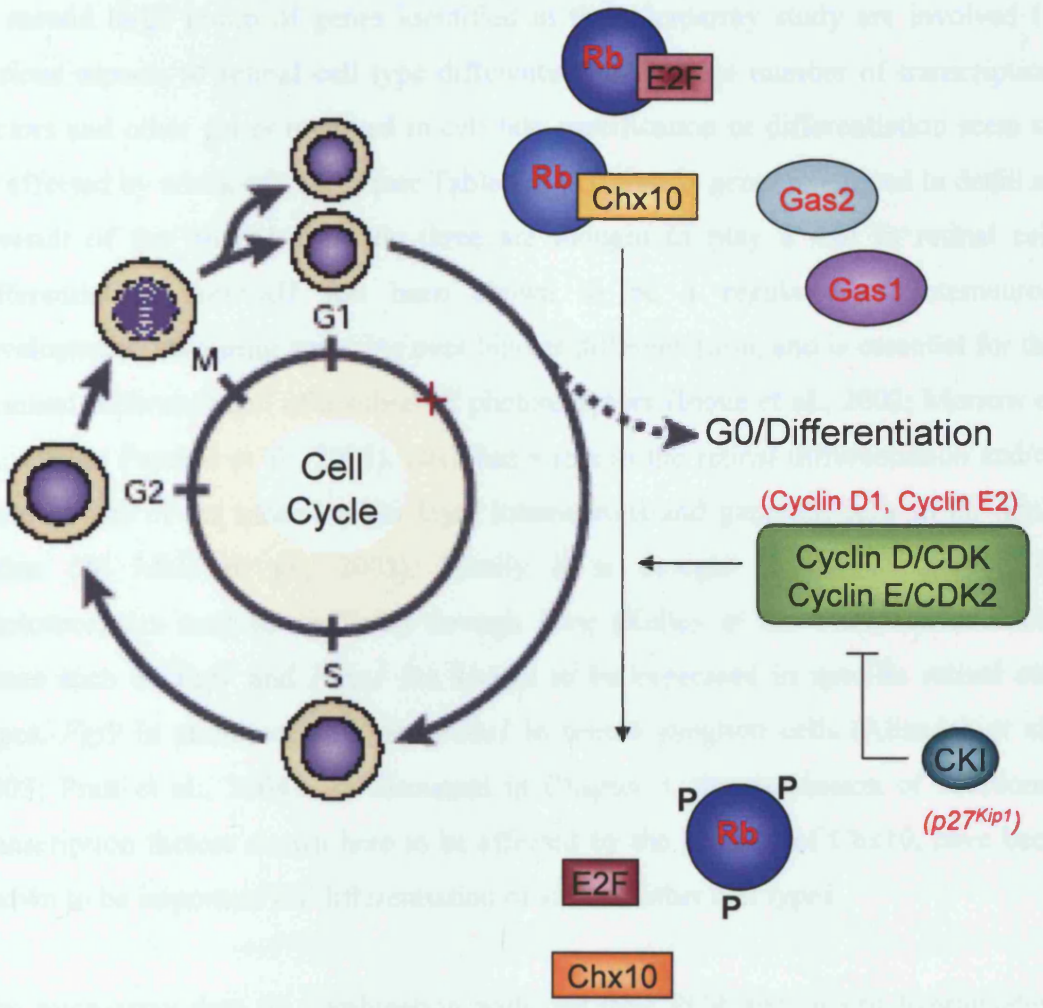

Figure 7.1: Interactions of cell cycle proteins known to interact with Chx10 or showing a change in expression in the Chx10$^{-/-}$ retina. Members of the pRB family are known to bind to Chx10, and thought to inhibit its binding to DNA. Cyclin D1 and E2 expression are down-regulated in the *Chx10*$^{-/-}$ retina, whilst p27^{Kip1} protein is up-regulated in the *Chx10*$^{-/-}$ retina, which may result in a failure to make the transition from G1 to S phase, even if cells don't enter G0 and differentiate. *Gas1* has been shown to be up-regulated in the *Chx10*$^{-/-}$ retina (Rowan et al, 2004), whilst *Gas2* expression is decreased. These factors are also important during G1. Cell cycle figure adapted from Livesey and Cepko, 2001.

7.1.2 Cell differentiation factors affected by a loss of Chx10

A second large group of genes identified in the microarray study are involved in various aspects of retinal cell type differentiation. A large number of transcription factors and other genes involved in cell fate specification or differentiation seem to be affected by a lack of Chx10 (see Table 3.5). Of the six genes examined in detail as a result of the microarray data, three are thought to play a role in retinal cell differentiation. *Neurod1* has been shown to be a regulator of interneuron development, favouring amacrine over bipolar differentiation, and is essential for the terminal differentiation of a subset of photoreceptors (Inoue et al., 2002; Morrow et al., 1999a; Pennesi et al., 2003). *Dlx2* has a role in the retinal differentiation and/or maintenance of the inner nuclear layer interneurons and ganglion cells in the adult retina (de Melo et al., 2005). Finally it is thought that differentiation of photoreceptors may be mediated through *Rxrg* (Kelley et al., 1994). In addition, genes such as *Fgf9* and *Foxc1* are known to be expressed in specific retinal cell types, *Fgf9* in photoreceptors and *Foxc1* in retinal ganglion cells (Alizadeh et al., 2003; Pratt et al., 2004). As discussed in Chapter 3, the expression of additional transcription factors shown here to be affected by the absence of Chx10, have been shown to be important for differentiation of various other cell types.

The microarray data, in combination with real-time PCR and *in situ* hybridisation suggest both *Neurod1* and *Dlx2* are positively regulated by the presence of Chx10, as they are both down-regulated in the *Chx10*$^{-/-}$ retina. In contrast, *Rxrg* seems to be negatively regulated by Chx10, as both microarray and real-time PCR data suggest its expression is increased in the *Chx10*$^{-/-}$ retina. How do these changes in gene expression result in the *Chx10*$^{-/-}$ phenotype? A decrease in retinal cells from all three retinal cell layers of the retina is observed in the *Chx10*$^{-/-}$ retina (Chapter 5). In addition, differentiation of many of the retinal cells types has been shown to be delayed. A significant proportion of genes known to affect retinal cell differentiation are down-regulated in the *Chx10*$^{-/-}$ retina (*Neurod1, Dlx2, Fgf9, and Foxc1*), and it follows that a down-regulation of expression of genes required for retinal cell differentiation results in a delay in differentiation. In addition, retinal cells such as rod photoreceptors show abnormal morphology in the *Chx10*$^{-/-}$ retina, and this may be caused by a lack of expression of genes required for normal differentiation.

Figure 7.2 summarises some of the changes in gene expression observed as a result of Chx10 absence in the *Chx10*$^{-/-}$ retina, and where in the retina they are usually expressed.

7.1.3 Genes expressed in the RPE are up-regulated in the *Chx10*$^{-/-}$ retina, suggesting a novel role for Chx10 in maintaining compartment boundaries

Of particular interest is that subsets of the cell specification genes identified in this study were RPE-specific genes. Both *Si* and *Dct* are usually expressed in the RPE, whose border with the retina is normally clearly defined. Silver expression is dependent on expression of the microphthalmia associated transcription factor (*Mitf*), a gene whose progressive restriction to the future RPE is thought to be instrumental for the specification of the mammalian optic vesicle into NR and RPE (Nguyen and Arnheiter, 2000). In addition, three more genes expressed in the RPE, *Fgf9*, *ApoE* and *Trpm1*, are also up-regulated in the *Chx10*$^{-/-}$ retina, and the human homologue of *Trpm1* maps to a microphthalmia locus (Chapter 4).

Whilst the roles of Chx10 in cell proliferation and bipolar cell specification have been established through various studies (Bone-Larson et al., 2000; Burmeister et al., 1996), two of the recent studies examining the Chx10 phenotype have focused on a novel role for Chx10 in the maintenance of compartment boundaries in the peripheral retina (Horsford et al., 2005; Rowan et al., 2004). These studies suggest that *Chx10*, required for neural retinal specification, and *Mitf*, required for RPE specification, are components of a pathway that determines and maintains the identity of the neural retina, and that the loss of Chx10 results in the progressively increased expression of RPE genes over time, and possibly transdifferentiation of the neural retina to RPE (Figure 7.3). The data obtained in Chapters 1 and 2 suggest that a loss of neural retinal identity may indeed have occurred early in development, or is occurring during development, resulting in the expression of RPE-specific genes at E11.5.

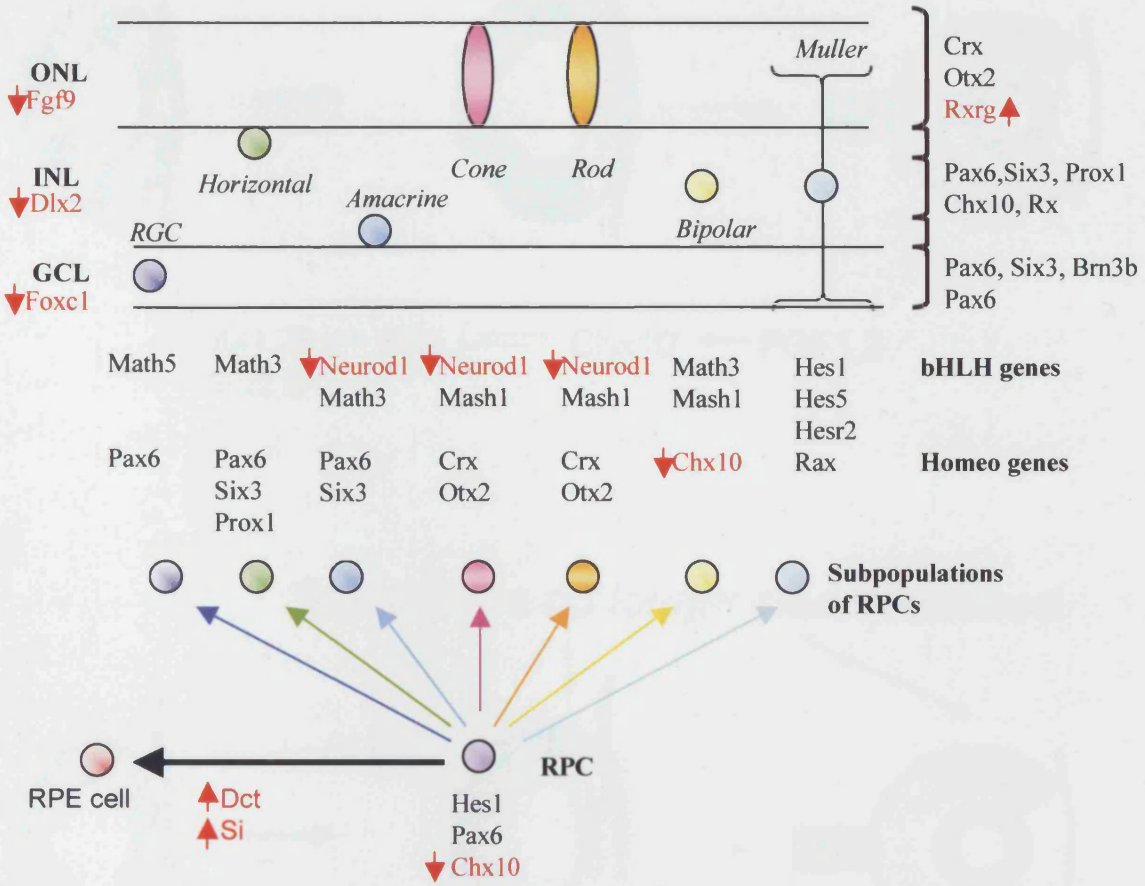

Figure 7.2: Cascade of progressive differentiation of retinal progenitor cells to the seven different cell types of the neural retina in the *Chx10*$^{-/-}$ retina. Chx10 and genes showing a change in expression as a result of lack of Chx10 are highlighted in red. Changes in gene expression of genes required for retinal differentiation are seen in all layers of the neural retina, which may contribute to the delayed differentiation and poor morphology of the different cell types, especially photoreceptors, as various genes affected by a lack of Chx10 are required for photoreceptor differentiation. In addition, an increase in RPE specific genes may lead to an expansion of the RPE-cell population, either early in development or through transdifferentiation. RPE = retinal pigmented epithelium, RPC = retinal progenitor cell, GCL = ganglion cell layer, INL = inner nuclear layer, ONL = outer nuclear layer. Compare to Figure 1.3.

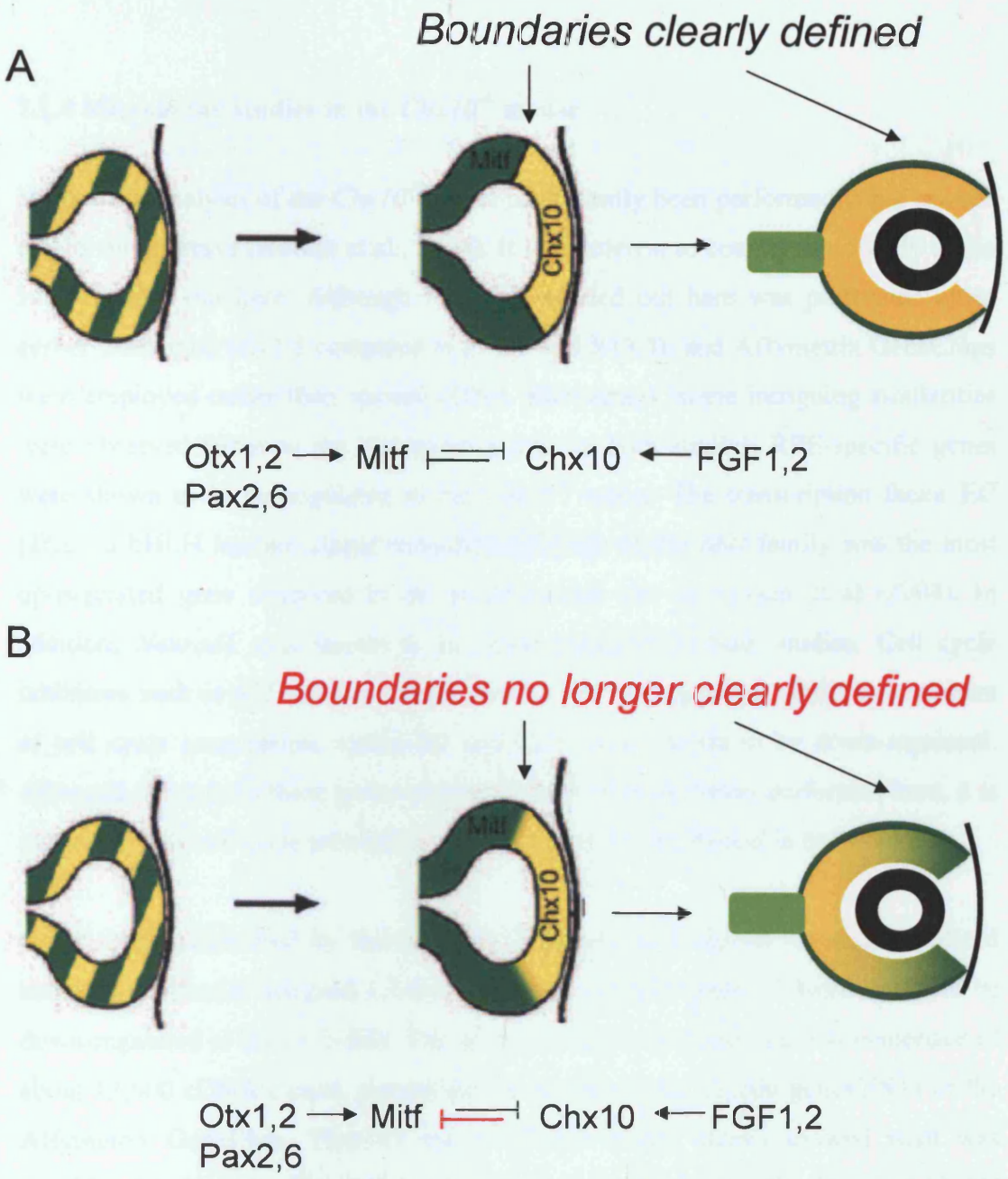

Figure 7.3: *Mitf-* and *Chx10*-mediated retinal tissue specification. In the wild type eye (*A*), all parts of the optic vesicle have the potential to become either neural retina or RPE, until the onset of *Chx10* and *Mitf* expression, induced by signals such as *FGF1* and *2* or *Otx1* and *2* respectively, when the inner layer of the optic cup acquires a retinal pigment epithelium identity (green), and the outer layer a neural retinal identity (yellow). The boundaries between the two cell layers are clearly defined by the inhibitory effect of the two genes on each other. In the *Chx10*$^{-/-}$ retina (*B*), the absence of *Chx10* reduces the inhibitory effect on *Mitf* expression, 'blurring' the boundaries between the presumptive neural retina and the presumptive RPE. As differentiation progresses, the periphery of the retina is seen to be expressing RPE-specific gene, suggesting it has acquired, or is acquiring, RPE identity. Figure adapted from Horsford et al, 2004.

7.1.4 Microarray studies in the *Chx10*$^{-/-}$ mouse

Microarray analysis of the *Chx10*$^{-/-}$ retina has recently been performed using spotted cDNA microarrays (Rowan et al., 2004). It is of interest to compare this study to the study carried out here. Although the study carried out here was performed at an earlier time point (E11.5 compared to E12.5 and E13.5), and Affymetrix GeneChips were employed rather than spotted cDNA microarrays, some intriguing similarities were observed between the two experiments. In both studies, RPE-specific genes were shown to be up-regulated in the *Chx10*$^{-/-}$ retina. The transcription factor EC (*Tfec*), a bHLH leucine-zipper transcription factor of the *Mitf* family was the most up-regulated gene observed in the study carried out by Rowan et al (2004). In addition, *Neurod1* was shown to be down-regulated in both studies. Cell cycle inhibitors such as *p57* and *Gas1* were shown to be up-regulated, whilst two markers of cell cycle progression, cyclin D1 and *E2f1*, were shown to be down-regulated. Although changes in these genes were not observed in the study performed here, it is intriguing that cell cycle proteins have been shown to be affected in both studies.

In the study performed by Rowan et al, 26 genes were shown to be up-regulated above an arbitrarily assigned 1.7-fold difference cut-off, whilst 21 were shown to be down-regulated at least 0.5-fold. The spotted microarray employed was composed of about 12,000 cDNA clones, comparable in number to the 12,000 genes/ESTs of the Affymetrix GeneChip. Thus 47 out of 12,000 cDNA clones showed what was considered to be a significant change in expression, compared to the 34 out of 12,000 genes/ESTs reported here.

Only two genes, *Neurod1* and Stathmin-like 2 (*Stmn2*), were shown to be significantly down-regulated in both studies, and only one gene, UDP-glucose ceramide glucosyltransferase (*Ugcg*), was shown to be significantly up-regulated in both studies. Taking into account the variation between the two studies, including a difference in time point and the use of different chips, such a small overlap is not particularly surprising. This overlap, together with the observation that similar groups of genes are represented, e.g. RPE-specific genes or cell cycle protein genes, and show similar changes in expression, lends validity to the results of the studies.

Microarray studies are becoming a more common tool for trying to elucidate how various eye phenotypes result from changes at a molecular level (Corbo and Cepko, 2005; Hollborn et al., 2005; Jones et al., 2000; Qian et al., 2005; Rattner and Nathans, 2005). It is encouraging that two experiments with similar aims and using similar tissues for examination, despite some fundamental differences, produce similar results. Both have resulted in the novel finding that RPE genes are up-regulated in the periphery of the *Chx10*$^{-/-}$ retina - suggesting a role for Chx10 in maintenance of compartment boundaries – and complement each other well. Such data are an indication of the power of array technology to reveal previously undiscovered molecular pathways and relationships.

7.2 Misspecification at the border between the neural retina and RPE may contribute to a decrease in proliferation in the periphery of the retina

The H3 and PCNA data obtained in Chapter 5 suggest that the periphery of the *Chx10*$^{-/-}$ retina is most seriously affected by a lack of proliferation, and the microarray and expression data presented in Chapters 3 and 4 indicate that expression of genes normally localised to the RPE expands into this area. Previously, a lack of proliferation has been reported in the periphery of the *Chx10*$^{-/-}$ retina (Bone-Larson et al., 2000; Burmeister et al., 1996), but it has thus far been unclear as to why this area of the retina was most seriously affected. It has been suggested that this phenomenon might be related to the central to peripheral gradient in which the retina matures, with cells of the central retina being the first to become post-mitotic and differentiate (Bone-Larson et al., 2000).

Whilst an effect on the central to peripheral gradient of maturation has not been excluded in this study, the data produced here suggest a correlation between the lack of proliferation observed in the *Chx10*$^{-/-}$ retina and the expansion of RPE gene expression into this same area. If tissue in the periphery of the retina is expressing RPE-specific genes, it may be acquiring an RPE identity, and its decreased rate of proliferation may be another manifestation of this process, as the RPE proliferates at a slower rate than the neural retina during development of the optic cup (Packer, 1967). Thus, the data obtained in this study support a model in which a decrease in proliferation observed in the periphery of the *Chx10*$^{-/-}$ retina is the result of a lack of

identity exhibited by RPCs in this area. This establishes a link between the role of Chx10 in proliferation of retinal progenitor cells and its role in establishing/maintaining neural retinal identity.

7.3 An altered pattern of proliferation in the Chx10 retina results in fewer retinal cells and a delay in their differentiation

In addition to identifying genes controlled by Chx10, in order to understand the molecular basis of the microphthalmia phenotype, a second aim of this study was to further characterise aspects of the phenotype at a cellular level. Specifically, I sought to examine how RPC proliferation is affected in the *Chx10*$^{-/-}$ retina. Several new observations were made in the studies discussed in Chapter 5:

1. The proportion of cells undergoing mitosis in the *Chx10*$^{-/-}$ retina changes little throughout development, and does not result in the exponential expansion of cell number observed in the wild type retina;
2. a larger proportion of RPCs in the *Chx10*$^{-/-}$ retina appears to reside in G1 phase of the cell cycle than is the case in the wild type retina;
3. a larger proportion of horizontal cell divisions occurs in the *Chx10*$^{-/-}$ retina compared to the wild type retina at E11.5; and,
4. differentiation of most retinal cell types is delayed in the *Chx10*$^{-/-}$ retina.

Whilst a decrease in proliferation has previously been observed in the periphery of the retina, as is observed in Chapter 5, the proportion of cells cycling in the central *Chx10*$^{-/-}$ retina is reported to be no different from that of the wild type (Bone-Larson et al., 2000; Burmeister et al., 1996). Why then, is the *Chx10*$^{-/-}$ retina so severely depleted of cells? Suggestions as to how this may be the case have included the following possibilities:

1. That increased cell death might result in a smaller population of RPCs;
2. a smaller number of cells are initially specified to become neural retinal cells, and that this, coupled with a decrease in proliferation in the periphery of the retina, inhibits the retina from attaining its full complement of cells (Bone-Larson et al., 2000); and,

3. there is a decrease in the rate of proliferation, through the extension of G1 of the cell cycle (Bone-Larson et al., 2000; Green et al., 2003).

It is unlikely that an increase in cell death in the *Chx10*$^{-/-}$ retina is the cause of the severely depleted RPC number. This and other studies have shown that apoptotic cell death is not a widespread phenomenon in the *Chx10*$^{-/-}$ retina, and that its occurrence may in fact be decreased (Robb et al., 1978; Theiler et al., 1976)(Chapter 5.2.7). The second possibility, that fewer cells are specified to become neural retina initially, is supported in this study by an increase in expression of RPE-specific genes, suggesting that, at least at the periphery of the retina, a proportion of cells might be specified to become RPE rather than neural retina. An increase in the length of G1 is also supported by this study. Evidence from the flow cytometry experiment performed in Chapter 5 suggests that a greater proportion of cells in the E11.5 *Chx10*$^{-/-}$ retina are in G1 phase of the cell cycle, compared to the wild type retina (Chapter 5.2.3).

If the cell cycle is merely delayed in the *Chx10*$^{-/-}$ retina, why does the retina not grow to its full size over a longer period of time? One model that is supported by the data obtained in these studies is that RPCs of the developing *Chx10*$^{-/-}$ retina are unable to expand in number due to an arrest in G1 of the cell cycle. The microarray data indicate that the cell cycle proteins affected by a lack of Chx10 are mainly important for the transition from G1 to S or from G1 to G0 and differentiation. If this mechanism is disrupted, it is possible that cells are temporarily unable either enter S phase to continue proliferating, or become post-mitotic and differentiate, reflected by a delay in the appearance of retinal neuron-specific markers. This model is illustrated in Figure 7.4.

7.4 Stem-cell like properties of cells proliferating in the adult *Chx10*$^{-/-}$ retina

A final aim of this study was to confirm whether stem cell-like cells reside in the CE of the eye, and whether more of these are present in the *Chx10*$^{-/-}$ retina than in the

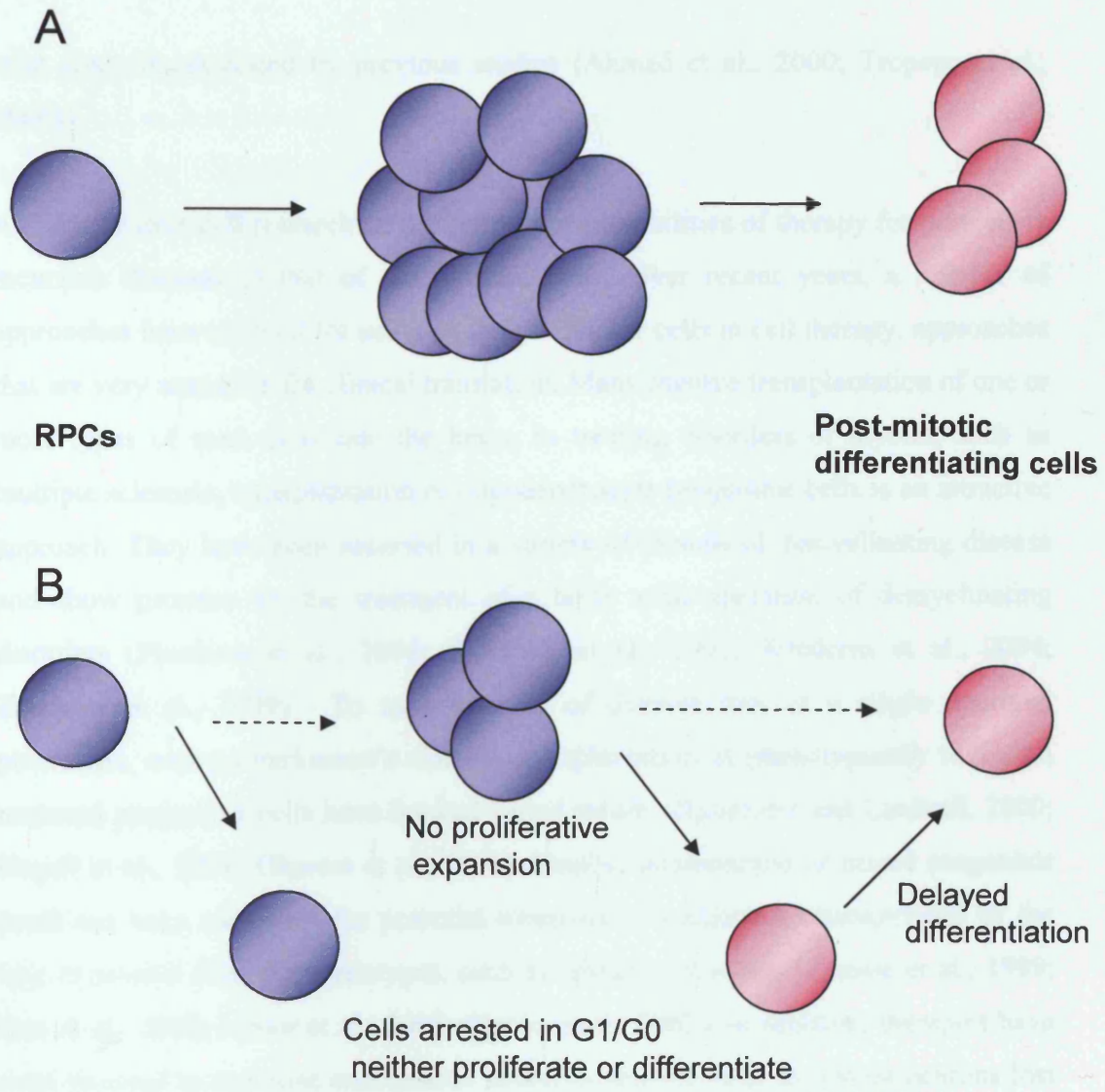

Figure 7.4: Model of how an arrest in G1/G0 of the cell cycle in RPCs of the *Chx10*$^{-/-}$ retina might result in a smaller population of retinal cells and delayed differentiation. *A*: In the wild type developing retina, RPCs proliferate symmetrically to produce an exponentially expanding population of RPCs, which will divide asymmetrically, and in time symmetrically, to produce post-mitotic differentiating cells in an organised manner, with various cell types being born at clearly defined times. *B*: In the *Chx10*$^{-/-}$ retina, RPCs may become arrested in G1/G0, and thus although they may divide symmetrically, long periods of time may exist between one division and the next, inhibiting proliferative expansion of RPCs. In a similar manner, differentiation of retinal cells may be delayed due to post-mitotic RPCs becoming arrested in G0. Whether this arrest is temporary or occurs in a certain percentage of the population of cells remains to be seen.

wild type, as suggested by previous studies (Ahmad et al., 2000; Tropepe et al., 2000).

An area of stem cell research now offering real possibilities of therapy for previously incurable diseases is that of neural stem cells. Over recent years, a number of approaches have evolved for using neural progenitor cells in cell therapy, approaches that are very attractive for clinical translation. Many involve transplantation of one or more types of stem cells into the brain. In treating disorders of myelin, such as multiple sclerosis, transplantation of oligodendrocyte progenitor cells is an attractive approach. They have been assessed in a variety of models of demyelinating disease and show promise for the treatment of a fairly wide spectrum of demyelinating disorders (Pluchino et al., 2004; Windrem et al., 2002; Windrem et al., 2004; Yandava et al., 1999). To treat diseases of discrete loss of a single neuronal phenotype, such as Parkinson's disease, transplantation of phenotypically restricted neuronal progenitor cells have booked varied results (Bjorklund and Lindvall, 2000; Hagell et al., 2002; Olanow et al., 1996). Finally, implantation of mixed progenitor pools has been examined for potential treatment of conditions characterized by the loss of several discrete phenotypes, such as spinal cord injury (Brustle et al., 1999; Han et al., 2004; Nistor et al., 2005; Ogawa et al., 2002). In addition, therapies have been directed to mobilise endogenous neural progenitor cells to restore neurons lost as a result of neurodegenerative diseases, in particular Huntington's disease (Chen et al., 2004; Curtis et al., 2003; Magavi et al., 2000). Together, these may present compelling strategies and near-term disease targets for cell-based neurological therapy.

Stem cells have also been characterised in the eye, where limbal stem cells replenish the cornea (Davanger and Evensen, 1971; Schermer et al., 1986; Tseng, 1989), and pigmented epithelial cells of the iris have been shown to re-enter the cell cycle and transdifferentiate to lens (Eguchi, 1988; Eguchi and Shingai, 1971; Imokawa and Brockes, 2003). Recently, the transplantation of limbal epithelial cells cultivated on amniotic membrane has been developed treatment for limbal stem cell deficiency, with encouraging results (Santos et al., 2005; Song et al., 2005). However, thus far, there has been no evidence that the mammalian retina can regenerate, or that any neural retinal progenitor-type cells exist in the mammalian retina, even though such

cells have been observed in lower vertebrates (see Chapter 1). Studies into transplant-based approaches for treatment of retinal degenerative conditions have been limited to the use of ES cells rather than more eye-specific cells (Banin et al., 2005; Meyer et al., 2005). Thus, the discovery that the CE of the mammalian eye might harbour self-renewing cells that could be induced to differentiate to various retinal cell types offers the first hope of developing therapies for retinal degenerative diseases.

Surprisingly, a large number of proliferating cells were observed throughout the *Chx10*$^{-/-}$ retina, and this is the first observation of proliferating cells in the adult mammalian retina *in vivo*. These cells seemed to continue to proliferate well into adulthood and showed self-renewing properties in culture. Moreover, they seemed to retain neurogenic properties, not only labelling with markers for neural progenitor cells and neuronal cells, but also with markers for the retinal specific amacrine cells.

No such cells were observed in the wild type retina. Proliferating cells were observed in the CE of both wild type and *Chx10*$^{-/-}$ retina, with a larger number seen in the *Chx10*$^{-/-}$ CE, but these did not co-label with any neurogenic markers, suggesting they have different properties to those proliferating cells observed in the *Chx10*$^{-/-}$ retina and that their ability to differentiate to various cell types, as shown in culture, may be restricted *in vivo*. The discovery of these cells, and their self-renewing and neurogenic properties, opens perspectives for devising mechanisms in which retinal cells can be regenerated after injury or degeneration. Further work needs to better define the properties of these cells. How is the *Chx10*$^{-/-}$ retina different to the wild type? Why do cells continue to proliferate in that environment? Can the properties of the *Chx10*$^{-/-}$ retina be utilised for the development of stem cell therapies for retinal degeneration or injury?

7.5 Considerations for future work

The work described here has revealed a variety of novel findings that pertain to the *Chx10*$^{-/-}$ phenotype. A number of genes that may be under Chx10 control have been identified, and the importance of Chx10 in directing retinal cell fate has been

highlighted by this study. In addition, proliferating cells with RPC-like qualities and neurogenic potential have been identified in the central retina of the *Chx10*$^{-/-}$ retina. Of course, these findings raise many new questions about the mechanisms in which Chx10 exerts its control, both on the RPC cell cycle and retinal cell differentiation.

Whilst a number of genes have been identified that are clearly under Chx10 control, whether this control is direct or indirect remains to be seen. *Neurod1* has 5 Chx10 binding sites within 5 kb of its start codon, and *Dlx2* has 3. Binding studies using Chx10 need to be carried out to examine whether Chx10 actually binds to these sites, which might suggest its direct, rather than indirect, control of these genes. Functional studies are also required, for example by manipulating the amount of these factors in cell culture of Chx10-deficient RPCs and examining whether they in some way rescue aspects the phenotype.

Thus far, only six of the 34 characterised genes that have shown a significant 1.5-fold change in expression in the microarray study performed here have been examined further. A number of other genes would be of interest to pursue, such as *Gas2* and *Ccne2*, with respect to Chx10's control of the cell cycle, or *ApoE*, another gene normally expressed in the RPE. *Fgf9* also shows a change in expression and as *Fgfs* are involved in various aspects of cell proliferation and differentiation, it would also be interesting to examine how *Fgf9* might be controlled by Chx10. A number of the genes showing a change in expression are currently being examined in this laboratory.

Many questions also remain unanswered as to how Chx10 regulates the cell cycle. The data suggest that the length of G1 is increased or cells are arrested in G1, and that *Chx10*$^{-/-}$ RPCs cycle abnormally during development, leading to a persistence of cycling cells after birth. However the mechanisms through which this occurs remain elusive. The cell culture studies initiated here should be expanded in order to further characterise how *Chx10*$^{-/-}$ RPCs are different to wild type, and how they respond to their environment, through the addition of growth factors for example. In addition, it would be beneficial to isolate the cycling cells observed in the adult *Chx10*$^{-/-}$ retina in culture, and compare them to embryonic RPCs in order to examine whether they are similar in nature and behaviour.

Finally, a population of proliferating cells has been identified in the adult *Chx10*$^{-/-}$ retina. This novel finding is of interest in light of the various stem cell studies that have been conducted on the mammalian retina. As described earlier, self-renewing cells with neurogenic potential have not previously been found in the mammalian retina. Stem cell-like cells have thus far only been isolated from the ciliary epithelium of the mammalian eye (Ahmad et al., 1999; Tropepe et al., 2000). Such cells are of great interest, as they may offer clues as to how cells in the mammalian retina might be regenerated after, for example, injury or degeneration. If the proliferating cells found in the *Chx10*$^{-/-}$ retina can self-renew and differentiate to specific retinal cell types, can they also integrate into the existing retinal structure? Can such cells be cultured indefinitely and be transplanted into an injured retina? Such questions are of great interest with respect to finding novel therapies for retinal degeneration, and cell culture and transplantation studies of these cells have been initiated in this and collaborating labs.

7.6 Final Thoughts

The study conducted here has produced a number of interesting and novel findings and offered some valuable clues as to how Chx10 affects retinal progenitor cell proliferation and differentiation. In addition, it has raised a number of new and interesting questions, which will form the basis of further work in this fast-evolving field. It is hoped this work will contribute to the current knowledge of eye development in general, and Chx10's involvement in this process in particular.

APPENDICES

Appendix 1

List of 293 genes that showed a greater than 1.5-fold expression between wild type and *Chx10*$^{-/-}$ E11.5 retinae in the experiment described in Chapter 3. 'Trend' indicates an increase (+) or decrease (-) in expression in the *Chx10*$^{-/-}$ retina as compared to the wild type, and 'Fold-change' indicates the fold change in expression. Of the 293 genes, 54 are expressed sequence tags ('EST') and 235 are characterised genes (eight genes are represented twice, these are marked with an asterisk).

Gene Title	Trend	Fold-Change	Genbank Accession Number
Actin, beta, cytoplasmic (*Actb*)	-	3.50	J04181
Adenylosuccinate synthetase like 1 (*Adssl1*)	+	1.92	M74495
Aortic preferentially expressed gene 1 (*Apeg1*)	+	2.03	U57098
Apolipoprotein E (*Apoe*)	+	4.70	D00466
ATPase, Ca++-sequestering (*Atp2c1*)	-	1.75	AV356516
ATP synthase, H+ transporting, mitochondrial F1 complex, delta subunit (*Atp5d*)	+	1.69	AV217314
ATP synthase, H+ transporting, mitochondrial F0 complex, subunit g (*Atp5l*)	-	2.17	Y17223
UDP-GlcNAc:betaGal beta-1,3-N-acetylglucosaminyltransferase 1 (*B3gnt1*)	+	2.46	AV315957
Biglycan (*Bgn*)	+	2.18	X53928
Basic helix-loop-helix domain containing, class B2 (*Bhlhb2*)	+	2.95	Y07836
Brain and kidney protein (*Bk*)	+	2.26	AW046243
BMP2 inducible kinase (*Bmp2k*)	-	1.79	AA673486
Budding uninhibited by benzimidazoles 1 homolog (S. cerevisiae) (*Bub1*)	-	1.70	AI428843
Nuclear DNA binding protein (*C1d*)	-	1.83	X95591
Calcium binding protein, intestinal (*Cai*)	+	1.89	Y00884
Catenin alpha 2 (*Catna2*)	-	1.73	D25281
Chromobox homolog 3 (Drosophila HP1 gamma) (*Cbx3*)	-	1.82	X56683
Cyclin E2 (*Ccne2*)	-	2.44	AF091432
Copper chaperone for superoxide dismutase (*Ccs*)	+	2.11	AV267263
CD8 antigen, beta chain 1 (*Cd8b1*)	-	1.60	X07698
Cadherin 4 (*Cdh4*)	-	2.53	X69966
Cadherin 8 (*Cdh8*)	-	5.99	X95600
Cyclin-dependent kinase inhibitor 1B (P27) (*Cdkn1b*)	+	1.50	U09968
C. elegans ceh-10 homeo domain containing homolog (*Chx10*)*	-	2.61	L34808
C. elegans ceh-10 homeo domain containing homolog (*Chx10*)*	-	2.70	AV246437
Creatine kinase, mitochondrial 1, ubiquitous (*Ckmt1*)	-	1.59	Z13969
Claudin 1 (*Cldn1*)	-	2.75	AI604314

Gene Title	Trend	Fold-Change	Genbank Accession Number
Claudin 6 (*Cldn6*)	-	2.43	AF087824
CCR4-NOT transcription complex, subunit 7 (*Cnot7*)	+	3.31	AI931748
Coactosin-like 1 (Dictyostelium) (*Cotl1*)	+	3.05	AI837006
Carnitine palmitoyltransferase 1a, liver (*Cpt1a*)	+	2.78	AF017175
Cellular retinoic acid binding protein I (*Crabp1*)	-	2.29	X15789
cAMP responsive element binding protein 1 (*Creb1*)	-	2.53	X67719
Cellular repressor of E1A-stimulated genes 1 (*Creg1*)	+	2.01	AF084524
Casein kinase 1, gamma 2 (*Csnk1g2*)	+	1.79	AW121446
Chondroitin sulfate proteoglycan 2 (*Cspg2*)	-	1.83	D45889
Cathepsin C (*Ctsc*)	+	1.82	U74683
Cytochrome P450, family 1, subfamily b, polypeptide 1 (*Cyp1b1*)	-	3.41	X78445
Cytochrome P450, family 4, subfamily v, polypeptide 3 (*Cyp4v3*)	+	3.35	AA212964
DNA segment, Chr 2, ERATO Doi 93, expressed (*D2Ertd93e*)	-	1.94	C77278
DNA segment, Chr 6, Wayne State University 176, expressed (*D6Wsu176e*)*	+	1.59	AA733372
DNA segment, Chr 6, Wayne State University 176, expressed (*D6Wsu176e*)*	-	2.07	AA733372
Death-associated kinase 3 (*Dapk3*)	-	1.80	AB007143
D site albumin promoter binding protein (*Dbp*)	+	1.97	AW047343
Dopachrome tautomerase (*Dct*)	+	4.80	X63349
DEAD (Asp-Glu-Ala-Asp) box polypeptide 6 (*Ddx6*)	-	5.65	D50494
DEK oncogene (DNA binding) (*Dek*)	-	2.12	AA733594
Diacylglycerol kinase, alpha (*Dgka*)	+	1.76	AF085219
Distal-less homeobox 2 (*Dlx2*)	-	13.83	M80540
DnaJ (Hsp40) homolog, subfamily B, member 9 (*Dnajb9*)*	-	1.61	AI835630
DnaJ (Hsp40) homolog, subfamily B, member 9 (*Dnajb9*)*	-	2.48	AW120711
Dual specificity phosphatase 16 (*Dusp16*)	-	1.85	AV234570
ER degradation enhancer, mannosidase alpha-like 1 (*Edem1*)	-	1.95	AW212878
Eukaryotic translation initiation factor 1A (*Eif1a*)	-	2.73	U28419
Elongation of very long chain fatty acids (FEN1/Elo2, SUR4/Elo3, yeast)-like 2 (*Elovl2*)	-	1.90	AI317360
Enamelin (*Enam*)	-	1.48	U82698
Enolase 2, gamma neuronal (*Eno2*)	+	2.28	AC002397
Ectonucleoside triphosphate diphosphohydrolase 4 (*Entpd4*)	+	1.69	AI851172
Eph receptor A4 (*Epha4*)	-	1.70	X65138
Epoxide hydrolase 2, cytoplasmic (*Ephx2*)	+	1.81	Z37107
Endogenous retroviral sequence 4 (with leucine t-RNA primer) (*Erv4*)	-	1.44	Y12713
Exocyst complex component 8 (*Exoc8*)	+	1.67	AI591555
Fatty acid binding protein 3, muscle and heart (*Fabp3*)	+	2.88	X14961
Farnesyl diphosphate synthetase (*Fdps*)	-	1.83	AW045533

Gene Title	Trend	Fold-Change	Genbank Accession Number
Fibroblast growth factor 9 (*Fgf9*)	-	2.75	U33535
Fibroblast growth factor 15 (*Fgf15*)	-	2.48	AF007268
Fibroblast growth factor receptor 2 (*Fgfr2*)	+	1.74	AV363696
Fragile histidine triad gene (*Fhit*)	+	1.80	AF047699
Forkhead box C1 (*Foxc1*)	-	2.33	AF045017
Forkhead box C2 (*Foxc2*)*	-	2.29	X74040
Forkhead box C2 (*Foxc2*)*	-	2.61	AV251191
Forkhead box G1 (*Foxg1*)	-	3.57	U36760
Friend virus susceptibility 4 (*Fv4*)	-	2.12	C78850
Frizzled homolog 4 (Drosophila) (*Fzd4*)	+	2.07	AW122897
Growth arrest and DNA-damage-inducible 45 alpha (*Gadd45a*)	-	2.00	U00937
Growth arrest specific 2 (*Gas2*)	-	2.15	M21828
GATA-binding protein 3 (*Gata3*)	-	2.27	X55123
Glia maturation factor, beta (*Gmfb*)	-	2.12	AA756568
Guanine nucleotide binding protein, beta 2 (*Gnb2*)	+	1.31	U34960
G protein-coupled receptor 49 (*Gpr49*)	-	2.95	AF110818
G protein-coupled receptor 143 (*Gpr143*)	+	3.91	X98352
G protein-coupled receptor 175 (*Gpr175*)	+	2.50	AI842363
G-rich RNA sequence binding factor 1 (*Grsf1*)	+	1.78	AV293460
Glutathione S-transferase, alpha 4 (*Gsta4*)	+	1.80	L06047
Glutathione S-transferase, theta 2 (*Gstt2*)	+	2.06	X98056
Hyaluronan synthase 2 (*Has2*)	-	2.39	U52524
Histone 1, H2ba (*Hist1h2ba*)	-	1.58	X90778
Histone 2, H3c2 (*Hist2h3c2*)	-	3.25	Z30939
Histone 2, H3c2; histone 1, H3g; histone 1, H3f; histone1, H3c; histone1, H3d; histone 1, H3b; histone 1, H3e; histone 1, H3h; histone 1, H3i; histone 1, H3a (*Hist2h3c2, Hist1h3g, Hist1h3f, Hist1h3c, Hist1h3d, Hist1h3b, Hist1h3e, Hist1h3h, Hist1h3i, Hist1h3a*)	-	3.70	M32459
Hexokinase 1 (*Hk1*)	-	3.79	J05277
Homeo box C4 (*Hoxc4*)	-	1.79	X69019
Heparan sulfate (glucosamine) 3-O-sulfotransferase 1 (*Hs3st1*)	+	2.32	AF019385
Heat shock protein 1A (*Hspa1a*)	+	2.76	M12571
Heat shock protein 1B (*Hspa1b*)	+	3.22	AF109906
Intracisternal A particles, Il3 linked (*Iap11-1*)	-	1.85	X04120
Inhibitor of DNA binding 1 (*Idb1*)	-	1.95	M31885
Interferon gamma inducible protein 30 (*Ifi30*)	+	1.88	AI844520
Insulin-like growth factor binding protein 5 (*Igfbp5*)	+	2.41	L12447
Inner centromere protein (*Incenp*)	-	1.50	AW045530
Indolethylamine N-methyltransferase (*Inmt*)	+	3.26	M88694
Insulinoma-associated 1 (*Insm1*)	-	2.14	AF044669
IL2-inducible T-cell kinase (*Itk*)	-	1.58	D14042
Integrin alpha 4 (*Itga4*)	-	1.71	X53177
Integrin alpha V (*Itgav*)	+	2.97	U14135
Potassium voltage-gated channel, subfamily Q, member 2 (*Kcnq2*)	-	2.21	AB000503
K+ voltage-gated channel, subfamily S, 1 (*Kcns1*)	+	1.78	AF008573

Gene Title	Trend	Fold-Change	Genbank Accession Number
Keratin complex 1, acidic, gene 10 (*Krt1-10*)	+	1.76	V00830
Kinectin 1 (*Ktn1*)	-	3.18	AV380640
Laminin B1 subunit 1 (*Lamb1-1*)	+	1.83	AV357656
Lamin A (*Lmna*)	+	1.72	D49733
Leukotriene B4 12-hydroxydehydrogenase (*Ltb4dh*)	+	1.84	AA596710
Mannosidase 1, alpha (*Man1a*)*	+	1.67	AI021125
Mannosidase 1, alpha (*Man1a*)*	+	2.05	U04299
Maternal embryonic leucine zipper kinase (*Melk*)	-	2.06	L76158
Microsomal glutathione S-transferase 1 (*Mgst1*)	+	1.84	AW124337
Mitochondrial ribosomal protein L54 (*Mrpl54*)	-	1.34	AW060257
MutS homolog 6 (E. coli) (*Msh6*)	-	1.37	AF031087
Metastasis-associated gene family, member 2 (*Mta2*)	-	1.62	AW048332
Myeloblastosis oncogene (*Myb*)	-	2.31	M12848
Myosin, heavy polypeptide 9, non-muscle (*Myh9*)	+	1.68	AW125698
Myosin X (*Myo10*)	+	2.81	AJ249706
Myelin transcription factor 1 (*Myt1*)	-	1.79	AF004294
N-acetyl galactosaminidase, alpha (*Naga*)	+	2.18	AJ223966
NADH dehydrogenase (ubiquinone) 1 alpha subcomplex 11 (*Ndufa11*)	-	2.11	AI843074
Neurogenic differentiation 1 (*Neurod1*)	-	8.26	U28068
Neuroblastoma myc-related oncogene 1 (*Nmyc1*)	-	1.82	M12731
Neuronatin (*Nnat*)	-	2.39	X83569
Non-POU-domain-containing, octamer-binding protein (*Nono*)	-	1.81	AI316087
Notch gene homolog 1, (Drosophila) (*Notch1*)	-	1.72	AV374287
Nuclear protein 1 (*Nupr1*)	-	4.20	AI852641
Osteoglycin (*Ogn*)	-	1.62	D31951
One cut domain, family member 1 (*Onecut1*)	-	2.22	U95945
OTU domain, ubiquitin aldehyde binding 1 (*Otub1*)	+	1.65	AI838318
Paired box gene 9 (*Pax9*)	-	2.56	X84000
Purkinje cell protein 4 (*Pcp4*)	+	1.67	X17320
Paternally expressed 10 (*Peg10*)	-	1.75	AI836610
Pleckstrin homology-like domain, family A, member 1 (*Phlda1*)	-	3.04	U44088
Plakophilin 2 (*Pkp2*)	-	1.53	AW208938
Pleiomorphic adenoma gene-like 1 (*Plagl1*)*	-	1.97	X95504
Pleiomorphic adenoma gene-like 1 (*Plagl1*)*	-	1.63	X95503
Phospholipase D3 (*Pld3*)	+	2.12	AF026124
Polo-like kinase homolog, (Drosophila) (*Plk1*)	-	1.47	AV305987
Polo-like kinase, pseudogene 1 (*Plk-ps1*)	-	2.67	U73170
Polyamine-modulated factor 1 (*Pmf1*)	-	1.78	AW060657
Peroxisome proliferator activated receptor alpha (*Ppara*)	-	1.75	X57638
Peroxisome proliferative activated receptor, gamma, coactivator 1 alpha (*Ppargc1a*)	+	1.90	AF049330
Peroxiredoxin 6 peroxiredoxin 6, related sequence 1 (*Prdx6 Prdx6-rs1*)	-	1.86	AF093853
Pituitary tumor-transforming 1 (*Pttg1*)	-	1.89	AF071209

Gene Title	Trend	Fold-Change	Genbank Accession Number
Prospero-related homeobox 1 (*Prox1*)	-	1.98	AF061576
Prostate tumor over expressed gene 1 (*Ptov1*)	+	1.41	AI838337
Protein kinase C, alpha (*Prkca*)	-	2.35	M25811
Protein kinase C, beta 1 (*Prkcb1*)*	+	2.56	X53532
Protein kinase C, beta 1 (*Prkcb1*)*	+	2.50	X59274
Protein kinase C, delta binding protein (*Prkcdbp*)	+	2.03	AW048944
PRP19/PSO4 homolog (S. cerevisiae) (*Prp19*)	+	1.74	AW122465
Protein tyrosine kinase 9 (*Ptk9*)	-	1.77	U82324
Protein tyrosine kinase 9-like (A6-related protein) (*Ptk9l*)	+	1.81	Y17808
Protein tyrosine phosphatase, receptor type, S (*Ptprs*)	+	1.43	X82288
Purine rich element binding protein A (*Pura*)	+	2.00	U02098
RAB7, member RAS oncogene family (*Rab7*)	+	1.64	X89650
RAD51 homolog (S. cerevisiae) (*Rad51*)	-	1.78	D13803
RAN GTPase activating protein 1 (*Rangap1*)	-	1.89	U20857
RNA binding motif protein 4 (*Rbm4*)	-	1.77	U89506
REST corepressor 1 (*Rcor1*)	-	2.07	AV356223
Regenerating islet-derived 2 (*Reg2*)	-	1.53	AV051312
Reelin (*Reln*)	+	3.90	AV263736
Renin-binding protein (*Renbp*)	+	2.46	AA600645
Ring finger protein 13 (*Rnf13*)	-	1.80	AF037205
Ring finger protein 138 (*Rnf138*)	-	1.80	AW209763
Roundabout homolog 3 (Drosophila) (*Robo3*)	+	3.29	AF060570
Rho-associated coiled-coil forming kinase 1 (*Rock1*)	-	1.75	AA647393
Ribosomal protein L27a (*Rpl27a*)	-	3.41	X05021
Ribosomal protein S15a (*Rps15a*)	-	2.27	AF085809
Ribosomal protein S28 *(Rps28)*	+	1.81	U11248
Reticulon 1 (*Rtn1*)	-	2.43	AW123115
Retinoid X receptor gamma (*Rxrg*)	+	17.93	X66225
S100 calcium binding protein A1 (*S100a1*)	+	4.50	AF087687
Sarcoma amplified sequence (*Sas*)	+	1.56	AI844321
Secretory carrier membrane protein 3 (*Scamp3*)	+	1.97	AF005036
Stearoyl-Coenzyme A desaturase 1 (*Scd1*)*	-	2.05	M21285
Stearoyl-Coenzyme A desaturase 1 (*Scd1*)*	-	1.90	M21285
Syndecan 4 (*Sdc4*)	+	2.80	D89571
SEC63-like (S. cerevisiae) (*Sec63*)	-	1.98	C76102
Selenium binding protein 1 selenium binding protein 2 (*Selenbp1* *Selenbp2*)	+	1.71	AV366872
Selenoprotein P, plasma, 1 (*Sepp1*)	-	1.61	AF021345
Sarcoglycan, gamma (dystrophin-associated glycoprotein) (*Sgcg*)	-	1.53	AB024922
SH2 domain binding protein 1 (tetratricopeptide repeat containing) (*Sh2bp1*)	-	2.03	AV375731
Silver (*Si*)	+	3.54	U14133
Solute carrier family 2 (facilitated glucose transporter), member 4 (*Slc2a4*)	+	2.18	M23383
Solute carrier family 19 (sodium/hydrogen exchanger), member 1 (*Slc19a1*)	+	1.86	L23755
Solute carrier family 22 (organic cation	+	2.16	AB012808

Gene Title	Trend	Fold-Change	Genbank Accession Number
transporter), member 17 (*Slc22a17*)			
Solute carrier family 23 (nucleobase transporters), member 3 (*Slc23a3*)	+	1.65	AV222871
Solute carrier organic anion transporter family, member 5A1 (*Slco5a1*)	-	1.93	AA407151
SWI/SNF-related, matrix-associated actin-dependent regulator of chromatin, subfamily a, containing DEAD/H box 1 (*Smarcad1*)	-	1.69	AV381829
Sphingomyelin phosphodiesterase, acid-like 3A (*Smpdl3a*)	+	2.42	Y08135
Small nuclear ribonucleoprotein polypeptide G (*Snrpg*)	-	2.14	AW060597
Sphingosine kinase 1 (*Sphk1*)	+	2.95	AF068748
Secreted phosphoprotein 1 (*Spp1*)	+	2.38	X13986
Small proline-rich protein 2F (*Sprr2f*)	-	2.03	AJ005564
Serine racemase (*Srr*)	-	1.68	AI840579
Signal sequence receptor, gamma (*Ssr3*)	-	1.98	AW227650
ST8 alpha-N-acetyl-neuraminide alpha-2,8-sialyltransferase 3 (*St8sia3*)	-	2.25	X80502
START domain containing 10 (*Stard10*)	+	1.72	AW049732
Signal transducer and activator of transcription 1 (*Stat1*)	-	1.37	U06924
Signal transducer and activator of transcription 6 (*Stat6*)	+	3.02	L47650
Stathmin-like 2 (*Stmn2*)	-	2.21	AI839868
Suppressor of zeste 12 homolog (Drosophila) (*Suz12*)	-	1.88	AA797843
Synaptotagmin binding, cytoplasmic RNA interacting protein (*Syncrip*)	-	1.72	AF093821
Synaptotagmin 11 (*Syt11*)	-	1.60	AB026808
Tubulin cofactor a (*Tbca*)	-	1.96	U05333
Transcription elongation factor B (SIII), polypeptide 2 (*Tceb2*)	-	1.79	AA795613
Transcription factor 20 (*Tcf20*)	+	1.99	AI847906
T-complex-associated testis expressed 2 (*Tcte2*)	-	1.38	U46151
T-complex-associated testis expressed 3 (*Tcte3*)	-	1.96	U21673
Cytoplasmic tyrosine kinase, Dscr28C related (Drosophila) (*Tec*)	+	2.38	X55663
Endothelial-specific receptor tyrosine kinase (*Tek*)	+	1.72	X71426
Transferrin receptor (*Tfrc*)	-	1.47	X57349
Thioesterase superfamily member 2 (*Them2*)	+	1.92	AW060827
THO complex 4 (*Thoc4*)	+	1.62	U89876
Thimet oligopeptidase 1 (*Thop1*)	+	1.80	AW047185
Thymocyte protein thy28 (*Thy28*)	-	1.55	AI050598
Transducin-like enhancer of split 1, homolog of Drosophila E(spl) (*Tle1*)	-	2.48	U61362
Transmembrane 4 superfamily member 8 (*Tm4sf8*)	+	2.18	AI843488
Transmembrane protein 30B (*Tmem30b*)	+	2.13	AA619554
Thymosin, beta 10 (*Tmsb10*)	-	2.64	AI852553
Tenascin C (*Tnc*)	-	2.30	X56304
Transient receptor potential cation channel,	+	3.34	AF047714

Gene Title	Trend	Fold-Change	Genbank Accession Number
subfamily M, member 1 (*Trpm1*)			
Thyroid stimulating hormone receptor (*Tshr*)	-	5.75	U02602
Tubulin, beta 2 (*Tubb2*)	-	1.64	AV351758
Ubiquitin-like 5 (*Ubl5*)	-	1.80	AW124386
UDP-glucose ceramide glucosyltransferase (*Ugcg*)	+	2.30	D89866
Vascular endothelial growth factor B (*Vegfb*)	+	1.84	U43836
WAP four-disulfide core domain 2 (*Wfdc2*)	+	1.93	AW121336
Zinc finger protein 54 (*Zfp54*)	+	2.12	AF080070
Zinc finger protein 101 (*Zfp101*)	-	1.78	U07861
Zinc finger protein 106 (*Zfp106*)	-	1.39	AF060245
Zinc finger protein 260 (*Zfp260*)	-	1.93	D45210
Zinc finger protein 281 (*Zfp281*)	-	1.70	AI850113
EST	+	2.73	AI606967
EST	+	2.60	AA266467
EST	+	2.51	AA607758
EST	+	2.50	AA717225
EST	+	2.39	AI845874
EST	+	2.33	AF015811
EST	+	2.26	W40747
EST	+	2.22	AV251613
EST	+	2.20	AV240248
EST	+	2.09	AA691628
EST	+	2.08	AA656550
EST	+	2.07	AI839150
EST	+	2.00	AV303935
EST	+	1.96	AI020029
EST	+	1.89	AV339602
EST	+	1.84	AA763466
EST	+	1.79	M31649
EST	+	1.70	C80138
EST	+	1.63	AV347226
EST	+	1.49	AI846236
EST	-	4.18	AW214136
EST	-	3.51	AW122834
EST	-	3.41	AW123796
EST	-	2.33	AA867778
EST	-	2.28	AW061337
EST	-	2.26	AV027707
EST	-	2.18	AV293047
EST	-	2.12	AA738737
EST	-	2.12	AV293047
EST	-	2.09	AW125284
EST	-	2.09	AI153421
EST	-	1.98	AI645050
EST	-	1.94	AA600542
EST	-	1.93	AW228316
EST	-	1.87	AA189811
EST	-	1.83	AA607053
EST	-	1.82	AV279579
EST	-	1.80	AA674798
EST	-	1.75	AI604097

Gene Title	Trend	Fold-Change	Genbank Accession Number
EST	-	1.75	AW259499
EST	-	1.75	X16670
EST	-	1.74	AA691185
EST	-	1.73	C77386
EST	-	1.66	AI850846
EST	-	1.62	AI854606
EST	-	1.54	AW047329
EST	-	1.52	D10627
EST	-	1.48	AV062425
EST	-	1.48	AW045808
EST	-	1.47	AU045946
EST	-	1.47	W91754
EST	-	1.45	AW047921
EST	-	1.36	AJ003132
EST	-	1.36	AI852409
EST	-	1.31	AV365271

Appendix 2

Amplification curves for RT-PCR experiments described in Chapter 4.

RT-PCR amplification curves for silver and dopachrome tautomerase. Amplification curves depicted as cycle number versus Delta Rn (baseline corrected normalised fluorescence). Amplification curves shown for cDNA from all 3 cDNA pools. *Chx10*$^{-/-}$ amplification curves are consistently to the left of the wild type curves. With the exception of silver, Pool 1, all PCRs were run as duplicates. *Chx10*$^{-/-}$ amplification curves are consistently to the left of the wild type curves.

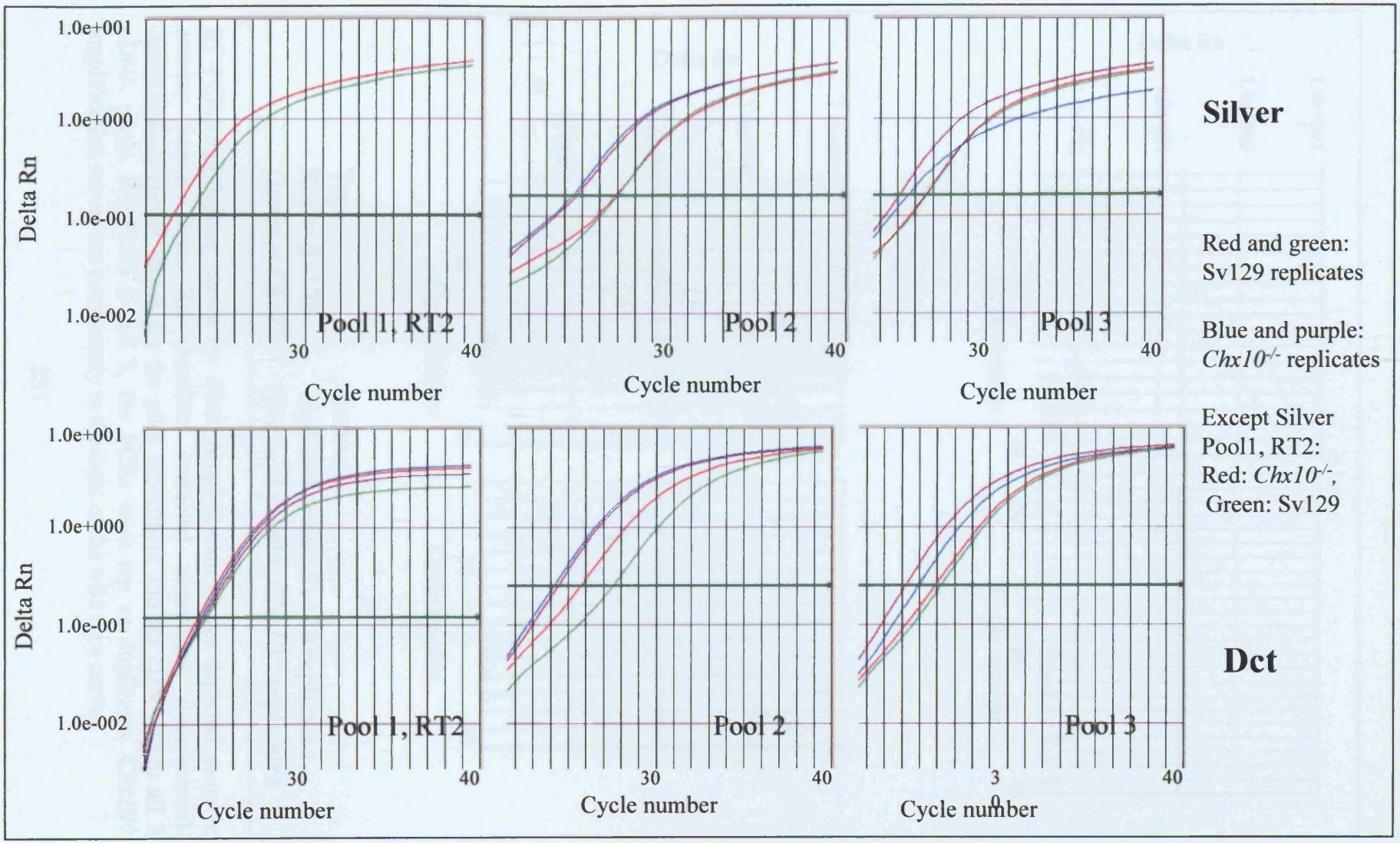
1.0e+001
1.0e+000
1.0e-001
1.0e-002
Delta Rn
Pool 1, RT2
Pool 2
Pool 3
30
40
Cycle number
Silver
Red and green:
Sv129 replicates
Blue and purple:
Chx10-/- replicates
Except Silver
Pool1, RT2:
Red: Chx10-/-,
Green: Sv129
Dct

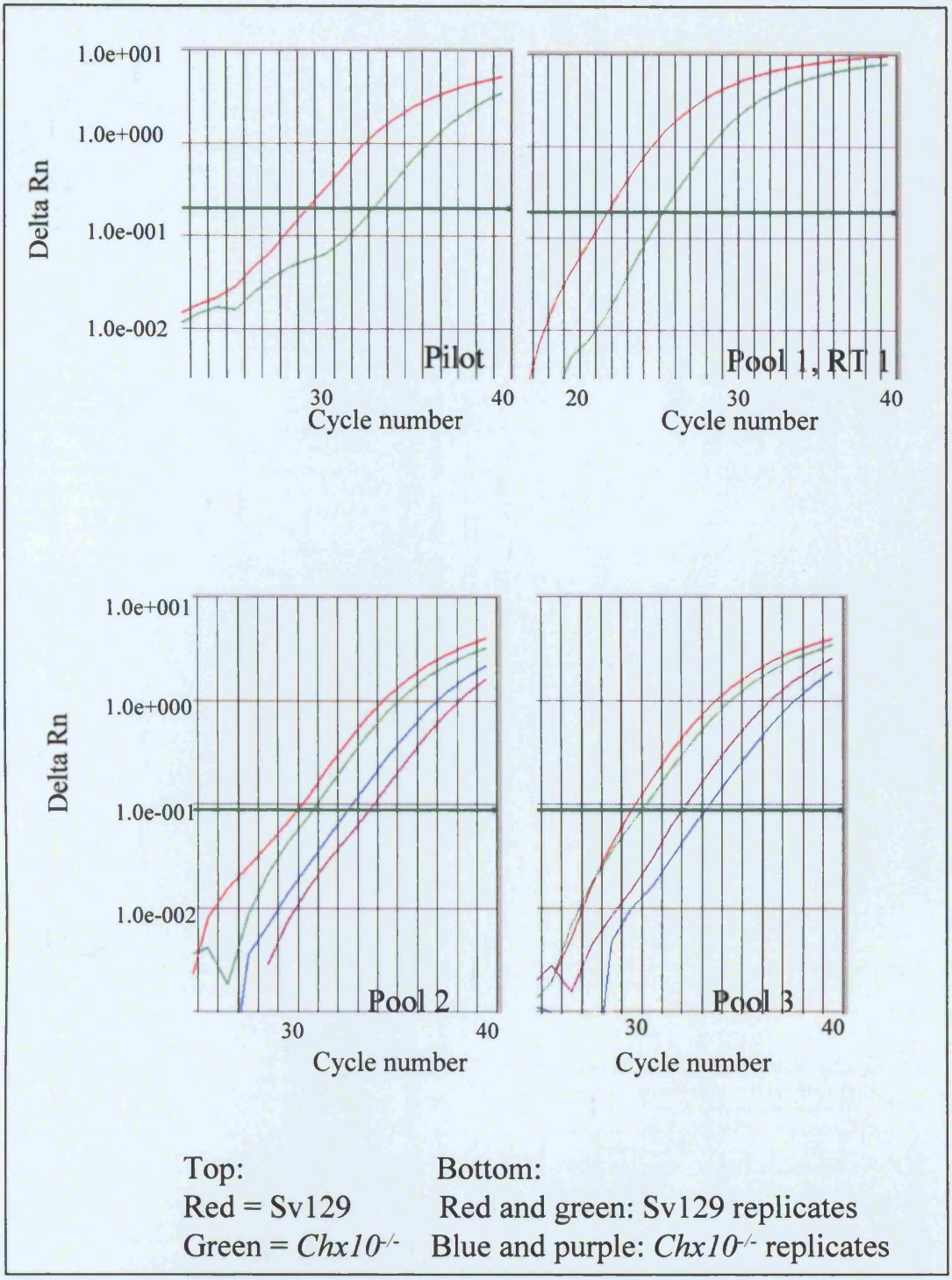

RT-PCR amplification curves for *Dlx2*. Amplification curves depicted as cycle number versus Delta Rn (baseline corrected normalised fluorescence). Amplification curves shown for the pilot experiment and for cDNA from all 3 cDNA pools. For Pools 2 and 3, the PCRs were run as duplicates. *Chx10*$^{-/-}$ amplification curves are consistently to the right of the wild type curves.

RT-PCR amplification curves for *Neurod1*. Amplification curves depicted as cycle number versus Delta Rn (baseline corrected normalised fluorescence). Amplification curves shown for cDNA from all 3 pools. *Chx10*$^{-/-}$ amplification curves are consistently to the right of the wild type curves. cDNA from pools 2 and 3 were run twice (top right and bottom left) and the RT repeated for both pools and run as well (bottom right). H_2O controls were used in all experiments, with fluorescence above the threshold level considered as contamination. H_2O controls are shown on bottom left graphs.

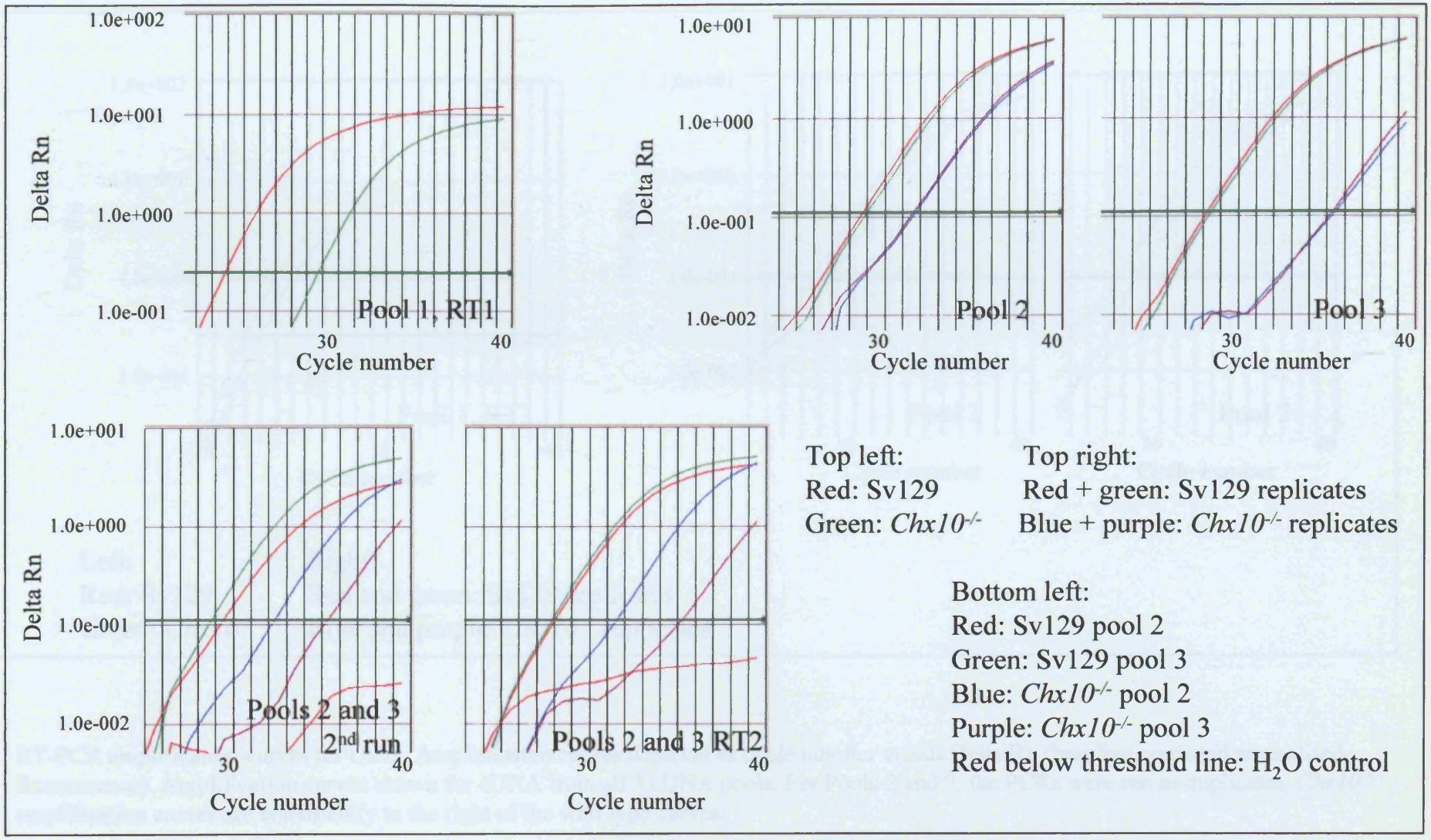
1.0e+002
1.0e+001
1.0e+000
1.0e-001
Delta Rn
Pool 1, RT1
30
40
Cycle number
1.0e+001
1.0e+000
1.0e-001
1.0e-002
Delta Rn
Pool 2
30
40
Cycle number
Pool 3
30
40
Cycle number
1.0e+001
1.0e+000
1.0e-001
1.0e-002
Delta Rn
Pools 2 and 3
2nd run
30
40
Cycle number
Pools 2 and 3 RT2
30
40
Cycle number
Top left:
Red: Sv129
Green: Chx10-/-
Top right:
Red + green: Sv129 replicates
Blue + purple: Chx10-/- replicates
Bottom left:
Red: Sv129 pool 2
Green: Sv129 pool 3
Blue: Chx10-/- pool 2
Purple: Chx10-/- pool 3
Red below threshold line: H2O control

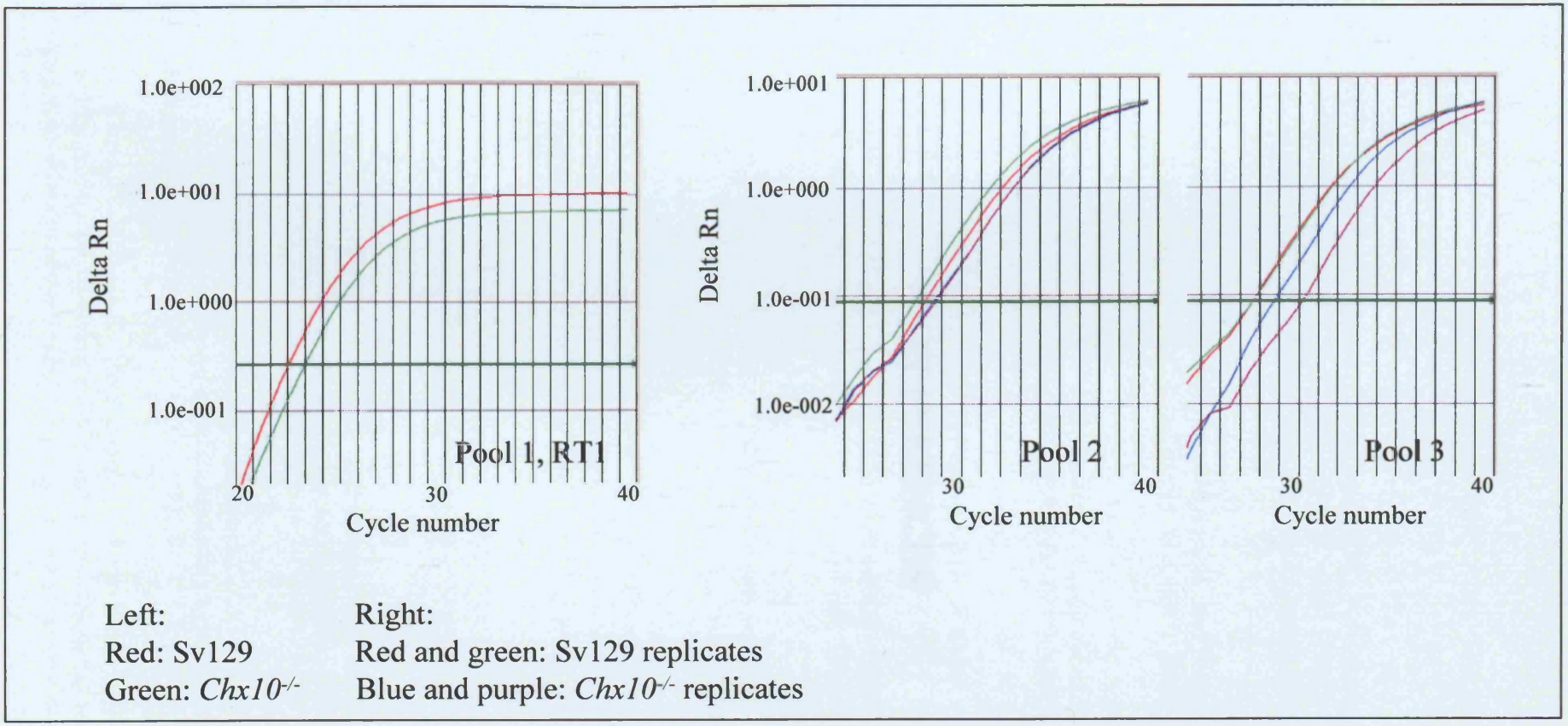

RT-PCR amplification curves for *Cdh8*. Amplification curves depicted as cycle number versus Delta Rn (baseline corrected normalised fluorescence). Amplification curves shown for cDNA from all 3 cDNA pools. For Pools 2 and 3, the PCRs were run as duplicates. *Chx10*$^{-/-}$ amplification curves are consistently to the right of the wild type curves.

REFERENCES

Reference List

Adams,M.D., Kelley,J.M., Gocayne,J.D., Dubnick,M., Polymeropoulos,M.H., Xiao,H., Merril,C.R., Wu,A., Olde,B., Moreno,R.F., and . (1991). Complementary DNA sequencing: expressed sequence tags and human genome project. Science *252*, 1651-1656.

Adema,G.J., Bakker,A.B., de Boer,A.J., Hohenstein,P., and Figdor,C.G. (1996). pMel17 is recognised by monoclonal antibodies NKI-beteb, HMB-45 and HMB-50 and by anti-melanoma CTL. Br. J Cancer *73*, 1044-1048.

Ahmad,I., Dooley,C.M., Thoreson,W.B., Rogers,J.A., and Afiat,S. (1999). In vitro analysis of a mammalian retinal progenitor that gives rise to neurons and glia. Brain Res. *831*, 1-10.

Ahmad,I., Tang,L., and Pham,H. (2000). Identification of neural progenitors in the adult mammalian eye. Biochem. Biophys. Res. Commun. *270*, 517-521.

Alexiades,M.R. and Cepko,C.L. (1997). Subsets of retinal progenitors display temporally regulated and distinct biases in the fates of their progeny. Development *124*, 1119-1131.

Alizadeh,M., Miyamura,N., Handa,J.T., and Hjelmeland,L.M. (2003). Human RPE cells express the FGFR2IIIc and FGFR3IIIc splice variants and FGF9 as a potential high affinity ligand. Exp. Eye Res. *76*, 249-256.

Anderson,D.H., Ozaki,S., Nealon,M., Neitz,J., Mullins,R.F., Hageman,G.S., and Johnson,L.V. (2001). Local cellular sources of apolipoprotein E in the human retina and retinal pigmented epithelium: implications for the process of drusen formation. Am. J. Ophthalmol. *131*, 767-781.

Arimatsu,Y., Naegele,J.R., and Barnstable,C.J. (1987). Molecular markers of neuronal subpopulations in layers 4, 5, and 6 of cat primary visual cortex. J. Neurosci. *7*, 1250-1263.

Ashery-Padan,R., Marquardt,T., Zhou,X., and Gruss,P. (2000). Pax6 activity in the lens primordium is required for lens formation and for correct placement of a single retina in the eye. Genes Dev. *14*, 2701-2711.

Austin,C.P., Feldman,D.E., Ida,J.A., Jr., and Cepko,C.L. (1995). Vertebrate retinal ganglion cells are selected from competent progenitors by the action of Notch. Development *121*, 3637-3650.

Azadi,S., Zhang,Y., Caffe,A.R., Holmqvist,B., and van Veen,T. (2002). Thyroid-beta2 and the retinoid RAR-alpha, RXR-gamma and ROR-beta2 receptor mRNAs; expression profiles in mouse retina, retinal explants and neocortex. Neuroreport *13*, 745-750.

Bailey,T.J., El Hodiri,H., Zhang,L., Shah,R., Mathers,E.H., and Jamrich,M. (2004). Regulation of vertebrate eye development by Rx genes. Int. J. Dev. Biol. *48*, 761-770.

Banin,E., Obolensky,A., Idelson,M., Hemo,I., Reinhardtz,E., Pikarsky,E., Ben Hur,T., and Reubinoff,B. (2005). Retinal Incorporation and Differentiation of Neural Precursors Derived from Human Embryonic Stem Cells. Stem Cells. 0: 200500091 published online 25 August 2005.

Barbieri,A.M., Broccoli,V., Bovolenta,P., Alfano,G., Marchitiello,A., Mocchetti,C., Crippa,L., Bulfone,A., Marigo,V., Ballabio,A., and Banfi,S. (2002). Vax2 inactivation in mouse determines alteration of the eye dorsal-ventral axis, misrouting of the optic fibres and eye coloboma. Development *129*, 805-813.

Barnstable,C.J., Hofstein,R., and Akagawa,K. (1985). A marker of early amacrine cell development in rat retina. Brain Res. *352*, 286-290.

Bateman,J.B. (1984). Microphthalmos. Int. Ophthalmol. Clin. *24*, 87-107.

Baxter,L.L. and Pavan,W.J. (2003). Pmel17 expression is Mitf-dependent and reveals cranial melanoblast migration during murine development. Gene Expr. Patterns. *3*, 703-707.

Becker,L.A. and Coolidge,F.L. (1991). On the proper interpretation of residualized interaction means in an analysis of variance: A reply to Rosnow and Rosenthal. Pscyhological Reports 483-490.

Belliveau,M.J. and Cepko,C.L. (1999). Extrinsic and intrinsic factors control the genesis of amacrine and cone cells in the rat retina. Development *126*, 555-566.

Belliveau,M.J., Young,T.L., and Cepko,C.L. (2000). Late retinal progenitor cells show intrinsic limitations in the production of cell types and the kinetics of opsin synthesis. J Neurosci *20*, 2247-2254.

Bermejo,E. and Martinez-Frias,M.L. (1998). Congenital eye malformations: clinical-epidemiological analysis of 1,124,654 consecutive births in Spain. Am. J. Med. Genet. *75*, 497-504.

Berson,J.F., Harper,D.C., Tenza,D., Raposo,G., and Marks,M.S. (2001). Pmel17 initiates premelanosome morphogenesis within multivesicular bodies. Mol Biol Cell *12*, 3451-3464.

Bessant,D.A., Khaliq,S., Hameed,A., Anwar,K., Mehdi,S.Q., Payne,A.M., and Bhattacharya,S.S. (1998). A locus for autosomal recessive congenital microphthalmia maps to chromosome 14q32. Am. J. Hum. Genet. *62*, 1113-1116.

Bhattacharyya,K.K., Coenen,M.J., and Bahn,R.S. (2005). Thyroid transcription factor-1 in orbital adipose tissues: potential role in orbital thyrotropin receptor expression. Thyroid *15*, 422-426.

Bjorklund,A. and Lindvall,O. (2000). Cell replacement therapies for central nervous system disorders. Nat Neurosci *3*, 537-544.

Blixt,A., Mahlapuu,M., Aitola,M., Pelto-Huikko,M., Enerback,S., and Carlsson,P. (2000). A forkhead gene, FoxE3, is essential for lens epithelial proliferation and closure of the lens vesicle. Genes Dev *14*, 245-254.

Bone-Larson,C., Basu,S., Radel,J.D., Liang,M., Perozek,T., Kapousta-Bruneau,N., Green,D.G., Burmeister,M., and Hankin,M.H. (2000). Partial rescue of the ocular retardation phenotype by genetic modifiers. J. Neurobiol. *42*, 232-247.

Bora,N., Conway,S.J., Liang,H., and Smith,S.B. (1998). Transient overexpression of the Microphthalmia gene in the eyes of Microphthalmia vitiligo mutant mice. Dev Dyn. *213*, 283-292.

Bovolenta,P., Mallamaci,A., Briata,P., Corte,G., and Boncinelli,E. (1997). Implication of OTX2 in pigment epithelium determination and neural retina differentiation. J Neurosci *17*, 4243-4252.

Brancolini,C., Bottega,S., and Schneider,C. (1992). Gas2, a growth arrest-specific protein, is a component of the microfilament network system. J. Cell Biol. *117*, 1251-1261.

Brickell,P.M. and Tickle,C. (1989). Morphogens in chick limb development. Bioessays *11*, 145-149.

Brownell,I., Dirksen,M., and Jamrich,M. (2000). Forkhead Foxe3 maps to the dysgenetic lens locus and is critical in lens development and differentiation. Genesis. *27*, 81-93.

Brustle,O., Jones,K.N., Learish,R.D., Karram,K., Choudhary,K., Wiestler,O.D., Duncan,I.D., and McKay,R.D. (1999). Embryonic stem cell-derived glial precursors: a source of myelinating transplants. Science *285*, 754-756.

Budd,P.S. and Jackson,I.J. (1995). Structure of the mouse tyrosinase-related protein-2/dopachrome tautomerase (Tyrp2/Dct) gene and sequence of two novel slaty alleles. Genomics *29*, 35-43.

Bumsted,K.M. and Barnstable,C.J. (2000). Dorsal retinal pigment epithelium differentiates as neural retina in the microphthalmia (mi/mi) mouse. Invest Ophthalmol Vis Sci *41*, 903-908.

Bumsted,K.M., Rizzolo,L.J., and Barnstable,C.J. (2001). Defects in the MITF(mi/mi) apical surface are associated with a failure of outer segment elongation. Exp. Eye Res *73*, 383-392.

Bunt-Milam,A.H. and Saari,J.C. (1983). Immunocytochemical localization of two retinoid-binding proteins in vertebrate retina. J. Cell Biol. *97*, 703-712.

Burmeister,M., Novak,J., Liang,M.Y., Basu,S., Ploder,L., Hawes,N.L., Vidgen,D., Hoover,F., Goldman,D., Kalnins,V.I., Roderick,T.H., Taylor,B.A., Hankin,M.H., and McInnes,R.R. (1996). Ocular retardation mouse caused by Chx10 homeobox null allele: impaired retinal progenitor proliferation and bipolar cell differentiation. Nat. Genet. *12*, 376-384.

Busby,A., Dolk,H., Collin,R., Jones,R.B., and Winter,R. (1998). Compiling a national register of babies born with anophthalmia/microphthalmia in England 1988-94. Arch. Dis. Child Fetal Neonatal Ed *79*, F168-F173.

Cao,S.X., Dhahbi,J.M., Mote,P.L., and Spindler,S.R. (2001). Genomic profiling of short- and long-term caloric restriction effects in the liver of aging mice. Proc. Natl. Acad. Sci. U. S. A *98*, 10630-10635.

Castilla,E.E. (1994). Clusters of ophthalmia. No further clues from global investigation. BMJ *308*, 206.

Cataisson,C., Joseloff,E., Murillas,R., Wang,A., Atwell,C., Torgerson,S., Gerdes,M., Subleski,J., Gao,J.L., Murphy,P.M., Wiltrout,R.H., Vinson,C., and Yuspa,S.H. (2003). Activation of cutaneous protein kinase C alpha induces keratinocyte apoptosis and intraepidermal inflammation by independent signaling pathways. J. Immunol. *171*, 2703-2713.

Cayouette,M. and Raff,M. (2003a). The orientation of cell division influences cell-fate choice in the developing mammalian retina. Development *130*, 2329-2339.

Cayouette,M. and Raff,M. (2003b). The orientation of cell division influences cell-fate choice in the developing mammalian retina. Development *130*, 2329-2339.

Cayouette,M., Whitmore,A.V., Jeffery,G., and Raff,M. (2001). Asymmetric segregation of Numb in retinal development and the influence of the pigmented epithelium. J. Neurosci. *21*, 5643-5651.

Cederberg,A., Gronning,L.M., Ahren,B., Tasken,K., Carlsson,P., and Enerback,S. (2001). FOXC2 is a winged helix gene that counteracts obesity, hypertriglyceridemia, and diet-induced insulin resistance. Cell *106*, 563-573.

Cepko,C.L., Austin,C.P., Yang,X., Alexiades,M., and Ezzeddine,D. (1996). Cell fate determination in the vertebrate retina. Proc. Natl. Acad. Sci. U. S. A *93*, 589-595.

Chattopadhyay,S., Kingsley,E., Serour,A., Curran,T.M., Brooks,A.I., and Pearce,D.A. (2004). Altered gene expression in the eye of a mouse model for batten disease. Invest Ophthalmol Vis Sci *45*, 2893-2905.

Chen,J., Magavi,S.S., and Macklis,J.D. (2004). Neurogenesis of corticospinal motor neurons extending spinal projections in adult mice. Proc Natl Acad Sci U S A *101*, 16357-16362.

Chenn,A. and McConnell,S.K. (1995). Cleavage orientation and the asymmetric inheritance of Notch1 immunoreactivity in mammalian neurogenesis. Cell *82*, 631-641.

Chow,L., Levine,E.M., and Reh,T.A. (1998). The nuclear receptor transcription factor, retinoid-related orphan receptor beta, regulates retinal progenitor proliferation. Mech. Dev. *77*, 149-164.

Chow,R.L. and Lang,R.A. (2001). Early eye development in vertebrates. Annu. Rev. Cell Dev. Biol. *17*, 255-296.

Chu,Y., Humphrey,M.F., and Constable,I.J. (1993). Horizontal cells of the normal and dystrophic rat retina: a wholemount study using immunolabelling for the 28-kDa calcium-binding protein. Exp. Eye Res. *57*, 141-148.

Collavin,L., Buzzai,M., Saccone,S., Bernard,L., Federico,C., DellaValle,G., Brancolini,C., and Schneider,C. (1998). cDNA characterization and chromosome mapping of the human GAS2 gene. Genomics *48*, 265-269.

Collinson,J.M., Hill,R.E., and West,J.D. (2000). Different roles for Pax6 in the optic vesicle and facial epithelium mediate early morphogenesis of the murine eye. Development *127*, 945-956.

Condie,B.G. and Capecchi,M.R. (1993). Mice homozygous for a targeted disruption of Hoxd-3 (Hox-4.1) exhibit anterior transformations of the first and second cervical vertebrae, the atlas and the axis. Development *119*, 579-595.

Condie,B.G. and Capecchi,M.R. (1994). Mice with targeted disruptions in the paralogous genes hoxa-3 and hoxd- 3 reveal synergistic interactions. Nature *370*, 304-307.

Constantine, L. and Harrington, C. (2001) Use of GeneChip high-density oligonucleotide arrays for gene expression monitoring. Life Science News Online, Amersham Biosciences, Articles by Application .

Corbo,J.C. and Cepko,C.L. (2005). A Hybrid Photoreceptor Expressing Both Rod and Cone Genes in a Mouse Model of Enhanced S-Cone Syndrome. PLoS Genet *1*, e11.

Costa,T., Scriver,C.R., and Childs,B. (1985). The effect of Mendelian disease on human health: a measurement. Am. J Med. Genet *21*, 231-242.

Cunningham,J.J., Levine,E.M., Zindy,F., Goloubeva,O., Roussel,M.F., and Smeyne,R.J. (2002). The cyclin-dependent kinase inhibitors p19(Ink4d) and p27(Kip1) are coexpressed in select retinal cells and act cooperatively to control cell cycle exit. Mol. Cell Neurosci. *19*, 359-374.

Curtis,M.A., Penney,E.B., Pearson,A.G., Roon-Mom,W.M., Butterworth,N.J., Dragunow,M., Connor,B., and Faull,R.L. (2003). Increased cell proliferation and neurogenesis in the adult human Huntington's disease brain. Proc Natl Acad Sci U S A *100*, 9023-9027.

Dattani,M.T., Martinez-Barbera,J.P., Thomas,P.Q., Brickman,J.M., Gupta,R., Wales,J.K., Hindmarsh,P.C., Beddington,R.S., and Robinson,I.C. (1999). HESX1: a novel gene implicated in a familial form of septo-optic dysplasia. Acta Paediatr. Suppl *88*, 49-54.

Davanger,M. and Evensen,A. (1971). Role of the pericorneal papillary structure in renewal of corneal epithelium. Nature *229*, 560-561.

de Melo,J., Du,G., Fonseca,M., Gillespie,L.A., Turk,W.J., Rubenstein,J.L., and Eisenstat,D.D. (2005). Dlx1 and Dlx2 function is necessary for terminal

differentiation and survival of late-born retinal ganglion cells in the developing mouse retina. Development *132*, 311-322.

de Melo,J., Qiu,X., Du,G., Cristante,L., and Eisenstat,D.D. (2003). Dlx1, Dlx2, Pax6, Brn3b, and Chx10 homeobox gene expression defines the retinal ganglion and inner nuclear layers of the developing and adult mouse retina. J. Comp Neurol. *461*, 187-204.

Dizhoor,A.M., Ray,S., Kumar,S., Niemi,G., Spencer,M., Brolley,D., Walsh,K.A., Philipov,P.P., Hurley,J.B., and Stryer,L. (1991). Recoverin: a calcium sensitive activator of retinal rod guanylate cyclase. Science *251*, 915-918.

Doetsch,F., Garcia-Verdugo,J.M., and Alvarez-Buylla,A. (1999). Regeneration of a germinal layer in the adult mammalian brain. Proc Natl Acad Sci U S A *96*, 11619-11624.

Dolle,P., Dierich,A., LeMeur,M., Schimmang,T., Schuhbaur,B., Chambon,P., and Duboule,D. (1993). Disruption of the Hoxd-13 gene induces localized heterochrony leading to mice with neotenic limbs. Cell *75*, 431-441.

Dolle,P., Fraulob,V., Kastner,P., and Chambon,P. (1994). Developmental expression of murine retinoid X receptor (RXR) genes. Mech Dev *45*, 91-104.

Dolle,P., Price,M., and Duboule,D. (1992). Expression of the murine Dlx-1 homeobox gene during facial, ocular and limb development. Differentiation *49*, 93-99.

Dooley,C.M., James,J., Jane,M.C., and Ahmad,I. (2003). Involvement of numb in vertebrate retinal development: evidence for multiple roles of numb in neural differentiation and maturation. J. Neurobiol. *54*, 313-325.

Dorval,K.M., Bobechko,B.P., Ahmad,K.F., and Bremner,R. (2005). Transcriptional activity of the paired-like homeodomain proteins CHX10 and VSX1. J. Biol. Chem. *280*, 10100-10108.

Dowling,J.E. (1987). The retina. An approachable part of the brain. (Cambridge, Massachusetts: Belknop press of Harvard University Press).

Dressler,G.R., Deutsch,U., Chowdhury,K., Nornes,H.O., and Gruss,P. (1990). Pax2, a new murine paired-box-containing gene and its expression in the developing excretory system. Development *109*, 787-795.

Duboule,D. (1995). Vertebrate Hox genes and proliferation: an alternative pathway to homeosis? Curr. Opin. Genet. Dev. *5*, 525-528.

Duncan,L.M., Deeds,J., Hunter,J., Shao,J., Holmgren,L.M., Woolf,E.A., Tepper,R.I., and Shyjan,A.W. (1998). Down-regulation of the novel gene melastatin correlates with potential for melanoma metastasis. Cancer Res. *58*, 1515-1520.

Dyer,M.A. and Cepko,C.L. (2001). Regulating proliferation during retinal development. Nat. Rev. Neurosci. *2*, 333-342.

Eguchi,G. (1988). Cellular and molecular background of wolffian lens regeneration. Cell Differ Dev *25 Suppl*, 147-158.

Eguchi,G. and Shingai,R. (1971). Cellular analysis on localization of lens forming potency in the newt iris epithelium. Dev Growth Differ *13*, 337-349.

Eisenstat,D.D., Liu,J.K., Mione,M., Zhong,W., Yu,G., Anderson,S.A., Ghattas,I., Puelles,L., and Rubenstein,J.L. (1999). DLX-1, DLX-2, and DLX-5 expression define distinct stages of basal forebrain differentiation. J. Comp Neurol. *414*, 217-237.

Eng,S.R., Lanier,J., Fedtsova,N., and Turner,E.E. (2004). Coordinated regulation of gene expression by Brn3a in developing sensory ganglia. Development *131*, 3859-3870.

Fantes,J., Ragge,N.K., Lynch,S.A., McGill,N.I., Collin,J.R., Howard-Peebles,P.N., Hayward,C., Vivian,A.J., Williamson,K., van,H., V, and FitzPatrick,D.R. (2003). Mutations in SOX2 cause anophthalmia. Nat. Genet. *33*, 461-463.

Fantl,V., Stamp,G., Andrews,A., Rosewell,I., and Dickson,C. (1995). Mice lacking cyclin D1 are small and show defects in eye and mammary gland development. Genes Dev. *9*, 2364-2372.

Favor,J., Sandulache,R., Neuhauser-Klaus,A., Pretsch,W., Chatterjee,B., Senft,E., Wurst,W., Blanquet,V., Grimes,P., Sporle,R., and Schughart,K. (1996). The mouse Pax2(1Neu) mutation is identical to a human PAX2 mutation in a family with renal-coloboma syndrome and results in developmental defects of the brain, ear, eye, and kidney. Proc. Natl. Acad. Sci. U. S. A *93*, 13870-13875.

Ferda,P.E., Ploder,L.A., Yu,J.J., Arici,K., Horsford,D.J., Rutherford,A., Bapat,B., Cox,D.W., Duncan,A.M., Kalnins,V.I., Kocak-Altintas,A., Sowden,J.C., Traboulsi,E., Sarfarazi,M., and McInnes,R.R. (2000). Human microphthalmia associated with mutations in the retinal homeobox gene CHX10. Nat. Genet. *25*, 397-401.

Fischer,A.J. and Reh,T.A. (2000). Identification of a proliferating marginal zone of retinal progenitors in postnatal chickens. Dev. Biol. *220*, 197-210.

Fischer,A.J. and Reh,T.A. (2001). Muller glia are a potential source of neural regeneration in the postnatal chicken retina. Nat. Neurosci. *4*, 247-252.

Fischer,A.J., Wang,S.Z., and Reh,T.A. (2004). NeuroD induces the expression of visinin and calretinin by proliferating cells derived from toxin-damaged chicken retina. Dev. Dyn. *229*, 555-563.

Franz,T. and Besecke,A. (1991). The development of the eye in homozygotes of the mouse mutant Extra- toes. Anat Embryol. (Berl) *184*, 355-361.

Freund,C., Horsford,D.J., and McInnes,R.R. (1996). Transcription factor genes and the developing eye: a genetic perspective. Hum. Mol. Genet. *5 Spec No*, 1471-1488.

Fryns,J.P. (1995). Autosomal dominant simple microphthalmos: incomplete penetrance and variable expression in a large family. J. Med. Genet. *32*, 326.

Fuhrmann,S., Levine,E.M., and Reh,T.A. (2000). Extraocular mesenchyme patterns the optic vesicle during early eye development in the embryonic chick. Development *127*, 4599-4609.

Furukawa,T., Morrow,E.M., and Cepko,C.L. (1997). Crx, a novel otx-like homeobox gene, shows photoreceptor-specific expression and regulates photoreceptor differentiation. Cell *91*, 531-541.

Furukawa,T., Morrow,E.M., Li,T., Davis,F.C., and Cepko,C.L. (1999). Retinopathy and attenuated circadian entrainment in Crx-deficient mice. Nat. Genet *23*, 466-470.

Furukawa,T., Mukherjee,S., Bao,Z.Z., Morrow,E.M., and Cepko,C.L. (2000). rax, Hes1, and notch1 promote the formation of Muller glia by postnatal retinal progenitor cells. Neuron *26*, 383-394.

Furuse,M., Fujita,K., Hiiragi,T., Fujimoto,K., and Tsukita,S. (1998). Claudin-1 and -2: novel integral membrane proteins localizing at tight junctions with no sequence similarity to occludin. J. Cell Biol. *141*, 1539-1550.

Furuta,Y. and Hogan,B.L. (1998). BMP4 is essential for lens induction in the mouse embryo. Genes Dev *12*, 3764-3775.

Gage,F.H. (2000). Mammalian neural stem cells. Science *287*, 1433-1438.

Gallardo,M.E., Rodriguez,D.C., Schneider,A.S., Dwyer,M.A., Ayuso,C., and Bovolenta,P. (2004). Analysis of the developmental SIX6 homeobox gene in patients with anophthalmia/microphthalmia. Am. J Med. Genet A *129*, 92-94.

Geng,Y., Yu,Q., Sicinska,E., Das,M., Bronson,R.T., and Sicinski,P. (2001). Deletion of the p27Kip1 gene restores normal development in cyclin D1- deficient mice. Proc. Natl. Acad. Sci. U. S. A *98*, 194-199.

Ghose,S., Singh,N.P., Kaur,D., and Verma,I.C. (1991). Microphthalmos and anterior segment dysgenesis in a family. Ophthalmic Paediatr. Genet. *12*, 177-182.

Gibson-Brown,J.J., Agulnik,I., Silver,L.M., and Papaioannou,V.E. (1998). Expression of T-box genes Tbx2-Tbx5 during chick organogenesis. Mech Dev *74*, 165-169.

Gouge,A., Holt,J., Hardy,A.P., Sowden,J.C., and Smith,H.K. (2001). Foxn4--a new member of the forkhead gene family is expressed in the retina. Mech. Dev. *107*, 203-206.

Graham,C.A., Redmond,R.M., and Nevin,N.C. (1991). X-linked clinical anophthalmos. Localization of the gene to Xq27-Xq28. Ophthalmic Paediatr. Genet. *12*, 43-48.

Graw,J. (1996). Genetic aspects of embryonic eye development in vertebrates. Dev. Genet. *18*, 181-197.

Green,E.S., Stubbs,J.L., and Levine,E.M. (2003). Genetic rescue of cell number in a mouse model of microphthalmia: interactions between Chx10 and G1-phase cell cycle regulators. Development *130*, 539-552.

Gudas,J.M., Payton,M., Thukral,S., Chen,E., Bass,M., Robinson,M.O., and Coats,S. (1999). Cyclin E2, a novel G1 cyclin that binds Cdk2 and is aberrantly expressed in human cancers. Mol. Cell Biol. *19*, 612-622.

Hagell,P., Piccini,P., Bjorklund,A., Brundin,P., Rehncrona,S., Widner,H., Crabb,L., Pavese,N., Oertel,W.H., Quinn,N., Brooks,D.J., and Lindvall,O. (2002). Dyskinesias following neural transplantation in Parkinson's disease. Nat Neurosci *5*, 627-628.

Halder,G., Callaerts,P., and Gehring,W.J. (1995). Induction of ectopic eyes by targeted expression of the eyeless gene in Drosophila. Science *267*, 1788-1792.

Hamada,S. and Fujita,S. (1983). DAPI staining improved for quantitative cytofluorometry. Histochemistry *79*, 219-226.

Han,S.S., Liu,Y., Tyler-Polsz,C., Rao,M.S., and Fischer,I. (2004). Transplantation of glial-restricted precursor cells into the adult spinal cord: survival, glial-specific differentiation, and preferential migration in white matter. Glia *45*, 1-16.

Hanashima,C., Shen,L., Li,S.C., and Lai,E. (2002). Brain factor-1 controls the proliferation and differentiation of neocortical progenitor cells through independent mechanisms. J. Neurosci. *22*, 6526-6536.

Harris,W.A. (1997). Cellular diversification in the vertebrate retina. Curr. Opin. Genet. Dev. *7*, 651-658.

Hatakeyama,J. and Kageyama,R. (2004). Retinal cell fate determination and bHLH factors. Semin Cell Dev Biol *15*, 83-89.

Hatakeyama,J., Tomita,K., Inoue,T., and Kageyama,R. (2001). Roles of homeobox and bHLH genes in specification of a retinal cell type. Development *128*, 1313-1322.

Hatini,V., Tao,W., and Lai,E. (1994). Expression of winged helix genes, BF-1 and BF-2, define adjacent domains within the developing forebrain and retina. J Neurobiol *25*, 1293-1309.

Hendzel,M.J., Wei,Y., Mancini,M.A., Van Hooser,A., Ranalli,T., Brinkley,B.R., Bazett-Jones,D.P., and Allis,C.D. (1997). Mitosis-specific phosphorylation of histone H3 initiates primarily within pericentromeric heterochromatin during G2 and spreads in an ordered fashion coincident with mitotic chromosome condensation. Chromosoma *106*, 348-360.

Hill,R.E., Favor,J., Hogan,B.L., Ton,C.C., Saunders,G.F., Hanson,I.M., Prosser,J., Jordan,T., Hastie,N.D., and van,H., V (1991). Mouse small eye results from mutations in a paired-like homeobox- containing gene. Nature *354*, 522-525.

Hirsch,N. and Harris,W.A. (1997). Xenopus Pax-6 and retinal development. J. Neurobiol. *32*, 45-61.

Hodgkinson,C.A., Moore,K.J., Nakayama,A., Steingrimsson,E., Copeland,N.G., Jenkins,N.A., and Arnheiter,H. (1993). Mutations at the mouse microphthalmia locus are associated with defects in a gene encoding a novel basic-helix-loop-helix-zipper protein. Cell *74*, 395-404.

Hoefnagel,D., Keenan,M.E., and Allen,F.H. (1963). Heredofamilial bilateral anophthalmia. Arch. Ophthalmol. *69*, 760-764.

Hollborn,M., Tenckhoff,S., Jahn,K., Iandiev,I., Biedermann,B., Schnurrbusch,U.E., Limb,G.A., Reichenbach,A., Wolf,S., Wiedemann,P., Kohen,L., and Bringmann,A. (2005). Changes in retinal gene expression in proliferative vitreoretinopathy: glial cell expression of HB-EGF. Mol Vis *11*, 397-413.

Holt,C.E., Bertsch,T.W., Ellis,H.M., and Harris,W.A. (1988). Cellular determination in the Xenopus retina is independent of lineage and birth date. Neuron *1*, 15-26.

Honjo,M., Tanihara,H., Suzuki,S., Tanaka,T., Honda,Y., and Takeichi,M. (2000). Differential expression of cadherin adhesion receptors in neural retina of the postnatal mouse. Invest Ophthalmol. Vis. Sci. *41*, 546-551.

Hoover,F., Seleiro,E.A., Kielland,A., Brickell,P.M., and Glover,J.C. (1998). Retinoid X receptor gamma gene transcripts are expressed by a subset of early generated retinal cells and eventually restricted to photoreceptors. J. Comp Neurol. *391*, 204-213.

Horsford,D.J., Nguyen,M.T., Sellar,G.C., Kothary,R., Arnheiter,H., and McInnes,R.R. (2005). Chx10 repression of Mitf is required for the maintenance of mammalian neuroretinal identity. Development *132*, 177-187.

Hubank,M. and Schatz,D.G. (1994). Identifying differences in mRNA expression by representational difference analysis of cDNA. Nucleic Acids Res *22*, 5640-5648.

Hui,C.C. and Joyner,A.L. (1993). A mouse model of greig cephalopolysyndactyly syndrome: the extra-toesJ mutation contains an intragenic deletion of the Gli3 gene. Nat. Genet *3*, 241-246.

Hunter,J.J., Shao,J., Smutko,J.S., Dussault,B.J., Nagle,D.L., Woolf,E.A., Holmgren,L.M., Moore,K.J., and Shyjan,A.W. (1998). Chromosomal localization and genomic characterization of the mouse melastatin gene (Mlsn1). Genomics *54*, 116-123.

Hyatt,G.A. and Dowling,J.E. (1997). Retinoic acid. A key molecule for eye and photoreceptor development. Invest Ophthalmol. Vis. Sci. *38*, 1471-1475.

Hyatt,G.A., Schmitt,E.A., Marsh-Armstrong,N., McCaffery,P., Drager,U.C., and Dowling,J.E. (1996). Retinoic acid establishes ventral retinal characteristics. Development *122*, 195-204.

Hyer,J., Mima,T., and Mikawa,T. (1998). FGF1 patterns the optic vesicle by directing the placement of the neural retina domain. Development *125*, 869-877.

Imokawa,Y. and Brockes,J.P. (2003). Selective activation of thrombin is a critical determinant for vertebrate lens regeneration. Curr Biol *13*, 877-881.

Inoue,T., Hojo,M., Bessho,Y., Tano,Y., Lee,J.E., and Kageyama,R. (2002). Math3 and NeuroD regulate amacrine cell fate specification in the retina. Development *129*, 831-842.

Isaac,A., Rodriguez-Esteban,C., Ryan,A., Altabef,M., Tsukui,T., Patel,K., Tickle,C., and Izpisua-Belmonte,J.C. (1998). Tbx genes and limb identity in chick embryo development. Development *125*, 1867-1875.

Jackson,I.J., Chambers,D.M., Tsukamoto,K., Copeland,N.G., Gilbert,D.J., Jenkins,N.A., and Hearing,V. (1992). A second tyrosinase-related protein, TRP-2, maps to and is mutated at the mouse slaty locus. Embo J *11*, 527-535.

Janssen,J.J., Kuhlmann,E.D., van Vugt,A.H., Winkens,H.J., Janssen,B.P., Deutman,A.F., and Driessen,C.A. (1999). Retinoic acid receptors and retinoid X receptors in the mature retina: subtype determination and cellular distribution. Curr. Eye Res. *19*, 338-347.

Jean,D., Ewan,K., and Gruss,P. (1998). Molecular regulators involved in vertebrate eye development. Mech. Dev. *76*, 3-18.

Johns,P.R. (1977). Growth of the adult goldfish eye. III. Source of the new retinal cells. J Comp Neurol *176*, 343-357.

Johns,P.R. and Easter,S.S., Jr. (1977). Growth of the adult goldfish eye. II. Increase in retinal cell number. J Comp Neurol *176*, 331-341.

Jones,S.E., Jomary,C., Grist,J., Stewart,H.J., and Neal,M.J. (2000). Altered expression of secreted frizzled-related protein-2 in retinitis pigmentosa retinas. Invest Ophthalmol Vis Sci *41*, 1297-1301.

Kallen,B., Robert,E., and Harris,J. (1996). The descriptive epidemiology of anophthalmia and microphthalmia. Int. J. Epidemiol. *25*, 1009-1016.

Kastner,P., Grondona,J.M., Mark,M., Gansmuller,A., LeMeur,M., Decimo,D., Vonesch,J.L., Dolle,P., and Chambon,P. (1994). Genetic analysis of RXR alpha developmental function: convergence of RXR and RAR signaling pathways in heart and eye morphogenesis. Cell *78*, 987-1003.

Kavathas,P., Sukhatme,V.P., Herzenberg,L.A., and Parnes,J.R. (1984). Isolation of the gene encoding the human T-lymphocyte differentiation antigen Leu-2 (T8) by gene transfer and cDNA subtraction. Proc Natl Acad Sci U S A *81*, 7688-7692.

Kee,N., Sivalingam,S., Boonstra,R., and Wojtowicz,J.M. (2002). The utility of Ki-67 and BrdU as proliferative markers of adult neurogenesis. J. Neurosci. Methods *115*, 97-105.

Kelley,M.W., Turner,J.K., and Reh,T.A. (1994). Retinoic acid promotes differentiation of photoreceptors in vitro. Development *120*, 2091-2102.

Kelley,M.W., Turner,J.K., and Reh,T.A. (1995a). Regulation of proliferation and photoreceptor differentiation in fetal human retinal cell cultures. Invest Ophthalmol. Vis. Sci. *36*, 1280-1289.

Kelley, M. W., Williams, R. C., Turner, J. K., and Reh, T. A. The developing neural retina expresses the RXR gamma receptor and forms additional rod photoreceptors after exposure to retinoic acid. Soc.Neurosci. 21, 530. 1995b.
Ref Type: Abstract

Kenyon,K.L., Moody,S.A., and Jamrich,M. (1999). A novel fork head gene mediates early steps during Xenopus lens formation. Development *126*, 5107-5116.

Kim,W.Y., Fritzsch,B., Serls,A., Bakel,L.A., Huang,E.J., Reichardt,L.F., Barth,D.S., and Lee,J.E. (2001). NeuroD-null mice are deaf due to a severe loss of the inner ear sensory neurons during development. Development *128*, 417-426.

Kobayashi,M., Nishikawa,K., Suzuki,T., and Yamamoto,M. (2001). The homeobox protein Six3 interacts with the Groucho corepressor and acts as a transcriptional repressor in eye and forebrain formation. Dev. Biol. *232*, 315-326.

Kobayashi,T., Urabe,K., Orlow,S.J., Higashi,K., Imokawa,G., Kwon,B.S., Potterf,B., and Hearing,V.J. (1994). The Pmel 17/silver locus protein. Characterization and investigation of its melanogenic function. J Biol Chem *269*, 29198-29205.

Kohn,G., el Shawwa,R., and el Rayyes,E. (1988). Isolated "clinical anophthalmia" in an extensively affected Arab kindred. Clin. Genet. *33*, 321-324.

Konyukhov,B.V. and Sazhina,M.V. (1966). Interaction of the genes of ocular retardation and microphthalmia in mice. Folia Biol. (Praha) *12*, 116-123.

Konyukhov,B.V. and Sazhina,M.V. (1971). Genetic control over the duration of G 1 phase. Experientia *27*, 970-971.

Korematsu,K., Goto,S., Okamura,A., and Ushio,Y. (1998). Heterogeneity of cadherin-8 expression in the neonatal rat striatum: comparison with striatal compartments. Exp. Neurol. *154*, 531-536.

Korematsu,K. and Redies,C. (1997). Expression of cadherin-8 mRNA in the developing mouse central nervous system. J. Comp Neurol. *387*, 291-306.

Koshiba-Takeuchi,K., Takeuchi,J.K., Matsumoto,K., Momose,T., Uno,K., Hoepker,V., Ogura,K., Takahashi,N., Nakamura,H., Yasuda,K., and Ogura,T. (2000). Tbx5 and the retinotectum projection. Science *287*, 134-137.

Krauss,S., Johansen,T., Korzh,V., Moens,U., Ericson,J.U., and Fjose,A. (1991). Zebrafish pax[zf-a]: a paired box-containing gene expressed in the neural tube. EMBO J. *10*, 3609-3619.

Krezel,W., Ghyselinck,N., Samad,T.A., Dupe,V., Kastner,P., Borrelli,E., and Chambon,P. (1998). Impaired locomotion and dopamine signaling in retinoid receptor mutant mice. Science *279*, 863-867.

Krishan,A. (1975). Rapid flow cytofluorometric analysis of mammalian cell cycle by propidium iodide staining. J. Cell Biol. *66*, 188-193.

Krumlauf,R. (1993a). Hox genes and pattern formation in the branchial region of the vertebrate head. Trends Genet. *9*, 106-112.

Krumlauf,R. (1993b). Mouse Hox genetic functions. Curr. Opin. Genet. Dev. *3*, 621-625.

Kubo,F., Takeichi,M., and Nakagawa,S. (2005). Wnt2b inhibits differentiation of retinal progenitor cells in the absence of Notch activity by downregulating the expression of proneural genes. Development *132*, 2759-2770.

Kubota,R., Hokoc,J.N., Moshiri,A., McGuire,C., and Reh,T.A. (2002). A comparative study of neurogenesis in the retinal ciliary marginal zone of homeothermic vertebrates. Brain Res. Dev. Brain Res. *134*, 31-41.

Kurki,P., Ogata,K., and Tan,E.M. (1988). Monoclonal antibodies to proliferating cell nuclear antigen (PCNA)/cyclin as probes for proliferating cells by immunofluorescence microscopy and flow cytometry. J. Immunol. Methods *109*, 49-59.

Kwon,B.S., Chintamaneni,C., Kozak,C.A., Copeland,N.G., Gilbert,D.J., Jenkins,N., Barton,D., Francke,U., Kobayashi,Y., and Kim,K.K. (1991). A melanocyte-specific gene, Pmel 17, maps near the silver coat color locus on mouse chromosome 10 and is in a syntenic region on human chromosome 12. Proc Natl Acad Sci U S A *88*, 9228-9232.

Lauper,N., Beck,A.R., Cariou,S., Richman,L., Hofmann,K., Reith,W., Slingerland,J.M., and Amati,B. (1998). Cyclin E2: a novel CDK2 partner in the late G1 and S phases of the mammalian cell cycle. Oncogene *17*, 2637-2643.

Lee,C.S., May,N.R., and Fan,C.M. (2001). Transdifferentiation of the ventral retinal pigmented epithelium to neural retina in the growth arrest specific gene 1 mutant. Dev. Biol *236*, 17-29.

Lee,J.E., Hollenberg,S.M., Snider,L., Turner,D.L., Lipnick,N., and Weintraub,H. (1995). Conversion of Xenopus ectoderm into neurons by NeuroD, a basic helix-loop-helix protein. Science *268*, 836-844.

Lee,K.K., Tang,M.K., Yew,D.T., Chow,P.H., Yee,S.P., Schneider,C., and Brancolini,C. (1999). gas2 is a multifunctional gene involved in the regulation of apoptosis and chondrogenesis in the developing mouse limb. Dev Biol *207*, 14-25.

Lee,M.H., Williams,B.O., Mulligan,G., Mukai,S., Bronson,R.T., Dyson,N., Harlow,E., and Jacks,T. (1996a). Targeted disruption of p107: functional overlap between p107 and Rb. Genes Dev. *10*, 1621-1632.

Lee,Z.H., Hou,L., Moellmann,G., Kuklinska,E., Antol,K., Fraser,M., Halaban,R., and Kwon,B.S. (1996b). Characterization and subcellular localization of human Pmel 17/silver, a 110-kDa (pre)melanosomal membrane protein associated with 5,6,-

dihydroxyindole-2-carboxylic acid (DHICA) converting activity. J Invest Dermatol. *106*, 605-610.

Leitges,M., Schmedt,C., Guinamard,R., Davoust,J., Schaal,S., Stabel,S., and Tarakhovsky,A. (1996). Immunodeficiency in protein kinase cbeta-deficient mice. Science *273*, 788-791.

Li,H., Tierney,C., Wen,L., Wu,J.Y., and Rao,Y. (1997). A single morphogenetic field gives rise to two retina primordia under the influence of the prechordal plate. Development *124*, 603-615.

Liang,P. and Pardee,A.B. (1992). Differential display of eukaryotic messenger RNA by means of the polymerase chain reaction. Science *257*, 967-971.

Lillien,L. (1998). Neural progenitors and stem cells: mechanisms of progenitor heterogeneity. Curr Opin Neurobiol *8*, 37-44.

Liu,I.S., Chen,J.D., Ploder,L., Vidgen,D., van der Kooy,D., Kalnins,V.I., and McInnes,R.R. (1994a). Developmental expression of a novel murine homeobox gene (Chx10): evidence for roles in determination of the neuroretina and inner nuclear layer. Neuron *13*, 377-393.

Liu,I.S., Chen,J.D., Ploder,L., Vidgen,D., van der,K.D., Kalnins,V.I., and McInnes,R.R. (1994b). Developmental expression of a novel murine homeobox gene (Chx10): evidence for roles in determination of the neuroretina and inner nuclear layer. Neuron *13*, 377-393.

Liu,M., Pleasure,S.J., Collins,A.E., Noebels,J.L., Naya,F.J., Tsai,M.J., and Lowenstein,D.H. (2000a). Loss of BETA2/NeuroD leads to malformation of the dentate gyrus and epilepsy. Proc. Natl. Acad. Sci. U. S. A *97*, 865-870.

Liu,W., Khare,S.L., Liang,X., Peters,M.A., Liu,X., Cepko,C.L., and Xiang,M. (2000b). All Brn3 genes can promote retinal ganglion cell differentiation in the chick. Development *127*, 3237-3247.

Liu,Y., Dehni,G., Purcell,K.J., Sokolow,J., Carcangiu,M.L., Artavanis-Tsakonas,S., and Stifani,S. (1996). Epithelial expression and chromosomal location of human TLE genes: implications for notch signaling and neoplasia. Genomics *31*, 58-64.

Lockhart,D.J., Dong,H., Byrne,M.C., Follettie,M.T., Gallo,M.V., Chee,M.S., Mittmann,M., Wang,C., Kobayashi,M., Horton,H., and Brown,E.L. (1996). Expression monitoring by hybridization to high-density oligonucleotide arrays. Nat. Biotechnol. *14*, 1675-1680.

Loosli,F., Winkler,S., and Wittbrodt,J. (1999). Six3 overexpression initiates the formation of ectopic retina. Genes Dev *13*, 649-654.

Luo,L., Salunga,R.C., Guo,H., Bittner,A., Joy,K.C., Galindo,J.E., Xiao,H., Rogers,K.E., Wan,J.S., Jackson,M.R., and Erlander,M.G. (1999). Gene expression profiles of laser-captured adjacent neuronal subtypes. Nat. Med. *5*, 117-122.

Magavi,S.S., Leavitt,B.R., and Macklis,J.D. (2000). Induction of neurogenesis in the neocortex of adult mice. Nature *405*, 951-955.

Mahadevappa,M. and Warrington,J.A. (1999). A high-density probe array sample preparation method using 10- to 100-fold fewer cells. Nat. Biotechnol. *17*, 1134-1136.

Male,A., Davies,A., Bergbaum,A., Keeling,J., FitzPatrick,D., Mackie,O.C., and Berg,J. (2002). Delineation of an estimated 6.7 MB candidate interval for an anophthalmia gene at 3q26.33-q28 and description of the syndrome associated with visible chromosome deletions of this region. Eur J Hum. Genet *10*, 807-812.

Mangelsdorf,D.J., Borgmeyer,U., Heyman,R.A., Zhou,J.Y., Ong,E.S., Oro,A.E., Kakizuka,A., and Evans,R.M. (1992). Characterization of three RXR genes that mediate the action of 9-cis retinoic acid. Genes Dev. *6*, 329-344.

Manzow,S., Brancolini,C., Marks,F., and Richter,K.H. (1996). Expression of growth arrest-specific (Gas) genes in murine keratinocytes: Gas2 is specifically regulated. Exp. Cell Res *224*, 200-203.

Marquardt,T. and Gruss,P. (2002). Generating neuronal diversity in the retina: one for nearly all. Trends Neurosci. *25*, 32-38.

Martin,P., Carriere,C., Dozier,C., Quatannens,B., Mirabel,M.A., Vandenbunder,B., Stehelin,D., and Saule,S. (1992). Characterization of a paired box- and homeobox-containing quail gene (Pax-QNR) expressed in the neuroretina. Oncogene *7*, 1721-1728.

Martinez-Esparza,M., Jimenez-Cervantes,C., Bennett,D.C., Lozano,J.A., Solano,F., and Garcia-Borron,J.C. (1999). The mouse silver locus encodes a single transcript truncated by the silver mutation. Mamm. Genome *10*, 1168-1171.

Mathers,P.H., Grinberg,A., Mahon,K.A., and Jamrich,M. (1997). The Rx homeobox gene is essential for vertebrate eye development. Nature *387*, 603-607.

Matsuo,I., Kuratani,S., Kimura,C., Takeda,N., and Aizawa,S. (1995). Mouse Otx2 functions in the formation and patterning of rostral head. Genes Dev *9*, 2646-2658.

McAvoy,J.W., Chamberlain,C.G., de Iongh,R.U., Richardson,N.A., and Lovicu,F.J. (1991). The role of fibroblast growth factor in eye lens development. Ann. N. Y. Acad Sci *638*, 256-274.

McCabe,K.L., Gunther,E.C., and Reh,T.A. (1999). The development of the pattern of retinal ganglion cells in the chick retina: mechanisms that control differentiation. Development *126*, 5713-5724.

Meyer,J.S., Katz,M.L., Maruniak,J.A., and Kirk,M.D. (2005). Embryonic stem cell-derived neural progenitors incorporate into degenerating retina and enhance survival of host photoreceptors. Stem Cells. 0: 200500591 published online 25 August 2005.

Miyata,T., Maeda,T., and Lee,J.E. (1999). NeuroD is required for differentiation of the granule cells in the cerebellum and hippocampus. Genes Dev. *13*, 1647-1652.

Mochii,M., Ono,T., Matsubara,Y., and Eguchi,G. (1998). Spontaneous transdifferentiation of quail pigmented epithelial cell is accompanied by a mutation in the Mitf gene. Dev. Biol. *196*, 145-159.

Mody,M., Cao,Y., Cui,Z., Tay,K.Y., Shyong,A., Shimizu,E., Pham,K., Schultz,P., Welsh,D., and Tsien,J.Z. (2001). Genome-wide gene expression profiles of the developing mouse hippocampus. Proc. Natl. Acad. Sci. U. S. A *98*, 8862-8867.

Molday,R.S. (1989). Monoclonal antibodies to rhodopsin and other proteins or rod outer segments. Prog. Retin. Eye Res. *8*, 173-209.

Monaghan,A.P., Davidson,D.R., Sime,C., Graham,E., Baldock,R., Bhattacharya,S.S., and Hill,R.E. (1991). The Msh-like homeobox genes define domains in the developing vertebrate eye. Development *112*, 1053-1061.

Morata,G. (1993). Homeotic genes of Drosophila. Curr. Opin. Genet. Dev. *3*, 606-614.

Morle,L., Bozon,M., Zech,J.C., Alloisio,N., Raas-Rothschild,A., Philippe,C., Lambert,J.C., Godet,J., Plauchu,H., and Edery,P. (2000). A locus for autosomal dominant colobomatous microphthalmia maps to chromosome 15q12-q15. Am. J. Hum. Genet. *67*, 1592-1597.

Moroy,T. and Geisen,C. (2004). Cyclin E. Int J Biochem Cell Biol *36*, 1424-1439.

Morrison,D., FitzPatrick,D., Hanson,I., Williamson,K., van,H., V, Fleck,B., Jones,I., Chalmers,J., and Campbell,H. (2002). National study of microphthalmia, anophthalmia, and coloboma (MAC) in Scotland: investigation of genetic aetiology. J. Med. Genet. *39*, 16-22.

Morriss-Kay,G. (1993). Retinoic acid and craniofacial development: molecules and morphogenesis. Bioessays *15*, 9-15.

Morrow,E.M., Furukawa,T., Lee,J.E., and Cepko,C.L. (1999a). NeuroD regulates multiple functions in the developing neural retina in rodent. Development *126*, 23-36.

Morrow,E.M., Furukawa,T., Lee,J.E., and Cepko,C.L. (1999b). NeuroD regulates multiple functions in the developing neural retina in rodent. Development *126*, 23-36.

Moshiri,A., Close,J., and Reh,T.A. (2004). Retinal stem cells and regeneration. Int. J. Dev. Biol. *48*, 1003-1014.

Moshiri,A. and Reh,T.A. (2004). Persistent progenitors at the retinal margin of ptc+/- mice. J. Neurosci. *24*, 229-237.

Mutoh,H., Fung,B.P., Naya,F.J., Tsai,M.J., Nishitani,J., and Leiter,A.B. (1997). The basic helix-loop-helix transcription factor BETA2/NeuroD is expressed in mammalian enteroendocrine cells and activates secretin gene expression. Proc. Natl. Acad. Sci. U. S. A *94*, 3560-3564.

Nakamura,T., Yao,R., Ogawa,T., Suzuki,T., Ito,C., Tsunekawa,N., Inoue,K., Ajima,R., Miyasaka,T., Yoshida,Y., Ogura,A., Toshimori,K., Noce,T., Yamamoto,T., and Noda,T. (2004). Oligo-astheno-teratozoospermia in mice lacking Cnot7, a regulator of retinoid X receptor beta. Nat. Genet. *36*, 528-533.

Nakayama,A., Nguyen,M.T., Chen,C.C., Opdecamp,K., Hodgkinson,C.A., and Arnheiter,H. (1998). Mutations in microphthalmia, the mouse homolog of the human deafness gene MITF, affect neuroepithelial and neural crest-derived melanocytes differently. Mech. Dev. *70*, 155-166.

Nguyen,M. and Arnheiter,H. (2000). Signaling and transcriptional regulation in early mammalian eye development: a link between FGF and MITF. Development *127*, 3581-3591.

Nicoletti,I., Migliorati,G., Pagliacci,M.C., Grignani,F., and Riccardi,C. (1991). A rapid and simple method for measuring thymocyte apoptosis by propidium iodide staining and flow cytometry. J. Immunol. Methods *139*, 271-279.

Nistor,G.I., Totoiu,M.O., Haque,N., Carpenter,M.K., and Keirstead,H.S. (2005). Human embryonic stem cells differentiate into oligodendrocytes in high purity and myelinate after spinal cord transplantation. Glia *49*, 385-396.

Nornes,H.O., Dressler,G.R., Knapik,E.W., Deutsch,U., and Gruss,P. (1990). Spatially and temporally restricted expression of Pax2 during murine neurogenesis. Development *109*, 797-809.

Ogawa,Y., Sawamoto,K., Miyata,T., Miyao,S., Watanabe,M., Nakamura,M., Bregman,B.S., Koike,M., Uchiyama,Y., Toyama,Y., and Okano,H. (2002). Transplantation of in vitro-expanded fetal neural progenitor cells results in neurogenesis and functional recovery after spinal cord contusion injury in adult rats. J Neurosci Res *69*, 925-933.

Olanow,C.W., Kordower,J.H., and Freeman,T.B. (1996). Fetal nigral transplantation as a therapy for Parkinson's disease. Trends Neurosci *19*, 102-109.

Olofsson,B., Pajusola,K., von Euler,G., Chilov,D., Alitalo,K., and Eriksson,U. (1996). Genomic organization of the mouse and human genes for vascular endothelial growth factor B (VEGF-B) and characterization of a second splice isoform. J. Biol. Chem. *271*, 19310-19317.

Othman,M.I., Sullivan,S.A., Skuta,G.L., Cockrell,D.A., Stringham,H.M., Downs,C.A., Fornes,A., Mick,A., Boehnke,M., Vollrath,D., and Richards,J.E. (1998). Autosomal dominant nanophthalmos (NNO1) with high hyperopia and angle- closure glaucoma maps to chromosome 11. Am. J. Hum. Genet. *63*, 1411-1418.

Otto,F. and Tsou,K.C. (1985). A comparative study of DAPI, DIPI, and Hoechst 33258 and 33342 as chromosomal DNA stains. Stain Technol. *60*, 7-11.

Packer,S.O. (1967). The eye and skeletal effects of two mutant alleles at the microphthalmia locus of Mus musculus. J Exp. Zool. *165*, 21-45.

Papalopulu,N. and Kintner,C. (1996). A Xenopus gene, Xbr-1, defines a novel class of homeobox genes and is expressed in the dorsal ciliary margin of the eye. Dev Biol *174*, 104-114.

Paraoanu,L.E., Weiss,B., Robitzki,A.A., and Layer,P.G. (2005). Cytochrome-c oxidase is one of several genes elevated in marginal retina of the chick embryo. Neuroscience *132*, 665-672.

Payton,M. and Coats,S. (2002). Cyclin E2, the cycle continues. Int J Biochem Cell Biol *34*, 315-320.

Pearce,W.G. (1986). Corneal involvement in autosomal dominant coloboma/microphthalmos. Can. J. Ophthalmol. *21*, 291-294.

Pennesi,M.E., Cho,J.H., Yang,Z., Wu,S.H., Zhang,J., Wu,S.M., and Tsai,M.J. (2003). BETA2/NeuroD1 null mice: a new model for transcription factor-dependent photoreceptor degeneration. J. Neurosci. *23*, 453-461.

Pequignot,M.O., Provost,A.C., Salle,S., Taupin,P., Sainton,K.M., Marchant,D., Martinou,J.C., Ameisen,J.C., Jais,J.P., and Abitbol,M. (2003). Major role of BAX in apoptosis during retinal development and in establishment of a functional postnatal retina. Dev. Dyn. *228*, 231-238.

Perron,M. and Harris,W.A. (2000a). Determination of vertebrate retinal progenitor cell fate by the Notch pathway and basic helix-loop-helix transcription factors. Cell Mol. Life Sci. *57*, 215-223.

Perron,M. and Harris,W.A. (2000b). Retinal stem cells in vertebrates. Bioessays *22*, 685-688.

Peters,M.A. and Cepko,C.L. (2002). The dorsal-ventral axis of the neural retina is divided into multiple domains of restricted gene expression which exhibit features of lineage compartments. Dev Biol *251*, 59-73.

Pittack,C., Jones,M., and Reh,T.A. (1991). Basic fibroblast growth factor induces retinal pigment epithelium to generate neural retina in vitro. Development *113*, 577-588.

Pluchino,S., Furlan,R., and Martino,G. (2004). Cell-based remyelinating therapies in multiple sclerosis: evidence from experimental studies. Curr Opin Neurol *17*, 247-255.

Porter,F.D., Drago,J., Xu,Y., Cheema,S.S., Wassif,C., Huang,S.P., Lee,E., Grinberg,A., Massalas,J.S., Bodine,D., Alt,F., and Westphal,H. (1997). Lhx2, a LIM homeobox gene, is required for eye, forebrain, and definitive erythrocyte development. Development *124*, 2935-2944.

Porteus,M.H., Bulfone,A., Liu,J.K., Puelles,L., Lo,L.C., and Rubenstein,J.L. (1994). DLX-2, MASH-1, and MAP-2 expression and bromodeoxyuridine incorporation define molecularly distinct cell populations in the embryonic mouse forebrain. J. Neurosci. *14*, 6370-6383.

Pratt,T., Tian,N.M., Simpson,T.I., Mason,J.O., and Price,D.J. (2004). The winged helix transcription factor Foxg1 facilitates retinal ganglion cell axon crossing of the ventral midline in the mouse. Development *131*, 3773-3784.

Qian,J., Esumi,N., Chen,Y., Wang,Q., Chowers,I., and Zack,D.J. (2005). Identification of regulatory targets of tissue-specific transcription factors: application to retina-specific gene regulation. Nucleic Acids Res *33*, 3479-3491.

Qiu,M., Bulfone,A., Ghattas,I., Meneses,J.J., Christensen,L., Sharpe,P.T., Presley,R., Pedersen,R.A., and Rubenstein,J.L. (1997). Role of the Dlx homeobox genes in proximodistal patterning of the branchial arches: mutations of Dlx-1, Dlx-2, and Dlx-1 and -2 alter morphogenesis of proximal skeletal and soft tissue structures derived from the first and second arches. Dev. Biol. *185*, 165-184.

Qiu,M., Bulfone,A., Martinez,S., Meneses,J.J., Shimamura,K., Pedersen,R.A., and Rubenstein,J.L. (1995). Null mutation of Dlx-2 results in abnormal morphogenesis of proximal first and second branchial arch derivatives and abnormal differentiation in the forebrain. Genes Dev. *9*, 2523-2538.

Quinn,J.C., West,J.D., and Hill,R.E. (1996). Multiple functions for Pax6 in mouse eye and nasal development. Genes Dev *10*, 435-446.

Quiring,R., Walldorf,U., Kloter,U., and Gehring,W.J. (1994). Homology of the eyeless gene of Drosophila to the Small eye gene in mice and Aniridia in humans. Science *265*, 785-789.

Ragge,N.K., Brown,A.G., Poloschek,C.M., Lorenz,B., Henderson,R.A., Clarke,M.P., Russell-Eggitt,I., Fielder,A., Gerrelli,D., Martinez-Barbera,J.P., Ruddle,P., Hurst,J., Collin,J.R., Salt,A., Cooper,S.T., Thompson,P.J., Sisodiya,S.M., Williamson,K.A., FitzPatrick,D.R., van,H., V, and Hanson,I.M. (2005a). Heterozygous Mutations of OTX2 Cause Severe Ocular Malformations. Am. J. Hum. Genet. *76*, 1008-1022.

Ragge,N.K., Lorenz,B., Schneider,A., Bushby,K., de Sanctis,L., de Sanctis,U., Salt,A., Collin,J.R., Vivian,A.J., Free,S.L., Thompson,P., Williamson,K.A., Sisodiya,S.M., van,H., V, and FitzPatrick,D.R. (2005b). SOX2 anophthalmia syndrome. Am. J. Med. Genet. A *135*, 1-7.

Rando,R.R. (1994). Isomerization reactions of retinoids in the visual system. Pure & Appl. Chem. *66*, 989-994.

Ratajczak,M.Z., Kant,J.A., Luger,S.M., Hijiya,N., Zhang,J., Zon,G., and Gewirtz,A.M. (1992). In vivo treatment of human leukemia in a scid mouse model with c-myb antisense oligodeoxynucleotides. Proc. Natl. Acad. Sci. U. S. A *89*, 11823-11827.

Ratineau,C., Petry,M.W., Mutoh,H., and Leiter,A.B. (2002). Cyclin D1 represses the basic helix-loop-helix transcription factor, BETA2/NeuroD. J. Biol. Chem. *277*, 8847-8853.

Rattner,A. and Nathans,J. (2005). The genomic response to retinal disease and injury: evidence for endothelin signaling from photoreceptors to glia. J Neurosci *25*, 4540-4549.

Rauchman, M., Christian, C, Luo, P, Ma, L, Satokata, I, and Maas, R. Genetic interaction of Pax6 and msx genes in lens induction. Dev Biol [186], B4. 1997. Ref Type: Abstract

Reh,T.A. (1992). Cellular interactions determine neuronal phenotypes in rodent retinal cultures. J Neurobiol *23*, 1067-1083.

Reh,T.A. and Levine,E.M. (1998). Multipotential stem cells and progenitors in the vertebrate retina. J. Neurobiol. *36*, 206-220.

Resnikoff,S., Pascolini,D., Etya'ale,D., Kocur,I., Pararajasegaram,R., Pokharel,G.P., and Mariotti,S.P. (2004). Global data on visual impairment in the year 2002. Bull. World Health Organ *82*, 844-851.

Rhinn,M., Dierich,A., Shawlot,W., Behringer,R.R., Le Meur,M., and Ang,S.L. (1998). Sequential roles for Otx2 in visceral endoderm and neuroectoderm for forebrain and midbrain induction and specification. Development *125*, 845-856.

Rieger,D.K., Reichenberger,E., McLean,W., Sidow,A., and Olsen,B.R. (2001). A double-deletion mutation in the Pitx3 gene causes arrested lens development in aphakia mice. Genomics *72*, 61-72.

Robb,R.M., Silver,J., and Sullivan,R.T. (1978). Ocular retardation (or) in the mouse. Invest Ophthalmol. Vis. Sci. *17*, 468-473.

Robitaille,J., MacDonald,M.L., Kaykas,A., Sheldahl,L.C., Zeisler,J., Dube,M.P., Zhang,L.H., Singaraja,R.R., Guernsey,D.L., Zheng,B., Siebert,L.F., Hoskin-Mott,A., Trese,M.T., Pimstone,S.N., Shastry,B.S., Moon,R.T., Hayden,M.R., Goldberg,Y.P., and Samuels,M.E. (2002). Mutant frizzled-4 disrupts retinal angiogenesis in familial exudative vitreoretinopathy. Nat. Genet. *32*, 326-330.

Rosnow,R.L. and Rosenthal,R. (1989). Definition and interpretation of interaction effects. Psychological Bulletin 143-146.

Rowan,S. and Cepko,C.L. (2004). Genetic analysis of the homeodomain transcription factor Chx10 in the retina using a novel multifunctional BAC transgenic mouse reporter. Dev. Biol. *271*, 388-402.

Rowan,S., Chen,C.M., Young,T.L., Fisher,D.E., and Cepko,C.L. (2004). Transdifferentiation of the retina into pigmented cells in ocular retardation mice defines a new function of the homeodomain gene Chx10. Development *131*, 5139-5152.

Rutherford,A.D., Dhomen,N., Smith,H.K., and Sowden,J.C. (2004). Delayed expression of the Crx gene and photoreceptor development in the Chx10-deficient retina. Invest Ophthalmol Vis Sci *45*, 375-384.

Sadler,T.W. (1990). Langman's Medical Embryology. (Baltimore, MD: Williams & Wilkins).

Saga,Y., Kobayashi,M., Ohta,H., Murai,N., Nakai,N., Oshima,M., and Taketo,M.M. (1999). Impaired extrapyramidal function caused by the targeted disruption of retinoid X receptor RXRgamma1 isoform. Genes Cells *4*, 219-228.

Saha,M.S., Servetnick,M., and Grainger,R.M. (1992). Vertebrate eye development. Curr. Opin. Genet. Dev. *2*, 582-588.

Sandberg,M.L., Sutton,S.E., Pletcher,M.T., Wiltshire,T., Tarantino,L.M., Hogenesch,J.B., and Cooke,M.P. (2005). c-Myb and p300 regulate hematopoietic stem cell proliferation and differentiation. Dev. Cell *8*, 153-166.

Santos,M.S., Gomes,J.A., Hofling-Lima,A.L., Rizzo,L.V., Romano,A.C., and Belfort,R., Jr. (2005). Survival analysis of conjunctival limbal grafts and amniotic membrane transplantation in eyes with total limbal stem cell deficiency. Am. J Ophthalmol *140*, 223-230.

Schaumberg,D.A. and Dana,M.R. (1996). The epidemiology of blindness: a global overview. Practical Optometry *7*, 192-196.

Schedl,A., Ross,A., Lee,M., Engelkamp,D., Rashbass,P., van,H., V, and Hastie,N.D. (1996). Influence of PAX6 gene dosage on development: overexpression causes severe eye abnormalities. Cell *86*, 71-82.

Schermer,A., Galvin,S., and Sun,T.T. (1986). Differentiation-related expression of a major 64K corneal keratin in vivo and in culture suggests limbal location of corneal epithelial stem cells. J Cell Biol *103*, 49-62.

Schindler, D, Bisop, D. F., Wallace, S, Wolfe, D. E., and Desnick, R. J. Characterization of alph-N-acetylglactosaminidase deficiency: a new neurodegenerative lysosomal disease. Pediat.Res. 23, 333A only. 1988.
Ref Type: Abstract

Schneider,J.W., Gu,W., Zhu,L., Mahdavi,V., and Nadal-Ginard,B. (1994). Reversal of terminal differentiation mediated by p107 in Rb-/- muscle cells. Science *264*, 1467-1471.

Scholtz,C.L. and Chan,K.K. (1987). Complicated colobomatous microphthalmia in the microphthalmic (mi/mi) mouse. Development *99*, 501-508.

Schulte,D. and Cepko,C.L. (2000). Two homeobox genes define the domain of EphA3 expression in the developing chick retina. Development *127*, 5033-5045.

Schulte,D., Furukawa,T., Peters,M.A., Kozak,C.A., and Cepko,C.L. (1999). Misexpression of the Emx-related homeobox genes cVax and mVax2 ventralizes the retina and perturbs the retinotectal map. Neuron *24*, 541-553.

Schulze,A. and Downward,J. (2001). Navigating gene expression using microarrays--a technology review. Nat. Cell Biol. *3*, E190-E195.

Schwartzman,M.L., Balazy,M., Masferrer,J., Abraham,N.G., McGiff,J.C., and Murphy,R.C. (1987). 12(R)-hydroxyicosatetraenoic acid: a cytochrome-P450-

dependent arachidonate metabolite that inhibits Na+,K+-ATPase in the cornea. Proc. Natl. Acad. Sci. U. S. A *84*, 8125-8129.

Shen,M., Kawamoto,T., Yan,W., Nakamasu,K., Tamagami,M., Koyano,Y., Noshiro,M., and Kato,Y. (1997). Molecular characterization of the novel basic helix-loop-helix protein DEC1 expressed in differentiated human embryo chondrocytes. Biochem. Biophys. Res. Commun. *236*, 294-298.

Silva,A.O., Ercole,C.E., and McLoon,S.C. (2002). Plane of cell cleavage and numb distribution during cell division relative to cell differentiation in the developing retina. J Neurosci *22*, 7518-7525.

Silvestre,J.S., Tamarat,R., Ebrahimian,T.G., Le Roux,A., Clergue,M., Emmanuel,F., Duriez,M., Schwartz,B., Branellec,D., and Levy,B.I. (2003). Vascular endothelial growth factor-B promotes in vivo angiogenesis. Circ. Res. *93*, 114-123.

Simeone,A., Acampora,D., Mallamaci,A., Stornaiuolo,A., D'Apice,M.R., Nigro,V., and Boncinelli,E. (1993). A vertebrate gene related to orthodenticle contains a homeodomain of the bicoid class and demarcates anterior neuroectoderm in the gastrulating mouse embryo. Embo J *12*, 2735-2747.

Smith,R.S., Zabaleta,A., Kume,T., Savinova,O.V., Kidson,S.H., Martin,J.E., Nishimura,D.Y., Alward,W.L., Hogan,B.L., and John,S.W. (2000). Haploinsufficiency of the transcription factors FOXC1 and FOXC2 results in aberrant ocular development. Hum. Mol. Genet. *9*, 1021-1032.

Snow,R.L. and Robson,J.A. (1994). Ganglion cell neurogenesis, migration and early differentiation in the chick retina. Neuroscience *58*, 399-409.

Song,E., Yang,W., Cui,Z.H., Dong,Y., Sui,D.M., Guan,X.K., and Ma,Y.L. (2005). Transplantation of human limbal cells cultivated on amniotic membrane for reconstruction of rat corneal epithelium after alkaline burn. Chin Med. J (Engl.) *118*, 927-935.

Sowden,J.C., Holt,J.K., Meins,M., Smith,H.K., and Bhattacharya,S.S. (2001). Expression of Drosophila omb-related T-box genes in the developing human and mouse neural retina. Invest Ophthalmol Vis Sci *42*, 3095-3102.

Steel,K.P., Davidson,D.R., and Jackson,I.J. (1992). TRP-2/DT, a new early melanoblast marker, shows that steel growth factor (c-kit ligand) is a survival factor. Development *115*, 1111-1119.

Stoll,C., Alembik,Y., Dott,B., and Roth,M.P. (1992). Epidemiology of congenital eye malformations in 131,760 consecutive births. Ophthalmic Paediatr. Genet. *13*, 179-186.

Svendsen,P.C. and McGhee,J.D. (1995). The C. elegans neuronally expressed homeobox gene ceh-10 is closely related to genes expressed in the vertebrate eye. Development *121*, 1253-1262.

Swisshelm,K., Machl,A., Planitzer,S., Robertson,R., Kubbies,M., and Hosier,S. (1999). SEMP1, a senescence-associated cDNA isolated from human mammary

epithelial cells, is a member of an epithelial membrane protein superfamily. Gene *226*, 285-295.

Theiler,K., Varnum,D.S., Nadeau,J.H., Stevens,L.C., and Cagianut,B. (1976). A new allele of ocular retardation: early development and morphogenetic cell death. Anat. Embryol. (Berl) *150*, 85-97.

Tibber,M.S., Kralj-Hans,I., Savage,J., Mobbs,P.G., and Jeffery,G. (2004). The orientation and dynamics of cell division within the plane of the developing vertebrate retina. Eur. J. Neurosci. *19*, 497-504.

Tomarev,S.I., Callaerts,P., Kos,L., Zinovieva,R., Halder,G., Gehring,W., and Piatigorsky,J. (1997). Squid Pax-6 and eye development. Proc. Natl. Acad. Sci. U. S. A *94*, 2421-2426.

Tomita,K., Ishibashi,M., Nakahara,K., Ang,S.L., Nakanishi,S., Guillemot,F., and Kageyama,R. (1996). Mammalian hairy and Enhancer of split homolog 1 regulates differentiation of retinal neurons and is essential for eye morphogenesis. Neuron *16*, 723-734.

Tomita,K., Moriyoshi,K., Nakanishi,S., Guillemot,F., and Kageyama,R. (2000). Mammalian achaete-scute and atonal homologs regulate neuronal versus glial fate determination in the central nervous system. Embo J *19*, 5460-5472.

Tong,Q., Dalgin,G., Xu,H., Ting,C.N., Leiden,J.M., and Hotamisligil,G.S. (2000). Function of GATA transcription factors in preadipocyte-adipocyte transition. Science *290*, 134-138.

Toy,J., Norton,J.S., Jibodh,S.R., and Adler,R. (2002). Effects of homeobox genes on the differentiation of photoreceptor and nonphotoreceptor neurons. Invest Ophthalmol Vis Sci *43*, 3522-3529.

Toy,J., Yang,J.M., Leppert,G.S., and Sundin,O.H. (1998). The optx2 homeobox gene is expressed in early precursors of the eye and activates retina-specific genes. Proc Natl Acad Sci U S A *95*, 10643-10648.

Tropepe,V., Coles,B.L., Chiasson,B.J., Horsford,D.J., Elia,A.J., McInnes,R.R., and van der,K.D. (2000). Retinal stem cells in the adult mammalian eye. Science *287*, 2032-2036.

Truslove,G.M. (1962). A gene causing ocular retardation in the mouse. Journal of Embryology and Experimental Morphology *10*, 652-660.

Tseng,S.C. (1989). Concept and application of limbal stem cells. Eye *3 (Pt 2)*, 141-157.

Turner,D.L. and Cepko,C.L. (1987). A common progenitor for neurons and glia persists in rat retina late in development. Nature *328*, 131-136.

Turner,D.L., Snyder,E.Y., and Cepko,C.L. (1990). Lineage-independent determination of cell type in the embryonic mouse retina. Neuron *4*, 833-845.

Uchida,N., Honjo,Y., Johnson,K.R., Wheelock,M.J., and Takeichi,M. (1996). The catenin/cadherin adhesion system is localized in synaptic junctions bordering transmitter release zones. J Cell Biol *135*, 767-779.

van Diggelen,O.P., Schindler,D., Willemsen,R., Boer,M., Kleijer,W.J., Huijmans,J.G., Blom,W., and Galjaard,H. (1988). alpha-N-acetylgalactosaminidase deficiency, a new lysosomal storage disorder. J. Inherit. Metab Dis. *11*, 349-357.

Van Gelder,R.N., von Zastrow,M.E., Yool,A., Dement,W.C., Barchas,J.D., and Eberwine,J.H. (1990). Amplified RNA synthesized from limited quantities of heterogeneous cDNA. Proc. Natl. Acad. Sci. U. S. A *87*, 1663-1667.

Velculescu,V.E., Zhang,L., Vogelstein,B., and Kinzler,K.W. (1995). Serial analysis of gene expression. Science *270*, 484-487.

Vingolo,E.M., Steindl,K., Forte,R., Zompatori,L., Iannaccone,A., Sciarra,A., Del Porto,G., and Pannarale,M.R. (1994). Autosomal dominant simple microphthalmos. J. Med. Genet. *31*, 721-725.

Voronina,V.A., Kozhemyakina,E.A., O'Kernick,C.M., Kahn,N.D., Wenger,S.L., Linberg,J.V., Schneider,A.S., and Mathers,P.H. (2004). Mutations in the human RAX homeobox gene in a patient with anophthalmia and sclerocornea. Hum. Mol. Genet. *13*, 315-322.

Voronina, V. A. and Mathers, P. H. Mutations in the *RX* gene in a patient with anophthalmia. ARVO annual meeting . 2000.
Ref Type: Abstract

Vyas,A., Saha,B., Lai,E., and Tole,S. (2003). Paleocortex is specified in mice in which dorsal telencephalic patterning is severely disrupted. J. Comp Neurol. *466*, 545-553.

Walcott,J.C. and Provis,J.M. (2003). Muller cells express the neuronal progenitor cell marker nestin in both differentiated and undifferentiated human foetal retina. Clin. Experiment. Ophthalmol. *31*, 246-249.

Wallis,D.E., Roessler,E., Hehr,U., Nanni,L., Wiltshire,T., Richieri-Costa,A., Gillessen-Kaesbach,G., Zackai,E.H., Rommens,J., and Muenke,M. (1999). Mutations in the homeodomain of the human SIX3 gene cause holoprosencephaly. Nat Genet *22*, 196-198.

Walther,C. and Gruss,P. (1991). Pax-6, a murine paired box gene, is expressed in the developing CNS. Development *113*, 1435-1449.

Wang,E., Miller,L.D., Ohnmacht,G.A., Liu,E.T., and Marincola,F.M. (2000). High-fidelity mRNA amplification for gene profiling. Nat. Biotechnol. *18*, 457-459.

Warburg,M. (1993). Classification of microphthalmos and coloboma. J. Med. Genet. *30*, 664-669.

Watanabe,M., Rutishauser,U., and Silver,J. (1991). Formation of the retinal ganglion cell and optic fiber layers. J. Neurobiol. *22*, 85-96.

Wawersik,S., Purcell,P., Rauchman,M., Dudley,A.T., Robertson,E.J., and Maas,R. (1999). BMP7 acts in murine lens placode development. Dev Biol *207*, 176-188.

Weischenfeldt,J., Lykke-Andersen,J., and Porse,B. (2005). Messenger RNA surveillance: neutralizing natural nonsense. Curr Biol *15*, R559-R562.

Weiss,A.H., Kousseff,B.G., Ross,E.A., and Longbottom,J. (1989). Simple microphthalmos. Arch. Ophthalmol. *107*, 1625-1630.

Welsh,J., Chada,K., Dalal,S.S., Cheng,R., Ralph,D., and McClelland,M. (1992). Arbitrarily primed PCR fingerprinting of RNA. Nucleic Acids Res *20*, 4965-4970.

Wetts,R. and Fraser,S.E. (1988). Multipotent precursors can give rise to all major cell types of the frog retina. Science *239*, 1142-1145.

Wetts,R., Serbedzija,G.N., and Fraser,S.E. (1989). Cell lineage analysis reveals multipotent precursors in the ciliary margin of the frog retina. Dev Biol *136*, 254-263.

Wiggan,O., Taniguchi-Sidle,A., and Hamel,P.A. (1998). Interaction of the pRB-family proteins with factors containing paired- like homeodomains. Oncogene *16*, 227-236.

Windrem,M.S., Nunes,M.C., Rashbaum,W.K., Schwartz,T.H., Goodman,R.A., McKhann,G., Roy,N.S., and Goldman,S.A. (2004). Fetal and adult human oligodendrocyte progenitor cell isolates myelinate the congenitally dysmyelinated brain. Nat Med. *10*, 93-97.

Windrem,M.S., Roy,N.S., Wang,J., Nunes,M., Benraiss,A., Goodman,R., McKhann,G.M., and Goldman,S.A. (2002). Progenitor cells derived from the adult human subcortical white matter disperse and differentiate as oligodendrocytes within demyelinated lesions of the rat brain. J Neurosci Res *69*, 966-975.

Wodicka,L., Dong,H., Mittmann,M., Ho,M.H., and Lockhart,D.J. (1997). Genome-wide expression monitoring in Saccharomyces cerevisiae. Nat. Biotechnol. *15*, 1359-1367.

Wohrn,J.C., Puelles,L., Nakagawa,S., Takeichi,M., and Redies,C. (1998). Cadherin expression in the retina and retinofugal pathways of the chicken embryo. J. Comp Neurol. *396*, 20-38.

Wu,L.Y., Li,M., Hinton,D.R., Guo,L., Jiang,S., Wang,J.T., Zeng,A., Xie,J.B., Snead,M., Shuler,C., Maxson,R.E., Jr., and Liu,Y.H. (2003). Microphthalmia resulting from MSX2-induced apoptosis in the optic vesicle. Invest Ophthalmol. Vis. Sci. *44*, 2404-2412.

Xuan,S., Baptista,C.A., Balas,G., Tao,W., Soares,V.C., and Lai,E. (1995). Winged helix transcription factor BF-1 is essential for the development of the cerebral hemispheres. Neuron *14*, 1141-1152.

Yamamoto,M., Maehara,Y., Takahashi,K., and Endo,H. (1983). Cloning of sequences expressed specifically in tumors of rat. Proc Natl Acad Sci U S A *80*, 7524-7527.

Yamamoto,M., Wakatsuki,T., Hada,A., and Ryo,A. (2001). Use of serial analysis of gene expression (SAGE) technology. J Immunol. Methods *250*, 45-66.

Yandava,B.D., Billinghurst,L.L., and Snyder,E.Y. (1999). "Global" cell replacement is feasible via neural stem cell transplantation: evidence from the dysmyelinated shiverer mouse brain. Proc Natl Acad Sci U S A *96*, 7029-7034.

Ying,S., Jansen,H.T., Lehman,M.N., Fong,S.L., and Kao,W.W. (2000). Retinal degeneration in cone photoreceptor cell-ablated transgenic mice. Mol. Vis. *6*, 101-108.

Yokoyama,Y., Narahara,K., Tsuji,K., Ninomiya,S., and Seino,Y. (1992). Autosomal dominant congenital cataract and microphthalmia associated with a familial t(2;16) translocation. Hum. Genet. *90*, 177-178.

Young,R.W. (1985). Cell differentiation in the retina of the mouse. Anat Rec. *212*, 199-205.

Yun,K., Fischman,S., Johnson,J., Hrabe,d.A., Weinmaster,G., and Rubenstein,J.L. (2002). Modulation of the notch signaling by Mash1 and Dlx1/2 regulates sequential specification and differentiation of progenitor cell types in the subcortical telencephalon. Development *129*, 5029-5040.

Zamenhof,S. (1987). Quantitative studies of mitoses in fetal rat brain: orientations of the spindles. Brain Res *428*, 143-146.

Zhang,D.H., Cohn,L., Ray,P., Bottomly,K., and Ray,A. (1997). Transcription factor GATA-3 is differentially expressed in murine Th1 and Th2 cells and controls Th2-specific expression of the interleukin-5 gene. J. Biol. Chem. *272*, 21597-21603.

Zhang,J., Kleinschmidt,J., Sun,P., and Witkovsky,P. (1994). Identification of cone classes in Xenopus retina by immunocytochemistry and staining with lectins and vital dyes. Vis. Neurosci. *11*, 1185-1192.

Zhang, L, Mathers, P. H., and Jamrich, M. Function of the *Rx* gene is essential for the formation of retinal progenitor cells in mice. ARVO annual meeting . 2001. Ref Type: Abstract

Zhang,L., Mathers,P.H., and Jamrich,M. (2000). Function of Rx, but not Pax6, is essential for the formation of retinal progenitor cells in mice. Genesis. *28*, 135-142.

Zhao,S. and Overbeek,P.A. (1999). Tyrosinase-related protein 2 promoter targets transgene expression to ocular and neural crest-derived tissues. Dev Biol *216*, 154-163.

Zhao,Y., Hong,D.H., Pawlyk,B., Yue,G., Adamian,M., Grynberg,M., Godzik,A., and Li,T. (2003). The retinitis pigmentosa GTPase regulator (RPGR)- interacting protein:

subserving RPGR function and participating in disk morphogenesis. Proc. Natl. Acad. Sci. U. S. A *100*, 3965-3970.

Zheng,W. and Flavell,R.A. (1997). The transcription factor GATA-3 is necessary and sufficient for Th2 cytokine gene expression in CD4 T cells. Cell *89*, 587-596.

Zlotogora,J., Legum,C., Raz,J., Merin,S., and BenEzra,D. (1994). Autosomal recessive colobomatous microphthalmia. Am. J. Med. Genet. *49*, 261-262.

Zuber,M.E., Gestri,G., Viczian,A.S., Barsacchi,G., and Harris,W.A. (2003). Specification of the vertebrate eye by a network of eye field transcription factors. Development *130*, 5155-5167.